The Aza-HDDA Reaction and Other Adventures in Cycloaromatization Chemistry

A DISSERTATION

SUBMITTED TO THE FACULTY OF THE

UNIVERSITY OF MINNESOTA

BY

Severin Kelly Thompson

IN PARTIAL FULFILLMENT OF THE REQUIERMENTS FOR THE DEGREE OF

DOCTOR OF PHILOSOPHY

Thomas R. Hoye, Adviser

July 2019

Acknowledgments

Several of my friends and fellow graduate students can attest to my generally cynical nature. When encountering the inevitable frustrations of graduate school and research, it has often been tempting to succumb to cynicism, bitterness, and despair. Indeed, I have given more than a few people the impression that my experience in graduate school has been a tiring, depressing, and seemingly endless struggle. More significantly, I've occasionally given the impression that I've been forced to endure this alone.

In spite of this, I have to confess that this is far from the truth. I've been tremendously fortunate to have a strong support system throughout these years—both inside and outside of the Department of Chemistry. I've encountered countless people who, in one way or another, have helped me and have shaped me into the person—and the chemist—that I am today. While I have found it humbling to essentially condense several years of my life into one thesis, it is nothing when compared to this attempt to acknowledge 6 years of collaboration, help, and guidance in just a few pages. I can't possibly do justice to all the people who have helped me in a short acknowledgment section of my thesis, but I will do what I can.

I will start by thanking my parents, as they were the people who initially instilled in me the values that have helped me to succeed as a chemist. Throughout my life, my parents have been a tremendous source of support—encouraging me to learn while also giving me room to pursue my own interests. Even though I've often been like a ghost over the last few years, they have always been there to offer encouragement, support, and perspective. My extended family has also enriched my life. There were few things that could help me recover from the frustrations of graduate school as much as flying out to visit my grandmother Martha, playing Mario Kart with my brother Kai, visiting my aunt Denise and trying some of her amazing cooking, or playing a few rounds of golf with my uncle Chris.

There is no doubt that I would not have been able to get this far without the help of my colleagues in the Hoye group. While frustrations and disagreements are inevitable when stressed out graduate students are put into a relatively small space and forced to share equipment, I've been lucky to share the lab with a group of smart, motivated, and friendly people. I first joined the lab with fellow first years Juntian Zhang and Xiao Xiao. From then until now, they have been a continuing source of entertainment and have contributed much to our lab—Xiao for his maintenance of our LC-MS and Juntian for his outstanding work on the GC-MS. After joining the lab, I received invaluable guidance and advice from older graduate students—or as Juntian would say, "big brothers,"—Junhua Chen and Sean Ross. They were valued mentors and good friends.

I would also like to acknowledge a few other graduate students from the Hoye lab: Grant Fahnhorst, who is a year below me, is a rare breed of graduate student—one who excels at research AND is an outstanding lab citizen. I've greatly appreciated having him as a lab mate. Juntian Zhang, whom I previously mentioned, has been one of my closest friends and most valued colleagues. He, more than anyone else, has made the experience of graduate school relatively enjoyable. I'd like to finally thank my hood mate and girlfriend Mengyuan Jin, who has been a tremendous source of emotional support as I've been stressfully trying to finish everything up over the last few months.

I've additionally had the privilege of sharing our lab with several great postdocs. In particular, I'd like to thank Nick Ball–Jones, who has offered invaluable career advice and whom I will be joining shortly in the Bay Area, Vijay Gopalsamuthiram, who has patiently worked with me on prodrug projects in which I have no expertise, Rajasekhar "Reddy" Naredla, who was a good friend as well as my colleague on the PDDA project, fellow St. Cloud, MN native Bryce Sunsdahl, who got our previously defunct glovebox running and who can fix ANYTHING, and Hang Shen, who was one of my favorite "postdoctors" and a good friend with whom I still keep in touch.

Finally, I must acknowledge some of the outstanding undergraduate students that I have known in the Hoye lab. I'll start with Nguyen Doan, who was only with us for a few months as a visiting undergrad from Nanyang Technological University. His knowledge of organic chemistry was so vast that it was scary. I had the privilege of

sharing my hood with him and acting as an unofficial mentor. Besides being my friend, he showed me the tremendous value of being in a mutually beneficial mentorship. Vignesh Palani was a highly gifted and extraordinarily dedicated student whom I am proud to call my friend. I will always cherish our memories of telling jokes and playing pranks on lab mates. I look forward to joining him in the Bay Area and am excited to see where his skills as a chemist take him in his career. Last but not least, I want to express my gratitude to Mr. Quang Hong Luu Nguyen, who is unlike any other chemist—or any other person—that I've met. He is both a gifted chemist and a relatable person. Even though Quang graduated from the University of Minnesota over four years ago, we still talk every day (whether I want to or not). Vignesh and I even managed to play a few pranks on him after he left. Quang is a source of inspiration, amusement, and happiness all rolled up into one person who I am glad to call my friend.

Countless graduate students who are outside of the Hoye lab but inside of the Department of Chemistry were an integral part my graduate school experience. Whether it was talking about life, gossiping about faculty members, discussing research, or playing softball, my experiences with my fellow graduate students were both enriching and enjoyable. I'd like to first thank my roommate and fellow 6th year Tom Webber for making my hours outside of lab more enjoyable (and for encouraging me to play softball). I additionally count myself very lucky to share the 4th floor of Smith Hall with Steve Kirberger and Peter Ycas from the Pomerantz lab. I don't think anyone is willing to listen to and pretend to laugh at my jokes as much as Steve. Peter, besides having a great sense of humor, was always willing to talk about our shared hobby of cooking. He, more than anyone else, taught me the value of having interests outside of chemistry and of having people with whom you can talk your interests. I'd finally like to thank (in no particularly order) Evan Beaumier, J.T. Moore, Zach Gilbert, and Alex "Undergrad" Wheeler for their friendship and support.

I'd further like to express my gratitude to the outstanding faculty and staff here in the Department of Chemistry. I'll start by thanking Professors Steven Kass, Wayland

Noland, and Courtney Aldrich for serving on my committee. I have interacted with Professors Kass and Noland as part of my qualifying exams. They are knowledgeable and kind people whom I am glad to have met. While my interactions with Professor Aldrich have been far more limited, I did take a course on the chemistry of natural products with him, during which time I grew to appreciate his knowledge, accessibility, and enthusiasm.

I'd like to give a special thanks to the NMR Lab Director, Dr. Letitia Yao. She is highly competent, extremely reliable, and really fun to talk to. Additionally, having spent several years in the Hoye lab, she understrood several of the unique joys and struggles I experienced throughout graduate school. Letitia is even the reason that I have a job! She informed me of a job opportunity from one of her former colleagues and forwarded my cover letter to her! I really am fortunate to know Letitia and I hope that, some day, I can repay her for all she has done for me.

Lastly, it is with bittersweet emotions that I express my gratitude toward my adviser, Dr. Thomas Hoye. I entered graduate school largely unaware of the direction in which I would be headed. This changed within the first week of taking Tom's organic synthesis class. His enthusiasm, tremendous breadth of knowledge, as well as his passion for the teaching and practice of organic chemistry were inspiring. In my eyes, he was a god among mortals in the world of chemistry.

After having spent most of my waking hours in his lab over the past six years, I can say that my impression of Tom has changed significantly. In place of the initial idolization and almost childish admiration that I had for him, my feelings have matured into a far more restrained but also far more deep-seated and well-deserved respect.

As an advisor, Tom is an apparent contradiction: both hands-on and hands-off. As a teacher of organic chemistry, he is tremendously dedicated and accessible. He has committed countless hours in teaching me how to think about organic chemistry, how to objectively analyze experimental results, and—most importantly—how to be a competent problem solver. I will always appreciate the multiple occasions where he dropped whatever he was doing to teach me how to—among many other things—troubleshoot our

GC-MS, fix a defective solvent pump, clean a seized vacuum pump, or appropriately flange tubing for my MPLC.

At the same time, Tom is rather hands-off when it comes to project conception and project management. During the first few years of graduate school, this was often a source of frustration for me. I looked on in bitterness and self-pity as I watched a few of my colleagues in other labs—whose advisors would give them explicit instructions—succeed and publish while I struggled just to get think of ideas and get them off the ground. It is only recently that I've come to truly appreciate Tom's style. His tendency to step back—while at the same time remaining highly accessible to answer my questions and teach me—have allowed me to mature into a more knowledgeable and independent chemist who is sufficiently confident to conceive and pursue his own ideas.

While I could probably write a separate thesis covering the broad array of emotions that I've felt for Tom, I will finish by simply saying this: As I enter industry and move onto the next stage of my career, I will consider myself extraordinarily fortunate if I can find a mentor or colleague who is anywhere close to Tom. Thank you, Tom, for all that you have done for me. With great pride, I can officially declare that our collaboration has been both cordial and fruitful!

Abstract

Cycloaromatization reactions yield cyclic products that are aromatic but unstable, leaving these products prone to further reactions and functionalization. Their relevance in the antibiotic mechanism of enediyne natural products as well as their ability to access diversely functionalized arenes have made cycloaromatization reactions a point of significant focus in chemical research. One particularly interesting and synthetically valuable cycloaromatization reaction is the hexadehdyro-Diels–Alder (HDDA) reaction, in which a 1,3-diyne moiety engages a covalently attached alkyne (diynophile) in a formal [4 + 2] cycloaddition under thermal conditions. The product of this reaction, 1,2-didehydrobenzene—also known as benzyne—is capable of reacting with myriad "trapping" molecules to yield an array of functionalized benzenoid products.

This HDDA cascade, as well as other related cycloaromatization reactions, are the focus of this thesis. Reactions of HDDA-generated benzyne with various carbonyl moieties were studied. Among these benzyne-trapping reactions are "divergent" reactions, in which HDDA-generated benzyne is shown to react differently from benzyne generated by the more standard Kobayashi protocol. Additionally, novel benzyne reactions that are not reported in the literature are discussed (**Chapter 2**). Closely related to the HDDA reaction is the pentadehydro-Diels–Alder (PDDA) reaction, in which a 1,3-allenyne (as opposed to a 1,3-diyne) undergoes a [4 + 2] cycloaddition with a pendant alkyne to yield a precedented but understudied α,3-dehydrotoluene intermediate. Synthetic studies of this reaction revealed its ability to access functionalized benzene and pyridine products, while computational studies lent insight into its mechanism and energetics (**Chapter 3**). Finally, the incorporation of nitriles into the HDDA reaction was investigated. The replacement of an alkyne with a nitrile on either the diynophile or 1,3-diyne of an HDDA substrate gives *aza*-HDDA substrates that cyclize to 3,4-pyridyne (**Chapter 4**) and 2,3-pyridyne (**Chapter 5**) intermediates. The generation of these intermediates and their subsequent trapping reactions to produce diversely functionalized pyridine products are discussed.

Table of Contents

Acknowledgments
i

Abstract vi

Table of Contents vii

List of Figures x

List of Abbreviations xv

Chapter 1. Introduction to the HDDA Reaction **.....1**

1.1 **Benzyne 1**

1.1.1 The Structure and Early History of Benzyne.....1

1.1.2 Reactivity of Benzyne 3

1.1.2.1 Functionalization of Benzyne.....3

1.1.2.2 Regioselectivity of Benzyne-Trapping Reactions 5

1.1.3 Generation of Benzyne 8

1.2 **The Hexadehydro-Diels–Alder (HDDA) Reaction 10**

1.2.1 Dehydro-Diels–Alder (DDA) Reactions.....10

1.2.2 Early Reports of the HDDA Reaction 13

1.2.3 Serendipitous Rediscovery of the HDDA Reaction.....17

1.2.4 Synthetic Utility of the HDDA reaction 20

Chapter 2. Reactions of HDDA Benzyne with Carbonyl Moieties **.....25**

2.1 **Preface: Reactions of Benzyne with Aldehydes 25**

2.2 **Attempted Three-Component Reactions with HDDA-Benzyne and Aromatic Aldehydes.....27**

2.3 **Synthesis of Benzodioxane Products Through the HDDA Reaction.....28**

2.4 **Formation of Alkenyl Phenol Products from Aliphatic Aldehydes: A Novel Benzyne Reaction 29**

2.5 **α-Arylation of 1,3-Dicarbonyl Traps: A "Divergent" Benzyne Reaction.....31**

Chapter 3. The Pentadehydro-Diels–Alder (PDDA) Reaction **.....36**

3.1 **Preface: Dehydro-Diels–Alder Reactions with Allenes 36**

3.2 **Discovery of a Pentadehydro-Diels–Alder (PDDA) Reaction Cascade.....38**

3.3 Probing PDDA Reaction Energetics with DFT Calculations 39
3.3.1 Initial Experimental Evidence for the Proposed PDDA Reaction 39
3.3.2 DFT Support for the PDDA Reaction 41
3.3.3 Additional in silico Observations 42
3.4 **Additional Studies into the Synthetic Applications of the PDDA Reaction 44**
3.4.1 An Attempted Bimolecular HDDA–PDDA Cascade 44
3.4.2 Attempts to Synthesize Functionalized Pyridazines 47
Chapter 4. The Aza-HDDA Reaction **53**
4.1 **Preface: A Hypothetical Aza-HDDA Reaction 53**
4.2 **Previous Attempts at the Aza-HDDA Reaction 57**
4.3 The First Successful Aza-HDDA Reaction 59
4.4 Initial Computational Studies 61
4.4.1 Proposal for an In Silico Aza-HDDA "Assay" 61
4.4.2 DFT Insight Regarding a Stepwise vs. a Concerted aza-HDDA Reaction 64
4.3.3 Carrying Out the In Silico Aza-HDDA Assay on Candidate Substrates 66
4.4 **Synthesis and Testing of Additional Aza-HDDA Substrates 67**
4.4.1 A gem-Dimethylated Benzylic Nitrile Substrate. 69
4.4.2 A Dialkynyl Ketone Substrate 74
3.4.3 An Acyl Nitrile Substrate with a Cycloheptene Tether. 77
3.4.3 An Acyl Nitrile Substrate with a More Stable Benzene Tether 82
4.5 **Intermolecular Trapping of Pyridynes Generated by the aza-HDDA Reaction . 87**
4.5.1 A Benzoyl Nitrile Aza-HDDA Substrate 87
4.5.2 A gem-Dimethylated Allylic Nitrile Substrate with a Cycloheptenyl Tether 92
4.5.3 Aza-HDDA Test Reaction of an Allylic Nitrile Substrate (4069) 97
4.5.4 Intermolecular Trapping Reactions of an Allylic Nitrile Substrate (4019) 100
4.5.4 Failed Aza-HDDA Reactions of Substrate 4019 104
Chapter 5. The Class II Aza-HDDA Reaction **106**
5.1 **Preface: The Class II Aza-HDDA Reaction 106**
5.2 **Some Initial Considerations on the Reactivity of Class II aza-HDDA Substrates 107**
5.3 Insight from Preliminary DFT Calculations 108
5.3.1 Relative Energetics of Isomeric Pyridynes 108

5.3.2 Geometric Distortion of Pyridyne Species 108
5.3.3 Relative Energetics of the Class I and Class II Aza-HDDA Reactions 110
5.3.4 Mechanistic Insight into the Class II Aza-HDDA Reaction 111
5.4 **Synthesis of the First Class II aza-HDDA Test Substrate 113**
5.4.1 First Attempted Synthetic Route 113
5.4.2 Second Attempted Synthetic Route 117
5.5 **First Attempts To Carry Out Class II Aza-HDDA Reactions 118**
5.5.1 Successful Reactions 118
5.5.2 Failed Reactions 121
5.5.3 Summary of Implications from the Experimental and Theoretical Results 123
5.6 **Synthesis of a gem-Dimethylated Class II Aza-HDDA Test Substrate 123**
5.6.1 First Attempted Synthetic Route 123
5.6.2 A Second Attempted Synthetic Route: Longer but Effective 125
5.7 **Aza-HDDA Reactions of a gem-Dimethylated Class II Substrate 126**
Chapter 6. Experimental Procedures and Compound Characterization **129**
Chapter 7. Computational Data 204
Bibliography and Notes 284

List of Figures

Figure 1.1 | Generic representation of the resonance structures of benzyne and the reactivity of benzyne with a molecular "trap" T^1–T^2. 1

Figure 1.2 | Nucleophilic functionalization of benzyne in a bimolecular fashion (a) and trimolecular fashion (b). 4

Figure 1.3 | Two isomeric benzenoid products can form when an unsymmetrical trap is used with an unsymmetrical benzyne intermediate. 6

Figure 1.4 | Regioselectivity in trapping of distorted benzynes. 7

Figure 1.5 | The Kobayashi method: Generation of benzyne by exposure of trimethylsilyl phenyl triflate (**1010**) to a fluoride source. 9

Figure 1.6 | (a) The Diels – Alder reaction (top left) and variations of the dehydro-Diels–Alder reactions. (b) The first report of a dehydro-Diels–Alder reaction. 11

Figure 1.7 | Energetics of the Diels–Alder reaction (a) and of the variations of dehydro-Diels–Alder reaction (b-f). The reaction energy for each reaction is shown below the arrows; the ring strain is shown to the right of each product (values in $kcal \cdot mol^{-1}$, calculated by Johnson and coworkers). 12

Figure 1.8 | Flash vacuum pyrolysis of 1,3,8-nonatriyne (**1021**) to give indane (**1022**) and indene (**1023**). 14

Figure 1.9 | Deuterium labeling experiment supports the formation of indane (**1022**) via the benzyne **1021*** (path b) as opposed to a Bergman cyclization (path a). 15

Figure 1.10 | Selected example of a cycloaromatization reaction reported by Ueda and coworkers along with their proposed reaction mechanism. 16

Figure 1.11 | Rediscovery of the HDDA reaction from an attempted oxidation of alcohol **1027**. 17

Figure 1.12 | a) Generic illustration of the HDDA cascade. b) Examples of structures access from intramolecular trapping of HDDA-generated benzynes. 21

Figure 1.13 | Products of intramolecular HDDA benzyne trapping. a.) Products resulting from nucleophilic attack on HDDA benzyne. b.) Products for which the benzyne is trapped in a pericyclic reaction. 22

Figure 1.14 | Selected examples of products representative of notable advances in HDDA chemistry.....24
Figure 2.1 | (a) Aldehydes react with phenyl anions that result from the trapping of benzyne with a nucleophile. This can be done in an intramolecular fashion (b) or in a multicomponent reaction (c).....25
Figure 2.2 | The reaction of benzyne with aldehydes yields *ortho*-quinone methide products.....26
Figure 2.3 | Formation of benzodioxane products **2018**–**2020**. 29
Figure 2.4 | (a) The trapping of HDDA-benzyne with a 1,3-dicarbonyl compound results in an α-arylation product as a mixture of tautomers **2032a** and **2033b**. (b) Products **2033**–**2036** resulting from this reaction. The molar ratios of enol to keto tautomers for products **2035** and **2036** are shown in parenthesis. 33
Figure 2.5 | α-Arylation products that were not formed from the HDDA reaction. 34
Figure 2.6 | Reactive divergence of HDDA benzyne from Kobayashi benzyne. 35
Figure 3.1 | Simplified examples of dehydro-Diels–Alder reactions with allenes.....36
Figure 3.2 | The pentadehydro-Diels–Alder reaction. 37
Figure 3.3 | Proposed formation of benzylic amine **3008** from tetrayne **3006** through a PDDA pathway. 39
Figure 3.4 | Experimental results that support a proposed PDDA pathway. 40
Figure 3.5 | Relative free energies of intermediates in the proposed PDDA reactions of substrates **3016a-d**. The relative free energy values for all intermediates and TS structures resulting from a given substrate are referenced to their corresponding allenyne (**3017a–d**). Figure reproduced from ref 72. 42
Figure 3.6 | Bimolecular PDDA reactions between an allenyne **3022** and DMAD (a) and between **3022** and benzyne (b). The free energy of activation ($\Delta G^{\ddagger}$) for each reaction is shown below the respective TS structures. 45
Figure 3.7 | Generic representation of a proposed HDDA–PDDA cascade. 46
Figure 3.8 | (a) Proposed synthesis of functionalized pyridazines through the PDDA reaction. (b) DFT-calculated free energy of activation for a PDDA cyclization of cyanoallene nitrile **3032** to α,3-dehydrodiazatoluene **3033**. (c) DFT-calculated free

energy of activation for an HDDA cyclization of cyanoalkyne nitrile **3034** to pyridazyne **3035**. 48
Figure 3.9 | The relative free energies of relevant intermediates and TS structures in the PDDA cycloaromatization of cyanoallene **3032** to α,3-dehydrodiazatoluene **3033**, as determined by DFT calculations. An image of **3033** is shown to the right. 51
Figure 4.1 | The HDDA reaction (left) and a hypothetical aza-HDDA reaction (right).. 53
Figure 4.2 | Examples of marketed pharmaceutical drugs that contain a pyridine ring. . 54
Figure 4.3 | Nitrogen heterocyles that appear in FDA approved small molecule drugs. The number of drugs in which the each heterocycle appears is listed in bold. Pyridine (top left, dashed box) is second only to piperidine. (Figure reproduced from Njardarson et al.) 55
Figure 4.4 | *De novo* synthesis of pyridine rings from (a) condensation reactions (b) and cycloaddition reactions (both literal and formal). 56
Figure 4.5 | Previous unsuccessful attempted aza-HDDA reactions. 59
Figure 4.6 | The first successful aza-HDDA reaction. 60
Figure 4.7 | The same aza-HDDA reaction run under milder thermal conditions. 61
Figure 4.8 | The HDDA reaction occurs through a stepwise process (right) in preference to a concerted process (left). 62
Figure 4.9 | Hypothetical stepwise pathway of the aza-HDDA reaction. 63
Figure 4.10 | Relative free energies of TS structures **4014**$^{\ddagger}_{\textbf{concerted}}$ and **4014**‡**_a** for the concerted and stepwise aza-HDDA reactions of nitrile-diyne substrate **4014**. 64
Figure 4.11 | Calculated energetics of selected aza-HDDA substrate candidates. 67
Figure 4.12 | Calculated activation energy ($\Delta G^{\ddagger}$) for the aza-HDDA cycloaromatization of the benzylic nitrile substrate **4015**. 69
Figure 4.13 | Calculated free energy of activation ($\Delta G^{\ddagger}$) for the aza-HDDA reaction of acyl nitrile substrate **4018**. 77
Figure 4.14 | Selected methodology for the synthesis of acyl nitriles from aldehydes. .. 80
Figure 4.15 | a) Generation of reactive pyridyne intermediate **4062*** and *in situ* trapping of **4062*** (by reaction with trap T^2-T^1) to give generic functionalized pyridine **4064**. b) Selected examples pyridine products (**4064a**–**4064d**) produced from the aza-HDDA

reaction of substrate **4062**; the molar ratios of regioisomers for products **4064c** and **4064d** are shown in parentheses. 88
Figure 4.16 | a) The result of heating substrate **4062** in the presence of *n*-butylamine and b) examples of pyridine products that were not successfully formed from the aza-HDDA reaction with **4062** (traps shown in parentheses below each product). 91
Figure 4.17 | The effect of the acyl nitrile functionality (a) and the cycloheptene tether (b) on energy required for an aza-HDDA reaction to occur. 93
Figure 4.18 | Calculated free energy of activation ($\Delta G^{\ddagger}$) for computational substrate **4019**. 93
Figure 4.19 | a) Proposed steric clash between the cycloheptene ring and the OTBS trap in TS structure **4069**‡. b) DFT-computed distances between carbon 4 and hydrogen substitutents on the tether in pyridynes **4019*** and **4017***. c) Results of heating aza-HDDA substrate **4069** in the presence of furan. 99
Figure 4.20 | a) Generation of reactive pyridyne intermediate **4019*** and its *in situ* trapping (by reaction with trapping compound T^2-T^1) to give functionalized pyridine **4081**. b) Selected examples of pyridyne products (**4081a**–**4081d**) produced from the aza-HDDA reaction of substrate **4019**; the molar ratios of regioisomers for products **4081c** and **4081d** are shown in parentheses. c) Comparison to analogous results from substrate benzoyl nitrile substrate **4062**. 101
Figure 4.21 | a) Generation of reactive pyridyne intermediate **4019*** and its *in situ* trapping (by reaction with trapping compound T^2-T^1) to give functionalized pyridine **4081**. b) Additional examples of pyridyne products (**4081e**–**4081i**) produced from the aza-HDDA reaction of substrate **4019**; the molar ratios of regioisomers for products **4081e** and **4081f** are shown in parentheses. 103
Figure 4.22 | Pyridine products that were not accessible in meaningful yields from the aza-HDDA reaction of nitrile **4019**. Molecular traps are shown in parentheses below each product. 105
Figure 5.1 | The class I (a) and class II (b) aza-HDDA reactions 106

Figure 5.2 | Successful aza-HDDA reaction of class I substrate **5005** with a nucleophilic trap (Nu) in contrast with a potential Michael addition of the same nucleophilic trap to the analogous class II substrate **5008** and an Alder–Ene reaction to give **5009**. 108

Figure 5.3 | Isomeric aza-HDDA substrates **5010** (class I) and **5011** (class II) have similar calculated changes free energies (ΔG_{rxn}) in their cyclizations to pyridyne products **5010*** and **5011***, respectively. The analgous triyne HDDA reaction of **5012** to **5012*** is far more exergonic..... 109

Figure 5.4 | a) Computed geometric distortion in arynes **5010*, 5011*, and 5012*** as shown by the differences in bond angles ($\Delta\theta$) for carbons a and b. b.) Similar geometric distortions shown in unsubstituted benzyne, 3,4-pyridyne, and 2,3-pyridyne. 109

Figure 5.5 | Candidate class II Aza-HDDA substrates **5013** and **5014** , along with their previously studied class I analogs **4017** and **4015**. 110

Figure 5.6 | Calculated relative free energy values of candidate class II aza-HDDA substrate **5013**, its corresponing pyridyne (**5013***), and the concerted TS structure that connects them (**5013**‡). Images of the computed structures for **5013**‡ and **5013*** are also shown..... 111

Figure 5.6 | Calculated relative free energy values of candidate class II aza-HDDA substrate **5014**, its corresponing pyridyne (**5014***), and the concerted TS structure that connects them (**5014**‡). Images of the computed structures for **5014**‡ and **5014*** are also shown..... 113

Figure 5.7 | Two common methods used to synthesize cyanoalkynes from terminal alkynes and their potential applications to the synthesis of intermediate **5019**..... 115

Figure 5.8 | Initial pyridine products **5025a**–**5025d** formed from aza-HDDA reactions of class II substrate **5015**..... 119

Figure 5.9 | Reaction of aza-HDDA substrate **5015** with natural products tropinone (a) and colchicine (b). 121

Figure 5.10 | Examples of products which were not successfully synthesized in more than trace amounts from the aza-HDDA reaction with substrate **5015**..... 122

Scheme 5.7 | Synthesis of test substrate **5026**. 125

Figure 5.11 | Products from the class II aza-HDDA reaction of substrate **5026**..... 127

List of Abbreviations

$AgNO_3$ Silver nitrate

CuCN Cuprous cyanide

DBU 1,8-Diazabicyclo[5.4.0]undec-7-ene

***o*-DCB** *ortho*-Dichlorobenzene

1,2-DCE 1,2-Dichloroethane

DDA Dehydro-Diels–Alder (reaction)

DFT Density Functional Theory

DIBAL Diisobutylaluminum hydride

DMAD Dimethyl acetylenedicarboxylate

DMF Dimethylformamide

FVP Flash vacuum pyrolysis

GC-MS Gas chromatography mass spectrometry

HCl Hydrogen chloride

HCN Hydrogen cyanide

HDDA Hexadehydro-Diels–Alder (reaction)

HF Hydrofluoric Acid

HMBC Heteronuclear Multiple Bond Correlation

HPLC High-pressure liquid chromatography

HRMS High resolution mass spectrometry

HSQC Heteronuclear Single Quantum Coherence

IRC Intrinsic Reaction Coordinate

KCN Potassium cyanide

LC-MS Liquid chromatography mass spectrometry

LDA Lithium diisopropylamide

LiHMDS Lithium bis(trimethylsilyl)amide

MeCN Acetonitrile

MeI Methyl iodide

MeOH Methanol

MnO_2 Manganese (IV) oxide

MPLC Medium-pressure liquid chromatography

MsCl Mesyl chloride

Ms_2O Methansulfonic anhydride

n-BuLi n-butyllithium

$NaBH_4$ Sodium borohydride

NaCN Sodium cyanide

NaH Sodium hydride

$NaHCO_3$ Sodium bicarbonate

Nfom Non-first order multiplet

NIS N-iodosuccinimide

NMR Nuclear magnetic resonance

NOE Nuclear Overhauser Effect

^{n}Pr *n*-Propyl

PBr_3 Phosphorous tribromide

$Pb(OAc)_4$ Lead tetraacetate

PCC Pyridinium chlorochromate

PDC Pyridinium Dichromate

PDDA Pentadehydro-Diels–Alder (reaction)

TBAB Tetra-*n*-butylammonium bromide

TBAF Tetra-*n*-butylammonium fluoride

TBS *tert*-Butylsilyl

TEA Triethylamine

TES Triethylsilyl

THF Tetrahydrofuran

TLC Thin Layer Chromatography

TMSCN Trimethylsilyl cyanide

$TMSN_3$ Azidotrimethylsilane

TPCPD Tetraphenylcyclopentadienone

TS Transition state

Chapter 1. Introduction to the HDDA Reaction

1.1 Benzyne

1.1.1 The Structure and Early History of Benzyne

Reactive intermediates have for quite some time been the object of broad and intense interest among organic chemists. Although the instability of these reactive intermediates makes them challenging to directly observe and characterize, it also allows them to react with a wide variety of molecular "traps"—often with remarkable (and underappreciated)[1] selectivity. This renders them invaluable in the synthesis of small molecules. For this reason, there has been a tremendous cumulation of research aimed at taming these short-lived, highly reactive intermediates. These include (but are certainly not limited to) radicals, carbenes, carbanions, carbocations, and highly strained rings for use in organic synthesis.

Of the reactive intermediates frequently encountered in organic synthesis, arynes (didehydroarenes), which are derived by the formal removal of two substituents from an aromatic ring, are among the most ubiquitous. Of the possible didehydroarene isomers—i.e. *ortho*-, *meta*-, and *para*-didehydroarenes in which the two formally removed substituents are *ortho*, *meta*, and *para* to each other, respectively—*ortho*-didehydroarenes (1,2-didehydroarenes) are the most frequently-encountered in chemical research. In particular, 1,2-didehydro*benzene*, henceforth referred to as "benzyne" in this thesis, has been most extensively studied. The ability of benzynes to react with myriad molecular traps across their (formal) strained double bond and access a wide variety of

Figure 1.1 | Generic representation of the resonance structures of benzyne and the reactivity of benzyne with a molecular "trap" T^1–T^2.

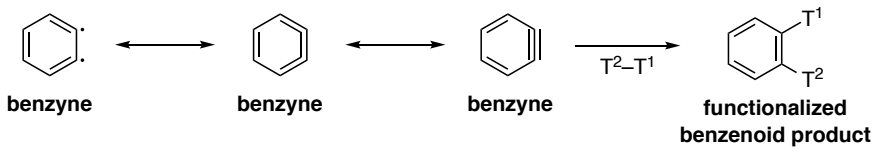

[1] Mayr, H.; Ofial, A. R., The Reactivity–Selectivity Principle: An Imperishable Myth in Organic Chemistry. *Angew. Chem. Int. Ed.* **2006,** *45*, 1844-1854.

functionalized benzenoid rings (generically illustrated in Figure 1) has made them the object of extensive research.

Although the first recorded postulation of an aryne as a reactive intermediate dates back to over a century ago,[2] it was not until the 1940s—several decades later—that research began to shed light onto this elusive species. During this time, Wittig reported an unusual substitution reaction of halobenzenes in the presence of phenyllithium (Scheme 1a).[3] Similarly, Bergstrom[4] (Scheme 1b) and Gilman[5] (Scheme 1c) showed several similar substitution reactions of halobenzenes that were exposed to amide bases in ammonia.

Scheme 1.1 | Benzene substitution reactions reported by Wittig (a), Bergstrom (b), and Gilman (c).

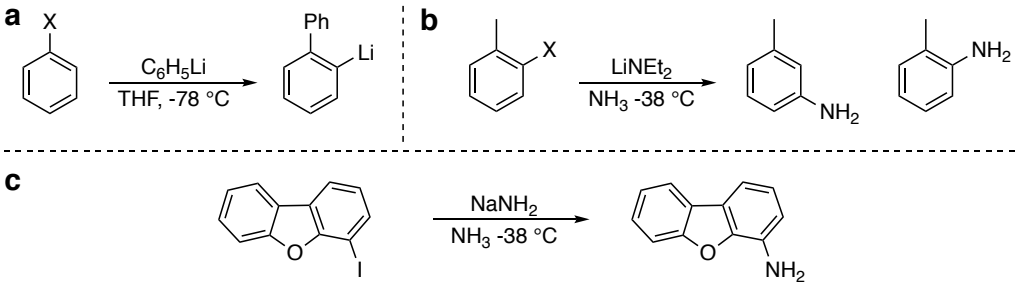

A seminal publication from Roberts in 1953[6] provided compelling mechanistic evidence that benzyne intermediates were responsible for the formation of these products. This publication details a labeling study in which ^{14}C-labelled chlorobenzene (**1001**) was subjected to the same reaction conditions of an amide base in liquid ammonia (Scheme 2a). The resulting ^{14}C-labelled aniline (**1002**) was then subjected to a 5-step derivatization to 1,5-diaminopropane (**1003**) and carbon dioxide (**1004**). Each of these products showed about half of the radioactivity of their aniline-^{14}C precursor (**1002**),

[2] Stoermer, R.; Kahlert, B., Ueber das 1- und 2-Brom-cumaron. *Ber. Dtsch. Chem. Ges* **1902,** *35*, 1633-1640.
[3] Wittig, G., Phenyl-lithium, der Schlüssel zu einer neuen Chemie metallorganischer Verbindungen. *Naturwissenschaften* **1942,** *30*, 696-703.
[4] Bergstrom, F. W.; Horning, C. H., The Action of Bases on Organic Halogen Compounds. V. The Action of Potassium Amide on Some Aromatic Halides (1). *J. Org. Chem.* **1946,** *11*, 334-340.
[5] Gilman, H.; Avakian, S., Dibenzofuran. XXIII. Rearrangement of Halogen Compounds in Amination by Sodamide 1. *J. Am. Chem. Soc.* **1945,** *67*, 349-351.
[6] Roberts, J. D.; Simmons, H. E.; Carlsmith, L. A.; Vaughan, C. W., Rearragement in the Reaction of Chlorobenzne-1-C14 with Potassium Amide 1. *J. Am. Chem. Soc.* **1953,** *75*, 3290-3291.

indicating that **1002** consisted of an even mixture two isotopomers (**1002a** and **1002b** in Scheme 2b). This even distribution of **1002a** and **1002b** could be definitively attributed to a symmetrical (when not considering the carbon-14 isotope) intermediate: benzyne **1001***.

Scheme 1.2 | a) Experiments from Roberts' seminal 1953 publication. The same carbon of intermediates **1002**, **1005**, and **1006**, (not necessarily the carbon-14 isotope) is labeled with a black dot. b) These experiments indicate the formation of a symmetrical benzyne (**1001***) intermediate.

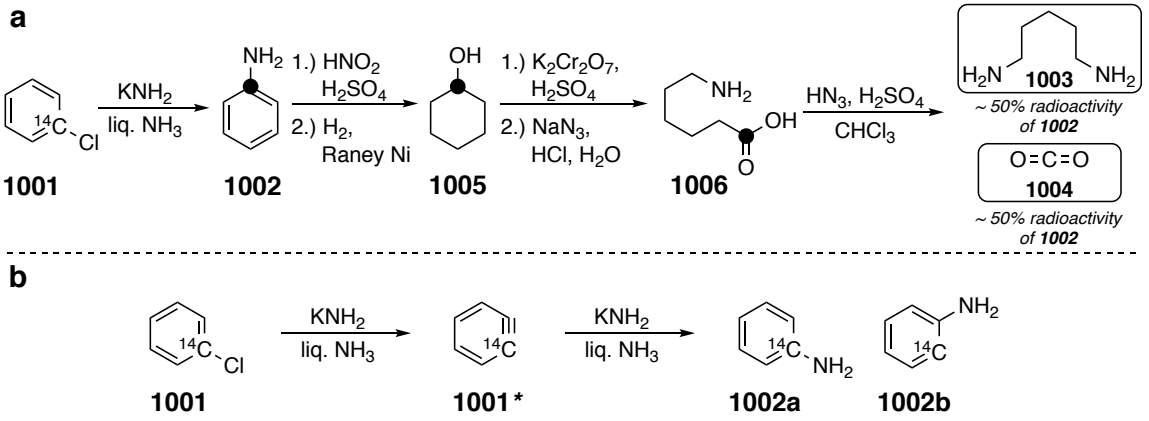

This paper and its preceding experiments were groundbreaking and proved to be just the beginning of an explosive foray into benzyne research. The next decade would see several review articles detailing new advances in benzyne chemistry,[7]a monograph of over 1000 studies that had been conducted on benzyne chemistry,[8] and even a natural product total synthesis that made use of a benzyne intermediate.[9]

1.1.2 Reactivity of Benzyne

1.1.2.1 Functionalization of Benzyne

These early forays into benzyne chemistry have ultimately evolved into over a half-century worth of research that has given tremendous insight into the reactivity of

[7] (a) Wittig, G.; Pohmer, L., Intermediäre Bildung von Dehydrobenzol (Cyclohexa-dienin). *Angewandte Chemie* **1955,** *67*, 348-348. (b) Wittig, G., 1,2-Dehydrobenzene. *Angew. Chem. Int. Ed.* **1965,** *4*, 731-737. (c) Heaney, H., The Benzyne and Related Intermediates. *Chem. Rev.* **1962,** *62*, 81-97.

[8] Hoffmann, R. W. Dehydrobenzene and Cycloalkynes. 11, Academic Press: New York, 1967.

[9] Kametani, T.; Ogasawara, K., Benzyne reaction. Part I. Total Syntheses of (±)-Cryptaustoline and (±)-Cryptowoline by the Benzyne Reaction. *J. Chem. Soc. C* **1967**, 2208-2208.

benzyne and has shown its extraordinary power in organic synthesis. While the reported reactions of benzyne are vast, they can generally be placed into one of three categories:

1.) Pericyclic reactions: The majority of pericyclic reactions with benzynes occur in a [4 + 2] manner with cyclic, electron-rich 1,3-dienes (such as furan), although there are also several examples of [2 + 2] reactions with alkenes and carbon-heteroatom double bonds, [3 + 2] cycloadditions with various 1,3-dipoles, and even ene reactions.

2.) Nucleophilic additions: Benzynes (as well as arynes in general) are highly electrophilic due to their low-lying, acetylenic LUMO.[10] Accordingly, they readily react with a wide variety of nucleophiles that are normally inert toward alkynes. Nucleophilic attack on benzyne typically results in a phenyl anion intermediate that is subsequently quenched by an electrophile (often a proton). This overall process can occur either in a bimolecular fashion, in which the nucleophile (Nu) and electrophile (El) are present in one trap (Figure 2a), or a trimolecular fashion (i.e. in a three-component reaction), where the nucleophile and electrophile are two distinct molecular entities (Figure 2b).

Figure 1.2 | Nucleophilic functionalization of benzyne in a bimolecular fashion (a) and trimolecular fashion (b).

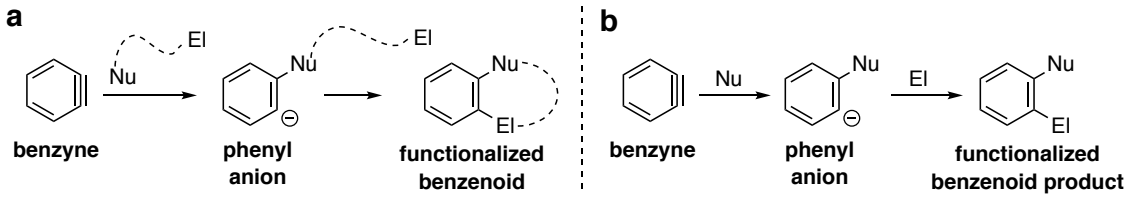

3.) Transition metal-mediated reactions:Although these reactions have been more recently discovered and researched over a shorter period of time, there is a healthy body of work detailing benzyne reactions that are catalyzed by transition metal complexes (usually palladium). Among the more established of these reactions are cyclotrimerizations of benzynes to form polycyclic arenes with a triphenylene core, as

[10] Leopold, D. G.; Miller, A. E. S.; Lineberger, W. C., Determination of the singlet-triplet splitting and electron affinity of o-benzyne by negative ion photoelectron spectroscopy. *J. Am. Chem. Soc.* **1986,** *108*, 1379-1384.

well of cyclization reactions of benzynes with varying equivalents of alkynes, alkenes, and other benzynes to form polycylic aromatic products. Even more valuable (from the perspective of small molecule synthesis) has been the development of benzyne carbopalladation reactions, which allow for rapid and facile access to diverse 1,2-functionalized benzenoid products that could not be directly accessed from benzyne in the absence of a palladium catalyst.

This broad array of benzyne reactions has greatly expanded the toolbox of the modern synthetic organic chemist by allowing for easy and efficient access to diversely functionalized benzenoid products. A strong testament to the synthetic utility of benzyne is the mere fact that dozens of successful natural product total syntheses have utilized benzyne chemistry.[11] Several review articles published within the last decade also highlight the general synthetic value of benzyne.[12]

1.1.2.2 Regioselectivity of Benzyne-Trapping Reactions

An additional issue that is related to benzyne functionalization must also be considered. The vast majority of benzyne-trapping reactions that have been carried out by synthetic organic chemists have not utilized simple, unsubstituted benzyne (C_6H_4) but rather substituted benzynes that are not symmetrical across the formal C≡C triple bond. Consequently, when an unsymmetrical benzyne trap is used, the issue of regioselectivity comes into play (Figure 3).

Numerous early examples of nucleophilic addition to unsymmetrically substituted benzynes indicated that the regioselectivity of addition depended primarily on inductive effects of the substituents on the benzyne ring.[8] Steric effects of the

---

[11] (a) Tadross, P. M.; Stoltz, B. M., A comprehensive history of arynes in natural product total synthesis. *Chem. Rev.* **2012,** *112*, 3550-3577. (b) Gampe, C. M.; Carreira, E. M., Arynes and Cyclohexyne in Natural Product Synthesis. *Angew. Chem. Int. Ed.* **2012,** *51*, 3766-3778.

[12] (a) Dubrovskiy, A. V.; Markina, N. A.; Larock, R. C., Use of benzynes for the synthesis of heterocycles. *Org. Biomol. Chem* **2013,** *11*, 191-218. (b) Sanz, R., Recent Applications of Aryne Chemistry to Organic Synthesis. A Review. *Org. Prep. Proced. Int* **2008,** *40*, 215-291. (c) García-López, J.-A.; Greaney, M. F., Synthesis of biaryls using aryne intermediates. *Chem. Soc. Rev.* **2016,** *45*, 6766-6798. (d) Alam, M. A.; Shimada, K.; Jahan, A.; Nasrin, D.; Zahan, M. K.-E.; Shahabuddin, M., The Advances and Applications of Arynes and Their Precursors to Synthesize the Heterocyclic Compounds: A Review. *American Journal of Heterocyclic Chemistry* **2017,** *3*, 47-54. (e) Bhunia, A.; Yetra, S. R.; Biju, A. T., Recent advances in transition-metal-free carbon-carbon and carbon-heteroatom bond-forming reactions using arynes. *Chem. Soc. Rev.* **2012,** *41*, 3140-52. (f) Bhojgude, S. S.; Bhunia, A.; Biju, A. T., Employing Arynes in Diels–Alder Reactions and Transition-Metal-Free Multicomponent Coupling and Arylation Reactions. *Acc. Chem. Res.* **2016,** *49*, 1658-1670.

benzyne substituents also affect the regioselectivity of benzyne-trapping reactions, although when inductive and steric effects are in opposition, inductive effects generally exert a stronger influence on the ultimate distribution of regioisomers.[13]

Figure 1.3 | Two isomeric benzenoid products can form when an unsymmetrical trap is used with an unsymmetrical benzyne intermediate.

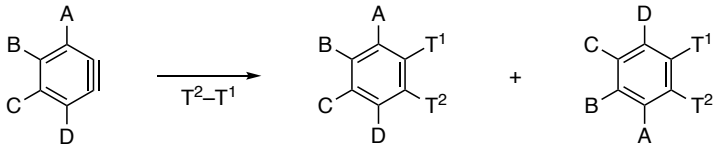

As computational methods and programs became more powerful, accurate, and accessible, several theoretical studies established a strong correlation between benzyne distortion and trapping regioselectivity[14,15] (as well as correlations between distortion

[13] (a) Castedo, L.; Guitian, E.; Saá, C.; Suau, R.; Saá, J. M., Regioselectivity in the [4+2] cycloaddition of benzyne. Synthesis of 11-substituted aporphines. *Tetrahedron Lett.* **1983,** *24*, 2107-2108. (b) Matsumoto, T.; Hosoya, T.; Katsuki, M.; Suzuki, K., New efficient protocol for aryne generation. Selective synthesis of differentially protected 1,4,5-naphthalenetriols. *Tetrahedron Lett.* **1991,** *32*, 6735-6736.

[14] For earlier examples, see: (a) Hamura, T.; Ibusuki, Y.; Sato, K.; Matsumoto, T.; Osamura, Y.; Suzuki, K., Strain-induced regioselectivities in reactions of benzyne possessing a fused four-membered ring. *Org. Lett.* **2003,** *5*, 3551-3554. (b) Garr, A. N.; Luo, D.; Brown, N.; Cramer, C. J.; Buszek, K. R.; VanderVelde, D., Experimental and theoretical investigations into the unusual regioselectivity of 4,5-, 5,6-, and 6,7-indole aryne cycloadditions. *Org. Lett.* **2010,** *12*, 96-9. (c) Cheong, P. H. Y.; Paton, R. S.; Bronner, S. M.; Im, G. Y. J.; Garg, N. K.; Houk, K. N., Indolyne and aryne distortions and nucleophilic regioselectivites. *J. Am. Chem. Soc.* **2010,** *132*, 1267-1269.

[15] For more recent examples, particularly for studies of the distortion and regioselectivity of various hetarynes, see: (a) Picazo, E.; Houk, K. N.; Garg, N. K., Computational predictions of substituted benzyne and indolyne regioselectivities. *Tetrahedron Lett.* **2015,** *56*, 3511-3514. (b) Medina, J. M.; Mackey, J. L.; Garg, N. K.; Houk, K. N., The Role of Aryne Distortions, Steric Effects, and Charges on Regioselectivities of Aryne Reactions. *J. Am. Chem. Soc.* **2014,** *136*, 15798-15805. (c) Goetz, A. E.; Garg, N. K., Enabling the Use of Heterocyclic Arynes in Chemical Synthesis. *J. Org. Chem.* **2014,** *79*, 846-851. (d) Goetz, A. E.; Garg, N. K., Regioselective reactions of 3,4-pyridynes enabled by the aryne distortion model. *Nat. Chem.* **2012,** *5*, 54. (e) Bronner, S. M.; Mackey, J. L.; Houk, K. N.; Garg, N. K., Steric Effects Compete with Aryne Distortion To Control Regioselectivities of Nucleophilic Additions to 3-Silylarynes. *J. Am. Chem. Soc.* **2012,** *134*, 13966-13969. (f) Goetz, A. E.; Bronner, S. M.; Cisneros, J. D.; Melamed, J. M.; Paton, R. S.; Houk, K. N.; Garg, N. K., An Efficient Computational Model to Predict the Synthetic Utility of Heterocyclic Arynes. *Angew. Chem. Int. Ed.* **2012,** *51*, 2758-2762. (g) Cheong, P. H. Y.; Paton, R. S.; Bronner, S. M.; Im, G. Y. J.; Garg, N. K.; Houk, K. N., Indolyne and aryne distortions and nucleophilic regioselectivites. *J. Am. Chem. Soc.* **2010,** *132*, 1267-1269.

and regioselectivity for strained cycloalkynes[16] and cycloallenes).[17] More specifically, substituted benzynes that have significantly different bond angles on the formal triple bond of the benzyne show higher regioselectivity. The carbon with the more obtuse bond angle has higher p character and a more positive charge, making it more prone to nucleophilic attack. The other carbon with the more acute bond angle has more s character, allowing it more effectively stabilize the developing negative charge that results from nucleophilic attack on the adjacent carbon (Figure 4). It should be noted that, although Figure 4 shows the regioselectivity of a reaction where a distorted benzyne is attacked by a nucleophile, this observed relationship between benzyne distortion and trapping regioselectivity applies to *all* benzyne reactions in which an unsymmetrical, sufficiently polarized trap is use—not only to those reactions in which the benzyne is trapped with a nucleophile.

In addition to the fact that this benzyne distortion model is interesting and gives significant insight into the regioselectivity of myriad benzyne-trapping reactions, it also

Figure 1.4 | Regioselectivity in trapping of distorted benzynes.

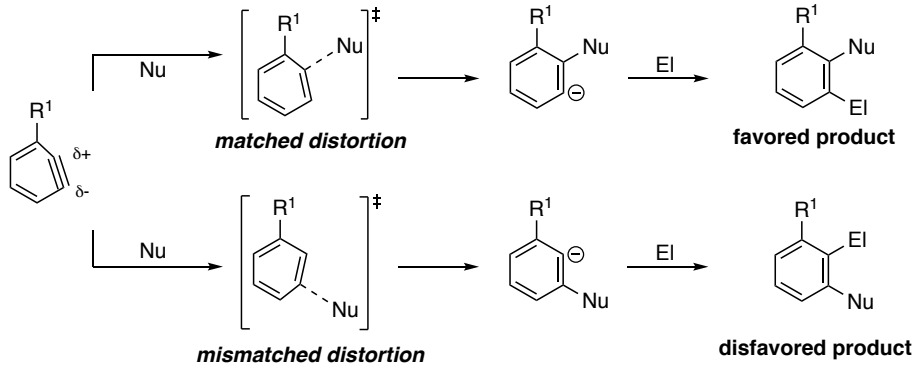

[16] (a) Medina, J. M.; McMahon, T. C.; Jiménez-Osés, G.; Houk, K. N.; Garg, N. K., Cycloadditions of cyclohexynes and cyclopentyne. *J. Am. Chem. Soc.* **2014,** *136*, 14706-9. (b) McMahon, T. C.; Medina, J. M.; Yang, Y.-F.; Simmons, B. J.; Houk, K. N.; Garg, N. K., Generation and Regioselective Trapping of a 3,4-Piperidyne for the Synthesis of Functionalized Heterocycles. *J. Am. Chem. Soc.* **2015**. (c) Shah, T. K.; Medina, J. M.; Garg, N. K., Expanding the Strained Alkyne Toolbox: Generation and Utility of Oxygen-Containing Strained Alkynes. *J. Am. Chem. Soc.* **2016,** *138*, 4948-4954.

[17] (a) Barber, J. S.; Styduhar, E. D.; Pham, H. V.; McMahon, T. C.; Houk, K. N.; Garg, N. K., Nitrone Cycloadditions of 1,2-Cyclohexadiene. *J. Am. Chem. Soc.* **2016,** *138*, 2512-2515. (b) Barber, J. S.; Yamano, M. M.; Ramirez, M.; Darzi, E. R.; Knapp, R. R.; Liu, F.; Houk, K. N.; Garg, N. K., Diels–Alder cycloadditions of strained azacyclic allenes. *Nat. Chem.* **2018,** *10*, 953-960. (c) Yamano, M. M.; Knapp, R. R.; Ngamnithiporn, A.; Ramirez, M.; Houk, K. N.; Stoltz, B. M.; Garg, N. K., Cycloadditions of Oxacyclic Allenes and a Catalytic Asymmetric Entryway to Enantioenriched Cyclic Allenes. *Angew. Chem. Int. Ed.* **2019,** *58*, 5653-5657.

has a more practical and valuable implication. The modern organic chemist generally has access to computational resources. If any synthetic chemist wishes to run a benzyne-trapping reaction that could result in a mixture of isomers and wishes to predict which isomer will be favored, he/she can determine the distortion of the benzyne *in silico*—a relatively simple task. This applies to benzynes that have any combination of varying substituents and that may be difficult to predict based on simple chemical intuition. As will be discussed in later chapters, this computational ability proved to be of significant value to the author of this thesis.

1.1.3 Generation of Benzyne

The types of functionalized benzenoid products that can be accessed *via* benzyne-trapping reactions depend not only on the inherent reactivity of any given benzyne (as discussed in the previous section), but also the method in which the benzyne in generated. Benzyne, of course, is a highly reactive, short-lived species that cannot be stored prior to use. Rather, it must be generated *in situ* from an appropriate precursor.

Most of the early methods used in benzyne generation involved the exposure to appropriately functionalized benzene rings to a strong base (Scheme 1.3). This base often effects an elimination reaction (such as a dehydrohalogenation when phenyl halides are used); alternatively, when an organolithium base is used, lithium halogen exchange occurs to access a phenyllithium intermediate that undergoes facile elimination (when a leaving group is adjacent to the lithium) to produce benzyne.

Scheme 1.3 | Selected examples of benzyne generation though the use of strong bases.

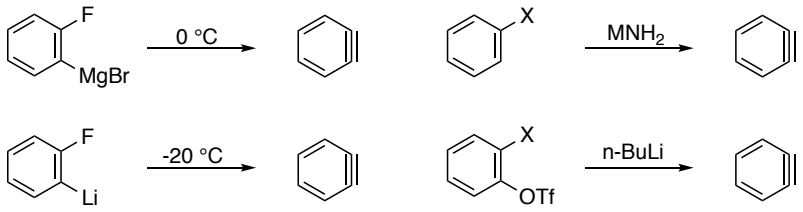

It goes without saying that the use of strong base significantly limits the scope of benzyne traps that can be used. Accordingly, a small number of benzyne precursors were developed that allowed for the generation of benzyne under milder conditions (due to the

formation of highly stable byproducts). Among these are 1-aminobenzotriazole (**1007**),[18] 1,2,3-benzothiadiazole (**1008**),[19] and benzenediazonium-2-carboxylate (**1009**)[20] (Scheme 1.4). However, inherent to these precursors were significant limitations such as difficulty in preparation, instability, use of toxic reagents (e.g. lead tetraacetate), and—in the case of precursor **1009**—significant shock sensitivity.[21]

Scheme 1.4 | Early examples of benzyne precursors that allow for benzyne generation under mild conditions

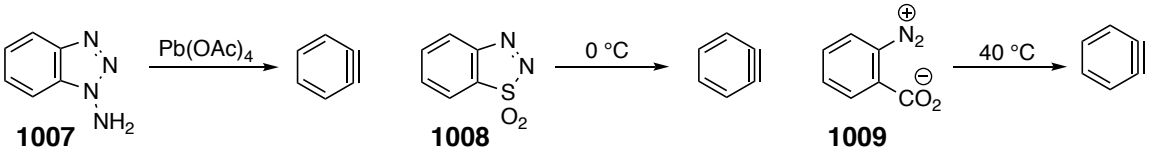

An additional method for benzyne generation was detailed in a humble 1983 publication[22] that, nevertheless, ultimately proved to be pioneering. In this paper, Kobayashi and co-workers show that trimethylsilyl phenyl triflate (**1010**), which is easily synthesized in three steps from *o*-chlorophenol (**1011**),[23] can be converted to benzyne simply by exposure to a fluoride source at room temperature (Figure 1.5). This newfound ability to generate benzyne under reasonable temperatures merely in the presence of a mildly basic fluoride source (often referred to as the Kobayashi method of benzyne

Figure 1.5 | The Kobayashi method: Generation of benzyne by exposure of trimethylsilyl phenyl triflate (**1010**) to a fluoride source.

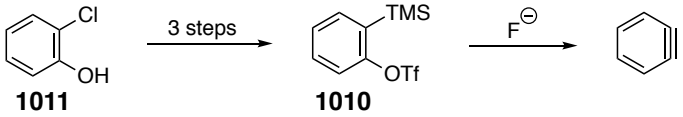

[18] Campbell, C. D.; Rees, C. W., Reactive intermediates. Part I. Synthesis and oxidation of 1- and 2-aminobenzotriazole. *J. Chem. Soc. C* **1969,** *0*, 742-742.
[19] Wittig, G.; Hoffmann, R. W., Dehydrobenzol aus 1.2.3-Benzothiadiazol-1.1-dioxyd. *Chemische Berichte* **1962,** *95*, 2718-2728.
[20] Stiles, M.; Miller, R. G.; Burckhardt, U., Reactions of Benzyne Intermediates in Non-basic Media. *J. Am. Chem. Soc.* **1963,** *85*, 1792-1797.
[21] Logullo, F. M.; Seitz, A. H.; Friedman, L., Benzenediazonium-2-carboxylate and Biphenylene. *Org. Synth.* **1968,** *48*, 12.
[22] Himeshima, Y.; Sonoda, T.; Kobayashi, H., Fluoride-induced 1,2-elimination of o-trimethylsilylphenyl triflate to benzyne under mild conditions. *Chem. Lett.* **1983**, 1211-1214.
[23] For a brief overview of the synthetic methods used to access various *o*-trimethylsilylphenyl triflate benzyne precursors, refer to Section 6 of ref. 12(a).

generation) represented a significant advance in the field of benzyne chemistry and is largely responsible for a revival of interest into benzyne research that continues today.

When considering this renaissance of benzyne research within the synthetic community—as well as considering the general value and tremendous remaining potential of benzyne in organic synthesis—it is clear that the development of novel benzyne-trapping reactions (or even novel variations on precedented benzyne reactions) is worth pursuing. Of even greater potential value would be the development of novel methods of benzyne generation. In both of these regards, the hexadehydro-Diels–Alder (HDDA) reaction has proven to be groundbreaking. Novel applications and variations of this HDDA reaction will be the focus of this thesis.

1.2 The Hexadehydro-Diels–Alder (HDDA) Reaction

1.2.1 Dehydro-Diels–Alder (DDA) Reactions

There are few named reactions in the realm of organic synthesis that are as iconic as the Diels–Alder reaction. This pericyclic reaction consists of a cycloaddition between a 1,3-diene and an alkene (also referred to as a dienophile). The simplest demonstration of a Diels–Alder reaction is the combination of 1,3-butadiene (**1012**) and ethylene (**1013**) to form cyclohexene (**1014**) (Figure 1.6). Since its original disclosure in 1928,[24] this reaction has found nearly unmatched use in the synthesis of both simple and complex organic compounds.[25]

Somewhat less well known than the standard Diels–Alder reaction are its related "dehydrogenated" variations. In these so-called dehydro-Diels–Alder (DDA) reactions, one or more of the alkenes in the original Diels–Alder reaction are replaced with an

---

[24] Diels, O.; Alder, K., Synthesen in der hydroaromatischen Reihe. *Justus Liebig's Annalen der Chemie* **1928,** *460*, 98-122.

[25] For just a few of the dozens of relatively recent reviews regarding the Diels–Alder reaction and its applications in organic synthesis, refer to (a) Nicolaou, K. C.; Snyder, S. A.; Montagnon, T.; Vassilikogiannakis, G., The Diels-Alder Reaction in Total Synthesis. *Angew. Chem. Int. Ed.* **2002,** *41*, 1668-1698. (b) Juhl, M.; Tanner, D., Recent applications of intramolecular Diels–Alder reactions to natural product synthesis. *Chem. Soc. Rev.* **2009,** *38*, 2983-2992. (c) Corey, E. J., Catalytic Enantioselective Diels–Alder Reactions: Methods, Mechanistic Fundamentals, Pathways, and Applications. *Angew. Chem. Int. Ed.* **2002,** *41*, 1650-1667. (d) Funel, J.-A.; Abele, S., Industrial applications of the Diels-Alder reaction. *Angew. Chem. Int. Ed.* **2013,** *52*, 3822-63. (e) Takao, K.-I.; Munakata, R.; Tadano, K.-i., Recent advances in natural product synthesis by using intramolecular Diels-Alder reactions. *Chem. Rev.* **2005,** *105*, 4779-807.

alkyne. It is interesting, and worth noting, that the first reported DDA reaction,[26] involving the conversion of 3-phenylpropiolic acid (**1015**) to form the polyaromatic product **1016** in acetic anhydride (Figure 1.6b) was reported over 3 decades before the original 1928 paper by Diels and Alder.

Simplified variations of the DDA are shown in Figure 1.6. Depending upon the degree of dehydrogenation—or, put more simply, how many alkenes have been replaced by alkynes—these reactions can be referred to as didehydro-, tetradehydro, or hexadehydro-Diels–Alder reactions. In general, DDA reactions give rise to strained cyclic products that are not stable under most standard reaction conditions. These products are prone either to undergo rearrangement reactions to more stable products (e.g. the rearrangement of cyclic allene **1017** and cyclic cumulene **1018** to benzene) or to reaction with a molecular trap. This latter result can occur with cyclic allenes (e.g. **1019**) and with conjugated cyclic cumulenes **1020** (which, it should be noted, is a resonance

Figure 1.6 | (a) The Diels – Alder reaction (top left) and variations of the dehydro-Diels–Alder reactions. (b) The first report of a dehydro-Diels–Alder reaction.

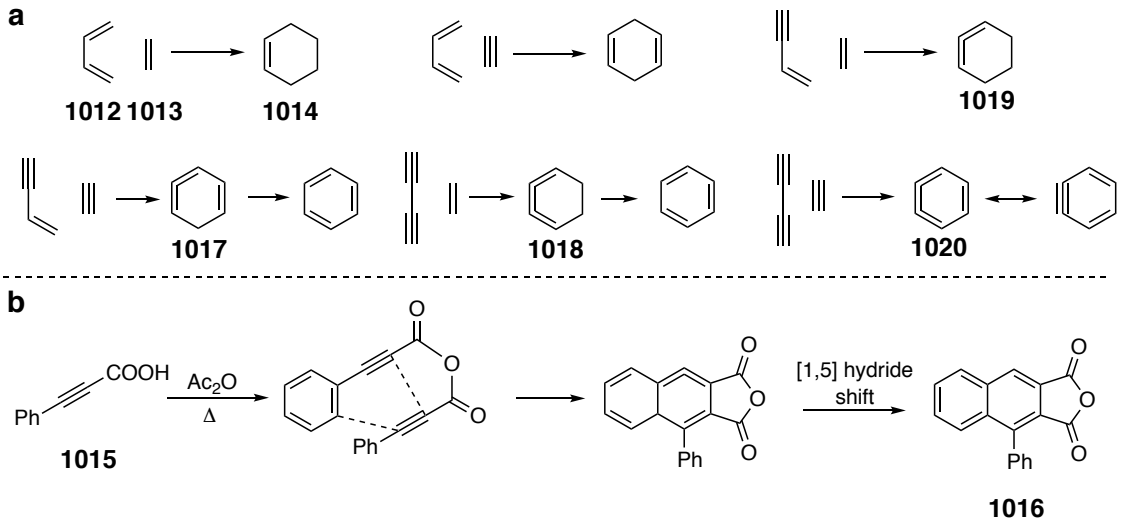

[26] Michael, A.; Bucher, J. E., Ueber die Einwirkung von Essigsäureanhydrid auf Säuren der Acetylenreihe. *Ber. Dtsch. Chem. Ges* **1895,** *28*, 2511-2512.

structure of benzyne). Largely due to this ability to access benzenoid products by way of these unstable cyclic intermediates, DDA reactions have found a modest but still appreciable niche in the field of organic synthesis.[27,28]

Variations of the DDA reaction are shown in Figure 1.7 (entries b-f), along with the internal energy of each reaction and the ring strain of each cyclic product.[29] Looking at these values it can be seen that DDA reactions are generally less exothermic than the original Diels–Alder reaction. This is to be expected, given the anticipated ring strain inherent to the products of DDA reactions Indeed, one can see that a lowering of reaction

Figure 1.7 | Energetics of the Diels–Alder reaction (a) and of the variations of dehydro-Diels–Alder reaction (b-f). The reaction energy for each reaction is shown below the arrows; the ring strain is shown to the right of each product (values in kcal•mol^{-1}, calculated by Johnson and coworkers).[29]

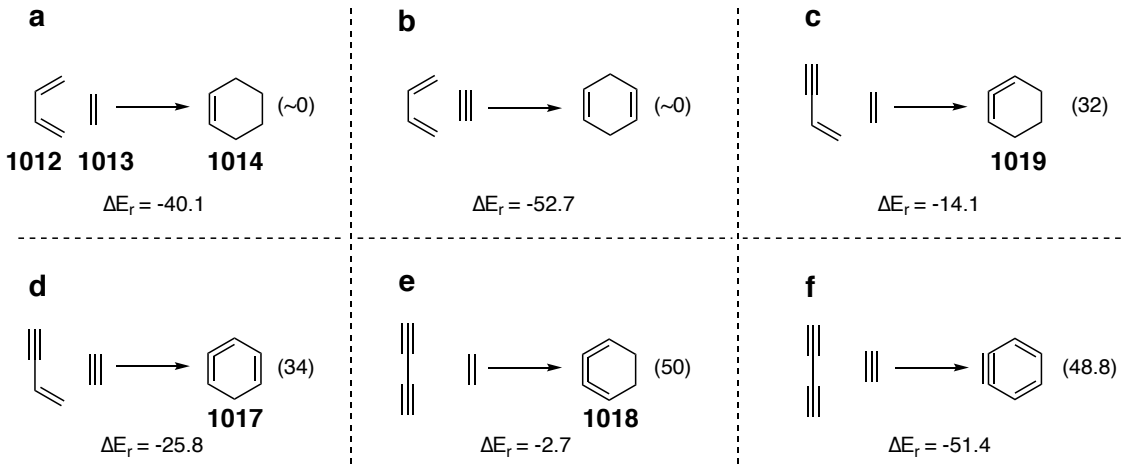

[27] Wessig, P.; Müller, G., The dehydro-Diels-Alder reaction. *Chem. Rev.* **2008,** *108*, 2051-63.

[28] For recent examples of applications of the DDA reaction in total synthesis, see (a) McGee, P.; Bétournay, G.; Barabé, F.; Barriault, L., A 11-Steps Total Synthesis of Magellanine through a Gold(I)-Catalyzed Dehydro Diels–Alder Reaction. *Angew. Chem. Int. Ed.* **2017,** *56*, 6280-6283. (b) Reddy, M. C.; Jeganmohan, M., Total synthesis of aristolactam alkaloids via synergistic C–H bond activation and dehydro-Diels–Alder reactions. *Chem. Sci.* **2017,** *8*, 4130-4135. (c) Chinta, B. S.; Sanapa, H.; Vasikarla, K. P.; Baire, B., Synthetic approach to seco-tetracenomycin natural products saccharothrixone A–C. *Tetrahedron Lett.* **2018,** *59*, 1970-1973. (d) Chinta, B. S.; Siraswar, A.; Baire, B., The dehydro Diels-Alder (DDA) reaction based approach to isofuranonaphthalenone, nodulones A-C and xestolactone A. *Tetrahedron* **2017,** *73*, 4178-4185. (e) Chinta, B. S.; Baire, B., Total synthesis of selaginpulvilins A and C. *Org. Biomol. Chem* **2018,** *16*, 262-265.

[29] Calculations run by Johnson and coworkers Ajaz, A.; Bradley, A. Z.; Burrell, R. C.; Li, W. H. H.; Daoust, K. J.; Bovee, L. B.; DiRico, K. J.; Johnson, R. P., Concerted vs stepwise mechanisms in dehydro-Diels-Alder reactions. *J. Org. Chem.* **2011,** *76*, 9320-8.

exothermicity generally accompanies increase in ring strain of the product for each respective reaction.

An outstanding exception to this trend is seen in the hexadehydro-Diels–Alder reaction (Figure 1.7f). Despite the enormous amount of ring strain present in the resulting benzyne—44.8 kcal•mol^{-1}relative to cyclohexene (**1014**), this reaction is, remarkably, even more exothermic than the Diels–Alder reaction! Almost any organic chemist would quickly attribute this to the aromaticity of the benzyne product. This is, indeed, probably the most significant contributing factor to the reaction exothermicity.

As a brief digression, it is important to consider the role of the alkyne moieties themselves. From a thermodynamic (as opposed to a kinetic) point of view, alkynes are very unstable species. In the same way that the conversion of two C=C doubles bonds to two C–C single bonds in the Diels–Alder reaction is largely responsible for its exothermicity, the formal conversion of two C≡C triple to two C=C double bonds also results in a significant thermodynamic sink. Furthermore, it should be noted that the conversion of an alkyne to an alkene is significantly more exothermic than the conversion of an alkene to an alkane.[30] This can be seen by comparing reactions **c** and **d** in Figure 1.7: while the products of each reaction both have a similar degree of ring strain, reaction **d**—which has two alkynes participating in the DDA reaction, as opposed to reaction **c**—is more exothermic by over 10 kcal•mol^{-1}. This seemingly minor point of thermodynamic alkyne instability, and the driving force it provides for certain DDA reactions, will become an important point of focus in later chapters of this thesis (Chapters 4 and 5).

1.2.2 Early Reports of the HDDA Reaction

Considering the previously-discussed ability of the most dehydrogenated variant of the DDA reaction (i.e. the hexadehydro-Diels–Alder reaction, Figure 1.7f) to access a

---

[30] As a demonstrative example, the heat of hydrogenation (ΔH°) of acetylene to ethane (1 atm, 25 °C) is –74.4 kcal•mol^{-1}l while the ΔH° of ethylene to ethane is –32.8 kcal•mol^{-1}. The ΔΔH° of these values (41.6 kcal•mol^{-1}), which can be taken to be the value of ΔH° for the hydrogenation acetylene to ethylene, is 8.8 kcal•mol^{-1} more exothermic than the hydrogenation of ethylene to ethane. ΔH° values for acetylene and ethylene were taken from: Roberts, J. D.; Caserio, M. C., Alkenes and Alkynes II. Oxidation and Reduction Reactions. Acidity of Alkynes. In *Basic Principles of Organic Chemistry*, Benjamin Inc.: Menlo Park, 1977; pp 405-444.

highly valuable benzyne intermediate—in what turns out to be a remarkably exothermic transformation—one might initially assume this to be a frequently exploited reaction in organic synthesis. However, until recently (as will be discussed later), it had been scarcely explored or described in the literature. A few scattered examples from the last few decades are presented below.

As described in a notable 1997 report, Johnson and coworkers observed that 1,3,8-nonatriyne (**1021**), when subjected to flash vacuum pyrolysis (FVP), yielded a mixture of indane (**1022**) and indene (**1023**), as shown in Figure 1.8.[31] They rationalized the formation of **1022** through a benzyne intermediate **1021***, which they presumed to form in a [4 + 2] cycloaromatization from **1021** (with indene (**1023**) presumably formed directly from indane (**1022**). In doing so, they became the first researchers recorded to attribute the formation of an observed benzenoid product to a hexadehydro-Diels–Alder reaction (although they did not refer to the reaction as such).

Figure 1.8 | Flash vacuum pyrolysis of 1,3,8-nonatriyne (**1021**) to give indane (**1022**) and indene (**1023**).

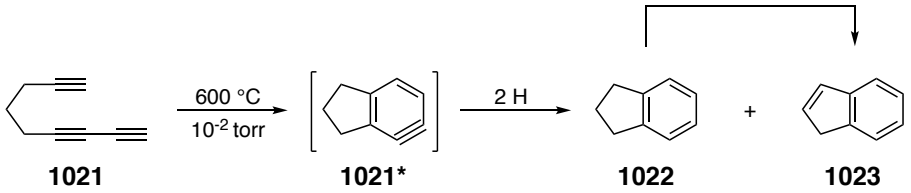

A deuterium labeling experiment was carried out to support this proposed mechanism (Figure 1.9). Specifically, deuterated 1,3,8-nonatriyne (**1021-d$_2$**) was synthesized and subjected to the same FVP conditions. This experiment was designed to rule out another plausible mechanism in which a 1,2-deuterium atom shift to form vinyl carbene **1024**—not unreasonable under FVP—which could then insert into the adjacent alkynyl C–D bond to access ene-diyne **1025**. This deuterated ene-diyne would then access deuteroindane (**1022-d$_2$_a**) through a Bergman cycloaromatization[32] (note that

[31] Bradley, A. Z.; Johnson, R. P., Thermolysis of 1,3,8-Nonatriyne: Evidence for Intramolecular [2 + 4] Cycloaromatization to a Benzyne Intermediate. *J. Am. Chem. Soc.* **1997,** *119*, 9917-9918.
[32] (a) Jones, R. R.; Bergman, R. G., p-Benzyne. Generation as an intermediate in a thermal isomerization reaction and trapping evidence for the 1,4-benzenediyl structure. *J. Am. Chem. Soc.* **1972,** *94*, 660-661. (b) Bergman, R. G., Reactive 1,4-dehydroaromatics. *Acc. Chem. Res.* **1973,** *6*, 25-31. (c) Grissom, J. W.;

Figure 1.9 | Deuterium labeling experiment supports the formation of indane (**1022**) via the benzyne **1021*** (path b) as opposed to a Bergman cyclization (path a).

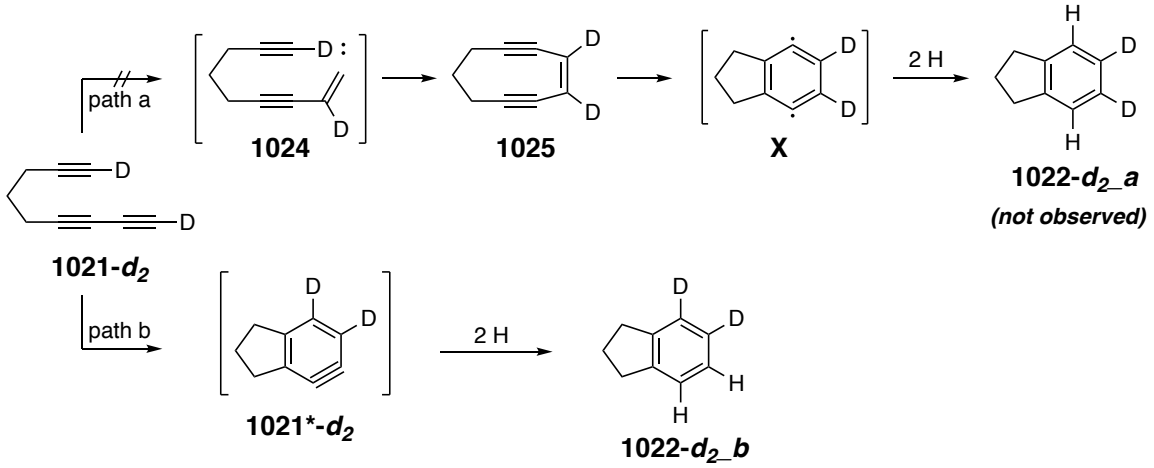

this occurs through a *para*-benzyne rather than an *ortho*-benzyne intermediate). As was anticipated, **1022-d$_2$_a** did not result from this reaction. Rather, its isotopomer **1022-d$_2$_b** was isolated, indicating the formation of an *ortho*-benzyne intermediate **1021*-d$_2$**.

Around the same time, Ueda and coworkers disclosed several reports describing cycloaromatizations of tetra-alkyne substrates to benzenoid products.[33] An example of one of these reported cycloaromatization reactions, along with the reaction pathway proposed by Ueda and coworkers, is shown in Figure 1.10. It should first be observed that the reaction is proposed to proceed through 1,2-didehydrobenzene diradicals **1025*a** and **1025*b**. Recall that the 1,2-didehydrobenzene diradical is one of the contributing resonance structures of benzyne (refer to Figure 1,1)—making this transformation a (stepwise) hexadehydro-Diels–Alder reaction. Of even greater importance is the fact that

Gunawardena, G. U.; Klingberg, D.; Huang, D., The chemistry of enediynes, enyne allenes and related compounds. *Tetrahedron* **1996,** *52*, 6453-6518.

[33] (a) Miyawaki, K.; Suzuki, R.; Kawano, T.; Ueda, I., Cycloaromatization of a non-conjugated polyenyne system: Synthesis of 5H-benzo[d]fluoreno[3,2-b]pyrans via diradicals generated from 1-[2-{4-(2-alkoxymethylphenyl)butan-1,3-diynyl}]phenylpentan-2,4-diyn-1-ols and trapping evidence for the 1,2-didehydroben. *Tetrahedron Lett.* **1997,** *38*, 3943-3946. (b) Miyawaki, K.; Kawano, T.; Ueda, I., Multiple cycloaromatization of novel aromatic enediynes bearing a triggering device on the terminal acetylene carbon. *Tetrahedron Lett.* **1998,** *39*, 6923-6926. (c) Ueda, I.; Sakurai, Y.; Kawano, T.; Wada, Y.; Futai, M., An unprecedented arylcarbene formation in thermal reaction of non-conjugated aromatic enetetraynes and DNA strand cleavage. *Tetrahedron Lett.* **1999,** *40*, 319-322. (d) Miyawaki, K.; Kawano, T.; Ueda, I., Domino thermal radical cycloaromatization of non-conjugated aromatic hexa- and heptaynes: synthesis of fluoranthene and benzo[a]rubicene skeletons. *Tetrahedron Lett.* **2000,** *41*, 1447-1451.

these reactions occurred under remarkably mild conditions—in stark contrast to Johnson's 600 °C FVP reaction. When a solution of tetrayne **1025** in benzene was left to stir at room temperature, it was converted to a mixture of benzenoid products **1026a** and **1026b**.

One might think that this apparent ability to form benzyne under such mild conditions would initiate significant efforts to explore the scope and general synthetic utility of this reaction. However, Ueda and coworkers never expanded this methodology beyond the synthesis of a handful of polycyclic benzenoid products. It is possible they

Figure 1.10 | Selected example of a cycloaromatization reaction reported by Ueda and coworkers along with their proposed reaction mechanism.[33]

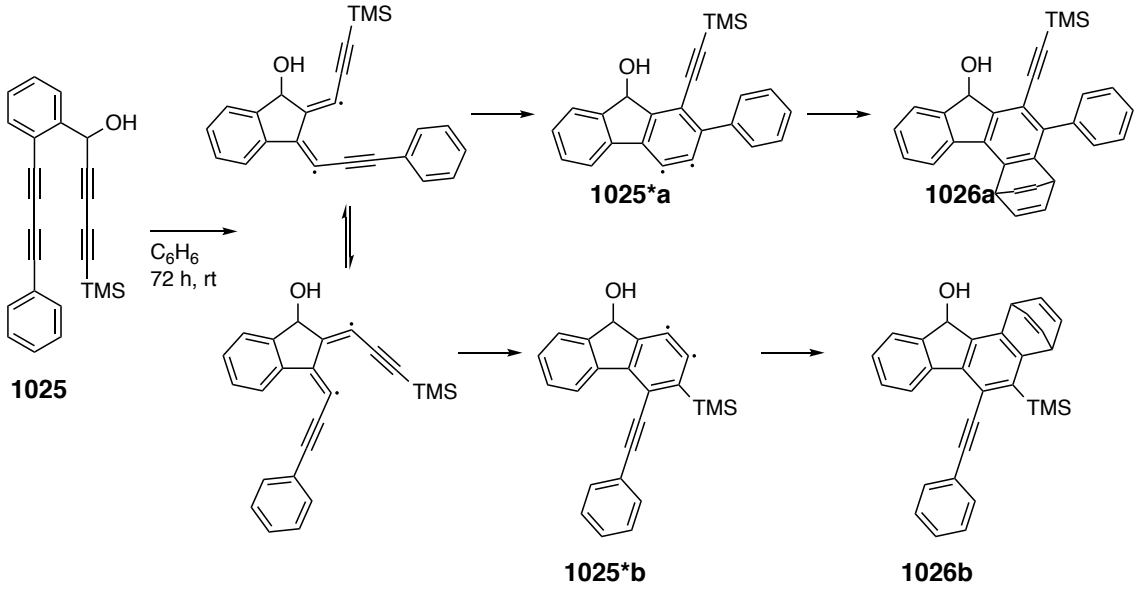

believed that only a limited number of polyyne substrates would undergo this reaction cascade; perhaps they did not appreciate the vast number of diversely functionalized benzenoid products that could accessed by this process; one might even consider the possibility that they, in looking at the reactive intermediate of this cascade (i.e. the benzyne intermediates) as a didehydrobenzene diradical rather than the more commonly drawn cyclic alkyne resonance contributor, simply failed to recognize it as the ubiquitous benzyne intermediate that is so commonly seen in organic synthesis. In any

case, the hexadehydro-Diels–Alder reaction—with few exceptions[34]—remained a source of synthetic potential that was left largely untapped by the synthetic community for well over a decade.

1.2.3 Serendipitous Rediscovery of the HDDA Reaction

In 2011, a researcher from the Hoye group attempted a simple oxidation of alcohol **1027** to ketone **1028** as part of a larger study into the chemistry ene-diyne natural products.[35] Surprisingly, this reaction was found to yield a benzenoid product rather than the anticipated ketone. One the structure of this product **1029** was determined, it quickly became apparent that it had formed through a benzyne intermediate. Specifically, the benzyne **1028*** formed from a hexadehydro-Diels–Alder reaction (which shall henceforth be consistently referred to as the HDDA reaction in this thesis) of the ketone **1028**. Nucleophilic attack of the fortuitously placed TBS ether to this benzyne, followed by a retro-Brook rearrangement of the zwitterion **1030**, yielded the observed product (Figure 1.11).

Figure 1.11 | Rediscovery of the HDDA reaction from an attempted oxidation of alcohol **1027**.

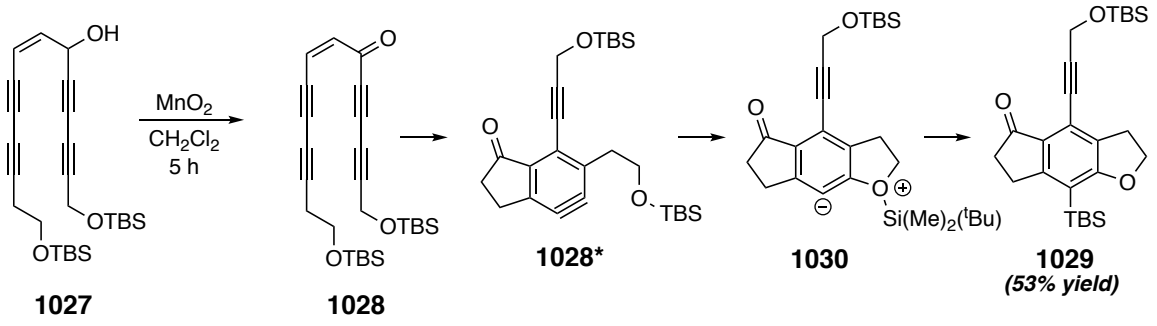

The novelty of this cascade was quickly realized. Not only did this constitute a new method of benzyne generation, but it was different from all previous methods in that it did not generate benzyne from an *ortho*-disubstituted benzene as a precursor. Furthermore, and perhaps more importantly, this HDDA reaction occurs in the absence of exogenous reagents—generating benzyne merely by heating an appropriate

[34] Tsui, J. A.; Sterenberg, B. T., A Metal-Templated 4 + 2 Cycloaddition Reaction of an Alkyne and a Diyne To Form a 1,2-Aryne. *Organometallics* **2009,** *28*, 4906-4908.
[35] Hoye, T. R.; Baire, B. B.; Niu, D.; Willoughby, P. H.; Woods, B. P., The hexadehydro-Diels–Alder reaction. *Nature* **2012,** *490*, 208.

precursor.[36] This could conceivably alter the reactivity of the benzyne itself, leading to novel or divergent modes of benzyne-trapping.

Quick to appreciate the synthetic potential of the HDDA reaction, Hoye and coworkers designed and tested several potential substrates to be used in this cascade. Several examples are shown in Scheme 1.4. Although these were just a few examples of HDDA reactions, they showed the applicability of this reaction for synthesizing a

Scheme 1.4 | Early examples of successfully run HDDA reactions. Scheme reproduced from ref 35.

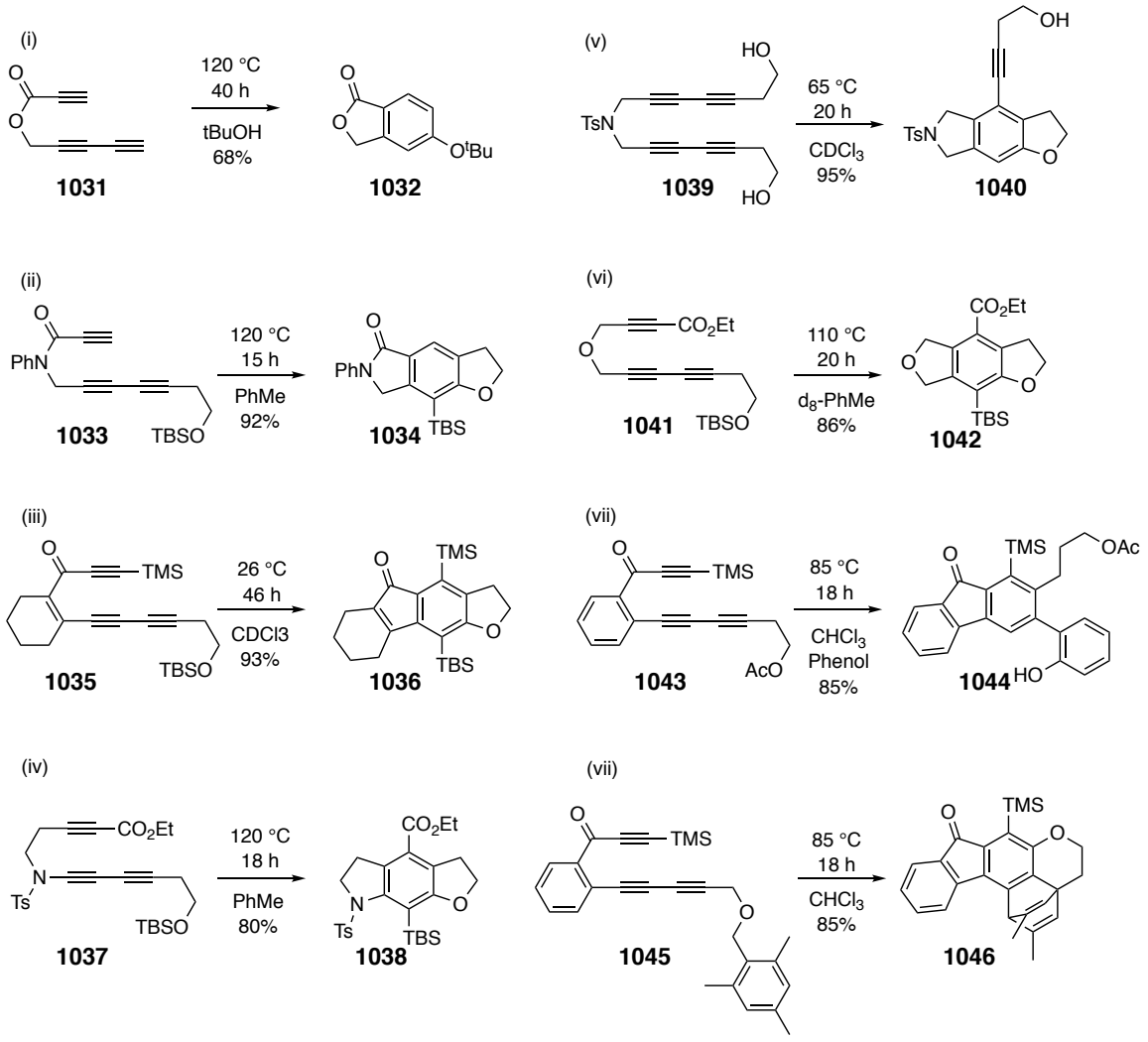

[36] Having said this, it is still advisable to—as one reviewer of this paper so aptly pointed out—never underestimate the power of mere heat.

variety of aromatic motifs such as phthalides (Scheme 1.4, entry i, **1032**), isoindolones (entry ii, **1034**), indenones (entry iii, **1036**), indolines (entry iv, **1038**), isoindolines (entry v, **1040**), benzofurans (entry vi, **1042**), and fluorenones (entries vii-viii, **1044** and **1046**).

On a related note, the variety of precursors are shown to be capable of initiating the HDDA cascade. Several conclusions can be drawn from looking at the array of HDDA substrates in Scheme 1.4. Among the most important are the following:

(i) Different functional groups inherent to the substrates are compatible with the conditions of the HDDA reaction. These include (but are not limited to) esters (**1031**), amides (**1033**), ketones (**1035**, **1043**, and **1045**), ethers (**1041**), and sulfonamides (**1037** and **1039**). Any functional group used in an HDDA substrate must, of course, be compatible with the intermediate benzyne. Any substrate containing even a modestly nucleophilic moiety would likely give poor yields, as this moiety would likely attack the benzyne.

(ii) Both tri-alkyne (triyne) and tetra-alkyne (tetrayne) substrates can undergo the HDDA reaction. It should be noted, however, that triynes seem to require a moiety that activates the diynophile (such as the carbonyl in substrates **1031**, **1033**, **1035**, **1043**, and **1045**).

(iii) The rate of the HDDA reaction—more specifically, the rate of the rate-determining benzyne formation step—shows significant variation based on the molecular "linker" that connects the 1,3-diyne moiety to its partner diynophile. Comparing the reaction conditions applied each to substrate **1031** and substrate **1033**, it can be seen that the activation energy of the reaction's rate-determining step is lowered simply by changing the linker from an ester to an amide. An even more impressive demonstration of this linker effect can be seen by comparing substrates **1043** and **1035**. While the former cyclizes to benzyne at an appreciable rate around 85 °C, while the later can be observed to cyclize at room temperature—a drastic change obtained simply by switching from one six-membered cyclic hydrocarbon linker to another. This last point of the "linker" effect in the HDDA reaction, which was later investigated by Woods *et*

al. in more detail,[37] will be a point of discussion in subsequent sections of this thesis.

Although not shown in Scheme 1.4, it is worth mentioning that HDDA reactions give significantly higher yields when the concentration of the HDDA substrate in the solvent is relatively low (generally 0.01–0.05 M). The use of such low concentrations likely inhibits side reactions involving benzyne dimerization to form phenylene—a reaction that has been known for quite some time.[7] At the same time, it should be noted that the low concentration of the benzyne intermediate at any given time during the reaction likely makes this, at most, a minor side reaction even at higher concentrations. Of greater importance is the decreased rate of the reaction between the benzyne intermediate with the alkynes of the HDDA substrate—a reaction that was recently studied in greater detail.[38]

1.2.4 Synthetic Utility of the HDDA reaction

Since the disclosure of these initial results by Hoye and coworkers, the HDDA reaction has proven to possess remarkable synthetic utility. While I will not comprehensively discuss the research on the HDDA reaction that been carried out[39], this section will briefly discuss the general synthetic versatility that has been unveiled over the past 7 years since Hoye's original publication.

Examples of molecular structures that have been accessed by the *intra*molecular trapping of HDDA-generated benzynes are shown in Figure 1.12b. A generic illustration of the HDDA cascade is shown in Figure 1.12a for reference. The products **1048**, **1049**, and **1050** result from an Alder-ene reaction,[40] a [4 + 2] cycloaddition,[41] and trapping by the hydroxyl group of a tethered phenol, respectively. While these reactions are precedented in the benzyne literature, their compatibility with the HDDA reaction is still

---

[37] Woods, B. P.; Baire, B.; Hoye, T. R., Rates of Hexadehydro-Diels–Alder (HDDA) Cyclizations: Impact of the Linker Structure. *Org. Lett.* **2014,** *16*, 4578-4581.
[38] Xiao, X.; Woods, B. P.; Xiu, W.; Hoye, T. R., Benzocyclobutadienes: An Unusual Mode of Access Reveals Unusual Modes of Reactivity. *Angew. Chem. Int. Ed.* **2018,** *57*, 9901-9905.
[39] For publications that review recent developments of the HDDA reaction, refer to: (a) Diamond, O. J.; Marder, T. B., Methodology and applications of the hexadehydro-Diels–Alder (HDDA) reaction. *Org. Chem. Front.* **2017,** *4*, 891-910. (b) Holden , C.; Greaney, M. F., The Hexadehydro-Diels–Alder Reaction: A New Chapter in Aryne Chemistry. *Angew. Chem. Int. Ed.* **2014,** *53*, 5746-5749.
[40] Karmakar, R.; Mamidipalli, P.; Yun, S. Y.; Lee, D., Alder-ene reactions of arynes. *Org. Lett.* **2013,** *15*, 1938-41.
[41] Pogula, V. D.; Wang, T.; Hoye, T. R., Intramolecular [4 + 2] Trapping of a Hexadehydro-Diels–Alder (HDDA) Benzyne by Tethered Arenes. *Org. Lett.* **2015,** *17*, 856-859.

Figure 1.12 | a) Generic illustration of the HDDA cascade. b) Examples of structures access from intramolecular trapping of HDDA-generated benzynes.

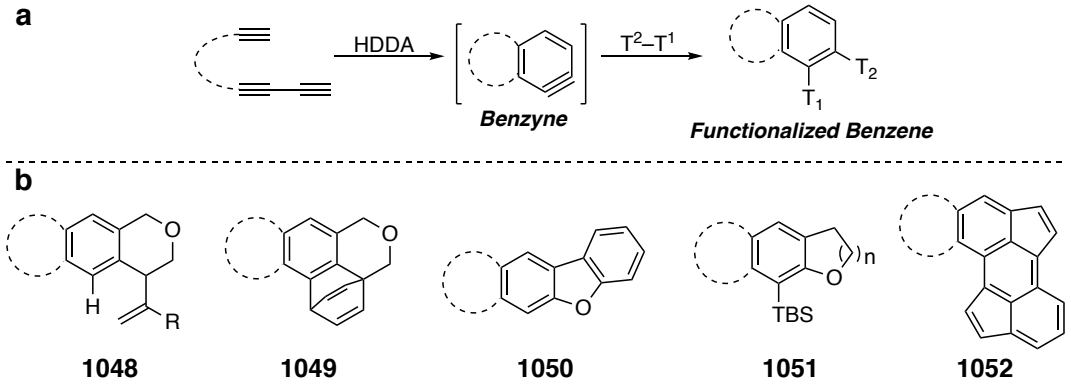

worth knowing. Furthermore, they allow for access to potentially useful molecular scaffolds.

On the other hand, structures **1051** and **1052** are the products of intramolecular benzyne-trapping reactions that were unprecedented. As described in previous paragraphs, **1051** is the result of a benzyne trapped by a tethered silyl ether. Far more interesting is the polyaromatic structure **1052**. This is the product of a "domino" HDDA reaction in which successive reactions of tethered 1,3-butadiyne units generate increasingly larger aryne moieties to ultimately produce a polycyclic aromatic hydrocarbon.[42]

As was seen in Scheme 1.4, HDDA substrates can be heated in the presence of exogenous compounds that are capable of trapping benzyne, resulting in *inter*molecularly-trapped benzenoid products. Examples of products that result from intermolecular nucleophilic attack on HDDA benzyne are shown in Figure 1.13a. While alcohols, amines, thiols and carboxylic acids (resulting in products **1053**, **1054**, **1055**, and **1056**, respectively) are precedented benzyne traps, it is worth knowing that they are compatible with the conditions of the HDDA reaction. Furthermore, the neutral (i.e.

[42] Xiao, X.; Hoye, T. R., The domino hexadehydro-Diels–Alder reaction transforms polyynes to benzynes to naphthynes to anthracynes to tetracynes (and beyond?). *Nat. Chem.* **2018,** *10*, 838-844.

reagent-free) conditions of the HDDA reaction often allowed for novel insight, as was the case for alcohol[43] and tertiary amine[44] traps.

It is worth mentioning the "divergent" reactivity that is occasionally observed with HDDA-generated benzyne. Specifically, HDDA benzyne has occasionally been shown to give different benzenoid products from benzynes generated through other protocols.This is well demonstrated in trapping with carboxylic acids, which give aryl ether products (e.g. **1056**) when heated with an HDDA benzyne precursor. This contrasts with the acylated phenol product (i.e. the product resulting from formal C–O insertion) that is obtained when carboxylic acids are reacted with Kobayashi benzyne. This product is presumably a result of the mildly basic conditions that are used to generate Kobayashi benzyne (refer to Section 1.1.3), which deprotonate the carboxylic acid and result in a distinct carboxylate trappings species. In contrast, HDDA benzyne, which is generated under neutral conditions, is directly trapped by the carboxylic acid itself.
Additional examples of molecular traps that give different products in the presence of HDDA benzyne will be briefly discussed in Chapter 2 of this thesis.

Figure 1.13 | Products of intramolecular HDDA benzyne trapping. a.) Products resulting from nucleophilic attack on HDDA benzyne. b.) Products for which the benzyne is trapped in a pericyclic reaction.

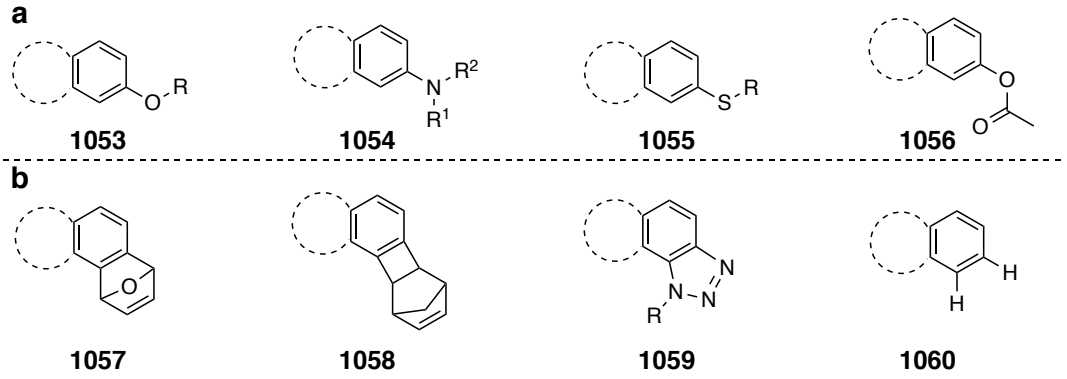

HDDA-generated benzyne are also capable of participating in pericyclic reactions with certain molecular traps, much like benzynes generated by other methods

[43] Willoughby, P. H.; Niu, D.; Wang, T.; Haj, M. K.; Cramer, C. J.; Hoye, T. R., Mechanism of the Reactions of Alcohols with o-Benzynes. *J. Am. Chem. Soc.* **2014,** *136*, 13657-13665.
[44] Ross, S. P.; Baire, B.; Hoye, T. R., Mechanistic Duality in Tertiary Amine Additions to Thermally Generated Hexadehydro-Diels–Alder Benzynes. *Org. Lett.* **2017,** *19*, 5705-5708.

(as discussed in Section 1.1.2.1). Representative examples of products that result from this process are shown in Figure 1.13b. These pericylic reactions include [4 + 2] reactions with a 4π diene (e.g. **1057** from furan),[45] [2 + 2] reactions with alkenes to yield benzocyclobutene products (e.g. **1058** from norbornene), and 1,3-dipolar cycloadditions[45] (e.g. **1059** from a substituted azide). Of particular note is the dihydrobenzene product **1060**, which is the product of concerted dihydrogen transfer from a cyclic alkane[46]—a relatively rare example of a dyotropic reaction.[47] This is a relatively rare example in which the HDDA reaction was used to unveil a fundamentally novel benzyne-trapping reaction.

Lastly, products that are representative of notable advances in HDDA chemistry are shown in Figure 1.14. While a fully comprehensive discussion of the products that have been formed through the HDDA reaction will not be included in this thesis,[39] these products are at least worth mentioning in passing. In no particular order, these include products that the result of: benzyne bromination with ammonium bromide salts to make aryl bromides (**1061**),[35] benzyne dichlorination with dilithium tetrachlorocuprate to make *o*-dichlorobenzenoid products (**1062**),[48] trapping of benzyne with α,β-unsaturated enals to make benzopyrans (**1063**),[49] trapping of benzyne with thioamides to make dihydrobenzothiazino heterocycles (**1064**),[50] phenol-ene reactions with benzyne to construct biaryl moieties (**1065**),[51] three component reactions of benzyne with tertiary

---

[45] Chen, J.; Baire, B.; Hoye, T. R., Cycloaddition reactions of azide, furan, and pyrrole units with benzynes generated by the hexadehydro-Diels–Alder (HDDA) reaction. *Heterocycles* **2014,** *88*, 1191-1200.
[46] Niu, D.; Willoughby, P. H.; Woods, B. P.; Baire, B.; Hoye, T. R., Alkane desaturation by concerted double hydrogen atom transfer to benzyne. *Nature* **2013,** *501*, 531-4.
[47] (a) Reetz, M. T., Dyotropic Rearrangements, a New Class of Orbital-Symmetry Controlled Reactions. Type II. *Angew. Chem. Int. Ed* **1972,** *11*, 130-131. (b) Fernández, I.; Sierra, M. A.; Cossío, F. P., In-Plane Aromaticity in Double Group Transfer Reactions. *J. Org. Chem.* **2007,** *72*, 1488-1491. (c) Fernández, I.; Cossío, F. P.; Sierra, M. A., Dyotropic Reactions: Mechanisms and Synthetic Applications. *Chem. Rev.* **2009,** *109*, 6687-6711.
[48] Niu, D.; Wang, T.; Woods, B. P.; Hoye, T. R., Dichlorination of (hexadehydro-Diels-Alder generated) benzynes and a protocol for interrogating the kinetic order of bimolecular aryne trapping reactions. *Org. Lett.* **2014,** *16*, 254-7.
[49] Wang, T.; Oswood, C. J.; Hoye, T. R., Trapping of Hexadehydro-Diels–Alder Benzynes with Exocyclic, Conjugated Enals as a Route to Fused Spirocyclic Benzopyran Motifs. *Synlett* **2017,** *28*, 2933-2935.
[50] Palani, V.; Chen, J.; Hoye, T. R., Reactions of Hexadehydro-Diels–Alder (HDDA)-Derived Benzynes with Thioamides: Synthesis of Dihydrobenzothiazino-Heterocyclics. *Org. Lett.* **2016,** *18*, 6312-6315.
[51] Zhang, J.; Niu, D.; Brinker, V. A.; Hoye, T. R., The Phenol–Ene Reaction: Biaryl Synthesis via Trapping Reactions between HDDA-Generated Benzynes and Phenolics. *Org. Lett.* **2016,** *18*, 5596-5599.

amines[52] and sulfides[53] to make structurally complex benzenoid products (**1066** and **1067**), hydroalkynylation reactions of benzyne to make aryl acetylene products (**1068**),[54] trapping of benzyne with complex natural products to give structurally complex, multifunctional benzenoid products (e.g. **1069** by trapping with tropinone),[55] trapping of benzyne with perylenes to product polyaromatic hydrocarbons (**1070**),[56] and reactions of benzyne with tetraphenylcyclopentadienone to yield blue-emitting, highly conjugated benzenoid products (**1071**) that possess potentially useful luminescent characteristics.[57]

Figure 1.14 | Selected examples of products representative of notable advances in HDDA chemistry.

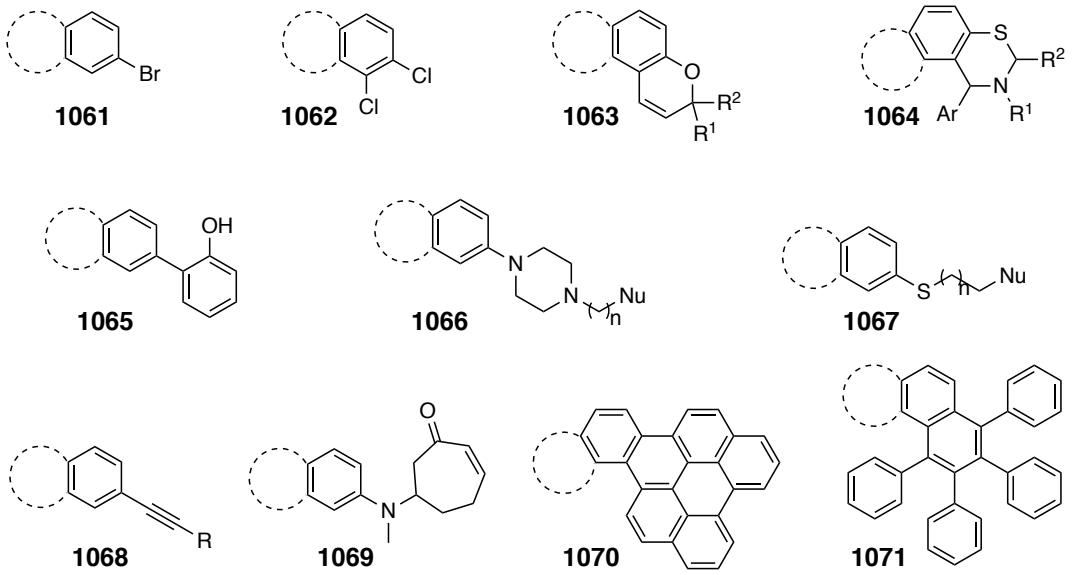

[52] Ross, S. P.; Hoye, T. R., Multiheterocyclic Motifs via Three-Component Reactions of Benzynes, Cyclic Amines, and Protic Nucleophiles. *Org. Lett.* **2018,** *20*, 100-103.
[53] Hoye, J. C.; Vignesh, P.; Thomas, R., Reactions of HDDA-Derived Benzynes with Sulfides: Mechanism, Modes, and Three-Component Reactions. *J. Am. Chem. Soc.* **2016,** *138*, 4318–4321.
[54] Xiao, X.; Wang, T.; Xu, F.; Hoye, T. R., CuI-Mediated Bromoalkynylation and Hydroalkynylation Reactions of Unsymmetrical Benzynes: Complementary Modes of Addition. *Angew. Chem. Int. Ed.* **2018,** *57*, 16564-16568.
[55] Ross, S. P.; Hoye, T. R., Reactions of hexadehydro-Diels–Alder benzynes with structurally complex multifunctional natural products. *Nat. Chem.* **2017,** *9*, 523-530.
[56] Xu, F.; Xiao, X.; Hoye, T. R., Reactions of HDDA-Derived Benzynes with Perylenes: Rapid Construction of Polycyclic Aromatic Compounds. *Org. Lett.* **2016,** *18*, 5636-5639.
[57] Xu, F.; Kyle, W. H.; Russell, J. H.; Hoye, T. R., Blue-Emitting Arylalkynyl Naphthalene Derivatives via a Hexadehydro-Diels–Alder Cascade Reaction. *J. Am. Chem. Soc.* **2016,** *138*, 12739–12742.

Chapter 2. Reactions of HDDA Benzyne with Carbonyl Moieties

2.1 Preface: Reactions of Benzyne with Aldehydes

Among countless precedented benzyne reactions sits the trapping of benzyne with aldehyde compounds. In the vast majority of these reported reactions, the aldehyde acts as an electrophile that traps the phenyl anion **2001**, which results from an initial nucleophilic trapping reaction of benzyne **2002** (Figure 2.1a). The products of this class of reaction are usually benzylic alcohols such as **2003**.

An intramolecular variation of this chemistry is demonstrated by work from Okuma and coworkers (Figure 2.1).[58] Here, benzyne is initially trapped by salicylaldehyde (**2004**) to give zwitterionic intermediate **2005**, which rapidly undergoes an annulation reaction to intermediate **2006** before ultimately yielding xanthol **2007**. Such chemistry can also be done in a multicomponent fashion, as shown in the research

Figure 2.1 | (a) Aldehydes react with phenyl anions that result from the trapping of benzyne with a nucleophile. This can be done in an intramolecular fashion (b) or in a multicomponent reaction (c).

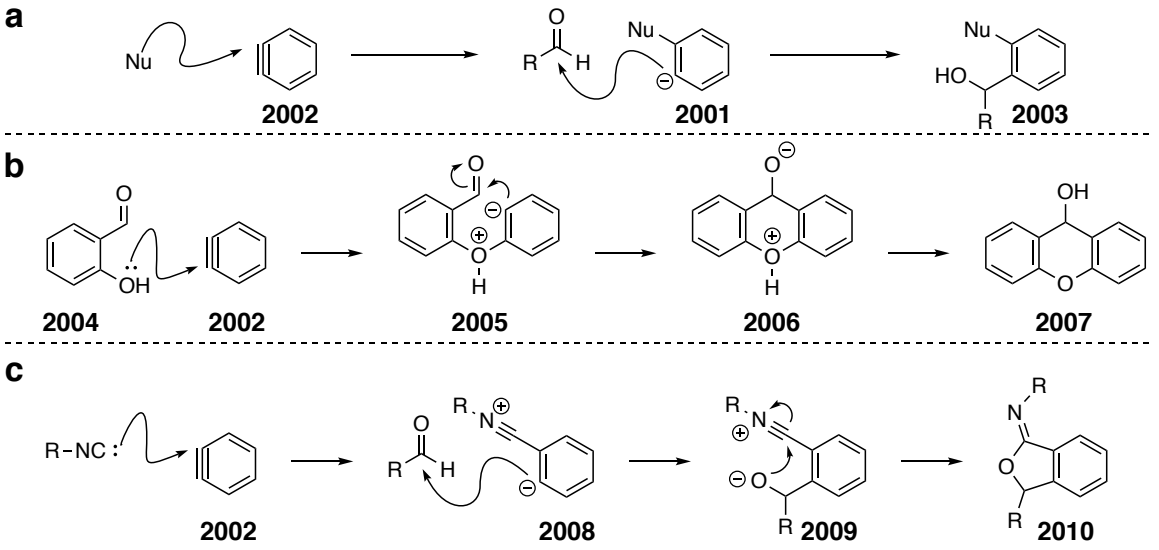

[58] Okuma, K.; Nojima, A.; Matsunaga, N.; Shioji, K., Reaction of Benzyne with Salicylaldehydes: General Synthesis of Xanthenes, Xanthones, and Xanthols. *Org. Lett.* **2009,** *11*, 169-171.

of Yoshida and coworkers (Figure 2.1c).[59] In this work, benzyne was trapped with isocyanide to access the zwitterionic nitrilium **2008**. This intermediate then reactions with an aldehyde to give the benzylic alkoxide **2009**, which ultimately yields the iminofuran product **2010** by a ring-closing reaction.

Less common are reactions in which aldehydes react *directly* with benzyne. Such reactions proceed through a formal [2 + 2] cycloaddition to access an unstable benzoxetene intermediate that is prone to *in situ* ring-opening in a retro [2 + 2] manner to give an *ortho*-quinone methide species (Figure 1.16). *o*-Quinone methides, like benzynes, are electrophilic reactive intermediates whose utility in organic synthesis is well-precedented.[60] The development of a process to react benzynes with aldehydes and to trap the resulting *o*-quinone methides *in situ* would hold remarkable value for the rapid synthesis of diversely-substituted benzenoid products. However, the need to selectively trap the *o*-quinone methide intermediate over the benzyne presents a significant challenge and is likely responsible for the scarcity of precedence examples for such a process.[61]

Figure 2.2 | The reaction of benzyne with aldehydes yields *ortho*-quinone methide products

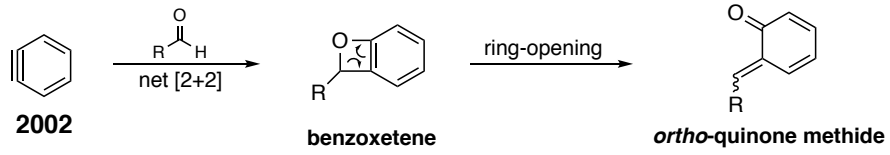

[59] Yoshida, H.; Fukushima, H.; Ohshita, J.; Kunai, A., Arynes in a three-component coupling reaction: straightforward synthesis of benzoannulated iminofurans. *Angew. Chem. Int. Ed.* **2004,** *43*, 3935-8.
[60] (a) Rokita, S. E. Quinone Methides. 1, Wiley: Hoboken, 2009. (b) Willis, N. J.; Bray, C. D., ortho-Quinone Methides in Natural Product Synthesis. *Chem. Eur. J.* **2012,** *18*, 9160-9173. (c) Yang, B.; Gao, S., Recent advances in the application of Diels–Alder reactions involving o-quinodimethanes, aza-o-quinone methides and o-quinone methides in natural product total synthesis. *Chem. Soc. Rev.* **2018,** *47*, 7926-7953. (d) Singh, M. S.; Nagaraju, A.; Anand, N.; Chowdhury, S., ortho-Quinone methide (o-QM): a highly reactive, ephemeral and versatile intermediate in organic synthesis. *RSC Adv.* **2014,** *4*, 55924-55959. (e) Bai, W.-J.; David, J. G.; Feng, Z.-G.; Weaver, M. G.; Wu, K.-L.; Pettus, T. R. R., The Domestication of ortho-Quinone Methides. *Acc. Chem. Res.* **2014**.
[61] (a) Yoshida, H.; Watanabe, M.; Fukushima, H.; Ohshita, J.; Kunai, A., A 2:1 Coupling Reaction of Arynes with Aldehydes via *o*-Quinone Methides: Straightforward Synthesis of 9-Arylxanthenes. *Org. Lett.* **2004,** *6*, 4049-4051. (b) Yoshida, H.; Ito, Y.; Ohshita, J., Three-component coupling using arynes and DMF: straightforward access to coumarins via ortho-quinone methides. *Chem. Commun.* **2011,** *47*, 8512-8512.

The viability of generating and trapping *o*-quinone methides through the use of HDDA-generated benzynes is demonstrated by the reaction in Scheme 2.1. In this cascade, triyne **2010** is heated in the presence of benzaldehyde (2 equiv) and ethyl vinyl ether (10 equiv.). The benzaldehyde traps the benzyne from the initial HDDA cycloaromatization to give *o*-quinone methide intermediate **2011**, which then reacts with ethyl vinyl ether (presumably in a [4 + 2] cycloaddition) to yield chromane **2012** in 70% yield as a mixture of syn- and anti-stereoisomers.

Scheme 2.1 | The three-component reaction between HDDA benzyne, benzaldehyde, and ethyl vinyl ether yields chromane **2012**.

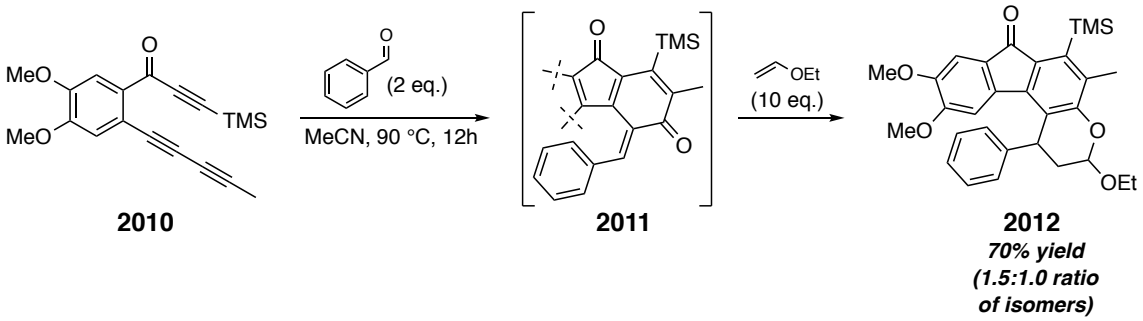

2010 **2011** **2012**

70% yield (1.5:1.0 ratio of isomers)

2.2 Attempted Three-Component Reactions with HDDA-Benzyne and Aromatic Aldehydes

Various aromatic aldehydes were shown to give similarly good results when ethyl vinyl ether was used as the third-component in the reaction. Unfortunately, the aforementioned problem of selective trapping proved to be significant. When heated in the presence of HDDA substrate **2010** and an aromatic aldehyde, most third-component traps showed a preference for benzyne-trapping over trapping of the *o*-quinone methide intermediate. Examples demonstrating this problem are shown in Scheme 2.2. The use of *tert*-butylamine as the third-component, for example, yielded aryl amine **2013** while the desired three-component reaction product **2014** was not observed. Even the replacement of the successfully-employed ethyl vinyl ether with cyclohexene failed to give tractable amounts of the desired product **2015**.[62] Rather, the predominant product of this reaction **2016** was the result of dihydrogen transfer from cyclohexene to the HDDA-benzyne.[46] In

[62] The use of styrene also did not yield the desired three-component reaction product.

each reaction, changing the stoichiometry of the trapping reagents did not give improved results.

Scheme 2.2 | Selected three-component reactions which failed to yield desired products.

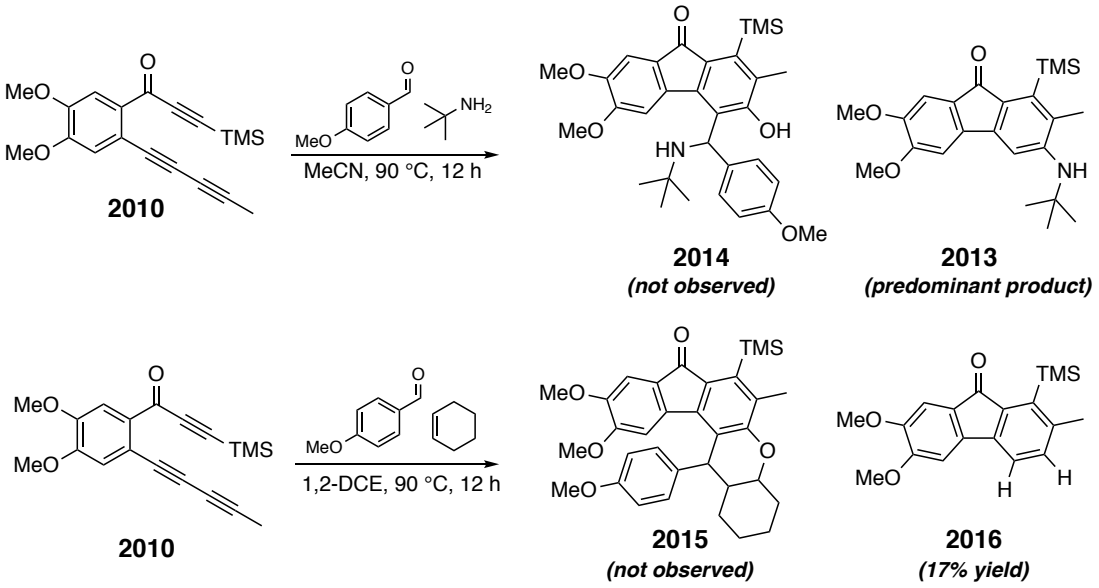

2.3 Synthesis of Benzodioxane Products Through the HDDA Reaction

In experimenting with the stoichiometry of the traps in these reactions, I frequently observed by LC/MS the formation of products whose masses indicated that they were formed from the trapping of benzyne with *two* equivalents of aromatic aldehyde. These products were ultimately identified as benzodioxanes (illustrated generically in Figure 2.3 as **2017**). Their formation presumably occurs through the trapping of *o*-quinone methide **2011** with an additional equivalent of the same aldehyde (Figure 2.3a).

Having identified these products, I felt that this chemistry was worth pursuing further. Not only is the precedence for this reaction quite limited,[63] but these benzo-1,3-dioxane products could potentially be further functionalized. I ran additional reactions in which the HDDA substrate **2010** was heated solely in the presence of aromatic aldehydes (10 equivalents). Selected products from these reactions are shown in Figure 2.3b.

[63] There are only two reported examples of such a reaction in the literature: (a) Heaney, H.; McCarty, C. T., Reactions of arynes with carbonyl compounds. *J. Chem. Soc. D: Chem. Comm.* **1970**, 123a-123a. (b) Jyuzo, N.; Masayuki, Y.; Osamu, S., Reaction of benzyne generated from 1-(2-carboxylphenyl)-3,3-dimethyltriazene with benzaldehyde and some other carbonyl compounds. *Chem. Lett.* **1973,** *2*, 451-454.

Although this reaction did indeed yield the desired benzodioxane products **2018** and **2019** when benzaldehyde and thiophencarboxaldehyde were respectively used, the yields are quite modest when considering the excess of aldehyde trap.

Furthermore, the scope of this reaction is limited by the degree of aromaticity in the aromatic aldehyde trap. The use of furfural is a case in point; heating **2010** in the presence of 10 equivalents of furfural only gave benzodioxane **2020** in 3% yield. The major product of this reaction was instead **2021**—the result of a [4 + 2] trapping event.

Figure 2.3 | Formation of benzodioxane products **2018**–**2020**.

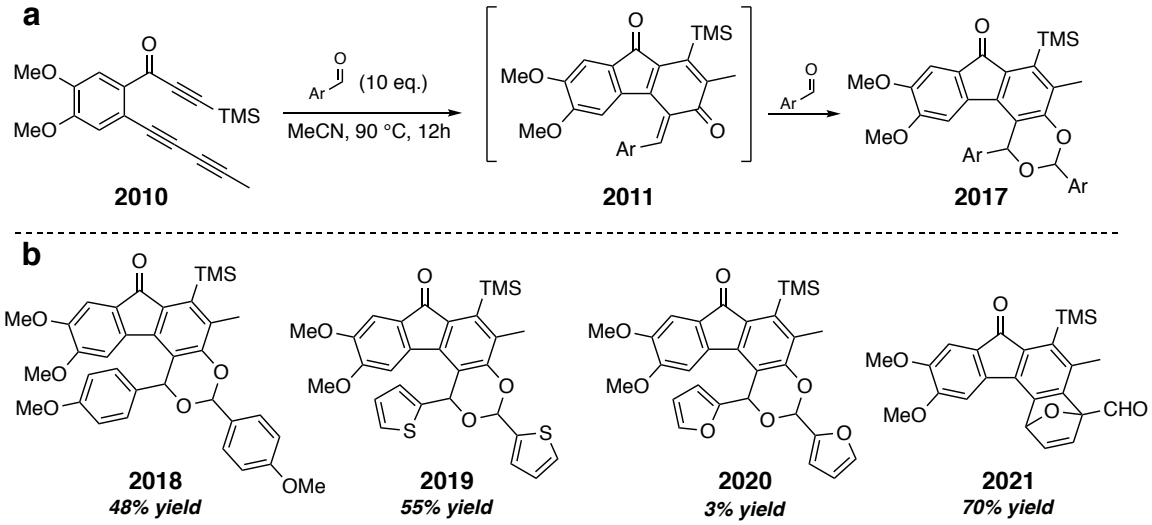

2.4 Formation of Alkenyl Phenol Products from Aliphatic Aldehydes: A Novel Benzyne Reaction

In an attempt to expand the scope of this reaction, I decided to heat HDDA substrate **2010** in the presence of both an aromatic aldehyde and an aliphatic aldehyde. Based on the hypothesis that an aromatic aldehyde would more readily trap the HDDA-benzyne than an aliphatic aldehyde,[64] I anticipated that the "mixed" benzodioxane **2022** would form (Scheme 2.3). However, no such product was observed when **2010** was

[64] This proposed preference was based on the assumption that the partial positive charge on the carbonyl carbon, which would develop increasing positive charge during the trapping even, would be more effectively stabilized by an aryl rather than an alkyl substituent.

heated in the presence of *p*-methoxybenzaldehyde (2 equivalents) and isobutyraldehyde (10 equivalents).[65]

Scheme 2.3 | Unexpected formation of alkenyl phenol product **2023**.

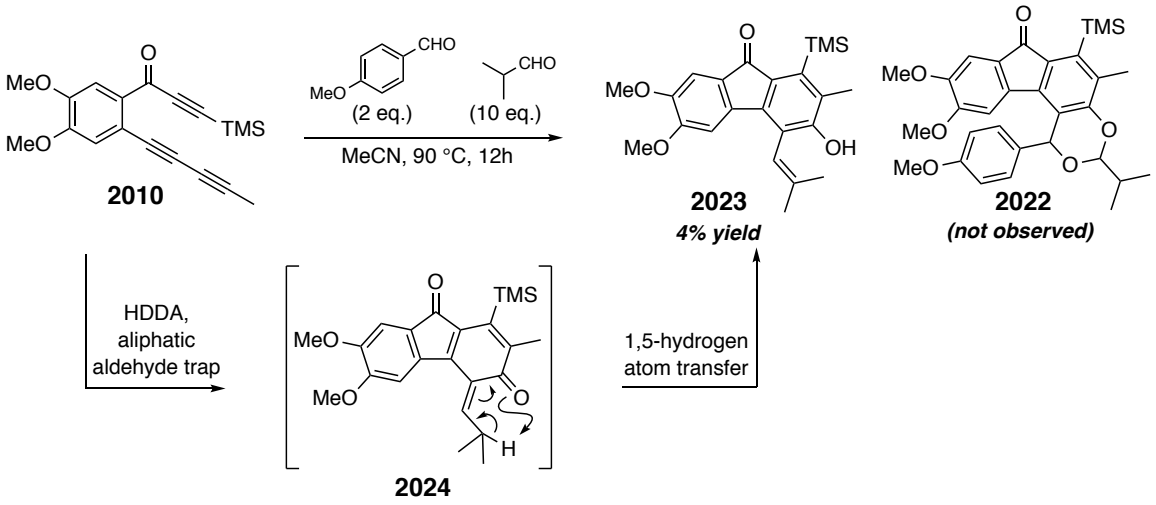

Interestingly, a barely isolable amount of the alkenyl phenol product **2023** was identified as part of the crude reaction mixture. The formation of this product was intriguing; it can be rationalized by the formation of *o*-quinone methide intermediate **2024** followed by a 1,5-hydrogen atom transfer. Despite the extremely low yield of this product, this transformation was not reported in the literature and constituted a novel benzyne reaction—an exciting realization when considering the decades worth of research that have been devoted to benzyne chemistry.

Heating **2010** solely in the presence of isobutyraldehyde gave **2023** in a more desirable but still modest yield of 29%.[66] The use of *n*-butyraldehyde resulted in the formation of alkenyl phenol **2025** in a slightly better yield of 38% (Scheme 2.4).[67] The observed preference for the formation of **2025** as a trans alkene is notable; no cis alkene analog of **2025** was isolated or seen in the crude reaction mixture. Despite the novelty of

[65] The use of acetaldehyde, formaldehyde, and acetone as the third-component also failed to yield their desired mixed benzodioxane products.

[66] When this same reaction was carried out in acetonitrile (like the HDDA reactions in Figure 2.3) rather than benzene, the yield of product **2023** was merely 5%.

[67] Similarly, when acetonitrile was used as the reaction solvent instead of benzene, the yield was significantly lower (11%).

this reaction, the modest yields observed for products **2023** and **2025** were somewhat disconcerting.

A potential factor contributing to these low yields was identified from the observed aryl ester side products **2026** and **2027** (Scheme 2.4). Recall from Section 1.2.4 that HDDA-generated benzyne reacts with carboxylic acid traps to give aryl esters—the result of formal insertion of the benzyne C≡C triple bond into the O–H bond of the carboxylic acid. While no carboxylic acid impurities were detected in the commercial sources of butyraldehyde or isobutyraldehyde, it seems reasonable that they could form under the elevated temperatures of the HDDA reaction as a result of autooxidation of the weak aldehyde C–H bond.[68] The reactions were rerun in benzene that had been thoroughly sparged with nitrogen gas. While this did almost completely eliminate the formation of aryl ester products **2026** and **2027**, it—unfortunately—did not mitigate the problem of low alkenyl phenol yield.

Scheme 2.4 | HDDA reactions with aliphatic aldehyde traps.

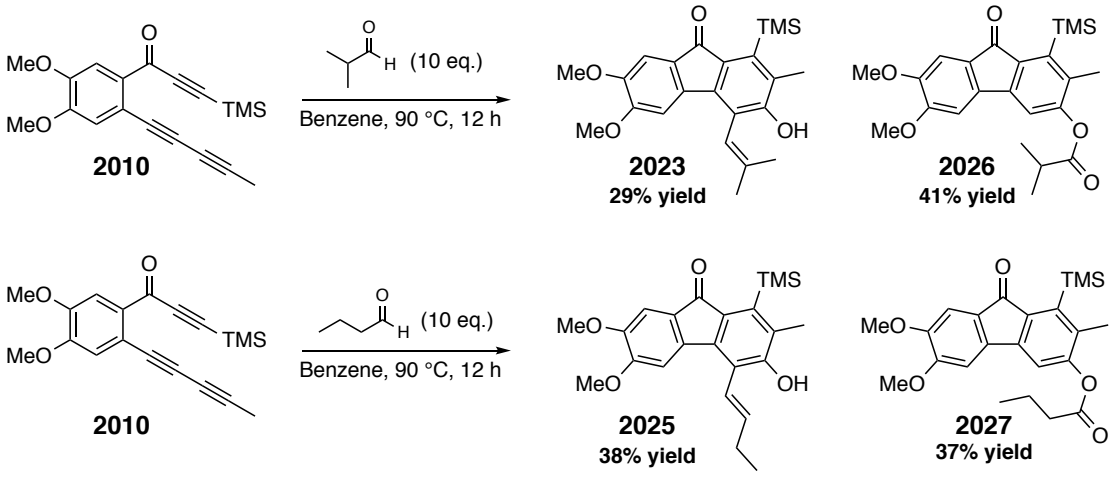

2.5 α-Arylation of 1,3-Dicarbonyl Traps: A "Divergent" Benzyne Reaction

Synthesis of the highly conjugated alkenyl phenol product **2028** was attempted by heating triyne **2010** in the presence of phenylacetaldehyde (Scheme 2.5). This, strangely, resulted in a complex mixture of products with no observed formation of the anticipated

[68] Vanoye, L.; Favre-Réguillon, A.; Aloui, A.; Philippe, R.; de Bellefon, C., Insights in the aerobic oxidation of aldehydes. *RSC Adv.* **2013,** *3*, 18931-18937.

product **2028**. Even more surprising was the isolation of a trace amount compound **2029**—a formal C–H insertion product.

When comparing this result to those from the isobutyraldehyde and butyraldehyde trapping reactions in Scheme 2.4, one might consider the keto–enol equilibrium for each aldehyde trapping species. One would naturally expect for phenylacetaldehyde to have a lower ketone:enol ratio than what is seen for isobutyraldehyde or butyraldehyde. Accordingly, if enol tautomers of aldehydes were, in some manner, able to cleanly react with benzyne, one could expect that the product of such a reaction would form in higher amounts when phenylacetaldehyde is used as the benzyne trap. With that having been said, it could be proposed that the formation of **2029** is the result of a hetero-ene reaction between enol tautomer **2030** and the HDDA benzyne that arises from **2010** (Scheme 2.5). This could proceed through a concerted process, as is demonstrated in the transition state structure **2031**, or a stepwise process (not shown).

Scheme 2.5 | Proposed formation of the observed α-arylation product **2029** through a hetero-ene reaction between HDDA benzyne and enol **2030**.

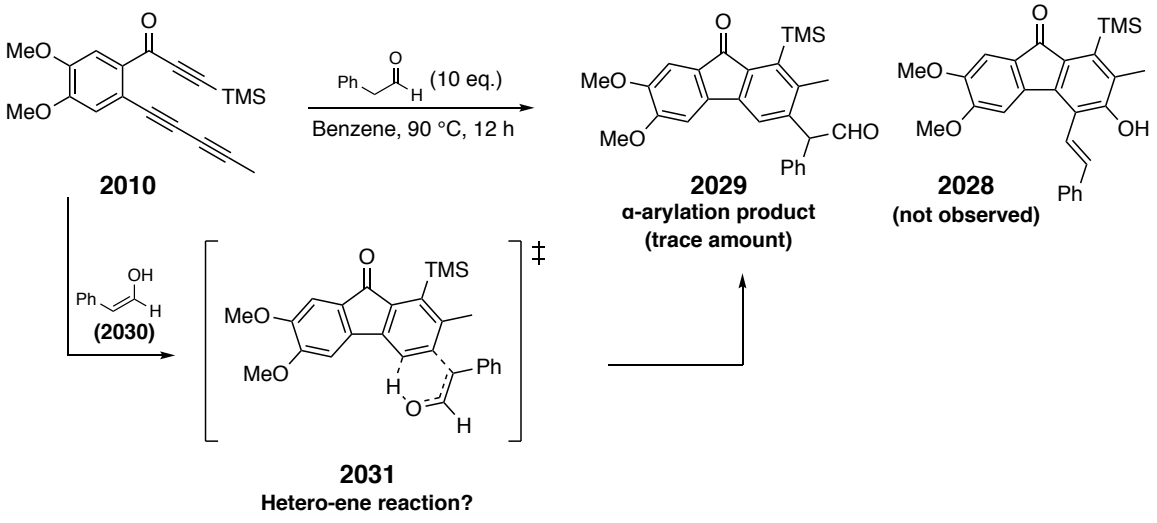

If this proposal were true, it could be expected that a carbonyl-containing compound whose equilibrium is even more favorable to the enol tautomer would give a higher yield of a product analogous to **2029**. Accordingly, I attempted several reactions in which **2010** was heated in the presence of a compound with a 1,3-dicarbonyl moiety

(Figure 2.4). These reactions were expected to yield products **2032**, either as a vinylogous acid **2032a**, its tautomer **2032b**, or a mixture of these two isomers.

Indeed, the use of ethyl acetoacetate as a trap produced product **2033** in a low (but still improved) yield of 11%. The use of acetylacetone gave a somewhat higher yield (27%) of α-arylation product **2034**. In each of these cases, only the enol tauomer of the product was observed. Dimedone, whose enol tautomer is nearly as favored as its keto tautomer, was an even more effective trap—resulting in a 52% yield of **2035** as a 5.5:1 molar ratio of tautomers. While it was hoped that 4-hydroxycoumarin—which shows a practically exclusive preference for its enol tautomer—would give a still higher yield, it resulted in a similar 54% yield of **2036**. Interestingly, this product appeared to exist as a mixture of keto and enol tautomers.

Figure 2.4 | (a) The trapping of HDDA-benzyne with a 1,3-dicarbonyl compound results in an α-arylation product as a mixture of tautomers **2032a** and **2033b**. (b) Products **2033**–**2036** resulting from this reaction. The molar ratios of enol to keto tautomers for products **2035** and **2036** are shown in parenthesis.

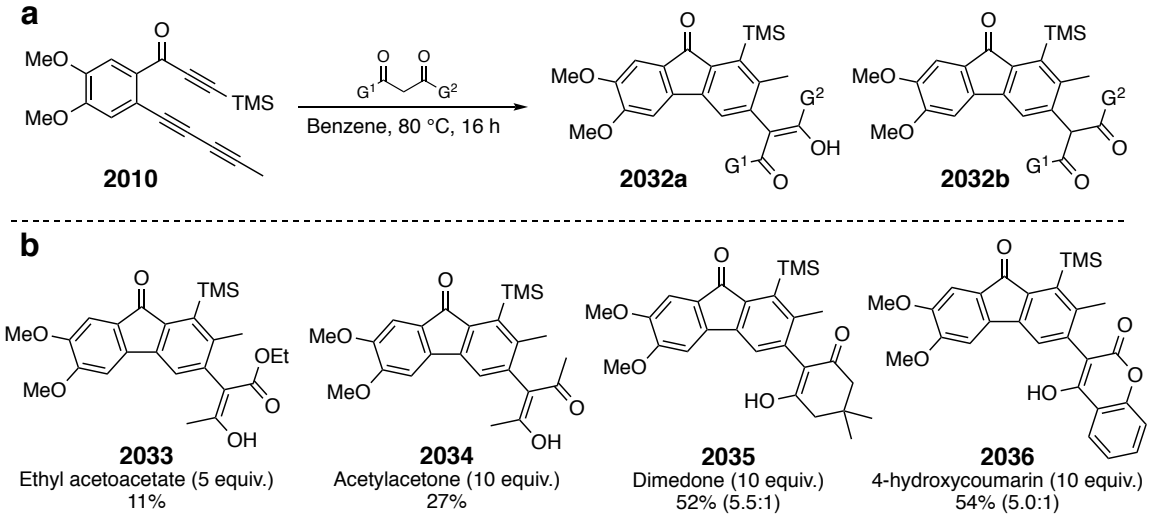

Additional HDDA reactions were attempted with malononitrile, diethylmalonate, chloroacetone, and nitromethane to form products **2037**, **2038**, **2039**, and **2040**, respectively (Figure 2.5). While these traps contain acidic α-C–H bonds, they either have an equilibrium that heavily favors the keto over the enol tautomer or they are simply

incapable of forming an enol tautomer. As expected, the use of these traps failed to yield an observable amount of their corresponding HDDA products.

Figure 2.5 | α-Arylation products that were not formed from the HDDA reaction.

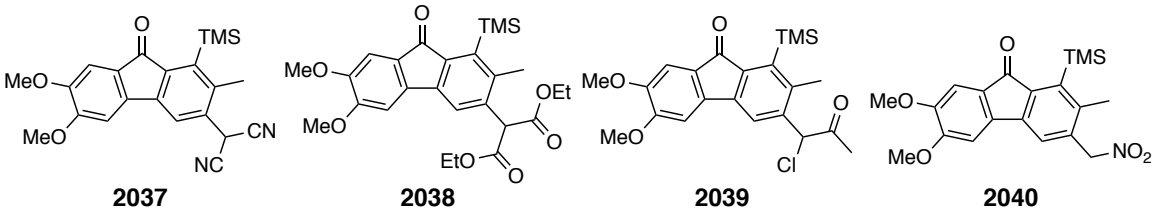

2037 Malononitrile (10 equiv.) | **2038** Diethylmalonate (10 equiv.) | **2039** Chloroacetone (10 equiv.) | **2040** Nitromethane (solvent)

While the yields of products **2033**–**2036** are not impressive, especially when considering the molar excess of the 1,3-dicarbonyl traps used, these reactions are an illustrative example of reactive "divergence" in the HDDA reaction. Recall from Section 1.2.4 that certain benzyne traps (such as carboxylic acids) yield different benzenoid products depending on whether the benzyne is generated by the HDDA reaction or by the more conventional protocol from Kobayashi and coworkers (discussed in Section 1.1.3, Figure 1.5). The work in this section shows that 1,3-dicarbonyl compounds (**2041**) fall into this category of benzyne traps, as they give α-arylation products **2042** with the HDDA reaction but yield C–C σ-bond insertion products **2043** with Kobayashi benzyne (Figure 2.6).[69,70,71]

---

[69] (a) Tambar, U. K.; Stoltz, B. M., The Direct Acyl-Alkylation of Arynes. *J. Am. Chem. Soc.* **2005,** *127*, 5340-5341. (b) Tadross, P. M.; Virgil, S. C.; Stoltz, B. M., Aryne Acyl-Alkylation in the General and Convergent Synthesis of Benzannulated Macrolactone Natural Products: An Enantioselective Synthesis of (−)-Curvularin. *Org. Lett.* **2010,** *12*, 1612-1614. (c) Yoshida, H.; Watanabe, M.; Ohshita, J.; Kunai, A., Facile insertion reaction of arynes into carbon–carbon σ-bonds. *Chem. Commun.* **2005**, 3292-3294.

[70] In contrast to other 1,3-dicarbonyl compounds, molecular traps that contain a protic amide (such as β-keto amides and malonamide esters) yield α-arylation products from reaction with Kobayashi benzyne: (a) Mohanan, K.; Coquerel, Y.; Rodriguez, J., Transition-Metal-Free α-Arylation of β-Keto Amides via an Interrupted Insertion Reaction of Arynes. *Org. Lett.* **2012,** *14*, 4686-4689. (b) Dhokale, R. A.; Thakare, P. R.; Mhaske, S. B., Transition-Metal-Free C-Arylation at Room Temperature by Arynes. *Org. Lett.* **2012,** *14*, 3994-3997. (c) Gupta, E.; Kant, R.; Mohanan, K., Decarbethoxylative Arylation Employing Arynes: A Metal-Free Pathway to Arylfluoroamides. *Org. Lett.* **2017,** *19*, 6016-6019.

[71] It should also be noted that, while they are not 1,3-dicarbonyl compounds per se, β-enamino esters and ketones yield α-arylation products under the Kobayashi conditions: (a) Ramtohul, Y. K.; Chartrand, A., Direct C-Arylation of β-Enamino Esters and Ketones with Arynes. *Org. Lett.* **2007,** *9*, 1029-1032. (b) Picazo, E.; Anthony, S. M.; Giroud, M.; Simon, A.; Miller, M. A.; Houk, K. N.; Garg, N. K., Arynes and Cyclic Alkynes as Synthetic Building Blocks for Stereodefined Quaternary Centers. *J. Am. Chem. Soc.* **2018,** *140*, 7605-7610.

Figure 2.6 | Reactive divergence of HDDA benzyne from Kobayashi benzyne.

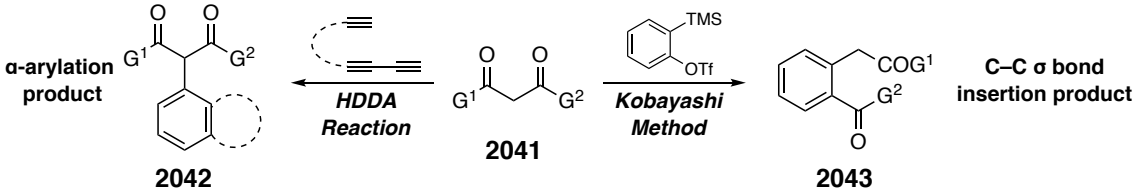

As is the case with carboxylic acid traps, this divergence can be attributed to the basic reaction conditions inherent to the Kobayashi protocol. Under these basic conditions, the molecular trap compound exists predominantly as an enolate ion pair in solution rather than a 1,3-dicarbonyl compound or its enol tautomer. Such enolate ions react with benzyne in a [2 + 2] to form a benzocyclobutene intermediate, which ring-opens to give its corresponding product **2043**.

Chapter 3. The Pentadehydro-Diels–Alder (PDDA) Reaction

The studies presented in this chapter are part of a collaboration between Dr. Teng Wang, Dr. Rajasekhar Naredla, and the author of this thesis. Regarding our published work,[72] Dr. Wang initiated the project, both Dr. Wang and Dr. Naredla carried out the synthetic work, while the author of this thesis performed the computational studies. This published, collaborative work will be the topic of Sections 3.1 – 3.3. Section 3.4 will discuss additional, unpublished synthetic work that was performed solely by the author of this thesis.

3.1 Preface: Dehydro-Diels–Alder Reactions with Allenes

In section 1.2.1, dehydro-Diels–Alder (DDA) reactions were discussed as part of an introduction to the HDDA reaction. All of the reactions discussed were examples in which one or more alkenes of the standard "diene + dienophile" Diels–Alder reaction had been replaced by an alkyne. This resulted in didehydro-, tetradehydro-, and—of course—hexadehydro-Diels–Alder reactions. Not discussed in this section were examples of DDA reactions possessing levels of "dehydroness" that are, in a sense, between those found in di-, tetra-, and hexadehydro-Diels–Alder reactions. Specifically, these are Diels–Alder reactions in which one or more of the alkenes has been replaced by an *allene* rather than an alkyne. Hypothetical examples of these reactions are shown in Figure 3.1.

Figure 3.1a shows a Diels–Alder reaction between a 1,3-diene and an allene to the stable diene product **3001**. As is the case with several of the DA reactions discussed in Chapter 1, some allene DA reactions yield intermediates that are capable of rearranging to more stable aromatic products. Such is the case in the "tridehydro"-Diels–Alder

Figure 3.1 | Simplified examples of dehydro-Diels–Alder reactions with allenes.

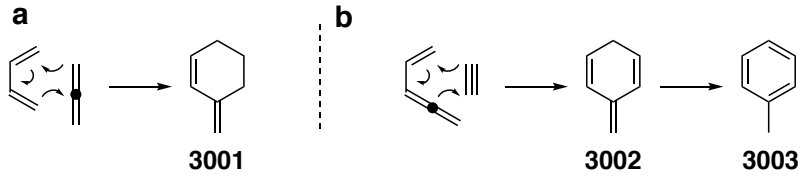

reaction shown in Figure 3.1b, which yields an exocyclic alkene **3002** that rearomatizes to toluene **3003**. While they are not as common as the DDA reactions discussed in

[72] Wang, T.; Naredla, R. R.; Thompson, S. K.; Hoye, T. R., The pentadehydro-Diels–Alder reaction. *Nature* **2016,** *532*, 484.

Chapter 1, these allene DDA reactions are still well-precedented.[73] Notice that the most oxidized of these allene DDA reactions—which can be referred to as a pentadehydro Diels–Alder (PDDA) reaction—gives a cyclic product **3004** that is both highly strained and incapable of rearrangement to a stable benzenoid product (Figure 3.2). This product, known as an α,3-dehydrotoluene, is a reactive intermediate—much like the benzyne that is accessed through the HDDA reaction. Unlike benzyne, which react with molecular traps to give *ortho*-functionalized benzene products, α,3-dehydrotoluenes yield aromatized products **3005** that are functionalized on the benzene ring and in the benzylic position.

Figure 3.2 | The pentadehydro-Diels–Alder reaction.

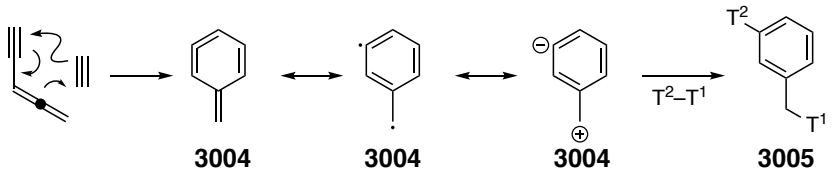

α,3-Dehydrotoluene intermediates are precedented. They have been spectroscopically characterized and their synthetic uses have been studied—although not nearly to the same extent as benzynes. Their generation is possible only from very specific substrates.[74,75,76] Until the work reported in this chapter, there were no examples

[73] Krause, N.; Hashmi, A. S. K. Modern Allene Chemistry. Wiley-VCH: Weinheim, 2004.

[74] (a) Myers, A. G.; Kuo, E. Y.; Finney, N. S., Thermal generation of .alpha.,3-dehydrotoluene from (Z)-1,2,4-heptatrien-6-yne. *J. Am. Chem. Soc.* **1989,** *111*, 8057-8059. (b) Myers, A. G.; Dragovich, P. S.; Kuo, E. Y., Studies on the thermal generation and reactivity of a class of (.sigma.,.pi.)-1,4-biradicals. *J. Am. Chem. Soc.* **1992,** *114*, 9369-9386.

[75] This cycloaromatization is probably most well-known for being integral to the mechanism of cytotoxicity for certain ene-diyne natural products such as neocarzinostatin. For relevant references, see: (a) Myers, A. G.; Proteau, P. J.; Handel, T. M., Stereochemical assignment of neocarzinostatin chromophore. Structures of neocarzinostatin chromophore-methyl thioglycolate adducts. *J. Am. Chem. Soc.* **1988,** *110*, 7212-7214. (b) Nagata, R.; Yamanaka, H.; Murahashi, E.; Saito, I., DNA cleavage by acyclic eneyne-allene systems related to neocarzinostatin and esperamicin-calicheamicin. *Tetrahedron Lett.* **1990,** *31*, 2907-2910. (c) Nicolaou, K. C.; Maligres, P.; Shin, J.; De Leon, E.; Rideout, D., DNA-cleavage and antitumor activity of designed molecules with conjugated phosphine oxide-allene-ene-yne functionalities. *J. Am. Chem. Soc.* **1990,** *112*, 7825-7826.

[76] One limitation in using the Myers–Saito reaction to access α,3-dehydrotoluene products is the tendency of certain allenyl enyne substrate to undergo a Schmittel cyclization. (a) Schmittel, M.; Strittmatter, M.; Kiau, S., Switching from the Myers reaction to a new thermal cyclization mode in enyne-allenes. *Tetrahedron Lett.* **1995,** *36*, 4975-4978. (b) Schmittel, M.; Keller, M.; Kiau, S.; Strittmatter, M., A Surprising Switch from the Myers–Saito Cyclization to a Novel Biradical Cyclization in Enyne–Allenes: Formal Diels–Alder and Ene Reactions with High Synthetic Potential. *Chem. Eur. J.* **1997,** *3*, 807-816.

in the literature of α,3-dehydrotoluene generation from a cycloaddition—a process we have termed a PDDA reaction).

3.2 Discovery of a Pentadehydro-Diels–Alder (PDDA) Reaction Cascade

The symmetrical tetrayne **3006** is a well-established HDDA substrate that is capable of forming functionalized benzenoid products through the HDDA reaction at the (relatively) low temperature of 70 °C. This is demonstrated by the reaction in which **3006** is heated in methanol at 70 °C to yield a mixture of isomeric benzenoid products **3007a** and **3007b** in 84% yield (Scheme 3.1a). A researcher in our lab observed that when **3006** was dissolved in piperidine at room temperature, it was converted—with a half-life of about 15 hours— to a compound that had the mass of an adduct of **3006** + piperidine. Much to our surprise, analysis by NMR spectroscopy revealed this adduct to be the benzylic amine **3008**.

Scheme 3.1 | a) HDDA reaction of tetrayne **3006** with methanol at 70 °C. b) Conversion of **3006** to benzylic amine **3008** at room temperature.

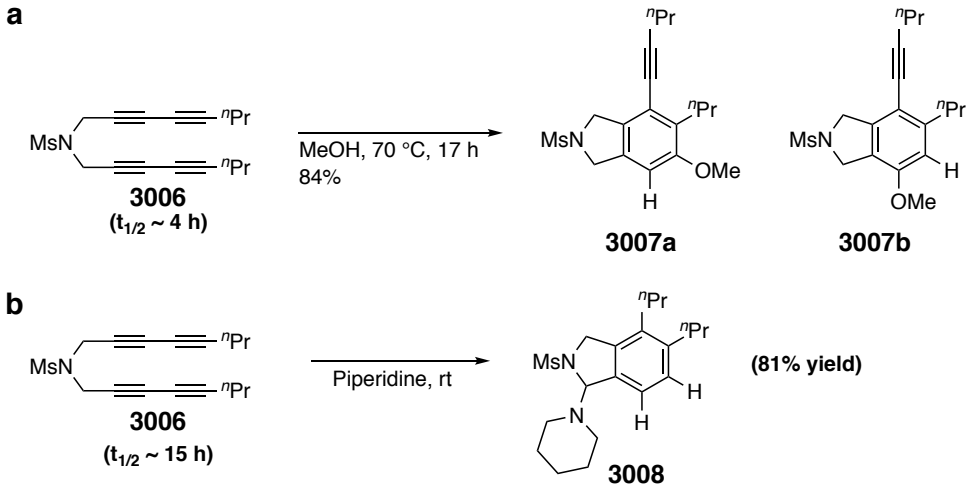

The (previously-discussed) precedence on α,3-dehydrotoluene chemistry was a sufficient basis on which to propose a pathway for the formation of product **3008** (Figure 3.3). The piperidine is sufficiently basic to deprotonate one of the chemically identical activated methylene groups in tetrayne **3006**. Such a deprotonation ultimately results in an isomerization to the diyne-allenyne intermediate **3009**. A PDDA reaction of this

intermediate would result in the α,3-dehydrotoluene analog **3010**, the trapping of which with piperidine would yield the observed product **3008**.

Figure 3.3 | Proposed formation of benzylic amine **3008** from tetrayne **3006** through a PDDA pathway.

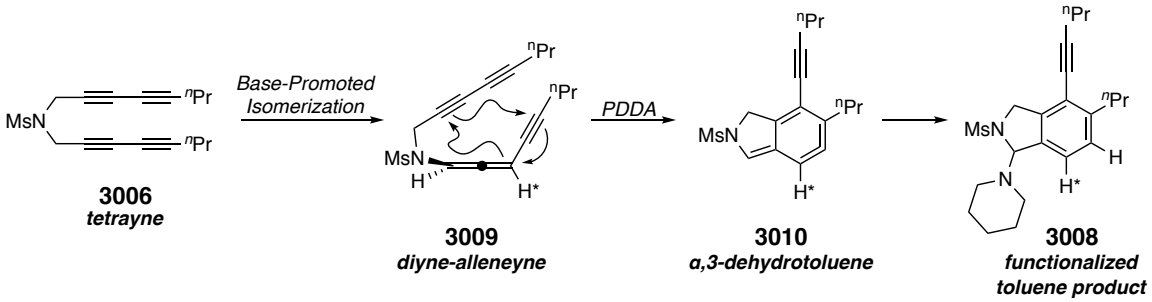

Subsequent work demonstrated a respectable scope for this reaction when different sulfonamine-tethered tetrayne substrates were exposed to 1,8-diazabicyclo[5.4.0]undec-7-ene (DBU) in different protic, nucleophilic solvents such as piperidine, diethylamine, *n*-butylamine, pyrrolidine, morpholine, methanol, and water. Far more exciting was the demonstration that nitriles could be incorporated into this cycloaromatiztion/trapping cascade to give functionalized picoline products (i.e. alkyl-pyridine products functionalized at the α position of the alkyl ring). The mere fact that nitriles are capable of participating in this cycloaromatization is notable, given their relative thermodynamic stability compared to alkynes.[77,78] Cyano substrates showed a similar scope in the PDDA reaction to the aforementioned tetrayne substrates.

3.3 Probing PDDA Reaction Energetics with DFT Calculations

3.3.1 Initial Experimental Evidence for the Proposed PDDA Reaction

While the proposed PDDA pathway is a reasonable explanation for the formation of the benzene and pyridine products that were observed, it proved difficult to provide experimental evidence for this mode of product formation. Formation of the observed

[77] While there exist countless examples of incorporations of alkynes into cycloaromatization processes, there are only a few examples of cycloaromatization reactions that involve nitriles. This will be an important premise to the work presented in Chapters 4 and 5.

[78] Given the remarkable ease with which nitriles were incorporated into the PDDA reaction, it is interesting to note the following reported failure to incorporate a nitrile into a Myers–Saito cyclizaion: Gillmann, T.; Heckhoff, S., Aza-enyne allenes: Thermal reaction behavior of 2,4,5-hexatrienenitriles. *Tetrahedron Lett.* **1996,** *37*, 839-840.

products could potentially be explained by hydroamination of either the alkyne or allenyne precursor by the employed amine base prior to cycloaromatization. The apparent instability of the putative allenyne intermediate, which could not be observed spectroscopically, made it difficult to provide compelling evidence. If the PDDA cycloaromatization were indeed responsible for product formation, its activation barrier would be very low.

There were a small number of experimental results that lent credence to the proposed PDDA pathway. Exposure of substrate **3006** to 5 equivalents of DBU in deuterated chloroform resulted in deuterated dichloroalkene product **3011** (Figure 3.4a). Deuteration occurred at the position of the arene ring corresponding to the nucleophilic *sp*-hybridized carbon of the α,3-dehydrotoluene intermediate **3010** in the putative PDDA pathway. The dichloroalkene moiety can be interpreted to form from attack of a trichloromethyl anion on the electrophilic α-position of **3010** to give intermediate **3012**, followed by elimination induced by DBU to yield the product **3011**. A cyano substrate was found to yield an analogous dichloroalkene product when exposed to the same conditions (not shown).

An additional experiment showed that dissolving nitrile-diyne **3013** in piperidine did not yield an analogous α-amino picoline product. Rather, the vinylamine **3014** was formed in 42% yield. Such a product would be expected from the amination of allene

Figure 3.4 | Experimental results that support a proposed PDDA pathway.

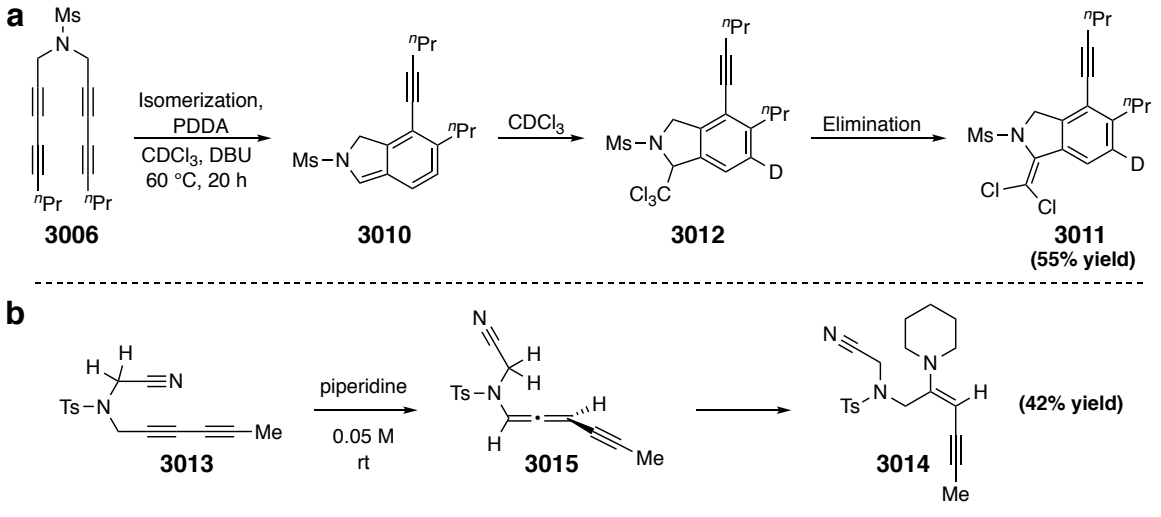

3015 with piperidine, and it could be argued that such a reaction would predominate in cases where the rate of allene-yne cyclization (in this case, of **3015**) is slow.

3.3.2 DFT Support for the PDDA Reaction

While these results were consistent with product formation from a PDDA reaction, they only constituted limited support this proposed pathway. Accordingly, I carried out DFT calculations to investigate the intermediates of this transformation. While these *in silico* results would not provide definitive proof that a PDDA reaction was occurring, they could lend further support to this proposed pathway if the reaction energetics were consistent with what was observed experimentally. The novelty of the transformations that were being observed experimentally—and the novelty of the pathway though which they were proposed to occur—made computational investigations a worthwhile endeavor.

A summary of results from the DFT calculations (run at the UB3LYP-D3BJ/6-311+G(d,p) level of theory) is shown in Figure 3.5. Four substrates **3016a**–**d**, variants of which had been investigated experimentally, were investigated. The relative free energies of all intermediates and TS structures in the proposed stepwise PDDA pathway were calculated.

The most important results of these computational investigations are the free energies of activation ($\Delta G^{\ddagger}$) for the conversion of allenyne intermediates **3017a–d** to their corresponding diradical intermediates **3019a–d**. The $\Delta G^{\ddagger}$ values for allenynes **3017a** and **3017d**, respectively, are 17.8 and 18.0 kcal•mol^{-1}—corresponding to respective half-lives of 1.26 and 1.77 seconds at 25 °C. These remarkably low $\Delta G^{\ddagger}$ values are consistent with the fact that both **3016a** and **3016d**—the diyne precursors to these allenyne species—are shown experimentally to give benzene and pyridine products, respectively, at room temperature.

In contrast, the respective $\Delta G^{\ddagger}$ values for **3017b** and **3017c** are 25.0 and 23.5 kcal•mol^{-1}—giving respective half-lives of 2.79 days and 5.32 hours at the same temperature. Indeed, diyne substrates **3016b** and **3016c** did not yield their anticipated aromatized products. Recall from Figure 3.4b that diyne substrate **3013** yielded the vinyl amine product **3014** when dissolved in piperidine—indicating that the presumed allenyne

formed from **3015** reacted with piperidine. This observation, when considered along with the computational results, indicates that the cyclization rate of **3015** is sufficiently slow to be outcompeted by amine trapping to give vinyl allene **3014**—and further supports the proposal of a PDDA reaction.

Figure 3.5 | Relative free energies of intermediates in the proposed PDDA reactions of substrates **3016a-d**. The relative free energy values for all intermediates and TS structures resulting from a given substrate are referenced to their corresponding allenyne (**3017a–d**). Figure reproduced from ref 72.

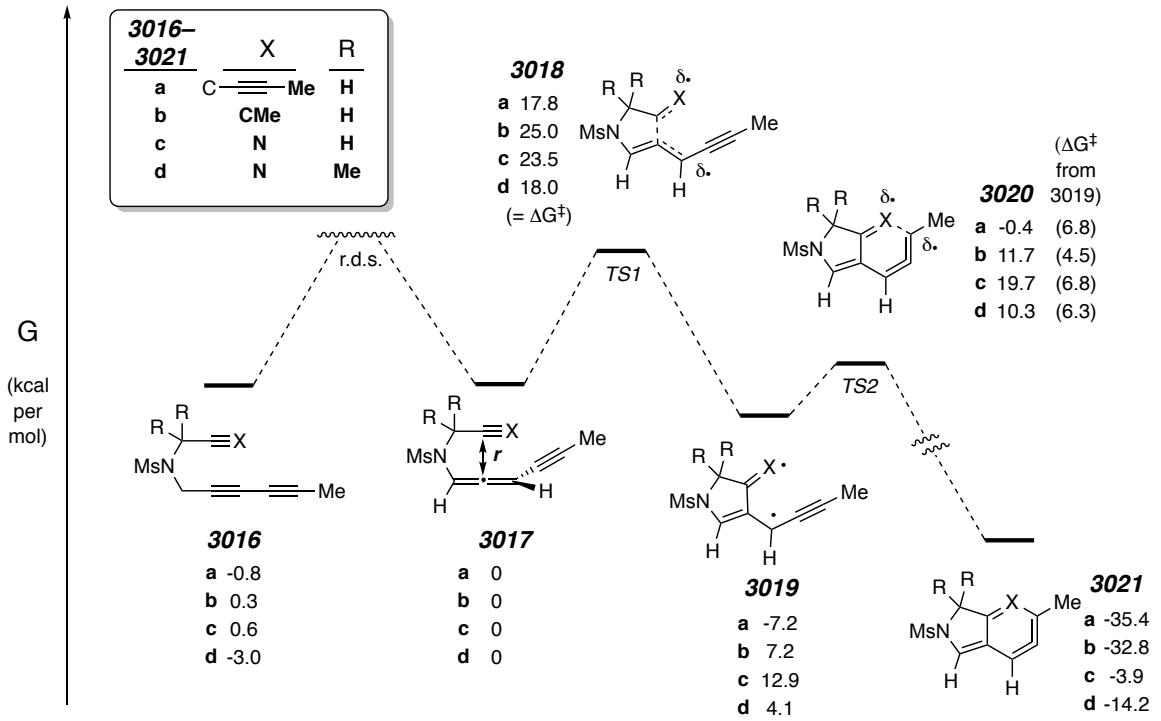

3.3.3 Additional *in silico* Observations

There are a number of additional observations from the DFT calculations that do not necessarily give additional evidence for a PDDA pathway, but are still interesting in their own right. They lend insight into both the hypothetical PDDA reaction as well as cycloaromatization reactions that will be discussed in the following chapters of this thesis. Some takeaways from these *in silico* results are as follows:

(i) The free energy change in the PDDA transformation (i.e. ΔG° from **3017a–b** to **3021a–b**) is quite large (around –35 kcal•mol^{-1}). This is similar to the typical ΔG° values observed for HDDA transformations of triyne substrates to benzynes, which

usually fall between –35 and –50 kcal•mol^{-1} (depending on the substrate). In contrast, the cyclization of allenynes containing a nitrile group (**3017c** and **3017d**) were significantly less exergonic. This emphasizes the thermodynamic instability of alkynes (discussed in section 1.2.1) when compared to nitriles, and will be an important point of discussion in Chapters 4 and 5.

(ii) Related to the thermodynamic instability of alkynes are the relative free energies ($\Delta G°$) of diynes **3016a–d** compared to allenynes **3017a–d**. The calculations show that these species are similar in energy—meaning that the high potential energy inherent in diyne substrates is also present in their tautomeric allenynes and acts as a thermodynamic driving force for the PDDA reaction.

(iii) When comparing nitrile allenyne substrates **3017c** and **3017d**, it can be seen that the cyclization of **3017d** to **3021d** is significantly more exergonic (by over 10 kcal•mol^{-1}) than the analogous conversion of **3017c** to **3021c**. Additionally, the free energy of activation ($\Delta G^{‡}$) of this process is significantly lower for **3017d** (by 5.5 kcal•mol^{-1}). While these substrates only differ by a *gem*-dimethyl moiety, which is present in **3017d** but absent in **3017c**, the DFT results clearly show the power of the Thorpe–Ingold effect.[79] This phenomenon, and its importance to the success of certain cycloaromatization reactions, will also be demonstrated in Chapters 4 and 5.

(iv) Last are the mechanistic implications of these DFT calculations. The computational results indicate that the PDDA reaction occurs through a stepwise process. The PDDA process appears to initiate with a rate-limiting C–C formation to give an unstable diradical intermediate (**3019a–d**), which rapidly undergoes a ring closing reaction through a low energy TS structure (**3020a–d**) to give the α,3-dehydrotoluene intermediates (**3021a–d**).

Interestingly, attempts to locate *concerted* TS structures for the direct conversion of allenynes **3017a–d** to α,3-dehydrotoluenes **3021a–d** consistently met with failure. More specifically, several TS structure searches starting from various guess geometries that imitated the hypothetical concerted TS structures consistently ultimately converged

[79] Jung, M. E.; Piizzi, G., gem-Disubstituent Effect: Theoretical Basis and Synthetic Applications. *Chem. Rev.* **2005,** *105*, 1735-1766.

to the stepwise TS structures (i.e. **3018a–d**). While I will stop short of drawing definitive conclusions about the mechanism of the PDDA reaction based on these preliminary calculations, I will say these calculations suggest that a concerted PDDA TS structure either does not exist or is prohibitively high in energy. This is in contrast to the HDDA reaction, where an energetically feasible concerted mechanism does exist but is outcompeted by the stepwise pathway, which proceeds through a lower energy rate-determining step.

It is also worth briefly mentioning that the computed TS structures **3018a–d** reaction had no open shell character. In other words, there were no unpaired electrons and no diradical character in these TS structures—in spite of the fact that these TS structures lead to (open shell) diradical intermediates **3017a–d** (this was confirmed by IRC calculations). This is also a contrast to the HDDA reaction, for which the TS structures connecting substrates to their corresponding diradical intermediates have open shell character.

3.4 Additional Studies into the Synthetic Applications of the PDDA Reaction

3.4.1 An Attempted Bimolecular HDDA–PDDA Cascade

While the HDDA reaction has proven to be a tremendously fruitful source of research for our lab, one ambitious but difficult goal that to this day has not been reached is the development of a bimolecular HDDA reaction—that is, a reaction in which a 1,3-diyne species and a separate species (i.e. a compound that is not covalently attached to the 1,3-diyne) containing a diyneophilic alkyne moiety react with each other in a bimolecular fashion to form benzyne. The high $\Delta G^{\ddagger}$ of such a process, which is roughly calculated to be 50–60 $kcal \cdot mol^{-1}$ (depending on the substrate) and the potential for undesired side reactions make the development of such a process quite difficult.

Recall from sections 5.2 and 5.3 that the PDDA reactions of certain substrates were observed to proceed at room temperature. DFT calculations further showed remarkably small $\Delta G^{\ddagger}$ values for these substrates corresponding to half-lives of just a few seconds. Accordingly, it occurred to me that a bimolecular PDDA reaction would be far more plausible than a bimolecular HDDA reaction. Such bimolecular PDDA reactions in

which stable, pre-synthesized allenyne substrates were to react with alkyne substrates could potentially expand the general synthetic utility of the PDDA reaction.

I carried out DFT calculations to probe the energetics of such a process, first by modeling a PDDA reaction between hexa-1,2-dien-4-yne (**3022**) and dimethyl acetylenedicarboxylate (DMAD) to intermediate **3023** (Figure 3.6a). As anticipated, the $\Delta G^{\ddagger}$ value for this process (32.2 kcal•mol^{-1}) was computed to be significantly lower than the typical value for an intermolecular HDDA reaction—which, recall, falls around 50–60 kcal•mol^{-1}. Although this result was encouraging, 32.2 kcal•mol^{-1} is still a fairly high value.[80] Although this reaction could occur without resorting to unreasonably high temperatures, it seems likely that it could still be outcompeted by other reactions (e.g. a dimerization between two molecules of **3022** or a [2 + 2] reaction between the allene of **3022** and DMAD)

Figure 3.6 | Bimolecular PDDA reactions between an allenyne **3022** and DMAD (a) and between **3022** and benzyne (b). The free energy of activation ($\Delta G^{\ddagger}$) for each reaction is shown below the respective TS structures.

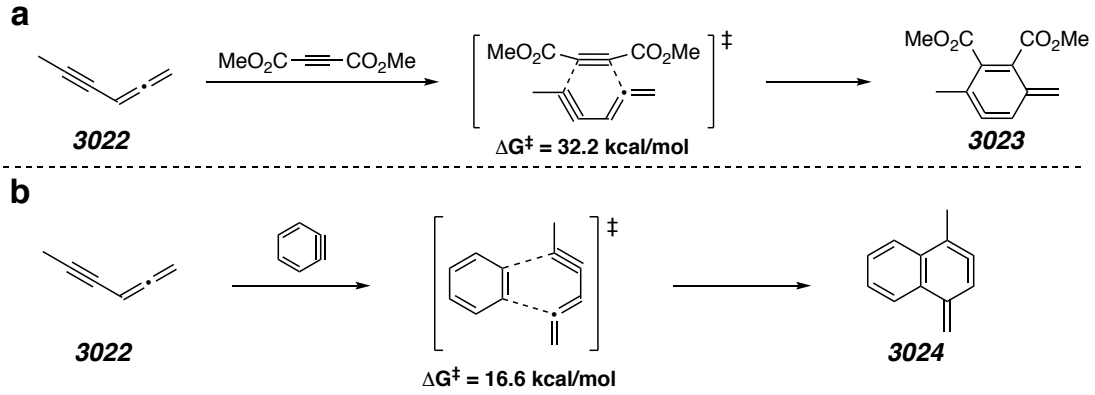

It further occurred to me that a reaction between an allenyne and the strained triple bond of benzyne would (formally) constitute an intermolecular PDDA reaction. The strain inherent to this formal triple bond, as well as its electron-deficient nature bond should make for a more facile PDDA reaction. Indeed, $\Delta G^{\ddagger}$ for the concerted PDDA reaction between **3022** and benzyne to form **3024** was computed to be a miniscule 16.6

[80] Admittedly, the formation of **3023** could occur through a competitive stepwise process. I did not attempt to locate the TS structures and intermediates for such a process.

kcal•mol^{-1} (Figure 3.6b). Bolstered by these results, I was determined to effect this type of transformation by way of an HDDA–PDDA cascade, which is generically illustrated in Figure 3.7.

Figure 3.7 | Generic representation of a proposed HDDA–PDDA cascade.

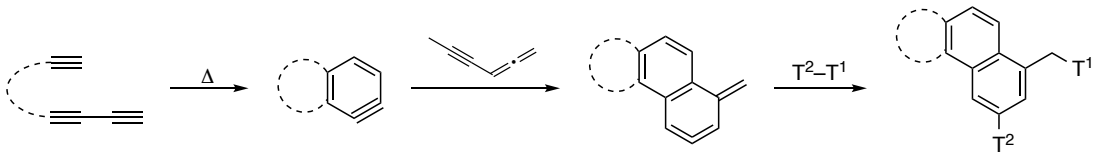

I proposed to first attempt this transformation by dissolving an HDDA substrate with an allenyne in 1,4-cyclohexadiene and heating the resulting solution. In this reaction, a benzyne, which would first be generated in the rate-determining HDDA reaction, would then ideally react in a selective manner with the allenyne to further generate a α,3-dehydrotoluene intermediate. This intermediate would then hopefully be trapped by the 1,4-cyclohexadiene, which is a known α,3-dehydrotoluene trap. The attempted reaction is shown in Scheme 3.2. Triyne HDDA substrate **3025** was chosen due to its availability (from previous research of the HDDA reaction, Chapter 2) while 2-methyldodeca-2,3-dien-5-yne (**3026**), which was synthesized in two steps, was chosen for its low volatility and lack of additional functional groups that might interfere with the desired reaction.

Scheme 3.2 | Attempted HDDA–PDDA cascade reaction.

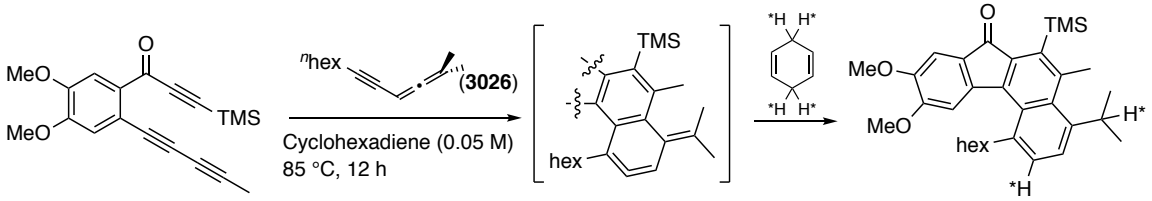

3025 ***3027*** ***3028*** ***(Not observed)***

Unfortunately, the formation of the naphthalene product **3028** was not observed, nor was any evidence for the formation of α,3-dehydrotoluene **3027** obtained. Rather, a complex mixture of products was seen, none of which could be identified after purification by MPLC. While the 1,4-cyclohexadiene could undergo an undesired side

reaction with the HDDA-generated benzyne,[81] significant amounts of the expected products from this reaction were not observed in the crude material. It is possible that, although the TS structure connecting the HDDA-benzyne to α,3-dehydrotoluene intermediate **3027** was computed to be low in energy, the allenyne **3026** may simply undergo side reactions with benzyne that have a lower energy barriers.[82]

3.4.2 Attempts to Synthesize Functionalized Pyridazines

Arguably the most valuable synthetic aspect of the PDDA reaction is the ability to access functionalized pyridine products. The thermodynamic stability of nitriles, when compared to alkynes, makes their incorporation into cycloaromatization reactions quite rare—yet recall that DFT calculations indicated the cyclization of the cyano substrate **3017d** to the α,3-dehydroazatoluene **3021d** (Figure 3.5) occurs with a half-life of consumption corresponding to less than 2 seconds at 25 °C!

Given the experimentally and computationally demonstrated ability of nitriles to participate in the PDDA reaction under remarkably mild thermal conditions, one might be so bold as to consider incorporating *two* nitriles into this reaction. Such a process, which is illustrated in Figure 3.8a, would involve the generation of a α,3-dehydrodiazatoluene intermediate **3030** from a tethered cyanoallene nitrile **3029** followed by trapping of the intermediate to give a functionalized pyridazine **3031**. Not only would the direct incorporation of two nitriles into one cycloaromatized product be unprecedented, but it would additionally constitute a novel synthetic method for pyridazine rings—a privileged structure in medicinal chemistry.[83]

Simple DFT calculations were run to quickly assess the viability of this process. A TS structure was located that connected cyanoallene **3032** to its corresponding diradical in a stepwise PDDA reaction (this TS structure is analogous to structures **3018a–d** in Figure 3.5). Remarkably, this TS structure was found to a mere 18.9

---

[81] Cyclic olefins are known to undergo Alder-Ene reactions with arynes: Chen, Z.; Liang, J.; Yin, J.; Yu, G.-A.; Liu, S. H., Alder-ene reaction of aryne with olefins. *Tetrahedron Lett.* **2013,** *54*, 5785-5787. This type of reaction was also observed when triyne **3025** was heated by itself in 1,4-cyclohexadiene.

[82] Heating HDDA substrates in the presence of an added 1,3-diyne trap also does not result in an analogous HDDA–HDDA cascade, as the 1,3-diyne moiety more readily forms an alkynyl benzocyclobutadiene product in lieu of a naphthalyne product (ref 29). The 1,3-diyne trap must be tethered to the benzyne precursor in order for this HDDA–HDDA cascade to occur (ref 38).

[83] Wermuth, C. G., Are pyridazines privileged structures? *Med. Chem. Commun.* **2011,** *2*, 935-941.

kcal•mol^{-1} higher in free energy than **3032** (Figure 3.8b), corresponding to a half-life of 8.1 seconds at 25 °C. This calculated $\Delta G^{\ddagger}$ is only 0.9 kcal•mol^{-1} higher than that for the PDDA cyclization of experimentally-verified substrate **3017d**. The synthesis of functionalized pyridazines through the PDDA reaction not only seemed plausible, but

Figure 3.8 | (a) Proposed synthesis of functionalized pyridazines through the PDDA reaction. (b) DFT-calculated free energy of activation for a PDDA cyclization of cyanoallene nitrile **3032** to α,3-dehydrodiazatoluene **3033**. (c) DFT-calculated free energy of activation for an HDDA cyclization of cyanoalkyne nitrile **3034** to pyridazyne **3035**.

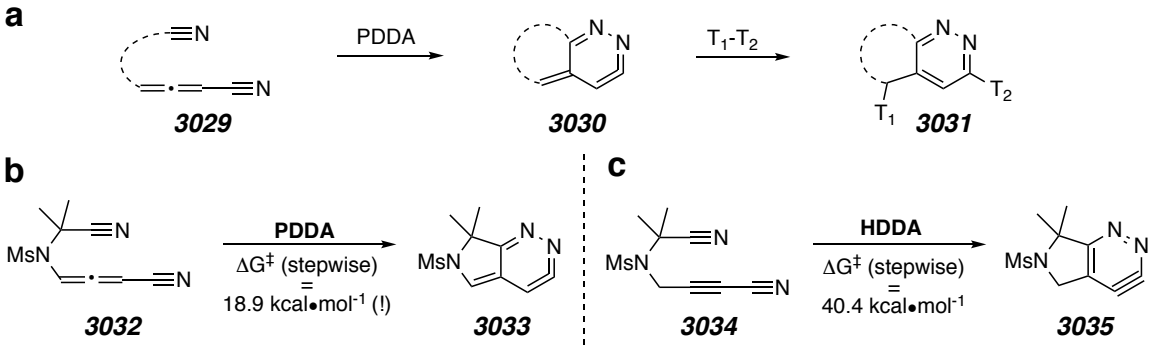

well within reach. As an aside, it is worth noting the stark difference in energetics for the analgous HDDA transformation of dinitrile **3034** to the pyridazyne **3035 (**Figure 3.8c). The $\Delta G^{\ddagger}$ value for the rate-determining step of the process was calculated to be a prohibitively high 40.4 kcal•mol^{-1}—corresponding to half-life of 1.35 hour at 250 °C.

In order to attempt this transformation experimentally, cyanoalkyne **3034** was synthesized[84] and then dissolved in piperidine (Scheme 3.3a). Remarkably, this resulted in consumption of the substrate over the course of 50 minutes at room temperature. Two distinct products were observed by TLC and ^{1}H NMR spectroscopy, neither of which corresponded to the desired pyridazine **3036**. While neither of these products could be identified, the crude NMR spectrum seemed to indicate that they resulted from the addition of piperidine to the cyanoalkene generated *in situ* (i.e. **3032**). The same cyanoalkyne substrate was again dissolved in piperidine, this time in the presence of

[84] The installation of the cyanoalkyne moiety proved to be somewhat troublesome but will be not be discussed here. The synthesis of cyanoalkyne substrates will be covered in more detail in Chapter 5.

DBU (Scheme 3.3b). These conditions resulted in significantly faster consumption of **3034**, as well as the formation of products distinct from those formed in the previous reaction. Unfortunately, pyridazine **3036** was, again, not seen to under from these conditions.

Scheme 3.3 | Initial attempts to synthesize pyridazine products through the PDDA reaction.

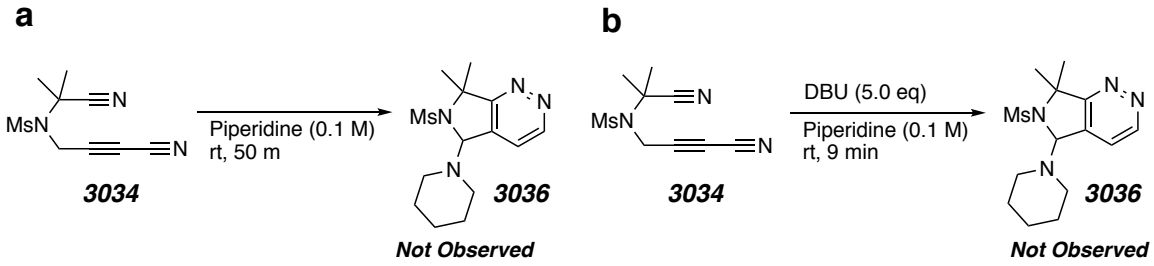

Not deterred by these initial failures, I designed and synthesized an additional substrate **3037**. It was anticipated that a PDDA reaction would yield either the *O*-silylhemiaminal **3038** directly from trapping of the α,3-dehydrodiazatoluene or the ketone **3039** from the *in situ* desilylation/elimination of **3038**. Dissolving **3037** in piperidine resulted in its remarkably fast consumption, which is not surprising considering the highly acidic methine C–H. While this reaction encouragingly yielded a predominant product, the crude ^{1}H NMR spectrum shown that it was neither **3038** nor **3039**.

Scheme 3.4 | An additional attempt to access pyridazine products using the PDDA reaction results in an unexpected cycloaromatization reaction to give naphthalene **3040**.

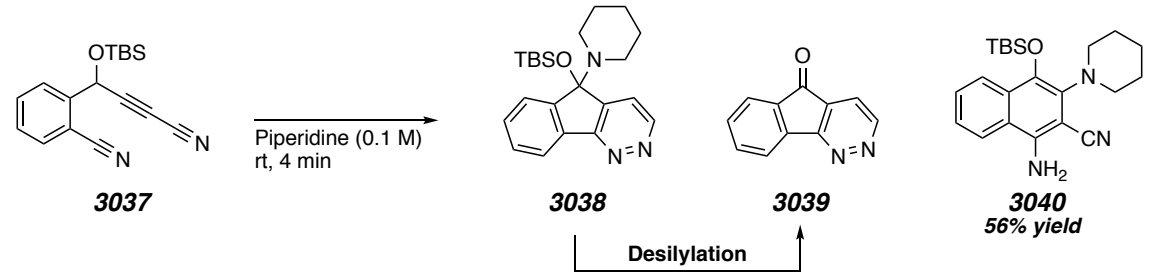

Rather, the product was ultimately identified as the tetrasubstituted naphthalene **3040**—the result of an unexpected cycloaromatization that is distinct from the PDDA reaction. The formation of this product could initiate either with conjugate addition of the

piperidine to the cyanoalkyne or from addition of the piperidine to the allene that is formed *in situ*. Considering the fast rate of the reaction, the latter proposal seems more likely. This initial event would be followed by an anionic ring closure and tautomerization to give **3040**. Although an interesting cycloaromatization in its own right, this transformation was not without precedence; Reux et al. demonstrated a bimolecular variation of this transformation (Scheme 3.5).[85]

Scheme 3.5 | Cycloaromatization reaction reported by Reux et al.

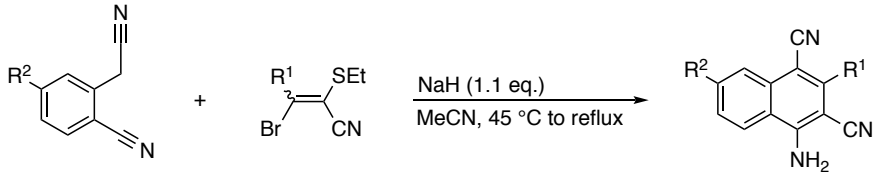

Considering how promising these reactions appeared based on DFT calculations, these experimental failures were particularly disappointing. Furthermore, it was not clear *why* the desired PDDA reaction, which should occur quickly, was not at all successful. In search of an explanation, I opted to go back and more thoroughly investigate the energetics of this pyridazyne-forming PDDA reaction *in silico*. The results from these DFT calculations are shown in Figure 3.9.

To further model the stepwise PDDA reaction of cyanoallene **3032**, the free energies (G) of diyne **3034**, diradical **3042**, and α,3-dehydrodiazatoluene **3033** relative to **3032** were calculated (Figure 3.9)—as was done when modeling the PDDA reactions of substrates **3017a–d** (Figure 3.5). The relative free energies of TS structures **3041** and **3043**, were also calculated.

For the most part, this potential energy surface is similar to that calculated for the PDDA cycloaromatization of allenynes **3017a–d** to α,3-dehydrotoluenes **3021a–d** (Figure 3.5); the free energy differences (ΔG) between the cyanoallene **3032**, cyanonitrile **3034**, and the diradical species **3024** are relatively small. However, a glaring and crucial point of divergence is the relative free energy of the α,3-dehydrodiazatoluene **3033**—it is incredibly high in energy relative to all the other ground state species in the pathway. In

[85] Reux, D.; Pochat, F., Single step synthesis of 2,4-dicyanonaphthylamines from synthetic equivalents of α-cyanoalkynes. *J. Chem. Soc., Chem. Commun.* **1991**, 1419-1420.

contrast to the cyclization of the allenyne **3017d** to α,3-azadehydrotoluene **3021d** in Figure 3.5, which is modestly exergonic by -14.2 kcal•mol^{-1}—and in contrast to the PDDA cycloaromatization of allenyne-diyne **3017a**, which is exergonic by -35.4 kcal•mol^{-1} ,–**3033** is 33.1 kcal•mol^{-1} *higher* in free energy than its cyanoallene precursor **3017**!

Figure 3.9 | The relative free energies of relevant intermediates and TS structures in the PDDA cycloaromatization of cyanoallene **3032** to α,3-dehydrodiazatoluene **3033**, as determined by DFT calculations. An image of **3033** is shown to the right.

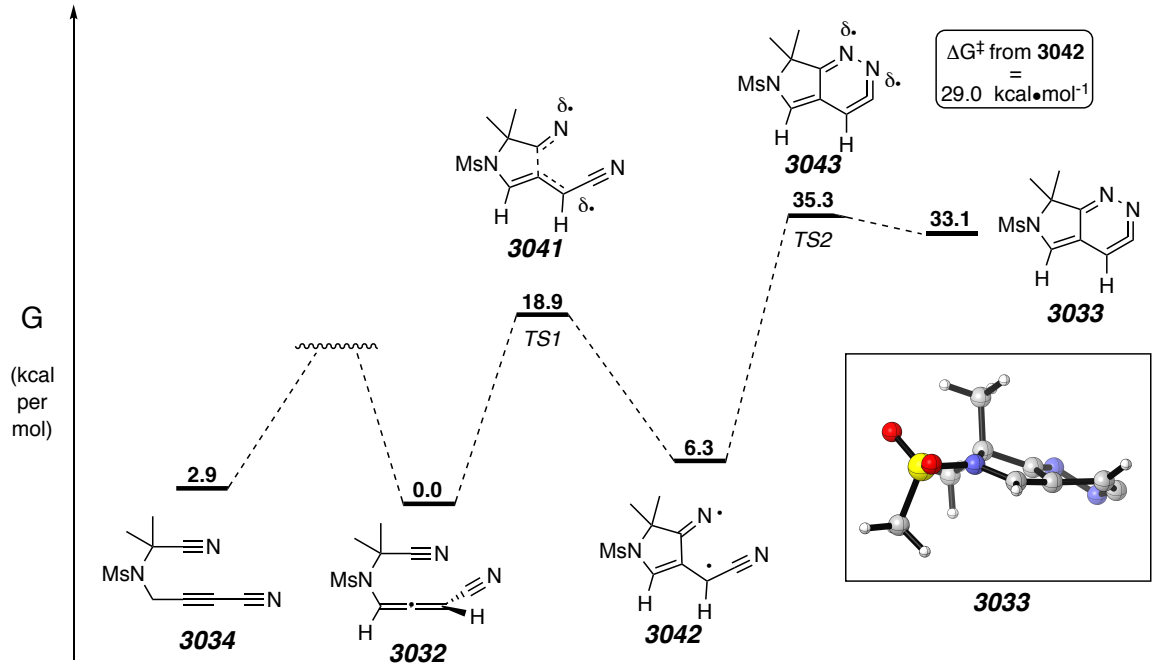

It is somewhat difficult to account for these differences in ΔG across substrates. Looking at the geometry of **3033** (shown in Figure 3.9), it is clear that the 6-membered diazacycle is not planar—indicating the aromaticity that generally acts to stabilize the products of cycloaromatization reactions may be significantly diminished in this case. However, it must be noted that the PDDA products **3021a–d,** despite being lower in energy than their allenyne precursors **3017a–d**, were also distorted to some degree from planarity.

While difficult to explain, the striking calculated endergonicity of this bis-nitrile PDDA reaction offers a sufficient explanation for the previous synthetic failures to access

functionalized pyridazine products. The formation of α,3-dehydrodiazatoluene **3033** is simply outcompeted by reactions with lower energy barriers (e.g. trapping of the cyanoallene with the nucleophilic piperidine trap.

Chapter 4. The Aza-HDDA Reaction

4.1. Preface: A Hypothetical Aza-HDDA Reaction

Since the seminal HDDA publication by Hoye et al. in 2012,[35] dozens of published works have appeared—from our lab and others—describing advances in HDDA chemistry (refer to Section 1.2.4). The vast majority of these publications focus on synthetic advances in benzyne chemistry that were made possible through the HDDA reaction. Specifically, they describe either novel benzyne-trapping reactions or novel variations of precedented benzyne-trapping reactions to access useful molecular scaffolds.

A fundamentally novel advance in HDDA chemistry would be to utilize the HDDA reaction in order to generate a reactive intermediate that is different from benzyne. Hypothetically, this could be achieved simply by replacing an alkyne in any HDDA substrate **4001** with a nitrile to give substrate **4002**. The HDDA cycloaromatization of such a substrate would yield a 1,2-didehydropyridine (or pyridyne) intermediate **4002*** in lieu of the HDDA-benzyne **4001*** that would be expected from **4001** (Figure 4.1).[86] The realization of this hypothetical cycloaromatization—an aza-HDDA reaction—would constitute a significant advance in HDDA chemistry. Presumably, the trapping reactions of HDDA-benzyne that have been developed to access myriad functionalized benzenoid products could also be applied to the aza-HDDA reaction to produce analogous functionalized pyridine products.

Figure 4.1 | The HDDA reaction (left) and a hypothetical aza-HDDA reaction (right).

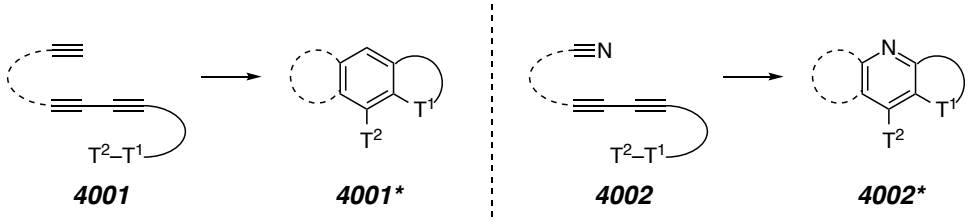

The ability to access functionalized pyridine products renders this hypothetical aza-HDDA reaction particularly attractive, as pyridines find applications in several areas

[86] The nitrile could also replace the end alkyne of the 1,3-diyne to make a substrate in which an alkyne is tethered to a cyanoalkyne moiety. The aza-HDDA reactions of such substrates will be the topic of the following chapter in this thesis (Chapter 5).

of chemical research such as coordination chemistry, materials chemistry, and organocatalysis. Far more important is their overwhelming presence in bioactive compounds as well as their tremendous value in medicinal chemistry. This value is partially demonstrated by their prevalence in pharmaceutical drugs including (but not limited to) imatinib, roflumilast, loratidine, lansoprazole, crizotinib, mirtazapine, esomeprazole, and pioglitazone (Figure 4.2).

Figure 4.2 | Examples of marketed pharmaceutical drugs that contain a pyridine ring.

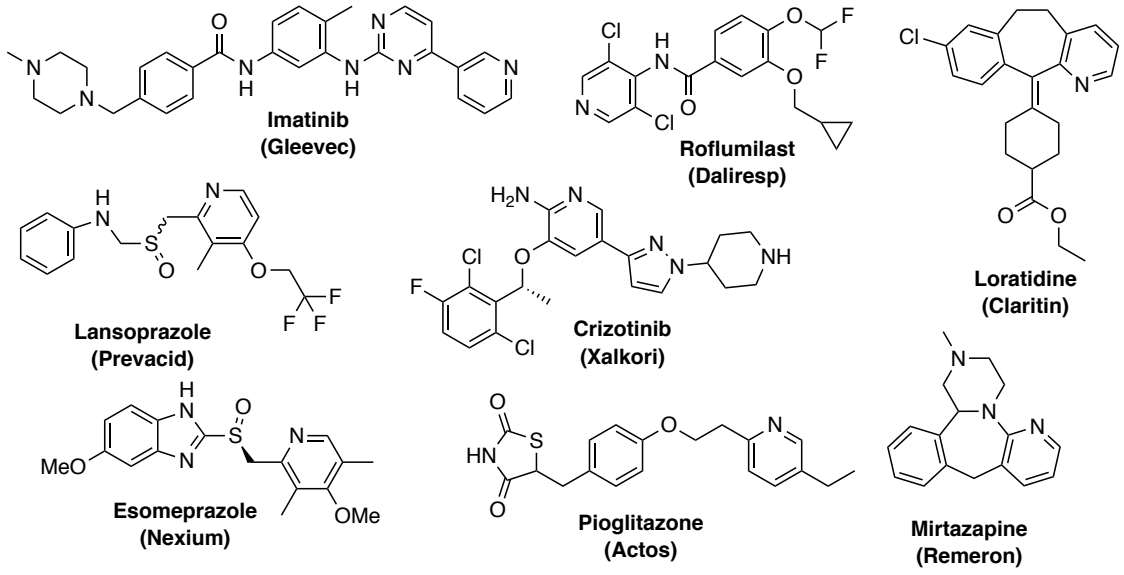

The value of pyridine moieties in pharmaceutical drugs is more objectively demonstrated in a perspective article on nitrogen heterocyclies by Njardarson et al.[87] Nitrogen heterocycles are among the most prevalent components of small molecule therapeutics—with 59% of U.S. FDA approved small molecule drugs containing at least one nitrogen heterocycle. Even among these nitrogen heterocycles, pyridine is particularly valuable. It is present in 62 FDA approved drugs—second only to piperidine (Figure 4.3).

[87] Vitaku, E.; Smith, D. T.; Njardarson, J. T., Analysis of the Structural Diversity, Substitution Patterns, and Frequency of Nitrogen Heterocycles among U.S. FDA Approved Pharmaceuticals. *J. Med. Chem.* **2014,** *57*, 10257-10274.

Figure 4.3 | Nitrogen heterocyles that appear in FDA approved small molecule drugs. The number of drugs in which the each heterocycle appears is listed in bold. Pyridine (top left, dashed box) is second only to piperidine. (Figure reproduced from Njardarson et al.[87])

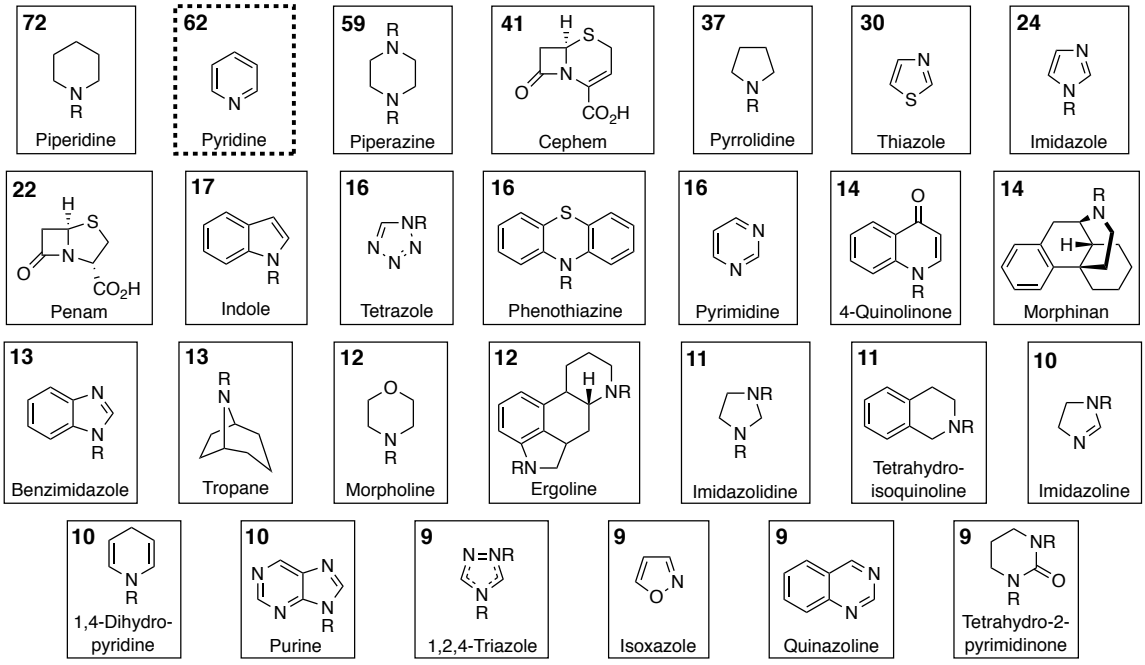

In spite of this value of the pyridine moiety, methods for the *de novo* synthesis of pyridine rings are somewhat limited. While there are several procedures through which pyridine rings can be functionalized,[88] the synthesis of pyridine rings themselves is more difficult—further adding to the synthetic value of a potential aza-HDDA reaction. Examples of methods for pyridine ring construction are shown in Figure 4.4. The majority of pyridine-forming reactions are condensation reactions (examples shown in Figure 4.4a), many of which require harsh thermal or basic conditions to proceed—significantly hindering their synthetic applicability.

The methods for accessing pyridine rings through cycloaddition reactions (both formal and literal) can often be run under milder conditions (examples shown in Figure

[88] (a) Murakami, K.; Yamada, S.; Kaneda, T.; Itami, K., C–H Functionalization of Azines. *Chem. Rev.* **2017,** *117*, 9302-9332. (b) Allais, C.; Grassot, J.-M.; Rodriguez, J.; Constantieux, T., Metal-Free Multicomponent Syntheses of Pyridines. *Chem. Rev.* **2014,** *114*, 10829-10868. (c) Bull, J. A.; Mousseau, J. J.; Pelletier, G.; Charette, A. B., Synthesis of Pyridine and Dihydropyridine Derivatives by Regio- and Stereoselective Addition to N-Activated Pyridines. *Chem. Rev.* **2012,** *112*, 2642-2713.

4.4b), although they are significantly rarer than condensation reactions. One notable example is the Boger pyridine synthesis (Figure 4.4b, left), which forms a pyridine ring through a [4 + 2] cycloaddition between a substituted enamine and a 1,2,4- triazine ring. Subsequent extrusion of N_2, followed by rearomatization through elimination of the exocylic amine yields a substituted pyridine product. Currently, the most common and most extensively researched method for *de novo* pyridine ring synthesis involves transition metal-mediated [2 + 2 + 2] cycloadditions between alkynes and nitriles (Figure 4.4, right).[89,90] While it can generally be run under generally mild conditions, this

Figure 4.4 | *De novo* synthesis of pyridine rings from (a) condensation reactions (b) and cycloaddition reactions (both literal and formal).

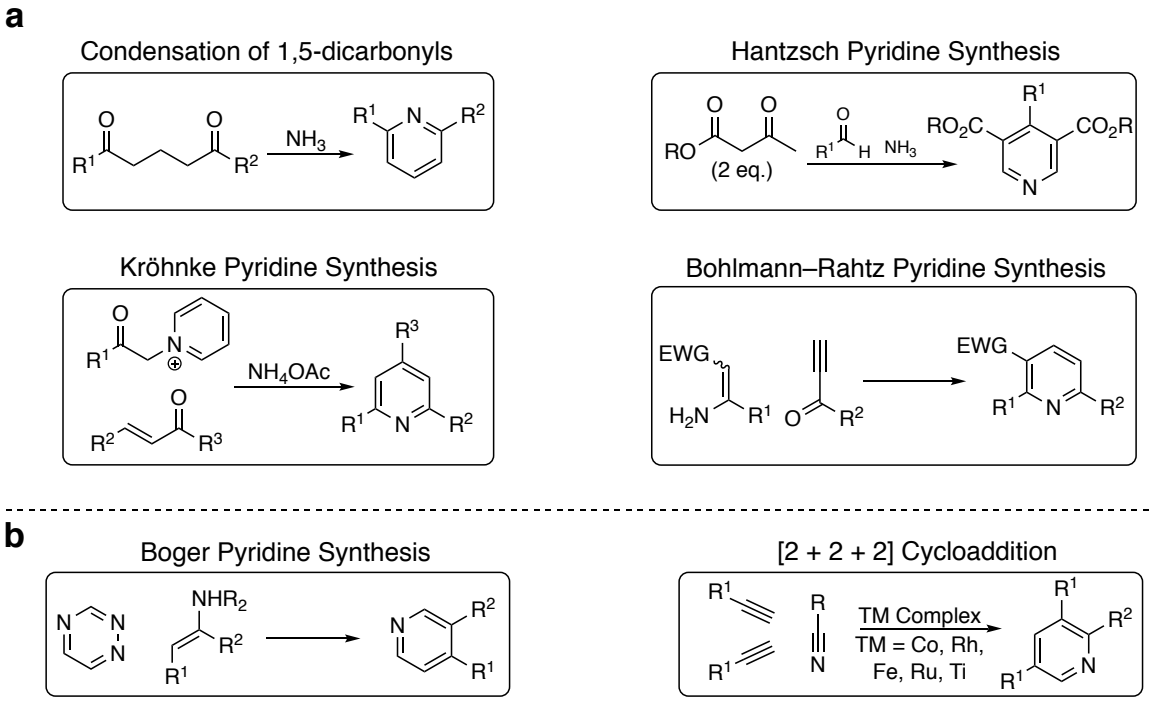

[89] For the original report of this reaction—sometimes referred to as the Bönnemann reaction—see: Bönnemann, H.; Brinkmann, R.; Schenkluhn, H., Eine einfache, kobalt-katalysierte Pyridin-Synthese. *Synthesis* **1974,** *1974*, 575-577.

[90] For relatively recent reviews on this chemistry, see: (a) Varela, J. A.; Saá, C., Construction of Pyridine Rings by Metal-Mediated [2 + 2 + 2] Cycloaddition. *Chem. Rev.* **2003,** *103*, 3787-3802. (b) Heller, B.; Hapke, M., The fascinating construction of pyridine ring systems by transition metal-catalysed [2 + 2 + 2] cycloaddition reactions. *Chem. Soc. Rev.* **2007,** *36*, 1085-1094. (c) Domínguez, G.; Pérez-Castells, J., Recent advances in [2+2+2] cycloaddition reactions. *Chem. Soc. Rev.* **2011,** *40*, 3430-3444. (d) Varela, J. A.; Saá, C., Recent Advances in the Synthesis of Pyridines by Transition-Metal-Catalyzed [2+2+2] Cycloaddition. *Synlett* **2008,** *2008*, 2571-2578.

methodology often suffers from poor selectivity (when the formation of several different pyridine isomers is possible).

One final but important point to consider when contemplating the potential value of an aza-HDDA reaction is the divergent nature of pyridine synthesis that is possible. While the aforementioned methods of pyridine synthesis converge several starting materials to give one specific pyridine product, any given aza-HDDA substrate would generate a single corresponding pyridyne intermediate that—by itself—is capable of directly forming an array of functionalized pyridine products. While the generation[91] and synthetic applications[92] of pyridyne have been studied, this hetaryne does not have nearly the amount of precedence that is seen for benzyne; it remains significantly underutilized as a synthetic tool. An aza-HDDA reaction would likely allow for new insight into pyridyne chemistry as well as unprecedented pyridyne reactions—much like the HDDA reaction allows for the development of novel benzyne chemistry.

4.2. Previous Attempts at the Aza-HDDA Reaction

Due to the tremendous potential value of the aza-HDDA reaction, and because it is a natural—almost obvious—extension of the triyne HDDA reaction, several researchers in our lab have attempted to bring this chemistry to fruition. While the realization of this reaction would bring high rewards, one can anticipate several potential difficulties. Most prominent among these issues is the thermodynamic stability of the

---

[91] (a) Levine, R.; Leake, W. W., Rearrangement in the Reaction of 3-Bromopyridine with Sodium Amide and Sodioacetophenone. *Science* **1955,** *121*, 780-780. (b) May, C.; Moody, C. J., A new precursor to 3,4-didehydropyridine, and its use in the synthesis of the antitumour alkaloid ellipticine. *Journal of the Chemical Society, Perkin Transactions 1* **1988**, 247-250. (c) Snieckus, V.; Tsukazaki, M., Synthetic Connections to the Directed ortho Metalation Reaction. 3,4-Pyridynes from 4-Trialkylsilyl-3-pyridyl Triflates. *Heterocycles* **1992,** *33*, 533-536. (d) Vinter-Pasquier, K.; Jamart-Grégoire, B.; Caubère, P., Complex Base-Induced Generation of 3,4-Didehydropyridine Derivatives: New Access to Aminopyridines or Pyridones. *Heterocycles* **1997,** *45*, 2113-2129. (e) Walters, M. A.; Shay, J. J., 2,3-Pyridyne Formation by Fluoride-Induced Desilylation-Elimination. *Synth. Commun.* **1997,** *27*, 3573-3579. (f) Lin, W.; Chen, L.; Knochel, P., Preparation of functionalized 3,4-pyridynes via 2-magnesiated diaryl sulfonates. *Tetrahedron* **2007,** *63*, 2787-2797.

[92] (a) Goetz, A. E.; Garg, N. K., Regioselective reactions of 3,4-pyridynes enabled by the aryne distortion model. *Nat. Chem.* **2012,** *5*, 54. (b) Enamorado, M. F.; Ondachi, P. W.; Comins, D. L., A Five-Step Synthesis of (S)-Macrostomine from (S)-Nicotine. *Org. Lett.* **2010,** *12*, 4513-4515. (c) Díaz, M.; Cobas, A.; Guitián, E.; Castedo, L., Synthesis of Ellipticine by Hetaryne Cycloadditions − Control of Regioselectivity. *European Journal of Organic Chemistry* **2001,** *2001*, 4543-4549. (d) Zoltewicz, J. A.; Nisi, C., Trapping of 3,4-pyridyne by thiomethoxide ion in ammonia. *J. Org. Chem.* **1969,** *34*, 765-766. (e) May, C.; Moody, C. J., A concise synthesis of the antitumour alkaloid ellipticine. *J. Chem. Soc., Chem. Commun.* **1984**, 926-927.

nitrile moiety vis-à-vis that seen in a typical alkyne.[93,94] In stark contrast to alkynes, the incorporation of nitriles into thermal pericyclic reactions is exceedingly rare.[72,95,96,97]

For this reason, it is perhaps not surprising that, while three distinct aza-HDDA substrates were synthesized by previous researchers in our lab, they all failed to yield their anticipated pyridine products (Figure 4.5). Entries 1 and 2 contain aza-HDDA substrates **4003** and **4005**, respectively, each of which contains a covalently attached silyl ether—a very effective trap of HDDA-generated benzyne.[98] Heating the former substrate to 150 °C resulted in "an ambiguous mixture of products," none of which was identified as pyridine **4004**. In contrast, **4005** neither decomposed nor did it yield the anticipated

---

[93] The thermodynamic instability of alkynes (as demonstrated by DFT calculations related to DDA reactions) was briefly discussed in section 1.2.1. The relative stability of alkynes compared to nitrile was shown as part of the *in silico* studies of the PDDA reaction in section 3.3.2.

[94] An additional demonstrative example of this can be seen in the (computed) $\Delta H°$ value for the addition of H_2 to ethyne (to ethene) vs. that for its addition to hydrogen cyanide (to methanimine). The former is -47.1 kcal•mol^{-1} while the latter is -11.7 kcal•mol^{-1}. Lan, Y.; Danheiser, R. L.; Houk, K. N., Why Nature Eschews the Concerted [2 + 2 + 2] Cycloaddition of a Nonconjugated Cyanodiyne. Computational Study of a Pyridine Synthesis Involving an Ene–Diels–Alder–Bimolecular Hydrogen-Transfer Mechanism. *J. Org. Chem.* **2012,** *77*, 1533-1538.

[95] While there do exist scattered examples of the participation of nitriles in the Diels–Alder reaction, they required either prohibitively high temperatures or the use of strongly activated nitriles such as tosyl cyanide. (a) Boger, D. L.; Weinreb, S. M. Hetero Diels–Alder Methodology in Organic Synthesis. Academic Press: San Diego, 1987. (b) van Leusen, A. M.; Jagt, J. C., Cycloaddition reactions of sulfonyl cyanides. *Tetrahedron Lett.* **1970,** *11*, 971-973. (c) Sasaki, M.; Hamzik, P. J.; Ikemoto, H.; Bartko, S. G.; Danheiser, R. L., Formal Bimolecular [2 + 2 + 2] Cycloaddition Strategy for the Synthesis of Pyridines: Intramolecular Propargylic Ene Reaction/Aza Diels–Alder Reaction Cascades. *Org. Lett.* **2018,** *20*, 6244-6249.

[96] Nitriles are known to undergo thermal 1,3-dipolar cycloadditions with azides to give tetrazoles. As is the case with nitrile Diels–Alder reactions, activated cyano groups such as tosyl and acyl nitriles are required for the reactions to proceed at reasonable temperatures. (a) Huisgen, R., 1,3-Dipolar Cycloadditions. Past and Future. *Angew. Chem. Int. Ed* **1963,** *2*, 565-598. (b) Demko, Z. P.; Sharpless, K. B., A Click Chemistry Approach to Tetrazoles by Huisgen 1,3-Dipolar Cycloaddition: Synthesis of 5-Sulfonyl Tetrazoles from Azides and Sulfonyl Cyanides. *Angew. Chem. Int. Ed.* **2002,** *41*, 2110-2113. (c) Demko, Z. P.; Sharpless, K. B., A Click Chemistry Approach to Tetrazoles by Huisgen 1,3-Dipolar Cycloaddition: Synthesis of 5-Acyltetrazoles from Azides and Acyl Cyanides. *Angew. Chem. Int. Ed.* **2002,** *41*, 2113-2116. (d) Himo, F.; Demko, Z. P.; Noodleman, L.; Sharpless, K. B., Mechanisms of Tetrazole Formation by Addition of Azide to Nitriles. *J. Am. Chem. Soc.* **2002,** *124*, 12210–12216.

[97] Rare examples of the participation of unactivated nitriles can been seen in the following two publications: Sakai, T.; Danheiser, R. L., Cyano Diels−Alder and Cyano Ene Reactions. Applications in a Formal [2 + 2 + 2] Cycloaddition Strategy for the Synthesis of Pyridines. *J. Am. Chem. Soc.* **2010,** *132*, 13203-13205. (b) You, X.; Xie, X.; Chen, H.; Li, Y.; Liu, Y., Cyano-Schmittel Cyclization through Base-Induced Propargyl-Allenyl Isomerization: Highly Modular Synthesis of Pyridine-Fused Aromatic Derivatives. *Chem. Eur. J.* **2015,** *21*, 18699-18705.

[98] Hoye, T. R.; Baire, B.; Wang, T., Tactics for probing aryne reactivity: mechanistic studies of silicon–oxygen bond cleavage during the trapping of (HDDA-generated) benzynes by silyl ethers. *Chem. Sci.* **2014,** *5*, 545-545.

pyridine **4006**; it remained inert even when heated to increasingly high temperatures. Entry 3 gives an example of the attempted generation and *intermolecular* trapping of an aza-HDDA pyridine intermediate to access pyridine **4007** from nitrile **4008**. Unfortunately, this attempt resulted in "extensive decomposition." Due to these failures, as well as the aforementioned rarity of nitrile participation in cycloaromatizations in the literature, research into the aza-HDDA reaction was abandoned for several years in our lab.

Figure 4.5 | Previous unsuccessful attempted aza-HDDA reactions.

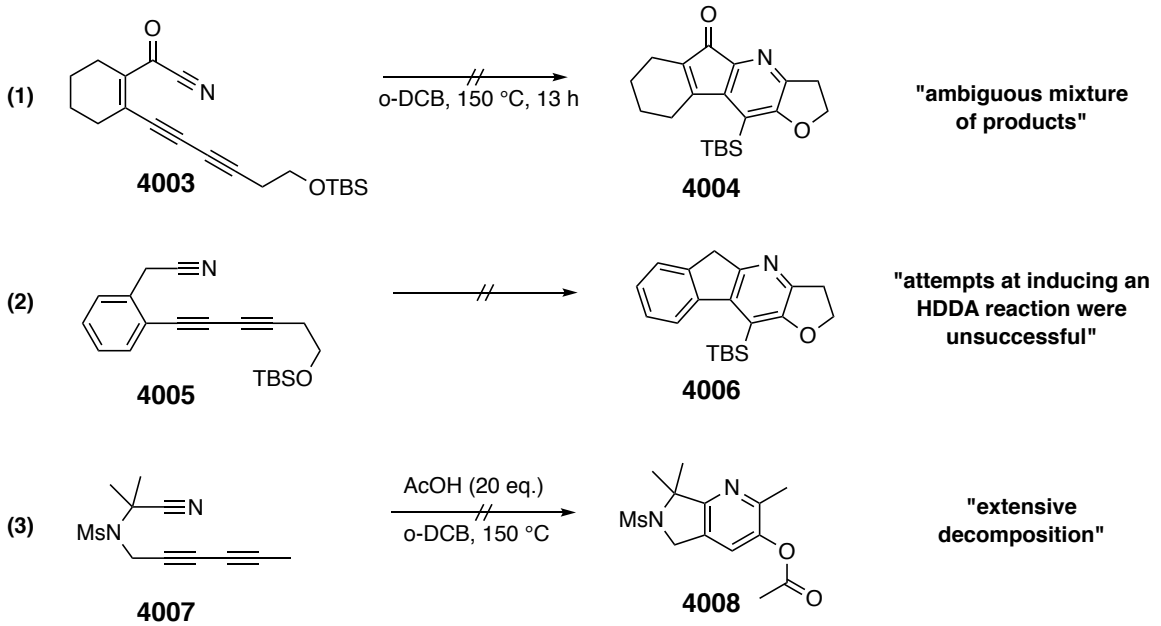

4.3 The First Successful Aza-HDDA Reaction

Among the previous unsuccessful aza-HDDA attempts (Figure 4.5), entry 3 example showed the most potential for improvement. While both nitrile substrates **4003** and **4005** failed to produce their anticipated pyridine products in the presence of a tethered silyl ether trap, **4007** was heated in the presence of 30 molar equivalents of acetic acid. I deduced that designing a substrate analogous to **4007** that contained a covalently attached silyl ether trap (e.g. **4009** in Figure 4.6) such as those found in **4003** and **4005**, could facilitate trapping of the pyridyne intermediate.

Fortunately, several grams of a terminal alkyne precursor to **4009** remained from my efforts to synthesize novel PDDA substrates (discussed in Section 3.4.2), and I was

able to synthesize several hundred milligrams of it. This candidate aza-HDDA substrate was dissolved in *o*-DCB to give a 0.05 M solution that (in a sealed culture tube) was subjected to increasingly high temperatures in a sand bath. Eventually, TLC analysis showed the formation of a new compound at 220 °C. The solution was heated at this temperature for 48 hours, during which time it turned black/heterogenous and most of the starting material **4009** was gradually consumed. Gratifyingly, purification by column chromatography gave the desired pyridine product **4010** in 19% yield in what constitutes the first recorded example of a successful aza-HDDA reaction (Figure 4.6). As small amount of the desilylated pyridine product **4011** was also observed.

Figure 4.6 | The first successful aza-HDDA reaction.

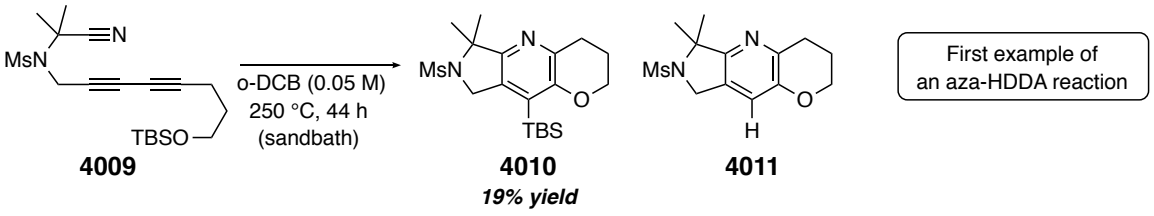

4009 **4010** ***19% yield*** **4011**

With this modest but encouraging result, the same substrate was again heated, this time at a concentration of 0.01 M in *o*-DCB and at a temperature of 225 °C. Additionally, the solution was heated in a microwave reactor rather than a sand bath. A microwave reactor was chosen due to its ability to reach the high temperatures (up to 250 °C) that would potentially be necessary to test aza-HDDA substrates. More importantly, while sand baths are prone to temperature fluctuations and hot spots, microwave reactors allow for precise temperature control and generally do not give rise to hot spots within the reaction (assuming that the reaction solution is homogeneous). This would not only give a potentially cleaner reaction, but would allow for much more accurate estimation of the thermal half-life for any aza-HDDA substrate.

As anticipated, the use of a microwave reactor yielded pyridines **4010** and **4011** in a still mediocre but significantly higher yield of 36% and 10%, respectively (Figure 4.7). While this initial test reaction yielded the desired pyridine product in a modest yield, it demonstrated that nitriles tethered to 1,3-diynes are, under certain circumstances, capable of undergoing a thermal HDDA cycloaromatization to access pyridyne reactive

intermediates—opening the door to the development of the potentially groundbreaking aza-HDDA reaction.

Figure 4.7 | The same aza-HDDA reaction run under milder thermal conditions.

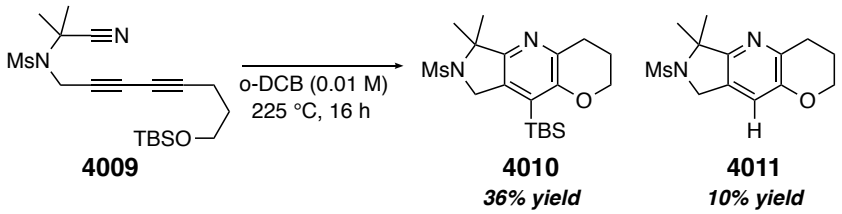

4009 **4010** ***36% yield*** **4011** ***10% yield***

4.4 Initial Computational Studies

4.4.1 Proposal for an *In Silico* Aza-HDDA "Assay"

Motivated by these encouraging initial results, I set about planning the syntheses of additional aza-HDDA substrates that would hopefully cyclize at lower temperatures and give functionalized pyridine products in higher yields. Naturally, one could design countless potential substrates to be used in the aza-HDDA reaction. Even when substituting an alkyne with a nitrile on precedented HDDA substrates, the number of aza-HDDA substrate candidates is more than can be synthesized within a viable period of time. This necessitated a rationale or method for determining which potential substrates were worth taking the effort to synthesize and test.

One fortunate aspect of probing the viability of individual aza-HDDA substrates is the mechanistic simplicity of the aza-HDDA reaction itself. Given the linearity of nitriles and alkynes, most potential substrates have relatively few degrees of freedom (and therefore a relatively small number of conformers)—making it significantly less burdensome to determine the Boltzmann-averaged energy of the array of conformers for any given substrate. More importantly, the aza-HDDA reaction is a unimolecular process that proceeds by applying heat, rather than through the use of exogenous reagents or catalysts. These combined features allow for the ability to gain insight into the energetics—and by extension, the synthetic utility—of potential aza-HDDA reactions through the use of DFT calculations in a relatively simple manner.

Regarding the mechanism of the HDDA cycloaromatization itself, it is well-established through both theoretical[99] and experimental[100] studies that the HDDA reaction occurs through a stepwise process. This process is drawn generically in Figure 4.8. A triyne substrate **4012** will cyclize to its corresponding benzyne **4012*** by way of a diradical intermediate $\mathbf{4012_{diradical}}$. In this process, the formation of the diradical from its triyne via transition state (TS) structure $\mathbf{4012^{‡}\_a}$ is the rate-determining step, while the

Figure 4.8 | The HDDA reaction occurs through a stepwise process (right) in preference to a concerted process (left).

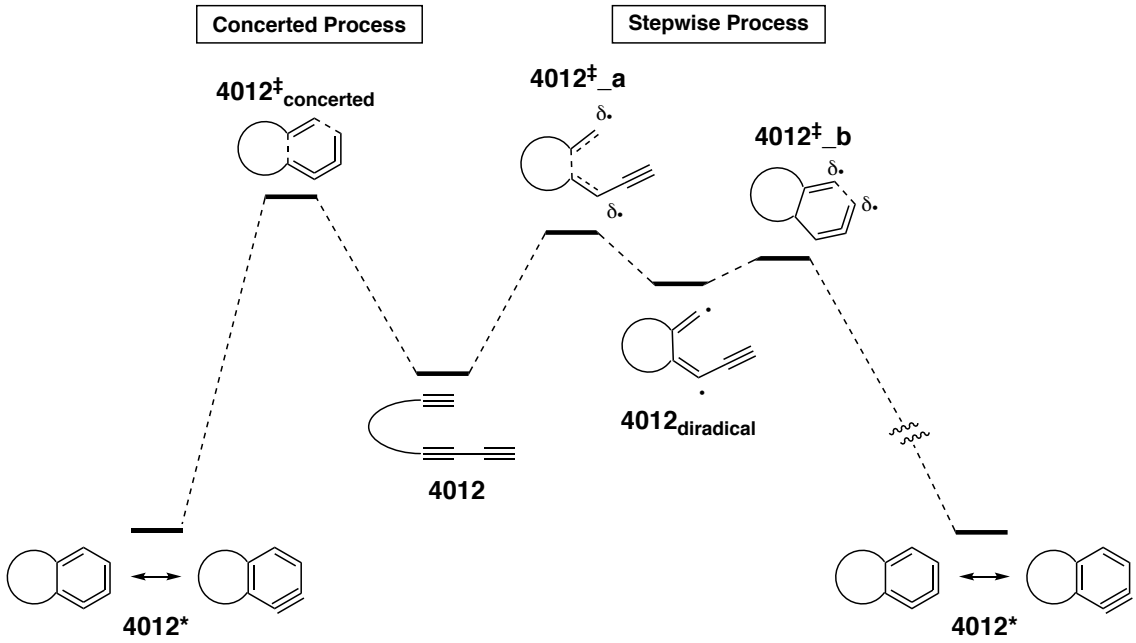

ring-closure of the diradical to the benzyne through TS structure $\mathbf{4012^{‡}\_b}$ is rapid (usually just a few 39.5 kcal•mol^{-1}). It should be noted that the HDDA reaction can also proceed through a concerted TS structure $\mathbf{4012^{‡}_{concerted}}$, although it is higher in energy

[99] (a) Marell, D. J.; Furan, L. R.; Woods, B. P.; Lei, X.; Bendelsmith, A. J.; Cramer, C. J.; Hoye, T. R.; Kuwata, K. T., Mechanism of the Intramolecular Hexadehydro-Diels–Alder Reaction. *J. Org. Chem.* **2015,** *80*, 11744-11754. (b) Liang, Y.; Hong, X.; Yu, P.; Houk, K. N., Why Alkynyl Substituents Dramatically Accelerate Hexadehydro-Diels–Alder (HDDA) Reactions: Stepwise Mechanisms of HDDA Cycloadditions. *Org. Lett.* **2014,** *16*, 5702-5705. (c) Yu, P.; Yang, Z.; Liang, Y.; Hong, X.; Li, Y.; Houk, K. N., Distortion-Controlled Reactivity and Molecular Dynamics of Dehydro-Diels–Alder Reactions. *J. Am. Chem. Soc.* **2016,** *138*, 8247-8252. (d) Chen, M.; He, C. Q.; Houk, K. N., Mechanism and Regioselectivity of an Unsymmetrical Hexadehydro-Diels–Alder (HDDA) Reaction. *J. Org. Chem.* **2019,** *84*, 1959-1963.

[100] Wang, T.; Niu, D.; Hoye, T. R., The Hexadehydro-Diels–Alder Cycloisomerization Reaction Proceeds by a Stepwise Mechanism. *J. Am. Chem. Soc.* **2016,** *138*, 7832-7835.

than **4012‡_a** for almost all HDDA substrates.The analogous stepwise pathway for the aza-HDDA cyclization of a generic nitrile-diyne **4013** to pyridyne **4013*** is shown in Figure 4.9. Assuming that the mechanism of any given aza-HDDA reaction resembles the stepwise mechanism of its triyne analog, finding the free energy of activation ($\Delta G^{\ddagger}$) for the rate-determining step of an aza-HDDA reaction would simply involve calculating the free energy difference (ΔG) between **4013** and the TS structure **4013‡_a**. The Eyring equation (top right box in Figure 4.9) can then be used to determine a rate constant for this process at any given temperature. Assuming first-order kinetics, this rate constant can be easily translated into a reaction half-life (i.e. the half-life of consumption for **4013** at any given temperature, (bottom right box in Figure 4.9). This information approximates the temperature to which any aza-HDDA substrate must be heated before cycloaromatization to the corresponding pyridyne intermediate can proceed at an appreciable rate. To summarize, one can obtain a DFT-derived estimate of the reactivity of any given aza-HDDA substrate by simply calculating the free energies of **4013** and **4013‡_a**. This is essentially a simple *in silico* assay that can save the time and effort of synthesizing a substrate whose aza-HDDA energetic barrier ($\Delta G^{\ddagger}$) is prohibitively high.

Figure 4.9 | Hypothetical stepwise pathway of the aza-HDDA reaction.

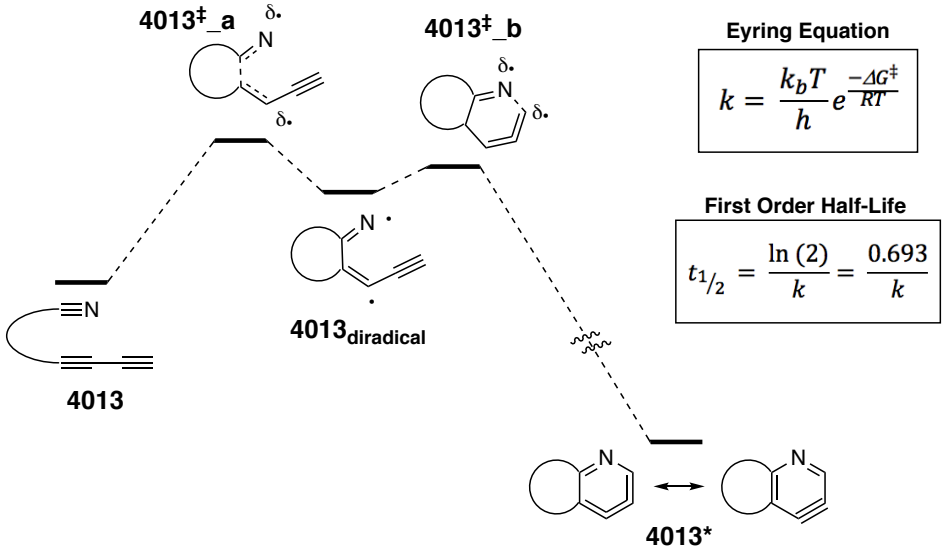

4.4.2 DFT Insight Regarding a Stepwise vs. a Concerted aza-HDDA Reaction

DFT studies were initiated by calculating $\Delta G^{\ddagger}$ for the experimentally validated substrate **4009** (Section 4.3). Recall that **4009** was observed by TLC monitoring to gradually reach near complete consumption over a period of about 16 hours. In order to facilitate the calculations, the siloxypropyl group of **4009** was changed to a simpler methyl group—giving test substrate **4014**. It was assumed that this truncation would not have a significant effect on the calculated $\Delta G^{\ddagger}$. Somewhat surprisingly, $\Delta G^{\ddagger}$ was calculated to be 37.8 kcal•mol^{-1} (Figure 4.10). For the procedure described in the previous paragraph, this translates to a half-life of 43 minutes at 225 °C—somewhat shorter than expected based on experimental results. Again, when the substrate **4009** was heated in *o*-DCB at 225 °C, it was consumed over a period of about 16 hours—roughly indicating a half-life of, say, 4–5 hours.

Figure 4.10 | Relative free energies of TS structures **4014$^{\ddagger}_{\text{concerted}}$** and **4014‡_a** for the concerted and stepwise aza-HDDA reactions of nitrile-diyne substrate **4014**.

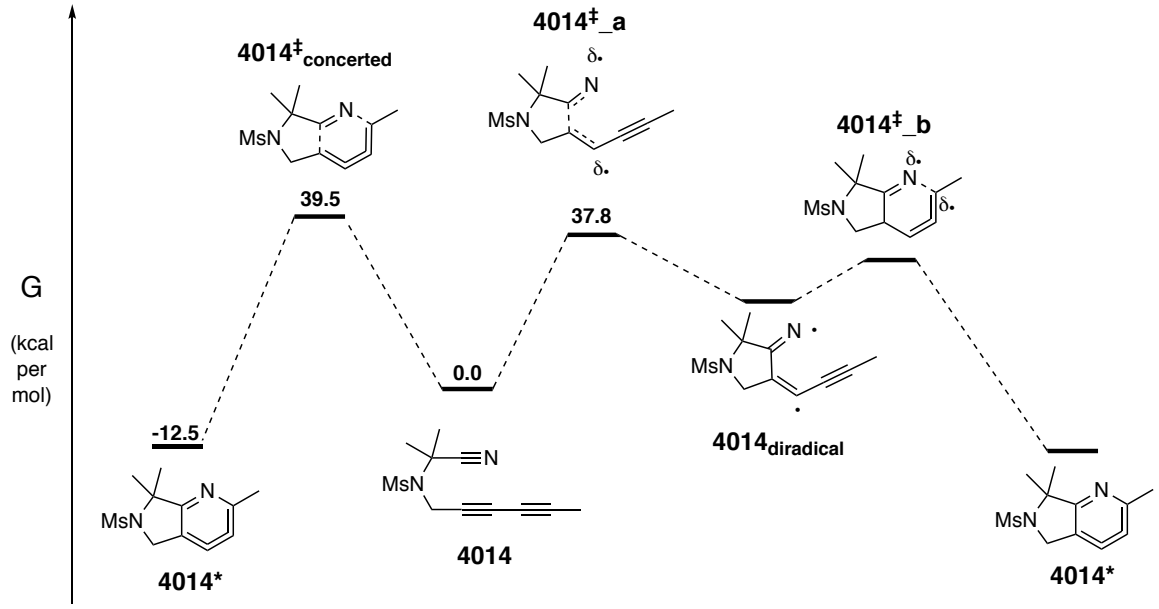

Somewhat surprised by this result, I attempted to find a *concerted* TS structure and compare the $\Delta G^{\ddagger}$ values for the stepwise and concerted aza-HDDA processes. Indeed, a concerted TS structure **4014$^{\ddagger}_{\text{concerted}}$** was located and $\Delta G^{\ddagger}$ was calculated to be 39.5 kcal•mol^{-1}—slightly higher than that calculated for the stepwise process. This $\Delta G^{\ddagger}$

gives a computationally-predicted half-life of 4.0 hours at 225 °C, which correlates with the experimental half-life much more closely.

This result was somewhat puzzling. Given the well-established preference of HDDA substrates to access benzyne via a stepwise, diradical pathway, it was anticipated that the aza-HDDA reaction would exhibit the same preference. Indeed, for substrate **4014**, the calculated $\Delta G^{\ddagger}$ for the first C-C bond forming step (i.e. the rate determining step) in the stepwise pathway was lower than that for the concerted aza-HDDA process. Yet, its experimental half-life correlates more closely to the calculated concerted $\Delta G^{\ddagger}$ value.

Initially, I considered that the applied basis set (6-31+G(d,p)) and the functional (M06–2X) might be ill-suited to calculate free energies of activation for this aza-HDDA rection. After all, the difference between the rate-determining free energies of activation for the concerted and stepwise pathways ($\Delta\Delta G^{\ddagger}$) was a relatively modest 1.7 kcal•mol^{-1}, which leaves room for error. Unfortunately, at this point **4014** was the only substrate for which computational and experimental data could be compared—making it difficult to draw definitive mechanistic conclusions.

An additional *in silico* observation—perhaps the most surprising observation—offered a potential explanation for the closer correlation of the experimental half-life to that of the calculated concerted aza-HDDA reaction. Recall that the established stepwise pathway of the HDDA reaction proceeds through a single (diradical) intermediate, which connects the triyne substrate to its corresponding benzyne intermediate. Further recall that while the first step of this pathway (to form the diradical) is rate-determining, the second (and final) step, which links the diradical to the benzyne, has a very low free energy of activation (typical just a few kcal•mol^{-1}). Although optimized geometries for nitrile-diyne **4014**, TS structure **4014‡_a**, diradical **4014$_{\text{diradical}}$**, and pyridyne **4014*** could be computed, the TS structure corresponding to this ring closure **4014X‡_b**, which is normally very easy to find, could not be located. In fact, attempts to bring the carbon and

nitrogen atoms of the forming C–N bond closer together resulted in the cleavage of the C–C bond that was formed in the first (diradical-forming) step.[101]

Ultimately, these computational observations suggest that, while **4014** is capable of forming the diradical **4014$_{\text{diradical}}$** under thermal conditions, this diradical is incapable of closing to form pyridyne **4014***—making it impossible for the pyridyne to form through the conventional stepwise mechanism. This offers an explanation for why the experimental half-life of **4014** correlates more closely to that computed for the concerted aza-HDDA reaction of **4014**. The inability to form a pyridyne from its diradical precursor was also observed in all other nitrile-diyne substrates that were subjected to analogous DFT studies (Section 4.3.3).

This apparent stark contrast to the mechanism of the triyne HDDA reaction is certainly interesting and could potentially offer a partial explanation for the observed reluctance of nitriles to participate in the HDDA reaction. While the TS structure **4014‡_a** to form the diradical **4014$_{\text{diradical}}$** is lower in energy than **4014$^{‡}_{\text{concerted}}$**, it ultimately cannot lead to the pyridyne product **4014***. This having been said, it should be noted that, while these observations are interesting, they have not been explored in depth—nor have they been supplemented with experiments. Accordingly, I will stop short of drawing any definitive mechanistic conclusions on the aza-HDDA reaction.

4.3.3 Carrying Out the *In Silico* Aza-HDDA Assay on Candidate Substrates

With the insight gained from the DFT calculations described in Section 4.3.2, I began to carry out DFT calculations to test potential aza-HDDA substrates. $\Delta G^{‡}$ for the concerted aza-HDDA reaction of each substrate was calculated, along with the change in free energy (ΔG_{rxn}) for each aza-HDDA reaction. The computational results for selected substrates are summarized in Figure 4.11. While these results will be discussed in more detail in the following sections, some general results are worth initially pointing out.

Perhaps most immediately noticeable is the change in free energy (ΔG_{rxn}) of these reactions. The ΔG_{rxn} value for each substrate is shown in parenthesis to the right of each

---

[101] This computational process involves starting from the geometry of the diradical **4014$_{\text{diradical}}$**, and optimizing the geometry of the structure as the distance between the carbon atom and nitrogen atom of the forming C–N bond is gradually decreased. It was observed that the C–C bond that was formed in the first step to access **4014$_{\text{diradical}}$** started to cleave as the new C–N bond was formed.

reaction. While the general exergonicity is notable—considering that a stable nitrile-diyne substrate converted to a highly unstable aryne intermediate—these ΔG_{rxn} values are quite small when compared to the HDDA reaction of triynes, which generally range from about -35 to -50 kcal•mol^{-1} depending on the substrate.

Figure 4.11 | Calculated energetics of selected aza-HDDA substrate candidates.

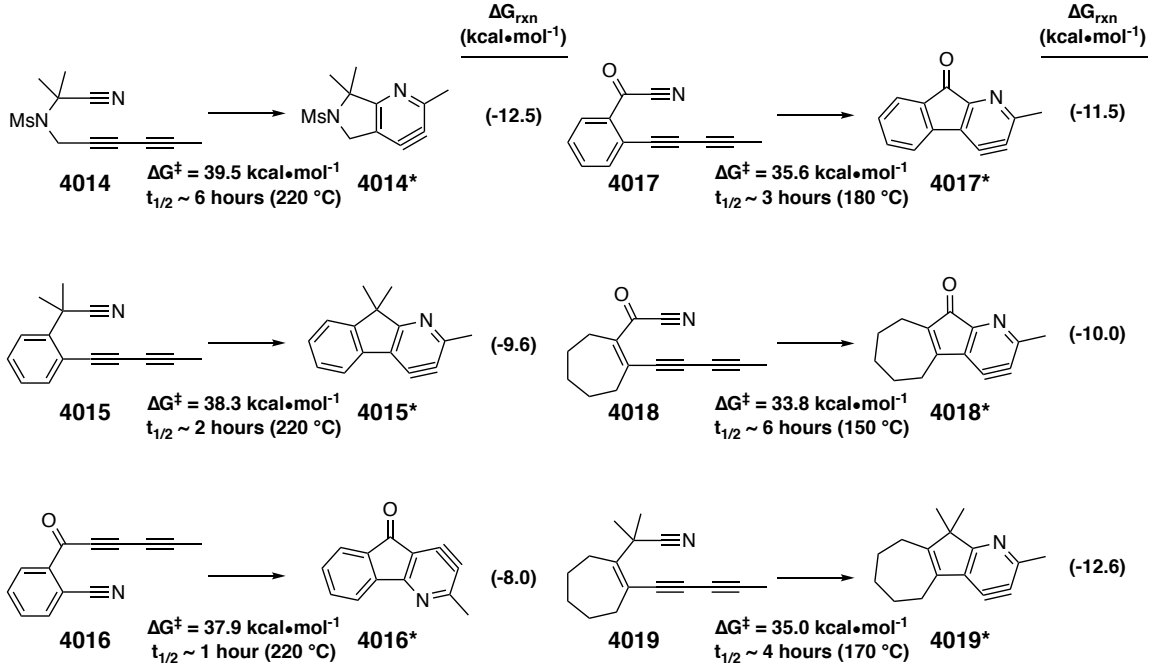

Most important are the calculated $\Delta G^{\ddagger}$ values for the aza-HDDA reaction of substrates **4015**–**4019**, which are shown below each reaction along with their corresponding half-lives. The $\Delta G^{\ddagger}$ values for these substrates are all lower than that for the experimentally-verified substrate **4014**—indicating that they are likely to be sufficiently competent aza-HDDA substrates. Particularly promising are substrates **4017**–**4019**, which are predicted to cyclize between 150 and 180 °C. All of these substrates **4015**–**4019** were ultimately tested experimentally for their potential ability to synthesized functionalized pyridines through the aza-HDDA reaction. The syntheses of these substrates and the results of these test reactions are presented in the following sections.

4.4 Synthesis and Testing of Additional Aza-HDDA Substrates

In order to experimentally probe the potential synthetic value of each candidate **4015**–**4019**, I chose to first synthesize and test analogs that contained a covalently

tethered TBS ether trap. This was the same approach that was used to test the first successful aza-HDDA substrate (Section 4.3). Substrates that yielded their corresponding silyl pyridine products in sufficiently high yields would be subjected to *intermolecular* pyridyne-trapping reactions so that the substrate scope could be further explored.

As a brief note, I will say that—although the focus of this chapter is specifically the aza-HDDA reactions of various nitrile-diyne substrates—the synthesis of these substrates was not trivial. Although they at first glance do not appear to be particularly complex, the syntheses of these substrates ultimately required a significant amount of time and effort. Anyone who has had to repeatedly plan, execute, troubleshoot, and revise either the total synthesis of a complex natural product or even the synthesis of a relatively simple small molecule can certainly understand this. For this reason, I will describe the synthesis of each substrate in some detail.

Additionally, individual reactions that were run in the pursuit of these substrates occasionally yielded interesting and unexpected side products. These side products often provided valuable insight and helped to guide the synthetic approach to the targeted substrates. At times, these side products were even the apparent result of unprecedented reactions. It is not uncommon for new reactions and methodologies to be serendipitously discovered in the synthetic pursuit of a natural product or small molecule—a fact which offers significant justification for the pursuit of total synthesis and synthetic research in general.[102] Indeed, the HDDA reaction—which has developed into an extraordinarily fruitful and useful methodology—was itself discovered in an unrelated synthetic pursuit of a small molecule. Accordingly, unexpected reactions that were observed during the syntheses of various aza-HDDA substrates are worth mentioning and offer another reason to describe these syntheses in some detail.

---

[102] (a) Armaly, A. M.; DePorre, Y. C.; Groso, E. J.; Riehl, P. S.; Schindler, C. S., Discovery of Novel Synthetic Methodologies and Reagents during Natural Product Synthesis in the Post-Palytoxin Era. *Chem. Rev.* **2015,** *115*, 9232-9276. (b) Nicolaou, K. C.; Vourloumis, D.; Winssinger, N.; Baran, P. S., The Art and Science of Total Synthesis at the Dawn of the Twenty-First Century. *Angew. Chem. Int. Ed.* **2000,** *39*, 44-122. (c) Nicolaou, K. C.; Snyder, S. A., The Essence of Total Synthesis. *Proc Natl Acad Sci* **2004,** *101*, 11929-11936.

4.4.1 A *gem*-Dimethylated Benzylic Nitrile Substrate.

While the computed activation energy of substrate **4015** (Figure 4.12) was calculated to be similar to that for the methanesulfonamide-tethered substrate **4014**, it was hoped that the effective replacement of a methanesulfonyl group with a benzene ring would make the substrate more soluble and more stable, perhaps resulting in more appealing yields.

The actual aza-HDDA substrate that was to be synthesized (substrate **4020)** differed from the substrate investigated *in silico* (substrate **4015**) in two ways: First, as mentioned before, experimental substrate **4020** contained a pendant TBS ether trap. Secondly, **4020** had methoxy substituents in the 4- and 5-positions of the aromatic ring. Based on previous experience synthesizing HDDA substrates (e.g. substrate **2010** in Chapter 2) it was anticipated that placement of methoxy groups in these positions would make it more likely for the intermediates in the synthesis of **4020** to be crystalline. This would allow for more scalable purification by recrystallization while having minimal effect on the aza-HDDA reaction that was to be tested. Thus, the synthesis of aza-HDDA substrate **4020** was initiated.

Figure 4.12 | Calculated activation energy ($\Delta G^{\ddagger}$) for the aza-HDDA cycloaromatization of the benzylic nitrile substrate **4015**.

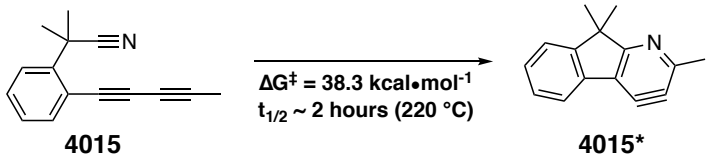

The optimized synthesis of **4020** started is shown in Scheme 4.1. It started with a precedented bromination of 3,4-dimethoxybenzyl alcohol (**4021**).[103] This reaction was chosen for its ability to conveniently access an appropriately bis-functionalized intermediate in one step. Just as important is its remarkable ease of scalability: the product **4022** crashes out of solution as the reaction progresses and can be directly isolated simply by filtering and washing with cold methanol. The use of glacial acetic acid was important as the use of older (i.e. wetter) sources resulted in several side

[103] Trost, B. M.; O'Boyle, B. M.; Hund, D., Investigation of a Domino Heck Reaction for the Rapid Synthesis of Bicyclic Natural Products. *Chem. Eur. J.* **2010,** *16*, 9772-9776.

products, making it difficult for the product to crystallize out of solution. This is possibly, in part, due to competing oxidation reactions resulting from the exposure of **4021** to a mixture of bromine and water.[104,105] When glacial acetic acid was used, this reaction was successfully run on a 400 mmol scale to give the dibromide **4022** in 70% yield.

Scheme 4.1 | Synthesis of substrate **4020**

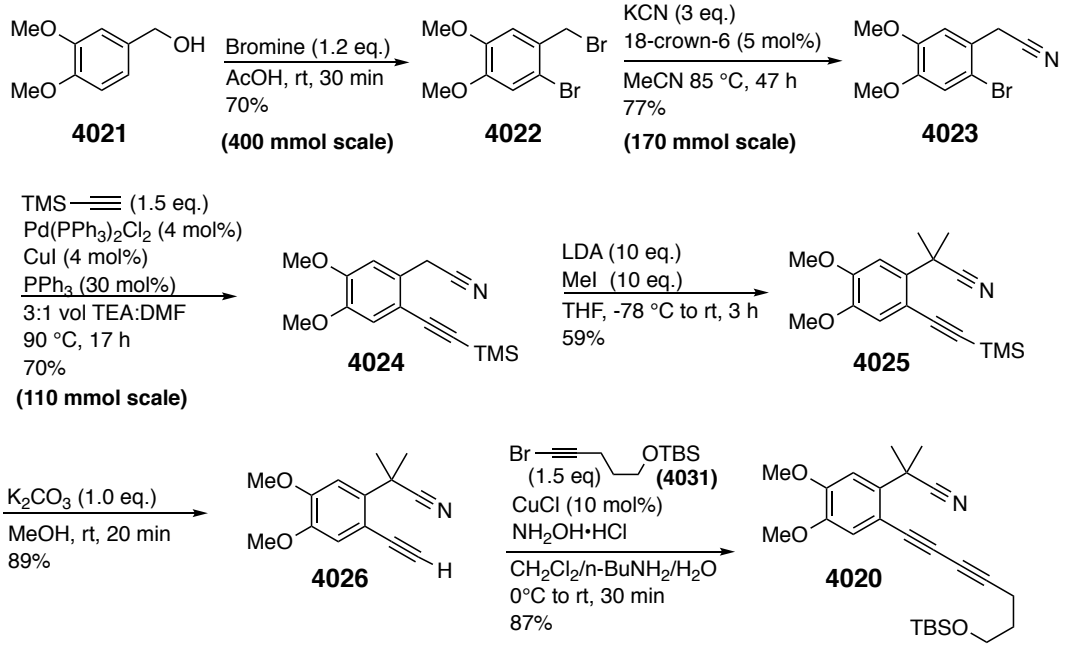

After this first step, attempts were made to access the benzylic nitrile **4023** by refluxing in a mixture of water and ethanol in the presence of sodium cyanide. Unfortunately, this method only gave the desired nitrile in 19% yield. Several side products were observed by GC-MS and their tentative assignments (based solely on mass) are shown in Scheme 4.2. Fortunately, **4023** could be obtained in good yields through other conventional methods such as refluxing the dibromide **X** with NaCN in DMF or by refluxing in acetonitrile in the presence KCN and 18-crown-6 ether. Ultimately, the later of these two methods was used on a 170 mmol scale to give **4023** in 77% yield.

---

[104] Deno, N. C.; Potter, N. H., Mechanism of oxidation of alcohols by aqueous bromine. *J. Am. Chem. Soc.* **1967,** *89*, 3555-3556.

[105] Palou, J., Oxidation of some organic compounds by aqueous bromine solutions. *Chem. Soc. Rev.* **1994,** *23*, 357-357.

Scheme 4.2 | Tentatively assigned products from the initial attempted cyanation of **4022**.

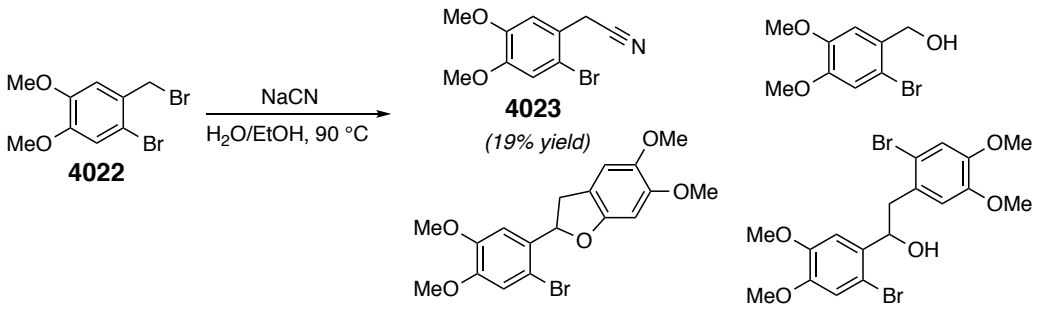

The subsequent Sonogashira reaction to access **4024** was predictably challenging. The aryl bromide precursor **4023** was not only *ortho*-substituted but further contained two electron-donating methoxy groups. Standard conditions[106] resulted in low conversion of **4023** to **4024** before apparent catalyst decomposition occured. However, the use of an alternative solvent mixture (DMF/TEA) along with the addition of triphenylphosphine (30 mol%) allowed for the efficient synthesis of **4024** in 70% yield. Although the removal of such a large amount of triphenylphosphine could potentially hinder the scalable purification of any reaction, in this case it was easily removed by treatment of the crude reaction material with hydrogen peroxide (to convert the triphenylphosphine to triphenylphosphine oxide) followed by selective crystallization of the product **4024** in MeOH. This allowed for the reaction to be run and purified on a 110 mmol scale.

Installation of the *gem*-dimethyl moiety to access the intermediate **4025** at the benzylic position proved to be fairly straightforward on smaller scales (up to 5 mmol). Exposure of the nitrile **4024** to 10 equivalents each of LDA and methyl iodide consistently yielded **4025** in yields ranging from about 60 to 70%. The use of fewer equivalents (2–5 eq.) of LDA or methyl iodide often yielded a mixture of **4025** and the mono-methylated intermediate leading to **4025**. These two products were inseparable even by normal phase HPLC.

Despite the general success and reproducibility of this reaction, an interesting problem was observed during scale up. When the reaction was scaled up (to a 50 mmol

[106] When saying "standard conditions," I refer to Sonogashira reaction conditions that I have used in the synthesis of HDDA substrates. Specifically, the conditions involve coupling of an aryl bromide with 1.1–1.5 equivalents of terminal alkyne in the presence of 1–2 mol% of $Pd(PPh_3)_2Cl_2$ and CuI using triethylamine as the solvent.

scale), a side product was observed along with the desired product **4025** (the molar ratio of **4025** to this side product observed in the crude product was 2.5:1.0). The side product was identified as the phenyl nitrile **4027** (Scheme 4.3a). This was a surprising transformation and, indeed, a search of the literature yielded no precedence for this type of reaction.

Scheme 4.3 | a) Side product **4027** observed during the methylation of the benylic nitrile **4024** and b) proposed mechanism for the formation **4027**.

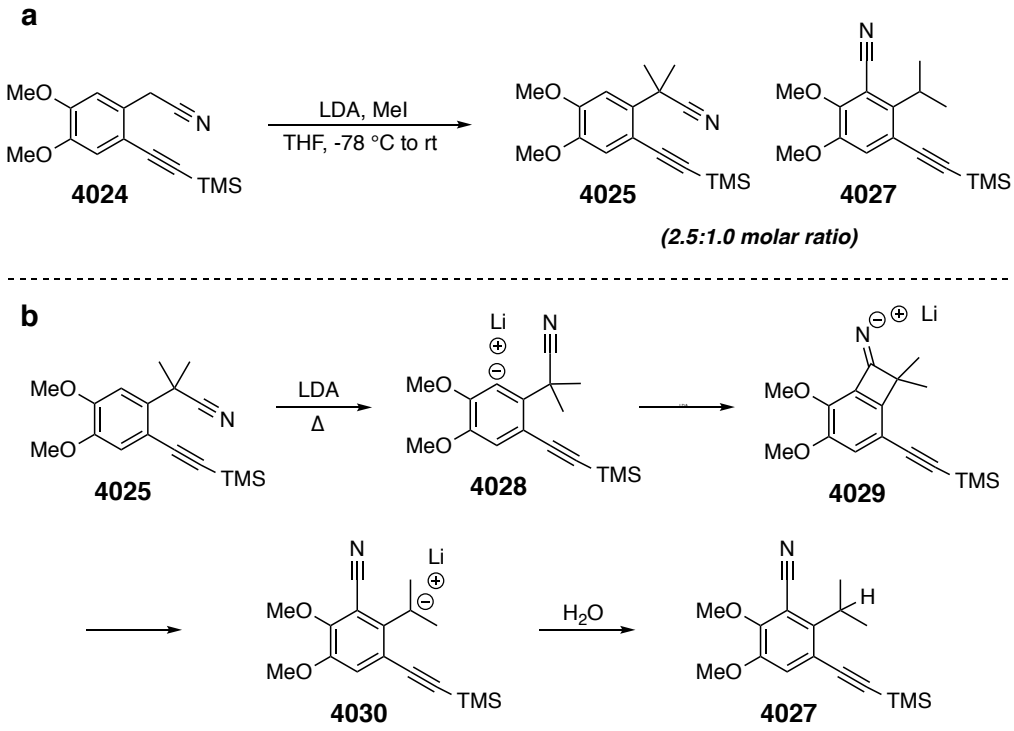

While running this reaction, I observed that a viscous slurry formed, which made it difficult to effectively stir the reaction mixture—as is often the case when running large scale reactions. This offers an explanation for the formation of **4027**. I hypothesize that, because of the ineffective mixing during the reaction, hot spots formed in the reaction mixture, allowing for the deprotonation of the arene by LDA to give the ion pair **4028**. This intermediate would then be capable of a ring closure (facilitated by the Thorpe–Ingold effect[79] to access the fused-ring intermediate **4029**, which could then generate the benzylic anion **4030**. Protonation of this intermediate would then yield the observed phenyl nitrile **4027**. In subsequent runs, the reaction mixture was made more dilute in

THF so as to make it less viscous and allow for more effective stirring. This seemed to be an effective solution, as **4027** was not observed in these reactions.

After the synthesis of several grams of the *gem*-dimethylated benzylic nitrile **4025** was completed, the final steps of the synthesis were carried out. Fortunately, these two steps proceeded smoothly. Exposure of **4024** to K_2CO_3 in MeOH cleanly desilylated the alkyne to give **4025** in 89% yield. Finally, **4025** was coupled to ((5-bromopent-4-yn-1-yl)oxy)(*tert*-butyl)dimethylsilane (**4031**) in a Cadiot–Chodkiewicz reaction to synthesize several hundred milligrams of the targeted aza-HDDA substrate **4020** in 87% yield.

Like the methanesulfonamide-tethered substrate **4009** in Section 4.3, test substrate **4020** was dissolved in *o*-DCB (0.01 M) and the resulting solution was heated in a microwave reactor at increasing temperature intervals. After each heating increment, the reaction mixture was cooled and analyzed by TLC. Gratifyingly, after heating the solution at 200 °C for 10 minutes, the solution took on a light yellow tint and TLC faintly showed the appearance of one new spot. Qualitatively, the reaction seemed to show a more appreciable conversion of the starting material to this new product when the solution was heated to 220 °C. As the solution was heated higher (to 240 °C) the reaction began to turn black and other spots appeared on the TLC plate. Both GC-MS and ^{1}H NMR spectroscopy of the crude material indicated that the desired aza-HDDA pyridine was the predominant product out of a mixture of products.

With this encouraging result in hand, a larger amount of **4020** was dissolved in *o*-DCB and heated in a microwave reactor. This time, the solution was heated consistently at 220 °C and monitored by TLC until **4020** was consumed. After 18 hours of heating, the crude reaction mixture was purified to give the anticipated aza-HDDA pyridine (**4032**) in 38% yield (Scheme 4.4). While it was encouraging to see an additional substrate that was capable of undergoing an aza-HDDA reaction, the yield and overall cleanliness of the reaction left much to be desired. The synthesis and testing of additional substrates were still needed.

Scheme 4.4 | Aza-HDDA reaction of benzylic nitrile **4020** to give pyridine **4032**.

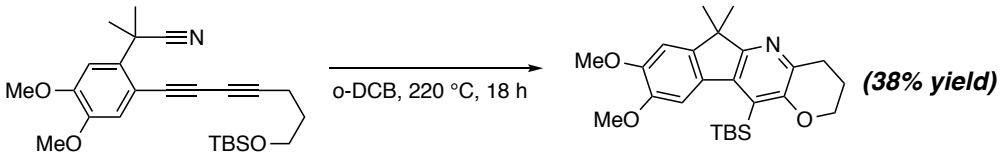

4020 **4032**

4.4.2 A Dialkynyl Ketone Substrate

Similar to computationally-tested substrates **4014** and **4015**, the free energy of activation energy of the dialkynyl ketone substrate **4016** (Figure 4.11) was predicted by DFT calculations to have a relatively high aza-HDDA $\Delta G^{\ddagger}$ value (37.9 kcal•mol^{-1}; $t_{1/2}$ = 7.44 hours at 220 °C) . Given the low yields of these previous substrates, it seemed unlikely that any experimental analogs **4016** would undergo a clean aza-HDDA reaction at similarly high temperatures. However, a successful aza-HDDA reaction of this substrate would yield a functionalized aza-fluorenone moiety. Given the prevalence and utility of aza-fluorenones as bidendate ligand precursors,[107] fluorescent probes,[108] and—in particular—as bioactive natural products,[109] an analog of **4016** seemed a worthy target for synthesis and for testing as an aza-HDDA substrate.

---

[107] Zhang, L.; Li, B., A series of 4,5-diazafluoren-9-one-derived ligands and their Cu(I) complexes: Synthesis, characterization and photophysical properties. *Inorganica Chimica Acta* **2009,** *362*, 4857-4861.

[108] (a) Ye, F.; Tran, C.; Jullien, L.; Le Saux, T.; Haddad, M.; Michelet, V.; Ratovelomanana-Vidal, V., Synthesis of Fluorescent Azafluorenones and Derivatives via a Ruthenium-Catalyzed [2 + 2 + 2] Cycloaddition. *Org. Lett.* **2018,** *20*, 4950-4953. (b) Gao, M.; Su, H.; Lin, Y.; Ling, X.; Li, S.; Qin, A.; Tang, B. Z., Photoactivatable aggregation-induced emission probes for lipid droplets-specific live cell imaging. *Chem. Sci.* **2017,** *8*, 1763-1768.

[109] (a) Mueller, D.; Davis, R. A.; Duffy, S.; Avery, V. M.; Camp, D.; Quinn, R. J., Antimalarial Activity of Azafluorenone Alkaloids from the Australian Tree Mitrephora diversifolia. *J. Nat. Prod.* **2009,** *72*, 1538-1540. (b) Wijeratne, E. M. K.; De Silva, L. B.; Kikuchi, T.; Tezuka, Y.; Gunatilaka, A. A. L.; Kingston, D. G. I., Cyathocaline, an Azafluorenone Alkaloid from Cyathocalyx zeylanica. *J. Nat. Prod.* **1995,** *58*, 459-462. (c) Hufford, C. D.; Liu, S.; Clark, A. M.; Oguntimein, B. O., Anticandidal Activity of Eupolauridine and Onychine, Alkaloids from Cleistopholis patens. *J. Nat. Prod.* **1987,** *50*, 961-964. (d) Koyama, J.; Morita, I.; Kobayashi, N.; Osakai, T.; Usuki, Y.; Taniguchi, M., Structure–activity relations of azafluorenone and azaanthraquinone as antimicrobial compounds. *Bioorg. Med. Chem. Lett.* **2005,** *15*, 1079-1082. (e) Manpadi, M.; Uglinskii, P. Y.; Rastogi, S. K.; Cotter, K. M.; Wong, Y.-S. C.; Anderson, L. A.; Ortega, A. J.; Van slambrouck, S.; Steelant, W. F. A.; Rogelj, S.; Tongwa, P.; Antipin, M. Y.; Magedov, I. V.; Kornienko, A., Three-component synthesis and anticancer evaluation of polycyclic indenopyridines lead to the discovery of a novel indenoheterocycle with potent apoptosis inducing properties. *Org. Biomol. Chem* **2007,** *5*, 3865-3872. (f) Addla, D.; Bhima; Sridhar, B.; Devi, A.; Kantevari, S., Design, synthesis and antimicrobial evaluation of novel 1-benzyl 2-butyl-4-chloroimidazole embodied 4-azafluorenones via molecular hybridization approach. *Bioorg. Med. Chem. Lett.* **2012,** *22*, 7475-7480. (g)

The synthesis of a related test substrate **4033** is shown in Scheme 4.5. It should be noted that the tethered silyl either trap that was used in previous substrates **4020** and **4009** was not initially used to test this new substrate. This was done to avoid potential problems with selective cleavage of a secondary TES ether (like that seen in intermediate **4037**) in the presence of a primary TBS ether. Instead, a tethered *p*-methoxybenzene trap was employed, as it (as well as other tethered arenes) have been shown to act as effective traps of HDDA-generated benzyne.[41]

Scheme 4.5 | Synthesis and testing of aza-HDDA substrate **4033** to give aza-fluorenone product **4039**.

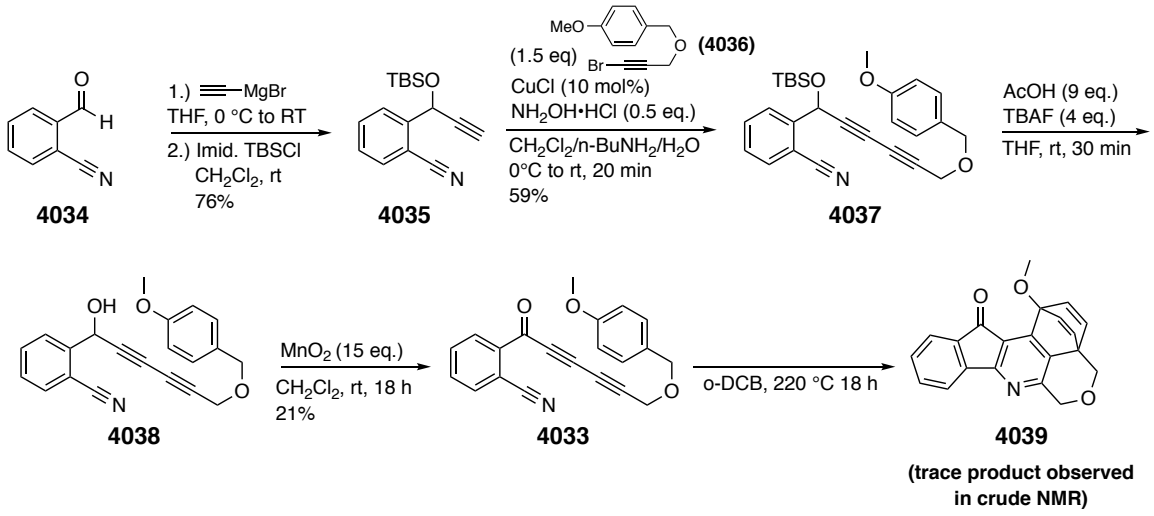

The synthesis commenced with a precedented[110] conversion of *o*-cyanobenzaldehyde (**4034**) to the propargylic silyl ether (**4035**) in 76% yield. This intermediate was then coupled with 1-(((3-bromoprop-2-yn-1-yl)oxy)methyl)-4-methoxybenzene (**4036**; synthesized in 2 steps) to give diyne intermediate **4037** in 59% yield. Deprotection of the TBS ether proved to be difficult presumably due to the sensitivity of the benzylic propargylic secondary alcohol in **4037**. Attempts with several standard TBS ether deprotection conditions (TBAF, NH_4F, hydrofluoric acid, as well as varying mixtures of AcOH/THF/H_2O) either resulted in low conversion, substrate

Goulart, M. O. F.; Santana, A. E. G.; De Oliveira, A. B.; De Oliveira, G. G.; Maia, J. G. S., Azafluorenones and azaanthraquinone from Guatteria dielsiana. *Phytochemistry* **1986,** *25*, 1691-1695.

[110] You, X.; Xie, X.; Chen, H.; Li, Y.; Liu, Y., Cyano-Schmittel Cyclization through Base-Induced Propargyl-Allenyl Isomerization: Highly Modular Synthesis of Pyridine-Fused Aromatic Derivatives. *Chem. Eur. J.* **2015,** *21*, 18699-18705.

decomposition, or tautomerization of the desired alcohol to its corresponding enones. Ultimately, the use of reaction conditions in which TBAF was buffered with acetic acid, followed by oxidation of the crude alcohol **4038** with MnO_2 allowed to the isolation of the desired aza-HDDA substrate **4033** in a sufficient 21% yield.

While this substrate did undergo an aza-HDDA reaction to give the congested polycylic product **4039** at 220 °C, only a trace amount of this product was isolated from the reaction. This result was disappointing and surprising considering how this substrate performed even more poorly than the previously tested aza-HDDA substrates, which cyclized at similar temperatures. Hoping the tethered *para*-methoxy benzene may simply have been an inadequate trap for this pyridyne, I decided to synthesize an analogous substrate with a covalently attached TBS ether trap—as was done for the previously tested aza-HDDA substrates.

The synthesis and testing of this alternate substrate **4040** are shown in Scheme 4.6. Fortuntaly, the bis-silylether **4041** (synthesized in 3 steps) cleanly gave the alcohol **4042** when exposed to excess HF-Pyridine complex. Subsequent oxidation with MnO_2 produced the test substrate **4040** in 68% yield. Heating a solution of **4040** in *o*-DCB (0.01 M) at 220 °C gradually consumed the substrate and yielded the aza-fluorenone **4043** in 33% yield (Scheme 4.6). Although this reaction was a significant improvement over the aza-HDDA reaction of substrate **4033**, the yield of 33% was still suboptimal. Accordingly, I continued to synthesize additional aza-HDDA test substrates in pursuit of a clean, high-yielding aza-HDDA reaction.

Scheme 4.6 | (a) Synthesis of aza-HDDA substrate **4040**. (b) Aza-HDDA reaction of **4040** to give aza-fluorenone **4043**.

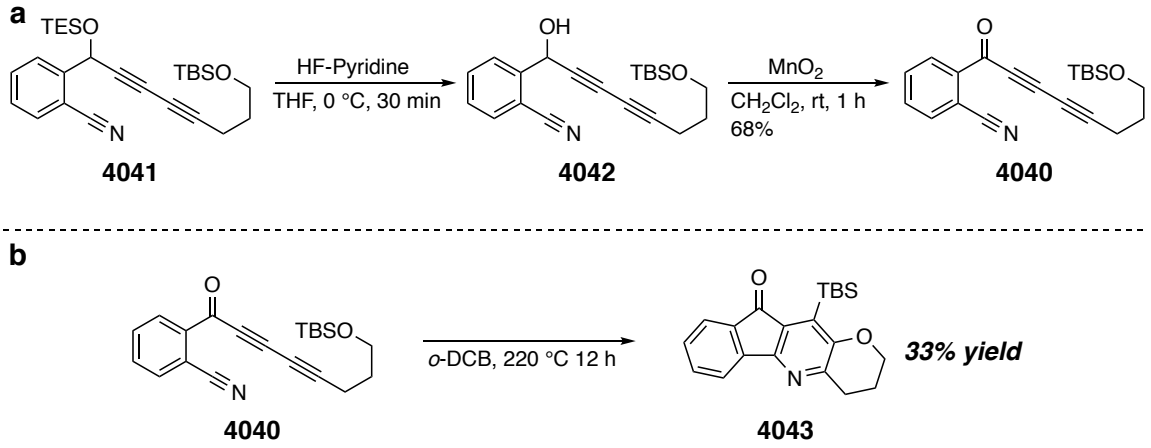

3.4.3 An Acyl Nitrile Substrate with a Cycloheptene Tether.

As is shown in Figure 4.13, it is predicted by DFT calculations that the potential aza-HDDA substrate **4018** in which an acyl nitrile is tethered to a 1,3-diyne *via* a cycloheptene ring has a remarkably low activation energy ($\Delta G^{\ddagger}$) of 33.8 kcal•mol^{-1}. This is particularly impressive when compared to the activation energies of the three previously-discussed substrates computed substrates **4014**–**4016**, all of which fall around 38–39.5 kcal•mol^{-1} (Figure 4.11).

Figure 4.13 | Calculated free energy of activation ($\Delta G^{\ddagger}$) for the aza-HDDA reaction of acyl nitrile substrate **4018**.

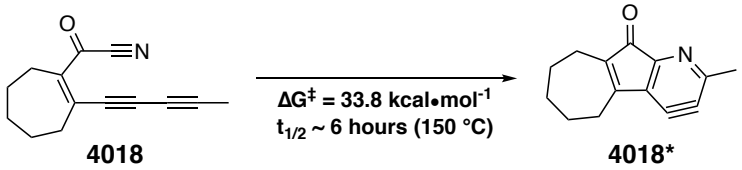

The relatively low energy barrier can likely be attributed to two structural features inherent to the substrate **4018**:

1.) The cycloheptenyl tether itself significantly lowers the activation energy. Previous work done by Hoye and coworkers showed that the use of a cycloheptene (7-membered ring) tether in place of a more conventional cyclohexene (6-membered ring) tether in an HDDA substrate results in a twentyfold increase of the rate constant (*k*) for the corresponding HDDA reaction of that substrate.[37]

2.) The nitrile is part of an acyl nitrile moiety. While diynophiles in triyne HDDA substrates are not "activated" by adjacent carbonyl moieties—in constrast to what is usually seen for dieneophiles for conventional Diels–Alder reactions—the nitrile moiety of any given aza-HDDA substrate may be more easily activated.

With the promising *in silico* result shown in Figure 4.13, the synthesis of a aza-HDDA test substrate **4044** was initiated (Scheme 4.7). This synthesis began with a Vilsmeier–Haack reaction carried out on cycloheptenone (**4045**) to give the beta-chloroenal **4046** in 89% yield. The high yield and scalability of this reaction are worth noting, specifically when compared the synthesis to its bromoenal analog. The initially planned synthesis of aza-HDDA substrate **4044** started with an analogous bromoenal because, unlike beta-chloroenals, beta-bromoenals have been shown to act as effective coupling partners with terminal 1,3-diynes in the Sonogashira reaction.[111] However, despite literature precedence, this intermediate proved to be difficult to synthesize in appreciable amounts. Multiple attempts to affect a higher yielding transformation by varying the stoichiometry of the reagents (DMF and PBr_3), changing the order of addition, using different reaction temperatures, and vigorously drying the $CHCl_3$ solvent all resulted consistently low yields.

Scheme 4.7 | Synthesis of the cycloheptene-tethered acyl nitrile aza-HDDA substrate **4044**.

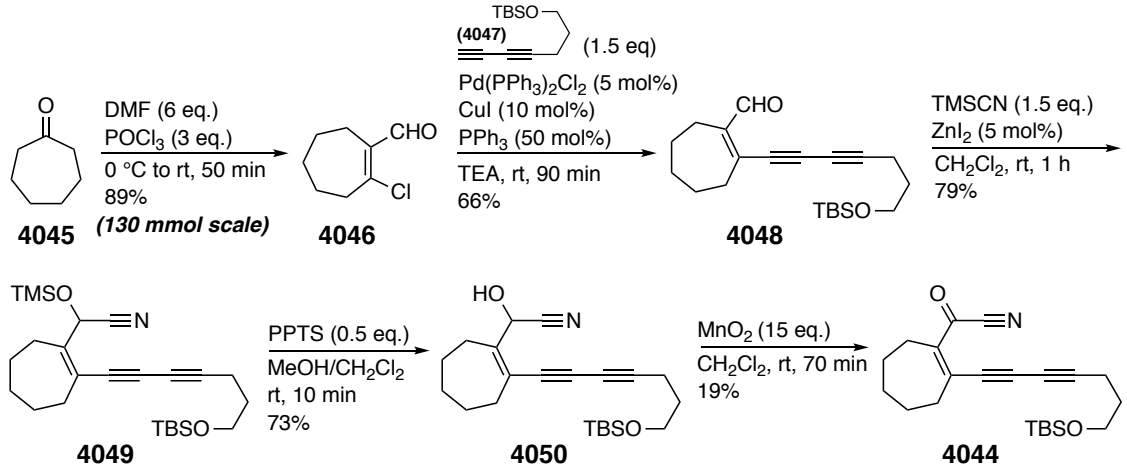

[111] Tomás-Mendivil, E.; Heinrich, C. F.; Ortuno, J.-C.; Starck, J.; Michelet, V., Gold-Catalyzed Access to 1*H*-Isochromenes: Reaction Development and Mechanistic Insight. *ACS Catalysis* **2017,** *7*, 380-387.

More important than the scalable synthesis of **4046** was its ability to effectively participate in a Sonogashira reaction with a terminal 1,3-diyne. Because **4046** is an electron deficient chloroalkene, it was conceivable that it would act as a competent coupling partner in this desired transformation. Indeed, **4046** was effectively coupled with *tert*-butyl(hepta-4,6-diyn-1-yloxy)dimethylsilane (**4047**, synthesized in 4 steps) to give highly conjugated enal intermediate **4048** in 66% yield. The addition of PPh_3 to the reaction mixture proved important to produce this product in good yield.

Accessing the synthetic target **4044** appeared, at first glance, to be a simple matter of converting an aldehyde to an acyl nitrile. Due to the prevalence of acyl nitrile moieties in the aza-HDDA work presented in this thesis and due to the somewhat esoteric nature of acyl nitriles, a brief overview of precedented synthetic methods that are used to access acyl nitriles is merited.

While the high electrophilicity of acyl nitriles makes them practically nonexistent in natural products or commercially-relevant small molecules, it has—on several occasions—rendered them useful as synthetic intermediates. Acyl nitriles are, in most cases, synthesized from an analogous aromatic or conjugated aldehyde *via* a cyanohydrin intermediate (shown generically in Figure 4.14). A simple and well-known demonstration of this—and one of the earliest uses of an acyl nitrile in a total synthesis—was developed in E. J. Corey's lab as part of the synthesis of an insect juvenile hormone.[112,113] Hydrogen cyanide—generated *in situ* from sodium cyanide and acetic acid—transforms an aldehyde to a cyanohydrin that is then oxidized by manganese dioxide to form an acyl nitrile. With methanol as the solvent, the acyl nitrile then rapidly undergoes methanolysis to access the corresponding methyl ester. This overall transformation is often referred to as a Corey–Ganam–Gilman oxidation (Figure 4.14a).

---

[112] Corey, E. J.; Katzenellenbogen, J. A.; Gilman, N. W.; Roman, S. A.; Erickson, B. W., Stereospecific total synthesis of the dl-C18 Cecropia juvenile hormone. *J. Am. Chem. Soc.* **1968,** *90*, 5618-5620.
[113] Corey, E. J.; Gilman, N. W.; Ganem, B. E., New methods for the oxidation of aldehydes to carboxylic acids and esters. *J. Am. Chem. Soc.* **1968,** *90*, 5616-5617.

Figure 4.14 | Selected methodology for the synthesis of acyl nitriles from aldehydes.

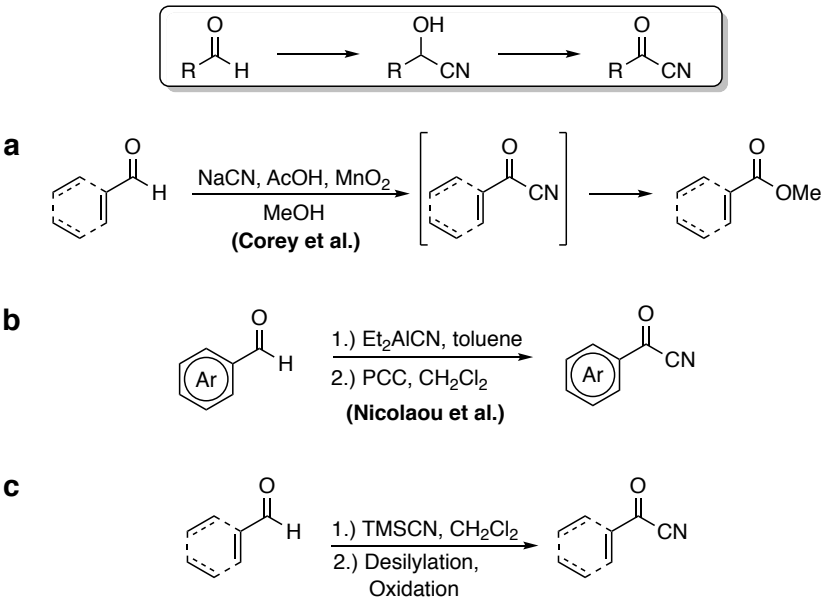

A more recent and more synthetically convenient methodology utilizes diethylaluminum cyanide (Figure 4.14b). While this reagent is more commonly associated with the hydrocyanation of α,β-unsaturated ketones[114,115], it can also be used to form cyanohydrins from sterically hindered and sensitive aldehyde substrates.[116] Of note is the use of this reagent on complex benzaldehyde intermediates, and the subsequent PCC oxidation of the resulting cyanohydrin, in the total synthesis of several coleophomone natural products[117,118].

Lastly, trimethylsilyl cyanide (TMSCN) can also act as a convenient reagent to access acyl nitriles—largely due to its ease of handling and wide functional group compatibility (Figure 4.14c). Exposure of aldehydes to TMSCN under mild conditions

---

[114] Nagata, W.; Yoshioka, M., Alkylaluminum cyanides as potent reagents for hydrocyanation. *Tetrahedron Lett.* **1966,** *7*, 1913-1918.
[115] Nagata, W.; Yoshioka, M.; Hirai, S., Hydrocyanation. IV. New hydrocyanation methods using hydrogen cyanide and an alkylaluminum, and an alkylaluminum cyanide. *J. Am. Chem. Soc.* **1972,** *94*, 4635-4643.
[116] Nicolaou, K. C.; Vassilikogiannakis, G.; Kranich, R.; Baran, P. S.; Zhong, Y.-L.; Swaminathan, N., New Synthetic Technology for the Mild and Selective One-Carbon Homologation of Hindered Aldehydes in the Presence of Ketones. *J. Am. Chem. Soc.* **2000,** *2*, 1895-1898.
[117] Nicolaou, K. C.; Vassilikogiannakis, G.; Montagnon, T., The Total Synthesis of Coleophomones B and C. *Angew. Chem. Int. Ed.* **2002,** *41*, 3276-3281.
[118] Nicolaou, K. C.; Montagnon, T.; Vassilikogiannakis, G.; Mathison, C. J. N., The Total Synthesis of Coleophomones B, C, and D. *J. Am. Chem. Soc.* **2005,** *127*, 8872–8888.

results in the formation of an *O*-silyl cyanohydrin[119] that can either be desilylated and oxidized to yield the corresponding acyl nitrile or—in some cases—directly oxidized to the acyl nitrile (usually by PDC[120,121] or DDQ[122,123]).

Returning to the synthesis of aza-HDDA substrate **4044**, the several attempts that were made to convert aldehyde **4048** directly to a cyanohydrin—most of which involved exposing the substrate to a cyanide salt and an acid source—resulted either in low conversion or substrate decomposition. Exposure of the aldehyde to TMSCN did yield small amounts *O*-trimethylsilyl cyanohydrin **4049**, albeit at a prohibitively low rate of conversion. Fortunately, as was demonstrated in the initial development of this methodology by Evans and coworkers,[119] it was found that the addition of 1–5 mol% of a catalyst (either KCN/18-crown-6 ether, tetra-*n*-butylammonium cyanide, or ZnI_2) dramatically enhanced the rate of this reaction (although KCN/18-crown-ether also resulted in several uncharacterized side reactions). Ultimately, the use of 5 mol% ZnI_2 and 1.5 equivalents of TMSCN allowed for the clean conversion of aldehyde **4048** to *O*-silylcyanohydrin **4049** in 79% yield.

While it was initially hoped that **4049** could be directly oxidized to the acyl nitrile **4044** , experimental attempts were unsuccessful. DDQ, rather than yielding the desired acyl nitrile, surprisingly gave the deprotected cyanohydrin **4050** in low yield. The use of PDC gave rise to uncharacterized side products. It is worth noting that when certain allylic *O*-silyl cyanohydrins are oxidized with PDC in DMF, the corresponding butenolides emerge as the predominant products (Scheme 4.8).[121] While no butenolide was observed in the attempted conversion of **4049** to **4044** with PDC, side oxidations such as those observed in Scheme 4.8 could be partially responsible failure of the reaction.

---

[119] Evans, D. A.; Truesdale, L. K.; Carroll, G. L., Cyanosilylation of aldehydes and ketones. A convenient route to cyanohydrin derivatives. *J. Chem. Soc., Chem. Commun.* **1973,** *0*, 55-55.
[120] Cossfo, F. P.; Aizpurua, J. M.; Palomo, C., Synthetic applications of chromium(VI) reagents in combination with chlorotrimethylsilane. *Can. J. Chem.* **1986,** *64*, 225-231.
[121] Corey, E. J.; Schmidt, G., A simple route to Δ2-butenolides from conjugated aldehydes. *Tetrahedron Lett.* **1980,** *21*, 731-734.
[122] Janosik, T.; Johnson, A.-L.; Bergman, J., Synthesis of the marine alkaloids rhopaladins A, B, C and D. *Tetrahedron* **2002,** *58*, 2813-2819.
[123] Kandemir, H.; Wood, K.; Kumar, N.; Black, D. S., Synthesis of 5-(7′-indolyl)oxazoles and 2,5-di-(7′-indolyl)oxazoles. *Tetrahedron* **2013,** *69*, 2193-2198.

Scheme 4.8 | Oxidation of allylic *O*-silyl cyanohydrins to butenolides demonstrated by Corey and Schmidt.

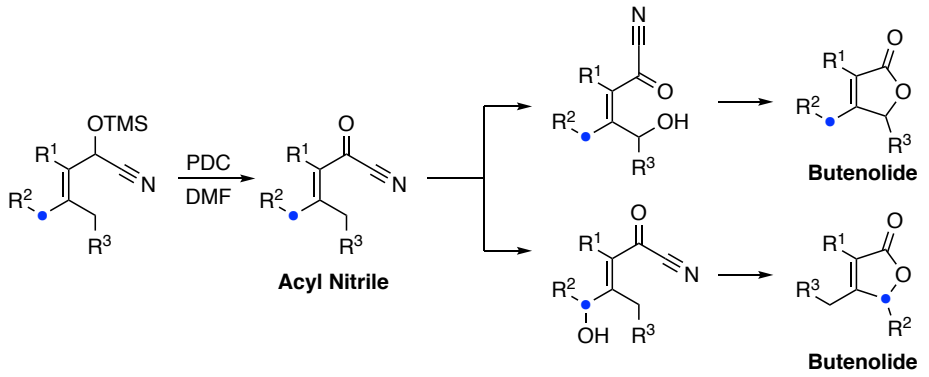

Despite this initial setback, *O*-silyl cyanohydrin **4049** could be cleanly deprotected by PPTS in MeOH/CH_2Cl_2 to give cyanohydrin **4050**, which was sufficiently stable to silica gel chromatography to be purified in 73% yield. Unfortunately, the oxidation of **4050** yielded only a small amount of the acyl nitrile **4044** (19% yield). While this reaction seemed to proceed cleanly, **4044** was shown to be inherently unstable even at room temperature; leaving a purified sample of **4044** under high vacuum overnight resulted in decomposition of most of the sample, which necessitated repurification.

Unfortunately, this instability of **4044** manifested itself in the results of its aza-HDDA cycloaromatization (Scheme 4.9). Despite the fact that the anticipated pyridine product **4051** was formed at the incredibly low temperature of 120 °C (!), the yield was a poor 29%. The remarkably fast consumption of **4044** (within 20 minutes) is certainly due to its inherent instability rather than a low energetic barrier to the aza-HDDA reaction.

Scheme 4.9 | Aza-HDDA reaction of acyl nitrile substrate **4044**.

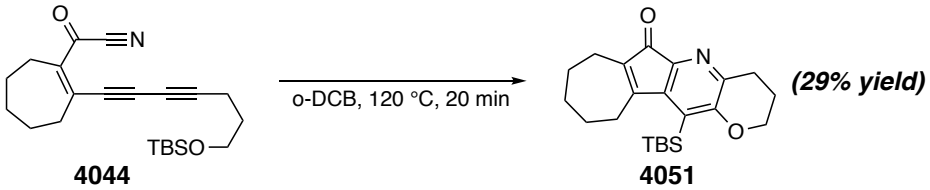

4044 **4051**

3.4.3 An Acyl Nitrile Substrate with a More Stable Benzene Tether

The instability of acyl nitrile **4044** and its consequently poor performance as an aza-HDDA substrate was a frustrating disappointment. Nevertheless, it seemed plausible that this problem could be fixed by designing and synthesizing a related acyl nitrile

substrate with a different tether that would impart greater stability and, hopefully, allow for a more successful aza-HDDA reaction. In this regard, the benzoyl nitrile substrate **4052** (Scheme 4.10b,), which was previously studied *in silico* as substrate **4017** (Scheme 4.10a) appears to be a good candidate. It is clear that the replacement of a cycloheptene tether with an aromatic ring raises the $\Delta G^{\ddagger}$ value of the aza-HDDA reaction (compare 35.6 kcal/mol for benzoyl nitrile **4017** to 33.8 kcal/mol for cycloheptene-tethered analog **4018**). However, this increase is rather modest, and it was hoped that test substrate **4052** would undergo a relatively clean aza-HDDA reaction.

The initial attempt to synthesize a benzoyl nitrile test substrate is shown in Scheme 4.10b. The first three steps (from **4053** to **4054**) were relatively straightforward reactions that were precedented and that I had carried out previously in the synthesis of triyne HDDA substrate **2010** (Chapter 2). As was done for the synthesis of the previous substrate **4044**, the installation of the acyl nitrile moiety was in **4052** was reserved for the last step of the synthesis, due to the high electrophilicity and general instability exhibited

Scheme 4.10 | a) Computed $\Delta G^{\ddagger}$ value for the aza-HDDA reaction of benzoyl nitrile **4017** and b) initially planned synthesis of benzoyl nitrile test substrate **4052**.

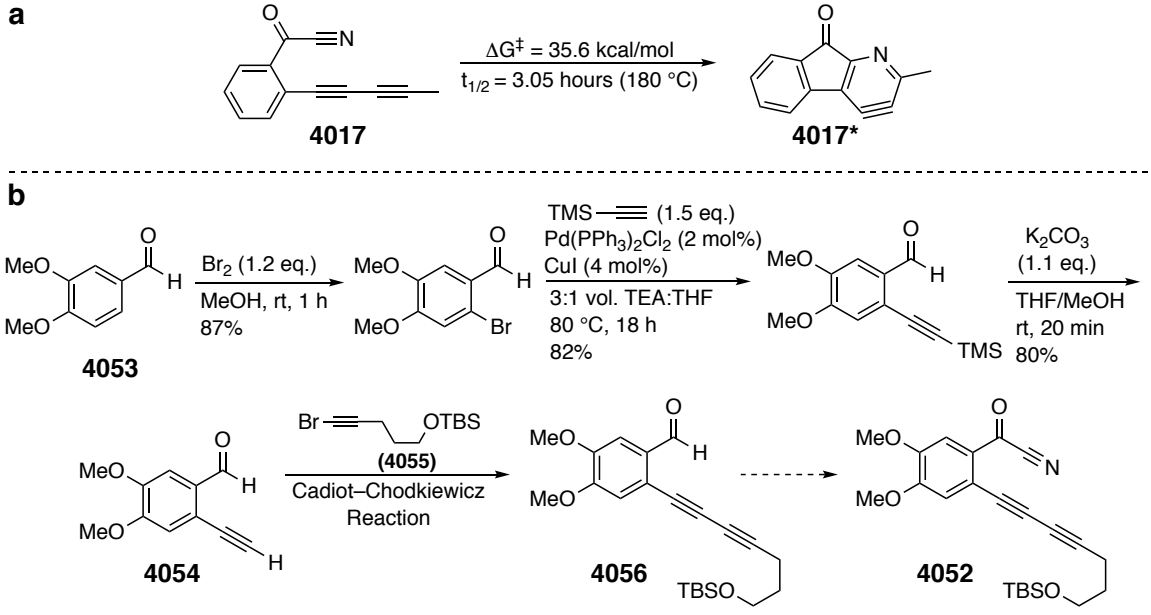

by acyl nitriles. Accordingly, attempts were made to couple ((5-bromopent-4-yn-1-yl)oxy)(*tert*-butyl)dimethylsilane (**4055**) with terminal alkyne **4054** to give the diyne intermediate **4056**.

The Cadiot–Chodkiewicz reaction has a reasonably high tolerance for a variety of functional groups that are not sensitive to strongly basic conditions, and the use of aqueous *n*-butylamine as the solvent in this coupling has become standard in the synthesis of HDDA substrates. Nevertheless, exposure of **4054** to bromoalkyne **4055**, CuCl, and hydroxylamine hydrochloride in aqueous *n*-butylamine resulted in full consumption of the starting material with no product formation (Scheme 4.11a).

It seemed plausible that the aldehyde functionality in **4054** was a liability in this reaction, and that the iminium intermediate formed *in situ* either from **4054** and *n*-butylamine (or diyne product **4056** and *n*-butylamine) was undergoing side reactions. Indeed, a Cadiot–Chodkiewicz reaction in which 1-bromopropyne was coupled with an analogous benzylic *alcohol* **4057** yielded the diyne-ol product **4058** in 75% yield (Scheme 4.11b), indicating that the aldehyde was the reason for the failure of the synthesis

Scheme 4.11 | a) Attempted synthesis of diyne intermediate **4056** through a Cadiot–Chodkiewicz coupling. b) Synthesis of an analogous diyne **4059** through an effective (reductive) protection of the aldehyde group.

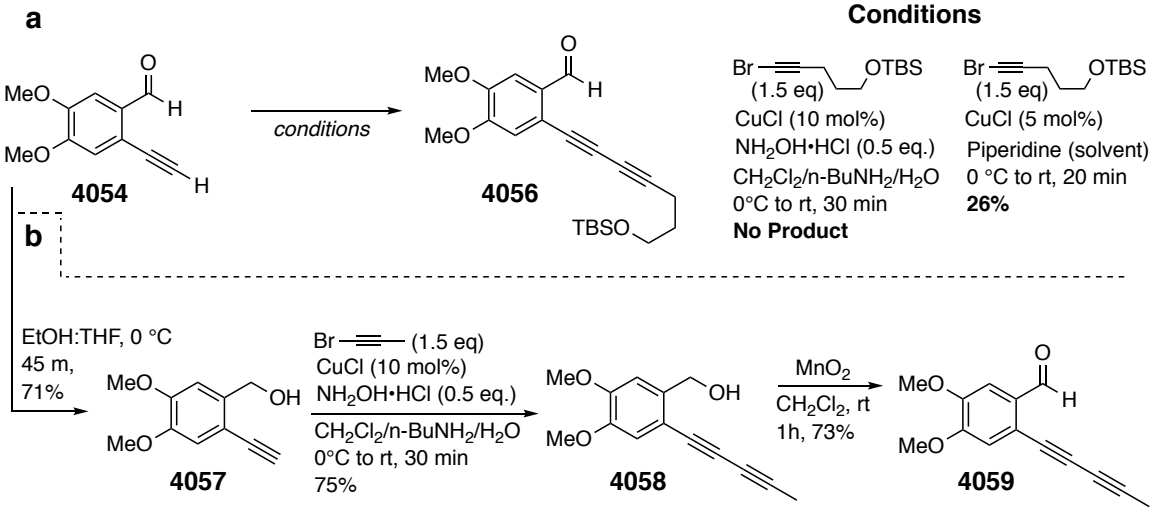

of **4056**. Subsequent oxidation of **4058** with MnO_2 produced aldehyde **4059** in 73% yield. While **4056** could also be synthesized in an analogous protection/deprotection sequence, it seemed conceivable that simply changing the amine base used in the coupling reaction (and hence the nature of the putative iminium ion formed during the reaction) could also facilitate its formation. It is well-known that the choice of amine base is frequently of critical importance in the Cadiot–Chodkiewicz reaction.[124]

I chose to use a slightly different set of Cadiot–Chodkiewicz conditions, in which rigorously degassed piperidine (rather than *n*-butylamine) is used as the solvent. These conditions have also been used on several occasions to synthesize HDDA substrates.[125] Gratifyingly, these conditions did indeed give diyne **4056**, albeit in a rather low yield of 26% (Scheme 4.11a). While this yield was low, it provided sufficient material to pursue the synthesis of the synthetic target **4052**.

Scheme 4.12 | Completion of the synthesis of benzoyl nitrile aza-HDDA test substrate **4052**.

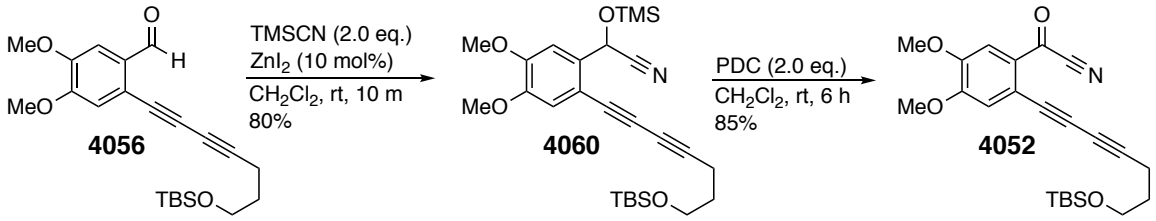

The completion of the synthesis of **4052** is shown in Scheme 4.12. As was done before in the synthesis of substrate **4044** (Section 3.4.3), conversion of the aldehyde moiety in **4056** to an acyl nitrile moiety proceeded through the corresponding *O*-trimethylsilyl cyanohydrin **4060**. Exposure of **4056** to TMSCN in the presence of a substiochiometric amount of ZnI_2 gave **4060** in 80% yield. In contrast to the synthesis of **4044**, where the *O*-silyl cyanohydrin intermediate needed to be desilylated before oxidation to the acyl nitrile, exposure of **4060** to PDC yielded the target benzoyl nitrile **4052** in 85% yield.

---

[124] Sindhu, K. S.; Thankachan, A. P.; Sajitha, P. S.; Anilkumar, G., Recent developments and applications of the Cadiot–Chodkiewicz reaction. *Org. Biomol. Chem* **2015,** *13*, 6891-6905.
[125] Baire, B.; Niu, D.; Willoughby, P. H.; Woods, B. P.; Hoye, T. R., Synthesis of complex benzenoids via the intermediate generation of o-benzynes through the hexadehydro-Diels-Alder reaction. *Nat. Protoc.* **2013,** *8*, 501-508.

With the synthesis completed, the aza-HDDA test substrate **4052** was dissolved in *o*-dichlorobenzene to give a 0.01 M solution. Starting at 130 °C, this solution was subjected to increasingly high temperatures. While TLC showed no change in the solution at 130 ° or 150 °C, conversion to one predominant product was observed after heating at 170 °C for 30 minutes.

Scheme 4.13 | Heating substrate **4052** yields the pyridine **4061** via the aza-HDDA reaction in good yield.

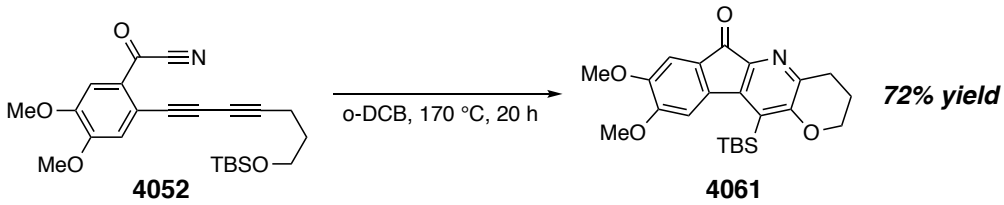

4052 **4061**

As illustrated in Scheme 4.13, heating the solution overnight at 170 °C for 20 hours resulted in full consumption of **4052** and apparent conversion to a predominant product. To my delight, the ^{1}H NMR spectrum of the crude material showed remarkably clean formation—72% yield based on an internal standard—of the desired pyridine product **4061**. A subsequent experiment showed that heating **4052** at 175 °C resulted in its full consumption over 8 hours and gave a similarly good (isolated) yield of 66%.

These results were immensely encouraging. The high yield of this reaction showed that, not only were nitriles capable of participating in the HDDA reaction, but that they could do so in a synthetically practical manner. Furthermore, the (relatively) low temperature required was a promising indication that this a variety of molecular traps other than silyl ethers could be used to access functionalized pyridine products. Naturally, the next step was to trap the reactive pyridyne intermediate from this substrate with other compounds in a bimolecular (i.e. intermolecular) fashion.

4.5 Intermolecular Trapping of Pyridynes Generated by the aza-HDDA Reaction

4.5.1 A Benzoyl Nitrile Aza-HDDA Substrate

In order to investigate the viability of intermolecular pyridyne-trapping reactions, an analog of the benzoyl nitrile **4052** was first synthesized. This analog **4062** simply contained a methyl substituent in place of the siloxypropyl group present in **4052**. In contrast to the synthesis of **4052**, where only a small amount (~5–10 mg) of material was necessary to test for an aza-HDDA reaction, at least several hundred milligrams of material would now be necessary to test run multiple reactions and to scale up successful reactions. The previous synthetic route, whose aforementioned low-yielding Cadiot–Chodkiewicz reaction (Scheme 4.11, **4054** to **4056**) would likely prove to be a synthetic bottleneck, seemed inadequate to meet this need.

Accordingly, a more efficient synthetic route to aza-HDDA substrate **4062** was developed (Scheme 4.14). Specifically, the conversion of 6-bromoveratraldehyde (**4063**)

Scheme 4.14 | Modified synthesis to produce aza-HDDA substrate **4062**.

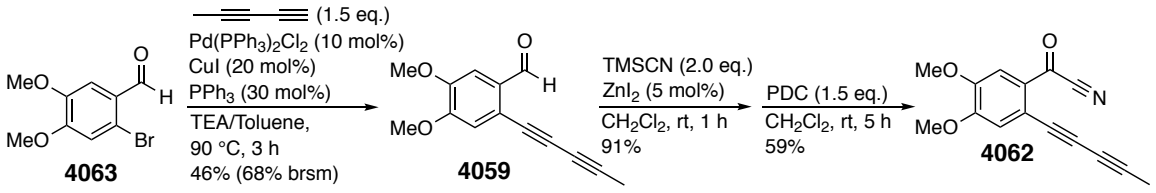

To diyne intermediate **4059** was reduced from 3 steps to 1 step by subjecting it to a Sonogashira coupling with 1,3-pentadiyne. While this approach was considered before in the synthesis of **4052**, it was not pursued due to the presumed difficulty of coupling a thermally unstable terminal 1,3-diyne with a relatively electron rich aryl bromide. Despite these misgivings, **4059** was isolated in 46% yield (although a relatively high loading of the palladium (II) precatalyst was required). This ultimately allowed for the synthesis about a gram of aza-HDDA substrate **4062**.

Selected examples of pyridine products obtained from aza-HDDA reactions of **4062** are shown in Figure 4.15. Products **4064a** and **4064b** were obtained by heating **4062** in the presence of the non-protic, non-nucleophilic traps furan and cyclooctane, respectively. Trapping with 3 equivalents of furan, a 4π diene that is known to react with

benzyne) in a [4 + 2] cycloaddition,[126] gave **4064a** in 55% yield. Interestingly, attempts to increase the yield by using a higher excess of furan actually gave significantly lower

Figure 4.15 | a) Generation of reactive pyridyne intermediate **4062*** and *in situ* trapping of **4062*** (by reaction with trap T^2-T^1) to give generic functionalized pyridine **4064**. b) Selected examples pyridine products (**4064a**–**4064d**) produced from the aza-HDDA reaction of substrate **4062**; the molar ratios of regioisomers for products **4064c** and **4064d** are shown in parentheses.

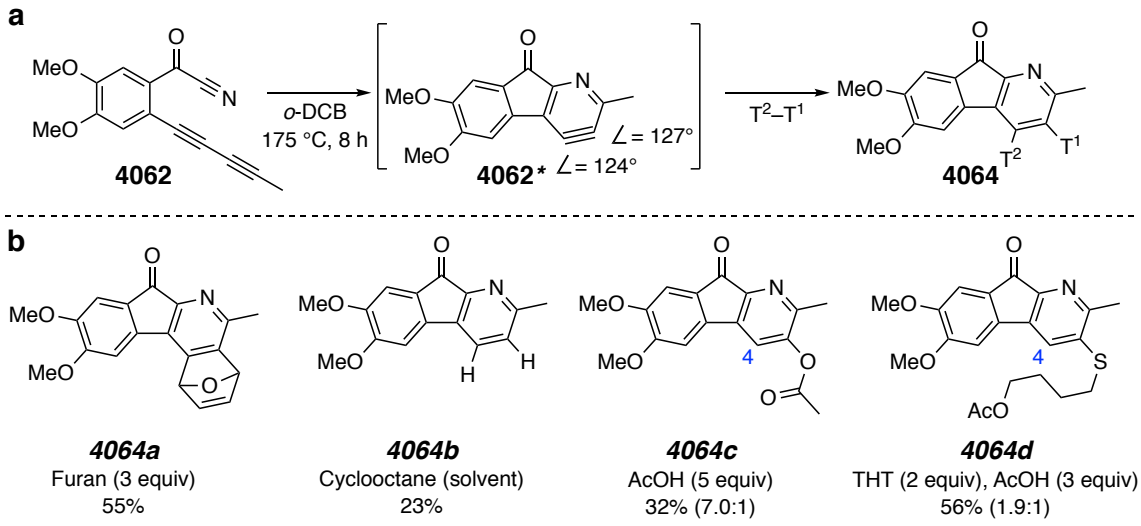

yields of **4064a**. This was shown to be caused by subsequent Diels–Alder reactions of the furan trap with **4064a** itself. While these side reactions have not occurred to a significant degree when trapping most HDDA benzynes with furan, it is not surprising that they occurred at the high temperature required for the aza-HDDA reaction of **4062**. This highlights a shortcoming of the aza-HDDA reaction with regard to its prerequisite high temperatures. Heating **4062** in cyclooctane solvent yielded the pyridine **4064b** by means of a concerted dihydrogen transfer from cyclooctane to the pyridyne intermediate.[46] While this has been shown to be an effective trap of several HDDA-generated benzynes, the yield of this reaction was disappointingly low (23%); the cause of this poor yield was not determined.

[126] Wittig, G.; Pohmer, L., Intermediäre Bildung von Dehydrobenzol (Cyclohexa-dienin). *Angewandte Chemie* **1955,** *67*, 348-348.

Products **4064c** and **4064d** are the results of trapping pyridyne **4062*** with protic, nucleophilic traps. Heating **4062** in the presence of 5 equivalents of glacial acetic acid produced pyridine **4064c** as a mixture of regioisomers (7.0:1 molar ratio, major product drawn in Figure 4.15b). The ratio of regioisomers in this reaction is noteworthy. Recall from Section 1.1.2.2 that the regioselectivity of a reaction in which an unsymmetrical aryne is trapped by a nucleophile is intimately related to the geometric distortion of the aryne—specifically, the difference between the bond angles on the formal triple bond of the aryne. The geometry of pyridyne **4062***, as determined by DFT calculations, shows a very modest degree of distortion, with a difference of about 3°. Accordingly, a nearly even distribution of regioisomers was expected for **4064c**. Nevertheless, acetic acid showed a clear preference for trapping at carbon 3 (compound drawn in Figure 4.15b) over carbon 4 (The structure of each isomer was determined through an NOE experiment). The reason for this is not immediately clear. It is possible that the inner "concave" portion the pyridine **4062*** results in significant steric hindrance in the vicinity of carbon 4, making it more difficult for nucleophiles to trap the pyridine at this position. At the same time, it should be noted that product **4064d** was formed as a much more even (1.9:1) ratio of regioisomers.

In addition to the surprising regioselectivity, it is also worth mentioning that this pyridiyne-trapping reaction with acetic acid was shown to be quite sensitive to the reaction conditions. The use of even slightly wet acetic acid predominantly gave rise to the benzofuranone product **4066** (Scheme 4.15). This presumably forms via the carboxylic acid intermediate **4065**, which itself could arise from the reaction of water with the acyl nitrile or from the mixed anhydride that results from the reaction of acetic acid with the acyl nitrile.

Scheme 4.15 | Side reaction of **4062** to form benzofuranone **4066** in the presence of acetic acid.

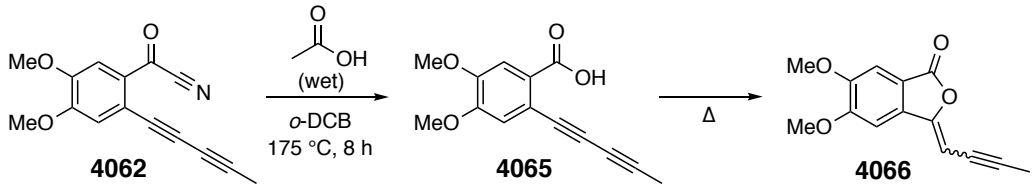

Heating **4062** in the presence of tetrahydrothiophene (THT) and acetic acid[53] resulted in the relatively clean formation of aryl thioether pyridine product **4064d** as a 1.9:1 molar ratio of regioisomers. The success of this reaction shows that certain three-component reactions can be carried out with this aza-HDDA substrate. This is quite important, given the value of multicomponent trapping reactions of arynes in accessing diverse molecularly complex structures.[127] Perhaps of greater insight is the observation that the soft thioether nucleophile of tetrahydrothiophene showed a greater preference for reacting with the pyridyne intermediate over the acyl nitrile. This is not particularly surprising, given the soft nature of arynes in general. However, it does demonstrate that, in spite of the problematic acyl nitrile functionality, substrate **4062** (as well as other potential acyl nitrile substrates) are compatible with sufficiently soft nucleophiles.

Despite these initial successes, it quickly became clear that the range of products obtainable from **4062** was quite limited. This is, in some cases, due to incompatibility of the trap or the product with the high temperature required for the reaction. However, the greater liability lies with the electrophilic acyl nitrile moiety, which excludes the use of many standard nucleophilic aryne traps. This is well-demonstrated through the failed attempt to use *n*-butylamine in order to access aminopyridine **4067** (Figure 4.16), which instead cleanly formed the amide **4068**.

Examples of pyridine products that could not be accessed in more than trace amounts are shown in Figure 4.16 b. In each of these cases, the reaction gave rise to several uncharacterized side products rather than a predominant, easily identified side product. The reasons for the failure of each reaction is not definitive, although—again—either the high reaction temperature or the acyl nitrile functionality seem to be the most likely causes of failure. In the cases of attempted trapping with catechol and mesitol, the modestly nucleophilic nature of the phenolic hydroxyl groups may render these traps incompatible with **4062**. Similarly, the attempted three component reaction with DABCO

[127] Bhojgude, S. S.; Biju, A. T., Arynes in transition-metal-free multicomponent coupling reactions. *Angew. Chem. Int. Ed.* **2012,** *51*, 1520-2.

Figure 4.16 | a) The result of heating substrate **4062** in the presence of *n*-butylamine and b) examples of pyridine products that were not successfully formed from the aza-HDDA reaction with **4062** (traps shown in parentheses below each product).

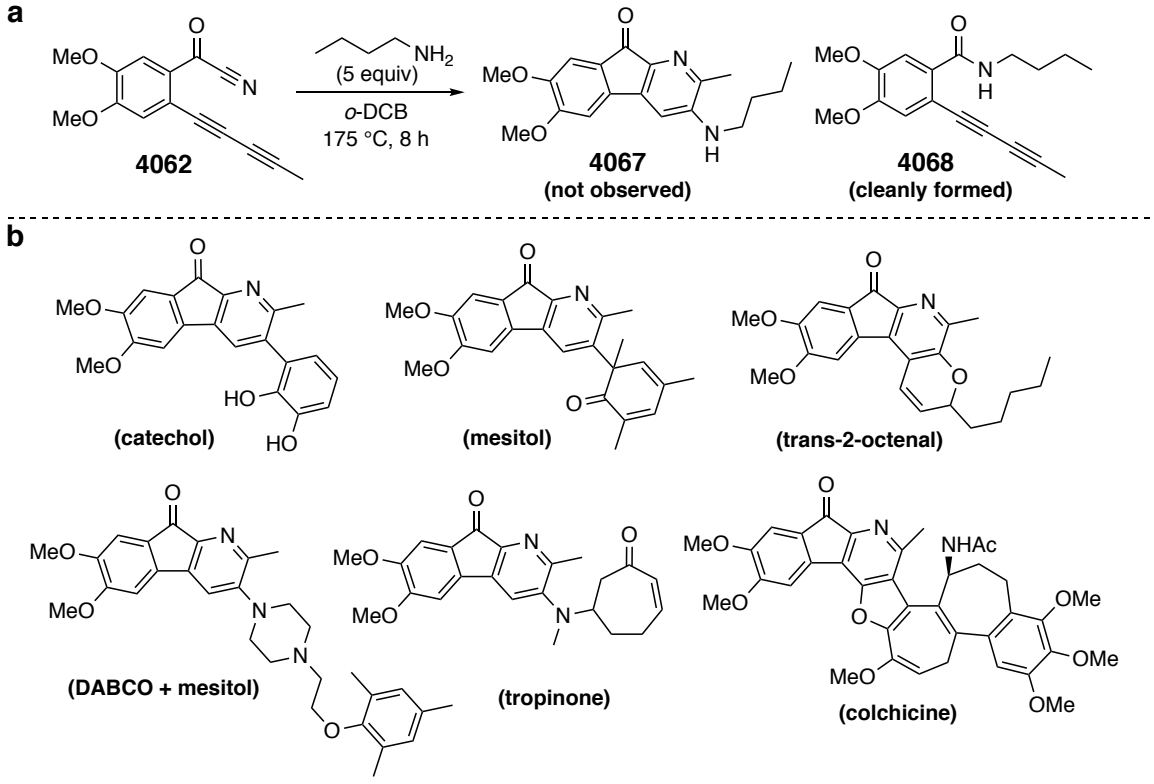

and mesitol traps likely failed due to a reaction between nucleophilic tertiary amine on DABCO and the acyl nitrile in **4062**.

Failure of the natural products tropinone and colchicine[55] to cleanly react with pyridyne could conceivably be attributed to either to the temperature or the acyl nitrile. Like DABCO, tropinone contains a nucleophilic tertiary amine. Colchicine is somewhat nucleophilic both at the carbonyl on its tropolone ring was well as the nitrogen atom on its amide functionality. Even in the absence of an acyl nitrile group, the chances of these structurally and functionally complex being sufficiently stable at such high temperatures seems slim.

The mere fact that various functionalized pyridine products were shown to be accessible in generally satisfactory yields through the aza-HDDA methodology was itself a great success and a significant step forward. However, it was clear that the number of

pyridine products accessible specifically from the substrate **4062** would be highly limited. Humbled by this sobering reality, but also bolstered by the demonstrated ability to access these pyridine products, I was determined to design and synthesize yet another substrate that could overcome these limitations and expand the synthetic utility of the aza-HDDA reaction.

4.5.2 A *gem*-Dimethylated Allylic Nitrile Substrate with a Cycloheptenyl Tether

Looking back on each of the previous aza-HDDA substrates tested *in silico* (Figure 4.11), there are a few well-defined structural features that allow for each substrate to undergo its corresponding aza-HDDA reaction at a lower temperature. For example, due to the Thorpe-Ingold effect, the presence of *gem*-dimethyl groups in substrates **4014** and **4015** is allows for the cycloaromatization of these substrates at approximately 220 °C. The significant activating effect of the acyl nitrile functionality is also demonstrated when comparing the benzylic *gem*-dimethylated nitrile **4015** to the benzoyl nitrile substrate **4017**. While they solely differ from each other at the benzylic position, the **4017** is predicted to cyclize to its aza-HDDA pyridyne **4017*** at a temperature that is over 40 °C lower than that for **4015**. Similarly, comparing the substrates **4017** and **4018** shows the significant improvement obtained by simply replacing a benzene tether present in substrate with a cycloheptene ring. These comparisons are shown in Figure 4.17.

However, it has also been demonstrated that certain functional groups, while lowering the activation energy for an aza-HDDA reaction, can also cause unintended problems. In particular, the acyl nitrile functionality—while allowing for a lower

Figure 4.17 | The effect of the acyl nitrile functionality (a) and the cycloheptene tether (b) on energy required for an aza-HDDA reaction to occur.

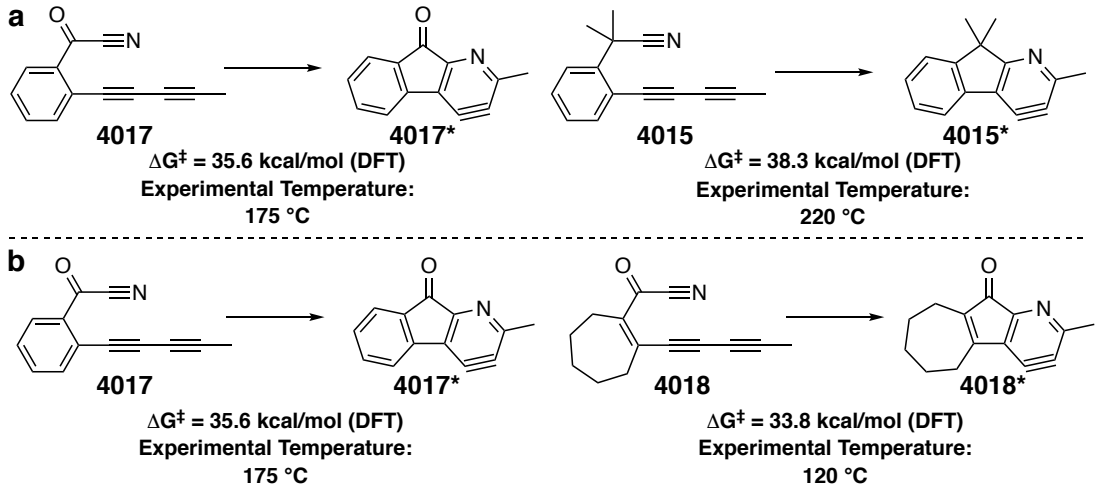

reaction temperature—caused inherent substrate instability of **4044** and was sensitive to several pyridyne-trapping compounds when substrate **4062** was tested. These limitations almost completely negated the benefit of the lower reaction temperatures.

With this experimental insight gained during the syntheses and reactions of the previous aza-HDDA substrates, I aimed to synthesize a substrate that made use of structural features that would lower the temperature necessary for an aza-HDDA reaction to occur—while at the same time avoiding any functionalities that would render the substrate unstable to the reaction conditions. Specifically, I chose to target a substrate that was tethered by a cycloheptene ring and fitted with a *gem*-dimethyl group (compound **4019**, Figure 4.11). Encouragingly, DFT calculations indicated that the aza-HDDA

Figure 4.18 | Calculated free energy of activation ($\Delta G^{\ddagger}$) for computational substrate **4019**.

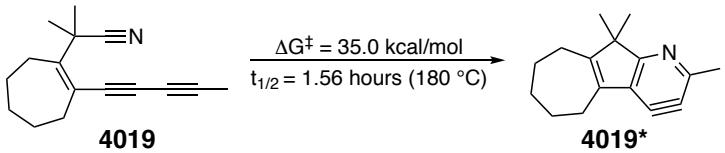

reaction of **4019** to its pyridyne **4019*** has a similar ($\Delta G^{\ddagger}$) to that for the benzoyl nitrile substrate **4017**. It was hoped that this "next-generation" substrate **4019** would cyclize at a

similar temperature while being sufficiently stable to react with a wider variety of trapping reagents.

As before, the actual test substrate that was to be experimentally investigated contained a siloxypropyl group on the diyne terminus (compound **4069**, Scheme 4.16). The initially planned synthesis of **4069** is shown in Scheme 4.16. The first three steps to access the allylic alcohol intermediate **4071** were straightforward. As was done in the synthesis of substrate **4044**, a Vilsmeier–Haack reaction was used to access choroenal **4046** from cycloheptenone (**4045**). As was also done before, **4046** was then subjected to a Sonogashira reaction—this time with ethynyltrimethylsilane to give the conjugated enal **4070** in 86% yield. Subsequent reduction of the aldehyde with $NaBH_4$ smoothly gave the allylic alcohol **4071** in 85% yield.

Scheme 4.16 | Planned synthesis of aza-HDDA test substrate **4069**.

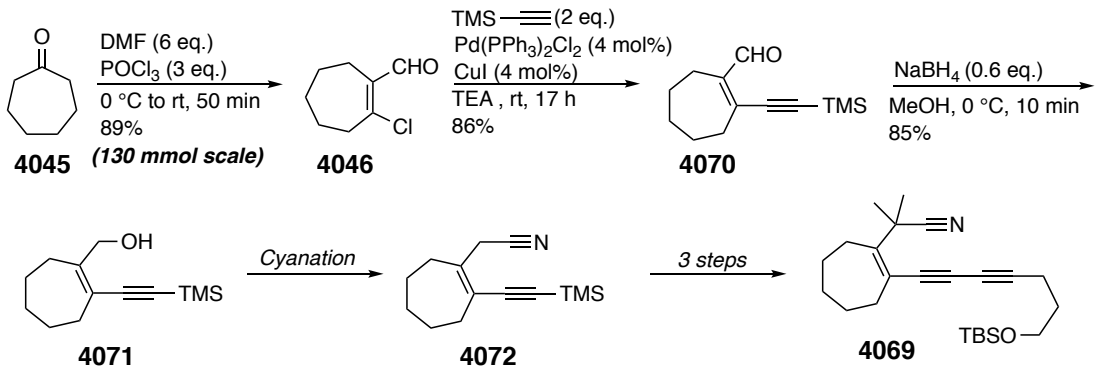

Conversion of allylic alcohols to better leaving groups and the subsequent displacement of these leaving groups with cyanide anions is a generally simple reaction that can be achieved by dozens of potential methods. Unfortunately, effecting this presumably simple transformation on alcohol **4071** to access the allylic nitrile **4072** proved to be more problematic than anticipated. Attempts were first made to access the allylic bromide **4073** (Scheme 4.17). Although the conjugated ene-yne moiety present in **4071** precluded any attempts to brominate with Br_2 or HBr, the Appel reaction[128] gave the desired product in 72% yield. The use of PBr_3 buffered with pyridine was also found to work, giving **4073** in 65% yield without the formation of the PPh_3 byproduct

[128] Appel, R., Tertiary Phosphane/Tetrachloromethane, a Versatile Reagent for Chlorination, Dehydration, and P-N Linkage. *Angew. Chem. Int. Ed.* **1975,** *14*, 801-811.

associated with the Appel reaction. Unfortunately, **4073** was observed to be rather unstable. It would extensively decompose when subjected to SiO_2 chromatography and would change from a light yellow oil to a black residue within a matter of hours (both when neat and when in solution). Perhaps due to this instability, exposure of **4073** to cyanide nucleophiles (NaCN, KCN, CuCN, and TMSCN) under an array of reaction conditions gave, at best, a small amount of desired product.

Scheme 4.17 | Failed attempt to access the allylic cyanide **4072** via the allylic bromide **4073**.

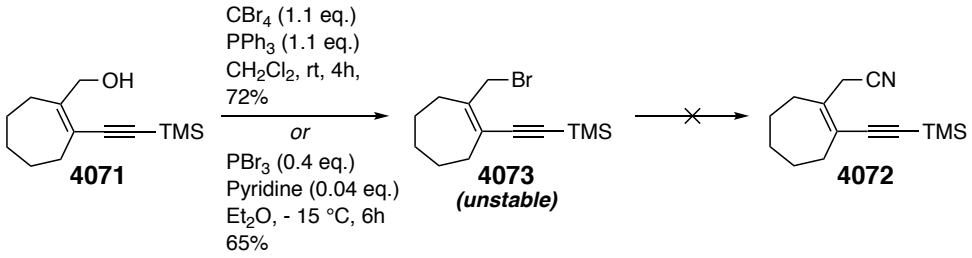

This failure prompted me to try the more direct approach of a Mitsunobu reaction,[129] which would convert the alcohol **4071** to the desired nitrile **4072** in one step. To avoid the dangers and complications of using hydrogen cyanide (HCN), I chose to use acetone cyanohydrin as a safer, more stable, and more easily handled source of HCN.[130] While this did give a small amount of nitrile **4702**, the yield was low (28%). The use of excess (~ 10 molar equivalents) DIAD, PPh_3 and acetone cyanohydrin did not give a higher yield (Scheme 4.18).

Scheme 4.18 | Attempted synthesis of nitrile **4072** through a Mitsunobu reaction.

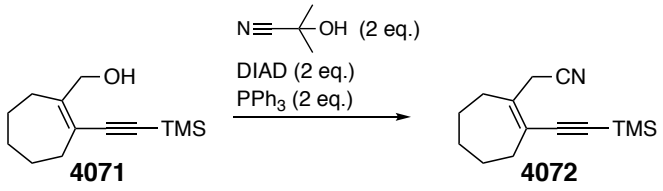

[129] (a) Mitsunobu, O.; Masaaki Yamada, Preparation of Esters of Carboxylic and Phosphoric Acid via Quaternary Phosphonium Salts. *Bull. Chem. Soc. Jpn.* **1967,** *40*. (b) Hughes, D. L., The Mitsunobu Reaction. *Org. React.* **1992,** *42*, 335.

[130] Wilk, B. K., A Convenient Preparation of Alkyl Nitriles by the Mitsunobu Procedure. *Synth. Commun.* **2006,** *23*, 2481-2484.

This Mitsunobu reaction, while inefficient, could likely be used to synthesize a sufficient amount of the nitrile **4072** to eventually access enough aza-HDDA substrate **4069** to run a small scale test reaction. However, the likelihood that this substrate would be used in several intermolecular pyridyne-trapping reactions meant that a more efficient synthesis of the **4072** would eventually need to be developed.

Scheme 4.19 | Synthesis of allylic mesylate **4074** that resulted in an unanticipated oxetane side product **4075**.

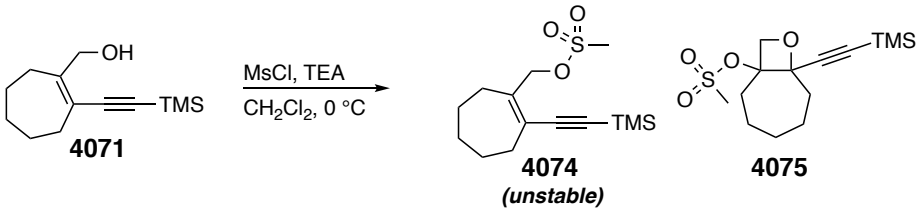

With this in mind, I again attempted to activate the alcohol **4071** for cyanation—this time as the allylic mesylate **4074** instead of the allylic bromide **4073**. While mesylation reactions of alcohols are generally straightforward, this transformation presented a few problems. Like the previous allylic bromide **4073**, the **4074** showed signs of instability. Furthermore, this reaction was prone to give side products. Besides the predictable problem of allylic chloride formation, this reaction would frequently yield another side product that was eventually determined to be the oxetane **4075** (Scheme 4.19). This transformation from **4071** to **4075** is noteworthy. It is without precedence in the literature—unsurprising given that it is an oxidation that occurs merely in the presence of mesyl chloride (MsCl) and TEA.

Despite these problems, it was found that the use of freshly prepared methanesulfonic anhydride (Ms_2O) cleanly yielded the allylic mesylate **4074** while limiting (but not completely eliminating) the formation of **4075**. Like allylic bromide **4073**, mesylate **4074** was subjected to several cyanation reaction conditions that were either irreproducible or gave unacceptably low yields. Fortunately, the use of biphasic reaction conditions in which **4074** was mixed with KCN and tetra-*n*-butylammonium bromide (TBAB) in CH_2Cl_2 and H_2O consistently yielded the desired nitrile **4072** in an acceptable 49% yield and on a sufficiently large scale.

Scheme 4.20 | Completion of the synthesis of aza-HDDA substrate **4069**.

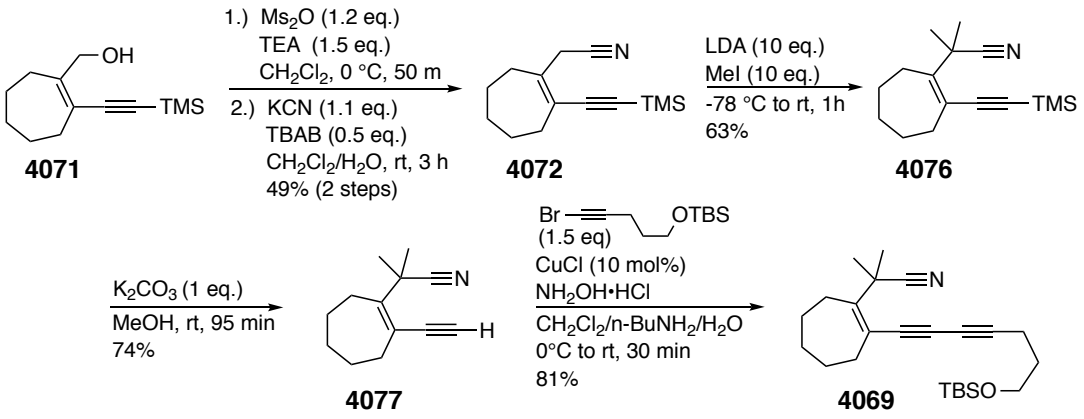

With this problematic cyanation reaction solved, the synthesis of aza-HDDA test substrate was swiftly completed (Scheme 4.20). Methylation of **4072** with excess LDA and MeI installed the important *gem*-dimethyl group and gave the intermediate **4076** in 63% yield. Desilylation to give terminal alkyne **4077** followed by a Cadiot–Chodkiewicz coupling finally yielded the test substrate **4069**.

4.5.3 Aza-HDDA Test Reaction of an Allylic Nitrile Substrate (4069)

Substrate **4069** was dissolved in *o*-DCB and heated at gradually increasing temperatures until signs of conversion to the anticipated pyridine product were observed by TLC. Promisingly, modest signs of conversion were observed after heating the solution at 150 °C for 2 hours. Heating at 175 °C for 7 hours resulted in full consumption of the starting material, as well as a golden yellow color of the solution which is characteristic of most clean HDDA reactions. While these were encouraging indications of a clean aza-HDDA reaction, the actual yield of the silyl pyridine **4078** turned out to be disappointingly low at 27% (Scheme 4.21).

Scheme 4.21 | Reaction of aza-HDDA test substrate **4069** to give silyl pyridine **4078** and *o*-DCB-trapped pyridine **4079**.

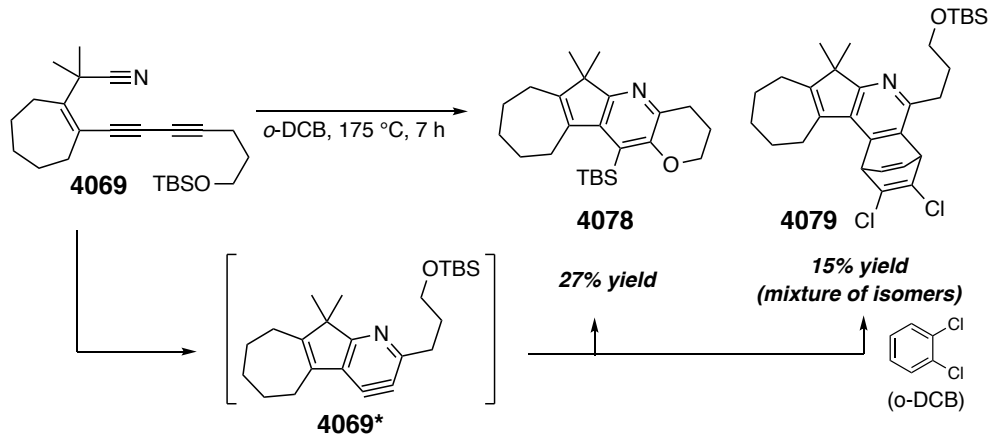

In spite of this initially devastating result, an additional aza-HDDA product **4079** was observed that lent insight into the reaction. Formation of this bridged dichloroalkene product is the result of a [4 + 2] cycloaddition between the *o*-DCB solvent and pyridyne **4069***. While this reaction did also occur when the previous aza-HDDA substrates were heated in *o*-DCB, no more than trace amounts of analogous dichoroalkene products were observed. Given the aromatic, electron deficient nature or *o*-DCB, this is to be expected. Indeed, *o*-DCB is a relatively common choice of solvent for HDDA reactions because of its general reluctance to trap benzyne. And yet, when substrate **4069**—which contains a covalently attached silyl ether trap—is heated in *o*-DCB, the dichloroalkene **4079** constitutes over a third of the HDDA product mixture. It is also worth remembering that the previously discussed benzoyl nitrile aza-HDDA substrate **4052** (which also contains a silyl ether trap), when heated under nearly the exact same conditions, cleanly yielded the expected silyl pyridine **4061**(Scheme 4.13).

This, of course, begs the question: why does **4069** give such a low yield of pyridine **4078**. One potential answer concerns the cycloheptene ring. While silyl ethers are normally effective aryne traps (when molecularly tethered to the aryne), the bulky TBS group could be an ineffective trap if the aryne is sterically hindered. In this case, it seemed possible that, in the TS structure **4069**‡, the cycloheptene ring was hindering the

approach of the *tert*-butylsilyl group to carbon 4 of the pyridyne ring (illustrated in Figure 4.19a).

Figure 4.19 | a) Proposed steric clash between the cycloheptene ring and the OTBS trap in TS structure **4069‡**. b) DFT-computed distances between carbon 4 and hydrogen substitutents on the tether in pyridynes **4019*** and **4017***. c) Results of heating aza-HDDA substrate **4069** in the presence of furan.

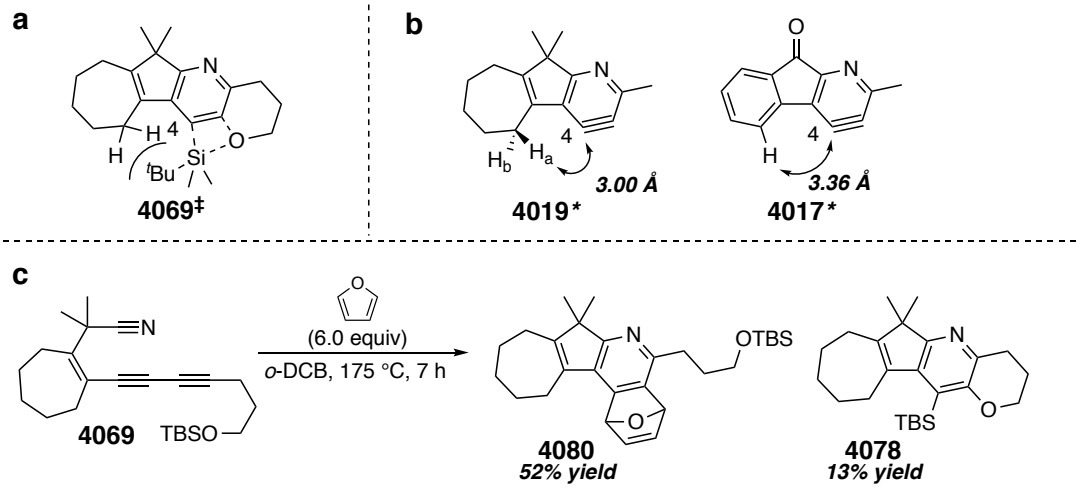

DFT calculations were utilized in order to investigate this hypothesis (Figure 4.19b). The greatest potential point of steric hindrance in TS structure **4069‡** is the adjacent methylene group on the cycloheptene ring. The distance between carbon 4 of the pyridyne and H_a in **4019*** is computed to be 3.00 Å (Boltzmann-averaged over four conformers of **4019***). In contrast, in pyridyne **4017*** (from benzoyl nitrile substrate **4017**) shows a much larger distance of 3.36 Å between carbon 4 and the adjacent hydrogen on the benzene ring. This difference of almost 0.4 Å is remarkable and lends significant credibility to the claim that the cycloheptene ring is responsible for the low yield of the trial aza-HDDA reaction with substrate **4069**.

With this insight, I chose to again heat a solution of **4069** in *o*-DCB—this time in the presence of several equivalents of a furan trap (Figure 4.19c). Gratifyingly, this yielded predominantly the furan-trapped product **4080** in 52% yield along with the silyl pyridine **4078** in 13% yield, giving a respectable combined aza-HDDA yield of 65%. Only a trace amount of the pyridine product resulting from trapping of the pyridyne with

o-DCB was observed in the crude ^{1}H NMR spectrum. It now seemed clear that pyridyne **4069*** was capable of reacting with molecular traps that were not sterically hindered and that this cyccloheptene-tether *gem*-dimethylated allylic nitrile substrate could be used to access a variety of functionalized pyridine products through the aza-HDDA reaction.

4.5.4 Intermolecular Trapping Reactions of an Allylic Nitrile Substrate (4019)

Several hundred milligrams of aza-HDDA substrate **4019** were synthesized for testing. Notice that in this case the experimental aza-HDDA substrate has the same structure as its computational analog in Figure 4.11. The synthetic route (not shown) was identical to that for the siloxypropyl-substituted substrate **4069**, save for the last step where bromopropyne was coupled to the terminal alkyne **4077** rather than ((5-bromopent-4-yn-1-yl)oxy)(*tert*-butyl)dimethylsilane (Scheme 4.20). Initially, the same reactions that yielded successful pyridine products from benzoyl nitrile substrate **4062** were attempted. These results are shown in Figure 4.20b (along with the analogous results from substrate **4062** in Figure 4.20c).

It can be seen that the yields of pyridine products from substrate **4019** (**4081a**–**4081d**) are generally higher than those from substrate **4062** (**4064a**–**4064d)**. Heating **4019** in the presence of furan gave pyridine **4081a** in 72% yield—a slightly higher yield than that obtained for **4064a** (although a slightly higher excess of furan was used). At the same time, the yield of dihydrogen transfer product **4081b** is over twice that obtained for the analogous product **4064b** (53% yield vs. 23% yield). A similar contrast is seen between acetic acid-trapped products **4081c** and **4064c**. The absence of a sensitive acyl nitrile moiety in **4081c** allows for a larger excess of acetic acid in the reaction, resulting in a yield of 65% (compared to 32% for **4064c**). Lastly, the yield of **4081d** is similar to that of **4061d**, although a different third component trap (methyl cyanoacetate, MCA) was used. These similar yields are likely a reflection of the compatibility of the acyl nitrile substrate with the soft tetrahydrothiophene nucleophile.

Figure 4.20 | a) Generation of reactive pyridyne intermediate **4019*** and its *in situ* trapping (by reaction with trapping compound T^2-T^1) to give functionalized pyridine **4081**. b) Selected examples of pyridyne products (**4081a**–**4081d**) produced from the aza-HDDA reaction of substrate **4019**; the molar ratios of regioisomers for products **4081c** and **4081d** are shown in parentheses. c) Comparison to analogous results from substrate benzoyl nitrile substrate **4062**.

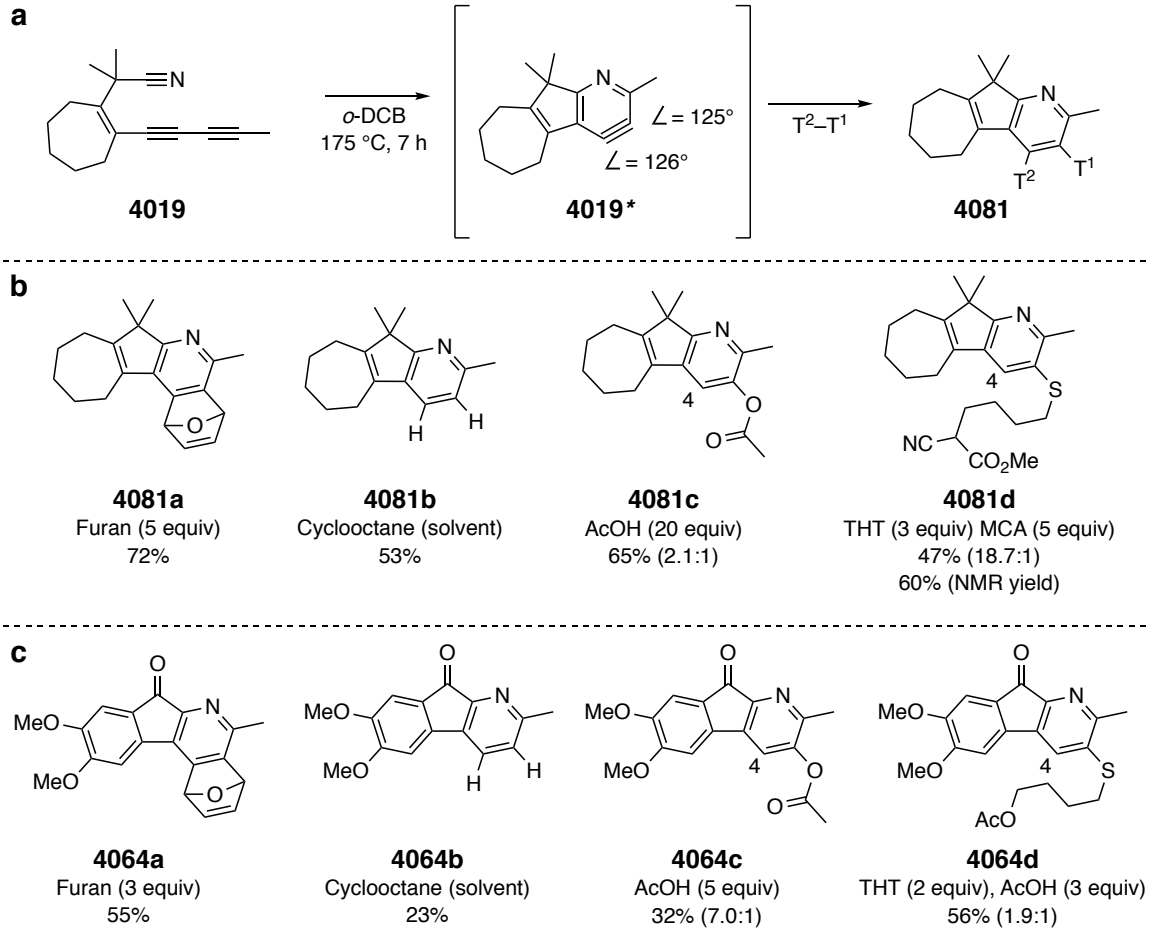

The relative degrees of regioselectivity should also be briefly noted. Recall from Section 4.5.3 that the cycloheptene ring in pyridyne **4019*** seems to introduce significant steric hindrance in the vicinity of carbon 4 (refer to Figure 4.19b) and appeared to be responsible for the poor aza-HDDA yield of silyl ether-trapped pyridine product **4078** (from substrate **4069**). For this same reason, when trapping pyridyne **4019*** with a compound that can result in two isomeric pyridine products (i.e. two distinct regioisomers

that are functionalized either at carbon 3 or carbon 4), one would expect a much higher ratio of products than what is seen from the benzoyl nitrile substrate **4062**—in spite of the absence of significant distortion in pyridyne **4019***. Looking specifically at products **4081c** and **4081d**, one would expect the formation of a significantly higher amount of pyridine product that results from nucleophilic attack at C3 (these specific isomers of **4081c** and **4081d** are those drawn in Figure 4.20b).

While this isomer is indeed the predominant isomer formed of pyridines the **4081c**, the isomeric ratio (2.1:1) is paradoxically *lower* than that observed for pyridines **4064c** (7.0:1). While acetic acid is not a particularly bulky trap and, accordingly, might not be expected to yield a particularly high ratio of isomeric pyridine products, one would at least expect it to give a higher ratio than what is seen for pyridine products **4081c**. This anomalous result remains unexplained. In stark contrast, product **4081d** was formed in a remarkably higher ratio (18.7:1) than product **4064d** (1.9:1). This is not particularly surprising. The nucleophile in this three-component reaction that actually engages the pyridyne intermediate **4019*** is tetrahydrothiophene. The steric clash between the cycloheptene ring of **4019*** and the α-methylene of tetrahydrothiophene is likely the source of such high regioselectivity.

With the encouraging yields of products **4081a–4081d**, additional reactions were attempted (Figure 4.21b). Products **4081e** and **4081f** were both obtained as a mixture of regioisomers. They were synthesized by heating substrate **4019** in the presence of *n*-butylamine and mesitol (2,4,6-trimethylphenol), respectively. The modestly high ratio of **4081e** regioisomers (7.7:1), again, likely results from steric hindrance of carbon 4 by the cycloheptene ring. The low isomer ratio of products **4081f** is quite surprising, given the bulky nature of the mesitol trap. This reason for this low ratio remains unclear.

However, more important than the ratio of regioisomers for these two products are their yields. Recall that previous reactions to trap pyridine generated from benzoyl nitrile substrate **4062** with *n*-butylamine and mesitol were unsuccessfully attempted. With substrate **4019**, not only are the corresponding pyridine products observed, but they are formed in good yields—clearly showing the positive effect of replacing an acyl nitrile moiety with a *gem*-dimethyl nitrile.

Figure 4.21 | a) Generation of reactive pyridyne intermediate **4019*** and its *in situ* trapping (by reaction with trapping compound T^2-T^1) to give functionalized pyridine **4081**. b) Additional examples of pyridyne products (**4081e**–**4081i**) produced from the aza-HDDA reaction of substrate **4019**; the molar ratios of regioisomers for products **4081e** and **4081f** are shown in parentheses.

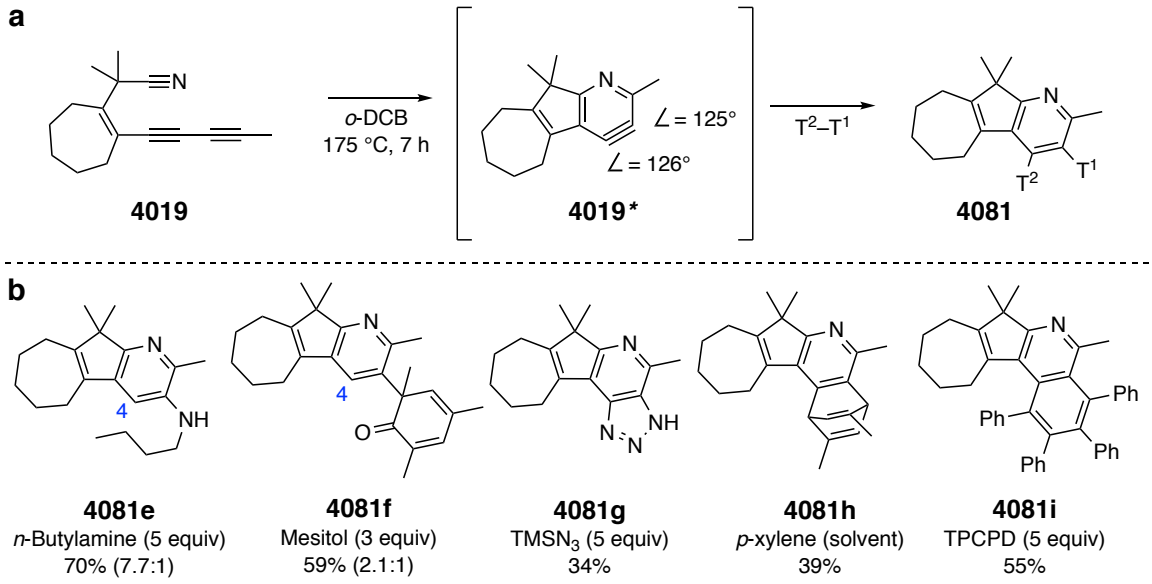

Additional aza-HDDA products **4081g–4081i** are also shown in Figure 4.21b. The triazolopyridine **4081g** is formed in a modest 34% yield through a formal dipolar cycloaddition between azidotrimethylsilane ($TMSN_3$) and pyridyne **4019***, followed by cleavage of the trimethylsilyl group in the resulting product during chromatographic purification.[45] Much like *ortho*-dichlorobenzene in Scheme 4.21, *para*-Xylene is capable of trapping arynes as a 4π diene in a [4 + 2] cycloaddition. Indeed, heating **4019** in *para*-xylene results in the formation of pyridine **4081h** in 39% yield as one sole isomer. Lastly, the isoquinoline derivative **4081i** was formed in 55% yield through the use of a tetraphenylcyclopentadienone (TPCPD) trap. This highly conjugated, fluorescent product is formed through an initial [4 + 2] cycloaddition between the pyridyne **4019*** and TPCPD to give norbornenone adduct **4082** followed by a chelotropic elimination to extrude carbon monoxide, which occurs readily under the high temperature of this aza-

HDDA reaction(Scheme 4.22).[131] This cascade has been effectively employed with HDDA-generated *benzynes* to access naphthalene derivatives with promising photophysical properties[57] the extension of this trapping reaction to the aza-HDDA reaction is, accordingly, of significant potential value.

Scheme 4.22 | Formation of isoquinoline product **4081i** from pyridyne **4019*** and TPCPD.

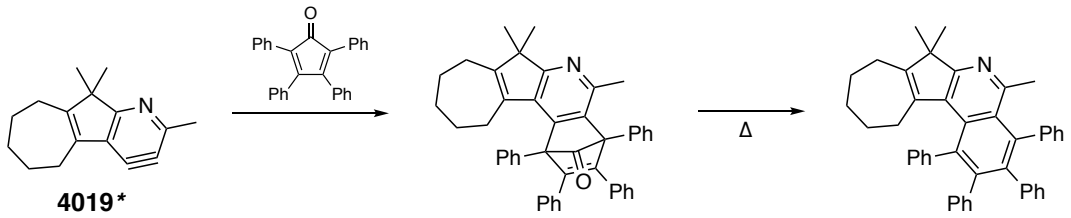

4.5.4 Failed Aza-HDDA Reactions of Substrate 4019

While the use of nitrile **4019** as an aza-HDDA substrate has clearly allowed for a greater diversity of accessible pyridine products, it is still necessary to acknowledge several attempted reactions that failed to yield their desired products in more than a trace yield. These anticipated products of these failed reaction reactions are shown in Figure 4.22. The molecular traps for five of these products (catechol, octenal, DABCO/mesitol, tropinone, and colchicine) were also heated in the presence of benzoyl nitrile substrate **4062**. The failure of these traps to produce a significant amount of pyridine product from either aza-HDDA substrates **4062** or **4019** may indicate that they are simply incompatible with the reaction temperature rather than the substrates themselves.

The use of norbornene and *tert*-butanol similarly failed to yield benzocyclobutene and phenyl ether products, respectively. Although it is initially tempting to consider that the benzocyclobutene product underwent a thermal ring-opening to an *o*-xylylene

[131] Pérez, I. P.; Agustín, C.; Diego, P.; Enrique, G.; Dolores, 1,7-Naphthodiyne: a new platform for the synthesis of novel, sterically congested PAHs. *Chem. Commun.* **2016,** *52*, 5534-5537.

intermediate,[132] this 4π conrotatory[133] reaction seems rather unlikely for the bridged ring product. Ultimately, I can offer no clear rational for the failure of these products to form.

Figure 4.22 | Pyridine products that were not accessible in meaningful yields from the aza-HDDA reaction of nitrile **4019**. Molecular traps are shown in parentheses below each product.

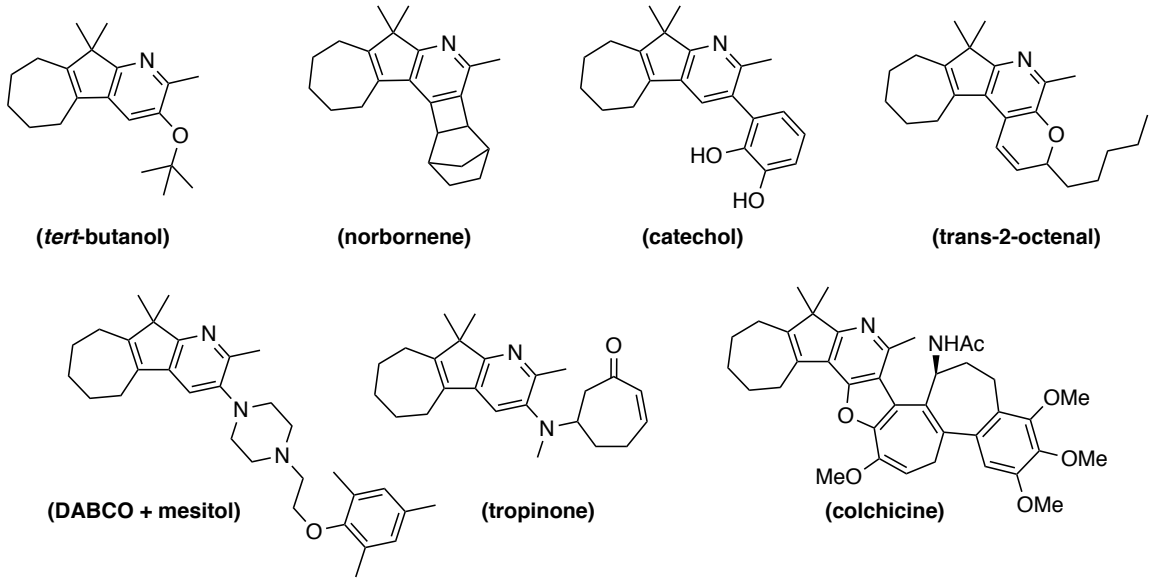

[132] Mehta, G.; Kotha, S., Recent chemistry of benzocyclobutenes. *Tetrahedron* **2001,** *57*, 625-659.
[133] Woodward, R. B.; Hoffmann, R., Conservation of Orbital Symmetry. *Angew. Chem. Int. Ed.* **1969,** *8*, 781-853.

Chapter 5. The Class II Aza-HDDA Reaction

5.1 Preface: The Class II Aza-HDDA Reaction

Having seen the results of the aza-HDDA reactions of the previous chapter, in which the substrates consisted of nitriles molecularly tethered to 1,3-diynes, it is natural to consider the following question: what would happen if one were to change the position of the nitrile? In other words, if one were to make a substrate—perhaps analogous to one of those seen in Chapter 4—in which an alkyne was tethered to a conjugated cyanoalkyne, would it also undergo an aza-HDDA reaction?

This hypothetical process, which shall be referred to as a class II aza-HDDA reaction, is illustrated in Figure 5.1b with the class I aza-HDDA reaction (Figure 5.1a). In contrast to the class I reaction, in which a functionalized pyridine **5002** is formed from nitrile-diyne **5001** *via* the 3,4-pyridyne intermediate **5001***, the class II aza-HDDA reaction would proceed through an isomeric 2,3-pyridyne intermediate **5003*** to form a pyridine product **5004** that is functionalized at the 2- and 3-positions. Also notice that, while the pyridynes resulting from class I aza-HDDA reactions can react with molecular traps in either an inter- or intramolecular fashion, class II pyridynes can only be trapped intermolecularly—as the lack of an open valency on the cyanoalkyne nitrogen of **5003** precludes the use of a covalently-attached trap.

Figure 5.1 | The class I (a) and class II (b) aza-HDDA reactions

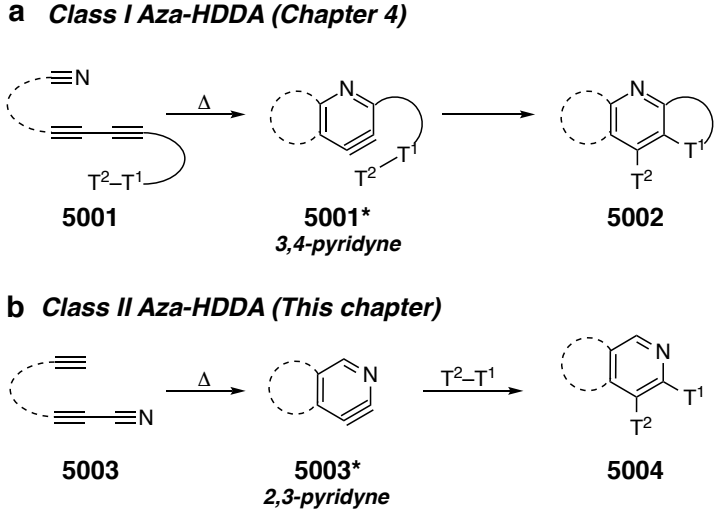

There are several reasons for which it worth exploring this potential extension of the aza-HDDA reaction. One reason, of course, is to simply see if it works. Because the class I and class II processes are, in a sense, isomeric, one may think that they should have similar energetics. Accordingly, one might conclude that class II substrates (i.e. **5003**) should successfully participate in aza-HDDA reactions simply because several class I substrates have been shown to work. This basic reasoning itself provides significant incentive to research the class II aza-HDDA reaction. Another (more practical) reason to initiate investigations into this chemistry is based simply in the idea of synthetic diversity. One of the primary driving forces behind the aza-HDDA research project in general (as well as behind HDDA chemistry as a whole) is to facilitate access to diverse arene products. The simple fact that the class II aza-HDDA reaction would allow for the synthesis of functionalized pyridine products that are isomeric to those obtained from the class I aza-HDDA reaction is also sufficient reason to see if it will work.

5.2 Some Initial Considerations on the Reactivity of Class II aza-HDDA Substrates

Again considering the fact that the class I and class II aza-HDDA reactions are "isomeric," one might assume that these two reactions would behave in a similar manner. For example, it might be assumed that for a set of isomeric aza-HDDA substrates—with one being a class I substrate and the other a class II substrate—the temperatures required for the cyclization to each corresponding pyridyne would be similar. Similarly, one might assume that each class of substrate would give similar results—i.e. that reactions which worked well with a class I substrate would work similarly well for its isomeric class II substrate.

This thinking would be somewhat misguided. Although isomeric, class I and class II substrates ultimately have different moieties that could manifest themselves in different ways under the conditions of any aza-HDDA reaction. Perhaps the most notable difference is the cyanoalkyne moiety present in any class II substrate. While the class I substrate **5005** tested in Chapter 4 (compound **4019** in Chapter 4) is capable of reacting with several nucleophilic traps to give pyridine products (e.g. **5006**), the conjugated

cyanoalkyne moiety in its analogous class II substrate **5007** could act as a potent Michael acceptor (to give, for example, **5008**). Additionally, **5007** could undergo a thermal Alder–Ene reaction to give allene product **5009**. (Figure 5.2).[134]

Figure 5.2 | Successful aza-HDDA reaction of class I substrate **5005** with a nucleophilic trap (Nu) in contrast with a potential Michael addition of the same nucleophilic trap to the analogous class II substrate **5008** and an Alder–Ene reaction to give **5009**.

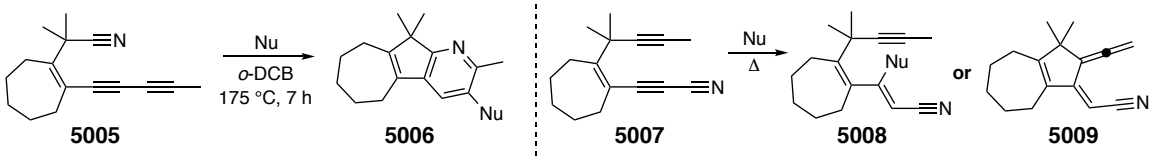

5.3 Insight from Preliminary DFT Calculations

5.3.1 Relative Energetics of Isomeric Pyridynes

One must indeed be hesitant to draw conclusions on the potential reactivity of any class II aza-HDDA substrate based simply on the observed reactivity of its analogous class I substrate. Having said this, it should still be noted that DFT calculations do at least show a similar change in free energy (i.e the difference in free energy between an aza-HDDA substrate and its corresponding pyridyne) between class I and class II aza-HDDA reactions. This is demonstrated in the calculated free energies of reaction (ΔG_{rxn}) for the cyclizations of octa-5,7-diynenitrile (**5010**) and octa-2,7-diynenitrile (**5011**) to pyidynes **5010*** and **5011***, respectively (Figure 5.3). The differences in free energies between these two processes ($\Delta\Delta G_{rxn}$) is merely 3.4 kcal•mol^{-1}. While this value is not insignificant (the ratio of pyridynes **5011*** to **5010*** in equilibrium would be about 250:1), the ΔG_{rxn} for each of these reactions pale in comparison to what is seen for the cycliczation of the triyne HDDA substrate nona-1,3,8-triyne (**5012**) to its benzyne **5012*** (Figure 5.3).

5.3.2 Geometric Distortion of Pyridyne Species

While the isomeric pyridynes **5010*** and **5011*** have similar free energies, they also were shown to have drastically different geometries (Figure 5.4). As was

[134] Karmakar, R.; Yun, S. Y.; Chen, J.; Xia, Y.; Lee, D., Benzannulation of Triynes to Generate Functionalized Arenes by Spontaneous Incorporation of Nucleophiles. *Angew. Chem. Int. Ed.* **2015,** *54*, 6582-6586.

Figure 5.3 | Isomeric aza-HDDA substrates **5010** (class I) and **5011** (class II) have similar calculated changes free energies (ΔG_{rxn}) in their cyclizations to pyridyne products **5010*** and **5011***, respectively. The analgous triyne HDDA reaction of **5012** to **5012*** is far more exergonic.

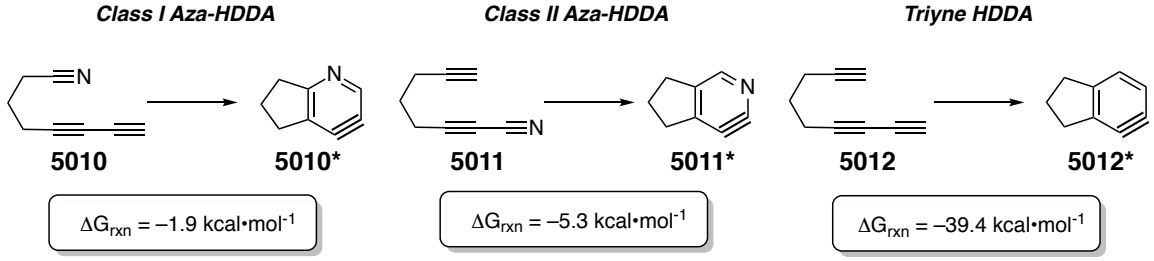

discussed in Chapter 4, 3,4-pyridynes tend to have a low level of geometric distortion. Specifically, the bond angle difference ($\Delta\theta$) between the two carbons on the formal triple bond of 3,4-pyridynes (shown as carbons "a" and "b" in Figure 5.4) is generally quite small. This is, indeed, observed in the structure of 3,4-pyridyne **5010***. In stark contrast, the 2,3-pyridyne **5011*** is a structure that shows tremendous geometrical distortion, with a $\Delta\theta$ value of 56.8°! The relative distortions of aryne structures **5010*, 5011*, and 5012*** are reflected in the computed geometries of the unsubstituted aryne species benzyne, 3,4-pyridiyne, and 2,3-pyridyne (Figure 5.4b).

Figure 5.4 | a) Computed geometric distortion in arynes **5010*, 5011*, and 5012*** as shown by the differences in bond angles ($\Delta\theta$) for carbons a and b. b.) Similar geometric distortions shown in unsubstituted benzyne, 3,4-pyridyne, and 2,3-pyridyne.

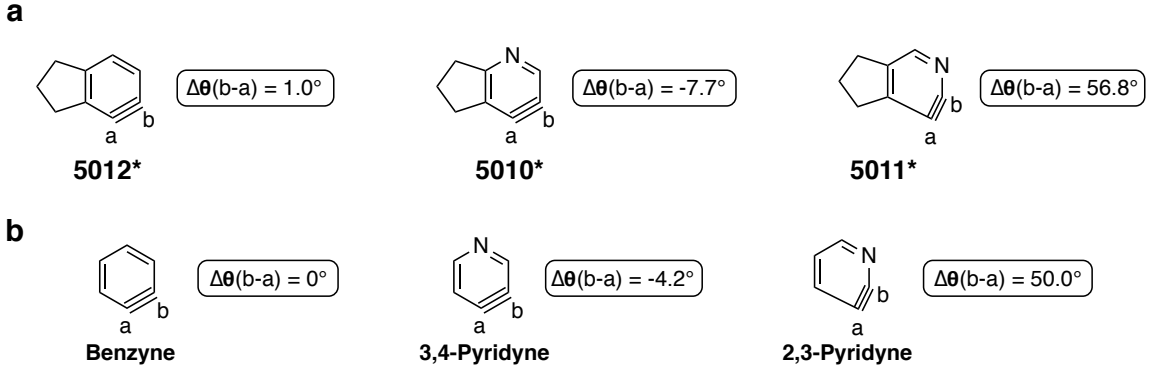

Recall, again, that the regioselectivity of an aryne trapping reaction is strongly dependent on the distortion of the aryne that is being trapped. Also recall that the more obtuse angle of a distorted aryne is more prone to nucleophilic attack or, in the case of traps that react with the aryne in a concerted fashion, the more electron rich portion of the trapping moiety. Given the tremendous distortion of 2,3-pyridynes, one would accordingly expect for class II aza-HDDA reactions to yield practically only one of two possible regioisomeric pyridine products.

5.3.3 Relative Energetics of the Class I and Class II Aza-HDDA Reactions

With sufficient motivation to initiate research into the class II aza-HDDA reaction, I first considered potential substrates. Two potential class II aza-HDDA substrates **5013** and **5014** are shown in Figure 5.5. Notice that these two substrates are analogous (although not strictly isomeric) to two of the class I aza-HDDA substrates (**4017** and **4015**) that were studied in Chapter 4. Indeed, these two class II candidate structures were chosen because of this analogy; even if they did not successfully form pyridine products from an aza-HDDA reaction, this failure would still be insightful.

Figure 5.5 | Candidate class II Aza-HDDA substrates **5013** and **5014** , along with their previously studied class I analogs **4017** and **4015**.

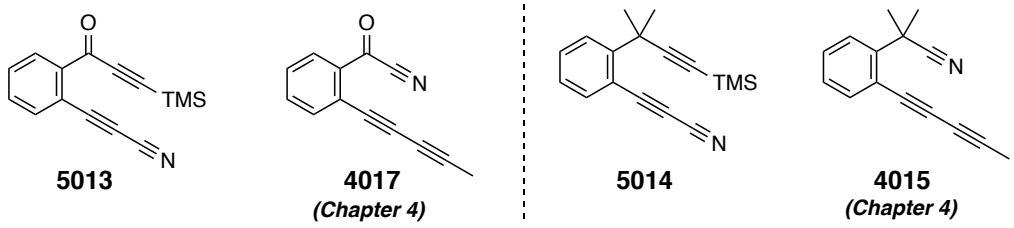

I first attempted to compute the free energy of activation ($\Delta G^{\ddagger}$) and the free energy of reaction (ΔG_{rxn}) for the cycloaromatization of **5013** to its pyridiyne **5013*** (Figure 5.6). It can first be seen that this transformation is only slightly exergonic (-6.9 kcal•mol^{-1})—similar to the cyclization of **5011** to **5011*** in Figure 5.3. It can also be seen that the pyridyne **5013**, like **5011***, has a highly distorted geometry (with a bond angle difference of nearly 60°).

Far more notable—and far more relevant to the potential synthetic use of this substrate—is the $\Delta G^{\ddagger}$ value of 30.0 kcal•mol^{-1}, which corresponds to a half-life of 25

minutes at 130 °C. This indicates that the aza-HDDA reaction of **5013** should occur at a temperature nearly 100 °C lower than the temperatures of several of the class I reactions in Chapter 4! Compare **5013** to its class I analog **4017**, which has a $\Delta G^{\ddagger}$ value of 35.6 kcal•mol^{-1} and whose experimental analog **4062** was found to cyclize at about 175 °C! This tremendous decrease in the activation energy in going from a class I to a class II aza-HDDA reaction provided more than enough incentive to further investigate the synthetic potential of the class II aza-HDDA reaction.

Figure 5.6 | Calculated relative free energy values of candidate class II aza-HDDA substrate **5013**, its corresponing pyridyne (**5013***), and the concerted TS structure that connects them (**5013**‡). Images of the computed structures for **5013**‡ and **5013*** are also shown.

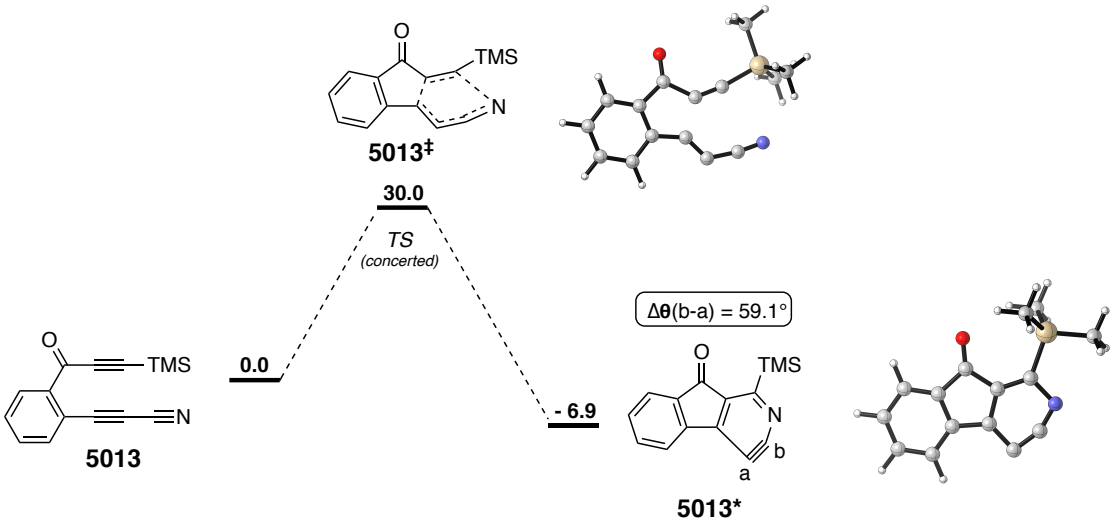

5.3.4 Mechanistic Insight into the Class II Aza-HDDA Reaction

The apparently concerted nature of this transformation is also worth mentioning. Notice that, although I have indicated in Figure 5.6 that the cycloaromatization of **5013** to **5013*** occurs through a concerted process, the geometry of the TS structure (**5013**‡) is highly asynchronous; it almost looks like a geometry that one would expect to see for a stepwise TS structure. However, a calculation of the intrinsic reaction coordinate (IRC) indicated that **5013**‡) does not pass through any energetic minima (i.e. intermediates) on the potential energy surface (PES) in its path to pyridyne **5013***. Additionally, the TS structure **5013**‡ was not calculated to be an open shell species, meaning it had no radical

or carbene character. Although this itself is not definitive proof that the TS structure is part of a concerted process (e.g. it could be a partially charged TS structure leading to a zwitterionic intermediate), it is consistent with a concerted process. Attempts to locate a diradical or zwitterionic intermediate linking **5013**‡ to **5013*** yielded no results.

One could speculate on a relationship between the apparently concerted yet highly asynchronous mechanism of this cycloaromatization and its relatively low calculated $\Delta G^{‡}$. Recall from the discussion in Sections 3.3.2 and 4.2 that the inherently stronger nature of the C≡N bond when compared to the C≡C bond makes its participation in cycloaromatization reactions much more difficult. Further recall that (according to DFT calculations) the class I aza-HDDA reaction seems to occur through a concerted process where formation of the new C–C bond occurs concomitantly with that of the new C–N bond (in other words, it is has a low degree of asynchronicity)—meaning that the nitrile is significantly "engaged" in the rate-determining step. Compare this with the nitrile in the TS structure **5013**‡, where both the alkynes are bending toward each other but the nitrile seems to be completely unengaged. It seems reasonable that this lack of engagement of the nitrile in the TS structure, and the consequent lack of distortion of the strong C≡N bond, is largely responsible for the relatively low $\Delta G^{‡}$ value for the cycloaromatization of **5013** to **5013***.

An analogous two-dimensional potential energy surface for the cycloaromatization of the other potential aza-HDDA substrate **5014** to its pyridyne **5014*** is shown in Figure 5.6. Although **5014** is almost structurally identical to the previous substrate **5013**, it seemed likely to give different *in silico* results due to the replacement of a ketone with a *gem*-dimethyl group in the important benzylic position. In spite of this, the free energy of activation ($\Delta G^{‡}$) is just 0.8 kcal•mol^{-1} higher than for the cycloaromatization of **5013**; this $\Delta G^{‡}$ value of 30.8 kcal•mol^{-1} gives a calculated half-life of 27 minutes at 140 °C. Such an almost insignificant difference suggests that the ketone moiety does *not* have a strong activating effect in the class II aza-HDDA reaction—which is similar to the triyne HDDA reaction but in contrast to the class I aza-HDDA reaction. Further similarities between the aza-HDDA reactions of **5013** and **5014** are seen

in the geometric distortion of aryne **5014***, which is almost the same as that of **5013***. The geometries of TS structures **5013**‡ and **5014**‡ are also very similar.

Figure 5.6 | Calculated relative free energy values of candidate class II aza-HDDA substrate **5014**, its corresponing pyridyne (**5014***), and the concerted TS structure that connects them (**5014**‡). Images of the computed structures for **5014**‡ and **5014*** are also shown.

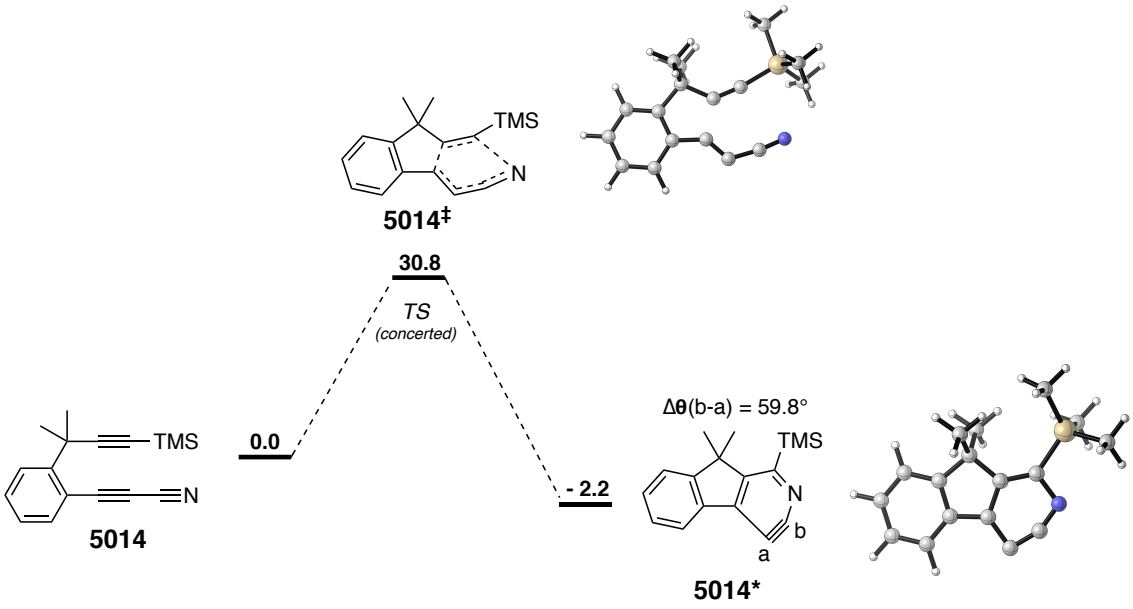

5.4 Synthesis of the First Class II aza-HDDA Test Substrate

5.4.1 First Attempted Synthetic Route

Synthetic efforts to a class II aza-HDDA substrate began with the attempted synthesis of compound **5015** (Scheme 5.1). As was the case with several of the previously described aza-HDDA substrates in Chapter 4, **5015** has minor structural differences from its analog that was investigated by DFT calculations (i.e. **5013**). Specifically, there are two methoxy groups on the 4- and 5-positions of the aromatic ring which allow for easier, more scalable purification of several synthetic intermediates (the methoxy groups in substrates **4020** and **4062** in Chapter 4 were present for the same reason). Additionally, the TMS group of *in silico* substrate **5013** is replaced by a TBS group in target **5015** to allow for a selective desilylation of a bis-silylalkyne intermediate in the planned synthesis.

Aldehyde **5016** was cleanly converted to alcohol intermediate **5017** in 92% yield when mixed with TBS-acetylide and an alkyllithium base. Exposure of **5017** to K_2CO_3 in

MeOH selectively cleaved the trimethylsilyl group. The secondary alcohol of this intermediate was then converted to an acetate, which was intended to act as a protecting group during the installation of the cyanoalkyne moiety.

Scheme 5.1 | Initially planned synthetic route to potential class II aza-HDDA substrate **5015**.

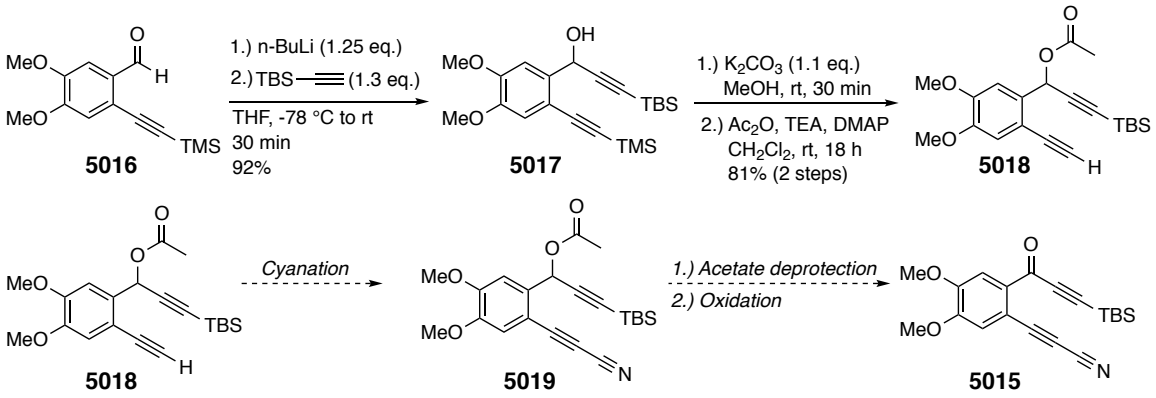

The resulting intermediate **5018** was to undergo a cyanation reaction to install the key cyanoalkyne. Although cyanoalkynes are not ubiquitous in synthetic organic chemistry, there several synthetic methods that can be used to access this moiety. Admittedly, most of these methods have rather niche applications and are rarely used.[135] Two of the more commonly used methods to synthesize cyanoalkynes, both of which start from a terminal alkyne, are shown in Figure 5.7. The first of these methods proceeds simply by deprotonation of a terminal alkyne followed by exposure of the resulting acetylide ion to an electrophilic cyano reagent (most commonly tosyl cyanide, cyanogen bromide, cyanogen chloride, phenyl cyanate, or cyanobenztriazole) (Figure 5.7a). The other method first halogenates the alkyne (either through iodination or bromination) to give a haloalkyne intermediate that is capable of cross-coupling with a metal cyanide reagent (cuprous cyanide being the most frequently used) (Figure 5.7b).

[135] For examples, see: (a) Casarini, A.; Dembech, P.; Reginato, G.; Ricci, A.; Seconi, G., Terminal 1-halo-1 and 1-pseudohalo-1-alkynes via bis(trimethylsilyl)peroxide (BTMSPO) promoted Umpolung transfer of Halides and pseudohalides. *Tetrahedron Lett.* **1991,** *32*, 2169-2170. (b) Kim, J.-G.; Lee, E. H.; Jang, D. O., One-pot synthesis of conjugated alkynenitriles from aldehydes. *Tetrahedron Lett.* **2007,** *48*, 2299-2301. (c) Yamamoto, Y.; Asatani, T.; Kirai, N., Copper-Catalyzed Stereoselective Hydroarylation of 3-Aryl-2-propynenitriles with Arylboronic Acids. *Advanced Synthesis & Catalysis* **2009,** *351*, 1243-1249. (d) Vatèle, J.-M., One-Pot Oxidative Conversion of Alcohols into Nitriles by Using a TEMPO/PhI(OAc)2/NH4OAc System. *Synlett* **2014,** *25*, 1275-1278.

Figure 5.7 | Two common methods used to synthesize cyanoalkynes from terminal alkynes and their potential applications to the synthesis of intermediate **5019**.

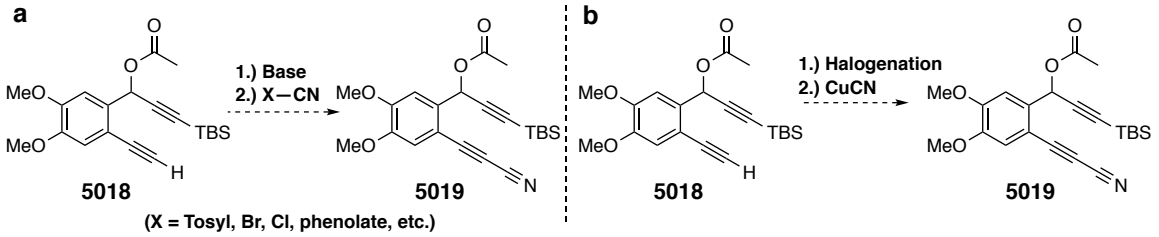

Application of the former method to terminal alkyne **5018** did not yield successful results, regardless of which cyanating reagent was used. In retrospect, the methine C–H bond, which is activated by the adjacent phenyl, alkynyl, and acetate groups, is likely more acidic than the terminal alkyne—making this methodology incompatible with **5018**. Attention was accordingly turned to the halogenation and cyanation of **5018** (Scheme 5.2). Initial attempts to iodinate the terminal alkyne with n-BuLi/I_2 and N-iodosuccinimide (NIS)/$AgNO_3$ met with failure. This was likely due to the afformentioned acidic methine group and the sensitivity of the alkynylsilane group to silver nitrate, respectively. Fortunately, the use of a morpholine-iodine complex in benzene[136] cleanly gave the desired iodoalkyne in 89% yield. Subsequent mixing of this intermediate with cuprous cyanide (CuCN) and lithium iodide (LiI) in refluxing THF over 2 days gradually yielded the desired cyanoalkyne **5019** (52%).

Scheme 5.2 | Synthesis of cyanoalkyne **5019** and failed acetate deprotections to give **5020**.

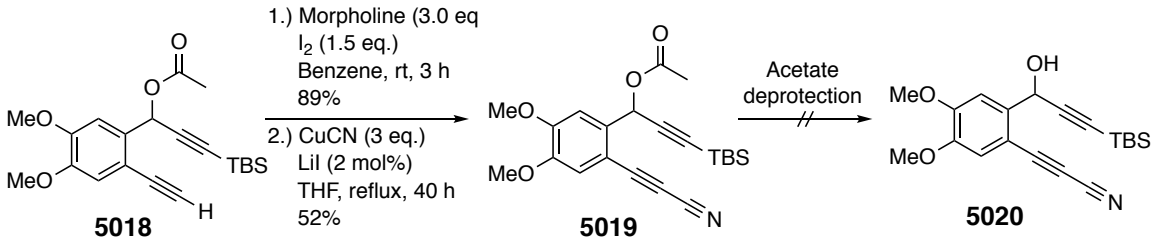

[136] Southwick, P. L.; Christman, D. R., Reactions of Iodine—Amine Complexes with Unsaturated Compounds. II. An Investigation of the Scope of the Reaction with the Iodine—Morpholine Complex. *J. Am. Chem. Soc.* **1953,** *75*, 629-632.

While **5019** was only 2 steps away the target substrate **5015**, the acetate deprotection needed to access the alcohol **5020** proved to be problematic. A series of test reactions using standard acetate deprotection protocols that were run under both acidic and basic conditions with various combinations of solvents at different temperatures either resulted in low conversion or extensive decomposition. Even the mild conditions of KCN in EtOH[137] resulted in a complex mixture of unidentified products. Although frustrating, this was not particularly surprising. While **5019** should be stable, the propargylic alcohol of **5020** can be expected to isomerize to a mixture of enones even under mildly basic or acidic conditions, due to the highly activate methine C–H bond.

As was discussed before, the cyanoalkyne Michael acceptor might also be expected to present problems. Indeed, this was seen in an attempt to deprotect the acetate group of **5019** through the use of Otera's catalyst.[138,139] Exposure of **5019** to several

Scheme 5.3 | Exposure of **5019** to Otera's catalyst ultimately yields cyclic ether **5021** through an intramolecular Michael addition.

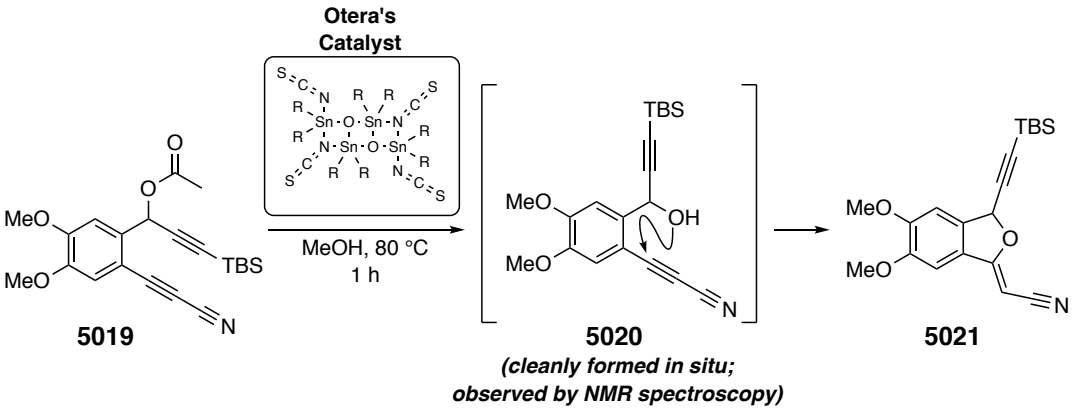

[137] Mori, K.; Tominaga, M.; Takigawa, T.; Matsui, M., A Mild Transesterification Method. *Synthesis* **1973,** *1973*, 790-791.

[138] (a) Otera, J.; Yano, T.; Kawabata, A.; Nozaki, H., Novel distannoxane-catalyzed transesterification and a new entry to α, β-unsaturated carboxylic acids. *Tetrahedron Lett.* **1986,** *27*, 2383-2386. (b) Otera, J.; Danoh, N.; Nozaki, H., Novel template effects of distannoxane catalysts in highly efficient transesterification and esterification. *J. Org. Chem.* **1991,** *56*, 5307-5311.

[139] For a good (albeit somewhat dated) overview of the use of organotin catalysts in transesterification reactions, refer to section VIII of the following review: Otera, J., Transesterification. *Chem. Rev.* **1993,** *93*, 1449-1470.

equivalents[140] of a variant of Otera's catalyst initially gave clean conversion to alcohol **5020**, which was observed by NMR analysis of the reaction mixture. Despite this initial gratifying observation, **5020** was subsequently observed to undergo an intramolecular Michael addition to give the 5-membered oxacyclic product **5021** under the relatively mild reaction conditions. Unfortunately, this reaction occurred at a similar rate to that for the initial acetate deprotection, making it difficult to isolate a useful amount of the alcohol **5020**.

5.4.2 Second Attempted Synthetic Route

Although there exist countless potential acetate deprotection conditions that could be tried, I opted to take my chances with a different protecting group. Specifically, I hoped that the secondary TES ether could be selectively cleaved in the presence of the alkynyl TBS silane in the intermediate **5024** (Scheme 5.4). Synthesis of this intermediate parallels that of the analogous acetylated intermediate **5019**. The bis-silylated terminal alkyne intermediate **5022** was synthesized in 65% over 3 steps from the same aldhehyde starting material **5016** that was used before. From here, **5022** was iodinated with morpholine-iodine complex, the iodoalkyne product of which was coupled with CuCN to give the cyanoalkyne intermediate **5023** in a yield of 70% over 2 steps.

Scheme 5.4 | Successful synthesis of alcohol **5020**

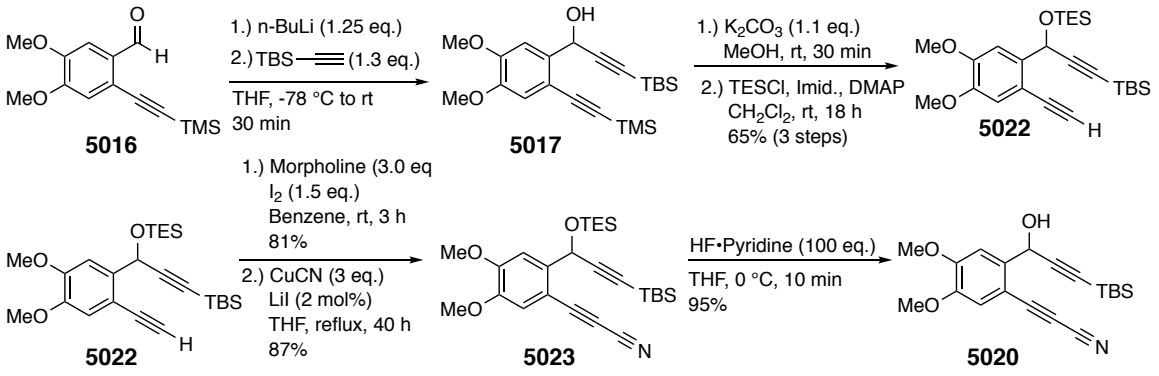

Fortunately, it was quickly discovered that exposure of **5023** (0.01 M in THF) to excess HF-Pyridine complex not only selectively cleaved the TES ether in the presence

[140] Several equivalents were used because the catalyst was several years old and this was a trial experiment. Otera's catalyst is usually capable of effectively catalyzing transesterification reactions at very low loadings.

of the TBS alkynylsilane, but did so without leading to side reactions or decomposition. The reaction was worked up simply by diluting in ethyl acetate and washing the resulting solution several times with water,[141] resulting in a 95% yield of alcohol **5020**.

The final oxidation to aza-HDDA substrate **5015** with manganese dioxide (MnO_2) gave surprising results. Although **5015** was accessed in 43% yield, the formation of a purple side product was also observed. Although it is difficult to confidently determine the structure of this side product without an X-ray crystal structure, analysis of the ^{13}C NMR spectrum seemed to suggest the indenone structure **5024** A search of the literature gave no precedence for such a transformation and the author of this thesis finds himself incapable of proposing a reasonable mechanism.

Scheme 5.5 | Oxidation of alcohol **5020** with MnO_2 to give aza-HDDA substrate **5015** and tentatively assigned side product **5024**.

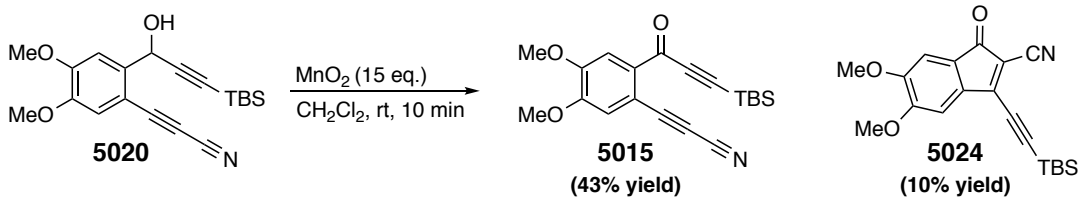

5.5 First Attempts To Carry Out Class II Aza-HDDA Reactions

5.5.1 Successful Reactions

In spite of the synthetic setbacks, I was ultimately able to obtain several hundred milligrams of **5015**. Because an intramolecular trap could not be molecularly tethered to the cyano moiety, the substrate **5015** was first heated in the presence of compounds that could trap the anticipated 2,3-pyridyne in an intermolecular fashion. It was first found that, when dissolved in *o*-DCB (0.01 M) and heated at 120 °C in the presence of 20 equivalents of furan, **5015** was cleanly converted to the desired product **5025a** in 81% yield (Figure 5.8)! The half-life of this substrate at 120 °C was determined to be approximately 30 minutes—reasonably close to the computed half-life of 25 minutes at 130 °C.

[141] Attempts to neutralize the hydrogen fluoride with a mildly basic workup of $NaHCO_3$ resulted in the formation of the aforementioned cyclic ether **5021**.

tert-Butyl alcohol was tested next as a pyridyne trap. Not only did this trap give the pyridine **5025b** in a high 75% yield but additionally showed the practically exclusive formation of one of two possible regioisomers. Specifically, the *tert*-butyl alcohol trap showed an extremely high preference for nucleophilic attack at C2 (as determined by an NOE experiment). Recall that the analogous HDDA substrate which was tested *in silico* **5013** was anticipated to yield a 2,3-pyridiyne intermediate **5013*** that was highly distorted (Figure 5.6). The structure of the 2,3-pyridyne **5015*** that is accessed from substrate **5015** was found to be similarly distorted by DFT calculations (Figure 5.8). Accordingly, one would indeed expect for the trapping of this pyridyne to be highly regioselective, with a strong preference for nucleophilic attack at the C2-position—as was observed experimentally.

Figure 5.8 | Initial pyridine products **5025a**–**5025d** formed from aza-HDDA reactions of class II substrate **5015**.

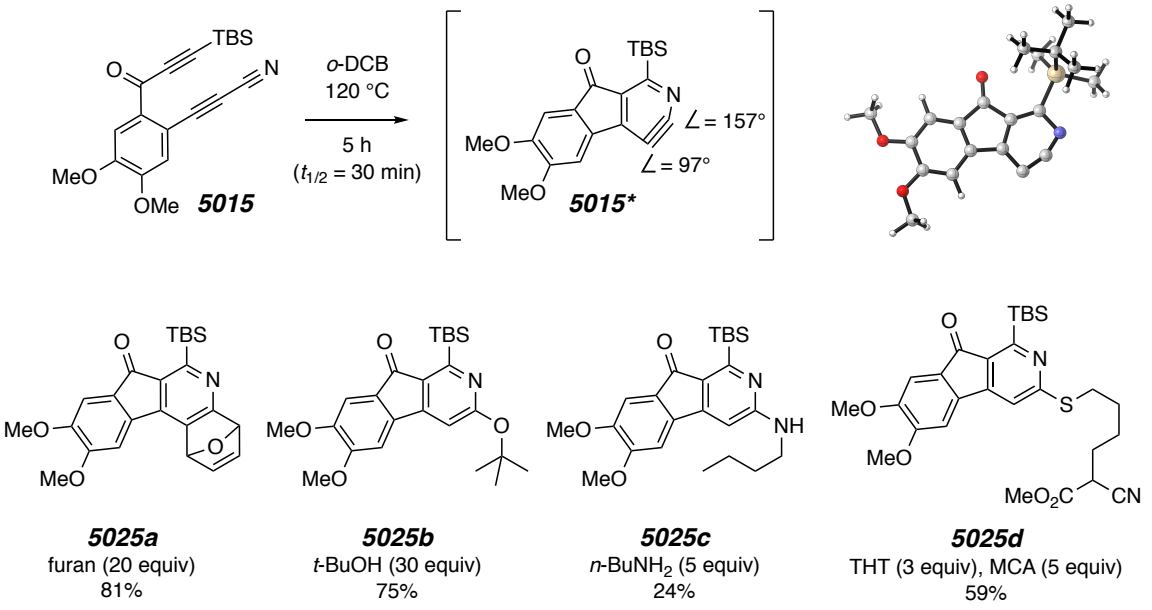

This high regioselectivity was also observed when *n*-butylamine was used to trap the pyridyne intermediate, yielding the 2-aminopyridine product **5025c**. However, the yield for this reaction was much lower (24%). It is suspected that the unhindered primary amine trap (in constrast to the *tert*-butyl alcohol nucleophile) formed side products from conjugate addition to one or both of the two potential Michael acceptors in substrate

5015. The use of a bulkier amine trap (piperidine) was also attempted to address this problem but gave even worse results, possibly due to the increased basicity of the amine.[142]

As was done with previous class I aza-HDDA substrates, a three-component reaction with a sulfide trap was attempted. Heating **5015** in the presence of tetrahydrothiophene and methyl cyanoacetate gave the aryl sulfide product **5025d** in 59% yield. Again, the regioisomer of **5025d** drawn in Figure 5.8 was the only HDDA product that was detected. This reaction is particularly notable for the apparent selective mode of trapping by tetrahydrothiophene; despite the potential for this soft nucleophile to react with either of the soft yne-one or cyanoalkyne Michael acceptors, product **5025d** is still formed in good yield.

In attempts to access more structurally and functionally complex pyridine products from the aza-HDDA reaction aza-HDDA reactions were also attempted with natural products.[55] The reaction of **5015** with tropinone gratifyingly gave the amino pyridine product **5025e** in 68% yield (Figure 5.9a). This transformation occurs through initial trapping of the pyridyne **5015*** with the tertiary amine group present in tropinone to form betaine **5025e'**. This intermediate is poised to undergo an intramolecular Hofmann elimination (arrows drawn in Figure 5.9a) to afford **5025e**. The cleanliness of this transformation is also noteworthy when considering that, while the primary *n*-butylamine and secondary piperidine traps failed to give their corresponding functionalized pyridine products, the tertiary amine moiety of tropinone works effectively. As expected, this reaction resulted in the formation of one sole regioisomer.

An attempt to trap pyridyne **5015*** with colchicine produced the highly functionalized pyridine product **5025f**—albeit in a very modest 32% yield. This product results from a [1,5]-H shift of the intermediate **5025f'**. The reaction, as expected, resulted in the observation of only one of two possible regioisomers—although this isomer was isolated as a mixture of conformers. It can be speculated that high regioselectivity of this

[142] The addition of 5.0 molar equivalents of piperidine to a solution of substrate **5015** in *o*-DCB gave a black solution within a matter of seconds at room temperature.

Figure 5.9 | Reaction of aza-HDDA substrate **5015** with natural products tropinone (a) and colchicine (b).

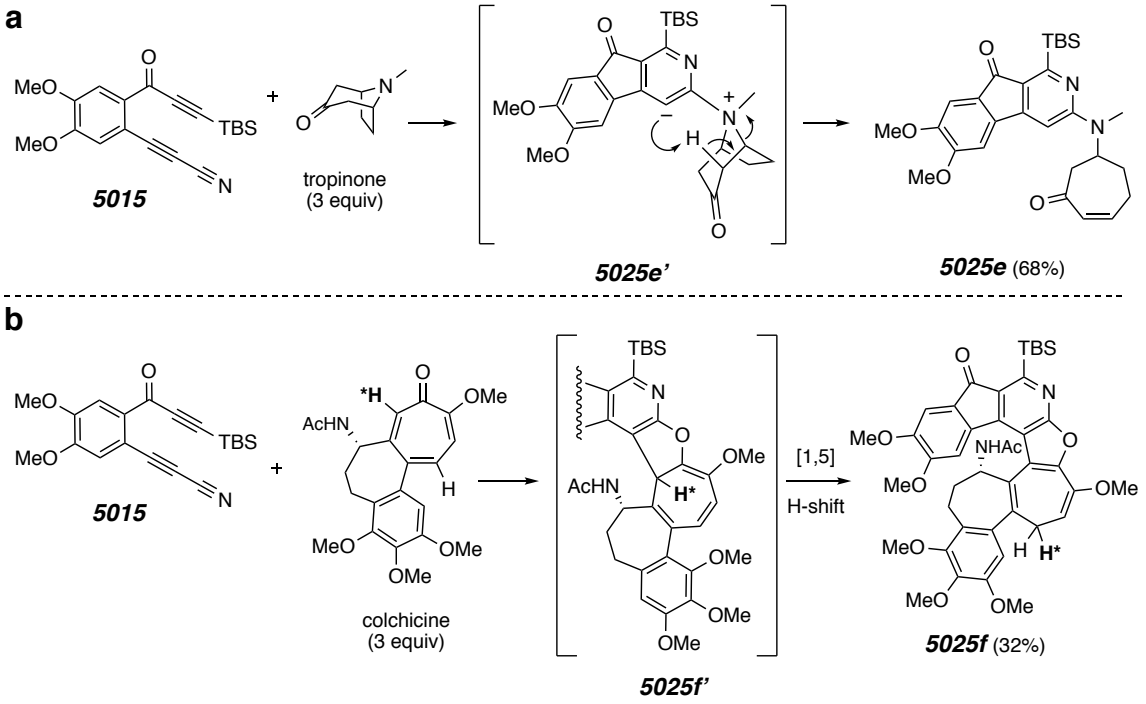

reaction is partially responsible for the low yield. Although the regioselectivity of aryne-trapping reactions is strongly dependent on the geometric distortion of the aryne (as has been discussion several times at this point), steric hindrance can also exert a significant effect—particularly when the aryne shows little distortion.[143] Observe that the electronically favored regioisomer **5025f** is in a "U" shape and appears to be sterically crowded. The alternate isomer, which is in an "S" shape (not shown), would be less crowded. This may simply be a reaction where the product heavily favored by steric factors and the product heavily favored by electronic factors are in contrast with each other—resulting in a low reaction yield.

5.5.2 Failed Reactions

Examples of products which could not be accessed in more than trace amounts are shown in Figure 5.10. Strangely, when pyridyne **5015*** was generated in cyclooctane solvent, the anticipated dihydrogen transfer product **5025g** was not observed. It seems

[143] Recall that this was seen to some extent in the reactions of the class I aza-HDDA substrates in Chapter 4.

possible that the highly distorted geometry of the pyridyne may make it difficult for concerted hydrogen transfer to occur. Similarly, the product of tetraphenylcyclopentadienone trapping **5025h** formed only as part of a mixture of uncharacterized products—further hinting at an incompatibility of the highly distorted pyridyne **5015*** with symmetrical concerted traps.[144] At the same time, if this were the case, one would expect that the furan-trapped pyridine product **5025a**—which also results from a concerted trapping mechanism—would not form in such a high yield.

The failed attempts to access products **5025i–5025m** suggest an incompatibility of substrate **5015** with acidic traps. While acetic acid is normally a very effective benzyne trap—and cleanly formed a pyridine product from class I aza-HDDA substrate **4019** (Chapter 4), it failed to yield a tractable amount of **5025i**. Similarly, catechol proved to be an ineffective trap to form **5025j**. Although the reaction of tetrahydrothiophene and

Figure 5.10 | Examples of products which were not successfully synthesized in more than trace amounts from the aza-HDDA reaction with substrate **5015**.

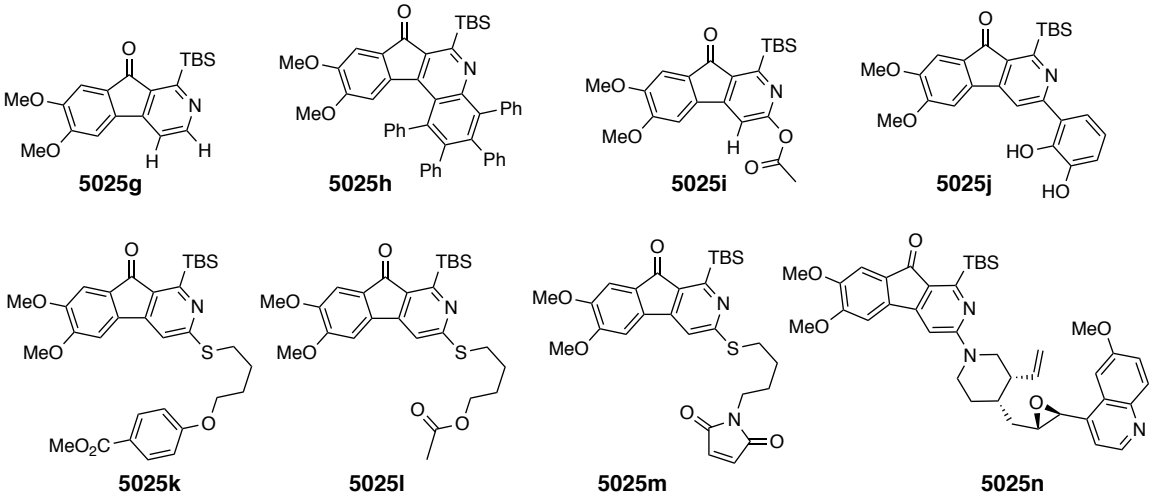

methyl cyanoacetate with pyridyne **5015*** cleanly formed product **5025d** (Figure 5.8), analogous three-component products were not observed when the third component was acidic (specifically, methyl paraben, acetic acid, and maleimide to form products **5025k**, **502lj**, and **5025m**, respectively).

[144] The anticipated product of this reaction would actually not be **5025h** but rather its carbonyl-bridged precursor that would give **5025h** through a chelotropic elimination of carbon monoxide.

Lastly, attempts to trap pyridyne **5015*** with the natural product quinine (also a tertiary amine trap) to access **5025n** were also unsuccessful—despite the clean formation of **5025e** from tropinone. On a related note, attempts at three-component reactions in which DABCO and a third protic nucleophile[52] were used as traps also met with failure (not shown in Figure 5.10).

5.5.3 Summary of Implications from the Experimental and Theoretical Results

Considering several of these failed attempted aza-HDDA reactions, it seems plausible that the class II aza-HDDA substrate scope could be significantly expanded by replacing the apparently sensitive alkynyl ketone (yneone) moiety of **5015**. Recall from Section 5.3 that the two candidate class II aza-HDDA substrates **5013** and **5014**, whose reaction energetics were investigated by DFT calculations, were very similar to each other from a structural point of view; the former was functionalized with a ketone in the benzylic position while the later contained a *gem*-dimethyl group. More importantly, the aza-HDDA free energy of activation ($\Delta G^{\ddagger}$) for the two substrates was computed to be quite similar (30.0 kcal•mol^{-1} for **5013** and 30.8 kcal•mol^{-1} for **5014**).

The implications of these results are that substrate **5014** should undergo an aza-HDDA reaction at a temperature similar to that observed for **5013**. At the same time, the replacement of the problematic yneone moiety with a more stable propargylic *gem*-dimethyl group may allow for a wider use of pyridyne-trapping compounds. Accordingly, I moved forward with cautious optimism to design and test this one additional class II aza-HDDA substrate.

5.6 Synthesis of a *gem*-Dimethylated Class II Aza-HDDA Test Substrate

5.6.1 First Attempted Synthetic Route

The initially planned synthetic route to an analog (compound **5026**) of the computational substrate **5014** is shown in Scheme 5.6. As was the case with substrate **5015**, **5025** contained two methoxy groups and a TBS group, both of which were not present in the computed substrate. As before, these groups were in the experimental target for the purpose of synthetic convenience.

The route in Scheme 5.6 was largely designed based on the fact that the dibromo starting material **5027**, which was functionalized appropriately for future reactions, could

Scheme 5.6 | Initially Planned Synthesis of Aza-HDDA test substrate **5026**.

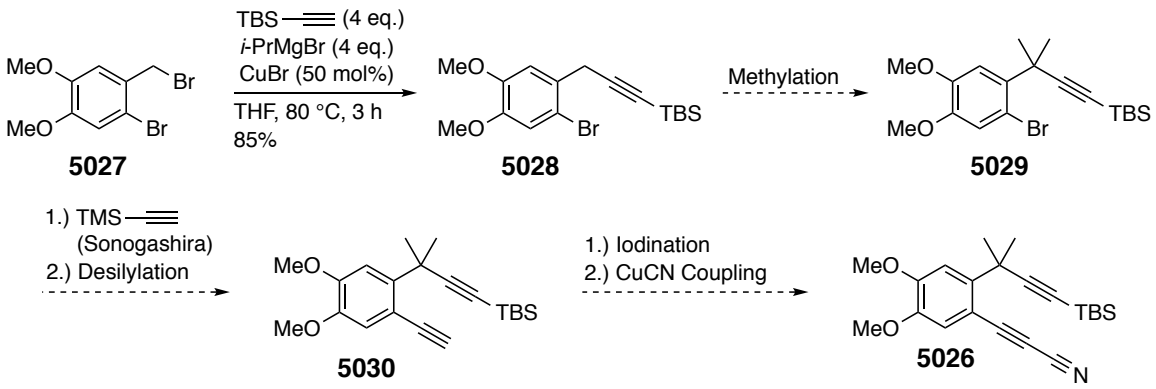

be quickly and conveniently synthesized on scale (refer to Section 4.4.1). In spite of this, and in spite of the confidence that the cyanoalkyne moiety could be efficiently installed on **5030**, it was clear that this synthesis could be challenging to execute effectively. As one example, the Sonogashira reaction to couple aryl bromide **5028** with TMS acetylene would likely be difficult—as the arene contained two electron donating groups and the bromide was ortho to hindered quaternary center.

Likely even more difficult would be the installation of the key *gem*-dimethyl group (i.e. conversion of **5028** to **5029**). While the methylene was both benzylic and propargylic—which should make it sufficiently acidic for several conventional strong bases to deprotonate[145]—the electron donating methoxy groups significantly reduce this acidity. Additionally, the methylene is adjacent to a bulky bromine group. Adding to these problems is the fact that two, not one, methyl groups must be installed.[146]

---

[145] Deprotonation and substitution on propargylic, benzylic methylenes is precedented but not very common. For a few examples, see (a) Miura, K.; Okajima, S.; Hondo, T.; Nakagawa, T.; Takahashi, T.; Hosomi, A., Acid-Catalyzed Cyclization of Vinylsilanes Bearing a Hydroxy Group: A New Method for Stereoselective Synthesis of Disubstituted Tetrahydrofurans1. *J. Am. Chem. Soc.* **2000,** *122*, 11348-11357. (b) Yan, J.; Zhu, J.; Matasi, J. J.; Herndon, J. W., Relative Asymmetric Induction in the Intramolecular Reaction between Alkynes and Cyclopropylcarbene−Chromium Complexes: Stereocontrolled Synthesis of Five-Membered Rings Fused to Oxygen Heterocycles. *J. Org. Chem.* **1999,** *64*, 1291-1301. (c) Feldman, K. S.; Bruendl, M. M.; Schildknegt, K.; Bohnstedt, A. C., Inter- and Intramolecular Addition/Cyclizations of Sulfonamide Anions with Alkynyliodonium Triflates. Synthesis of Dihydropyrrole, Pyrrole, Indole, and Tosylenamide Heterocycles. *J. Org. Chem.* **1996,** *61*, 5440-5452. (d) Tarasova, O. A.; Brandsma, L.; Nedolya, N. A.; Afonin, A. V.; Ushakov, I. A.; Klyba, L. V., New Approach to the Synthesis of Strained Cyclic Systems: I. Iminocyclobutenes and Iminothietanes from 1,3-Dilithio-3-phenylpropyne and Methyl Isothiocyanate. *Russ. J. Org.* **2003,** *39*, 1451-1457.

[146] Deprotonation/dialkylation of a benzylic, propargylic methylene is even more rare. Only two examples could be found in the literature: (a) Kinoshita, K.; Asoh, K.; FuruchiI, N.; Ito, T.; Kawada, H.; Ishii, N.; Sakamoto, H.; Hong, W.; Park, M.; Ono, Y.; Kato, Y.; Morikami, K.; Emura, T.; Oikawa, N. Tetracyclic

This, indeed, proved to be a significant problem. Exposure of intermediate **5028** to various strong bases (LDA, NaH, LiHMDS, and n-BuLi) and methylating reagents (MeI and dimethyl sulfate), at best, resulted in monomethylation. In no case was any dimethyl product **5029** observed.

5.6.2 A Second Attempted Synthetic Route: Longer but Effective

In the second attempted synthetic route, I chose to employ a nitrile moiety to act as a masked alkyne. From the synthesis of the class I aza-HDDA substrate **4020** (Section 4.4.1), I knew that the *gem*-dimethyl group could be installed on a benzylic nitrile to give intermediate **5031**.The reduction of the nitrile to an aldehyde, followed either by a Corey–Fuchs reaction or an Ohira–Bestmann homologation would yield the desired benzylic propargylic *gem*-dimethyl moiety. Indeed, reduction of the nitrile **5031** with DIBAL produced aldehyde **5032** in 79% yield. Although significant reaction optimization (not discussed here) was necessary, subjection of **5032** to Corey–Fuchs conditions gave the 1,1-dibromoalkene intermediate **5033** in an acceptable 73% yield. Elimination induced by n-BuLi subsequently produced the desired terminal alkyne **5034** in 95% yield.

Scheme 5.7 | Synthesis of test substrate **5026**.

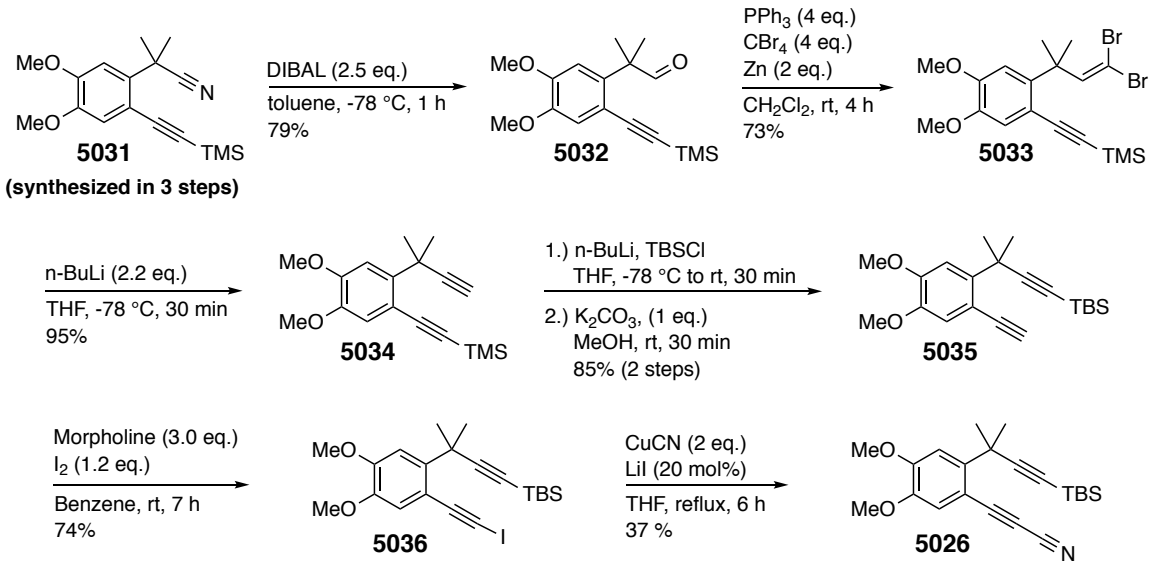

Compound. US2012083488, April 5th, 2012. (b) Aquila, B.; Dakin, L.; Ezhuthachan, J.; Lee, S.; Lyne, P.; Pontz, T.; Zheng, X. Quinazolineone Derivatives and Their Use as B-RAF Inhibitors WO2006024834 March 9th, 2006.

Conversion to the terminal phenylacetylene **5035** was a simple matter of silylation with TBSCl followed by TMS-desilylation with K_2CO_3 in MeOH.[147] From here, the cyanoalkyne moiety was installed using the same methodology that was used in the synthesis of yneone substrate **5015** (Section 5.4.2). Iodination of **5035** with morpholine and iodine gave iodoalkyne **5036** in 74% yield. Finally, coupling of this intermediate with CuCN in refluxing THF yielded the aza-HDDA substrate **5026** in a disappointing but still tractable 37% yield. While the synthetic sequence in Scheme 5.7 is long, it ultimately allowed for the synthesis of several hundred milligrams of **5026** to be used in the aza-HDDA reaction.

5.7 Aza-HDDA Reactions of a *gem*-Dimethylated Class II Substrate

The first observation regarding class II aza-HDDA substrate **5026** was rather surprising. While DFT calculations indicated that **5026** should undergo an aza-HDDA reaction at a similar rate to that observed for yneone substrate **5015**, experiment showed a half-life of 40 minutes at 170 °C (compared to 5 hours at 120 °C for **5015**). I cannot provide a suitable explanation for this significant contrast between theory and experiment.

Figure 5.11 shows products **5037a**–**5037h** that were formed from aza-HDDA reactions of substrate **5026**. Products **5037a**–**5037c** are analogous to products formed from the yneone substrate **5015** (products **5025a**–**5025c** in Figure 5.8). It should be noted that the yield of **5037a** (48%) is significantly lower than that of **5025a** (81%). This is largely due to the elevated temperature necessary for the aza-HDDA reaction of **5026** to occur, which resulted in additional Diels–Alder reactions of the furan trap with the desired product **5037a**. In contrast, the yield of **5037b** (57%) is higher than that observed for its aza-fluorenone analog **5025b** (24%)—presumably due to the lack of a sensitive yneone moiety in **5026**. Both **5037c** and **5037d** are each the result of a tetrahydrothiophene-initated three-component trapping reaction of pyridyne **5026***. While **5037c** is analogous to the product **5025c** formed from the yneone substrate, the use

[147] You may notice that intermediate **5034** itself could be converted to a cyanoalkyne aza-HDDA substrate. DFT calculations indicated that such a substrate would cyclize at tractable temperatures ($\Delta G^{\ddagger} = 32.8$ kcal•mol^{-1}). Unfortunately, the attempts to synthesize this substrate from **5034** (not discussed in this thesis) met with failure.

Figure 5.11 | Products from the class II aza-HDDA reaction of substrate **5026**.

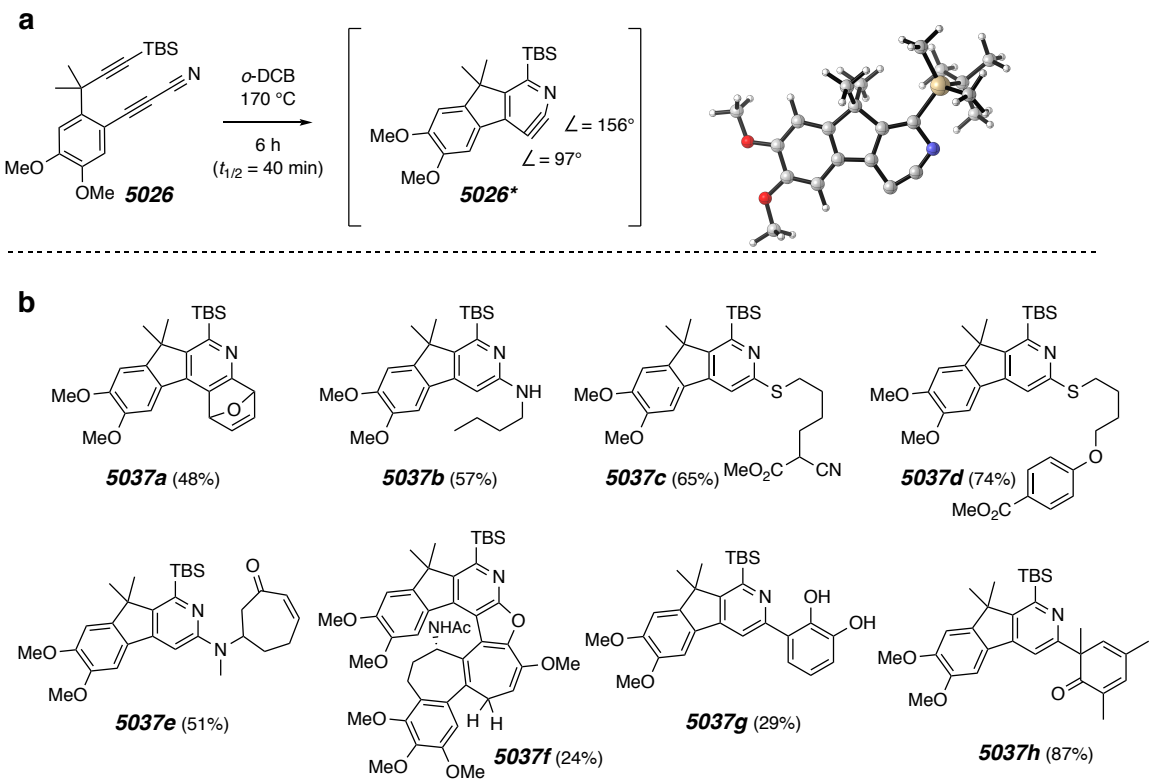

of methyl paraben as the third component (to form **5025d** in 74% yield) was incompatible with yneone **5015**—possibly due to the relative acidity of the phenol in the methyl paraben trap.

Like yneone **5015**, substrate **5026** was also heated in the presence of natural products tropinone and colchicine to give pyridines **5037e** and **5037f**, respectively. The mediocre yields of these reactions (51% and 24%, respectively) do not differ significantly from those produced from **5015**—indicating that neither the potentially advantageous stability of the *gem*-dimethyl group of **5026** nor the potentially detrimental high reaction temperature required for its cycloaromatization made a significant difference. The formation of products **5037g** and **5037h** from phenol-ene reactions was also successful. While **5037g**, which resulted from trapping **5026*** with catechol, was formed in a poor yield (29%) (partially due to issues of co-elution of catechol with the product), it did not produce a detectable amount of biaryl product at all when heated with yneone **5015**. The phenol-ene reaction with mesitol gave a comparably high yield (87%) of product **5037h**.

Finally, it should be noted that—as with pyridyne **5015*** from yneone substrate **5015**—the trapping of pyridyne **5026*** occurred with practically exclusive regioselectivity. Of the products **5037b**–**5037h**, the regioisomers drawn Figure 5.11b were the only regioisomers that were observed.

Chapter 6. Experimental Procedures and Compound Characterization

I. General Experimental Protocols

^{1}H and ^{13}C NMR spectra were recorded on Bruker Avance spectrometers (500 or 400 MHz). ^{1}H and ^{13}C NMR chemical shifts in $CDCl_3$ are referenced to TMS (0.00 ppm) and $CDCl_3$ (77.16 ppm), respectively. Non-first order multiplets are designated as "nfom"s. Proton resonances are reported with the following format: chemical shift in ppm (multiplicity, coupling constant values (*J*) in Hz, integral value, and assignment).

Infrared (IR) spectra were recorded as thin film samples on a Bruker Alpha II Spectrometer in the ATR mode. Absorption bands are reported in cm^{-1}.

HPLC-MS data were obtained on an Agilent 1100 series G1956B mass spectrometer in electrospray ionization (ESI) mode. The HPLC column (50 mm × 4.6 mm) contained a C18 stationary phase with a particle size of 3.5 μm.

HRMS data were collected on either i) a Thermo Orbitrap Velos in electron spray ionization (ESI), positive mode [sample introduction as a solution in methanol or acetonitrile; external standard (Pierce™ LTQ); mass accuracy <4 ppm] or ii) a Bruker BioTOF II (ESI-TOF) instrument in electrospray ionization (ESI) mode (PEG was added as an internal standard; sample was introduced as a solution in methanol or acetonitrile). Low resolution MS data were collected on an Advion expression compact mass spectrometer in atmospheric-pressure chemical ionization (APCI) mode (positive ion).

Medium pressure liquid chromatography (MPLC, 50-200 psi) was performed on hand-packed silica gel (25-35 μm, 60 Å pores) columns. A Fluid Metering Inc. pump outfitted with a Gilson UV detector and Waters R401 differential refractive index detector was used. Flash chromatography was performed on columns packed with silica gel (Agela, 40-63 μm).

Reaction temperatures refer to the temperature of the heating or cooling bath used. HDDA reactions were run in a culture tube fitted with a Teflon®-lined threaded cap, unless otherwise indicated. Reactions requiring anhydrous conditions were carried out under an atmosphere of nitrogen in oven-dried glassware. THF was distilled over a mixture of sodium and benzophenone immediately before use; anhydrous DMF and methylene chloride were obtained by vacuum transferring from CaH_2. 1,2-Dichlorobenzene was dried over molecular sieves and sparged with nitrogen gas prior to use.

***N*-(8-((*tert*-Butyldimethylsilyl)oxy)octa-2,4-diyn-1-yl)-*N*-(2-cyanopropan-2-yl)methanesulfonamide (4009)**

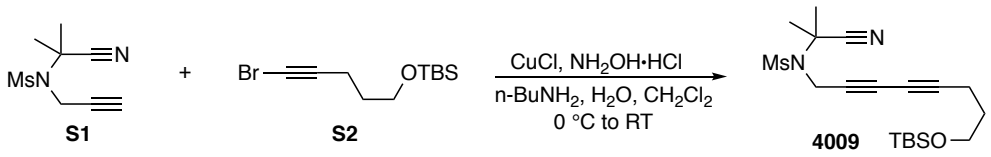

A 100 mL round-bottom flask containing CuCl (42.4 mg, 0.428 mmol), hydroxylamine hydrochloride (149 mg, 2.14 mmol), and a magnetic stir bar was purged with N_2 before being put under a slight positive N_2 pressure. *n*-Butylamine (15 mL) was added by syringe and the resulting solution was stirred in an ice bath for 20 minutes. A solution of nitrile **S1** (854 mg, 4.26 mmol) in CH_2Cl_2 (10 mL) was prepared and 2 mL of this solution were added to the reaction mixture by syringe, resulting in the formation of an off-white suspension. The remaining 8 mL of this solution were added to a solution of bromoalkyne **S2** (1.77 g, 6.39 mmol) in CH_2Cl_2 (15 mL) and the resulting mixture was added to the reaction mixture dropwise over 30 minutes. After addition was complete, the reaction flask was taken out of the ice bath and left to stir at r.t. After 15 minutes, the reaction mixture was quenched by the addition of saturated aqueous NH_4Cl solution (30 mL) and extracted with CH_2Cl_2 (2 x 25 mL). The extracts were washed with brine, dried with $MgSO_4$, and concentrated to a yellow oil. This oil was purified by flash column chromatography (3:1 hexanes:EtOAc) to give **4009** a white crystalline solid (1.60 g, 4.02 mmol, 94%).

^{1}H NMR (500 MHz, $CDCl_3$): δ 4.29 (t, J = 1.0 Hz, 2H, SO_2NCH_2), 3.67 (t, J = 5.9 Hz, 2H, $C{\equiv}CCH_2CH_2CH_2OSi$), 3.19 (s, 3H, CH_3SO_2N), 2.38 (tt, J = 7.0, 1.0 Hz, $C{\equiv}CCH_2CH_2CH_2OSi$), 1.92 [s, 6H, $NCH_2C(CH_3)_2C{\equiv}N$], 1.73 (tt, J = 7.0, 5.9 Hz, 2H, $C{\equiv}CCH_2CH_2CH_2OSi$), 0.90 [s, 9H, $OSi(C(CH_3)_3$], and 0.05 (s, 6H, $OSi(CH_3)_2$].

^{13}C NMR (125 MHz, $CDCl_3$): δ 120.5, 82.1, 71.6, 69.7, 64.2, 61.4, 54.0, 41.7, 36.4, 31.1, 29.0, 26.0, 18.4, 15.9, and -5.2.

HRMS (ESI-Orbitrap) Calculated for $C_{19}H_{33}N_2O_3SSi^+$ [M+H$^+$] 397.1976, found 397.1976; Calculated for $C_{19}H_{36}N_3O_3SSi^+$ [M+NH_4^+] 414.2241, found 414.2240.

TLC: R_f 0.35 (3:1 hexanes:EtOAc)

m.p. 55–56 °C.

9-(*tert*-Butyldimethylsilyl)-6,6-dimethyl-7-(methylsulfonyl)-2,3,4,6,7,8-hexahydropyrano[3,2-*b*]pyrrolo[3,4-*e*]pyridine (4010)

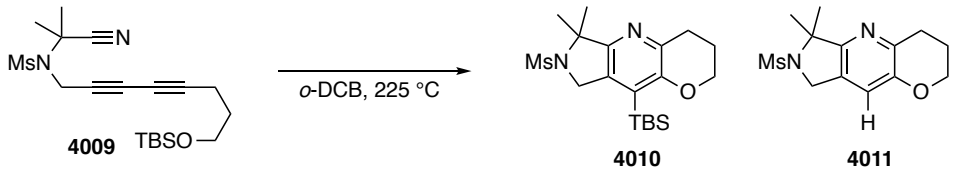

In 30 mL microwave vial equipped with a stir bar, the nitrile **4009** (72.0 mg, 0.182 mmol) was dissolved in dried, degassed *o*-DCB (18 mL). The vial was capped, placed in a microwave reactor, and heated at 225 °C for 16 hours (TLC monitoring). The resulting solution was concentrated to a black solid that was then purified by MPLC (2:1 hexanes:EtOAc) to give, in order of elution, the silyl pyridine **4010** (26.1 mg, 0.0658 mmol, 36%) as an off-white solid and the pyridine **4011** (5.1 mg, 0.0181 mmol, 10%) also as an off-white solid.

Data for 4010

^{1}H NMR (500 MHz, $CDCl_3$): δ 4.55 (s, 2H, SO_2NCH_2), 4.11 (t, J = 5.2 Hz, 2H, $ArCH_2CH_2CH_2O$), 2.95 (t, J = 7 Hz, 2H, $ArCH_2CH_2CH_2O$) 2.95 (s, 3H, CH_3SO_2N), 2.08 (br pent, J = 5.5 Hz, 2H, $ArCH_2CH_2CH_2O$), 1.70 (s, 6H, $NCH_2C(CH_3)_2Ar$), 0.90 [s, 9H, $ArSiC(CH_3)_3$], and 0.32 [s, 6H, $ArSi(CH_3)_2$].

^{13}C NMR (125 MHz, $CDCl_3$): δ 155.9, 154.4, 142.8, 131.4, 129.0, 67.6, 65.9, 52.4, 39.7, 28.9, 27.9, 27.0, 22.3, 18.6, and -2.8.

HRMS (ESI-Orbitrap) Calculated for $C_{19}H_{33}N_2O_3SSi^+$ [M+H$^+$] 397.1976, found 397.1973.

TLC: R_f 0.30 (2:1 hexanes:EtOAc)

Data for 4011

^{1}H NMR (500 MHz, $CDCl_3$): δ 6.95 (t, J = 1.0 Hz, ArH, 1H), 4.56 (dt, J = 1.1, 1.1 Hz, $MsNCH_2$, 2H), 4.19 (nfom, OCH_2, 2H), 2.97 (s, CH_3SO_2N, 3H), 2.96 (m, $ArCH_2$, 2H), 2.12 (nfom, OCH_2CH_2, 2H), and 1.72 (s, $C(CH_3)_2$, 6H).

^{13}C NMR (125 MHz, $CDCl_3$): δ 155.4, 151.3, 144.2, 126.0, 118.4, 68.6, 66.7, 50.4, 39.8, 28.6, 27.7, and 22.3.

HRMS (ESI-Orbitrap) Calculated for $C_{13}H_{19}N_2O_3S^+$ [M+H$^+$] 283.1111, found 283.1111.

m.p. 129–131°C.

2-(2-Bromo-4,5-dimethoxyphenyl)acetonitrile (4023)

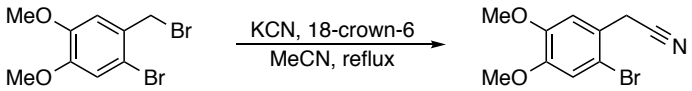

4022 **4023**

To a solution of the benzylic bromide **4022** (53.8 g, 174 mmol) in MeCN (350 mL), KCN (33.9 g, 521 mmol) and 18-crown-6 ether (2.32 g, 8.77 mmol) were added. The reaction mixture was vigorously stirred and left to reflux in an 85 °C oil bath. After 47 hours (TLC monitoring), the mixture was vacuum filtered and the filtrate was concentrated to give a light orange solid. This crude material was recrystallized from methanol to give the nitrile **4023** (34.4 g, 134 mmol, 77%) as a light yellow crystalline solid whose spectral data matched those in the literature.[148]

[148] Imbri, D.; Tauber, J.; Opatz, T., A High-Yielding Modular Access to the Lamellarins: Synthesis of Lamellarin G Trimethyl Ether, Lamellarin η and Dihydrolamellarin η. *Chem. Eur. J.* **2013,** *19*, 15080-15083.

2-(4,5-Dimethoxy-2-((trimethylsilyl)ethynyl)phenyl)acetonitrile (4024)

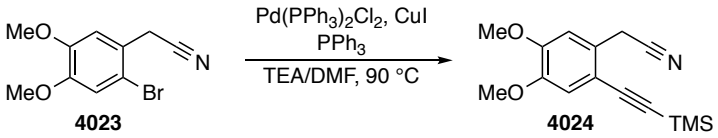

To a 1 L oven-dried round-bottom flask containing a stir bar, dry triethylamine (300 mL) and dry DMF (100 mL) were added. This solution was sparged with nitrogen at 0 °C. Subsequently, $Pd(PPh_3)_2Cl_2$ (2.32 g, 3.31 mmol), CuI (1.26 g, 6.64 mmol), PPh_3 (8.66 g, 33.0 mmol), aryl bromide **4023** (28.2 g, 110 mmol), and ethynyltrimethylsilane (30 mL, 220 mmol) were added sequentially. The flask was fitted with a reflux condenser, placed under a slight positive N_2 pressure, and lowered into a 90 °C oil bath. After 47 hours (GC monitoring) the reaction mixture was quenched by the addition of saturated aqueous NH_4Cl solution (500 mL) and further diluted with EtOAc (1 L). The organic layer was washed with additional portions of saturated aqueous NH_4Cl solution (2 x 500 mL), 5 wt% aqueous LiCl solution (5 x 500 mL), and 30% (w/w) aqueous H_2O_2 solution (100 mL), and brine; dried with $MgSO_4$; and concentrated. The residue dissolved in DCM, SiO_2 was added, and the mixture was concentrated to dryness. This material was loaded to the top of a plug of SiO_2 and eluted with 1:3 hexanes:EtOAc. The filtrate was concentrated to give a brown solid. This solid was recrystallized from MeOH to give silane **4024** (15.3 g, 56.0 mmol) as a slightly tan crystalline solid. The mother liquor was concentrated and the resulting solid was purified by flash chromatography (4:1 hexanes:EtOAc) to give additional **4024** (5.72 g, 20.9 mmol, 70%) as a white crystalline solid.

^{1}H NMR (500 MHz, $CDCl_3$): δ 6.96 (s, 1H, Ar*H3* or Ar*H6*), 6.92 (s, 1H, Ar*H3* or Ar*H6*), 3.92 (s, 3H, ArOC*H*$_3$), 3.88 (s, 3H, ArOC*H*$_3$*'*), 3.86 (s, 2H, ArC*H*$_2$CN), 0.27 [s, 9H, Si(CH_3)$_3$]

^{13}C NMR (125 MHz, $CDCl_3$): δ 150.1, 148.5, 125.5, 117.9, 114.81, 114.77, 111.0, 102.0, 99.5, 56.24, 56.22, 22.3, and 0.11.

IR (thin film): 3005, 2956, 2941, 2853, 2262, 2146, 1603, 1518, 1460, 1409, 1347, 1250, 1218, 1197, 1098, 997, 876, 837, 760, and 695 cm^{-1}.

HRMS (ESI-Orbitrap) Calculated for $C_{15}H_{20}NO_2Si^+$ [M+H$^+$] 274.1258, found 274.1258.

TLC: R_f 0.30 (4:1 hexanes:EtOAc)

m.p. 123–124 °C.

2-(4,5-Dimethoxy-2-((trimethylsilyl)ethynyl)phenyl)-2-methylpropanenitrile (4025) and 2-Isopropyl-5,6-dimethoxy-3-((trimethylsilyl)ethynyl)benzonitrile (4027)

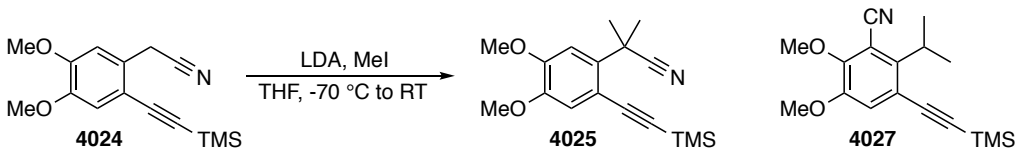

A 1L 3-neck round-bottom flask containing a stir bar was fitted with a pressure-equalizing dropping funnel and placed under a slight N_2 pressure. Diisopropylamine (36 mL, 260 mmol) was dissolved in 200 mL of THF and the resulting solution was cooled in a dry ice/acetone bath until the temperature reached –70 °C. To this stirred solution, n-BuLi solution in hexanes (100 mL, 250 mmol) was added by cannula over a period of 10 minutes. A solution of the benzylic nitrile **4024** (6.84 g, 25.0 mmol) and MeI (16 mL, 260 mmol) in 50 mL of THF was added dropwise from the dropping funnel over a period of 15 minutes (such that the temperature did not rise above – 50 °C). After the addition was complete, the resulting mixture was taken out of the cold bath and left to stir. As the mixture warmed, it gradually changed from orange and heterogeneous to purple and nearly homogeneous. One hour following removal from the cold bath, the reaction mixture was quenched by the addition of saturated aqueous ammonium chloride solution (300 mL), which was accompanied by dissipation of the purple color, and extracted with EtOAc (300 mL). The combined extracts were washed with brine, dried with $MgSO_4$, and concentrated to a dull orange solid. The solid was recrystallized from methanol to give **4025** (2.62 g, 8.69 mmol), as a white crystalline solid. The mother liquor was concentrated and the resulting solid purified by flash column chromatography (5:1 hexanes:EtOAc) to give additional **4025** (1.84 g, 6.10 mmol, 59%) as a white crystalline solid.

Data for 4025

^{1}H NMR (500 MHz, $CDCl_3$): δ 7.05 (s, 1H, Ar*H3* or Ar*H6*), 7.01 (s, 1H, Ar*H3* or Ar*H6*), 3.92 (s, 3H, ArOC*H*$_3$), 3.88 (s, 3H, ArOC*H*$_3$'), 1.93 [s, 6H, ArC(C*H*$_3$)$_2$], and 0.27 (s, 9H, Si(C*H*$_3$)$_3$).

^{13}C NMR (125 MHz, $CDCl_3$): δ 149.4, 147.8, 135.2, 124.2, 117.7, 113.1, 109.6, 103.8, 101.3, 56.2, 56.1, 37.7, 27.3, and -0.2.

IR (thin film): 2998, 2960, 2934, 2849, 2233, 2145, 1601, 1518, 1462, 1445, 1381, 1342, 1264, 1246, 1223, 1190, 1160, 1069, 992, 863, 837, 754, 696, and 655 cm^{-1}.

HRMS (ESI-Orbitrap) Calculated for $C_{17}H_{24}NO_2Si^+$ [M+H$^+$] 302.1571, found 302.1576.

TLC: R_f 0.30 (5:1 hexanes:EtOAc)

m.p. 105–106 °C.

The formation of the phenyl nitrile **4027** was occasionally observed as a side product. This tended to correlate with experiments in which the heterogeneous reaction mixture was being inefficiently stirred (and, perhaps, local warming). Presumably lithiation at C6 in **4025** allowed for intramolecular cyano group transfer.

Data for 4027.

^{1}H NMR (500 MHz, $CDCl_3$): δ7.13 (s, Ar*H*, 1H), 4.00 (s, OCH_3, 3H), 3.86 (s, OCH_3', 3H), 3.60 (septet, J = 7.3 Hz, C*H*Me_2, 1H), 1.46 [d, J = 7.3 Hz, CH(CH_3)$_2$, 6H], and 0.26 [s, Si(CH_3)$_3$, 9H].

^{13}C NMR (125 MHz, $CDCl_3$): δ152.6 (C5), 149.8 (C6), 146.5 (C2), 121.7 (C4), 118.0 (C1), 115.3 (CN), 107.2 (C3), 102.7 (ArC≡C), 99.8 (C≡CSi), 61.8 (H_3*C*C5), 56.3 (H_3*C*C6), 32.7 (Ar*C*H), 20.7 [CH(*C*H_3)$_2$], and -0.20 [Si(CH_3)$_3$]. (assignments based on HMBC analyses)

HRMS (ESI-Orbitrap) Calculated for $C_{17}H_{24}NO_2Si^+$ [M+H$^+$] 302.1571, found 302.1573.

TLC: R_f 0.50 (4:1 hexanes:EtOAc)

m.p. 59–62 °C.

2-(2-Ethynyl-4,5-dimethoxyphenyl)-2-methylpropanenitrile (4026)

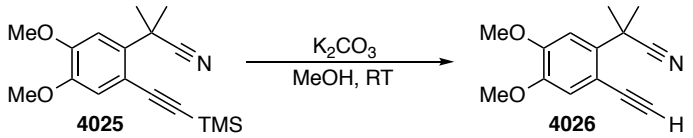

In a 50 mL round-bottom flask containing a stir bar, the alkynyl silane **4025** (836 mg, 2.77 mmol) was dissolved in 30 mL of MeOH. K_2CO_3 (384 mg, 2.78 mmol) was added and resulting mixture was stirred at room temperature. After 20 minutes, the reaction mixture was diluted with EtOAc (100 mL) and quenched by the addition of H_2O (50 mL). The organic layer was treated with brine and Na_2SO_4 before being concentrated to an orange oil. This oil was purified by MPLC (4:1 hexanes:EtOAc) to give **4026** (558 mg, 2.47 mmol, 89%) as an off-white crystalline solid.

^{1}H NMR (400 MHz, $CDCl_3$): δ 7.053 (s, 1H, Ar*H3* or Ar*H6*), 7.048 (s, 1H, Ar*H3* or Ar*H6*), 3.93 (s, 3H, ArOC*H*$_3$), 3.88 (s, 3H, ArOC*H*$_3$'), 3.46 (s, 1H, ArC≡C*H*), and 1.93 [s, 6H, ArC(C*H*$_3$)$_2$].

^{13}C NMR (125 MHz, $CDCl_3$): δ 149.6, 147.9, 135.3, 124.2, 118.2, 112.1, 109.5, 84.1, 82.3, 56.2, 56.1, 37.6, and 27.5.

HRMS (ESI-Orbitrap) Calculated for $C_{14}H_{16}NO_2^+$ [M+H$^+$] 230.1176, found 230.1180.

m.p. 89–91 °C.

2-(2-(7-((*tert*-Butyldimethylsilyl)oxy)hepta-1,3-diyn-1-yl)-4,5-dimethoxyphenyl)-2-methylpropanenitrile (4020)

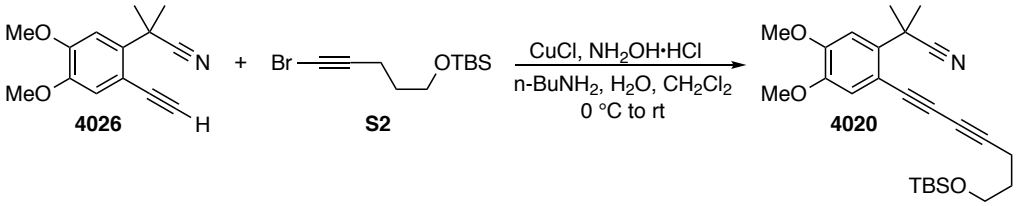

A 25 mL round-bottom flask containing CuCl (15.0 mg, 0.152 mmol), hydroxylamine hydrochloride (35.2 mg, 0.507 mmol), and a magnetic stir bar was purged with N_2 before being placed under a slight positive N_2 pressure. *n*-Butylamine solution (30% wt. in water, 5 mL) was added by syringe and the resulting solution was stirred in an ice bath for 5 minutes. A solution of nitrile **4026** (230 mg, 1.00 mmol) in CH_2Cl_2 (3 mL) was prepared and 0.5 mL of this solution was added to the reaction mixture by syringe. The remainder of this solution was added to a solution of bromoalkyne **S2** (417 mg, 1.50 mmol) in CH_2Cl_2 (3 mL), and the resulting mixture was added to the reaction flask dropwise by syringe over 10 minutes. After addition was complete, the reaction flask was taken out of the ice bath and left to stir at room temperature. After 20 minutes, the reaction mixture was diluted with CH_2Cl_2 (50 mL) and quenched by the addition of a mixture of brine and 30% aqueous NH_4OH solution (3:1 vol., 50 mL). The organic extract was washed with brine, dried with $MgSO_4$, and concentrated to leave a yellow oil. This oil was purified by MPLC (6:1 hexanes:EtOAc) to provide the 1,3-diyne **4020** (377 mg, 0.886 mmol, 87%) as a yellow oil.

^{1}H NMR (400 MHz, $CDCl_3$): δ 7.08 (s, *H*3 or *H*6 1H), 7.02 (s, *H*3 or *H*6 1H), 3.93 (s, OCH_3, 3H), 3.87 (s, OCH_3', 3H), 3.72 (t, J = 5.9 Hz, OCH_2, 2H), 2.48 (t, J = 7.1 Hz, ≡CCH_2, 2H), 1.92 [s, (CH_3)$_2$CH, 6H], 1.78 (tt, J = 5.9, 7.1 Hz, ≡CCH$_2$CH_2, 2H), 0.90 [s, C(CH_3)$_3$, 9H], and 0.07 [s, Si(CH_3)$_2$, 6H].

^{13}C NMR (125 MHz, $CDCl_3$): δ 149.7, 147.9, 136.3, 124.2, 118.3, 111.6, 109.7, 86.5, 80.8, 72.7, 65.1, 61.4, 56.13, 56.07, 38.0, 31.3, 27.6, 26.0, 18.4, 16.3, and –5.3.

HRMS (ESI-Orbitrap) Calculated for $C_{25}H_{36}NO_3Si^+$ [M+H$^+$] 426.2459, found 426.2462.

TLC: R_f 0.40 (6:1 hexanes:EtOAc)

11-(*tert*-butyldimethylsilyl)-8,9-dimethoxy-6,6-dimethyl-2,3,4,6-tetrahydroindeno[2,1-*b*]pyrano[2,3-*e*]pyridine (4032)

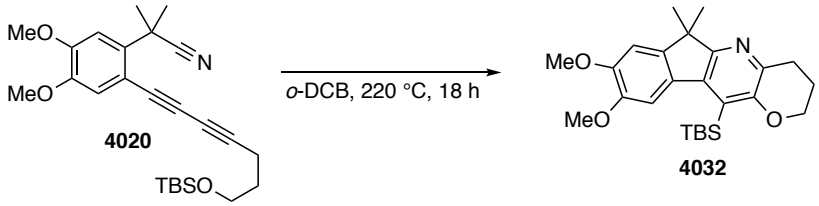

In 30 mL microwave vial equipped with a stir bar, nitrile **4020** (91.6 mg, 0.215 mmol) was dissolved in dried, degassed *o*-DCB (22 mL). The vial was capped, placed in a microwave reactor and heated at 220 °C for 18 hours (TLC monitoring). The resulting solution was concentrated to a black solid that was then purified by MPLC (3:1 hexanes:EtOAc) to give pyridine **4032** (34.5 mg, 0.0811 mmol, 38%) as a light yellow oil.

^{1}H NMR (400 MHz, $CDCl_3$): δ 7.46 (s, *H*10, 1H), 6.93 (s, *H7*, 1H), 4.11 (nfom, 2H), 3.96 (s, OCH_3 and OCH_3', 6H), 3.03 (t, J = 6.7 Hz, 2H), 2.11 (nfom, 2H), 1.45 [s, $C(CH_3)_2$, 6H], 1.11 (s, 9H), and 0.45 (s, 6H).

^{13}C NMR (125 MHz, $CDCl_3$): δ 163.7, 155.8, 149.0, 147.3, 147.0, 138.1, 138.0, 130.5, 127.8, 109.0, 105.6, 65.6, 56.5, 56.2, 45.3, 28.9, 28.2, 26.4, 22.7, 19.4, and 0.5.

HRMS (ESI-Orbitrap) Calculated for $C_{25}H_{36}NO_3Si^+$ [M+H$^+$] 426.2459, found 426.2463.

2-(8-((*tert*-Butyldimethylsilyl)oxy)octa-2,4-diynoyl)benzonitrile (4040)

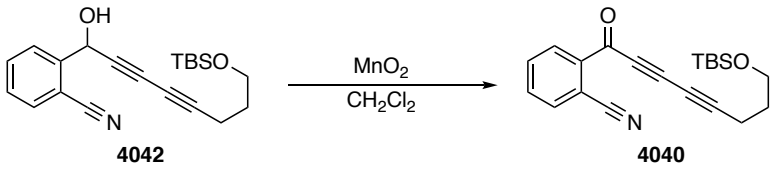

4042 **4040**

Alcohol **4042** (195 mg, 0.551 mmol) was dissolved in CH_2Cl_2 (5.5 mL). MnO_2 (90% purity, 531 mg, 5.50 mmol) was added and the mixture was stirred at room temperature. After 1 hour, the slurry was filtered through a silica gel plug with ethyl acetate and the filtrate was concentrated. The resulting oil was purified by MPLC (5:1 hexanes:EtOAc) to give the ketone **4040** (132 mg, 0.376 mmol, 68%) as a light yellow oil.

^{1}H NMR (500 MHz, $CDCl_3$): δ 8.29 (ddd, *J* = 7.6, 1.5, 0.6 Hz, 1H, Ar*H3*), 7.83 (ddd, *J* = 7.5, 1.5, 0.6 Hz, 1H, Ar*H6*), 7.76 (ddd, *J* = 7.6, 7.6, 1.4 Hz, 1H, Ar*H4*) 7.71 (ddd, *J* = 7.5, 7.5, 1.6 Hz, 1H, Ar*H5*), 3.71 (t, *J* = 5.8 Hz, 2H, C≡CCH$_2$CH$_2$C*H$_2$*), 2.54 (t, *J* = 7.0, 2H, C≡CC*H$_2$*CH$_2$CH$_2$), 1.81 (br app pent, *J* = 6 Hz, 2H, C≡CCH$_2$C*H$_2$*CH$_2$), 0.90 (s, 9H, OSi(C(C*H$_3$*)$_3$), and 0.07 (s, 6H, OSi(C*H$_3$*)$_2$).

^{13}C NMR (125 MHz, $CDCl_3$): δ 174.2, 138.0, 135.6, 133.7, 132.9, 132.7, 117.3, 111.4, 92.6, 80.7, 70.7, 64.1, 61.2, 30.8, 26.0, 18.4, 16.4, and -5.3.

TLC: R_f 0.35 (3:1 hexanes:EtOAc).

11-(*tert*-Butyldimethylsilyl)-3,4-dihydroindeno[1,2-*b*]pyrano[2,3-*e*]pyridin-10(2*H*)-one (4043)

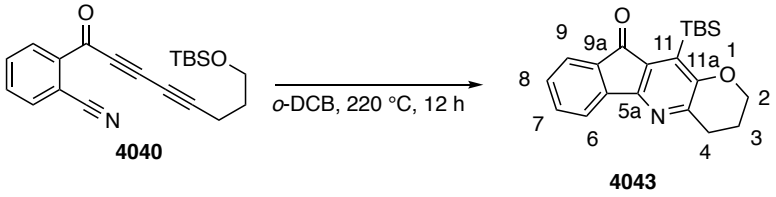

In 30 mL microwave vial equipped with a stir bar, the nitrile **4040** (37.7 mg, 0.107 mmol) was dissolved in dried, degassed *o*-DCB (11 mL). The vial was capped, placed in a microwave reactor and heated at 220 °C for 12 hours (TLC monitoring). The resulting solution was concentrated to a black solid that was then purified by MPLC (4:1 hexanes:EtOAc) to give the pyridine **4043** (12.4 mg, 0.0353 mmol, 33%) as a yellow solid.

^{1}H NMR (500 MHz, $CDCl_3$): δ 7.70 (ddd, *J* = 7.4, 0.8, 0.8 Hz, 1H, Ar*H6*), 7.58 (ddd, *J* = 7.3, 0.9, 0.9 Hz, 1H, Ar*H9*), 7.49 (ddd, *J* = 7.5, 7.5, 1.1 Hz, 1H, Ar*H7*), 7.29 (ddd, *J* = 7.4, 7.4, 0.9 Hz, 1H, Ar*H8*), 4.15 (br t, *J* = 5.2 Hz, 2H, C2H_2), 3.03 (t, *J* = 6.7 Hz, 2H), 2.11 [nfom (magnetic inequivalence) 2H, C3H_2], 0.97 (s, 9H), and 0.41 [s, 6H, $Si(CH_3)_2$],

^{13}C NMR (125 MHz, $CDCl_3$): δ 193.3 (C10), 157.4 (C11a), 157.3 (C5a), 146.4 (C4a), 143.7 (C9a), 136.7 (C11), 135.3 (C5b), 135.2 (C7), 134.3 (C10a), 129.7 (C8), 123.8 (C9), 119.8 (C6), 66.3 (C2), 29.7 (C4), 27.6 [SiC(CH_3)], 22.4 (C3), 19.3 [SiC(CH_3)], and -1.1 [Si(CH_3)$_2$].

HRMS (ESI-Orbitrap) Calculated for $C_{21}H_{26}NO_2Si^+$ [M+H$^+$], 352.1727, found 352.1726.

TLC: R_f 0.30 (4:1 hexanes:EtOAc)

2-(7-((*tert*-butyldimethylsilyl)oxy)hepta-1,3-diyn-1-yl)cyclohept-1-ene-1-carbaldehyde (4044)

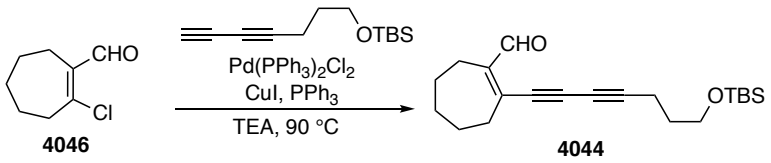

$Pd(PPh_3)_2Cl_2$ (71.0 mg, 0.101 mmol), CuI (38.9 mg, 0.204 mmol), and PPh_3 (263 mg, 1.00 mmol) were added to a 25 mL round-bottom flask containing a stir bar. The headspace was briefly flushed with N_2, the flask was capped with a rubber septum, and dry/degassed triethylamine (5 mL) was added by syringe. A solution of chloroenal **4046** (319 mg, 2.01 mmol) in dry/degassed triethylamine (3 mL) was added, followed by a solution of *tert*-butyl(hepta-4,6-diyn-1-yloxy)dimethylsilane (891 mg, 4.00 mmol) in dry/degassed triethylamine (3 mL). The flask was fitted with a reflux condenser, lowered into a 90 °C oil bath, and left to stir. After 90 minutes, the reaction mixture was diluted with EtOAc (50 mL) and quenched by the addition of saturated aqueous NH_4Cl solution (50 mL). The layers were separated and the EtOAc layer was washed with additional NH_4Cl solution (50 mL) and brine (50 mL), filtered through a SiO_2 plug with additional EtOAc as eluant, and concentrated to a reddish-black oil. This oil was purified by MPLC (50:1 hexanes:EtOAc) to give **4044** (459 mg, 1.33 mmol, 66%) as a reddish-orange oil.

^{1}H NMR (400 MHz, $CDCl_3$): δ 10.09 (s, 1H, C*H*O), 3.70 (t, *J* = 5.9 Hz, OCH_2), 2.60 (nfom, 2H, CH_2C=C-CH_2), 2.50 (nfom, 2H, CH_2C=C-CH_2), 2.48 (t, *J* = 7.1 Hz, 2H, ≡CCH_2), 1.79 (nfom, 2H, CH_2CH_2C=C-CH_2CH_2), 1.77 (tt, *J* = 7.1, 5.9 Hz, 2H, ≡CCH_2CH_2), 1.62 (nfom, 2H, CH_2CH_2C=C-CH_2CH_2), and 1.44 (br pent, *J* = ~6 Hz, 2H, C$H_2CH_2CH_2C$=C), 0.90 [s, 9H, C(CH_3)$_3$], and 0.08 [s, 6H, Si(CH_3)$_2$].

^{13}C NMR (125 MHz, $CDCl_3$): δ 191.8, 151.9, 144.7, 89.5, 85.4, 72.7, 65.0, 61.4, 37.2, 32.3, 31.3, 26.0, 25.8, 25.7, 24.5, 18.4, 16.4, and -5.2.

HRMS (ESI-Orbitrap) Calculated for $C_{21}H_{33}O_2Si^+$ [M+H$^+$] 345.2244, found 345.2244.

TLC: R_f 0.25 (50:1 hexanes:EtOAc)

2-(2-(7-((*tert*-Butyldimethylsilyl)oxy)hepta-1,3-diyn-1-yl)cyclohept-1-en-1-yl)-2-((trimethylsilyl)oxy)acetonitrile (4049)

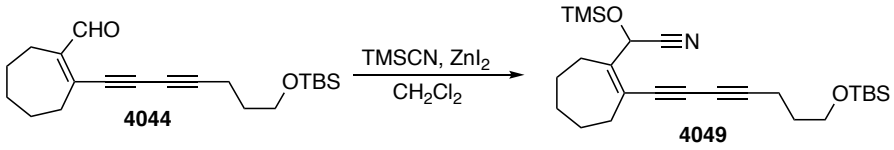

In an 8 mL culture tube containing a stir bar, aldehyde **4048** (275 mg, 0.797 mmol) was dissolved in CH_2Cl_2 (4.0 mL). TMSCN (0.20 mL, 1.60 mmol) and ZnI_2 (25.4 mg, 0.0796 mmol) were added and the resulting mixture was vigorously stirred at room temperature. After 1 hour (and after ^{1}H NMR analysis of an aliquot indicated full conversion), the resulting mixture was filtered through a SiO_2 plug with EtOAc and the eluent was concentrated to a brown oil. This oil was purified by MPLC (40:1 hexanes:EtOAc) to give the *O*-silylated cyanohydrin **4049** (281 mg, 0.633 mmol, 79%) as a yellow oil.

^{1}H NMR (400 MHz, $CDCl_3$): δ 5.59 (s, 1H, C=CC*H*CN), 3.70 (t, *J* = 5.9 Hz, 2H, OC*H*$_2$), 2.49 (ddd, *J* = 15.1, 7.9, 3.8 Hz, 1H, CH_2C=C-C*H*$_a$H$_b$), 2.46 (t, *J* = 7.0 Hz, 2H, C≡CC*H*$_2$), 2.40 (ddd, *J* = 14.7, 8.8, 2.7 Hz, 1H, CH_2C=C-CH$_a$*H*$_b$), 2.40–2.35 (m, 2H, C=C-CH$_2$), 1.76 (tt, *J* = 7.0, 5.9 Hz, 2H, C≡CCH$_2$C*H*$_2$), 1.83–1.69 (m, 2H, =CCH$_2$C*H*$_2$), 1.62-1.50 (m, 2H, =CCH$_2$CH$_2$C*H*$_2$), 0.90 [s, 9H, SiC(C*H*$_3$)$_3$], 0.20 [s, 9H, SiC(C*H*$_3$)$_3$], and 0.06 [s, 6H, Si(C*H*$_3$)$_2$].

^{13}C NMR (125 MHz, $CDCl_3$): δ 147.9, 125.8, 118.6, 87.1, 80.7, 73.4, 64.8, 64.2, 61.4, 34.5, 32.2, 31.3, 29.0, 26.4, 26.0, 25.8, 18.4, 16.2, -0.2, and -5.3.

TLC: R_f 0.35 (40:1 hexanes:EtOAc)

2-(2-(7-((*tert*-Butyldimethylsilyl)oxy)hepta-1,3-diyn-1-yl)cyclohept-1-en-1-yl)-2-hydroxyacetonitrile (4050)

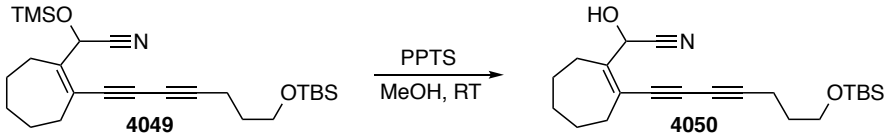

In a 100 mL round-bottom flask containing a stir bar and the *O*-silylated cyanohydrin **4049** (310 mg, 0.637 mmol) was dissolved in MeOH (30 mL). PPTS (161 mg, 0.069 mmol) was added and the resulting solution was stirred at room temperature. After 10 minutes, TLC analysis showed that the starting material was almost consumed and that another, more polar side product (presumably the diol) was also forming. Accordingly, the reaction solution was diluted with CH_2Cl_2 (50 mL) and quenched with H_2O (50 mL). The resulting layers were separated and the aqueous layer was extracted with additional CH_2Cl_2 (50 mL). The combined organic extracts were treated with brine, dried with Na_2SO_4, and concentrated to an orange oil. This oil was purified by MPLC (8:1 hexanes:EtOAc) to give cyanohydrin **4050** (173 mg, 0.467 mmol, 73%) as a light yellow oil.

^{1}H NMR (500 MHz, $CDCl_3$): δ 5.68 (d, *J* = 4.8 Hz, 1H, C*H*OH), 3.69 (t, *J* = 5.9 Hz, 2H, OCH_2), 2.50 (ddd, *J* = 15.2, 7.8, 3.2 Hz, 1H, CH_2C=C-CH_aH$_b$), 2.45 (t, *J* = 7.1 Hz, 2H, C$H_2CH_2CH_2O$), ca. 2.44 (m, *J*'s obscured by overlap, 1H, CH_2C=C-CH_aH_b), 2.42 (*J*'s obscured by overlap, 1H, C=CC'H_aH$_b$), 2.40 (ddd, *J* = 14.9, 11.1, 5.0 Hz, 1H, C=CC'H_aH_b), 2.24 (d, *J* = 4.9 Hz, 1H, O*H*), 1.76 (tt, *J* = 7.1, 5.8 Hz, 2H, C≡CCH_2CH_2), 1.83–1.72 (m, 2H), 1.66-1.52 (m, 4H), 0.90 [s, 9H, SiC(CH_3)$_3$], and 0.06 [s, 6H, Si(CH_3)$_2$].

^{13}C NMR (125 MHz, $CDCl_3$): δ 146.6, 127.4, 118.1, 87.6, 81.0, 73.1, 64.8, 64.0, 61.5, 34.6, 32.2, 31.3, 29.1, 26.5, 26.0, 25.7, 18.4, 16.3, and -5.2.

TLC: R_f 0.35 (8:1 hexanes:EtOAc)

2-(7-((*tert*-Butyldimethylsilyl)oxy)hepta-1,3-diyn-1-yl)cyclohept-1-ene-1-carbonyl cyanide (4044)

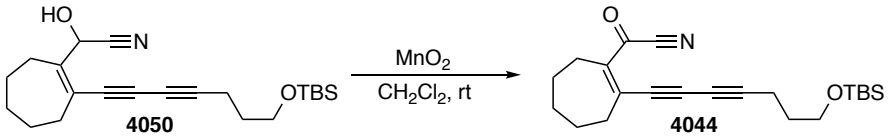

In an 16 mL culture tube containing a stir bar, the cyanohydrin **4050** (156 mg, 0.419 mmol) was dissolved in CH_2Cl_2 (4 mL). MnO_2 (90% purity, 608 mg, 6.29 mmol) was added to this solution, and the resulting mixture was vigorously stirred at room temperature. After 70 minutes, TLC analysis indicated that most of the starting material was consumed but also showed that several side products were forming. Accordingly, the mixture was filtered through a plug of SiO_2 with EtOAc and the filtrate was concentrated to a yellow-orange oil. This oil was purified by MPLC (20:1 hexanes:EtOAc) to give the acyl nitrile **4044** (28.7 mg, 0.0777 mmol, 19%) as a bright yellow oil.

^{1}H NMR (500 MHz, $CDCl_3$): δ 3.69 (t, J = 5.9 Hz, 2H, OCH_2), 2.68 (m, 4H, CH_2C=CCH_2), 2.51 (t, J = 7.1 Hz, 2H, C≡CCH_2), 1.84–1.79 (m, 2H), 1.77 (tt, J = 7.2, 5.9 Hz, 2H, C≡CCH_2CH_2), 1.65 (br app pent, J ~ 5.5 Hz, 2H, =CCH_2CH_2), 1.51 (br app pent, J ~ 5.5 Hz, 2H, =CCH_2CH_2CH_2), 0.89 [s, 9H, SiC(CH_3)$_3$], and 0.06 [s, 6H, Si(CH_3)$_2$].

^{13}C NMR (125 MHz, $CDCl_3$): δ 166.5, 147.2, 145.9, 114.2, 94.0, 93.0, 73.4, 65.4, 61.4, 39.1, 31.9, 31.2, 27.7, 26.0, 25.7, 25.3, 18.3, 16.7, and -5.2.

TLC: R_f 0.35 (20:1 hexanes:EtOAc)

12-(*tert*-Butyldimethylsilyl)-2,3,4,7,8,9,10,11-octahydro-6*H*-azuleno[2,1-*b*]pyrano[2,3-*e*]pyridin-6-one (4051)

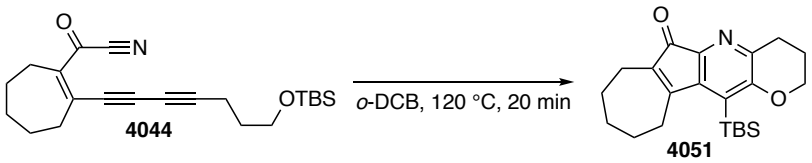

In a 50 mL culture tube, the acyl nitrile **4044** (28.3 mg, 0.0766 mmol) was dissolved in *o*-dichlorobenzene (7.7 mL). The culture tube was sealed with a Teflon-lined cap and placed in a 120 °C oil bath. TLC analysis indicated that the starting material was consumed after 20 minutes. The reaction solution was filtered through a plug of SiO_2 with hexanes (to elute the *o*-dichlorobenzene) followed by EtOAc. The EtOAc filtrate was concentrated to a dull orange oil. This oil was then purified by MPLC (3:1 hexanes:EtOAc) to give the pyridine **4051** (8.1 mg, 0.0219 mmol, 29%) as a yellow crystalline solid.

^{1}H NMR (500 MHz, $CDCl_3$): δ 4.13 (nfom, 2H, OCH_2), 2.95 (t, J = 6.6 Hz, 2H, ArCH_2), 2.70 (nfom, 2H, C=CCH_2), 2.45 (nfom, 2H, CH_2C=C), 2.05 (nfom, 2H, ArCH$_2$CH_2), 1.85 (nfom, 2H, CH_2CH$_2$C=C), 1.61 (nfom, 2H, =CCH$_2$CH_2), 1.53 (nfom, 2H, =CCH$_2$CH$_2$CH_2), 1.03 [s, 9H, SiC(CH_3)$_3$], and 0.30 [s, 6H, Si(CH_3)$_2$].

^{13}C NMR (125 MHz, $CDCl_3$): δ 194.9*, 163.0 (C11a), 158.4* (C12a), 148.1 (C5a), 143.2* (C11b), 138.8 (C6a or C4a), 138.6 (C4a or C6a), 129.6*(C12), 66.3, 32.2, 30.8 (C11), 28.4, 28.2, 27.0, 26.2, 23.4 (C7), 22.2, 18.7, and 0.9. *These resonances, each for a non-hydrogen-bearing carbon, were of low intensity in the 1D spectrum but their presence was confirmed by HMBC analysis.

HRMS (ESI-Orbitrap) Calculated for $C_{22}H_{32}NO_2Si^+$ [M+H$^+$] 370.2197, found 370.2200.

TLC: R_f 0.30 (3:1 hexanes:EtOAc)

m.p. 160–163 °C

2-(7-((*tert*-Butyldimethylsilyl)oxy)hepta-1,3-diyn-1-yl)-4,5-dimethoxybenzaldehyde (4052)

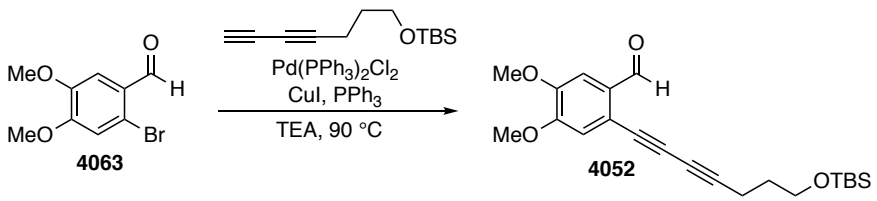

Spectral Data for 4052

^{1}H NMR (400 MHz, $CDCl_3$): δ 10.33 (s, 1H, C*H*O), 7.38 (s, 1H, Ar*H6*), 7.01 (s, 1H, Ar*H3*), 3.95 (s, 3H, OCH_3), 3.94 (s, 3H, OCH_3'), 3.72 (t, *J* = 5.8 Hz, 2H, OCH_2), 2.49 (t, *J* = 7.0 Hz, 2H, C≡CCH_2), 1.79 (tt, *J* = 6.0, 7.2 Hz, 2H, C≡CCH$_2$CH_2), 0.91 [s, 9H, C(CH_3)$_3$], and 0.08 [s, 6H, Si(CH_3)$_2$].

^{13}C NMR (125 MHz, $CDCl_3$): δ 189.9, 153.5, 150.2, 132.0, 120.2, 115.2, 108.2, 86.5, 79.9, 70.1, 64.9, 61.4, 56.3, 56.2, 31.3, 26.0, 18.3, 16.2, and -5.3.

HRMS (ESI-Orbitrap) Calculated for $C_{22}H_{31}O_4Si^+$ [M+H$^+$] 387.1986, found 387.1985

TLC: R_f 0.35 (11:1 hexanes:EtOAc)

2-(2-(7-((*tert*-Butyldimethylsilyl)oxy)hepta-1,3-diyn-1-yl)-4,5-dimethoxyphenyl)-2-((trimethylsilyl)oxy)acetonitrile (4060)

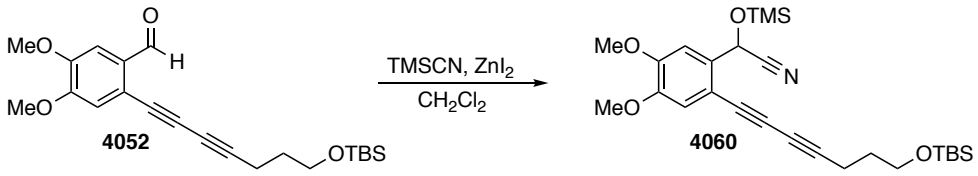

In a 2 dram glass vial containing a stir bar, aldehyde **4056** (105 mg, 0.272 mmol) was dissolved in CH_2Cl_2 (1.0 mL). TMSCN (68 μL, 0.54 mmol) and ZnI_2 (9.5 mg, 0.030 mmol) were added and the resulting mixture was vigorously stirred at room temperature. After 10 minutes, TLC analysis indicated that the reaction was complete. The slurry was filtered through a SiO_2 plug with 1:1 hexanes:EtOAc and the eluent was concentrated to a yellow oil. This oil was purified by MPLC (8:1 hexanes:EtOAc) to give the *O*-silylated cyanohydrin **4060** (106 mg, 0.218 mmol, 80%) as a light yellow oil.

^{1}H NMR (400 MHz, $CDCl_3$): δ 7.14 (s, 1H, Ar*H3* or Ar*H6*), 6.94 (s, 1H, Ar*H3* or Ar*H6*), 5.84 (s, 1H, ArC*H*CN), 3.95 (s, 3H, ArOCH_3), 3.87 (s, 3H, ArOCH_3'), 3.72 (t, J = 5.9 Hz, 2H, OCH_2), 2.48 (t, J = 7.0 Hz, 2H, C≡CCH_2), 1.79 (tt, J = 7.0, 5.9 Hz, 2H, C≡CCH$_2$CH_2), 0.91 [s, 9H, SiC(CH_3)$_3$], 0.23 [s, 9H, Si(CH_3)$_3$], and 0.08 [s, 6H, Si(CH_3)$_2$].

^{13}C NMR (125 MHz, $CDCl_3$): δ 150.7, 149.6, 132.9, 119.1, 115.1, 112.7, 109.9, 86.2, 79.2, 71.0, 64.9, 61.7, 61.4, 56.23, 56.19, 31.3, 26.0, 18.4, 16.2, -0.1, and -5.2.

TLC: R_f 0.30 (8:1 hexanes:EtOAc)

2-(7-((*tert*-Butyldimethylsilyl)oxy)hepta-1,3-diyn-1-yl)-4,5-dimethoxybenzoyl cyanide (4052)

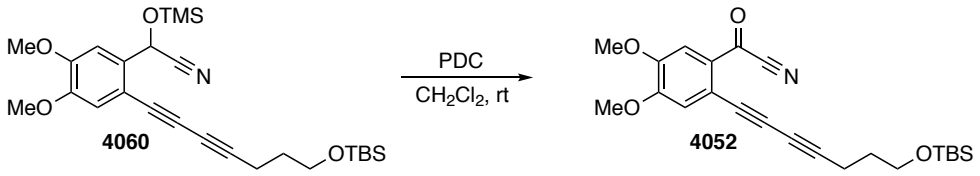

In an 8 mL culture tube containing a stir bar, the *O*-silyl cyanohydrin **4060** (88.7 mg, 0.183 mmol) was dissolved in CH_2Cl_2 (1.5 mL). PDC (137 mg, 0.365 mmol) was added to this solution, and the resulting mixture was vigorously stirred at room temperature. After 6 hours, the mixture was filtered through a plug of SiO_2 with EtOAc and the filtrate was concentrated to an orange oil. This oil was purified by MPLC (5:1 hexanes:EtOAc) to give the acyl nitrile **4052** (63.6 mg, 0.155 mmol, 85%) as a bright orange oil.

^{1}H NMR (500 MHz, $CDCl_3$): δ 7.51 (s, 1H, Ar*H6*), 7.09 (s, 1H, Ar*H3*), 3.984 (s, 3H, ArOCH_3), 3.978 (s, 3H, ArOCH_3*'*), 3.71 (t, *J* = 5.9 Hz, 2H, OCH_2) 2.50 (t, *J* = 7.1 Hz, 2H, C≡CCH_2), 1.79 (tt, *J* = 7.1, 5.9 Hz, 2H, C≡CCH$_2$CH_2), 0.90 [s, 9H, SiC(CH_3)$_3$], and 0.07 [s, 6H, Si(CH_3)$_2$].

^{13}C NMR (125 MHz, $CDCl_3$): δ 164.6, 154.9, 149.8, 128.3, 118.9, 117.7, 113.8, 113.5, 88.5, 82.5, 71.2, 65.3, 61.5, 56.7, 56.5, 31.3, 26.0, 18.4, 16.4, and -5.2.

HRMS (ESI-Orbitrap) Calculated for $C_{23}H_{30}NO_4Si^+$ [M+H$^+$] 412.1939, found 412.1946.

TLC: R_f 0.35 (5:1 hexanes:EtOAc)

11-(*tert*-Butyldimethylsilyl)-8,9-dimethoxy-3,4-dihydroindeno[2,1-*b*]pyrano[2,3-*e*]pyridin-6(2*H*)-one (4061)

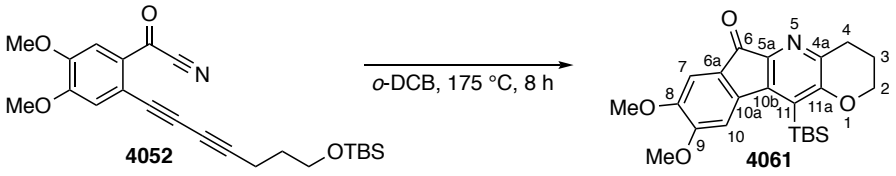

In a 16 mL culture tube, acyl nitrile **4052** (32.6 mg, 0.0792 mmol) was dissolved in *o*-dichlorobenzene (7.9 mL). The culture tube was sealed with a Teflon-lined cap and placed in a 175 °C oil bath. TLC analysis indicated that the starting material was consumed after 8 hours. The reaction solution was filtered through a plug of SiO_2 with hexanes (to elute the *o*-dichlorobenzene) followed by EtOAc. The EtOAc filtrate was concentrated to a dark red solid. This oil was then purified by MPLC (1:1 hexanes:EtOAc) to give the pyridine **4061** (21.6 mg, 0.0525 mmol, 66%) as an orange crystalline solid.

^{1}H NMR (500 MHz, $CDCl_3$): δ 7.26 (s, 1H, Ar*H7*), 7.25 (s, 1H, Ar*H10*), 4.19 (br t, *J* = 5.2 Hz, 2H, OCH_2), 4.00 (s, 3H, ArOCH_3), 3.92 (s, 3H, ArOCH_3'), 3.01 (t, *J* = 6.6 Hz, 2H, ArCH_2CH$_2$), 2.10 (nfom, 2H, ArCH$_2$CH_2), 1.09 [s, 9H, SiC(CH_3)$_3$], and 0.44 [s, 6H, Si(CH_3)$_2$].

^{13}C NMR (125 MHz, $CDCl_3$): δ 191.3 (C6), 159.5 (C11a), 153.5 (C8 or C9), 149.5 (C8 or C9), 146.5, 145.9, 140.8 (C4a), 138.2, 129.1 (C11), 127.4, 109.2 (C10), 107.1 (C7), 66.5 (C2), 56.6 (O*C*H$_3$), 56.4 (O*C*H$_3$'), 28.6 (C4), 28.0 [SiC(*C*H$_3$)$_3$], 22.1 (C3), 19.3 [Si*C*(CH$_3$)$_3$], and 0.2 [Si(*C*H$_3$)$_2$]. (the indicated carbon assignments were deduced from analysis of HMBC data)

HRMS (ESI-Orbitrap) Calculated for $C_{23}H_{30}NO_4Si^+$ [M+H$^+$] 412.1939, found 412.1945.

m.p. 196–197 °C

4,5-Dimethoxy-2-(penta-1,3-diyn-1-yl)benzaldehyde (4059)

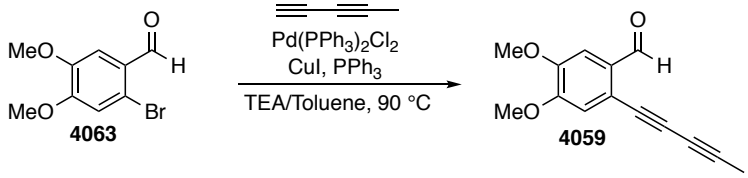

To an oven-dried 500 mL round-bottom flask with a stir bar were added $Pd(PPh_3)_2Cl_2$ (703 mg, 1.00 mmol), CuI (380 mg, 2.00 mmol), and PPh_3 (788 mg, 3.00 mmol). The headspace was briefly flushed with N_2 and dry/degassed triethylamine (100 mL), bromoaldehyde **4063** (2.45 g, 10.0 mmol), and 1,3-pentadiyne (20 mmol; prepared as a solution in 260 mL of toluene by NaOH-promoted deprotection of 2-methylhepta-3,5-diyn-2-ol) were added. The flask was fitted with a reflux condenser, placed under a positive N_2 pressure, and lowered into a 90 °C oil bath. After 1.5 hours, ^{1}H NMR analysis of an aliquot indicated that the reaction had not proceeded to complete conversion; analysis after 3 hours indicated essentially no further conversion. Accordingly, the reaction mixture was diluted with EtOAc (300 mL) and quenched by the addition of saturated aqueous NH_4Cl solution (200 mL). The organic layer was treated with additional portions of saturated aqueous NH_4Cl solution (2 x 200 mL), washed with brine, dried with $MgSO_4$, and concentrated to give a dark brown solid. This solid was purified by flash column chromatography (50:1 hexanes:EtOAc) to give the diyne **4059** (1.06 g, 4.64 mmol, 46%, 68% brsm) as a tan solid.

^{1}H NMR (500 MHz, $CDCl_3$): δ 10.33 (s, 1H, ArC*H*O), 7.38 (s, 1H, Ar*H6*), 7.00 (s, 1H, Ar*H3*), 3.95 (s, 3H, ArOC*H*$_3$), 3.94 (s, 3H, ArOC*H*$_3$*'*), and 2.06 (s, 3H, C≡CC*H*$_3$).

^{13}C NMR (125 MHz, $CDCl_3$): δ 190.0, 153.6, 150.2, 132.1, 120.3, 115.3, 108.3, 82.5, 80.0, 69.6, 64.1, 56.4, 56.3, and 4.8.

HRMS (ESI-Orbitrap) Calculated for $C_{14}H_{13}O_3^+$ [M+H$^+$] 229.0859, found 229.0856.

2-(4,5-Dimethoxy-2-(penta-1,3-diyn-1-yl)phenyl)-2-((trimethylsilyl)oxy)acetonitrile

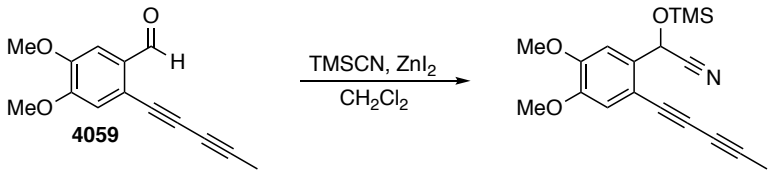

In an 8 mL culture tube fitted with a stir bar, aldehyde **4059** (182 mg, 0.797 mmol) was dissolved in CH_2Cl_2 (4.0 mL). To this solution, TMSCN (0.20 mL, 1.6 mmol) and ZnI_2 (13.2 mg, 0.0414 mmol) were added. The resulting solution was left to vigorously stir at room temperature. After 1 hour, the reaction solution was filtered through a SiO_2 plug with EtOAc and the filtrate was concentrated to give the *O*-silylated cyanohydrin (238 mg, 0.726 mmol, 91%) as a brown oil. This material was not further purified, but taken on to the next reaction.

^{1}H NMR (500 MHz, $CDCl_3$): δ 7.14 (s, 1H, Ar*H3* or Ar*H6*), 6.94 (s, 1H, Ar*H3* or Ar*H6*), 5.84 [s, 1H, ArC*H*(CN)OSi], 3.95 (s, 3H, ArOCH_3), 3.88 (s, 3H, ArOCH_3'), 2.05 (s, 3H, C≡CCH_3), and 0.23 [s, 9H, OSi(CH_3)$_3$].

^{13}C NMR (125 MHz, $CDCl_3$): δ 150.7, 149.6, 132.8, 119.1, 115.1, 112.7, 109.9, 82.2, 79.3, 70.4, 64.1, 61.7, 56.3, 56.2, 4.8, and -0.1.

4,5-Dimethoxy-2-(penta-1,3-diyn-1-yl)benzoyl cyanide (4062)

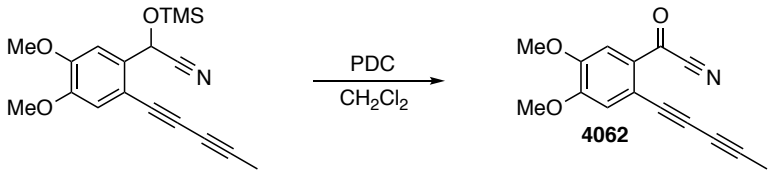

In a 50 mL round-bottom flask containing a stir bar, the *O*-silylated cyanohydrin (1.42 g, 4.34 mmol) was dissolved in 15 mL of CH_2Cl_2. PDC (2.45 g, 6.60 mmol) was added and the resulting mixture was vigorously stirred at room temperature. After 5 hours (TLC monitoring), the mixture was filtered through a plug of SiO_2 with EtOAc and the filtrate was concentrated to provide a bright yellow solid. This solid was purified by MPLC (4:1 hexanes:EtOAc) to yield the acyl nitrile **4062** (648 mg, 2.56 mmol, 59%) as a neon yellow, crystalline solid.

^{1}H NMR (500 MHz, $CDCl_3$): δ 7.51 (s, 1H, Ar*H6*), 7.09 (s, 1H, Ar*H3*), 3.984 (s, 3H, ArOCH_3), 3.979 (s, 3H, ArOCH_3'), and 2.07 (s, 3H, C≡CCH_3).

^{13}C NMR (125 MHz, $CDCl_3$): δ 164.5, 154.8, 149.7, 128.3, 118.8, 117.6, 113.6, 113.4, 84.4, 82.5, 70.6, 64.4, 56.7, 56.4, and 5.0.

HRMS (ESI-Orbitrap) Calculated for $C_{15}H_{12}NO_3^+$ [M+H$^+$] 254.0812, found 254.0816.

TLC: R_f 0.35 (2:1 hexanes:EtOAc)

m.p. 160–161 °C.

9,10-Dimethoxy-5-methyl-1,4-dihydro-7*H*-1,4-epoxyindeno[2,1-*c*]isoquinolin-7-one (4064a)

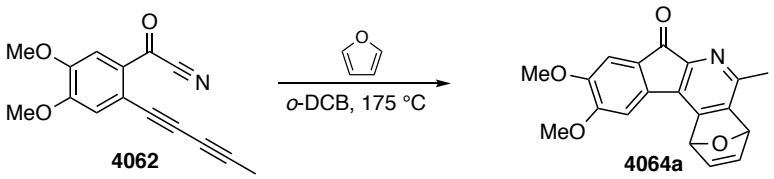

In a 50 mL flame-dried culture tube, acyl nitrile **4062** (35.2 mg, 0.139 mmol) and furan (30 µL, 0.41 mmol) were dissolved in 14 mL *o*-DCB. The culture tube was sealed with a Teflon-lined cap and placed in a 175 °C oil bath. After 7 hours the solution was filtered through a plug of SiO_2 with hexanes (to elute the *o*-dichlorobenzene) followed by EtOAc. The EtOAc filtrate was concentrated and the residue was purified by MPLC (1:2 hexanes:EtOAc) to give the pyridine derivative **4064a** (24.6 mg, 0.0766 mmol, 55%) as an orange crystalline solid.

^{1}H NMR (500 MHz, $CDCl_3$): δ 7.29 (s, 1H, *H8*), 7.10 (dd, *J* = 5.6, 1.8 Hz, 1H, *H2*), 7.07 (dd, *J* = 5.5, 1.8 Hz, 1H, *H3*), 6.91 (s, 1H, *H11*), 6.04 (dd, *J* =1.8, 0.7 Hz, 1H, *H4*), 5.84 (dd, *J* = 1.8, 0.8 Hz, 1H, *H1*), 4.06 (s, 3H, C9OC*H*$_3$), 3.93 (s, 3H, C10OC*H*$_3$), and 2.55 (s, 3H, ArC*H*$_3$).

^{13}C NMR (125 MHz, $CDCl_3$): δ 191.0, 155.3, 152.3, 150.2, 149.5, 147.8, 144.7, 142.8, 141.2, 136.9, 129.0, 126.4, 107.8, 105.1, 80.3, 80.2, 56.7, 56.4, and 21.0.

HRMS (ESI-Orbitrap) Calculated for $C_{19}H_{16}NO_4^+$ [M+H$^+$] 322.1074, found 322.1078.

TLC: R_f (1:2 hexanes:EtOAc)

6,7-Dimethoxy-2-methyl-9H-indeno[2,1-b]pyridin-9-one (4064b)

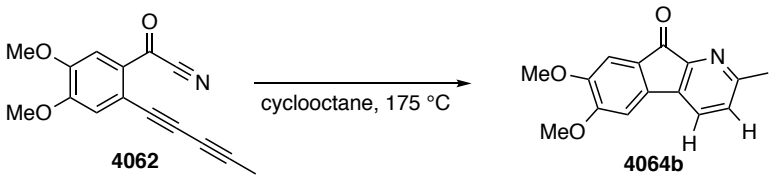

In a 50 mL flame-dried culture tube, the acyl nitrile **4062** (50.0 mg, 0.1974 mmol) was dissolved in 10 mL of cyclooctane. The culture tube was sealed with a Teflon-lined cap and placed in an oil bath held at 175 °C. After 7 hours the solution was passed through a plug of SiO_2 with hexanes (to first elute the cyclooctane) followed by EtOAc. The EtOAc was removed and the residue was purified by MPLC (50:1 CH_2Cl_2:MeOH) to give the pyridine derivative **4064b** (11.6 mg, 0.0454 mmol, 23%) as an orange crystalline solid. No other discrete components were observed to elute on silica gel.

^{1}H NMR (400 MHz, $CDCl_3$): δ 7.56 (d, *J* = 7.8 Hz, 1H, *H4*), 7.26 (s, 1H, *H8*), 7.11 (d, *J* = 7.8 Hz, 1H, *H3*), 6.96 (s, 1H, *H5*), 4.02 (s, 3H, OC*H*$_3$), 3.92 (s, 3H, OC*H*$_3$'), and 2.60 (s, 3H, ArC*H*$_3$).

^{13}C NMR (125 MHz, $CDCl_3$): δ 192.4, 158.6, 155.3, 153.9, 150.1, 137.5, 137.1, 126.7, 126.2, 125.4, 107.8, 104.0, 56.6, 56.4, and 24.2.

HRMS (ESI-Orbitrap) Calculated for $C_{15}H_{14}NO_3^+$ [M+H$^+$] 256.0968, found 256.0970.

TLC: R_f 0.25 (50:1 CH_2Cl_2:MeOH)

6,7-Dimethoxy-2-methyl-9-oxo-9*H*-indeno[2,1-*b*]pyridin-3-yl acetate (4064c-major)
and
6,7-Dimethoxy-2-methyl-9-oxo-9*H*-indeno[2,1-*b*]pyridin-4-yl acetate (4064c-minor)

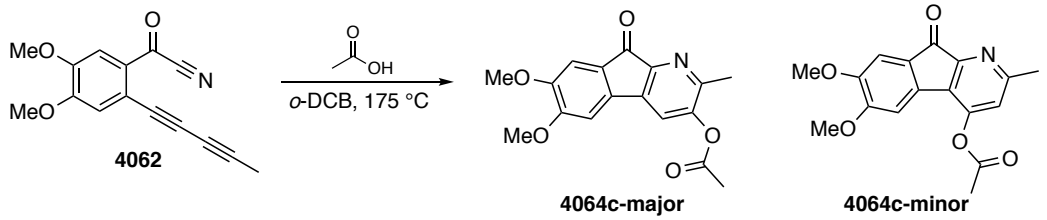

In a 50 mL flame-dried culture tube, the acyl nitrile **4062** (101 mg, 0.398 mmol) and acetic acid (114 μL, 1.99 mmol) were dissolved in dry, degassed *o*-DCB (40 mL). The culture tube was sealed with a Teflon-lined cap and placed in a 175 °C oil bath. After 8 hours (TLC monitoring) the solution was concentrated to a black oil. This oil was purified by MPLC (1:2 hexanes:EtOAc) to give, in order of elution, **4064c-major** (35.2 mg, 0.112 mmol, 28%) as a bright red crystalline solid and **4064c-minor** (5.1 mg, 0.016 mmol, 4%) as a dull yellow solid.

Data for 4064c-major

^{1}H NMR (400 MHz, $CDCl_3$): δ 7.42 (s, 1H, Ar*H4*), 7.25 (s, 1H, Ar*H8*), 6.92 (s, 1H, Ar*H5*), 4.00 (s, 3H, C6OC*H*$_3$), 3.92 (s, 3H, C7OC*H*$_3$), 2.48 (s, 3H, ArC*H*$_3$), and 2.39 [s, 3H, CH_3(C=O)O].

^{13}C NMR (125 MHz, $CDCl_3$): δ 190.8, 168.6, 155.2, 150.7, 150.7, 150.3, 148.1, 139.2, 136.2, 126.0, 120.6, 107.7, 104.2, 56.6, 56.4, 21.1, and 19.3.

HRMS (ESI-Orbitrap) Calculated for $C_{17}H_{16}NO_5^+$ [M+H$^+$] 314.1023, found 314.1018.

TLC: R_f 0.40 (1:3 hexanes:EtOAc)

4-((6,7-Dimethoxy-2-methyl-9-oxo-9*H*-indeno[2,1-*b*]pyridin-3-yl)thio)butyl acetate (4064d-major) and 4-((6,7-Dimethoxy-2-methyl-9-oxo-9*H*-indeno[2,1-*b*]pyridin-4-yl)thio)butyl acetate (4064d-minor)

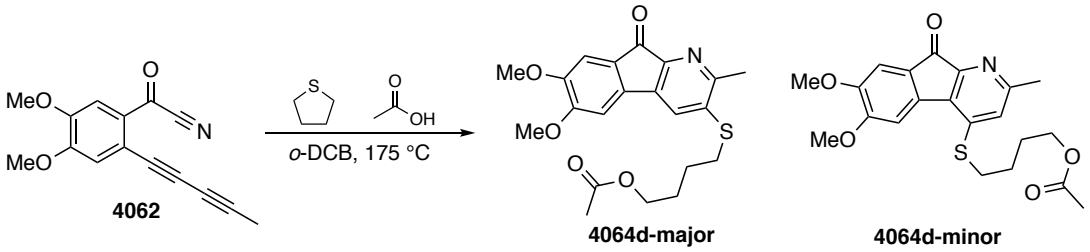

In a 50 mL culture tube, acyl nitrile **4062** (78.5 mg, 0.310 mmol), tetrahydrothiophene (55 µL, 0.62 mmol), and glacial acetic acid (53 µL, 0.93 mmol) were dissolved in *o*-dichlorobenzene (15 mL). The culture tube was sealed with a Teflon-lined cap and placed in a 175 °C oil bath for 8 hours. After this time, the solution was filtered through a plug of SiO_2 with hexanes (to elute the *o*-dichlorobenzene) followed by EtOAc. The EtOAc filtrate was concentrated and purified by flash column chromatography (1:1.5 hexanes:EtOAc + 1% TEA) to give, in order of elution, the isomeric pyridines **4064d-major** (46.3 mg, 0.115 mmol, 37%) and **4064d-minor** (23.8 mg, 0.0592 mmol, 19%), each as an orange crystalline solid as an orange residue.

Data for **4064d-major**:

^{1}H NMR (400 MHz, $CDCl_3$): δ 7.37 (s, 1H,), 7.22 (s, 1H), 6.97 (s, 1H), 4.15 (br t, J = 6.1 Hz, 1H, C*H*$_2$OC=O), 4.04 (s, 3H), 3.92 (s, 3H), 3.07 (t, J = 7.0 Hz, 2H, SC*H*$_2$CH$_2$), 2.58 (s, 3H, ArC*H*$_3$), 2.06 (s, 3H, C*H*$_3$CO$_2$CH$_2$), and 1.85–1.90 (m, 4H, SCH$_2$C*H*$_2$C*H*$_2$).

^{13}C NMR (125 MHz, $CDCl_3$): δ 191.7 171.2, 154.84, 154.81, 150.1, 149.1, 138.8, 138.1, 136.5, 125.9, 122.1, 107.5, 104.0, 63.6, 56.6, 56.3, 31.4, 28.0, 25.0, 22.8, and 21.1.

HRMS (ESI-Orbitrap) Calculated for $C_{21}H_{24}NO_5S^+$ [M+H$^+$] 402.1370, found 402.1375.

TLC: R_f 0.35 (1:1 hexanes:EtOAc + 10% TEA)

m.p. 154–156 °C

Data for **4064d-minor**:

^{1}H NMR (400 MHz, $CDCl_3$): δ 7.48 (s, 1H,), 7.28 (s, 1H), 6.92 (s, 1H), 4.15 (br t, J = 6 Hz, 1H, C*H*$_2$OC=O), 4.04 (s, 3H), 3.92 (s, 3H), 3.14 (br t, J = 7 Hz, 2H, SC*H*$_2$CH$_2$), 2.58 (s, 3H, ArC*H*$_3$), 2.06 (s, 3H, C*H*$_3$CO$_2$CH$_2$), and 1.85–1.90 (m, 4H, SCH$_2$C*H*$_2$C*H*$_2$).

^{13}C NMR (125 MHz, $CDCl_3$): δ 192.1, 171.1, 157.9, 154.7, 153.5, 149.4, 142.6, 138.0, 134.2, 125.0, 121.9, 108.1, 107.7, 63.6, 56.6, 56.5, 30.9, 28.0, 25.3, 24.3, and 21.1.

HRMS (ESI-Orbitrap) Calculated for $C_{21}H_{24}NO_5S^+$ [M+H$^+$] 402.1370, found 402.1370.

TLC: R_f 0.25 (1:1 hexanes:EtOAc + 10% TEA);

(2-((Trimethylsilyl)ethynyl)cyclohept-1-en-1-yl)methanol (4071)

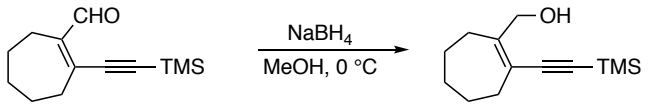

4070 **4071**

Aldehyde **4070** (4.28 g, 19.4 mmol) was dissolved in MeOH (30 mL) and cooled in an ice bath for 10 minutes. $NaBH_4$ (681 mg, 18.0 mmol) was then added in portions over one minute, and the resulting mixture was stirred in ice bath. After 5 minutes, the reaction mixture was quenched by the addition of H_2O (40 mL) and extracted with EtOAc (3 x 50 mL). The combined EtOAc extracts were treated with brine, dried with Na_2SO_4, and concentrated. The resulting oil was purified by flash column chromatography (5:1 hex:EtOAc) to give alcohol **4071** (3.65 g, 16.4 mmol, 85%) as a golden oil.

^{1}H NMR (500 MHz, $CDCl_3$): δ 4.34 (s, 2H, C*H*$_2$OH), 2.36 (nfom, 2H, CH_2C=C-C*H*$_2$), 2.34 (nfom, C*H*$_2$C=C-CH_2 *2H*), 1.75 (br pent, *J* = 5.9 Hz, 2H), 1.55 (m, 2H), 1.50 (br pent, *J* = 5.5 Hz, 2H), and 0.19 (s, 9H, Si(C*H*$_3$)$_3$).

^{13}C NMR (125 MHz, $CDCl_3$): δ 151.7, 123.0, 105.9, 97.9, 66.7, 34.8, 32.5, 31.4, 26.5, 26.4, and 0.2.

IR (thin film): 3333 (broad), 2921, 2850, 2133, 1448, 1248, 1050, 1018, 993, 838, 756, and 697 cm^{-1}.

HRMS (ESI-Orbitrap) Calculated for $C_{13}H_{23}OSi^+$ [M+H$^+$] 223.1513, found 223.1513.

2-(2-((Trimethylsilyl)ethynyl)cyclohept-1-en-1-yl)acetonitrile (4072)

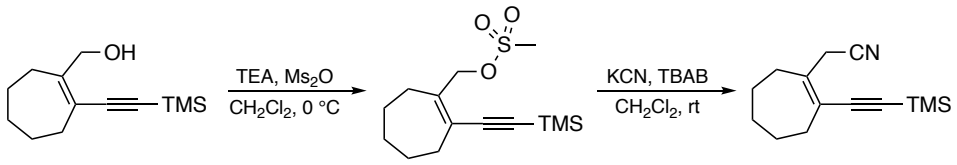

4071 **4074** **4072**

In a flame-dried 250 mL round-bottom flask, the allylic alcohol **4071** (3.00 g, 13.5 mmol) was dissolved in dry CH_2Cl_2 (135 mL) and the resulting solution was cooled in a 0 °C ice bath. Triethylamine (2.8 mL, 20 mmol) was added followed by recently prepared[i] methanesulfonic anhydride (2.86 g, 16.4 mmol). After 50 minutes, ^{1}H NMR analysis of an aliquot indicated that the reaction was complete. At this point, the reaction mixture was diluted with additional CH_2Cl_2 (100 mL), which was washed with water (2 x 100 mL) and brine, dried over $MgSO_4$, and concentrated to a light yellow residue. This material was shown by ^{1}H NMR analysis to be predominantly the allylic mesylate **4074**. This material showed signs of instability (discoloration over several hours) and was carried on to the next step without further purification or delay.

Data for a crude sample of the mesylate 4074.

^{1}H NMR (500 MHz, $CDCl_3$): 4.97 (s, 2H, C*H*$_2$OSO$_2$), 3.03 (s, 3H, SO$_3$C*H*$_3$), 2.40 (nfom, 2H, CH$_2$C=C-C*H*$_2$), 2.35 (nfom, 2H, C*H*$_2$C=C-CH$_2$), 1.76 (br pent, J ~ 6 Hz, 2H), 1.61–1.51 (m, 4H), and 0.20 [s, 9H, Si(C*H*$_3$)$_3$].

The crude mesylate **4074** was dissolved in 70 mL of CH_2Cl_2. To this solution, water (70 mL), potassium cyanide (697 mg, 14.8 mmol), and tetra-*n*-butylammonium bromide (2.18 g, 6.76 mmol) were added. The resulting biphasic mixture was vigorously stirred at room temperature. After 3 hours (TLC monitoring), the CH_2Cl_2 layer was separated, washed with water (2 x 100 mL) and brine, dried over $MgSO_4$, and concentrated to a reddish-orange residue. This material was purified by flash column chromatography (20:1 hexanes:EtOAc) to give the allylic nitrile **4072** (1.53 g, 6.60 mmol, 49%) as a light yellow oil.

^{1}H NMR (500 MHz, $CDCl_3$): δ 3.45 (s, 2H, C*H*$_2$CN), 2.37 (m, 4H, C*H*$_2$C=C-C*H*$_2$), 1.76 (br pent, J ~ 6 Hz, 2H, C*H*$_2$CH$_2$C=C-CH$_2$CH$_2$), 1.56 (m, 4H, C*H*$_2$C*H*$_2$CH$_2$C=C-CH$_2$), and 0.20 [s, 9H, Si(C*H*$_3$)$_3$].

^{13}C NMR (125 MHz, $CDCl_3$): δ 139.8, 126.1, 117.6, 105.1, 99.7, 34.2, 33.1, 32.0, 26.0, 25.9, 25.8, and 0.1.

IR (thin film): 2924, 2852, 2249, 2135, 1449, 1414, 1248, 1030, 840, 758, and 698 cm^{-1}.

HRMS (ESI-Orbitrap) Calculated for $C_{14}H_{22}NSi^+$ [M+H$^+$] 232.1516, found 232.1511.

TLC: R_f 0.25 (15:1 hexanes:EtOAc)

2-Methyl-2-(2-((trimethylsilyl)ethynyl)cyclohept-1-en-1-yl)propanenitrile (4076)

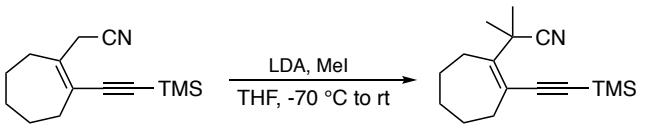

4072 **4076**

A 250 mL 3-neck round-bottom flask containing a stir bar was fitted with a pressure-equalizing dropping funnel and placed under a slight N_2 pressure. Diisopropylamine (9.8 mL, 69 mmol) was dissolved in 100 mL of THF and the resulting solution was cooled in a dry ice/acetone cold bath for 10 minutes. To this stirred solution, n-BuLi solution in hexanes (27 mL, 68 mmol) was added by syringe over a period of 5 minutes. A solution of the allylic nitrile **4072** (1.53 g, 6.61 mmol) in THF (30 mL) was added through the dropping funnel over about a minute. To this mixture, MeI (4.1 mL, 66 mmol) was added dropwise by syringe over a period of 5 minutes. Shortly after the addition of MeI was complete, a white solid precipitated. The flask was removed from the cold bath and the slurry was allowed to stir. When close to room temperature, the solution became homogeneous. At this point, if the solution color was dark (purple to black), additional MeI was added by syringe until the solution took on a light yellow-orange color. Once this color was obtained, reaction completion was confirmed by GC-MS. The reaction was quenched by the addition of saturated aqueous ammonium chloride solution (150 mL). The THF layer was separated, washed with brine, dried with Mg_2SO_4, and concentrated to a dull orange oil. This oil was purified by flash column chromatography (20:1 hexanes:EtOAc) to give the dimethylated allylic nitrile **4076** (1.08 g, 4.16 mmol, 63%) as a light yellow oil.

^{1}H NMR (500 MHz, $CDCl_3$): δ 2.46–2.41 (m, 4H, C*H*$_2$C=C-C*H*$_2$), 1.75 (br pent, J = ~ 6 Hz, 2H, C*H*$_2$CH$_2$C=C-CH$_2$CH$_2$), 1.71 [s, 6H, C(C*H*$_3$)$_2$], 1.56 (br pent, J = ~ 5 Hz, 2H, CH$_2$CH$_2$C=C-CH$_2$C*H*$_2$), 1.51 (br pent, J = ~ 5 Hz, C*H*$_2$CH$_2$CH$_2$C=C), and 0.19 [s, 9H, Si(C*H*$_3$)$_3$].

^{13}C NMR (125 MHz, $CDCl_3$): δ 148.5, 124.5, 123.3, 106.0, 103.5, 39.4, 37.1, 32.1, 31.9, 27.1, 26.2, 25.8, and -0.2.

IR (thin film): 2957, 2924, 2854, 2232, 2134, 1444, 1248, 1105, 1015, 834, 758, and 699 cm^{-1}.

HRMS (ESI-Orbitrap) Calculated for $C_{16}H_{26}NSi^+$ [M+H$^+$] 260.1829, found 260.1830.

TLC: R_f 0.25 (30:1 hexanes:EtOAc)

2-(2-Ethynylcyclohept-1-en-1-yl)-2-methylpropanenitrile (4077)

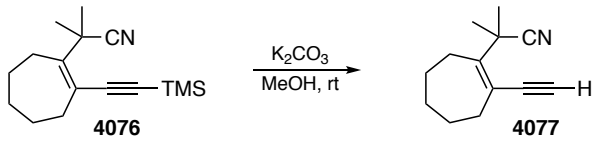

4076 **4077**

In a 50 mL round-bottom flask, the alkynyl silane **4076** (589 mg, 2.27 mmol) was dissolved in MeOH (15 mL). K_2CO_3 (174 mg, 1.26 mmol) was added and the resulting mixture was vigorously stirred at room temperature. After 90 minutes (TLC monitoring), the mixture was diluted with EtOAc (50 mL) and treated with H_2O (50 mL). The layers were separated and the aqueous layer was extracted with additional EtOAc (50 mL). The combined organic extracts were treated with brine, dried over Mg_2SO_4, and concentrated to leave a pale yellow oil. This oil was purified by MPLC (20:1 hexanes:EtOAc) to give the terminal alkyne **4077** (316 mg, 1.69 mmol, 74%) as a clear oil.

^{1}H NMR (500 MHz, $CDCl_3$): δ 3.45 (s, 1H, C≡C*H*), 2.47–2.44 (m, 4H, CH_2C=C-CH_2), 1.76 (br pent, J = ~ 6 Hz, 2H, CH_2CH$_2$C=C-CH$_2$CH$_2$), 1.70 [s, 6H, C(CH_3)$_2$], 1.57 (br pent, J = ~5 Hz, 2H, CH$_2$CH$_2$C=C-CH$_2$CH_2), and 1.52 (br pent, J = ~5 Hz, 2H, CH$_2$CH$_2$C=C-CH$_2$CH$_2$CH_2).

^{13}C NMR (125 MHz, $CDCl_3$): 148.9, 124.3, 122.3, 86.5, 84.4, 39.2, 37.2, 31.8, 31.7, 27.1, 26.1, and 25.6.

IR (thin film): 3282, 2979, 2923, 2853, 2233, 2084, 1443, 1389, 1366, 1214, 1197, 991, 965, 832, 695, and 625 cm^{-1}.

HRMS (ESI-Orbitrap) Calculated for $C_{13}H_{18}N^+$ [M+H$^+$] 188.1434, found 188.1434.

TLC: R_f 0.40 (10:1 hexanes:EtOAc)

2-(2-(7-((*tert*-Butyldimethylsilyl)oxy)hepta-1,3-diyn-1-yl)cyclohept-1-en-1-yl)-2-methylpropanenitrile (4069)

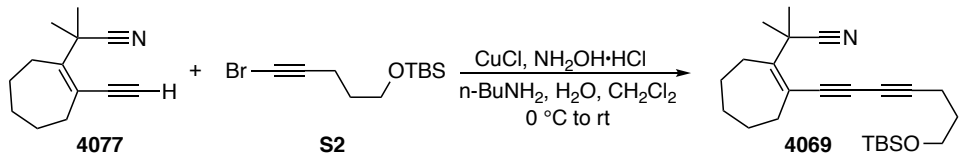

A 25 mL round-bottom flask containing CuCl (19.5 mg, 0.197 mmol), hydroxylamine hydrochloride (31.5 mg, 0.453 mmol), and a magnetic stir bar was purged with N_2 before being placed under a slight positive N_2 pressure. *n*-Butylamine solution (30% wt. in water, 5 mL) was added by syringe and the resulting mixture was stirred in an ice bath for 5 minutes. A solution of the nitrile **4077** (164 mg, 0.874 mmol) in CH_2Cl_2 (4 mL) was prepared and 1 mL of this solution was added to the reaction mixture by syringe. A yellow precipitate was formed. The remainder of this solution of X was added to a solution of the bromoalkyne **S2** (363 mg, 1.31 mmol) in CH_2Cl_2 (4 mL), and the resulting solution of both reactants was added to the reaction flask dropwise by syringe over 5 minutes. After addition was complete, the reaction flask was taken out of the ice bath and allowed to warm to room temperature. After 30 minutes, the reaction mixture was diluted with CH_2Cl_2 (50 mL) and treated with a mixture of brine and 30% aqueous NH_4OH solution (3:1 vol., 2 x 50 mL). The organic extract was washed with brine, dried with $MgSO_4$, and concentrated to leave an orange oil. This oil was purified by MPLC (30:1 hexanes:EtOAc) to provide the 1,3-diyne **4069** (271 mg, 0.705 mmol, 81%) as a clear oil.

^{1}H NMR (500 MHz, $CDCl_3$): δ 2.69 (t, J = 6.0 Hz, 2H, OCH_2), 2.48–2.42 (m, 4H, CH_2C=C-CH_2), 2.44 (t, J = 7.1 Hz, 2H, C≡CCH_2), 1.75 (tt, J = 7.1 Hz, 6.0 Hz, 2H, C≡CCH$_2$CH_2), 1.75 (m, 2H, CH_2CH$_2$C=C-CH$_2$CH$_2$), 1.70 [s, 6H, C(CH_3)$_2$], 1.58–1.49 (m, 4H, CH$_2$CH$_2$C=C-CH$_2$CH_2CH_2), 0.89 [s, 9H, SiC(CH_3)$_3$], and 0.06 [s, 6H, Si(CH_3)$_2$].

^{13}C NMR (125 MHz, $CDCl_3$): Contains some impurity peak (tolerable, but could be better) δ 150.7, 124.2, 121.9, 87.3, 83.1, 74.8, 65.4, 61.5, 39.8, 37.0, 32.4, 31.8, 31.4, 27.3, 26.2, 26.0, 25.8, 18.4, 16.3, and -5.3.

IR (thin film): 2951, 2927, 2855, 2252, 2233, 1463, 1443, 1253, 1102, 1068, 963, 911, 833, 775, 732, and 662 cm^{-1}.

HRMS (ESI-Orbitrap) Calculated for $C_{24}H_{38}NOSi^+$ [M+H$^+$] 384.2717, found 384.2723.

TLC: R_f 0.50 (10:1 hexanes:EtOAc)

12-((*tert*-Butyldimethylsilyl)oxy)-6,6-dimethyl-3,4,6,7,8,9,10,11-octahydro-2*H*-azuleno[2,1-*b*]pyrano[2,3-*e*]pyridine (4078)
and
5-(3-((*tert*-Butyldimethylsilyl)oxy)propyl)-2,3-dichloro-7,7-dimethyl-1,4,7,8,9,10,11,12-octahydro-1,4-ethenoazuleno[2,1-*c*]isoquinoline (4079)
and
5-(3-((*tert*-butyldimethylsilyl)oxy)propyl)-1,2-dichloro-7,7-dimethyl-1,4,7,8,9,10,11,12-octahydro-1,4-ethenoazuleno[2,1-c]isoquinoline (4079')

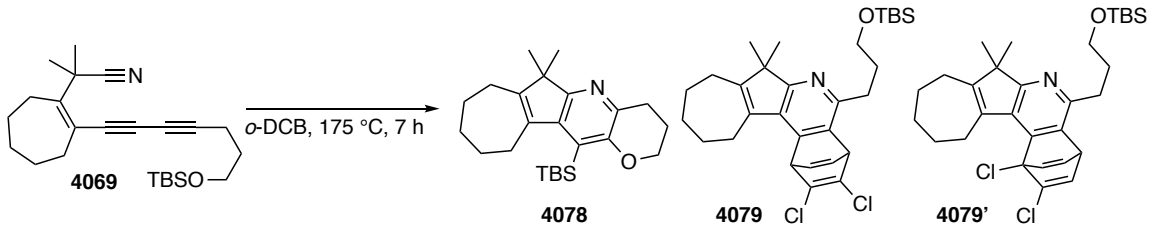

In a 50 mL culture tube, the nitrile **4069** (152 mg, 0.396 mmol) was dissolved in *o*-dichlorobenzene (40 mL). The culture tube was sealed with a Teflon-lined cap and placed in a 175 °C oil bath. After 7 hours (TLC monitoring), the solution was filtered through a plug of SiO_2 with hexanes (to elute the *o*-dichlorobenzene) followed by EtOAc. The EtOAc filtrate was concentrated to a dull orange oil. This oil was purified by MPLC (10:1 hexanes:EtOAc) to give, in order of elution, the dichloroalkene **4079,** containing a minor amount of the coeluting isomer **4079'**, (31.3 mg, 0.0590 mmol, 15%, ca. 6:1 ratio) and the aryl silane **4078** (41.2 mg, 0.107 mmol, 27%), each as a light yellow oil.

Data for the major dichloroalkene 4079

^{1}H NMR (400 MHz, $CDCl_3$): δ 6.95 (ddd, *J* = 6.6, 5.8, 1.6 Hz, 1H), 6.89 (ddd, *J* = 6.6, 5.8, 1.7 Hz, 1H), 5.42 (dd, *J* = 5.8, 1.6 Hz, 1H, C1*H*), 5.08 (dd, *J* = 5.9, 1.7 Hz, 1H, C4*H*), 3.70 (ddd, *J* = 10.2, 6.0, 6.0 Hz, 1H, OCH_aH$_b$), 3.64 (ddd, *J* = 10.2, 6.3, 6.3 Hz, 1H, OCH$_a$$H_b$), 2.97 (ddd, *J* = 13.5, 8.9, 7.0 Hz, 1H, ArCH_aH$_b$), 2.92 (ddd, *J* = 13.3, 8.5, 6.0 Hz, 1H, ArCH$_a$$H_b$), 2.92–2.81 (m, 2H, =CC12H$_2$), 2.37 (nfom, 2H, CH$_2$C=C-C8H_2'), 1.90-1.81 (m, 6H), 1.76-1.70 (m, 2H), 1.19 [s, 3H, C(CH_3)(CH$_3$)], 1.16 [s, 3H, C(CH$_3$)(CH_3)], 0.94 [s, 9H, SiC(CH_3)$_3$], 0.08 [s, 3H, Si(CH_3)(CH$_3$)], and 0.07 [s, 3H, Si(CH$_3$)(CH_3)].

^{13}C NMR (125 MHz, $CDCl_3$): δ 169.0, 155.3, 148.3, 143.7, 139.3, 138.2, 136.4, 135.6, 135.1, 134.0, 129.6, 62.6, 52.2, 51.8, 34.2, 31.1, 30.0, 28.9, 27.1, 26.3, 26.2, 26.1, 25.1, 22.5, 22.4, 18.5, -5.0, and -5.1.

IR (thin film): 2955, 2926, 2856, 1629, 1580, 1470, 1462, 1392, 1379, 1254, 1095, 1023, 963, 836, 775, 753, and 732 cm^{-1}.

HRMS (ESI-Orbitrap) Calculated for $C_{30}H_{42}{}^{35}Cl_2NOSi^+$ [M+H$^+$] 530.2407, found 530.2397.

TLC: R_f 0.30 (8:1 hexanes:EtOAc)

Selected NMR data attributed to the minor dichloroalkene 4079'

^{1}H NMR (400 MHz, $CDCl_3$): δ 6.90 (dd, *J* = 6.5, 6.5 Hz, 1H, C1HC=C*H*C4), 6.77 (dd, *J* = 6.5, 6.5 Hz, 1H, C3*H*), 6.70 (dd, *J* = 6.8, 2.0 Hz, 1H, C1*H*C=CHC4), 5.07 (dd, *J* = 6.4, 2.0 Hz, 1H, C4*H*), 3.14 (ddd, *J* = 15.7, 8.8 Hz, 1H, C12H_aH_b), 1.18 [s, 3H, C(CH_3)(CH_3)], 1.15 [s, 3H, C(CH_3)(CH_3)], and 0.93 [s, 9H, SiC(CH_3)$_3$].

LCMS In the chromatogram of this sample of coeluting isomers, two peaks, each with a mass of 530 ($M+H^+$) and a distribution of ions consistent with the isotopomers of a dichloride, were observed in an ca. 6:1 ratio, consistent with the ratio observed in the ^{1}H NMR spectrum.

TLC: R_f 0.30 (8:1 hexanes:EtOAc)

Data for the aryl silane 4078

^{1}H NMR (400 MHz, $CDCl_3$): broad peak at 1.70 δ 4.06 (nfom, 2H, CH_2O), 2.97 (t, *J* = 6.7 Hz, 2H, ArCH_2), 2.63 (nfom, 2H, C11H_2C=C-CH_2'), 2.38 (nfom, 2H, CH_2C=C-C7H_2'), 2.06 (nfom, 2H, OCH_2CH_2), 1.83 (br app pent, *J* ~ 6 Hz, 2H), 1.56 (br app pent, *J* ~ 6 Hz, 2H), 1.49 (br app pent, *J* ~ 6 Hz, 2H), 1.20 [s, 6H, C(CH_3)$_2$], 1.04 [s, 9H, SiC(CH_3)$_3$], and 0.29 [s, 6H, Si(CH_3)$_2$].

^{13}C NMR (125 MHz, $CDCl_3$): δ 163.6, 157.1, 155.6, 142.7, 138.6, 134.9, 126.5, 65.4, 48.5, 32.9, 29.2, 28.6, 28.6, 28.1, 27.0, 26.9, 22.8, 22.4, 18.8, and 1.2.

IR (thin film): 2955, 2923, 2852, 1612, 1562, 1519, 1462, 1444, 1386, 1330, 1315, 1259, 1248, 1211, 1170, 1150, 1101, 1065, 1042, 987, 908, 832, 808, 775, 731, and 683 cm^{-1}.

HRMS Calculated for $C_{24}H_{38}NO_2Si^+$ [$M+H^+$] 400.2666, found 400.2654.

5-(3-((*tert*-butyldimethylsilyl)oxy)propyl)-7,7-dimethyl-1,4,7,8,9,10,11,12-octahydro-1,4-epoxyazuleno[2,1-*c*]isoquinoline (4080)

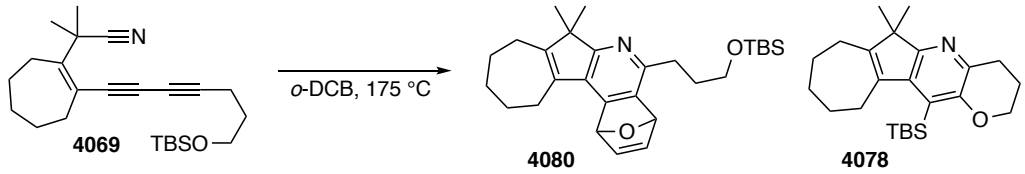

In a 50 mL flame-dried culture tube, the nitrile **4069** (29.1 mg, 0.0759 mmol) and furan (33 µL, 0.45 mmol) were dissolved in 7.5 mL of dry *o*-DCB. The culture tube was sealed with a Teflon-lined cap and placed in a 175 °C oil bath. After 7 hours (TLC monitoring) the solution was concentrated to leave a dark orange oil. This oil was purified by flash column chromatography (10:1 hexanes:EtOAc) to give, in order of elution, **4080** (furan-trapped product) (17.8 mg, 0.0395 mmol, 52%) as a white crystalline solid and **4078** (aryl silane) (3.8 mg, 0.13 mmol, 13%) as a pale yellow oil.

Data for **4080**

^{1}H NMR (400 MHz, $CDCl_3$): 7.09 (dd, *J* = 5.5, 1.8 Hz, 1H, *H2* or *H3*), 6.96 (dd, *J* = 5.5, 1.8 Hz, 1H, *H2* or *H3*), 6.05 (dd, *J* = 1.8, 0.8 Hz, 1H, *H1*), 5.84 (dd, *J* = 1.8, 0.8 Hz, 1H *H4*), 3.63 (ddd, *J* = 10.3, 6.3, 6.3 Hz, 1H, OCH_aH$_b$), 3.58 (ddd, *J* = 10.3, 6.3, 6.3 Hz, 1H, OCH$_a$$H_b$), 2.88 (ddd, *J* = 13.5, 8.3, 6.9 Hz, 1H, ArCH_aH$_b$), 2.82 (ddd, *J* = 13.5, 8.3, 6.5 Hz, 1H, ArCH$_a$$H_b$), 2.70 (ddddd, *J* = 15.7, 8.8, 3.0, 1.1, 1.1 Hz, 1H, CH_2C=C-C12H_aH$_b$), 2.60 (ddddd, 15.7, 8.0, 3.0, 1.0, 1.0 Hz, CH_2C=C-C12H$_a$$H_b$), 2.36 (nfom, 2H, C=CC8$H_2$), 1.94-1.61 (m, 8H), 1.19 (s, 3H, CH_3CCH$_3$), 1.17 (s, 3H, CH_3CCH$_3$), 0.92 [s, 9H, SiC(CH_3)$_3$], 0.07 [s, 3H, Si(CH_3)(CH$_3$)], and 0.06 [s, 3H, Si(CH$_3$)(CH_3)].

^{13}C NMR (125 MHz, $CDCl_3$): δ 170.2, 155.0, 146.7, 146.5, 143.1, 141.4, 138.6, 133.7, 129.6, 80.6, 80.3, 62.3, 50.7, 33.5, 31.27, 31.26, 28.1, 27.6, 27.2, 26.4, 26.1, 22.6, 22.2, 18.5, -5.03, and -5.06.

IR (thin film): 3016, 2954, 2926, 2854, 2246, 2168, 2136, 1598, 1513, 1460, 1445, 1388, 1341, 1250, 1205, 1160, 1093, 1007, 877, 834, 774, 731, 703, 670, and 660 cm^{-1}.

HRMS (ESI-Orbitrap) Calculated for $C_{28}H_{42}NO_2Si^+$ [M+H$^+$] 452.2979, found 452.2971.

TLC: R_f 0.25 (8:1 hexanes:EtOAc)

2-Methyl-2-(2-(penta-1,3-diyn-1-yl)cyclohept-1-en-1-yl)propanenitrile (4019)

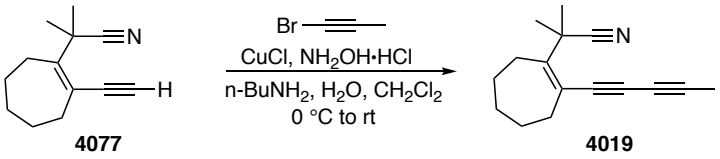

4077 **4019**

A 50 mL round-bottom flask containing CuCl (16.0 mg, 0.162 mmol), hydroxylamine hydrochloride (55.1 mg, 0.793 mmol), and a magnetic stir bar was purged with N_2 before being placed under a slight positive N_2 pressure. *n*-Butylamine solution (30 wt.% in water, 8 mL) was added by syringe and the resulting mixture was stirred in an ice bath for 5 minutes. A solution of the nitrile **4077** (292 mg, 1.56 mmol) in CH_2Cl_2 (8 mL) was prepared and 1 mL of this solution was added to the reaction mixture by syringe. A yellow homogeneous solution was formed. The remainder of the solution of **4077** was added to a solution of the 1-bromopropyne(366 mg, 3.08 mmol) in hexanes (2 mL) and the resulting solution of both reactants was added to the reaction flask dropwise by syringe over 5 minutes. After addition was complete, the reaction flask was removed from the ice bath and allowed to warm to room temperature. After 25 minutes, the reaction mixture was diluted with CH_2Cl_2 (50 mL) and treated with a mixture of brine and 30% aqueous NH_4OH solution (3:1 vol., 2 x 50 mL), which was sufficient for the final aqueous wash to no longer be blue. The organic extract was washed with brine, dried with $MgSO_4$, and concentrated to leave a yellow oil. This oil was purified by MPLC (30:1 hexanes:EtOAc) to provide the 1,3-diyne **4019** (288 mg, 1.28 mmol, 82%) as a clear oil.

^{1}H NMR (400 MHz, $CDCl_3$): δ 2.47–2.42 (m, 4H, C*H*$_2$C=C-C*H*$_2$), 2.01 (s, 3H, C≡CC*H*$_3$), 1.75 (br app pent, J = ~ 6 Hz, 2H, C*H*$_2$CH$_2$C=C-CH$_2$CH$_2$), 1.69 [s, 6H, C(C*H*$_3$)$_2$], and 1.58–1.49 (m, 4H, CH$_2$CH$_2$C=C-CH$_2$C*H*$_2$C*H*$_2$).

^{13}C NMR (125 MHz, $CDCl_3$): δ 150.8, 124.3, 121.9, 83.3, 83.2, 74.3, 64.5, 39.7, 36.9, 32.2, 31.8, 27.3, 26.2, 25.8, and 4.9.

IR (thin film): 2979, 2922, 2852, 2260, 2340, 2232, 2145, 1442, 1389, 1366, 1213, 1195, 1158, 990, 963, 868, and 833 cm^{-1}.

HRMS (ESI-Orbitrap) Calculated for $C_{16}H_{20}N^+$ [M+H$^+$] 226.1590, found 226.1583.

TLC: R_f 0.35 (10:1 hexanes:EtOAc)

5,7,7-Trimethyl-1,4,7,8,9,10,11,12-octahydro-1,4-epoxyazuleno[2,1-*c*]isoquinoline (4081a)

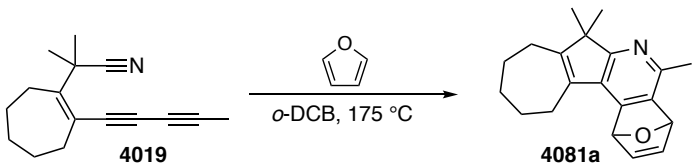

In a 50 mL flame-dried culture tube, the nitrile **4019** (27.0 mg, 0.120 mmol) and furan (44 µL, 0.61 mmol) were dissolved in dry, degassed *o*-DCB (12 mL). The culture tube was sealed with a Teflon-lined cap and placed in a 175 °C oil bath. After 7 hours the solution was concentrated under vacuum to a brown oil. This oil was purified by MPLC (2:1 hexanes:EtOAc) to give the pyridine derivative **4081a** (25.5 mg, 0.0869 mmol, 72%) as a pale yellow crystalline solid.

^{1}H NMR (400 MHz, $CDCl_3$): δ 7.02 (dd, *J* = 5.6, 1.8 Hz, 1H, *H2* or *H3*), 6.97 (dd, *J* = 5.6, 1.9 Hz, 1H, *H2* or *H3*), 6.06 (dd, *J* = 1.8, 0.8 Hz, 1H, *H1* or *H4*), 5.80 (dd, *J* = 1.8, 0.8 Hz, 1H, *H1* or *H4*), 2.69 (ddddd, *J* = 15.8, 8.5, 3.3, 1.2, 1.2 Hz, 1H, CH_2C=C-C12H_aH$_b$), 2.60 (ddddd, *J* = 15.8, 8.0, 3.3, 1, 1 Hz, 1H, CH_2C=C-C12H$_a$$H_b$), 2.51 (s, 3H, ArC$H_3$), 2.36 (nfom, 2H, C=CC8$H_2$), 1.89–1.61 (m, 4H, C9-11H_2), 1.20 (s, 3H, CH_3CCH_3), and 1.18 (s, 3H, CH_3CCH_3).

^{13}C NMR (125 MHz, $CDCl_3$): δ 170.2 (C6a), 154.9 (C7a), 146.9, 142.9 (C3 or C2), 142.5 (C5), 141.4 (C2 or C3), 138.6, 133.7 (C12a), 129.5, 80.6 (C1 or C4), 80.3 (C4 or C1), 50.6, 31.2, 28.0, 27.6, 27.2, 26.3, 22.6, 22.3, and 21.1. (assignments based on analysis of HMBC data)

IR (thin film): 3014, 2959, 2921, 2852, 1621, 1597, 1445, 1408, 1397, 1346, 1280, 1159, 1032, 927, 910, 874, 853, 820, 730, 709, and 658 cm^{-1}.

HRMS (ESI-Orbitrap) Calculated for $C_{20}H_{24}NO^+$ [M+H$^+$] 294.1852, found 294.1846.

TLC: R_f 0.25 (2:1 hexanes:EtOAc).

m.p. 121–122 °C.

Reaction performed on a >1 mmol scale

In a 150 mL flame-dried glass pressure vessel, the nitrile **4019** (255 mg, 1.13 mmol) and furan (0.41 mL , 5.6 mmol) were dissolved in dry, degassed *o*-DCB (110 mL). The vessel was sealed using a PTFE plug that contained an O-ring and placed in a 175 °C oil bath. After 7 hours the solution was concentrated under vacuum to a brown oil. This oil was purified by MPLC (2:1 hexanes:EtOAc) to give the pyridine derivative **4081a** (233 mg, 0.794 mmol, 70%) as a pale yellow crystalline solid.

2,10,10-Trimethyl-5,6,7,8,9,10-hexahydroazuleno[2,1-*b*]pyridine (4081b)

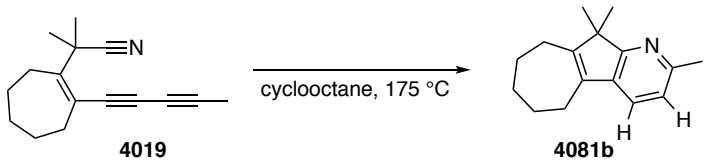

4019 **4081b**

In a 50 mL flame-dried culture tube, the nitrile **4019** (35.7 mg, 0.159 mmol) was dissolved in 16 mL of cyclooctane that had been sparged with N_2. The culture tube was sealed with a Teflon-lined cap and placed in a 175 °C oil bath. After 7 hours, the solution was passed through a plug of SiO_2 with hexanes (to first elute the cyclooctane) followed by EtOAc. The EtOAc was removed and the residue was purified by flash column chromatography (30:1 hexanes:EtOAc + 1% TEA) to give the pyridine derivative **4081b** (19.0 mg, 0.0835 mmol, 53%) as a clear oil.

^{1}H NMR (400 MHz, $CDCl_3$): δ 7.26 (d, *J* = 7.7 Hz, 1H, C4*H*), 6.94 (d, *J* = 7.7 Hz, 1H, C3*H*), 2.56 (s, 3H, ArC*H*$_3$), 2.52 (nfom, 2H, C*H*$_2$C=C-CH$_2$'), 2.37 (nfom, 2H, CH$_2$C=C-C*H*$_2$'), 1.88–1.81 (m, 2H), 1.70–1.62 (m, 4H), and 1.22 [s, 6H, C(CH$_3$)$_2$].

^{13}C NMR (125 MHz, $CDCl_3$): δ 171.8, 153.4, 152.5, 135.0, 134.2, 124.9, 120.6, 50.3, 31.7, 27.9, 27.4, 26.6, 26.0, 24.4, and 21.9.

IR (thin film): 3040, 2959, 2918, 2849, 1621, 1579, 1443, 1412, 1370, 1353, 1157, 1124, 827, and 790 cm^{-1}.

HRMS (ESI-Orbitrap) Calculated for $C_{16}H_{22}N^+$ [M+H$^+$] 228.1747, found 228.1741.

TLC: R_f 0.35 (10:1 hexanes:EtOAc + 1% TEA).

2,10,10-Trimethyl-5,6,7,8,9,10-hexahydroazuleno[2,1-*b*]pyridin-3-yl acetate (4081c-major)
and
2,10,10-Trimethyl-5,6,7,8,9,10-hexahydroazuleno[2,1-*b*]pyridin-4-yl acetate (4081c-minor)

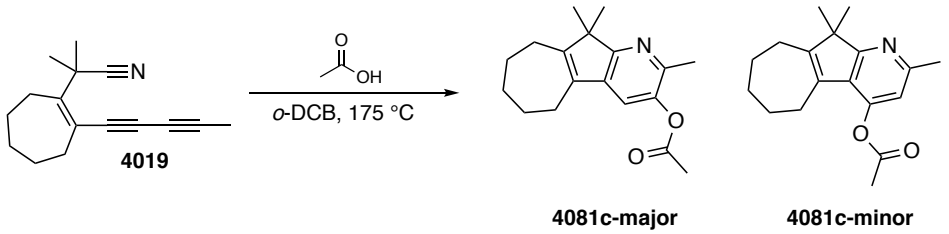

In a 50 mL flame-dried culture tube, the nitrile **4019** (102 mg, 0.453 mmol) and acetic acid (0.52 mL, 9.1 mmol) were dissolved in dry, degassed *o*-DCB (45 mL). The culture tube was sealed with a Teflon-lined cap and placed in a 175 °C oil bath. After 7 hours (TLC monitoring) the solution was concentrated to a brown oil. This oil was purified by MPLC (4:1 hexanes:EtOAc) to give, in order of elution, **4081c-major** (56.4 mg, 0.198 mmol, 44%) and **4081c-minor** (27.5 mg, 0.0964 mmol, 21%) each as a light yellow oil.

Data for 4081c-major

^{1}H NMR (400 MHz, $CDCl_3$): δ 7.03 (s, 1H, Ar*H*), 2.48 (nfom, 2H, C*H*$_2$C=C-CH$_2$'), 2.42 (s, 3H, ArC*H*$_3$) 2.38 (nfom, 2H, CH$_2$C=C-C*H*$_2$'), 2.34 [s, 3H, C*H*$_3$(C=O)O], 1.86–1.80 (m, 2H), 1.69–1.61 (m, 4H), and 1.21 [s, 6H, C(C*H*$_3$)$_2$].

^{13}C NMR (125 MHz, $CDCl_3$): δ 169.5, 169.0, 155.4, 144.6, 144.2, 137.1, 133.9, 118.7, 50.1, 31.6, 27.7, 27.2, 26.7, 26.1, 21.8, 21.1, and 19.1.

IR (thin film): 2961, 2921, 2851, 1764, 1622, 1581, 1468, 1440, 1423, 1368, 1202, 1160, 1137, 1043, 1007, and 914 cm^{-1}.

HRMS (ESI-Orbitrap) Calculated for $C_{18}H_{24}NO_2^+$ [M+H$^+$] 286.1802, found 286.1795.

TLC: R_f 0.30 (4:1 hexanes:EtOAc)

Data for 4081c-minor

^{1}H NMR (400 MHz, $CDCl_3$): 6.66 (s, 1H, Ar*H*), 2.68 (nfom, 2H, C*H*$_2$C=C-CH$_2$'), 2.54 (s, 3H, ArC*H*$_3$), 2.35 (nfom, 2H, CH$_2$C=C-C*H*$_2$'), 2.32 [s, 3H, C*H*$_3$(C=O)O], 1.84–1.78 (m, 2H), 1.70–1.61 (m, 4H), and 1.22 [s, 6H, C(C*H*$_3$)$_2$].

^{13}C NMR (125 MHz, $CDCl_3$): δ 175.0, 169.0, 155.0, 154.3, 149.8, 133.2, 126.0, 115.2, 50.9, 31.4, 27.4, 27.2, 27.0, 26.0, 24.2, 21.9, and 21.2.

IR (thin film): 2962, 2922, 2851, 1770, 1616, 1595, 1577, 1442, 1368, 1353, 1194, 1165, 1120, 1026, and 896 cm^{-1}.

HRMS (ESI-Orbitrap) Calculated for $C_{18}H_{24}NO_2^+$ [M+H$^+$] 286.1802, found 286.1793.

TLC: R_f 0.25 (4:1 hexanes:EtOAc)

Methyl 2-cyano-6-((2,10,10-trimethyl-5,6,7,8,9,10-hexahydroazuleno[2,1-*b*]pyridin-3-yl)thio)hexanoate (4081d-major)
and
Methyl 2-cyano-6-((2,10,10-trimethyl-5,6,7,8,9,10-hexahydroazuleno[2,1-*b*]pyridin-4-yl)thio)hexanoate (4081d-minor)

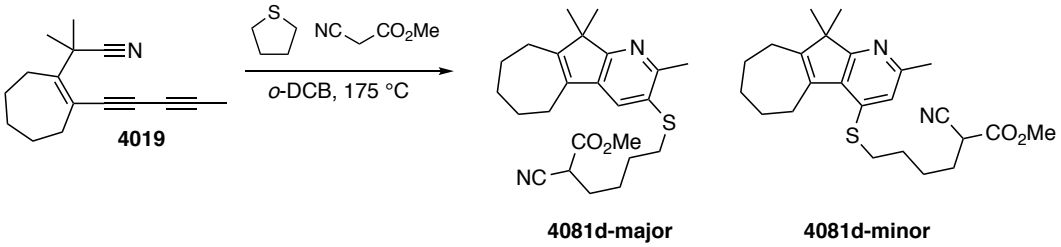

In a 50 mL flame-dried culture tube, the nitrile **4019** (79.5 mg, 0.353 mmol), tetrahydrothiophene (100 µL, 1.13 mmol), and methyl cyanoacetate (166 µL, 1.88 mmol) were dissolved in 35 mL of dry *o*-DCB. The culture tube was sealed with a Teflon-lined cap and placed in a 175 °C oil bath. After 7 hours, the solution was concentrated to a brown oil. HLC/MS analysis of this sample indicated a 17:1 ratio of two compounds of identical mass, which are presumed to be **4081d-major** and **4081d-minor**. This oil was purified by flash column chromatography (3:1 hexanes:EtOAc) to give **4081d-major** (68.2 mg, 0.165 mmol, 47%) as a light yellow oil.

Data for 4081d-major

^{1}H NMR (400 MHz, $CDCl_3$): δ 7.31 (s, 1H, Ar*H*), 3.82 (s, 3H, CO_2CH_3), 3.51 (dd, *J* = 7.5, 6.4 Hz, 1H, C*H*CN), 2.88 (br t, *J* = 6.6 Hz, 2H, SCH_2), 2.66 (s, 3H, $ArCH_3$), 2.53 (nfom, 2H, $C5H_2C$=C-CH_2), 2.37 (nfom, 2H, CH_2C=C-$C9H_2$), 2.01–1.94 (m, 2H), 1.87–1.82 (m, 2H), 1.72–1.63 (m, 8H), and 1.21 [s, 6H, $C(CH_3)_2$].

^{13}C NMR (125 MHz, $CDCl_3$): δ 169.9, 166.5, 154.6, 152.5, 136.2, 133.9, 128.0, 126.8, 116.3, 53.6, 50.2, 37.3, 33.6, 31.6, 29.5, 28.4, 27.7, 27.3, 26.6, 26.05, 25.98, 23.2, and 21.8.

IR (thin film): 2957, 2920, 2851, 2250, 1748, 1552, 1437, 1417, 1371, 1353, 1262, 1207, 1180, and 999 cm^{-1}.

HRMS (ESI-Orbitrap) Calculated for $C_{24}H_{33}Cl_2N_2O_2S^+$ [M+H$^+$] 413.2257, found 413.2248.

***N*-Butyl-2,10,10-trimethyl-5,6,7,8,9,10-hexahydroazuleno[2,1-*b*]pyridin-3-amine (4081e-major)**
and
***N*-Butyl-2,10,10-trimethyl-5,6,7,8,9,10-hexahydroazuleno[2,1-*b*]pyridin-4-amine (4081e-minor)**

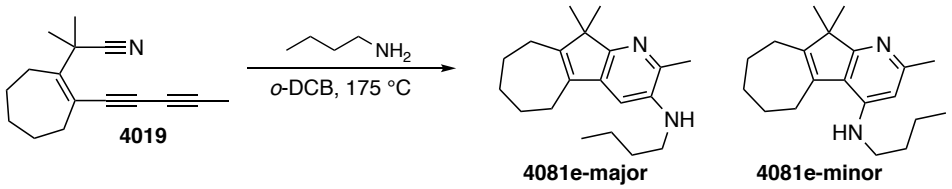

In a 50 mL flame-dried culture tube, the nitrile **4019** (56.3 mg, 0.250 mmol) and *n*-butylamine (123 µL, 1.24 mmol) were dissolved in 25 mL of dry *o*-DCB. The culture tube was sealed with a Teflon-lined cap and placed in a 175 °C oil bath. After 7 hours the solution was concentrated to a brown oil. This oil was purified by flash column chromatography (15:1 hexanes:EtOAc + 2% TEA) to give, in order of elution, **4081e-major** (46.0 mg, 0.155 mmol, 62%) and **4081e-minor** (6.0 mg, 0.020 mmol, 8%), each as a light yellow oil.

Data for 4081e-major

^{1}H NMR (400 MHz, $CDCl_3$): δ 6.68 (s, 1H, Ar*H*), 3.32 (br s, 1H, N*H*), 3.16 (t, *J* = 7.0 Hz, 2H, NHC*H*$_2$), 2.53 (nfom, 2H, C*H*$_2$C=C-CH$_2$'), 2.40 (s, 3H, ArC*H*$_3$) 2.35 (nfom, 2H, CH$_2$C=C-C*H*$_2$'), 1.86–1.81 (m, 2H), 1.70–1.62 (m, 6H), 1.47 (dq, *J* = 7.6, 7.6 Hz, 2H, NHCH$_2$CH$_2$C*H*$_2$CH$_3$) 1.19 [s, 6H, C(CH$_3$)$_2$], and 0.98 (t, *J* = 7.4 Hz, 3H, NHCH$_2$CH$_2$CH$_2$C*H*$_3$).

^{13}C NMR (125 MHz, $CDCl_3$): δ 159.5, 154.0, 141.1, 137.5, 136.3, 134.4, 107.1, 49.5, 44.0, 31.9, 31.9, 27.9, 27.4, 26.7, 26.1, 22.2, 20.5, 20.4, and 14.1.

IR (thin film): 3423, 3348, 3052, 2956, 2918, 2855, 1591, 1469, 1446, 1372, 1352, 1322, 1273, 1246, 1221, 1207, 1159, 1137, 983, 964, 858, and 733 cm^{-1}.

HRMS (ESI-Orbitrap) Calculated for $C_{20}H_{31}N_2^+$ [M+H$^+$] 299.2482, found 299.2475.

TLC: R_f 0.25 (3:1 hexanes:EtOAc + 1% TEA)

Data for 481e-minor

^{1}H NMR (400 MHz, $CDCl_3$): Contains grease, acetone, and DCM δ 6.21 (s, 1H, ArH), 4.39 (br t, *J* ~ 5 Hz, 1H, N*H*), 3.14 (td, *J* = 7.1, 5.2 Hz, 2H, N*H*C*H*$_2$), 2.81-2.77 (m, 2H, C*H*$_2$C=C-CH$_2$'), 2.46 (s, 3H, ArC*H*$_3$), 2.33 (nfom, 2H, nfom, 2H, CH$_2$C=C-C*H*$_2$'), 1.85-1.76 (m, 4H), 1.74–1.69 (m, 2H), 1.64 (tt, *J* = 7.2, 7.2 Hz, 2H, NHCH$_2$C*H*$_2$CH$_2$CH$_3$), 1.45 (dq, *J* = 7.6, 7.6 Hz, 2H, NHCH$_2$CH$_2$C*H*$_2$CH), 1.17 [s, 6H, C(C*H*$_3$)$_2$], and 0.98 (t, *J* = 7.3 Hz, 3H, NHCH$_2$CH$_2$CH$_2$C*H*$_3$).

HRMS (ESI-Orbitrap) Calculated for $C_{20}H_{31}N_2^+$ [M+H$^+$] 299.2482, found 299.2476.

TLC: R_f 0.30 (3:1 hexanes:EtOAc + 1% TEA)

2,4,6-Trimethyl-6-(2,10,10-trimethyl-5,6,7,8,9,10-hexahydroazuleno[2,1-*b*]pyridin-3-yl)cyclohexa-2,4-dien-1-one (4081f-major)
and
2,4,6-Trimethyl-6-(2,10,10-trimethyl-5,6,7,8,9,10-hexahydroazuleno[2,1-*b*]pyridin-4-yl)cyclohexa-2,4-dien-1-one (4081f-minor)

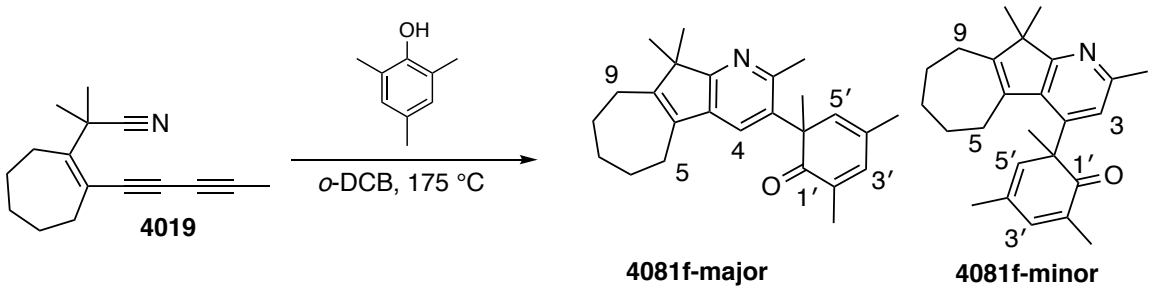

In a 50 mL flame-dried culture tube, the nitrile **4019** (63.5 mg, 0.282 mmol) and 2,4,6-trimethylphenol (115 mg, 0.844 mmol) were dissolved in dry, degassed *o*-DCB (28 mL). The culture tube was sealed with a Teflon-lined cap and placed in a 175 °C oil bath. After 7 hours (TLC monitoring) the solution was concentrated to a brown oil. This oil was purified by MPLC (4:1 hexanes:EtOAc) to give, in order of elution, **4081f-major** (41.2 mg, 0.114 mmol, 40%) and **4081f-minor** (19.5 mg, 0.0539 mmol, 19%), each as an off-white crystalline solid.

Data for 4081f-major

^{1}H NMR (400 MHz, $CDCl_3$): δ 7.42 (s, 1H, Ar*H*), 6.83 (dq, *J* = 2.5, 1.5 Hz, 1H, H3'), 5.87 (dq, *J* = 2.5, 1.6 Hz, H5'), 2.57 (m, 2H, C5*H*$_2$C=C-CH$_2$'), 2.37 (m, 2H, CH$_2$C=C-C9*H*$_2$'), 2.09 (s, 3H, ArC*H*$_3$), 1.98 (br d, *J* = 1.4 Hz, 3H, C2'*H*$_3$), 1.95 (d, *J* = 1.6 Hz, 3H, C4'*H*$_3$), 1.85 (br app sext, *J* ~ 6 Hz, 2H, C*H*$_2$CH$_2$C=C-CH$_2$CH$_2$), 1.69 (br pent, *J* ~ 6 Hz, 2H, CH$_2$CH$_2$C=C-CH$_2$C*H*$_2$ or C*H*$_2$CH$_2$CH$_2$C=C), 1.65 (br pent, *J* ~ 6 Hz, 2H, CH$_2$CH$_2$C=C-CH$_2$C*H*$_2$ or C*H*$_2$CH$_2$CH$_2$C=C), 1.56 (s, 3H, C6'*H*$_3$), 1.20 (s, 3H, C*H*$_3$CCH$_3$), and 1.19 (s, 3H, CH$_3$CC*H*$_3$).

^{13}C NMR (125 MHz, $CDCl_3$): δ 204.2, 169.8, 153.9, 151.5, 141.9, 140.2, 135.5, 134.4, 133.9, 132.9, 127.4, 123.0, 54.0, 50.0, 31.8, 27.9, 27.4, 26.6, 26.0, 25.0, 22.3, 21.75, 21.74 21.1, and 15.8.

IR (thin film): 2963, 2920, 2851, 2249, 1664, 1649, 1581, 1562, 1468, 1446, 1377, 1363, 1240, 1163, 1025, 940, 912, 829, and 731 cm^{-1}.

HRMS Calculated for $C_{25}H_{32}NO^+$ [M+H$^+$] 362.2478, found 362.2472.

TLC: R_f 0.45 (2:1 hexanes:EtOAc)

Data for 4081f-minor

^{1}H NMR (400 MHz, $CDCl_3$): 7.00 (s, 1H, Ar*H*), 6.72 (dq, *J* = 3.0, 1.5 Hz, 1H, H3'), 6.08 (dq, *J* = 2.6, 1.6 Hz, H5'), 2.58 (s, 3H, ArC*H*$_3$), 2.32 (ddd, *J* = 15.1, 7.0, 3.1 1H, C9*H*$_a$H$_b$C=C-CH$_2$'), 2.30 (ddd, *J* = 15.2, 7.4, 3.1, 1H, C9H$_a$*H*$_b$C=C-CH$_2$'), 2.05 (ddd, *J* = 15.3, 7.5, 3.4 1H, C5*H*$_a$H$_b$C=C-CH$_2$'), 2.03 (ddd, *J* = 15.1, 8.0, 3.1, 1H, CH$_a$*H*$_b$C=C-CH$_2$'), 1.99 (br d, *J* = 1.4, 0.6 Hz, 3H, C2'*H*$_3$) 1.91 (d, *J* = 1.6 Hz, 3H, C4'*H*$_3$), 1.81–1.68 (m, 2H), 1.62 (s, 3H, C6'*H*$_3$), 1.54 (ddddd, *J* =

11.3, 8.0, 8.0, 3.3, 3.3 Hz, 1H, CH_aH$_b$), 1.45 (ddddd, J = 11.6, 8.2, 8.2, 3.6, 3.6 Hz, 1H, CH$_a$$H_b$), 1.36–1.28 (m, 1H, C$H_aH_b$), 1.27–1.21 (m, 1H, C$H_aH_b$), 1.20 (s, 3H, C$H_3CCH_3$), and 1.18 (s, 3H, CH$_3CCH_3$).

^{13}C NMR (125 MHz, $CDCl_3$): δ 203.1, 172.9, 155.5, 152.4, 142.2, 140.8*, 140.2, 136.4, 133.3, 132.5 (C2*), 127.6, 119.8, 55.6, 49.3, 32.9, 27.1, 26.9, 26.5, 26.4, 26.3, 24.5, 22.1, 22.0, 21.2, and 16.1. *These substituted carbon resonances were of low intensity in the 1D spectrum but were identified by HMBC.

IR (thin film): 2961, 2920, 2850, 1667, 1650, 1616, 1583, 1448, 1376, 1361, 1241, 1033, 911, 822, and 732 cm^{-1}.

HRMS Calculated for $C_{25}H_{32}NO^+$ [M+H$^+$] 362.2478, found 362.2474.

TLC: R_f 0.30 (2:1 hexanes:EtOAc)

4,6,6-Trimethyl-6,7,8,9,10,11-hexahydro-3*H*-azuleno[2,1-*b*][1,2,3]triazolo[4,5-*d*]pyridine (4081g)

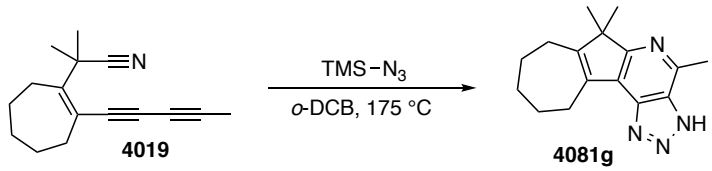

In a 50 mL flame-dried culture tube, the nitrile **4019** (89.5 mg, 0.397 mmol), azidotrimethylsilane (263 µL, 1.98 mmol), and 4 4'-di-*tert*-butylbiphenyl (23.0 mg, 0.0863 mmol) were dissolved in dry, degassed *o*-DCB (40 mL). The culture tube was sealed with a Teflon-lined cap and placed in a 175 °C oil bath. After 7 hours (TLC monitoring) the solution was concentrated to a brown oil. The yield of pyridine **4081g,** based on NMR analysis, was 39% using 4 4'-di-*tert*-butylbiphenyl resonances as an internal standard. This oil was purified by flash column chromatography (25:1 CH_2Cl_2:MeOH) to give the pyridine **4081g** (40.7 mg, 0.136 mmol, 34%) as an off-white crystalline solid. This compound was only sparingly soluble in $CDCl_3$.

^{1}H NMR (400 MHz, $CDCl_3$): δ 12.30 (br s, 1H), 3.04 (s, 3H, ArC*H*$_3$), 2.92 (br s, 2H, C*H*$_2$C=C-CH$_2$'), 2.45 (nfom, 2H, CH$_2$C=C-C*H*$_2$'), 1.91–1.87 (m, 2H), 1.84–1.79 (m, 2H), 1.74–1.69 (m, 2H), and 1.29 [s, 6H, C(C*H*$_3$)$_2$].

^{13}C NMR (125 MHz, $CDCl_3$): δ 166.3, 155.1, 145.9, 142.2, 132.2, 51.9, 31.2, 28.7, 27.4, 27.4, 26.5, 21.5 20.4. The solubility of **X** was found to be poor in a variety of solvents and a sufficiently concentrated NMR sample with which to obtain quality 1D ^{13}C data could not be obtained. Accordingly, the ^{13}C NMR chemical shifts were obtained from HMBC and HSQC spectra. The chemical shifts of two C_{sp2}-carbons could not be identified.

IR (thin film): 3400–2300 (broad), 3111, 2963, 2920, 2851, 1622, 1444, 1356, 1334, 1277, 1241, 1061, 977, and 731 cm^{-1}.

HRMS Calculated for $C_{16}H_{21}N^+$ [M+H$^+$] 269.1761, found 269.1753.

TLC: R_f 0.30 (2:3 hexanes:EtOAc)

m.p. 210–216 °C (decomp).

2,5,7,7,13-Pentamethyl-1,4,7,8,9,10,11,12-octahydro-1,4-ethenoazuleno[2,1-*c*]isoquinoline (4081h)

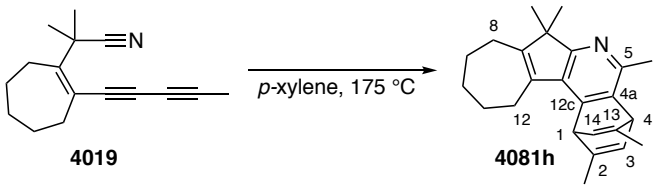

In a 16 mL flame-dried culture tube, the nitrile **4019** (30.3 mg, 0.134 mmol) was dissolved in *p*-xylene (13 mL). The culture tube was sealed with a Teflon-lined cap and placed in a 175 °C oil bath. After 7 hours, the solution was concentrated to an orange oil. This oil was purified by MPLC (2:1 hexanes:EtOAc) to give the pyridine **4081h** (17.3 mg, 0.0522 mmol, 39%) as a colorless oil.

^{1}H NMR (400 MHz, $CDCl_3$): δ 6.34 (dq, *J* = 5.9, 1.8 Hz, 1H), 6.25 (dq, *J* = 5.8, 1.8 Hz, 1H), 5.08 (dd, *J* = 5.9, 1.9 Hz, 1H, *H4*), 4.65 (dd, *J* = 5.9, 1.9 Hz, 1H, *H1*), 2.91 (m, 2H, C12H_2C=C-C8H_2), 2.59 (s, 3H, ArCH_3), 2.35 (m, 2H, C12H_2C=C-C8H_2), 1.916 (d, *J* =1.8 Hz, 3H, C*2*CH_3 or C*13*CH_3), 1.912 (d, *J* = 1.8 Hz, 3H, C*2*CH_3 or C*13*CH_3), 1.83 (m, 4H), 1.70 (br pent, *J* ~ 6 Hz, 2H), 1.169 (s, 3H, CH_3CCH$_3$), and 1.167 (s, 3H, CH$_3$CCH_3).

^{13}C NMR (125 MHz, $CDCl_3$): δ 167.7, 153.6, 150.7, 149.3, 147.1, 143.0, 138.6, 134.6, 131.5, 130.1, 128.7, 50.4, 49.7, 49.6, 30.3, 29.0, 27.3, 26.4, 25.0, 22.6, 22.5, 21.1, 19.8, and 19.4.

IR (thin film): 3051, 2961, 2924, 2852, 1700, 1582, 1441, 1406, 1378, 1360, 1266, 1207, 1193, 1034, 1004, 861, 789, 736, and 703 cm^{-1}.

HRMS Calculated for $C_{24}H_{30}N^+$ [M+H$^+$] 332.2373, found 332.2363.

5,7,7-trimethyl-1,2,3,4-tetraphenyl-7,8,9,10,11,12-hexahydroazuleno[2,1-*c*]isoquinoline (4081i)

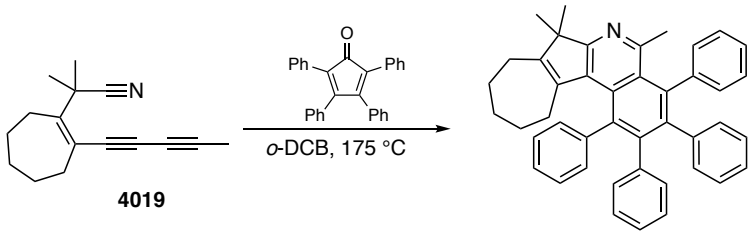

4019 **4081i**

In a 16 mL flame-dried culture tube, the nitrile **4019** (24.2 mg, 0.107 mmol) and tetraphenylcyclopentadienone (205 mg, 0.533 mmol) were dissolved in dry, degassed *o*-DCB (11 mL). The culture tube was sealed with a Teflon-lined cap and placed in a 175 °C oil bath. After 7 hours (TLC monitoring) the solution was concentrated to a purple solid. This solid was purified by MPLC (10:1 hexanes:EtOAc) to give the pyridine **4081i** (34.2 mg, 0.0588 mmol, 55%) as a fluorescent yellow crystalline solid.

^{1}H NMR (400 MHz, $CDCl_3$): δ 7.11–7.04 (m, 6H, Ar*H*), 7.02–6.98 (m, 2H, Ar*H*), 6.93–6.80 (m, 8H, Ar*H*), 6.65–6.60 (m, 4H, Ar*H*), 2.27 (nfom, 2H, C8H_2C=C-C12H_2'), 2.17 (s, 3H, ArCH_3), 1.52–1.46 (m, 4H), 1.42 (nfom, 2H, C8H_2C=C-C12H_2'), 1.31 [s, 6H, C(CH_3)$_2$], and 1.10 (br pent, J ~ 6 Hz, 2H).

^{13}C NMR (125 MHz, $CDCl_3$): δ 165.2, 154.1, 153.2, 142.6, 141.2, 141.0, 140.7, 140.6, 139.7, 139.3, 138.5, 135.3, 133.2, 131.9, 131.8, 131.6, 131.4, 130.0, 127.6, 127.3, 126.9, 126.9, 126.6, 126.5, 126.3, 125.5, 125.2, 50.3, 30.7, 28.5, 28.4, 27.3, 25.99, 25.96, and 22.2.

IR (thin film): 3080, 3055, 3023, 2958, 2922, 2856, 2243, 2205, 1945, 1877, 1803, 1753, 1600, 1547, 1531, 1490, 1442, 1391, 1370, 1204, 1134, 1073, 1027, 905, 813, 774, 729, 697, 648, 584 and 552 cm^{-1}.

HRMS (ESI-Orbitrap) Calculated for $C_{44}H_{40}N^+$ [M+H^+] 582.3155, found 582.3146.

TLC R_f 0.30 (10:1 hexanes:EtOAc)

***tert*-Butyl(3-(2-ethynyl-4,5-dimethoxyphenyl)-3-((triethylsilyl)oxy)prop-1-yn-1-yl)dimethylsilane (5022)**

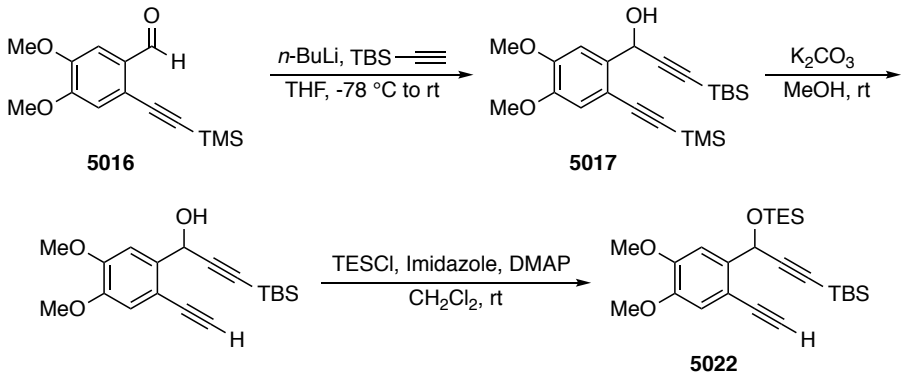

A solution of *tert*-butyl(ethynyl)dimethylsilane (7.4 mL, 40 mmol) in THF (75 mL) was cooled in a dry ice/acetone bath. n-BuLi (38 mmol, 2.5 M in hexanes) was added dropwise. After ca. 5 min, aldehyde **5016** (8.01 g, 30.5 mmol) in THF (25 mL) was added dropwise to this solution over 10 minutes. The resulting mixture was stirred in the cold bath for an additional 5 minutes and then allowed to warm to room temperature. After 30 minutes, the reaction mixture was quenched with a saturated aqueous NH_4Cl solution (100 mL), extracted with EtOAc (3 x 150 mL). The organic extracts were washed with brine and concentrated to give a viscous orange oil. This sample was used directly in the next step.

Data for the crude sample of alcohol 5017

^{1}H NMR (500 MHz, $CDCl_3$): 7.27 (s, 1H), 6.94 (s, 1H) 5.87 (d, J = 4.8 Hz, 1H), 3.92 (s, 3H), 3.88 (s, 3H), 2.62 (d, J = 4.8 Hz, 1H), 0.96 (s, 9H), 0.27 (s, 9H), 0.15 (s, 3H), and 0.14 (s, 3H).

K_2CO_3 (4.64 g, 33.6 mmol) was added to a solution of this crude material in MeOH (150 mL). The resulting suspension was stirred at room temperature for 30 minutes before being diluted with H_2O, extracted with EtOAc (2 x 200 mL), treated with brine, dried with Na_2SO_4, and concentrated to give a tan solid. This crude material was directly submitted to the next step.

Data for a crude sample of the monosilyl intermediate

^{1}H NMR (500 MHz, $CDCl_3$): 7.29 (s, 1H), 6.98 (s, 1H), 5.88 (d, J = 5.0 Hz, 1H), 3.92 (s, 3H), 3.89 (s, 3H), 3.29 (s, 1H), 2.42 (d, J = 5.0 Hz, 1H), 0.95 (s, 9H), 0.15 (s, 3H), and 0.14 (s, 3H).

This sample of # was dissolved in dry CH_2Cl_2 (100 mL). TESCl (5.8 mL, 35 mmol), imidazole (2.73 g, 40.1 mmol), and DMAP (699 mg, 5.72 mmol) were added sequentially, and the resulting solution was stirred overnight at room temperature. After 18 hours, the mixture was quenched with saturated aqueous NH_4Cl solution (100 mL) and extracted with additional CH_2Cl_2 (100 mL). The combined organic extracts were washed with brine, dried with Na_2SO_4, and concentrated. The resulting oil was purified by flash column chromatography (15:1 hexanes:EtOAc) to give **5022** as a yellow oil (11.5 g, 25.9 mmol, 65%), which slowly crystalized at room temperature over the course of several months.

^{1}H NMR (500 MHz, $CDCl_3$): δ 7.26 (s, 1H, ArH6), 6.92 (s, 1H, ArH3), 5.83 (s, 1H, ArC*H*C≡CSi), 3.91 (s, 3H, ArOC*H*$_3$), 3.87 (s, 3H, ArOC*H*$_3$'), 3.23 (s, 1H, ArC≡C*H*), 0.97 [t, *J* = 7.9 Hz, 9H, OSi($CH_aH_bCH_3$)], 0.92 [s, 9H, C≡CSi(C(C*H*$_3$)$_3$], 0.72 [dq, *J* = 15.2, 7.7 Hz, 3H, OSi(C*H*$_a$H$_b$CH$_3$)$_3$], 0.67 [dq, 3H, *J* = 15.4, 8.1 Hz, 3H, OSi($CH_aH_bCH_3$)], and 0.09 [s, 6H, Si(C*H*$_3$)$_2$].

^{13}C NMR (125 MHz, $CDCl_3$): δ 150.1, 148.2, 138.0, 114.6, 111.9, 109.8, 106.9, 88.2, 81.5, 80.7, 63.0, 56.1, 56.0, 26.2, 16.7, 6.94, 5.0, and -5.0.

IR (thin film): 3313 (sh), 3280 (br), 3000, 2953, 2933, 2933, 2877, 2856, 2171, 2105, 1603, 1510, 1462, 1396, 1357, 1301, 1259, 1211, 1097, 1058, 1005, 986, 824, 775, and 728 cm^{-1}.

HRMS (ESI-Orbitrap) Calculated for fragment $C_{19}H_{25}O_2Si^+$ [= $(M+H^+)-C_6H_{16}OSi]^+$ 313.1618, found 313.1619.

m.p. 33–36 °C

***tert*-Butyl(3-(2-(iodoethynyl)-4,5-dimethoxyphenyl)-3-((triethylsilyl)oxy)prop-1-yn-1-yl)dimethylsilane**

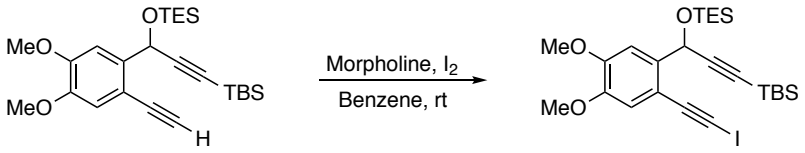

5022

In a 50 mL round-bottom flask, iodine (1.39 g, 5.49 mmol) was dissolved in benzene (15 mL). The flask was wrapped in aluminum foil. Morpholine (1.29 mL, 15.0 mmol) was added, the flask was capped with a rubber septum, and the resulting mixture was stirred for 30 minutes. A solution of alkyne **5022** (2.23 g, 5.02 mmol) in benzene (10 mL) was added by syringe, and the resulting solution was stirred. The reaction progress was monitored by APCI-MS until the terminal alkyne starting material was no longer observed. After 22 hours, the reaction mixture was filtered through Celite with Et_2O and the filtrate was concentrated. The resulting solid was purified by flash column chromatography (8:1 hexanes:EtOAc) to give the iodoalkyne (2.31 g, 4.05 mmol, 81%) as a white crystalline solid.

^{1}H NMR (400 MHz, $CDCl_3$): δ 7.25 (s, 1H, Ar*H6*), 6.88 (s, 1H, Ar*H3*), 5.79 (s, 1H, ArC*H*C≡C), 3.91 (s, 3H, ArOCH_3), 3.86 (s, 3H, ArOCH_3'), 0.98 [t, J = 8.0 Hz, 9H, OSi(CH_2CH_3)$_3$], 0.93 [s, 9H, C≡CSi(C(CH_3)$_3$], 0.73 [dq, J = 15.4, 7.8 Hz, 3H, OSi($CH_aH_bCH_3$)$_3$], 0.68 [dq, J = 15.6, 8.0 Hz, 3H, ($CH_aH_bCH_3$)], and 0.10 [s, 6H, C≡CSi(CH_3)$_2$].

^{13}C NMR (125 MHz, $CDCl_3$): δ 150.1, 148.2, 138.2, 114.8, 113.5, 109.8, 106.9, 92.0, 88.4, 63.0, 56.1, 56.0, 26.3, 16.7, 8.7, 7.0, 5.0, and -4.6.

IR (thin film): 3006, 2952, 2930, 2877, 2855, 2169, 1602, 1576, 1510, 1462, 1398, 1346, 1304, 1260, 1213, 1107, 1057, 1017, 988, 865, 837, 810, 775, 759, 725, 701, 689, 579, 466, and 421 cm^{-1}.

HRMS (ESI-Orbitrap) Calculated for fragment $C_{19}H_{24}IO_2Si^+$ [= $(M+H^+)-C_6H_{16}OSi]^+$ 439.0590, found 439.0589.

TLC: R_f 0.40 (5:1 hexanes:EtOAc)

m.p. 84–85 °C.

3-(2-(3-(*tert*-Butyldimethylsilyl)-1-((triethylsilyl)oxy)prop-2-yn-1-yl)-4,5-dimethoxyphenyl)propiolonitrile (5023)

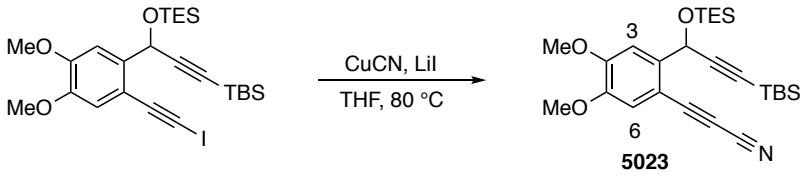

In a flame-dried 16 mL culture tube containing a stir bar, the iodoalkyne (571 mg, 1.00 mmol) was dissolved in THF (5.0 mL). CuCN (261 mg, 2.91 mmol) and LiI (28.0 mg, 0.209 mmol) were added. After flushing the headspace with N_2, the culture tube was sealed with a Teflon-lined cap and placed into a 90 °C oil bath, and the reaction mixture was vigorously stirred. The reaction progress was monitored by LC-MS until the iodoalkyne starting material was no longer observed. After 42 hours the reaction mixture was cooled and filtered through a silica gel plug with ethyl acetate and the filtrate was concentrated. The resulting oil was purified by MPLC (5:1 hexanes:EtOAc) to give the alkyne-nitrile **5023** (407 mg, 0.866 mmol, 87%) as a yellow oil.

^{1}H NMR (400 MHz, $CDCl_3$): δ 7.29 (s, 1H, Ar*H3*), 7.00 (s, 1H, Ar*H6*), 5.67 (s, 1H, ArC*H*C≡C), 3.95 (s, 3H, ArOC*H*$_3$), 3.89 (s, 3H, ArOC*H*$_3$'), 0.99 (t, *J* = 8.0 Hz, 9H, OSi(CH_2CH_3)$_3$), 0.93 (s, 9H, C≡CSi(C(CH_3)$_3$), 0.76 [dq, *J* = 15.4, 7.9 Hz, 3H, OSi($CH_aH_bCH_3$)$_3$], 0.71 [dq, *J* = 15.8, 8.0 Hz, 3H, ($CH_aH_bCH_3$)], and 0.11 [s, 6H, C≡CSi(CH_3)$_2$].

^{13}C NMR (125 MHz, $CDCl_3$): δ 152.6, 148.4, 141.8, 115.7, 109.9, 106.7, 105.9, 105.5, 89.7, 81.8, 66.9, 62.9, 56.3, 56.2, 26.2, 16.7, 6.9, 5.0, and -4.7.

IR (thin film): 3007, 2954, 2933, 2877, 2857, 2258, 2170, 2139, 1599, 1570, 1511, 1462, 1402, 1350, 1318, 1273, 1229, 1211, 1130, 1065, 1006, 874, 824, 808, 775, 728, and 677 cm^{-1}.

HRMS (ESI-Orbitrap) Calculated for fragment $C_{20}H_{24}NO_2Si^+$ [$(M+H^+)-C_6H_{16}OSi]^+$ 338.1571, found 338.1567.

TLC: R_f 0.25 (8:1 hexanes:EtOAc)

3-(2-(3-(*tert*-Butyldimethylsilyl)-1-hydroxyprop-2-yn-1-yl)-4,5-dimethoxyphenyl)propiolonitrile (5020)

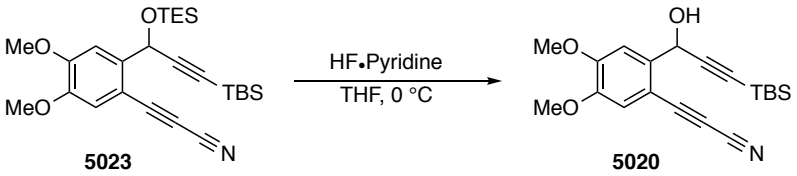

5023 **5020**

In a 50 mL polypropylene Falcon™ tube, silyl ether **5023** (407 mg, 0.866 mmol) was dissolved in THF (40 mL). The resulting solution was cooled in an ice bath for 10 minutes, after which time HF•pyridine (70 wt% HF, 2.9 g, 2.6 mL, 99 mmol) was added over 1 minute. After 10 minutes, the solution was diluted with EtOAc (100 mL), washed with H_2O (5 x 100 mL) and brine, dried with $MgSO_4$, and concentrated to give the alcohol **5020** as a brown amorphous solid of suitable purity for the next reaction (292 mg, 0.821 mmol, 95%).

^{1}H NMR (500 MHz, $CDCl_3$): δ 7.30 (s, 1H, ArH3), 7.04 [s, 1H, ArH6], 5.73 (d, *J* = 4.7 Hz, 1H, ArC*H*(OH)), 3.96 (s, 3H, ArOC*H*$_3$), 3.90 (s, 3H, ArOC*H*$_3$'), 2.33 (d, *J* = 4.8 Hz, 1H, O*H*), 0.95 [s, 9H, C≡CSi(C(C*H*$_3$)$_3$], and 0.14 [s, 6H, C≡CSi(C*H*$_3$)$_2$]

^{13}C NMR (125 MHz, $CDCl_3$): δ 152.6, 148.8, 140.1, 115.9, 110.1, 107.6, 105.7, 104.5, 90.9, 81.4, 66.9, 62.7, 56.3, 56.2, 26.1, 16.6, and -4.7.

IR (thin film): 3487 (broad), 3008, 2953, 2856, 2930, 2856, 2258, 2168, 2140, 1599, 1571, 1511, 1462, 1404, 1345, 1316, 1249, 1209, 1125, 1036, 1012, 977, 913, 869, 838, 825, 810, 775, 730, 702, 672, 614, and 492 cm^{-1}.

HRMS (ESI-Orbitrap) Calculated for $C_{20}H_{26}NO_3Si^+$ [M+H$^+$] 356.1676, found 356.1680.

TLC: R_f 0.20 (3:1 hexanes:EtOAc).

3-(2-(3-(*tert*-Butyldimethylsilyl)propioloyl)-4,5-dimethoxyphenyl)propiolonitrile (5015)
and
3-((*tert*-Butyldimethylsilyl)ethynyl)-5,6-dimethoxy-1-oxo-1*H*-indene-2-carbonitrile (5024)

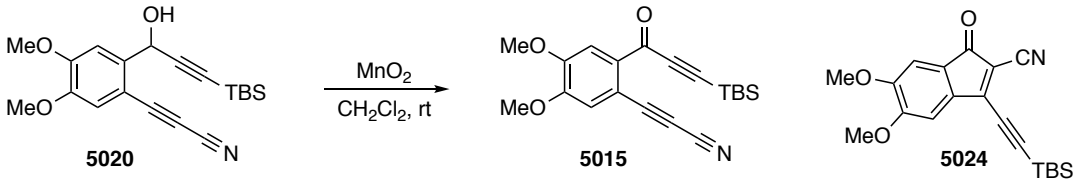

In an 50 mL culture tube equipped with a stir bar, alcohol **5020** (292 mg, 0.822 mmol) was dissolved in CH_2Cl_2 (15 mL). MnO_2 (90% purity, 1.59 g, 16.5 mmol) was added and the resulting mixture was vigorously stirred. After 10 minutes, the mixture was filtered through a plug of SiO_2 with EtOAc and the resulting solution was concentrated to a purple-grey solid. This solid was purified by MPLC (5:1 hexanes:EtOAc) to give ketone **5015** (126 mg, 0.357 mmol, 43%) as an off-white crystalline solid and indenone **5024** (29.8 mg, 0.0843 mmol, 10%) as a purple grey crystalline solid.

Data for ynone 5015

^{1}H NMR (400 MHz, $CDCl_3$): δ 7.75 (s, 1H, Ar*H3*), 7.14 (s, 1H, Ar*H6*), 3.99 (s, 3H, OCH_3), 3.98 (s, 3H, OCH_3'), 1.02 [s, 9H, C(CH_3)$_3$], and 0.26 [s, 6H, Si(CH_3)$_2$].

^{13}C NMR (125 MHz, $CDCl_3$): δ 174.1, 152.7, 151.2, 134.4, 118.1, 114.9, 110.7, 105.9, 101.6, 101.0, 81.6, 66.7, 56.7, 56.3, 26.2, 16.8, and -5.0.

IR (thin film): 2945, 2929, 2886, 2857, 2252, 2139, 1641, 1583, 1555, 1519, 1457, 1391, 1356, 1292, 1250, 1199, 1162, 1038, 1010, 991, 905, 872, 843, 826, 781, 759, 677, 636, 585, 515, 499, and 434 cm^{-1}.

HRMS (ESI-Orbitrap) Calculated for $C_{20}H_{24}NO_3Si^+$ [M+H$^+$] 354.1520, found 354.1518.

TLC: R_f 0.35 (3:1 hexanes:EtOAc).

m.p. 178–185 °C (decomp).

Data for the Indenone 5024

^{1}H NMR (400 MHz, $CDCl_3$): δ 7.10 (s, 1H), 6.89 (s, 1H), 3.98 (s, 3H), 3.93 (s, 3H), 1.06 (s, 9H), and 0.30 (s, 6H).

^{13}C NMR (125 MHz, $CDCl_3$): Get spectrum with higher S/N if convenient δ 188.8, 154.1, 152.3, 151.6, 135.2, 124.6, 121.4, 112.5, 111.1, 107.6, 106.4, 95.8, 56.7, 56.6, 26.2, 16.9, and -4.9.

HRMS (ESI-Orbitrap) Calculated for $C_{20}H_{24}NO_3Si^+$ [M+H$^+$] 354.1520, found 354.1529.

m.p. 171–173 °C

6-(*tert*-Butyldimethylsilyl)-9,10-dimethoxy-1,4-dihydro-7*H*-1,4-epoxyindeno[2,1-*c*]quinolin-7-one (5025a)

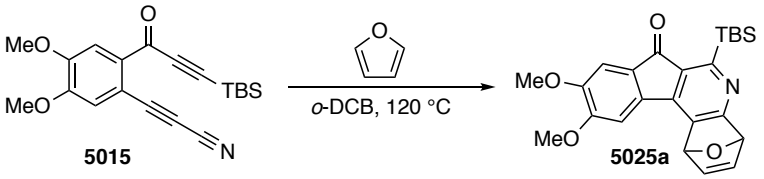

In a 16 mL flame-dried culture tube, the cyanoalkyne **5015** (30.0 mg, 0.0849 mmol) and furan (124 µL, 1.71 mmol) were dissolved in dried, degassed *o*-DCB (8.5 mL). The culture tube was sealed with a Teflon-lined cap and placed in a 120 °C oil bath. After 5 hours (TLC monitoring) the solution was filtered through a plug of SiO_2 with hexanes (to elute the *o*-dichlorobenzene) followed by EtOAc. The EtOAc filtrate was concentrated and the residue was purified by MPLC (3:2 hexanes:EtOAc) to give the pyridine derivative **5025a** (29.1 mg, 0.0690 mmol, 81%) as a bright yellow crystalline solid.

^{1}H NMR (500 MHz, $CDCl_3$): 7.23 (s, 1H, Ar*H8*), 7.13 (dd, *J* = 5.5, 1.7 Hz, 1H, *H2* or *H3*), 7.10 (dd, *J* = 5.5, 1.5 Hz, 1H, *H2* or *H3*), 6.96 (s, 1H, Ar*H11*), 6.12 (d, *J* = 1.5 Hz, 1H, *H1* or *H4*), 5.61 (d, *J* = 1.8 Hz, 1H, *H1* or *H4*), 4.05 (s, 3H, ArOC*H*$_3$), 3.94 (s, 3H, ArOC*H*$_3$'), 0.97 [s, 9H, ArSi(C(C*H*$_3$)$_3$], 0.42 [s, 3H, ArSi(C*H*$_3$)(CH_3)], and 0.40 [s, 3H, ArSi(CH_3)(C*H*$_3$)].

^{13}C NMR (125 MHz, $CDCl_3$): δ 192.6, 174.9, 160.4, 154.7, 151.4, 142.4, 141.7, 139.0, 135.9, 132.6, 131.5, 128.6, 106.8, 105.2, 82.6, 79.9, 56.6, 56.4, 27.3, 18.6, -4.69, and -4.71.

IR (thin film): 2953, 2927, 2888, 2852, 1707, 1641, 1589, 1560, 1495, 1462, 1393, 1325, 1304, 1260, 1244, 1216, 1142, 1092, 1063, 1025, 1004, 968, 870, 852, 832, 800, 788, 770, 733, 705, 688, 665, 633, and 575.

HRMS (ESI-Orbitrap) Calculated for $C_{24}H_{28}NO_4Si^+$ [M+H$^+$] 422.1782, found 422.1779.

TLC: R_f 0.45 (1:1 hexanes:EtOAc)

m.p. 148–150 °C.

3-(*tert*-Butoxy)-1-(*tert*-butyldimethylsilyl)-6,7-dimethoxy-9*H*-indeno[2,1-*c*]pyridin-9-one (5025b)

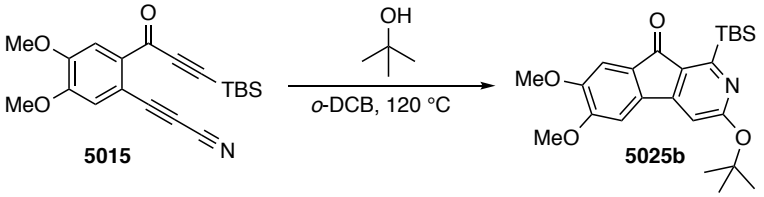

In a 16 mL flame-dried culture tube, the cyanoalkyne **5015** (28.7 mg, 0.0812 mmol) and *tert*-butanol (0.23 mL, 2.4 mmol) were dissolved in dried, degassed *o*-DCB (8.1 mL). The culture tube was sealed with a Teflon-lined cap and placed in a 120 °C oil bath. After 5 hours (TLC monitoring) the solution was filtered through a plug of SiO_2 with hexanes (to elute the *o*-dichlorobenzene) followed by EtOAc. The EtOAc filtrate was concentrated and the residue was purified by MPLC (5:1 hexanes:EtOAc) to give the pyridine derivative **5025b** (27.4 mg, 0.0641 mmol, 79%) as a bright yellow crystalline solid.

^{1}H NMR (500 MHz, $CDCl_3$): δ 7.19 (s, 1H, Ar*H8*), 7.00 (s, 1H, Ar*H5*), 6.59 (s, 1H, *H4*), 3.98 (s, 3H, ArOCH_3), 3.93 (s, 3H, ArOCH_3'), 1.63 [s, 9H, ArOC(CH_3)$_3$], 0.94 [s, 9H, ArSi(C(CH_3)$_3$], and 0.45 [s, 6H, Si(CH_3)$_2$].

^{13}C NMR (125 MHz, $CDCl_3$): δ 192.0, 165.3, 163.7, 154.3, 152.9, 151.4, 135.7, 130.4, 129.1, 106.4, 103.7, 103.6, 80.7, 56.5, 56.4, 28.7, 27.3, 18.6, and -4.3.

IR 2974, 2952, 2926, 2880, 2852, 1705, 1608, 1590, 1550, 1495, 1461, 1402, 1361, 1331, 1270, 1247, 1222, 1202, 1168, 1094, 1058, 1030, 1005, 960, 865, 841, 809, 794, 777, 694, 682, and 634.

HRMS (ESI-Orbitrap) Calculated for $C_{24}H_{34}NO_4Si^+$ [M+H$^+$] 428.2252, found 428.2257.

TLC: R_f 0.35 (1:2 hexanes:EtOAc)

m.p. 189–190 °C

3-(Butylamino)-1-(*tert*-butyldimethylsilyl)-6,7-dimethoxy-9*H*-indeno[2,1-*c*]pyridin-9-one (5025c)

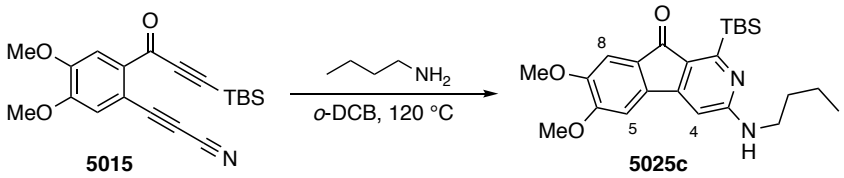

In a 16 mL flame-dried culture tube, the cyanoalkyne **5015** (35.0 mg, 0.0990 mmol) and *n*-butylamine (49 µL, 0.50 mmol) were dissolved in dried, degassed *o*-DCB (10 mL). The culture tube was sealed with a Teflon-lined cap and placed in a 120 °C oil bath. After 5 hours the solution was filtered through a plug of SiO_2 with hexanes (to elute the *o*-dichlorobenzene) followed by EtOAc. The EtOAc filtrate was concentrated and the residue was purified by MPLC (2:1 hexanes:EtOAc) to give the pyridine derivative **5025c** (10.2 mg, 0.0239 mmol, 24%) as a bright yellow oil.

^{1}H NMR (400 MHz, $CDCl_3$): δ 7.19 (s, 1H, Ar*H8*), 7.01 (s, 1H, Ar*H5*), 6.33 (s, 1H, Ar*H4*), 5.00 (br s, 1H, N*H*), 4.00 (s, 3H, C6OCH_3), 3.92 (s, 3H, C7OCH_3), 3.48 (br t, J = 7.0 Hz, 2H, CH_2NH), 1.65 (br pent, J ~ 7 Hz, 2H, CH_2CH$_2$NH) 1.44 (sext, J = 7.6 Hz, 2H, CH_2CH$_2$CH$_2$NH), 1.00 [s, 9H, ArSi(C(CH_3)$_3$], 0.97 (t, J = 7.3 Hz, 2H, CH_3CH$_2$), and 0.41 [s, 6H, Si(CH_3)$_2$]

^{13}C NMR (125 MHz, $CDCl_3$): δ 191.5 (C9), 166.7 (C1), 159.5 (C3), 153.6 (C6), 152.0* (br, C4a), 151.2 (C7), 135.1, 129.8, 126.8, 106.2, 103.5, 97.5* (br, C4), 56.5, 56.3, 42.0, 32.0, 27.2, 20.4, 18.3 (CMe_3), 14.0, and -5.1 ($Si(CH_3)_2$). *These resonances for non-hydrogen-bearing carbon resonances were of low intensity in the 1D spectrum but their presence were confirmed by HMBC analysis.

IR 3388, 2956, 2930, 2854, 1688, 1610, 1593, 1560, 1514, 1495, 1467, 1365, 1272, 1242, 1215, 1180, 1105, 1062, 1002, 839, and 824.

HRMS Calculated for $C_{24}H_{35}N_2O_3Si^+$ [M+H$^+$] 427.2411, found 427.2404.

TLC: R_f 0.30 (2:3 hexanes:EtOAc)

Methyl 6-((1-(*tert*-Butyldimethylsilyl)-6,7-dimethoxy-9-oxo-9H-indeno[2,1-c]pyridin-3-yl)thio)-2-cyanohexanoate (5025d)

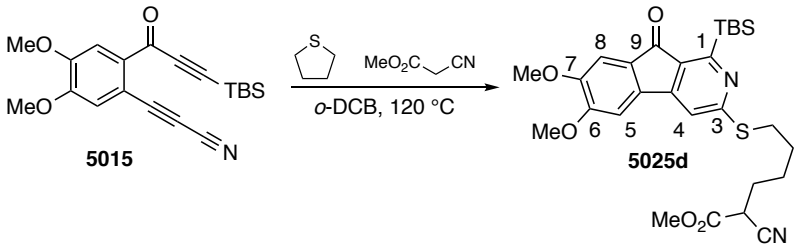

In a 50 mL flame-dried culture tube, the cyanoalkyne **5015** (29.7 mg, 0.0840 mmol,), tetrahydrothiophene (22 µL, 0.25 mmol), and methyl cyanoacetate (37 µL, 0.419 mmol) were dissolved in dry, degassed *o*-DCB (8.4 mL). The culture tube was sealed with a Teflon-lined cap and placed in a 120 °C oil bath. After 5 hours (TLC monitoring) the solution was concentrated to leave a dull orange oil. This oil was purified by MPLC (3:1 hexanes:EtOAc) to give the pyridine derivative **5025d** (26.8 mg, 0.0496 mmol, 59%) as an amorphous yellow solid.

^{1}H NMR (500 MHz, $CDCl_3$): δ 7.20 (s, 1H, ArH8), 7.11 (s, 1H, ArH4), 7.02 (s, 1H, ArH5), 4.01 (s, 3H, C6OC*H*$_3$), 3.93 (s, 3H, C7OC*H*$_3$), 3.83 (s, 3H, CO_2OC*H*$_3$), 3.52 (dd, *J* = 7.6, 7.0 Hz, 1H, C*H*CN), 3.30 (ddd, *J* = 13.6, 7.1, 7.1 Hz, 1H, SC*H*$_a$H$_b$), 3.27 (ddd, *J* = 13.7, 7.1, 7.1 Hz, 1H, SCH$_a$*H*$_b$), 1.99 (app q, *J* = 8 Hz, 2H, C3'*H*$_2$), 1.81 (tt, *J* = 7.4, 7.4 Hz, 2H, C5'*H*$_2$), 1.67–1.63 (m, 2H, C4'H$_2$), 0.97 [s, 9H, SiC(C*H*$_3$)$_3$], and 0.44 [s, 6H, Si(CH$_3$)$_2$].

^{13}C NMR (125 MHz, $CDCl_3$): δ 192.7(C9), 166.6(CO_2Me), 164.5(C1), 163.5(C3), 154.5(C7), 151.6(C6), 149.8(C9a,byvirtueofabsenceofHMBC), 135.9(C4b), 132.7(C4a), 128.3(C8a), 116.4(C≡N), 111.8(C4), 106.5(C8), 103.8(C5), 56.6(C6*C*H$_3$), 56.4(C7*C*H$_3$), 53.6(CO_2*C*H$_3$), 37.4(C2'), 29.6(C3'C5'orC6'), 29.5(C3'C5'orC6'), 29.3(C3'C5'orC6'), 27.2[C(*C*H$_3$)$_3$], 26.3(C4'), 18.4[*C*(Me$_3$)], and -4.8[Si(CH$_3$)$_2$].

IR 3009, 2929, 2249, 1732, 1711, 1596, 1575, 1492, 1473, 1405, 1387 1367, 1313, 1235, 1115, 1049, 1024, 972, 873, 844, 780, and 597 cm^{-1}.

HRMS (ESI-Orbitrap) Calculated for $C_{28}H_{37}N_2O_5SSi^+$ [M+H$^+$] 541.2187, found 541.2182.

TLC: R_f 0.30 (3:1 hexanes:EtOAc)

1-(*tert*-Butyldimethylsilyl)-6,7-dimethoxy-3-(methyl(3-oxocyclohept-4-en-1-yl)amino)-9*H*-indeno[2,1-*c*]pyridin-9-one (5025e)

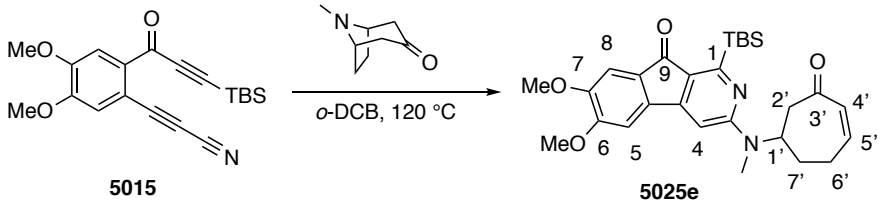

In a 50 mL flame-dried culture tube, the cyanoalkyne **5015** (30.0 mg, 0.0848 mmol) and tropinone (35.9 mg, 0.258 mmol) were dissolved in 8.5 mL of *o*-DCB. The culture tube was sealed with a Teflon-lined cap and placed in a 120 °C oil bath. After 5 hours (TLC monitoring) the solution was filtered through a plug of SiO_2 with hexanes (to elute the *o*-dichlorobenzene) followed by EtOAc. The EtOAc filtrate was concentrated and the residue was purified by MPLC (2:3 hexanes:EtOAc) to give the pyridine derivative **5025e** (28.6 mg, 0.0580 mmol, 68%) as a bright yellow crystalline solid.

^{1}H NMR (500 MHz, $CDCl_3$): δ 7.19 (s, 1H, Ar*H8*), 7.06 (s, 1H, Ar*H5*), 6.67 (ddd, *J* = 12.1, 6.2, 4.6 Hz, 1H, C5'*H*), 6.49 (s, 1H, Ar*H4*), 6.10 (ddd, *J* = 12.1, 2.0, 1.2 Hz, 1H, C4'*H*), 5.72 (br s, 1H, C1'*H*), 4.02 (s, 3H, OC*H*$_3$), 3.93 (s, 3H, OC*H*$_3$'), 3.09 (s, 3H, NC*H*$_3$), 2.93 (dd, *J* = 15.8, 5.8 Hz, 1H, C2'H_aH$_b$), 2.89 (dd, *J* = 15.8, 7.9 Hz, 1H, C2'H$_a$*H*$_b$), 2.62 (m, *J* = 18.8, 12.0, 6.2, 4.1, 1.4 Hz, 1H, C6'*Ha*Hb), 2.57 (ddddd, *J* = 18.7, 9.5, 4.1, 4.1, 2.3 Hz, 1H, C6'Ha*Hb*), 2.16 (nfom 1H, C7'Ha*Hb*), 2.01 (dddd, *J* = 13.9, 9.8, 9.8, 4.3 Hz, 1H, C7'Ha*Hb*), 0.97 [s, 9H, ArSi(C(C*H*$_3$)$_3$], 0.392 [s, 3H, ArSi(C*H*$_3$)(CH$_3$)], and 0.387 [s, 3H, ArSi(CH$_3$)(C*H*$_3$)].

^{13}C NMR (125 MHz, $CDCl_3$): δ 201.4, 191.5, 165.6, 158.8, 153.7, 152.7, 151.3, 146.1, 135.3, 132.6, 129.7, 126.2, 106.2, 103.5, 96.0, 56.6, 56.3, 50.4, 48.3, 30.84, 30.81, 28.5, 27.2, 18.2, and -5.1

IR 2929, 2892, 2853, 1691, 1643, 1581, 1532, 1492, 1462, 1415, 1369, 1314, 1240, 1209, 1173, 1079, 999, 986, 966, 874, 833, 768 ,728, 662, and 627.

HRMS (ESI-Orbitrap) Calculated for $C_{28}H_{37}N_2O_4Si^+$ [M+H$^+$] 493.2517, found 493.2512.

TLC: R_f 0.35 (1:2 hexanes:EtOAc).

m.p. 190-194 °C.

(*S*)-*N*-(6-(*tert*-Butyldimethylsilyl)-3,9,10,15,16,17-hexamethoxy-7-oxo-1,12,13,14-tetrahydro-7*H*-benzo[6',7']heptaleno[1',2':4,5]furo[2,3-*b*]indeno[1,2-*d*]pyridin-12-yl)acetamide (5025f)

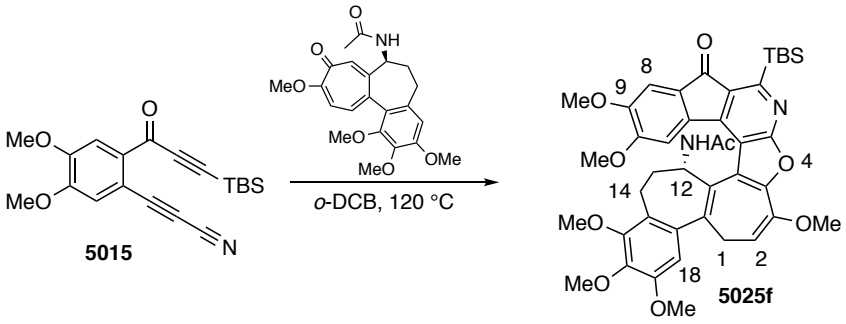

In a 16 mL flame-dried culture tube, the cyanoalkyne **5015** (29.2 mg, 0.083 mmol) and colchicine (99.1 mg, 0.224 mmol) were dissolved in 8.3 mL of *o*-DCB. The culture tube was sealed with a Teflon-lined cap and placed in a 120 °C oil bath. After 5 hours (TLC monitoring) the solution was filtered through a plug of SiO_2 with hexanes (to elute the *o*-dichlorobenzene) followed by EtOAc. The EtOAc filtrate was concentrated and the residue was purified by MPLC (1:3 hexanes:EtOAc) to give the pyridine derivative **5025f** (20.0 mg, 0.0266 mmol, 32%) as a bright yellow crystalline solid.

The ^{1}H NMR spectrum showed additional resonances that were attributed to a colchicine + pyridyne adduct. NOE shows this to be a minor conformer of **5025f** (rather than a different regioisomer).

^{1}H NMR (500 MHz, $CDCl_3$): δ 7.13 (s, 1H, Ar*H8*), 7.07 (s, 1H, Ar*H11*), 6.48 (s, 1H, Ar*H18*), 5.383 (dd, *J* = 6.1, 8.6 Hz, 1H, C2H), 5.376 (d, *J* = 10.4 Hz, 1H, N*H*), 5.16 (ddd, *J* = 6.2, 10.4, 11.8 Hz, 1H, C12*H*), 4.06 (s, 3H), 3.92 (s, 3H), 3.90 (s, 3H), 3.82 (s, 3H), 3.81 (s, 3H), 3.79 (s, 3H), 3.11 (dd, *J* = 13.8, 8.6 Hz, 1H, C1*Ha*Hb), 2.55 (dd, *J* = 13.9, 6.3 Hz, 1H, C1Ha*Hb*), 2.31-2.17 (m, 2H) 1.03 [s, 9H, ArSi(C(CH_3)$_3$]], 0.52 [ArSi(CH_3)(CH_3)], and 0.48 [ArSi(CH_3)(CH_3)].

^{13}C NMR (125 MHz, $CDCl_3$): δ 192.6, 168.8, 162.7, 162.2, 154.5, 153.8, 152.3, 151.4, 150.9, 148.5, 148.1, 140.2, 135.9, 135.2, 135.1, 132.3, 127.0, 125.0, 124.3, 116.8, 113.3, 109.2, 107.2, 106.9, 106.1, 61.0, 60.7, 56.34, 56.27, 56.1, 56.0, 48.6, 41.9, 32.0, 31.5, 27.4, 23.1, 18.6, -4.5, and -4.6.

IR 3365, 2934, 2854, 2341, 1709, 1661, 1591, 1558, 1495, 1462, 1401, 1358, 1324, 1310, 1262, 1222, 1196, 1139, 1096, 1057, 1022, 840, 821, 801, 785, and 680.

HRMS (ESI-Orbitrap) Calculated for $C_{42}H_{49}N_2O_9Si^+$ [M+H$^+$] 753.3202, found 753.3192.

TLC: R_f 0.25 (1:3 hexanes:EtOAc).

m.p. 294–297 °C (decomp).

2-(4,5-Dimethoxy-2-((trimethylsilyl)ethynyl)phenyl)-2-methylpropanal (5032)

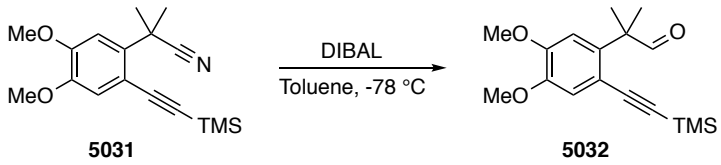

5031 **5032**

In a flame-dried 500 mL round-bottom flask containing a stir bar, nitrile substrate **5031** (6.04 g, 20.0 mmol) was dissolved in 100 mL of dry toluene. The flask was then fitted with a pressure-equalizing dropping funnel, placed under a positive N_2 pressure, and cooled in a dry ice/acetone bath for 15 minutes. To this stirred solution, DIBAL (1.4 M in toluene, 36 mL, 50 mmol) was added dropwise by the dropping funnel over 20 minutes. After 1 hour of being stirred in the cold bath, the reaction mixture was quenched by the addition of EtOAc (300 mL). After an additional 10 minutes in the cold bath the solution was warmed, washed with 2M aqueous HCl solution (5 x 150 mL) and brine, dried with $MgSO_4$, and concentrated to provide a reddish orange oil. This material was purified by flash column chromatography (4:1 hexanes:EtOAc), yielding aldehyde **5032** (4.83 g, 15.9 mmol, 79%) as a yellow oil, which slowly crystallized upon storage. The sample was observed to take on a reddish hue upon storage, although there was essentially no change observed in the ^{1}H NMR spectrum of such a sample.

^{1}H NMR (400 MHz, $CDCl_3$): δ 9.75 (s, 1H, C*H*O), 7.00 (s, 1H, Ar*H3*), 6.83 (s, 1H, Ar*H6*), 3.92 (s, 3H, ArOCH_3), 3.88 (s, 3H, ArOCH_3'), 1.49 (s, 6H, C(CH_3)$_2$), and 0.23 (s, 9H, Si(CH_3)$_3$).

^{13}C NMR (125 MHz, $CDCl_3$): δ 203.5, 149.7, 147.6, 139.2, 116.5, 114.5, 109.8, 104.3, 99.8, 56.11, 55.05, 50.5, 23.4, and -0.4.

IR (thin film) 2960, 2934, 2904, 2846, 2811, 2711, 2154, 1726, 1601, 1565, 1507, 1458, 1442, 1390, 1331, 1266, 1247, 1215, 1159, 1072, 1032, 993, 864, 841, 793, 760, 705, 638, 603, and 527.

HRMS (ESI-Orbitrap) Calculated for $C_{17}H_{25}O_3Si^+$ [M+H$^+$] 305.1567, found 305.1571

TLC: R_f 0.40 (4:1 hexanes:EtOAc)

m.p. 55–58 °C.

((2-(4,4-Dibromo-2-methylbut-3-en-2-yl)-4,5-dimethoxyphenyl)ethynyl)trimethylsilane (5033)

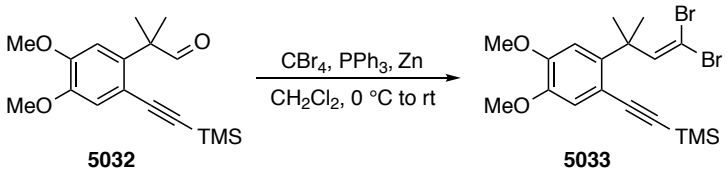

5032 **5033**

In an oven-dried 50 mL culture tube, zinc powder (1.36 g, 20.8 mmol) was dissolved in dry CH_2Cl_2 (6 mL). The culture tube was fitted with a rubber septum and placed under a slight positive N_2 pressure. PPh_3 (5.45 g, 20.8 mmol) was added and the resulting mixture was stirred in an ice bath for 5 minutes. A solution of CBr_4 (3.47 g, 10.5 mmol) in CH_2Cl_2 (6 mL) was then added by syringe. The mixture was taken out of the ice bath and stirred at room temperature for 10 minutes. After this time, a solution of the aldehyde **5032** (1.59 g, 5.22 mmol) in CH_2Cl_2 (6 mL) was added by syringe and the reaction mixture was allowed to stir at room temperature. After 4 hours, the reaction mixture was diluted with CH_2Cl_2 (25 mL) and filtered through Celite. The filtrate was washed with brine, dried with $MgSO_4$, and concentrated to a sticky yellow solid. This solid was purified by flash column chromatography (15:1 hexanes:EtOAc) to give dibromoalkene **5033** (1.75 g, 3.80 mmol, 73%), as an off-white crystalline solid.

^{1}H NMR (500 MHz, $CDCl_3$): δ 6.99 (s, 1H, Ar*H6*), 6.92 (s, 1H, C*H*=CBr_2), 6.84 (s, 1H, Ar*H3*), 3.90 (s, 3H, ArOC*H*$_3$), 3.87 (s, 3H, ArOC*H*$_3$'), 1.59 [s, 6H, ArC(C*H*$_3$)$_2$], and 0.28 [s, 9H, ArC≡CSi(C*H*$_3$)$_3$].

^{13}C NMR (125 MHz, $CDCl_3$): δ 148.9, 148.0, 146.7, 143.4, 116.9, 113.7, 109.8, 105.8, 99.3, 86.8, 55.96, 55.93, 42.8, 28.2, and 0.1.

IR (neat) 2995, 2959, 2936, 2909, 2846, 2144, 1602, 1568, 1509, 1460, 1442, 1392, 1333, 1262, 1221, 1160, 1134, 1073, 1040, 994, 855, 835, 774, 754, 697, 654, 619, 533, and 485.

HRMS (ESI-Orbitrap) Calculated for $C_{18}H_{25}{}^{79}Br_2O_2Si^+$ [M+H$^+$] 460.9965, found 460.9966.

m.p. 78–79 °C.

((4,5-Dimethoxy-2-(2-methylbut-3-yn-2-yl)phenyl)ethynyl)trimethylsilane (5034)

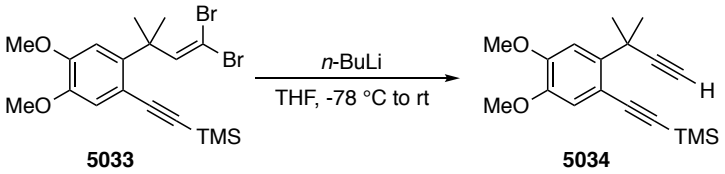

5033 **5034**

In a 100 mL oven-dried round-bottom flask containing a stir bar, the dibromoalkene **5033** (1.71 g, 3.72 mmol) was dissolved in THF (25 mL). The flask was fitted with a rubber septum, put under positive N_2 pressure, and cooled in a dry ice/acetone bath for 5 minutes. A solution of *n*-BuLi in hexanes (3.3 mL, 8.3 mmol) was added dropwise, by syringe, over a period of 10 minutes. The resulting solution was stirred for 30 minutes (GC-MS monitoring) in the cold bath before being quenched by the addition of saturated aqueous NH_4Cl solution (30 mL). The resulting layers were separated and the aqueous layer was extracted with additional EtOAc (50 mL). The combined organic layers were treated with brine, dried with $MgSO_4$, and concentrated to a yellow solid. This solid was purified by flash column chromatography (10:1 hexanes:EtOAc) and concentrated to give the terminal alkyne **5034** (1.06 g, 3.54, 95%) as a light yellow crystalline solid.

^{1}H NMR (400 MHz, $CDCl_3$): δ 7.38 (s, 1H, *H3*), 6.98 (s, 1H, *H6*), 3.91 (s, 3H, OC*H*$_3$), 3.87 (s, 3H, OC*H*$_3$*'*), 2.43 (s, 1H, C≡C*H*), 1.84 [s, 6H, C(C*H*$_3$)$_2$], and 0.25 [s, 9H, Si(CH$_3$)$_3$].

^{13}C NMR (125 MHz, $CDCl_3$): δ 149.0, 146.9, 140.5, 117.7, 112.6, 110.8, 105.6, 99.5, 91.3, 70.9, 56.1, 55.9, 37.1, 29.3, and -0.1.

IR (neat) 3244, 3087, 3000, 2968, 2932, 2903, 2845, 2144, 1602, 1568, 1508, 1462, 1441, 1385, 1331, 1258, 1245, 1216, 1187, 1158, 1065, 1040, 993, 939, 864, 834, 787, 754, 713, 697, 656, 580, 558, and 427.

HRMS (ESI-Orbitrap) Calculated for $C_{18}H_{25}O_2^+$ [M+H$^+$] 301.1618, found 301.1626.

TLC: R_f 0.25 (10:1 hexanes:EtOAc)

m.p. 80–81 °C

***tert*-Butyl(3-(2-ethynyl-4,5-dimethoxyphenyl)-3-methylbut-1-yn-1-yl)dimethylsilane (5035)**

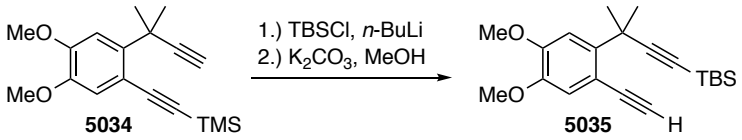

In a 50 mL flame-dried round-bottom flask containing a stir bar, alkyne **5034** (789 mg, 2.63 mmol) was dissolved in dry THF (15 mL). The flask was placed under a positive N_2 pressure and placed into a dry ice/acetone bath for 5 minutes. To the stirred reaction mixture, a solution of *n*-BuLi in hexanes (1.6 mL, 4.0 mmol) was added dropwise by syringe, followed by a solution of TBSCl (571 mg, 5.26 mmol) in 5 mL of dry THF. Subsequently, the flask was removed from the cold bath and left to stir at room temperature. After 30 minutes, the reaction mixture was quenched by the addition of saturated aqueous NH_4Cl solution (30 mL) and extracted with EtOAc (3 x 30 mL). The combined organic extracts were washed with brine (50 mL), dried with Na_2SO_4, and concentrated to leave a yellow oil (953 mg). This sample was used directly in the following desilylation reaction.

In a 50 mL flame-dried round-bottom flask containing a stir bar, the crude material from the previous reaction was dissolved in MeOH (12 mL). K_2CO_3 (352 mg, 2.55 mmol) was added to the reaction solution. The resulting mixture was vigorously stirred at room temperature for 1 hour. After this time the reaction mixture was quenched by the addition of H_2O (50 mL) and extracted with EtOAc (2 x 50 mL). The combined organic extracts were treated with brine (50 mL), dried with Na_2SO_4, and concentrated to give an orange oil. This oil was purified by flash column chromatography (10:1 hexanes:EtOAc) to give the alkyne **5035** (608 mg, 1.77 mmol, 67%) as a white crystalline solid.

^{1}H NMR (400 MHz, $CDCl_3$): δ 7.53 (s, *H*6, 1H), 6.99 (s, *H*3, 1H), 3.91 (s, OCH_3, 3H), 3.86 (s, OCH_3', 3H), 3.33 (s, ≡C*H*, 1H), 1.83 [s, (CH_3)$_2$CH, 6H], 0.96 [s, C(CH_3)$_3$, 9H], and 0.13 [s, Si(CH_3)$_2$, 6H].

^{13}C NMR (125 MHz, $CDCl_3$): δ 149.0, 146.8, 141.0, 118.2, 114.4, 111.3, 111.1, 85.2, 84.2, 82.3, 56.1, 55.8, 38.3, 29.6, 26.3, 16.7, and –4.3.

IR (neat) 3310, 3285, 3000, 2953, 2931, 2902, 2855, 2164, 2099, 1602, 1568, 1510, 1462, 1443, 1385, 1332, 1260, 1212, 1191, 1151, 1063, 1038, 985, 872, 836, 824, 810, 795, 774, 695, 671, 641, 586, and 564 cm^{-1}.

HRMS (ESI-Orbitrap) Calculated for $C_{21}H_{31}O_2Si^+$ [M+H$^+$] 343.2088, found 343.2087.

TLC: R_f 0.20 (30:1 hexanes:EtOAc)

m.p. 61–62 °C.

***tert*-Butyl(3-(2-(iodoethynyl)-4,5-dimethoxyphenyl)-3-methylbut-1-yn-1-yl)dimethylsilane (5036)**

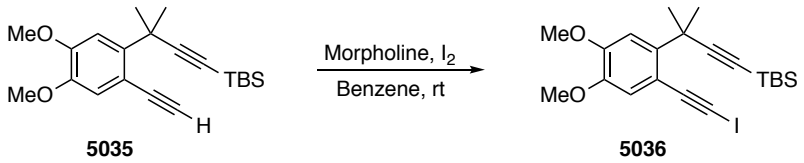

5035 **5036**

In a 50 mL round-bottom flask, iodine (439 mg, 1.73 mmol) was dissolved in benzene (10 mL). The flask was wrapped in aluminum foil. Morpholine (0.37 mL, 4.29 mmol) was added, the flask was capped with a rubber septum, and the resulting mixture was stirred for 5 minutes. A solution of alkyne **5035** (494 mg, 1.44 mmol) in benzene (10 mL) was added by syringe, and the resulting solution was stirred. The reaction progress was monitored by HPLC-MS until the terminal alkyne starting material was no longer observed. After 7 hours, the reaction mixture was filtered through Celite® with Et_2O and the filtrate was concentrated. The resulting solid was purified by MPLC (10:1 hexanes:EtOAc) to give the iodoalkyne **5036** (495 mg, 1.06 mmol, 74%) as a viscous orange oil.

^{1}H NMR (400 MHz, $CDCl_3$): Assign δ 7.47 (s, 1H), 6.94 (s, 1H), 3.90 (s, 3H, OC*H*$_3$), 3.86 (s, 3H, OC*H*$_3$*'*), 1.78 [s, 6H, C(C*H*$_3$)$_2$], 0.96 [s, 9H, SiC(CH_3)$_3$], and 0.14 [s, 6H, Si(CH_3)$_2$].

^{13}C NMR (125 MHz, $CDCl_3$): δ 149.1, 146.7, 141.5, 118.2, 114.2, 112.6, 111.0, 94.2, 85.0, 56.1, 55.8, 38.1, 29.8, 26.3, 16.7, 10.2, and -4.2.

IR (thin film): 3086, 2999, 2952, 2930, 2902, 2163, 1601, 1566, 1510, 1462, 1442, 1386, 1333, 1262, 1216, 1192, 1157, 1070, 991, 872, 836, 824, 811, 774, 733, 696, and 583.

HRMS (ESI-Orbitrap) Calculated for $C_{21}H_{30}IO_2Si^+$ [M+H$^+$] 469.1054, found 469.1052.

3-(2-(4-(*tert*-Butyldimethylsilyl)-2-methylbut-3-yn-2-yl)-4,5-dimethoxyphenyl)propiolonitrile (5026)

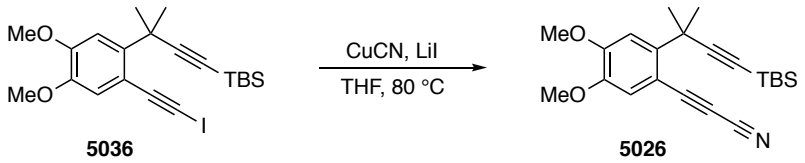

5036 **5026**

In a flame-dried 30 mL culture tube containing a stir bar, iodoalkyne **5036** (428 mg, 0.914 mmol) was dissolved in THF (8 mL). CuCN (165 mg, 1.84 mmol) and LiI (24.0 mg, 0.179 mmol) were added. After flushing the headspace with N_2, the culture tube was sealed with a Teflon-lined cap and placed into a 90 °C oil bath, and the reaction mixture was vigorously stirred. The reaction progress was monitored by HPLC-MS until the iodoalkyne starting material was no longer observed. After 6 hours the reaction mixture was cooled and filtered through a silica gel plug with ethyl acetate and the filtrate was concentrated. The resulting oil was purified by MPLC (15:1 hexanes:EtOAc) to give the alkyne-nitrile **5026** (125 mg, 0.340 mmol, 37%) as an off-white crystalline solid.

^{1}H NMR (500 MHz, $CDCl_3$): δ 7.35 (s, 1H, Ar*H3*), 7.06 (s, 1H, Ar*H6*), 3.94 (s, 3H, OCH_3), 3.89 (s, 3H, OCH_3'), 1.75 [s, 6H, (CH_3)$_2$C)], 0.96 [s, 9H, C(CH_3)$_3$], and 0.14 [s, 6H, Si(CH_3)$_2$].

^{13}C NMR (125 MHz, $CDCl_3$): δ 151.7, 147.2, 145.5, 118.8, 112.7, 110.7, 106.5, 106.1, 85.6, 83.6, 68.5, 56.3, 56.0, 37.6, 30.5, 26.2, 16.6, and -4.3.

IR (thin film): 3093, 2995, 2975, 2952, 2930, 2853, 2247, 2169, 2137, 1599, 1563, 1513, 1459, 1445, 1387, 1340, 1288, 1268, 1249, 1205, 1189, 1166, 1033, 1008, 916, 879, 836, 821, 808, 788, 774, 698, 671, 617, 562, 516, and 437.

HRMS (ESI-Orbitrap) Calculated for $C_{22}H_{30}NO_2Si^+$ [M+H$^+$] 368.2040, found 368.2040.

m.p. 109–110 °C.

6-(*tert*-Butyldimethylsilyl)-9,10-dimethoxy-7,7-dimethyl-4,7-dihydro-1*H*-1,4-epoxyindeno[2,1-*c*]quinolone (5037a)

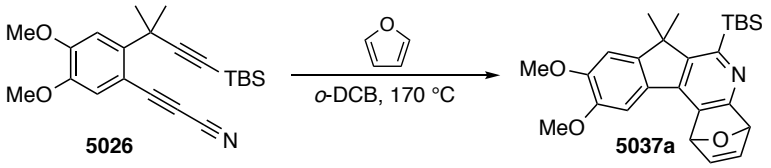

In a 16 mL flame-dried culture tube, the cyanoalkyne **18** (27.3 mg, 0.0743 mmol) and furan (108 μL, 1.49 mmol) were dissolved in dry, degassed *o*-DCB (7.4 mL). The culture tube was sealed with a Teflon-lined cap and placed in a 170 °C oil bath. After 6 hours (TLC monitoring) the solution was filtered through a plug of SiO_2, first with hexanes (to elute the *o*-dichlorobenzene) followed by EtOAc. The EtOAc filtrate was concentrated and the residue was purified by MPLC (3:1 hexanes:EtOAc) to give the pyridine derivative **19a** (15.6 mg, 0.0358 mmol, 48%) as a off-white crystalline solid.

^{1}H NMR (400 MHz, $CDCl_3$): δ 7.16 (dd, *J* = 5.5, 1.9 Hz, 1H, *H2* or *H3*), 7.14 (s, 1H, ArH*8*), 7.12 (dd, *J* = 5.5 Hz, 1.8 Hz, 1H, *H2* or *H3*), 6.88 (s, 1H, ArH*11*), 6.26 (dd, *J* = 1.8, 0.8 Hz, 1H, *H1* or *H4*), 5.62 (dd, *J* = 1.9, 0.8 Hz, 1H, *H1* or *H4*), 3.99 (s, 3H, ArOCH_3), 3.98 (s, 3H, ArOCH_3'), 1.55 [s, 3H, C(CH_3)(CH_3)], 1.54 [s, 3H, C(CH_3)(CH_3)], 0.91 [s, 9H, ArSi(C(CH_3)$_3$], 0.48 [s, 3H, ArSi(CH_3)(CH_3)], and 0.45 [s, 3H, ArSi(CH_3)(CH_3)].

^{13}C NMR (125 MHz, $CDCl_3$): δ 168.3, 153.6, 151.2, 151.0, 149.2, 149.0, 142.8, 142.8, 137.8, 131.4, 127.6, 105.4, 105.2, 82.7, 80.5, 56.6, 56.3, 47.8, 28.1, 27.8, 27.7, 18.2, -1.0, and -1.2.

IR 3004, 2956, 2929, 2893, 2853, 2254, 1633, 1609, 1560, 1498, 1464, 1352, 1320, 1272, 1255, 1207, 1176, 1064, 1012, 975, 910, 875, 858, 833, 809, 771, and 732.

HRMS (ESI-Orbitrap) Calculated for $C_{26}H_{34}NO_3Si^+$ [M+H$^+$] 436.2302, found 436.2293.

TLC: R_f (1:1 hexanes:EtOAc)

m.p. 179–181 °C

***N*-Butyl-1-(*tert*-butyldimethylsilyl)-6,7-dimethoxy-9,9-dimethyl-9*H*-indeno[2,1-*c*]pyridin-3-amine (5037b)**

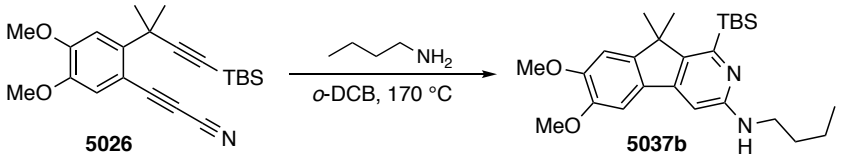

In a 16 mL flame-dried culture tube, the cyanoalkyne **5026** (29.5 mg, 0.0803 mmol) and *n*-butylamine (40 µL, 0.41 mmol) were dissolved in dry, degassed *o*-DCB (8.0 mL). The culture tube was sealed with a Teflon-lined cap and placed in a 170 °C oil bath. After 6 hours (TLC monitoring) the solution was filtered through a plug of SiO_2, first with hexanes (to elute the *o*-dichlorobenzene) followed by EtOAc. The EtOAc filtrate was concentrated and the residue was purified by MPLC (3:1 hexanes:EtOAc) to give the pyridine derivative **5037b** (20.2 mg, 0.0458 mmol, 57%) as a white crystalline solid.

^{1}H NMR (400 MHz, $CDCl_3$): δ 7.16 (s, 1H, Ar*H5*), 6.86 (s, 1H, Ar*H8*), 6.53 (s, 1H, Ar*H4*), 4.31 (t, *J* = 5.0 Hz, 1H, N*H*), 3.96 (s, 6H, ArOC*H*$_3$ and ArOC*H*$_3$'), 3.38 (td, *J* = 7.1, 5.0 Hz, 2H, C*H*$_2$NHAr), 1.69–1.60 (m, 2H, $NHCH_2CH_2CH_2CH_3$), 1.53 [s, 6H, $C(CH_3)_2$], 1.45 (dq, *J* = 7.3, 7.3 Hz, 2H, $NHCH_2CH_2CH_2CH_3$), 0.96 (t, *J* = 7.3 Hz, 3H, CH_2CH_3), 0.94 [s, 9H, $ArSi(C(CH_3)_3$], and 0.45 [s, 6H, $Si(CH_3)_2$].

^{13}C NMR (125 MHz, $CDCl_3$): δ 158.3, 156.1, 150.8, 149.5, 148.7, 147.9, 145.3, 129.0, 105.3, 103.2, 96.2, 56.3, 56.3, 46.9, 42.4, 32.4, 28.2, 27.8, 20.5, 18.1, 14.1, and -1.5.

IR 3395, 2957, 2928, 2855, 2254, 1607, 1562, 1496, 1462, 1441, 1428, 1358, 1342, 1273, 1255, 1197, 1159, 1094, 1034, 972, 906, 831, 804, 766, 728, 673, and 647 cm^{-1}.

HRMS (ESI-Orbitrap) Calculated for $C_{26}H_{41}N_2O_2Si^+$ [M+H$^+$] 441.2932, found 441.2921.

TLC: R_f 0.25 (25:1 CH_2Cl_2:MeOH)

m.p. 171–172 °C.

Methyl 6-((1-(*tert*-butyldimethylsilyl)-6,7-dimethoxy-9,9-dimethyl-9*H*-indeno[2,1-*c*]pyridin-3-yl)thio)-2-cyanohexanoate (5037c)

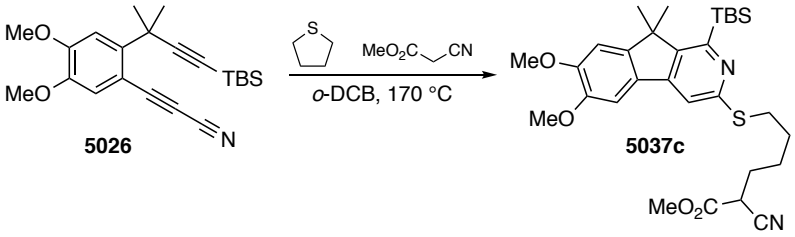

In a 16 mL flame-dried culture tube, the cyanoalkyne **5026** (29.5 mg, 0.0803 mmol), tetrahydrothiophene (21 μL, 0.24 mmol), and methyl cyanoacetate (35 μL, 0.40 mmol) were dissolved in dry, degassed *o*-DCB (8.0 mL). The culture tube was sealed with a Teflon-lined cap and placed in a 170 °C oil bath. After 6 hours (TLC monitoring) the solution was filtered through a plug of SiO_2 with hexanes (to elute the *o*-dichlorobenzene) followed by EtOAc. The EtOAc filtrate was concentrated and the residue was purified by MPLC (3:1 hexanes:EtOAc) to give the pyridine derivative **5037c** (28.9 mg, 0.0521 mmol, 65%) as a yellow crystalline solid.

^{1}H NMR (400 MHz, $CDCl_3$): δ 7.30 (s, 1H, Ar*H4*), 7.16 (s, 1H, Ar*H5*), 6.87 (s, 1H, Ar*H8*), 3.97 (s, 3H, C7OCH_3), 3.96 (s, 3H, C6OCH_3), 3.82 (s, 3H, CO_2CH_3), 3.52 (dd, J = 7.4, 6.5 Hz, 1H, C*H*CN), 3.30$^+$ (dt, J = 13, 7 Hz, 1H, SCH_aCH$_b$), 3.30$^-$ (dt, J = 13, 7 Hz, 1H, SCH$_a$CH_b), 1.99 (app q, J = 8 Hz, 2H, NCCHCH_2), 1.76 (br app pent, J ~ 7 Hz, SCH_2CH_2), 1.73-1.64 (m 2H, $SCH_2CH_2CH_2$), 1.55 [s, 6H, C(CH_3)$_2$], 0.93 [s, 9H, SiC(CH_3)$_3$], and 0.50 [s, 6H, Si(CH_3)$_2$].

^{13}C NMR (125 MHz, $CDCl_3$): δ 166.7, 160.3, 154.0, 151.8, 151.4, 149.0 (2x), 146.8, 127.9, 116.5, 111.6, 105.1, 103.3, 56.34, 56.31, 53.6, 47.5, 37.5, 29.8, 29.6, 29.1, 28.1, 27.4, 26.4, 18.1, and -1.3.

IR 2999, 2955, 2929, 2854, 2252,1749, 1611, 1585, 1523, 1494, 1462, 1385, 1372, 1343, 1299, 1254 ,1205, 1178, 1157, 1120, 1055, 1030, 912, 846, 833, 800, 771, 755, 732, 704, and 677 cm^{-1}.

HRMS (ESI-Orbitrap) Calculated for $C_{30}H_{43}N_2O_4SSi$+ [M+H$^+$] 555.2707, found 555.2695.

TLC: R_f 0.40 (2:1 hexanes:EtOAc).

m.p. 114–116 °C

Methyl 4-(4-((1-(*tert*-Butyldimethylsilyl)-6,7-dimethoxy-9,9-dimethyl-9*H*-indeno[2,1 *c*]pyridin-3-yl)thio)butoxy)benzoate (5037d)

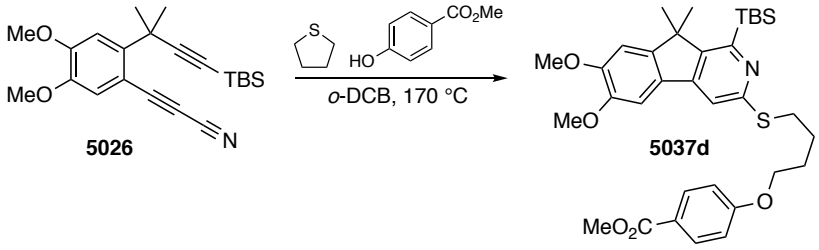

In a 16 mL flame-dried culture tube, the cyanoalkyne **5026** (29.1 mg, 0.0792 mmol), tetrahydrothiophene (21 μL, 0.24 mmol), and methyl paraben (60.2 mg, 0.396 mmol) were dissolved in dry, degassed *o*-DCB (7.9 mL). The culture tube was sealed with a Teflon-lined cap and placed in a 170 °C oil bath. After 6 hours (TLC monitoring) the solution was filtered through a plug of SiO_2 with hexanes (to elute the *o*-dichlorobenzene) followed by EtOAc. The EtOAc eluate was concentrated and the residue was purified by MPLC (4:1 hexanes:EtOAc) to give the pyridine derivative **5037d** (35.6 mg, 0.0586 mmol, 74%) as a clear oil.

^{1}H NMR (500 MHz, $CDCl_3$): δ 7.97 (d, *J* = 8.8 Hz, 2H, Ar*H2*'), 7.31 (s, 1H, Ar*H4*), 7.16 (s, 1H, Ar*H5*), 6.90 (d, *J* = 8.9 Hz, 2H, Ar*H3*'), 6.87 (s, 1H, Ar*H8*), 4.05 (t, *J* = 6.3 Hz, 2H, OCH_2), 3.97 (s, 3H, C7OCH_3), 3.95 (s, 3H, C6OCH_3), 3.88 (s, 3H, CO_2CH_3), 3.37 (t, *J* = 7.2 Hz, 2H, SCH_2), 2.02–1.96 (nfom, 2H, OCH_2CH_2), 1.94–1.88 (nfom, 2H, SCH_2CH_2), 1.56 [s, 6H, $C(CH_3)_2$], 0.93 (s, 9H, $C(CH_3)_3$), and 0.50 (s, 6H, $Si(CH_3)_2$). NOEs were observed between protons H4 and H5, H8 and its ortho-methoxy group, H8 and the geminal dimethyl group, and H5 and its ortho-methoxy group.

^{13}C NMR (125 MHz, $CDCl_3$): δ 167.1, 163.0, 160.3, 154.2, 151.7, 151.4, 149.0 (2x), 146.7, 131.7, 128.0, 122.5, 114.2, 111.6, 105.1, 103.3, 67.8, 56.3, 56.3, 52.0, 47.5, 29.4, 28.7, 28.1, 27.4, 26.9, 18.1, and -1.3.

HRMS (ESI-Orbitrap)

TLC: R_f 0.45 (3:1 hexanes:EtOAc).

6-((1-(*tert*-Butyldimethylsilyl)-6,7-dimethoxy-9,9-dimethyl-9*H*-indeno[2,1-*c*]pyridin-3-yl)(methyl)amino)cyclohept-2-en-1-one (5037e)

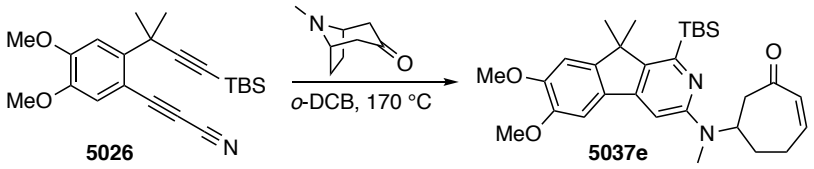

In a 50 mL flame-dried culture tube, the cyanoalkyne **5026** (22.6 mg, 0.0615 mmol) and tropinone (26.0 mg, 0.187 mmol) were dissolved in dry, degassed *o*-DCB (6.2 mL). The culture tube was sealed with a Teflon-lined cap and placed in a 170 °C oil bath. After 6 hours (TLC monitoring) the solution was filtered through a plug of SiO_2, first with hexanes (to elute the *o*-dichlorobenzene) followed by EtOAc. The EtOAc filtrate was concentrated and the residue was purified by MPLC (3:2 hexanes:EtOAc) to give the pyridine derivative **5037e** (15.9 mg, 0.0314 mmol, 51%) as an off-white crystalline solid.

^{1}H NMR (500 MHz, $CDCl_3$): δ 7.19 (s, 1H, *H*5), 6.86 (s, 1H, *H*8), 6.64 (s, 1H, *H*4), 6.64 (ddd, *J* = 12.1, 6.2, 4.6 Hz, 1H, *H*C=CHC=O) 6.08 (br d, *J* = 12.1 Hz), 5.69 (dddd, *J* = 10.1, 7.8, 6.1, 4.3 Hz, 1H, C*H*NMe), 3.98 (s, 3H, OCH_3), 3.97 (s, 3H, OCH_3'), 2.94 (s, 3H, NCH_3), 2.88 (dd, *J* = 15.8, 8.0 Hz, 1H, C2'H_aH$_b$), 2.86 (dddd, *J* = 15.8, 6.2, 0.8, 0.8 Hz, 1H, C2'H$_a$$H_b$), 2.61 (ddddd, *J* = 18.8, 10.4, 5.4, 4.1, 1.3 Hz, 1H, C6'H_aH$_b$), 2.54 (ddddd, *J* = 18.7, 9.2, 4.4, 4.4, 2.3 Hz, 1H, C6'H$_a$$H_b$), 2.12 (br dddd, *J* = 13.8, 4, 4, 4 Hz, 1H, C7'H_aH$_b$), 2.01 (dddd, *J* = 13.8, 9.8, 9.8, 4.1 Hz, 1H, C7'H$_a$$H_b$), 1.537 (s, 3H, C$H_3CCH_3$'), 1.535 (s, 3H, CH$_3CCH_3$'), 0.91 [s, 9H, C(C$H_3$)$_3$], 0.45 (s, 3H, C$H_3$SiCH$_3$'), and 0.43 (s, 3H, CH$_3SiCH_3$').

^{13}C NMR (125 MHz, $CDCl_3$): δ 202.3, 157.5, 155.3, 150.8, 149.3, 148.7, 148.3, 145.9, 144.7, 132.5, 129.0, 105.1, 103.0, 95.0, 56.3, 56.1, 49.4, 48.4, 46.8, 31.0, 30.1, 28.7, 27.9, 27.68, 27.64, 17.9, -1.54 and -1.55. (update shifts from the spectrum that will be in the SI)

IR 3067, 2955, 2925, 2892, 2854, 1650, 1595, 1531, 1493, 1461, 1414, 1311, 1259, 1199, 1162, 1073, 1034, 963, 844, 830, 800, 770, 678, 664, 651, and 616.

TLC R_f 0.55 (1:2 hexanes:EtOAc).

HRMS (ESI-Orbitrap) Calculated for $C_{30}H_{43}N_2O_3Si^+$ [M+H$^+$] 507.3037, found 507.3028.

m.p. 205–208 °C.

3-(1-(*tert*-Butyldimethylsilyl)-6,7-dimethoxy-9,9-dimethyl-9*H*-indeno[2,1-*c*]pyridin-3-yl)benzene-1,2-diol (5037g)

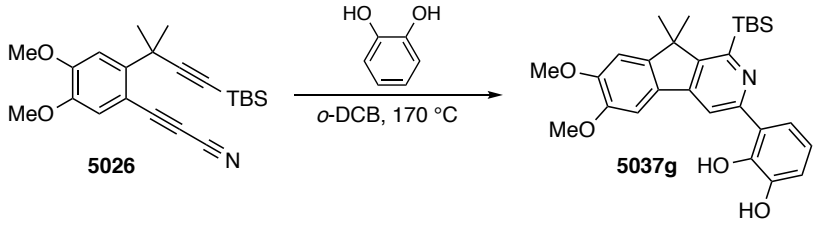

In a 16 mL flame-dried culture tube, the cyanoalkyne **5026** (22.2 mg, 0.0604 mmol) and catechol (20.0 mg, 0.182 mmol) were dissolved in dry, degassed *o*-DCB (6.0 mL). The culture tube was sealed with a Teflon-lined cap and placed in a 170 °C oil bath. After 6 hours (TLC monitoring) the solution was filtered through a plug of SiO_2, first with hexanes (to elute the *o*-dichlorobenzene) followed by EtOAc. The EtOAc filtrate was concentrated and the residue was purified by MPLC (5:1 hexanes:EtOAc) to give the pyridine derivative **5037g** (8.4 mg, 0.0175, 29%) as a light yellow oil.

^{1}H NMR (400 MHz, $CDCl_3$): δ 8.07 (s, 1H, Ar*H4'*), 7.50 (dd, *J* = 8.2, 1.5 Hz, 1H, Ar*H4*), 7.32 (s, 1H, Ar*H5'*), 6.97 (dd, *J* = 7.8, 1.4 Hz, 1H, ArH6), 6.91 (s, 1H, Ar*H8'*), 6.81 (dd, *J* = 8.0, 8.0 Hz, 1H, Ar*H5*), 5.89 (br s, 1H), 4.03 (s, 3H, C6OCH_3), 4.00 (s, 3H, C7OCH_3), 1.62 [s, 6H, C(CH_3)$_2$], 0.95 [s, 9H, SiC(CH_3)$_3$], and 0.65 [s, 6H, Si(CH_3)$_2$].

^{13}C NMR (125 MHz, $CDCl_3$):δ 156.2, 155.6, 153.2, 152.1, 149.5, 149.4, 148.63, 148.60, 146.2, 127.6, 118.2, 117.9, 116.8, 114.8, 108.7, 105.0, 103.5, 56.5, 56.4, 48.3, 28.0, 27.3, 18.5, and -1.3.

HRMS (ESI-Orbitrap) Calculated for $C_{28}H_{36}NO_4Si^+$ [M+H$^+$] 478.2408, found 478.2399.

TLC: R_f 0.40 (2:1 hexanes:EtOAc)

m.p. 213–214 °C

(*S*)-*N*-(6-(*tert*-Butyldimethylsilyl)-3,9,10,15,16,17-hexamethoxy-7,7-dimethyl-1,12,13,14-tetrahydro-7*H*-benzo[6',7']heptaleno[1',2':4,5]furo[2,3-*b*]indeno[1,2-*d*]pyridin-12-yl)acetamide (5037f)

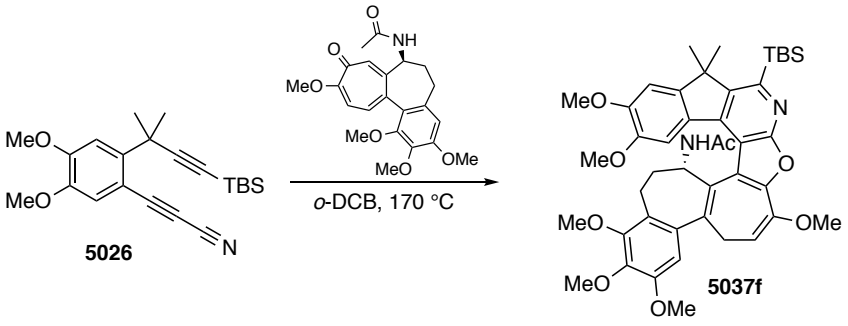

In a 16 mL flame-dried culture tube, the cyanoalkyne **5026** (28.7 mg, 0.0781 mmol), and colchicine (93.6 mg, 0.234 mmol) were dissolved in dry, degassed *o*-DCB (7.8 mL). The culture tube was sealed with a Teflon-lined cap and placed in a 170 °C oil bath. After 6 hours (TLC monitoring) the solution was concentrated to a brown oil. This oil was purified by MPLC (1:4 hexanes:EtOAc) to give the pyridine derivative **5037f** (14.3 mg, 0.0186 mmol, 24%) as a light orange solid.

The ^{1}H NMR spectrum shows two sets of resonances in a ratio of 8:1; this is interpreted as a mixture of interconverting conformers in the 7-membered F-ring; the sample shows a single, symmetrical peak when analyzed by reversed-phase HPLC.

^{1}H NMR (400 MHz, $CDCl_3$):
Data extracted for the major conformer: δ 7.38 (s, 1H, Ar*H11*), 6.82 (s, 1H, Ar*H8*), 6.49 (s, 1H, ArH18), 5.53 (d, *J* = 10.0 Hz, 1H, AcN*H*), 5.36 (dd, *J* = 8.5, 6.2 Hz, 1H, *H2*), 5.17 (ddd, *J* = 11.7, 10.0, 5.8 Hz, 1H, C*H*NHAc), 4.05 (s, 3H, ArOCH_3), 3.93 (s, 3H, C9OCH_3), 3.92 (s, 3H, C17OCH_3), 3.83 (s, 3H, ArOCH_3), 3.80 (s, 3H, ArOCH_3), 3.76 (s, 3H, C10OCH_3), 3.10 (dd, *J* = 13.7, 8.5 Hz, 1H, C1H_aH$_b$), 2.58 (dd, *J* = 13.7, 6.2 Hz, 1H, C1H$_a$$H_b$), 2.55-2.45 (nfom, 1H), 2.30-2.22 (m, 2H), 1.64 [s, 3H, C(CH_3)(CH$_3$)], 1.57 [s, 3H, C(CH$_3$)(CH_3)], ~1.56 (m, 1H), 1.01 [s, 9H, ArSi(C(CH_3)$_3$], 0.61 [ArSi(CH_3)(CH$_3$)], and 0.56 [ArSi(CH$_3$)(CH_3)]. (assigned OMe resonances and aromatic singlets based on NOE analysis)

Partial data set extracted for the minor conformer: δ 7.13 (s, 1H, Ar*H8*), 7.07 (s, 1H, Ar*H11*), 6.48 (s, 1H, Ar*H18*), 5.383 (dd, *J* = 6.1, 8.6 Hz, 1H, C2H), 5.376 (d, *J* = 10.4 Hz, 1H, N*H*), 5.16 (ddd, *J* = 6.2, 10.4, 11.8 Hz, 1H, C12*H*), 4.06 (s, 3H), 3.92 (s, 3H), 3.90 (s, 3H), 3.82 (s, 3H), 3.81 (s, 3H), 3.79 (s, 3H), 3.11 (dd, *J* = 13.8, 8.6 Hz, 1H, C1*Ha*Hb), 2.55 (dd, *J* = 13.9, 6.3 Hz, 1H, C1Ha*Hb*).

^{13}C NMR (125 MHz, $CDCl_3$): δ 168.3, 159.0, 157.1, 153.5, 151.3, 151.1, 150.9, 150.5, 149.3, 148.8, 148.4, 142.8, 140.2, 135.4, 134.1, 128.4, 125.6, 124.7, 117.1, 111.8, 108.3, 106.9, 106.3, 104.0, 60.9, 60.7, 56.2, 56.1, 56.0, 55.8, 49.1, 47.5, 41.6, 32.0, 31.6, 28.3, 27.5, 27.3, 22.9, 18.5, -0.96, and -0.98.

IR (thin film): 3442, 3325, 2931, 2853, 2250, 1667, 1593, 1561, 1495, 1459, 1412, 1399, 1322, 1266, 1245, 1228, 1208, 1192, 1135, 1116, 1096, 1062, 1018, 994, 938, 911, 831, 808, 799, 784, 729, 684, and 646 cm^{-1}.

HRMS (ESI-Orbitrap) Calculated for $C_{44}H_{55}N_2O_8Si^+$ [M+H$^+$] 767.3722, found 767.3704.

TLC: R_f 0.15 (1:4 hexanes:EtOAc).

6-(1-(*tert*-Butyldimethylsilyl)-6,7-dimethoxy-9,9-dimethyl-9*H*-indeno[2,1-*c*]pyridin-3-yl)-2,4,6-trimethylcyclohexa-2,4-dien-1-one (5037h)

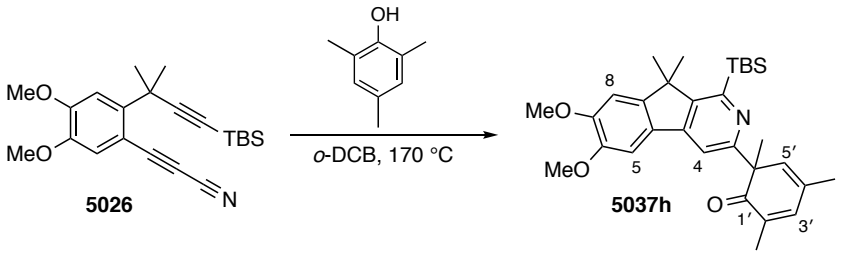

In a 16 mL flame-dried culture tube, the cyanoalkyne **5026** (23.9 mg, 0.0650 mmol), and 2,4,6-trimethylphenol (26.5 mg, 0.195 mmol) were dissolved in dry, degassed *o*-DCB (6.5 mL). The culture tube was sealed with a Teflon-lined cap and placed in a 170 °C oil bath. After 6 hours (TLC monitoring) the solution was filtered through a plug of SiO_2 with hexanes (to elute the *o*-dichlorobenzene) followed by EtOAc. The EtOAc filtrate was concentrated and the residue was purified by MPLC (4:1 hexanes:EtOAc) to give the pyridine derivative **5037h** (28.5 mg, 0.0566 mmol, 87%) as a light yellow crystalline solid.

^{1}H NMR (500 MHz, $CDCl_3$): δ 7.30 (s, 1H, Ar*H4*), 7.20 (s, 1H, Ar*H5*), 6.85 (s, 1H, Ar*H8*), 6.80 (dq, *J* = 2.8, 1.5 Hz, 1H, *H3'*), 6.15 (dq, *J* = 2.5, 1.6 Hz, 1H, *H5'*), 3.97 (s, 3H, C6OC*H*$_3$), 3.96 (s, 3H, C7OC*H*$_3$), 1.945 (d, *J* = 1.3 Hz, 3H, C2'C*H*$_3$ based on HMBC), 1.938 (d, *J* = 1.6 Hz, 3H, C4'C*H*$_3$ based on HMBC), 1.69 (s, 3H, C6'C*H*$_3$ based on NOE), 1.54 [s, 3H, C(C*H*$_3$)(CH_3)], 1.52 [s, 3H, C(CH_3)(C*H*$_3$)], 0.88 [s, 9H, ArSi(C(C*H*$_3$)$_3$], 0.46 [ArSi(C*H*$_3$)(CH_3)], and 0.42 [ArSi(CH_3)(C*H*$_3$)].

^{13}C NMR (125 MHz, $CDCl_3$): δ 204.6, 160.2, 158.6, 153.1, 151.0, 148.9, 148.6, 146.9, 143.2, 140.6, 132.0, 128.8, 126.1, 110.3, 105.0, 103.5, 56.9, 56.4, 56.3, 47.6, 28.0, 27.14, 27.11, 24.5, 21.4, 18.1, 15.8, -1.5, and -1.6.

HRMS (ESI-Orbitrap)

TLC: R_f 0.20 (4:1 hexanes:EtOAc).

Chapter 7. Computational Data

All DFT calculations were performed in Gaussian 09. All structures were optimized in and characterized by a frequency calculation (performed at 298 K) at the (U)M06-2X/6-31+G(d,p) level of theory with solvation treatment (SMD) using chloroform.

More explicitly, each computed species was subjected to an initial Monte Carlo conformational search in MacroModel (version 10.1) and Maestro (version 9.4) in the Schrodinger software suite. All resulting conformers were then subjected to the aformentioned DFT geometry optimization and frequency calculations. The DFT energies of each conformer were then used to determine the Boltzmann averaged energy of each species.

For open-shell calculations (i.e. for diradical and stepwise TS structures), the spin symmetry was broken by using the keyword "guess=(mix,always)." The triplet state energies of the same species were also calculated to correct for spin contamination and extract the pure singlet stat energy.

Listed on the following pages, one per page, are the free energy value (in Hartree atomic units), the Cartesian coordinates, the spin expectation value ($<S^2>$), and the imaginary frequencies of each conformer for each *in silico* species described in Chapters 4 and 5.

Energy and Geometry for 4014 (conformer 1)
Sum of electronic and thermal free energies = -1085.075491 a.u.

Center Number	Atomic Number	Atomic Type	Coordinates (Ångstroms)		
			X	Y	Z
1	7	0	0.975911	0.023132	0.550464
2	6	0	1.14367	1.389102	-0.014343
3	6	0	-0.063354	-0.236939	1.554393
4	16	0	1.535013	-1.31491	-0.294086
5	8	0	1.938729	-0.870455	-1.623327
6	6	0	2.995068	-1.801419	0.592921
7	8	0	0.546431	-2.378653	-0.148633
8	6	0	2.585397	1.565936	-0.329319
9	6	0	0.296428	1.656772	-1.267309
10	6	0	0.818497	2.43765	1.063262
11	7	0	3.707457	1.751671	-0.536031
12	6	0	-1.44091	-0.169624	1.046217
13	6	0	-2.585326	-0.118591	0.6489
14	6	0	-3.885229	-0.068652	0.189847
15	6	0	-5.028242	-0.031853	-0.214582
16	6	0	-6.402167	0.001336	-0.701706
17	1	0	0.108534	-1.233338	1.968504
18	1	0	0.062831	0.468028	2.378738
19	1	0	3.388659	-2.688987	0.092567
20	1	0	3.714697	-0.981959	0.549995
21	1	0	2.715458	-2.032749	1.622181
22	1	0	0.47064	2.680532	-1.610307
23	1	0	0.543332	0.963357	-2.06996
24	1	0	-0.758943	1.549705	-1.005341
25	1	0	1.072349	3.424284	0.670225
26	1	0	-0.251699	2.427025	1.285341
27	1	0	1.392378	2.264711	1.976768
28	1	0	-7.045739	-0.61372	-0.066624
29	1	0	-6.787308	1.024502	-0.698716
30	1	0	-6.45325	-0.385907	-1.723031

Energy and Geometry for 4014 (conformer 2)
Sum of electronic and thermal free energies = -1085.074935 a.u.

Center Number	Atomic Number	Atomic Type	Coordinates (Ångstroms)		
			X	Y	Z
1	7	0	1.099315	0.034601	0.629685
2	6	0	1.236328	1.327745	-0.097684
3	6	0	0.057536	-0.126149	1.653695
4	16	0	1.59593	-1.386584	-0.107677
5	8	0	1.921836	-2.318598	0.966412
6	6	0	0.205472	-2.079651	-0.981193
7	8	0	2.614041	-1.002318	-1.077635
8	6	0	2.685801	1.615885	-0.266459
9	6	0	0.55008	1.350042	-1.471081
10	6	0	0.692518	2.475727	0.770802
11	7	0	3.786145	1.94911	-0.38463
12	6	0	-1.321594	-0.065073	1.142591
13	6	0	-2.456314	-0.007588	0.717725
14	6	0	-3.745788	0.056491	0.231846
15	6	0	-4.879836	0.112071	-0.195347
16	6	0	-6.244616	0.176602	-0.703832
17	1	0	0.229013	-1.088799	2.143847
18	1	0	0.19966	0.634942	2.423779
19	1	0	0.586246	-2.972481	-1.48364
20	1	0	-0.56561	-2.353531	-0.259799
21	1	0	-0.168013	-1.35892	-1.708837
22	1	0	0.658477	2.343881	-1.912816
23	1	0	0.994928	0.624842	-2.154788
24	1	0	-0.514998	1.13941	-1.339952
25	1	0	0.903379	3.416143	0.25756
26	1	0	-0.389992	2.38564	0.888132
27	1	0	1.17509	2.4999	1.750081
28	1	0	-6.813559	-0.699735	-0.381443
29	1	0	-6.748632	1.073658	-0.334323
30	1	0	-6.243645	0.205131	-1.796949

Energy and Geometry for 4014 (conformer 3)
Sum of electronic and thermal free energies = -1085.074526 a.u.

Center Number	Atomic Number	Atomic Type	Coordinates (Ångstroms)		
			X	Y	Z
1	7	0	-1.232971	0.058684	-0.688231
2	6	0	-1.143488	1.441741	-0.158691
3	6	0	-0.235983	-0.375203	-1.685258
4	16	0	-1.774442	-1.165514	0.353217
5	8	0	-1.633585	-0.713514	1.73306
6	6	0	-3.503883	-1.316849	-0.026542
7	8	0	-1.127116	-2.403003	-0.069809
8	6	0	-0.112704	1.564477	0.914323
9	6	0	-0.734021	2.398791	-1.290649
10	6	0	-2.49225	1.913655	0.40546
11	7	0	0.683363	1.752421	1.731181
12	6	0	1.147258	-0.384928	-1.193065
13	6	0	2.287362	-0.371594	-0.780922
14	6	0	3.583521	-0.357176	-0.310754
15	6	0	4.724066	-0.345642	0.101618
16	6	0	6.093497	-0.334775	0.60159
17	1	0	-0.510048	-1.376254	-2.020477
18	1	0	-0.318529	0.283374	-2.551771
19	1	0	-3.878631	-2.147209	0.576454
20	1	0	-4.017883	-0.39218	0.234872
21	1	0	-3.600061	-1.537892	-1.090281
22	1	0	-0.76802	3.420284	-0.906581
23	1	0	0.277779	2.207377	-1.652527
24	1	0	-1.448751	2.307148	-2.113438
25	1	0	-2.393287	2.950869	0.73343
26	1	0	-3.240587	1.867655	-0.390874
27	1	0	-2.814648	1.321224	1.261597
28	1	0	6.414266	0.688219	0.816241
29	1	0	6.167899	-0.921119	1.521493
30	1	0	6.774183	-0.763843	-0.138935

Energy and Geometry for 4014 (conformer 4)
Sum of electronic and thermal free energies = -1085.074373 a.u.

Center Number	Atomic Number	Atomic Type	Coordinates (Ångstroms)		
			X	Y	Z
1	7	0	-0.876106	0.02587	-0.470049
2	6	0	-1.386454	1.39103	-0.178542
3	6	0	0.12531	-0.13419	-1.531211
4	16	0	-1.728641	-1.327263	0.020731
5	8	0	-1.447826	-2.390481	-0.940154
6	6	0	-0.997885	-1.796343	1.570629
7	8	0	-3.108207	-0.918192	0.263423
8	6	0	-1.921827	1.429117	1.205335
9	6	0	-0.223679	2.400634	-0.186462
10	6	0	-2.481969	1.813516	-1.16496
11	7	0	-2.303144	1.535638	2.291196
12	6	0	1.505951	-0.090256	-1.030476
13	6	0	2.647677	-0.075422	-0.622099
14	6	0	3.947559	-0.050702	-0.160014
15	6	0	5.090429	-0.027822	0.245943
16	6	0	6.464725	-0.000425	0.732647
17	1	0	-0.044626	-1.092453	-2.026501
18	1	0	-0.026278	0.635286	-2.294773
19	1	0	-1.520673	-2.694552	1.907162
20	1	0	0.059741	-2.00232	1.397481
21	1	0	-1.133317	-0.982716	2.284647
22	1	0	-0.608693	3.376115	0.119251
23	1	0	0.565268	2.09631	0.504203
24	1	0	0.190511	2.502039	-1.191759
25	1	0	-2.815286	2.830809	-0.943109
26	1	0	-2.066302	1.796851	-2.176706
27	1	0	-3.332448	1.132995	-1.112288
28	1	0	6.885155	-1.009576	0.749772
29	1	0	7.087035	0.623787	0.085538
30	1	0	6.502157	0.407635	1.746451

Energy and Geometry for 4014‡_a

$<S^2>$ = 0.608016

Imaginary Frequencies: -702.269 cm^{-1}

Sum of electronic and thermal free energies = -1085.015534 a.u.

Center Number	Atomic Number	Atomic Type	Coordinates (Ångstroms)		
			X	Y	Z
1	7	0	1.32297	0.071626	0.768395
2	6	0	0.992044	1.383573	0.172337
3	6	0	0.097505	-0.420307	1.416021
4	16	0	2.042331	-1.125559	-0.216239
5	8	0	1.531627	-1.075842	-1.58535
6	6	0	3.766842	-0.699721	-0.209132
7	8	0	1.903229	-2.37378	0.531626
8	6	0	-0.426636	1.194928	-0.453378
9	6	0	0.852427	2.409087	1.307696
10	6	0	1.975856	1.919693	-0.859948
11	7	0	-0.96412	1.753789	-1.3791
12	6	0	-1.078522	0.009241	0.551747
13	6	0	-2.305047	-0.33977	0.532491
14	6	0	-3.610825	-0.413286	0.205764
15	6	0	-4.80001	-0.493526	-0.077257
16	6	0	-6.209052	-0.582981	-0.421448
17	1	0	0.12652	-1.501326	1.539881
18	1	0	0.016159	0.036483	2.40495
19	1	0	4.271615	-1.572227	-0.631355
20	1	0	3.946699	0.173023	-0.833109
21	1	0	4.079387	-0.538224	0.822515
22	1	0	0.608134	3.382032	0.874954
23	1	0	0.065401	2.151967	2.019129
24	1	0	1.804073	2.481746	1.842051
25	1	0	1.591292	2.876536	-1.218933
26	1	0	2.945841	2.100262	-0.387457
27	1	0	2.085913	1.260563	-1.721633
28	1	0	-6.722483	0.351975	-0.179481
29	1	0	-6.327141	-0.780663	-1.490796
30	1	0	-6.686992	-1.395711	0.134468

Energy and Geometry for 4014$^{‡}_{concerted}$
Imaginary Frequencies: -486.3761 cm^{-1}
Sum of electronic and thermal free energies = -1085.012742 a.u.

Center Number	Atomic Number	Atomic Type	Coordinates (Ångstroms)		
			X	Y	Z
1	6	0	2.239303	-1.840254	-0.118156
2	6	0	3.487747	-1.411001	0.096646
3	6	0	4.010347	-0.284617	0.277242
4	7	0	2.373077	0.990806	0.139303
5	6	0	1.309291	0.489655	-0.064791
6	6	0	1.054146	-1.475075	-0.254944
7	6	0	5.097228	0.660625	0.531141
8	6	0	-0.39897	-1.581631	-0.450372
9	7	0	-0.946455	-0.29914	0.037844
10	6	0	-0.129278	0.881015	-0.350714
11	6	0	-0.223683	1.193112	-1.851714
12	6	0	-0.460886	2.106959	0.501206
13	16	0	-2.613094	-0.20894	0.128954
14	8	0	-3.103374	-1.562587	-0.121996
15	6	0	-2.942047	0.179634	1.830956
16	8	0	-3.114367	0.891603	-0.69177
17	1	0	6.039131	0.112597	0.617589
18	1	0	5.173857	1.381299	-0.287099
19	1	0	4.91528	1.210158	1.458462
20	1	0	-0.811315	-2.40218	0.138287
21	1	0	-0.63194	-1.758475	-1.50795
22	1	0	0.036719	0.318199	-2.45474
23	1	0	0.469622	2.000455	-2.100835
24	1	0	-1.242569	1.503251	-2.092519
25	1	0	-1.475015	2.455889	0.292779
26	1	0	-0.352341	1.879322	1.564778
27	1	0	0.236258	2.907464	0.245084
28	1	0	-2.542772	1.16766	2.05927
29	1	0	-4.028715	0.171929	1.943084
30	1	0	-2.48032	-0.58886	2.451647

Energy and Geometry for 4014* (conformer 1)

Sum of electronic and thermal free energies = -1085.139661 a.u.

Center Number	Atomic Number	Atomic Type	Coordinates (Ångstroms)		
			X	Y	Z
1	6	0	2.244613	-1.965184	-0.059853
2	6	0	3.364923	-1.418434	0.033383
3	6	0	3.602465	-0.043012	0.094125
4	7	0	2.465725	0.678957	0.037433
5	6	0	1.280886	0.090453	-0.062666
6	6	0	1.044105	-1.298098	-0.11986
7	6	0	4.924547	0.641101	0.204626
8	6	0	-0.411163	-1.61446	-0.224151
9	7	0	-0.992307	-0.257397	-0.315835
10	6	0	-0.021978	0.870632	-0.119571
11	6	0	-0.038145	1.816554	-1.320252
12	6	0	-0.227569	1.635504	1.190615
13	16	0	-2.612329	-0.116647	-0.094658
14	8	0	-3.212189	-1.27328	-0.757903
15	6	0	-2.957534	-0.29624	1.646775
16	8	0	-2.998205	1.235501	-0.489087
17	1	0	4.784409	1.722057	0.240471
18	1	0	5.447257	0.313056	1.107823
19	1	0	5.555474	0.387364	-0.652445
20	1	0	-0.76781	-2.163116	0.657538
21	1	0	-0.654433	-2.198392	-1.115416
22	1	0	0.103554	1.254636	-2.247623
23	1	0	0.771964	2.544823	-1.219739
24	1	0	-0.992389	2.345274	-1.369476
25	1	0	-1.171385	2.188742	1.171636
26	1	0	-0.21454	0.95667	2.049531
27	1	0	0.587442	2.354962	1.30871
28	1	0	-2.576764	0.574993	2.178361
29	1	0	-4.043668	-0.359719	1.74407
30	1	0	-2.493525	-1.216588	2.006785

Energy and Geometry for 4014* (conformer 2)
Sum of electronic and thermal free energies = -1085.139418 a.u.

Center Number	Atomic Number	Atomic Type	Coordinates (Ångstroms)		
			X	Y	Z
1	6	0	-2.230016	-1.976083	0.028474
2	6	0	-3.360031	-1.440253	0.017316
3	6	0	-3.616918	-0.068067	-0.019421
4	7	0	-2.486511	0.666551	-0.054844
5	6	0	-1.292181	0.090733	-0.050817
6	6	0	-1.037343	-1.294528	-0.004828
7	6	0	-4.950356	0.602694	-0.0265
8	6	0	0.428042	-1.579665	0.016087
9	7	0	0.986319	-0.244331	-0.314625
10	6	0	0.00865	0.876358	-0.045648
11	6	0	0.18953	1.532671	1.329454
12	6	0	0.040894	1.904101	-1.172118
13	16	0	2.586922	-0.030053	0.093692
14	8	0	2.858832	-0.496704	1.456643
15	6	0	3.41448	-1.131544	-1.028257
16	8	0	2.93792	1.347785	-0.245989
17	1	0	-5.519692	0.305776	-0.912473
18	1	0	-5.529019	0.306752	0.853435
19	1	0	-4.823575	1.685885	-0.027767
20	1	0	0.721934	-2.313129	-0.740231
21	1	0	0.751419	-1.932751	1.004365
22	1	0	-0.645691	2.216291	1.507462
23	1	0	1.120338	2.104083	1.367927
24	1	0	0.199142	0.780555	2.124283
25	1	0	-0.773098	2.619608	-1.02511
26	1	0	0.991797	2.439712	-1.171715
27	1	0	-0.094393	1.412986	-2.139833
28	1	0	4.482977	-0.987279	-0.852169
29	1	0	3.137862	-2.161569	-0.799012
30	1	0	3.148066	-0.858749	-2.049625

Energy and Geometry for 4014* (conformer 3)
Sum of electronic and thermal free energies = -1085.134586 a.u.

Center Number	Atomic Number	Atomic Type	Coordinates (Ångstroms)		
			X	Y	Z
1	6	0	-2.278578	-1.945433	-0.10626
2	6	0	-3.393476	-1.385361	-0.031609
3	6	0	-3.608082	-0.00638	0.044548
4	7	0	-2.459275	0.697857	0.021544
5	6	0	-1.28254	0.090501	-0.061516
6	6	0	-1.066079	-1.298406	-0.133638
7	6	0	-4.920966	0.697794	0.140226
8	6	0	0.38437	-1.634055	-0.191786
9	7	0	0.994629	-0.283068	-0.3504
10	6	0	0.036375	0.847485	-0.070622
11	6	0	0.232857	1.541425	1.281782
12	6	0	0.045216	1.858581	-1.219018
13	16	0	2.591521	-0.256757	0.119168
14	8	0	3.16611	-1.479863	-0.444224
15	6	0	3.282124	1.144373	-0.723243
16	8	0	2.756765	-0.043235	1.559259
17	1	0	-4.765398	1.776733	0.173957
18	1	0	-5.549031	0.449519	-0.720405
19	1	0	-5.4553	0.381578	1.04102
20	1	0	0.645083	-2.265771	-1.043534
21	1	0	0.707259	-2.136023	0.729334
22	1	0	1.16134	2.118544	1.308073
23	1	0	0.253562	0.817632	2.100007
24	1	0	-0.602987	2.230035	1.434999
25	1	0	-0.793323	2.549041	-1.091527
26	1	0	0.965622	2.446865	-1.231461
27	1	0	-0.062319	1.346856	-2.17926
28	1	0	2.897276	2.064353	-0.282532
29	1	0	4.359046	1.075901	-0.549504
30	1	0	3.057019	1.070965	-1.787326

Energy and Geometry for 4015 (conformer 1)
Sum of electronic and thermal free energies = -633.64245 a.u.

Center Number	Atomic Number	Atomic Type	Coordinates (Ångstroms)		
			X	Y	Z
1	6	0	0.677613	2.488195	0.000004
2	6	0	0.40047	1.109442	0.000004
3	6	0	1.464554	0.175219	0.000002
4	6	0	2.76908	0.674706	-0.000005
5	6	0	3.034151	2.043439	-0.000008
6	6	0	1.984652	2.956907	-0.000003
7	6	0	1.197661	-1.338004	0.000002
8	6	0	2.481261	-2.071896	0.000002
9	6	0	0.447522	-1.7896	1.273509
10	6	0	0.447528	-1.789589	-1.273512
11	7	0	3.457536	-2.692396	-0.000003
12	6	0	-0.986123	0.743481	0.000016
13	6	0	-2.181879	0.524172	0.000013
14	6	0	-3.529411	0.24188	0.000009
15	6	0	-4.716758	-0.010717	-0.000005
16	6	0	-6.142903	-0.313067	-0.000012
17	1	0	-0.156394	3.183023	0.00001
18	1	0	3.606977	-0.014629	-0.000007
19	1	0	4.063602	2.387457	-0.000013
20	1	0	2.178737	4.024562	-0.000003
21	1	0	0.330447	-2.876792	1.266892
22	1	0	0.999321	-1.498717	2.170857
23	1	0	-0.54413	-1.336167	1.304761
24	1	0	0.330431	-2.876779	-1.266895
25	1	0	-0.544115	-1.336135	-1.304776
26	1	0	0.999343	-1.498717	-2.170854
27	1	0	-6.623555	0.108441	-0.887187
28	1	0	-6.304388	-1.394532	-0.000065
29	1	0	-6.623548	0.108354	0.887207

Energy and Geometry for 4015 (conformer 2)
Sum of electronic and thermal free energies = -633.642126 a.u.

Center Number	Atomic Number	Atomic Type	Coordinates (Ångstroms)		
			X	Y	Z
1	6	0	-1.198247	2.360418	-0.109175
2	6	0	-0.725988	1.041012	-0.012462
3	6	0	-1.640785	-0.037309	0.046586
4	6	0	-3.004357	0.256979	0.004511
5	6	0	-3.465088	1.570586	-0.086268
6	6	0	-2.561184	2.627207	-0.144
7	6	0	-1.158249	-1.486736	0.204853
8	6	0	-0.161598	-1.793382	-0.846265
9	6	0	-0.512771	-1.689477	1.593056
10	6	0	-2.281989	-2.526261	0.031963
11	7	0	0.586875	-2.09677	-1.67469
12	6	0	0.693841	0.849831	0.017897
13	6	0	1.904099	0.74002	0.039791
14	6	0	3.272135	0.590884	0.066012
15	6	0	4.478166	0.455609	0.088425
16	6	0	5.926457	0.290966	0.109344
17	1	0	-0.475798	3.168949	-0.156721
18	1	0	-3.733389	-0.543828	0.039741
19	1	0	-4.533333	1.761145	-0.115684
20	1	0	-2.911458	3.651683	-0.217895
21	1	0	-0.163314	-2.720435	1.695705
22	1	0	0.329334	-1.015126	1.754958
23	1	0	-1.272395	-1.495814	2.355626
24	1	0	-1.852038	-3.529256	0.085034
25	1	0	-3.009165	-2.427282	0.842403
26	1	0	-2.79232	-2.417172	-0.928232
27	1	0	6.415114	1.142791	-0.371597
28	1	0	6.289979	0.21884	1.138097
29	1	0	6.214002	-0.619186	-0.424209

Energy and Geometry for 4015 (conformer 3)
Sum of electronic and thermal free energies = -633.642126 a.u.

Center Number	Atomic Number	Atomic Type	Coordinates (Ångstroms)		
			X	Y	Z
1	6	0	1.198229	-2.360417	-0.109182
2	6	0	0.725981	-1.041008	-0.012465
3	6	0	1.640787	0.037305	0.046591
4	6	0	3.004356	-0.256994	0.004523
5	6	0	3.465076	-1.570605	-0.08626
6	6	0	2.561164	-2.627218	-0.144002
7	6	0	1.15826	1.486736	0.204855
8	6	0	0.161618	1.793384	-0.846272
9	6	0	0.512774	1.689485	1.593052
10	6	0	2.282008	2.526252	0.031968
11	7	0	-0.586846	2.096768	-1.674706
12	6	0	-0.693847	-0.849818	0.017894
13	6	0	-1.904104	-0.740009	0.039791
14	6	0	-3.272141	-0.590873	0.066015
15	6	0	-4.478172	-0.455598	0.088427
16	6	0	-5.926463	-0.290959	0.109347
17	1	0	0.475773	-3.168942	-0.156734
18	1	0	3.733395	0.543806	0.039759
19	1	0	4.53332	-1.761172	-0.115671
20	1	0	2.91143	-3.651697	-0.2179
21	1	0	0.163323	2.720445	1.695695
22	1	0	-0.329335	1.015139	1.754951
23	1	0	1.272392	1.49582	2.355628
24	1	0	1.852063	3.529251	0.085032
25	1	0	3.009178	2.427272	0.842412
26	1	0	2.792345	2.417156	-0.928224
27	1	0	-6.289987	-0.218839	1.1381
28	1	0	-6.214011	0.619195	-0.424203
29	1	0	-6.415117	-1.142783	-0.371599

Energy and Geometry for 4015‡_a

$<S^2>$ = 0.64824

Imaginary Frequencies: -777.7187 cm^{-1}

Sum of electronic and thermal free energies = -633.582980 a.u.

Center Number	Atomic Number	Atomic Type	Coordinates (Ångstroms)		
			X	Y	Z
1	6	0	-0.872091	-2.289905	-0.066851
2	6	0	-0.667708	-0.906483	-0.043312
3	6	0	-1.744235	-0.019906	0.005255
4	6	0	-3.047959	-0.509294	0.030944
5	6	0	-3.259574	-1.887551	0.0041
6	6	0	-2.17644	-2.772729	-0.044867
7	6	0	-1.3401	1.433343	0.047952
8	6	0	0.195861	1.425559	-0.159106
9	6	0	-1.994043	2.256759	-1.065433
10	6	0	-1.631635	2.047272	1.425134
11	7	0	0.97372	2.327775	-0.365187
12	6	0	0.629943	-0.23201	-0.058385
13	6	0	1.853078	-0.615019	-0.004527
14	6	0	3.195569	-0.509005	0.018457
15	6	0	4.419925	-0.445596	0.039684
16	6	0	5.870785	-0.364057	0.063311
17	1	0	-0.02372	-2.966524	-0.105854
18	1	0	-3.892183	0.174059	0.070271
19	1	0	-4.272854	-2.277054	0.01986
20	1	0	-2.355077	-3.843217	-0.067549
21	1	0	-1.638041	3.289848	-1.028877
22	1	0	-1.765757	1.840272	-2.050397
23	1	0	-3.080527	2.257097	-0.930452
24	1	0	-1.286569	3.084577	1.456429
25	1	0	-2.710827	2.027535	1.609839
26	1	0	-1.134604	1.484844	2.220904
27	1	0	6.307633	-1.367696	0.065943
28	1	0	6.238161	0.170403	-0.817548
29	1	0	6.210066	0.163177	0.959594

Energy and Geometry for $4015^{‡}_{concerted}$

Imaginary Frequencies: -475.9891 cm^{-1}
Sum of electronic and thermal free energies = -633.581628 a.u.

Center Number	Atomic Number	Atomic Type	Coordinates (Ångstroms)		
			X	Y	Z
1	6	0	-2.175065	-1.965648	0
2	6	0	-1.151844	-1.006421	-0.000003
3	6	0	-1.453566	0.364864	0.000003
4	6	0	-2.788738	0.76583	0.000011
5	6	0	-3.807056	-0.185767	0.000014
6	6	0	-3.500498	-1.549627	0.000009
7	6	0	-0.302803	1.356359	-0.000004
8	6	0	1.023604	0.636226	-0.000001
9	6	0	0.243321	-1.319828	-0.000013
10	6	0	1.354583	-1.881984	-0.000017
11	6	0	2.688328	-1.757537	-0.000002
12	6	0	3.417377	-0.722408	0.000006
13	7	0	2.202699	0.808617	-0.000001
14	6	0	4.740053	-0.086104	0.000018
15	6	0	-0.344068	2.236377	-1.263989
16	6	0	-0.344066	2.236397	1.263966
17	1	0	-1.920129	-3.020464	-0.000004
18	1	0	-3.03984	1.823235	0.000014
19	1	0	-4.843829	0.136066	0.00002
20	1	0	-4.297269	-2.286768	0.000011
21	1	0	4.862268	0.543315	0.885685
22	1	0	5.511108	-0.860215	0.000024
23	1	0	4.862282	0.543317	-0.885645
24	1	0	-0.283871	1.625973	-2.169129
25	1	0	-1.281723	2.799431	-1.285083
26	1	0	0.490164	2.942968	-1.255866
27	1	0	0.490152	2.943004	1.255818
28	1	0	-1.28173	2.799435	1.285067
29	1	0	-0.283842	1.626009	2.169115

Energy and Geometry for 4016 (conformer 1

Sum of electronic and thermal free energies = -629.106968 a.u.

Center Number	Atomic Number	Atomic Type	Coordinates (Ångstroms)		
			X	Y	Z
1	6	0	3.44094	0.959909	-0.00852
2	6	0	2.538252	-0.107026	-0.003623
3	6	0	1.15037	0.140222	0.005715
4	6	0	0.701179	1.461154	0.009925
5	6	0	1.603642	2.522834	0.005691
6	6	0	2.972587	2.272011	-0.003606
7	6	0	0.176049	-0.991686	0.011744
8	6	0	-1.24012	-0.65478	0.007448
9	8	0	0.527935	-2.156944	0.019501
10	6	0	-2.434064	-0.432744	0.00312
11	6	0	-3.782437	-0.168219	-0.001957
12	6	0	-4.972616	0.068156	-0.006613
13	6	0	-6.400056	0.352134	-0.011124
14	6	0	3.111516	-1.430679	-0.010116
15	7	0	3.69201	-2.432103	-0.01668
16	1	0	4.505817	0.752876	-0.016215
17	1	0	-0.365348	1.661405	0.017136
18	1	0	1.234252	3.542856	0.009632
19	1	0	3.68182	3.093191	-0.00712
20	1	0	-6.965017	-0.536367	-0.305108
21	1	0	-6.726	0.658653	0.986793
22	1	0	-6.62454	1.159944	-0.712872

Energy and Geometry for 4016‡_a

$<S^2>$ = 0.620918

Imaginary Frequencies: -822.1578 cm^{-1}

Sum of electronic and thermal free energies = -629.051652 a.u.

Center Number	Atomic Number	Atomic Type	Coordinates (Ångstroms)		
			X	Y	Z
1	6	0	-2.663772	-1.575337	0.000132
2	6	0	-1.54613	-0.74444	0.0001
3	6	0	-1.680646	0.638794	-0.000078
4	6	0	-2.934973	1.244895	-0.000205
5	6	0	-4.057823	0.422841	-0.000168
6	6	0	-3.920372	-0.972751	-0.000008
7	6	0	-0.370796	1.321048	-0.000105
8	6	0	0.719986	0.285512	0.000043
9	8	0	-0.1796	2.516739	-0.000231
10	6	0	1.990888	0.404348	-0.000025
11	6	0	3.31127	0.164156	-0.000046
12	6	0	4.521211	-0.03366	-0.000071
13	6	0	5.951888	-0.272472	-0.000084
14	6	0	-0.132664	-1.210366	0.000277
15	7	0	0.394737	-2.300299	0.00055
16	1	0	-2.551434	-2.654525	0.000263
17	1	0	-3.019597	2.327208	-0.000329
18	1	0	-5.049987	0.862377	-0.000262
19	1	0	-4.809389	-1.595768	0.000011
20	1	0	6.497144	0.67647	0.000907
21	1	0	6.239116	-0.842338	0.888405
22	1	0	6.239384	-0.84065	-0.889568

Energy and Geometry for 4016$^{‡}_{concerted}$
Imaginary Frequencies: -503.5885 cm^{-1}
Sum of electronic and thermal free energies = -629.046533 a.u.

Center Number	Atomic Number	Atomic Type	Coordinates (Ångstroms)		
			X	Y	Z
1	6	0	0.610473	-0.581768	0.000025
2	6	0	0.622288	1.434484	0.000009
3	6	0	-0.806096	1.739999	0.000003
4	6	0	-1.600384	0.484832	-0.00001
5	6	0	-0.854613	-0.697713	0.000012
6	6	0	-2.991346	0.453126	-0.000029
7	6	0	-3.634414	-0.782398	-0.000026
8	6	0	-2.890079	-1.96637	-0.000002
9	6	0	-1.49603	-1.936202	0.000017
10	7	0	1.622815	-1.21737	0.000047
11	6	0	3.384379	-0.205701	-0.000001
12	6	0	3.047659	1.008318	-0.00003
13	6	0	1.859975	1.61286	0.000009
14	8	0	-1.274596	2.861997	0.000019
15	6	0	4.353406	-1.299568	-0.00003
16	1	0	-3.550054	1.383991	-0.000046
17	1	0	-4.718661	-0.827945	-0.000042
18	1	0	-3.401716	-2.923615	0.000003
19	1	0	-0.9138	-2.851675	0.000037
20	1	0	4.212003	-1.924394	-0.885935
21	1	0	5.36602	-0.889653	0.000013
22	1	0	4.211961	-1.924483	0.885804

Energy and Geometry for 4016* (conformer 1)
Sum of electronic and thermal free energies = -629.119688 a.u.

Center Number	Atomic Number	Atomic Type	Coordinates (Ångstroms)		
			X	Y	Z
1	6	0	0.621572	-0.201105	-0.000383
2	6	0	0.646415	1.224898	0.00011
3	6	0	-0.756892	1.739939	0.000357
4	6	0	-1.616977	0.511821	0.000219
5	6	0	-0.801555	-0.631122	-0.0003
6	6	0	-2.997749	0.415407	0.000512
7	6	0	-3.564419	-0.866017	0.00036
8	6	0	-2.753957	-2.002003	-0.000096
9	6	0	-1.355189	-1.899719	-0.000444
10	7	0	1.680232	-0.993777	-0.001648
11	6	0	2.933436	-0.476586	-0.002195
12	6	0	2.946597	0.917515	-0.001122
13	6	0	1.943857	1.666451	-0.000559
14	8	0	-1.118795	2.895877	0.00066
15	6	0	4.112255	-1.388936	0.001744
16	1	0	-3.617221	1.307388	0.000852
17	1	0	-4.643841	-0.977677	0.000606
18	1	0	-3.21453	-2.985136	-0.000167
19	1	0	-0.726923	-2.78482	-0.000788
20	1	0	3.78513	-2.427542	-0.055363
21	1	0	4.766967	-1.163134	-0.844782
22	1	0	4.694781	-1.242915	0.916687

Energy and Geometry for 4018 (conformer 1)
Sum of electronic and thermal free energies = -670.717019 a.u.

Center Number	Atomic Number	Atomic Type	Coordinates (Ångstroms)		
			X	Y	Z
1	6	0	-1.174266	-1.79982	-0.810091
2	6	0	-0.577933	-0.440014	-0.493653
3	6	0	-1.380176	0.649252	-0.334146
4	6	0	-2.882244	0.542194	-0.443908
5	6	0	-3.523945	-0.300725	0.672886
6	6	0	-3.425514	-1.810052	0.444483
7	6	0	-2.005778	-2.372294	0.353515
8	6	0	-0.878029	1.982699	0.034864
9	6	0	0.57183	2.313007	-0.051326
10	8	0	-1.594959	2.899598	0.388974
11	7	0	1.647419	2.731638	-0.108444
12	6	0	0.833811	-0.443599	-0.311534
13	6	0	2.033964	-0.585577	-0.167734
14	6	0	3.392673	-0.679354	0.004393
15	6	0	4.594958	-0.749591	0.159275
16	6	0	6.037022	-0.828255	0.345962
17	1	0	-0.359777	-2.484169	-1.054328
18	1	0	-1.807086	-1.710723	-1.702835
19	1	0	-3.141183	0.107243	-1.418199
20	1	0	-3.299296	1.55005	-0.423745
21	1	0	-4.58348	-0.030263	0.737611
22	1	0	-3.070119	-0.030699	1.63492
23	1	0	-3.955763	-2.055799	-0.486417
24	1	0	-3.957388	-2.327633	1.250977
25	1	0	-1.468194	-2.207959	1.296014
26	1	0	-2.070771	-3.456582	0.21341
27	1	0	6.552707	-0.32501	-0.476728
28	1	0	6.325607	-0.343051	1.282468
29	1	0	6.364251	-1.870887	0.376242

Energy and Geometry for 4018 (conformer 2)
Sum of electronic and thermal free energies = -670.716476 a.u.

Center Number	Atomic Number	Atomic Type	Coordinates (Ångstroms)		
			X	Y	Z
1	6	0	-1.172208	-1.798468	-0.813756
2	6	0	-0.577704	-0.438239	-0.495779
3	6	0	-1.381514	0.649457	-0.333593
4	6	0	-2.883601	0.539862	-0.440535
5	6	0	-3.521395	-0.306028	0.676273
6	6	0	-3.420799	-1.814837	0.445298
7	6	0	-2.000317	-2.374535	0.350508
8	6	0	-0.880828	1.983263	0.036084
9	6	0	0.568264	2.316071	-0.053605
10	8	0	-1.598445	2.898498	0.393063
11	7	0	1.643092	2.736279	-0.113369
12	6	0	0.834128	-0.440169	-0.314239
13	6	0	2.034294	-0.581583	-0.17003
14	6	0	3.392853	-0.675767	0.003082
15	6	0	4.59487	-0.74735	0.159398
16	6	0	6.036137	-0.830281	0.349882
17	1	0	-0.356996	-2.480895	-1.060939
18	1	0	-1.806992	-1.708705	-1.705031
19	1	0	-3.143846	0.105957	-1.414938
20	1	0	-3.302452	1.546922	-0.417895
21	1	0	-4.581278	-0.037581	0.743652
22	1	0	-3.06603	-0.036721	1.637779
23	1	0	-3.95254	-2.06004	-0.484895
24	1	0	-3.950149	-2.334568	1.252067
25	1	0	-1.46108	-2.210939	1.292198
26	1	0	-2.063751	-3.45868	0.208621
27	1	0	6.265168	-1.162627	1.366346
28	1	0	6.475249	-1.541056	-0.355396
29	1	0	6.497535	0.148633	0.193587

Energy and Geometry for 4018 (conformer 3)
Sum of electronic and thermal free energies = -670.715439 a.u.

Center Number	Atomic Number	Atomic Type	Coordinates (Ångstroms)		
			X	Y	Z
1	6	0	-0.617467	-2.03694	-0.705852
2	6	0	-0.254526	-0.579636	-0.489576
3	6	0	-1.219739	0.380933	-0.414886
4	6	0	-2.683023	0.037923	-0.560908
5	6	0	-3.239308	-0.817188	0.591595
6	6	0	-2.894847	-2.303277	0.479745
7	6	0	-1.401996	-2.638858	0.475281
8	6	0	-0.831233	1.7687	-0.120957
9	6	0	-1.948953	2.729077	0.143917
10	8	0	0.293123	2.220451	-0.051462
11	7	0	-2.756334	3.522822	0.37604
12	6	0	1.133549	-0.329498	-0.316508
13	6	0	2.342257	-0.274134	-0.176516
14	6	0	3.700676	-0.17226	-0.005474
15	6	0	4.901076	-0.07798	0.152914
16	6	0	6.340375	0.037339	0.345501
17	1	0	0.302923	-2.602419	-0.862671
18	1	0	-1.212653	-2.122638	-1.624843
19	1	0	-2.834602	-0.493366	-1.509878
20	1	0	-3.266575	0.958588	-0.638664
21	1	0	-4.329876	-0.715657	0.596441
22	1	0	-2.879685	-0.413808	1.54676
23	1	0	-3.341502	-2.695082	-0.444857
24	1	0	-3.37274	-2.8407	1.306728
25	1	0	-0.9357	-2.320204	1.416124
26	1	0	-1.293647	-3.727398	0.424475
27	1	0	6.57605	0.917124	0.950425
28	1	0	6.732241	-0.85002	0.85004
29	1	0	6.844079	0.137027	-0.620323

Energy and Geometry for 4018 (conformer 4

Sum of electronic and thermal free energies = -670.715447 a.u.

Center Number	Atomic Number	Atomic Type	Coordinates (Ångstroms)		
			X	Y	Z
1	6	0	-1.159634	-1.879539	-0.246294
2	6	0	-0.588678	-0.479123	-0.065673
3	6	0	-1.332858	0.657194	0.055373
4	6	0	-2.835799	0.702776	0.245861
5	6	0	-3.443827	-0.516056	0.945913
6	6	0	-3.696982	-1.695552	0.006139
7	6	0	-2.522302	-1.94653	-0.939948
8	6	0	-0.715761	2.00116	0.054129
9	6	0	0.668825	2.215764	-0.454494
10	8	0	-1.30582	3.017353	0.365992
11	7	0	1.689583	2.554307	-0.877736
12	6	0	0.837559	-0.48231	-0.001257
13	6	0	2.041787	-0.637752	0.077669
14	6	0	3.408089	-0.748843	0.15875
15	6	0	4.617299	-0.836001	0.22552
16	6	0	6.067964	-0.938619	0.30346
17	1	0	-1.19209	-2.373582	0.734987
18	1	0	-0.420751	-2.434249	-0.832046
19	1	0	-3.326969	0.877778	-0.722099
20	1	0	-3.039843	1.595703	0.841497
21	1	0	-4.386506	-0.216674	1.414891
22	1	0	-2.777656	-0.819589	1.762806
23	1	0	-4.600302	-1.508368	-0.586659
24	1	0	-3.890177	-2.595551	0.602131
25	1	0	-2.627965	-2.93288	-1.40274
26	1	0	-2.534388	-1.219393	-1.760652
27	1	0	6.535325	-0.076088	-0.179621
28	1	0	6.39161	-0.967641	1.347531
29	1	0	6.415101	-1.847854	-0.194699

Energy and Geometry for 4018 (conformer 5)
Sum of electronic and thermal free energies = -670.713279 a.u.

Center Number	Atomic Number	Atomic Type	Coordinates (Ångstroms)		
			X	Y	Z
`	6	0	1.162503	-1.879478	0.247845
2	6	0	0.589477	-0.480068	0.066398
3	6	0	1.331798	0.657322	-0.05559
4	6	0	2.834587	0.705375	-0.246624
5	6	0	3.444234	-0.512787	-0.946442
6	6	0	3.699485	-1.691543	-0.006279
7	6	0	2.525732	-1.943863	0.940624
8	6	0	0.7119	2.0001	-0.056177
9	6	0	-0.670146	2.212975	0.460144
10	8	0	1.297893	3.016449	-0.374938
11	7	0	-1.688971	2.549519	0.889597
12	6	0	-0.836764	-0.484855	0.001508
13	6	0	-2.040951	-0.640247	-0.078107
14	6	0	-3.407259	-0.750632	-0.160254
15	6	0	-4.616534	-0.83621	-0.227874
16	6	0	-6.067203	-0.937144	-0.306158
17	1	0	1.194986	-2.37441	-0.732982
18	1	0	0.424812	-2.434704	0.834634
19	1	0	3.32575	0.881385	0.721156
20	1	0	3.036941	1.598429	-0.842651
21	1	0	4.386311	-0.212181	-1.415849
22	1	0	2.77822	-0.817594	-1.762992
23	1	0	4.602859	-1.502836	0.58596
24	1	0	3.893656	-2.591512	-0.601998
25	1	0	2.633295	-2.929774	1.403912
26	1	0	2.537141	-1.216255	1.760924
27	1	0	-6.357631	-1.825822	-0.873379
28	1	0	-6.496443	-1.010983	0.696943
29	1	0	-6.485397	-0.055641	-0.799444

Energy and Geometry for 4018 (conformer 6)
Sum of electronic and thermal free energies = -670.711548 a.u.

Center Number	Atomic Number	Atomic Type	Coordinates (Ångstroms)		
			X	Y	Z
1	6	0	-1.161891	-1.819489	-0.990697
2	6	0	-0.595065	-0.465682	-0.607656
3	6	0	-1.455135	0.577442	-0.422528
4	6	0	-2.940006	0.354939	-0.571983
5	6	0	-3.544036	-0.50462	0.567725
6	6	0	-2.588334	-1.538531	1.172223
7	6	0	-1.92685	-2.497563	0.176683
8	6	0	-1.046772	1.913681	0.02611
9	6	0	0.381347	2.333116	-0.031692
10	8	0	-1.826549	2.758227	0.425174
11	7	0	1.438014	2.799796	-0.062222
12	6	0	0.809151	-0.422782	-0.389292
13	6	0	2.010709	-0.518085	-0.22005
14	6	0	3.367659	-0.569235	-0.018985
15	6	0	4.567972	-0.604749	0.160931
16	6	0	6.007236	-0.646628	0.378142
17	1	0	-0.353916	-2.470072	-1.329827
18	1	0	-1.835904	-1.67263	-1.839922
19	1	0	-3.116932	-0.135069	-1.534287
20	1	0	-3.449282	1.319464	-0.610884
21	1	0	-4.438419	-1.004738	0.179069
22	1	0	-3.877501	0.159475	1.372425
23	1	0	-3.136228	-2.131798	1.912249
24	1	0	-1.804147	-1.01309	1.730158
25	1	0	-1.226966	-3.13143	0.730942
26	1	0	-2.67984	-3.163458	-0.259419
27	1	0	6.226741	-0.966541	1.400676
28	1	0	6.478452	-1.349036	-0.314668
29	1	0	6.444324	0.343666	0.224071

Energy and Geometry for 4018 (conformer 7)
Sum of electronic and thermal free energies = -670.711374 a.u.

Center Number	Atomic Number	Atomic Type	Coordinates (Ångstroms)		
			X	Y	Z
1	6	0	-0.593599	-2.050272	-0.886417
2	6	0	-0.255548	-0.603734	-0.583327
3	6	0	-1.268084	0.308904	-0.493499
4	6	0	-2.694829	-0.145006	-0.682494
5	6	0	-3.223534	-0.999406	0.496214
6	6	0	-2.157713	-1.849531	1.194985
7	6	0	-1.328148	-2.760005	0.282937
8	6	0	-0.972287	1.700635	-0.137458
9	6	0	-2.159216	2.568323	0.144613
10	8	0	0.12068	2.219169	-0.035177
11	7	0	-3.035288	3.282075	0.387066
12	6	0	1.115582	-0.310614	-0.363979
13	6	0	2.317704	-0.20743	-0.196288
14	6	0	3.668562	-0.057536	-0.003186
15	6	0	4.863111	0.079327	0.167644
16	6	0	6.295972	0.246387	0.369279
17	1	0	0.320013	-2.594839	-1.130849
18	1	0	-1.222848	-2.062223	-1.782209
19	1	0	-2.747092	-0.72612	-1.608606
20	1	0	-3.354446	0.713315	-0.834235
21	1	0	-4.0277	-1.640844	0.118101
22	1	0	-3.674192	-0.336042	1.242858
23	1	0	-2.646839	-2.471928	1.951874
24	1	0	-1.478078	-1.187533	1.744412
25	1	0	-0.583002	-3.268089	0.903488
26	1	0	-1.966669	-3.539828	-0.146852
27	1	0	6.829612	0.104321	-0.574929
28	1	0	6.516351	1.248987	0.745283
29	1	0	6.668626	-0.487301	1.089476

Energy and Geometry for 4018‡_a

$<S^2>$ = 0.565895

Imaginary Frequencies: -759.5640 cm^{-1}

Sum of electronic and thermal free energies = -670.671867 a.u.

Center Number	Atomic Number	Atomic Type	Coordinates (Ångstroms)		
			X	Y	Z
1	6	0	-0.86632	-1.766182	-0.579251
2	6	0	-0.573526	-0.313481	-0.33667
3	6	0	-1.503994	0.666332	-0.278103
4	6	0	-2.986799	0.527108	-0.442528
5	6	0	-3.634184	-0.476671	0.522109
6	6	0	-3.322	-1.945007	0.223721
7	6	0	-1.865037	-2.371745	0.420288
8	6	0	-0.895664	1.974587	-0.028853
9	6	0	0.648927	1.817935	0.10685
10	8	0	-1.438198	3.04555	0.06789
11	7	0	1.517205	2.62056	0.327433
12	6	0	0.80394	0.137212	-0.1419
13	6	0	1.946227	-0.440342	-0.132109
14	6	0	3.281336	-0.581324	-0.04019
15	6	0	4.494854	-0.735132	0.038268
16	6	0	5.933272	-0.908915	0.131808
17	1	0	0.073211	-2.323106	-0.55027
18	1	0	-1.270721	-1.865782	-1.596743
19	1	0	-3.205217	0.224954	-1.476673
20	1	0	-3.432612	1.516165	-0.30177
21	1	0	-4.719289	-0.336293	0.467279
22	1	0	-3.335741	-0.234073	1.550084
23	1	0	-3.622619	-2.17164	-0.80917
24	1	0	-3.949355	-2.56792	0.871645
25	1	0	-1.541529	-2.137832	1.442438
26	1	0	-1.807914	-3.460346	0.314013
27	1	0	6.387985	-0.04255	0.621993
28	1	0	6.172425	-1.802139	0.716661
29	1	0	6.370337	-1.014009	-0.86527

Energy and Geometry for 4018‡$_{concerted}$

Imaginary Frequencies: -451.6078 cm^{-1}
Sum of electronic and thermal free energies = -670.663167 a.u.

Center Number	Atomic Number	Atomic Type	Coordinates (Ångstroms)		
			X	Y	Z
1	6	0	1.71739	-1.75618	0.033518
2	6	0	0.764654	-0.587941	0.00841
3	6	0	1.087616	0.727106	-0.079145
4	6	0	2.454985	1.348839	-0.06194
5	6	0	3.461072	0.561307	0.786577
6	6	0	4.051041	-0.663169	0.077645
7	6	0	3.030171	-1.489577	-0.711319
8	6	0	-0.090106	1.606723	-0.13424
9	6	0	-1.413979	0.834021	-0.073398
10	6	0	-0.652202	-0.855	0.056935
11	6	0	-1.641911	-1.636429	0.133553
12	6	0	-2.974046	-1.56811	0.146402
13	6	0	-3.885045	-0.718955	0.085034
14	7	0	-2.584703	1.081172	-0.086354
15	8	0	-0.082472	2.812111	-0.213416
16	6	0	-5.205851	-0.1058	0.049291
17	1	0	1.197581	-2.609565	-0.412203
18	1	0	1.908321	-2.028335	1.081476
19	1	0	2.339992	2.362808	0.333974
20	1	0	2.827625	1.468548	-1.088927
21	1	0	4.277753	1.227577	1.08275
22	1	0	2.962414	0.254098	1.714198
23	1	0	4.535347	-1.301626	0.82637
24	1	0	4.838482	-0.338463	-0.613241
25	1	0	2.794017	-0.989211	-1.658258
26	1	0	3.480722	-2.451109	-0.977594
27	1	0	-5.330017	0.466415	-0.873894
28	1	0	-5.973937	-0.882851	0.097629
29	1	0	-5.328333	0.575613	0.895579

Energy and Geometry for 4018* (conformer 1)
Sum of electronic and thermal free energies = -670.732606 a.u.

Center Number	Atomic Number	Atomic Type	Coordinates (Ångstroms)		
			X	Y	Z
1	6	0	1.730973	-1.72892	0.043398
2	6	0	0.774493	-0.577233	0.001194
3	6	0	1.051634	0.741849	-0.110666
4	6	0	2.383897	1.429196	-0.103054
5	6	0	3.41117	0.690168	0.76581
6	6	0	4.030458	-0.54691	0.100693
7	6	0	3.051141	-1.433609	-0.678636
8	6	0	-0.233529	1.513029	-0.144301
9	6	0	-1.354463	0.489147	-0.045191
10	6	0	-0.697747	-0.764791	0.046988
11	6	0	-1.645555	-1.750288	0.144522
12	6	0	-2.884793	-1.551096	0.145867
13	6	0	-3.527806	-0.320056	0.050847
14	7	0	-2.649078	0.712055	-0.047652
15	8	0	-0.361125	2.712876	-0.220613
16	6	0	-4.995934	-0.051961	0.053408
17	1	0	1.234754	-2.590934	-0.417556
18	1	0	1.912262	-2.010828	1.091259
19	1	0	2.226814	2.444269	0.277806
20	1	0	2.763007	1.546729	-1.127883
21	1	0	4.216429	1.380007	1.039824
22	1	0	2.919281	0.402088	1.703051
23	1	0	4.521961	-1.146385	0.876786
24	1	0	4.819731	-0.22705	-0.590635
25	1	0	2.814068	-0.966785	-1.642441
26	1	0	3.547121	-2.381834	-0.910574
27	1	0	-5.182601	1.002093	-0.156098
28	1	0	-5.497769	-0.667129	-0.698409
29	1	0	-5.426147	-0.302789	1.028061

Energy and Geometry for 4018* (conformer 2)
Sum of electronic and thermal free energies = -670.738298 a.u.

Center Number	Atomic Number	Atomic Type	Coordinates (Ångstroms)		
			X	Y	Z
1	6	0	1.767508	-1.659646	-0.587918
2	6	0	0.806982	-0.531633	-0.357589
3	6	0	1.085867	0.787306	-0.249441
4	6	0	2.400243	1.503092	-0.285683
5	6	0	3.631233	0.58761	-0.218441
6	6	0	3.521717	-0.452262	0.906397
7	6	0	2.865149	-1.781341	0.487053
8	6	0	-0.190108	1.543962	-0.032233
9	6	0	-1.309638	0.514037	-0.028114
10	6	0	-0.659334	-0.73013	-0.230714
11	6	0	-1.605018	-1.722541	-0.242899
12	6	0	-2.837266	-1.534834	-0.094711
13	6	0	-3.473865	-0.313493	0.107818
14	7	0	-2.596647	0.724703	0.129702
15	8	0	-0.309423	2.738247	0.11357
16	6	0	-4.933992	-0.060113	0.285585
17	1	0	2.234227	-1.511527	-1.568121
18	1	0	1.211383	-2.600007	-0.649168
19	1	0	2.420763	2.191992	0.569808
20	1	0	2.440254	2.142596	-1.177288
21	1	0	3.790722	0.090029	-1.182334
22	1	0	4.506813	1.223403	-0.054614
23	1	0	2.955089	-0.006853	1.733893
24	1	0	4.515249	-0.676552	1.308039
25	1	0	3.628376	-2.45875	0.088245
26	1	0	2.448291	-2.269127	1.374825
27	1	0	-5.107215	0.999631	0.476877
28	1	0	-5.484242	-0.356427	-0.612773
29	1	0	-5.324657	-0.647383	1.121477

Energy and Geometry for 4017 (conformer 1)
Sum of electronic and thermal free energies = -629.100177 a.u.

Center Number	Atomic Number	Atomic Type	Coordinates (Ångstroms)		
			X	Y	Z
1	6	0	-1.446931	-2.093433	0.101108
2	6	0	-0.892148	-0.80482	0.025272
3	6	0	-1.763802	0.305632	-0.050487
4	6	0	-3.150074	0.103406	-0.055106
5	6	0	-3.681385	-1.175816	0.028001
6	6	0	-2.824061	-2.275369	0.107385
7	6	0	-1.323093	1.717075	-0.130898
8	6	0	0.055393	2.102171	0.276727
9	8	0	-2.047657	2.626842	-0.472401
10	7	0	1.071506	2.543355	0.604534
11	6	0	0.532593	-0.695352	-0.01081
12	6	0	1.746887	-0.680191	-0.044845
13	6	0	3.119807	-0.618718	-0.075769
14	6	0	4.331716	-0.555391	-0.09883
15	6	0	5.78612	-0.476087	-0.123038
16	1	0	-0.777524	-2.945503	0.150561
17	1	0	-3.800557	0.969843	-0.113543
18	1	0	-4.756822	-1.317132	0.033486
19	1	0	-3.229998	-3.279827	0.172228
20	1	0	6.219352	-1.195056	0.577659
21	1	0	6.16408	-0.696386	-1.125145
22	1	0	6.116051	0.527204	0.159953

Energy and Geometry for 4017‡_a

$<S^2>$ = 0.603224

Imaginary Frequencies: -739.3973 cm^{-1}

Sum of electronic and thermal free energies = -629.049241 a.u.

Center Number	Atomic Number	Atomic Type	Coordinates (Ångstroms)		
			X	Y	Z
1	6	0	-1.176072	-1.996963	0.005578
2	6	0	-0.877515	-0.632263	0.004014
3	6	0	-1.91022	0.305919	-0.001947
4	6	0	-3.251981	-0.07392	-0.006558
5	6	0	-3.548217	-1.431566	-0.005195
6	6	0	-2.51365	-2.380382	0.001008
7	6	0	-1.401246	1.681979	-0.00197
8	6	0	0.159423	1.636681	0.005095
9	8	0	-2.017435	2.713504	-0.006059
10	7	0	0.96424	2.534437	0.008626
11	6	0	0.462063	-0.040777	0.006406
12	6	0	1.654113	-0.50853	0.006164
13	6	0	2.998909	-0.51661	0.003882
14	6	0	4.224551	-0.547383	0.000132
15	6	0	5.676046	-0.572875	-0.009788
16	1	0	-0.379258	-2.733904	0.010059
17	1	0	-4.032252	0.681136	-0.011133
18	1	0	-4.581474	-1.762488	-0.008819
19	1	0	-2.761958	-3.43738	0.002027
20	1	0	6.036647	-1.462126	-0.535944
21	1	0	6.065426	0.312941	-0.520869
22	1	0	6.065444	-0.58712	1.011853

Energy and Geometry for 4017$^{‡}_{concerted}$
Imaginary Frequencies: -478.9396 cm^{-1}
Sum of electronic and thermal free energies = -629.043760 a.u.

Center Number	Atomic Number	Atomic Type	Coordinates (Ångstroms)		
			X	Y	Z
1	6	0	-0.250391	-0.992317	-0.000014
2	6	0	-0.960627	0.797858	-0.000006
3	6	0	0.381839	1.530698	-0.000006
4	6	0	1.52467	0.602157	-0.000002
5	6	0	1.169666	-0.754153	-0.000008
6	6	0	2.858891	1.002476	0.000009
7	6	0	3.848066	0.024386	0.000014
8	6	0	3.497682	-1.332201	0.000009
9	6	0	2.164727	-1.73518	-0.000002
10	6	0	-1.306897	-1.674002	-0.000015
11	6	0	-2.632706	-1.541532	-0.000005
12	6	0	-3.457787	-0.599704	0.000006
13	7	0	-2.124691	1.072133	-0.000005
14	8	0	0.432453	2.735654	-0.00001
15	6	0	-4.7544	0.069843	0.00002
16	1	0	3.105827	2.059785	0.000013
17	1	0	4.894647	0.310195	0.000023
18	1	0	4.279223	-2.085872	0.000013
19	1	0	1.895966	-2.78607	-0.000006
20	1	0	-4.854765	0.701321	0.886655
21	1	0	-4.854776	0.70134	-0.8866
22	1	0	-5.549315	-0.680832	0.000017

Energy and Geometry for 4017* (conformer 1)

Sum of electronic and thermal free energies = -629.118488 a.u.

Center Number	Atomic Number	Atomic Type	Coordinates (Ångstroms)		
			X	Y	Z
1	6	0	0.299836	-0.834625	0
2	6	0	0.897021	0.456807	0
3	6	0	-0.233027	1.468908	0
4	6	0	-1.491701	0.659013	0
5	6	0	-1.168821	-0.709568	0
6	6	0	-2.805496	1.092937	0
7	6	0	-3.817525	0.123812	0
8	6	0	-3.498322	-1.234284	0
9	6	0	-2.16565	-1.670867	0
10	6	0	1.295737	-1.782489	0
11	6	0	2.519844	-1.522797	0
12	6	0	3.108627	-0.255312	0
13	7	0	2.187781	0.733049	0
14	8	0	-0.127969	2.672718	0
15	6	0	4.564071	0.069645	0
16	1	0	-3.039237	2.153596	0
17	1	0	-4.858407	0.430569	0
18	1	0	-4.29708	-1.96972	0
19	1	0	-1.924786	-2.729335	0
20	1	0	5.048294	-0.358167	-0.882849
21	1	0	4.704647	1.15106	-0.000008
22	1	0	5.048289	-0.358151	0.88286

Energy and Geometry for 4019 (conformer 1)
Sum of electronic and thermal free energies = -675.251937 a.u.

Center Number	Atomic Number	Atomic Type	Coordinates (Ångstroms)		
			X	Y	Z
1	6	0	0.430111	-2.173067	0.716821
2	6	0	0.140178	-0.69353	0.466112
3	6	0	1.139954	0.215029	0.41766
4	6	0	2.569068	-0.24542	0.635919
5	6	0	3.116323	-1.119933	-0.508953
6	6	0	2.706331	-2.589884	-0.410215
7	6	0	1.199242	-2.851512	-0.428181
8	6	0	0.985003	1.725672	0.192609
9	6	0	2.040996	2.13108	-0.76812
10	6	0	-0.341439	2.22932	-0.401555
11	6	0	1.245326	2.457204	1.530198
12	7	0	2.849026	2.464365	-1.526626
13	6	0	-1.252887	-0.424018	0.276077
14	6	0	-2.461138	-0.36753	0.138481
15	6	0	-3.822469	-0.251795	-0.030918
16	6	0	-5.022234	-0.146088	-0.186294
17	6	0	-6.463081	-0.023317	-0.375922
18	1	0	-0.523182	-2.685449	0.863845
19	1	0	0.992648	-2.281496	1.653809
20	1	0	2.638459	-0.804822	1.578601
21	1	0	3.217519	0.62681	0.752979
22	1	0	4.210426	-1.063498	-0.491351
23	1	0	2.795938	-0.698955	-1.470482
24	1	0	3.118868	-3.002945	0.52134
25	1	0	3.175014	-3.146292	-1.230281
26	1	0	0.769206	-2.531638	-1.386101
27	1	0	1.037251	-3.933052	-0.356216
28	1	0	-0.237756	3.29228	-0.637526
29	1	0	-0.607411	1.693225	-1.314975
30	1	0	-1.146139	2.120469	0.325993
31	1	0	1.228352	3.539844	1.376715
32	1	0	0.44952	2.185653	2.229093

33	1	0	2.207865	2.181229	1.96668
34	1	0	-6.756384	1.029114	-0.420421
35	1	0	-6.768782	-0.507052	-1.307928
36	1	0	-7.000321	-0.497255	0.450281

Energy and Geometry for 4019 (conformer 2)
Sum of electronic and thermal free energies = -675.251282 a.u.

Center Number	Atomic Number	Atomic Type	Coordinates (Ångstroms)		
			X	Y	Z
1	6	0	-1.03352	-2.121372	-0.660845
2	6	0	-0.474297	-0.717593	-0.467286
3	6	0	-1.271937	0.374461	-0.423762
4	6	0	-2.759706	0.20488	-0.636081
5	6	0	-3.466834	-0.510611	0.533659
6	6	0	-3.348003	-2.03497	0.472123
7	6	0	-1.921782	-2.589481	0.50341
8	6	0	-0.709992	1.78986	-0.178571
9	6	0	0.200012	1.77564	0.989414
10	6	0	0.063662	2.280009	-1.421291
11	6	0	-1.789593	2.835211	0.175744
12	7	0	0.870756	1.84335	1.930193
13	6	0	0.945247	-0.649101	-0.312112
14	6	0	2.158233	-0.676881	-0.21217
15	6	0	3.529722	-0.669477	-0.097145
16	6	0	4.739599	-0.65841	0.004171
17	6	0	6.192508	-0.644756	0.127339
18	1	0	-0.193514	-2.810421	-0.774514
19	1	0	-1.605089	-2.162414	-1.598249
20	1	0	-2.92473	-0.380089	-1.550884
21	1	0	-3.231853	1.171542	-0.806659
22	1	0	-4.530296	-0.24652	0.510925
23	1	0	-3.06678	-0.137778	1.485226
24	1	0	-3.833649	-2.380399	-0.451745
25	1	0	-3.915905	-2.470511	1.302577
26	1	0	-1.434599	-2.327622	1.451315

27	1	0	-1.980424	-3.683447	0.470855
28	1	0	0.448945	3.290234	-1.254636
29	1	0	0.89701	1.617107	-1.661236
30	1	0	-0.626462	2.30266	-2.26991
31	1	0	-1.303068	3.764352	0.483155
32	1	0	-2.405362	3.053869	-0.699622
33	1	0	-2.431813	2.493832	0.992218
34	1	0	6.660414	-0.539294	-0.855566
35	1	0	6.514508	0.191135	0.754553
36	1	0	6.547454	-1.574123	0.581267

Energy and Geometry for 4019 (conformer 3)
Sum of electronic and thermal free energies = -675.250892 a.u.

Center Number	Atomic Number	Atomic Type	Coordinates (Ångstroms)		
			X	Y	Z
1	6	0	-0.447658	-2.072153	-0.912413
2	6	0	-0.172651	-0.638032	-0.461178
3	6	0	-1.184906	0.226907	-0.225987
4	6	0	-2.617087	-0.252369	-0.38041
5	6	0	-3.040578	-1.317242	0.650901
6	6	0	-2.610605	-2.740485	0.293586
7	6	0	-1.101266	-2.948018	0.167278
8	6	0	-1.051747	1.674689	0.270078
9	6	0	-1.861047	2.518278	-0.644196
10	6	0	-1.664495	1.787372	1.686131
11	6	0	0.353121	2.299387	0.289924
12	7	0	-2.475214	3.199955	-1.349499
13	6	0	1.224335	-0.37514	-0.289106
14	6	0	2.436284	-0.326509	-0.186088
15	6	0	3.802857	-0.22022	-0.057578
16	6	0	5.008088	-0.123213	0.05533
17	6	0	6.456275	-0.012501	0.187832
18	1	0	0.50135	-2.518385	-1.217477
19	1	0	-1.088752	-2.053658	-1.803749
20	1	0	-2.760662	-0.656569	-1.391468

21	1	0	-3.295807	0.601227	-0.303882
22	1	0	-4.13335	-1.297079	0.732192
23	1	0	-2.644689	-1.044921	1.637741
24	1	0	-3.080041	-3.016088	-0.661264
25	1	0	-3.006811	-3.431988	1.046305
26	1	0	-0.608316	-2.760736	1.130377
27	1	0	-0.91598	-3.998813	-0.082346
28	1	0	-1.639589	2.828254	2.020413
29	1	0	-2.699094	1.438683	1.716438
30	1	0	-1.06536	1.182475	2.372611
31	1	0	0.261049	3.355259	0.560238
32	1	0	0.97264	1.807993	1.041319
33	1	0	0.845004	2.231043	-0.682177
34	1	0	6.924705	0.0827	-0.795872
35	1	0	6.721732	0.865884	0.782559
36	1	0	6.864954	-0.899475	0.679918

Energy and Geometry for 4019 (conformer 4)
Sum of electronic and thermal free energies = -675.250567 a.u.

Center Number	Atomic Number	Atomic Type	Coordinates (Ångstroms)		
			X	Y	Z
1	6	0	-1.072859	-2.001654	-0.9108
2	6	0	-0.506479	-0.646455	-0.507511
3	6	0	-1.294976	0.433375	-0.297337
4	6	0	-2.793442	0.286804	-0.45012
5	6	0	-3.439338	-0.618767	0.619451
6	6	0	-3.33489	-2.1133	0.308872
7	6	0	-1.912891	-2.665266	0.191909
8	6	0	-0.713823	1.776734	0.193078
9	6	0	0.437787	2.165154	-0.652293
10	6	0	-1.698963	2.959443	0.097239
11	6	0	-0.245123	1.653282	1.660288
12	7	0	1.30736	2.548398	-1.312842
13	6	0	0.909526	-0.624775	-0.311213
14	6	0	2.114196	-0.699005	-0.152268

15	6	0	3.476968	-0.74368	0.034886
16	6	0	4.67927	-0.777019	0.200777
17	6	0	6.123838	-0.812373	0.396288
18	1	0	-0.238335	-2.655326	-1.175309
19	1	0	-1.683773	-1.886703	-1.81632
20	1	0	-3.010171	-0.136631	-1.440555
21	1	0	-3.277382	1.26171	-0.430018
22	1	0	-4.50133	-0.358422	0.693806
23	1	0	-2.99202	-0.404332	1.598599
24	1	0	-3.859478	-2.304584	-0.638182
25	1	0	-3.873094	-2.675846	1.080762
26	1	0	-1.387379	-2.56798	1.150838
27	1	0	-1.978159	-3.737879	-0.023468
28	1	0	-1.183106	3.878417	0.386736
29	1	0	-2.087145	3.085367	-0.916527
30	1	0	-2.533195	2.807702	0.786839
31	1	0	0.172619	2.604085	2.003948
32	1	0	-1.110845	1.406626	2.281765
33	1	0	0.508085	0.872446	1.77803
34	1	0	6.633525	-0.3145	-0.433365
35	1	0	6.397713	-0.302894	1.324359
36	1	0	6.479139	-1.845027	0.450465

Energy and Geometry for 4019 (conformer 5)

Sum of electronic and thermal free energies = -675.249766 a.u.

Center Number	Atomic Number	Atomic Type	Coordinates (Ångstroms)		
			X	Y	Z

1	6	0	1.044435	-2.13602	0.250994
2	6	0	0.515013	-0.713969	0.060914
3	6	0	1.263347	0.409445	-0.056342
4	6	0	2.758682	0.403032	-0.312114
5	6	0	3.33396	-0.861634	-0.956901
6	6	0	3.582999	-2.005513	0.024605
7	6	0	2.396322	-2.229273	0.962579

8	6	0	0.624965	1.814297	-0.083003
9	6	0	-0.501933	1.921228	0.870568
10	6	0	1.595432	2.930141	0.377968
11	6	0	0.119034	2.133334	-1.504771
12	7	0	-1.34056	2.124179	1.641778
13	6	0	-0.916698	-0.670524	0.015875
14	6	0	-2.128563	-0.754554	-0.059762
15	6	0	-3.501663	-0.805535	-0.141321
16	6	0	-4.713242	-0.844653	-0.20983
17	6	0	-6.168683	-0.890268	-0.288467
18	1	0	1.077218	-2.65609	-0.716198
19	1	0	0.291398	-2.661427	0.846031
20	1	0	3.307376	0.64928	0.60881
21	1	0	2.95734	1.232806	-0.998179
22	1	0	4.275426	-0.599722	-1.451693
23	1	0	2.650858	-1.1886	-1.750254
24	1	0	4.481942	-1.796534	0.617417
25	1	0	3.784401	-2.922519	-0.542305
26	1	0	2.483794	-3.21309	1.435547
27	1	0	2.412998	-1.492695	1.775124
28	1	0	1.044274	3.870456	0.458684
29	1	0	2.031536	2.70153	1.353865
30	1	0	2.397094	3.076454	-0.347539
31	1	0	-0.294631	3.145166	-1.545036
32	1	0	0.963388	2.072635	-2.198514
33	1	0	-0.64769	1.42148	-1.818825
34	1	0	-6.518642	-1.925609	-0.321783
35	1	0	-6.613652	-0.403272	0.583792
36	1	0	-6.520947	-0.3767	-1.187351

Energy and Geometry for 4019 (conformer 6)
Sum of electronic and thermal free energies = -675.249476 a.u.

Center Number	Atomic Number	Atomic Type	Coordinates (Ångstroms)		
			X	Y	Z

1	6	0	0.562189	-2.263816	-0.213196

2	6	0	0.239859	-0.771915	-0.08364
3	6	0	1.146963	0.228619	0.01747
4	6	0	2.624439	-0.003922	0.286627
5	6	0	3.000112	-1.307238	0.996735
6	6	0	3.085594	-2.515689	0.065942
7	6	0	1.896197	-2.583592	-0.892052
8	6	0	0.734114	1.716925	-0.002197
9	6	0	1.919844	2.544779	-0.331234
10	6	0	-0.312008	2.110503	-1.069723
11	6	0	0.256681	2.141851	1.404528
12	7	0	2.800352	3.246084	-0.599272
13	6	0	-1.176108	-0.547612	-0.067694
14	6	0	-2.392265	-0.518755	-0.016172
15	6	0	-3.765572	-0.432782	0.03421
16	6	0	-4.976505	-0.351244	0.073562
17	6	0	-6.431167	-0.257379	0.118149
18	1	0	-0.249679	-2.696959	-0.80489
19	1	0	0.501557	-2.744775	0.77283
20	1	0	2.953697	0.824295	0.925316
21	1	0	3.199973	0.10856	-0.644428
22	1	0	2.269082	-1.494724	1.792526
23	1	0	3.965259	-1.163769	1.49412
24	1	0	3.128436	-3.430543	0.669422
25	1	0	4.016917	-2.473771	-0.511628
26	1	0	2.040946	-1.88229	-1.723059
27	1	0	1.839041	-3.582744	-1.336492
28	1	0	-0.349729	3.20019	-1.151724
29	1	0	-0.048747	1.69599	-2.04628
30	1	0	-1.303335	1.760847	-0.789398
31	1	0	0.03461	3.212661	1.424235
32	1	0	-0.652555	1.586467	1.648951
33	1	0	1.018014	1.92443	2.158896
34	1	0	-6.810086	0.243395	-0.777184
35	1	0	-6.877354	-1.254274	0.171184
36	1	0	-6.752709	0.31204	0.994612

Energy and Geometry for 4019 (conformer 7)
Sum of electronic and thermal free energies = -675.248171 a.u.

Center Number	Atomic Number	Atomic Type	Coordinates (Ångstroms)		
			X	Y	Z
1	6	0	0.993778	-2.150582	-0.896883
2	6	0	0.469965	-0.745537	-0.6335
3	6	0	1.327278	0.299843	-0.539659
4	6	0	2.799884	0.012327	-0.720198
5	6	0	3.418845	-0.690076	0.513648
6	6	0	2.483134	-1.690055	1.199355
7	6	0	1.838998	-2.727018	0.271847
8	6	0	0.85802	1.726719	-0.200259
9	6	0	0.01445	1.684044	1.016463
10	6	0	2.017799	2.684889	0.139313
11	6	0	0.042902	2.331101	-1.36321
12	7	0	-0.604128	1.704805	1.994605
13	6	0	-0.939613	-0.621561	-0.441516
14	6	0	-2.147975	-0.593409	-0.295224
15	6	0	-3.511827	-0.52704	-0.12292
16	6	0	-4.714479	-0.464881	0.031856
17	6	0	-6.158208	-0.390499	0.222604
18	1	0	1.591829	-2.128378	-1.813793
19	1	0	0.150275	-2.814833	-1.097102
20	1	0	3.363676	0.919363	-0.941041
21	1	0	2.920824	-0.638558	-1.591716
22	1	0	3.717896	0.065824	1.249475
23	1	0	4.336014	-1.196179	0.189896
24	1	0	1.689006	-1.139612	1.717535
25	1	0	3.042882	-2.21917	1.97884
26	1	0	2.615597	-3.375596	-0.151152
27	1	0	1.198145	-3.368216	0.885995
28	1	0	1.610733	3.634576	0.495502
29	1	0	2.668373	2.273448	0.915766
30	1	0	2.609882	2.886797	-0.7565
31	1	0	-0.279869	3.345015	-1.109528
32	1	0	0.683872	2.377623	-2.248455

33	1	0	-0.835945	1.727626	-1.596309
34	1	0	-6.680458	-0.888395	-0.59912
35	1	0	-6.445531	-0.876491	1.159235
36	1	0	-6.486008	0.651931	0.259938

Energy and Geometry for 4019 (conformer 8)
Sum of electronic and thermal free energies = -675.247866 a.u.

Center Number	Atomic Number	Atomic Type	Coordinates (Ångstroms)		
			X	Y	Z
1	6	0	0.415837	-2.04691	-1.100731
2	6	0	0.174303	-0.629137	-0.593798
3	6	0	1.237457	0.161688	-0.316224
4	6	0	2.625572	-0.409775	-0.548465
5	6	0	3.010819	-1.597771	0.381273
6	6	0	1.8417	-2.354284	1.019284
7	6	0	0.871922	-2.998125	0.024279
8	6	0	1.202268	1.568466	0.289812
9	6	0	2.055718	2.431563	-0.563929
10	6	0	-0.163409	2.267754	0.377747
11	6	0	1.835385	1.516811	1.700058
12	7	0	2.707452	3.126958	-1.220412
13	6	0	-1.206295	-0.322536	-0.381476
14	6	0	-2.412944	-0.226535	-0.251479
15	6	0	-3.770798	-0.06823	-0.089108
16	6	0	-4.967793	0.077107	0.054989
17	6	0	-6.406206	0.248549	0.224457
18	1	0	1.177084	-2.016239	-1.886147
19	1	0	-0.497095	-2.431114	-1.56166
20	1	0	3.376945	0.376354	-0.435747
21	1	0	2.69208	-0.727138	-1.594364
22	1	0	3.643874	-1.216662	1.19022
23	1	0	3.630203	-2.296546	-0.193473
24	1	0	1.285836	-1.665127	1.665976
25	1	0	2.244527	-3.131026	1.678782
26	1	0	1.338354	-3.875655	-0.439341

27	1	0	-0.005805	-3.358688	0.57267
28	1	0	-0.011477	3.292609	0.72828
29	1	0	-0.666074	2.302407	-0.590873
30	1	0	-0.802784	1.752699	1.096109
31	1	0	1.89556	2.523651	2.122534
32	1	0	1.199133	0.902609	2.343651
33	1	0	2.840097	1.087298	1.680291
34	1	0	-6.838261	-0.617461	0.733626
35	1	0	-6.619376	1.140794	0.819547
36	1	0	-6.896196	0.356706	-0.747339

Energy and Geometry for 4019 (conformer 9)
Sum of electronic and thermal free energies = -675.247684 a.u.

Center Number	Atomic Number	Atomic Type	Coordinates (Ångstroms)		
			X	Y	Z
1	6	0	-1.086994	-2.139756	-0.102889
2	6	0	-0.537608	-0.712004	-0.052846
3	6	0	-1.26774	0.428836	0.010761
4	6	0	-2.780161	0.462494	-0.105071
5	6	0	-3.429424	-0.674155	-0.903951
6	6	0	-3.630635	-1.964383	-0.11173
7	6	0	-2.383951	-2.353308	0.683329
8	6	0	-0.572743	1.789184	0.286065
9	6	0	0.504095	2.029399	-0.700269
10	6	0	-1.498959	3.018639	0.163447
11	6	0	0.020377	1.792855	1.71304
12	7	0	1.31056	2.305872	-1.483192
13	6	0	0.895373	-0.687795	-0.023632
14	6	0	2.109159	-0.777256	-0.012051
15	6	0	3.484534	-0.831094	-0.00357
16	6	0	4.697982	-0.871713	-0.000465
17	6	0	6.155475	-0.916852	-0.005333
18	1	0	-0.307588	-2.784388	0.312271
19	1	0	-1.211591	-2.455572	-1.147209
20	1	0	-3.050617	1.396506	-0.600169

21	1	0	-3.22737	0.52602	0.899766
22	1	0	-2.816528	-0.868327	-1.792348
23	1	0	-4.39966	-0.323791	-1.272186
24	1	0	-3.891318	-2.77128	-0.807259
25	1	0	-4.479735	-1.850946	0.573176
26	1	0	-2.329522	-1.770046	1.610969
27	1	0	-2.452682	-3.404421	0.982832
28	1	0	-0.922066	3.916182	0.400575
29	1	0	-1.905772	3.132843	-0.843674
30	1	0	-2.321067	2.942962	0.879722
31	1	0	0.516519	2.746512	1.913864
32	1	0	-0.800431	1.668717	2.425923
33	1	0	0.737708	0.984488	1.858225
34	1	0	6.508058	-1.874367	-0.398589
35	1	0	6.559734	-0.116088	-0.630791
36	1	0	6.547334	-0.794654	1.008241

Energy and Geometry for 4019 (conformer 10)
Sum of electronic and thermal free energies = -675.247655 a.u.

Center Number	Atomic Number	Atomic Type	Coordinates (Ångstroms)		
			X	Y	Z
1	6	0	-0.399318	2.169063	0.902587
2	6	0	-0.132761	0.701369	0.583682
3	6	0	-1.176794	-0.157528	0.508003
4	6	0	-2.563159	0.388713	0.794862
5	6	0	-3.102831	1.347317	-0.302898
6	6	0	-2.029877	2.085937	-1.107757
7	6	0	-1.051519	2.923761	-0.278278
8	6	0	-1.111184	-1.652407	0.175697
9	6	0	-2.216718	-1.923858	-0.776031
10	6	0	0.171309	-2.167582	-0.498504
11	6	0	-1.371677	-2.471214	1.461218
12	7	0	-3.067746	-2.148936	-1.527435
13	6	0	1.243808	0.397213	0.345987
14	6	0	2.446254	0.299092	0.182146

15	6	0	3.799106	0.137702	-0.01499
16	6	0	4.991336	-0.010578	-0.191944
17	6	0	6.423506	-0.186003	-0.404548
18	1	0	0.538312	2.658664	1.175235
19	1	0	-1.047943	2.226158	1.782126
20	1	0	-2.540553	0.911859	1.756099
21	1	0	-3.2742	-0.432603	0.91941
22	1	0	-3.773885	2.07076	0.174875
23	1	0	-3.712088	0.767801	-1.004929
24	1	0	-2.523963	2.738297	-1.836221
25	1	0	-1.463454	1.35231	-1.693514
26	1	0	-0.264354	3.2926	-0.945425
27	1	0	-1.563337	3.80643	0.123305
28	1	0	0.013669	-3.203906	-0.810492
29	1	0	0.433118	-1.573321	-1.376828
30	1	0	1.001504	-2.148246	0.208206
31	1	0	-1.405124	-3.53896	1.227224
32	1	0	-0.549303	-2.287075	2.157894
33	1	0	-2.311153	-2.188461	1.941655
34	1	0	6.766033	0.434566	-1.237347
35	1	0	6.982323	0.099854	0.491008
36	1	0	6.651747	-1.230162	-0.635637

Energy and Geometry for 4019 (conformer 11)
Sum of electronic and thermal free energies = -675.246195 a.u.

Center Number	Atomic Number	Atomic Type	Coordinates (Ångstroms)		
			X	Y	Z

1	6	0	-1.060299	-1.980166	-0.987766
2	6	0	-0.544703	-0.631156	-0.504092
3	6	0	-1.349559	0.419987	-0.221244
4	6	0	-2.862754	0.341483	-0.153123
5	6	0	-3.55848	-1.029671	-0.068063
6	6	0	-2.832621	-2.01837	0.84998
7	6	0	-1.740897	-2.806115	0.109506
8	6	0	-0.774669	1.787588	0.20623

9	6	0	0.411069	2.147124	-0.603205
10	6	0	-1.748885	2.967944	-0.025337
11	6	0	-0.381084	1.74115	1.697526
12	7	0	1.29412	2.540487	-1.239406
13	6	0	0.874734	-0.577239	-0.329035
14	6	0	2.079276	-0.650291	-0.168324
15	6	0	3.442605	-0.688061	0.016381
16	6	0	4.645725	-0.715113	0.177767
17	6	0	6.091247	-0.746327	0.36776
18	1	0	-0.222358	-2.544563	-1.40429
19	1	0	-1.756965	-1.810312	-1.813268
20	1	0	-3.299028	0.933154	-0.968861
21	1	0	-3.137849	0.876733	0.765683
22	1	0	-3.696233	-1.46905	-1.061407
23	1	0	-4.565975	-0.837882	0.315511
24	1	0	-3.546429	-2.721493	1.291405
25	1	0	-2.390329	-1.462732	1.687033
26	1	0	-0.990555	-3.16841	0.821401
27	1	0	-2.18098	-3.690912	-0.366064
28	1	0	-1.233444	3.903276	0.206538
29	1	0	-2.088167	3.009905	-1.063403
30	1	0	-2.616119	2.89198	0.632746
31	1	0	-0.006922	2.715637	2.024374
32	1	0	-1.270276	1.492783	2.28568
33	1	0	0.385628	0.985117	1.880666
34	1	0	6.378663	-1.602434	0.984569
35	1	0	6.602456	-0.827764	-0.595645
36	1	0	6.431822	0.166946	0.863398

Energy and Geometry for 4019 (conformer 12)
Sum of electronic and thermal free energies = -675.246109 a.u.

Center Number	Atomic Number	Atomic Type	Coordinates (Ångstroms)		
			X	Y	Z
1	6	0	-0.556972	-2.152462	-0.924789
2	6	0	-0.26603	-0.71254	-0.516769
3	6	0	-1.242922	0.193071	-0.277815
4	6	0	-2.720037	-0.155156	-0.210044
5	6	0	-3.168528	-1.614587	-0.006411
6	6	0	-2.265167	-2.394976	0.953361
7	6	0	-1.06344	-3.022533	0.230522
8	6	0	-0.91726	1.664368	0.058409
9	6	0	-2.148004	2.487709	-0.013222
10	6	0	-0.39259	1.776426	1.507679
11	6	0	0.055508	2.338761	-0.935062
12	7	0	-3.062476	3.194852	-0.064491
13	6	0	1.130959	-0.439996	-0.363418
14	6	0	2.338102	-0.358127	-0.224293
15	6	0	3.697383	-0.216925	-0.057119
16	6	0	4.895313	-0.086653	0.093258
17	6	0	6.334173	0.06612	0.275689
18	1	0	0.354372	-2.589079	-1.34131
19	1	0	-1.291955	-2.142251	-1.734269
20	1	0	-3.235616	0.28311	-1.076238
21	1	0	-3.102779	0.404051	0.655364
22	1	0	-3.248736	-2.144227	-0.961451
23	1	0	-4.185923	-1.568356	0.395231
24	1	0	-2.835156	-3.182932	1.456245
25	1	0	-1.916049	-1.715698	1.741895
26	1	0	-0.249976	-3.208161	0.941251
27	1	0	-1.349514	-3.995509	-0.186721
28	1	0	-0.218783	2.824255	1.768502
29	1	0	-1.110819	1.351076	2.214632
30	1	0	0.550157	1.231017	1.590722
31	1	0	0.117758	3.407863	-0.713877
32	1	0	1.054167	1.914406	-0.846053

33	1	0	-0.294622	2.21336	-1.962963
34	1	0	6.777309	0.580887	-0.581378
35	1	0	6.547247	0.649033	1.17603
36	1	0	6.813317	-0.911794	0.375966

Energy and Geometry for 4019‡_a

$<S^2>$ = 0.630254

Imaginary Frequencies: -784.8669 cm^{-1}

Sum of electronic and thermal free energies = -675.199361 a.u.

Center Number	Atomic Number	Atomic Type	Coordinates (Ångstroms)		
			X	Y	Z
1	6	0	-0.745851	-2.028729	-0.668018
2	6	0	-0.47284	-0.570117	-0.399081
3	6	0	-1.400855	0.398179	-0.312694
4	6	0	-2.87944	0.178315	-0.476448
5	6	0	-3.475113	-0.818671	0.532213
6	6	0	-3.145696	-2.286959	0.249765
7	6	0	-1.671246	-2.682458	0.368232
8	6	0	-0.855482	1.772144	-0.00509
9	6	0	0.675943	1.587343	0.101076
10	6	0	-1.149319	2.771793	-1.131902
11	6	0	-1.377225	2.299943	1.338633
12	7	0	1.56295	2.376747	0.323664
13	6	0	0.890752	-0.092583	-0.181281
14	6	0	2.057441	-0.628766	-0.164924
15	6	0	3.39989	-0.671859	-0.045843
16	6	0	4.619982	-0.735629	0.057378
17	6	0	6.067172	-0.803905	0.183568
18	1	0	0.207094	-2.563922	-0.696027
19	1	0	-1.1961	-2.132335	-1.665704
20	1	0	-3.0802	-0.185077	-1.495049
21	1	0	-3.400448	1.136051	-0.382739
22	1	0	-4.565105	-0.703965	0.516372
23	1	0	-3.142371	-0.549354	1.543383
24	1	0	-3.497085	-2.53719	-0.761724
25	1	0	-3.727041	-2.908863	0.940722

26	1	0	-1.302279	-2.45177	1.376216
27	1	0	-1.599915	-3.769542	0.246967
28	1	0	-0.703207	3.74243	-0.897823
29	1	0	-0.744159	2.41975	-2.085096
30	1	0	-2.230582	2.905535	-1.241009
31	1	0	-0.943723	3.281483	1.550426
32	1	0	-2.466829	2.403868	1.301107
33	1	0	-1.119756	1.619172	2.15548
34	1	0	6.551647	-0.353656	-0.687504
35	1	0	6.397441	-0.272177	1.080896
36	1	0	6.393283	-1.845914	0.261961

Energy and Geometry for 4019$^{\ddagger}_{\text{concerted}}$
Imaginary Frequencies: -481.5187 cm^{-1}
Sum of electronic and thermal free energies = -675.195832 a.u.

Center Number	Atomic Number	Atomic Type	Coordinates (Ångstroms)		
			X	Y	Z
1	6	0	-1.858472	-1.851572	-0.676213
2	6	0	-0.805015	-0.787209	-0.459108
3	6	0	-1.054121	0.53413	-0.359891
4	6	0	-2.442655	1.108631	-0.453506
5	6	0	-3.39069	0.614543	0.654739
6	6	0	-3.930701	-0.802465	0.442968
7	6	0	-2.893548	-1.928438	0.45571
8	6	0	0.12239	1.457657	-0.106175
9	6	0	1.402528	0.654025	-0.009394
10	6	0	0.571411	-1.152969	-0.306486
11	6	0	1.605092	-1.857547	-0.228691
12	6	0	2.92806	-1.813182	-0.037875
13	6	0	3.753388	-0.88696	0.169856
14	7	0	2.574919	0.795313	0.168197
15	6	0	5.082184	-0.322594	0.415466
16	6	0	-0.050801	2.205053	1.229848
17	6	0	0.298992	2.458206	-1.264294
18	1	0	-1.359848	-2.818126	-0.78346
19	1	0	-2.37748	-1.655409	-1.625094

20	1	0	-2.876602	0.850023	-1.430333
21	1	0	-2.393279	2.200494	-0.420042
22	1	0	-4.244248	1.300482	0.701796
23	1	0	-2.877705	0.679753	1.62326
24	1	0	-4.466407	-0.831453	-0.516737
25	1	0	-4.677224	-1.008019	1.219079
26	1	0	-2.3711	-1.948075	1.420804
27	1	0	-3.425756	-2.882368	0.365843
28	1	0	5.102484	0.205419	1.372701
29	1	0	5.821288	-1.127851	0.434701
30	1	0	5.347105	0.38801	-0.372095
31	1	0	0.80027	2.870555	1.398609
32	1	0	-0.963824	2.807914	1.206505
33	1	0	-0.117301	1.501514	2.064726
34	1	0	0.455125	1.933916	-2.211312
35	1	0	1.161916	3.101283	-1.071587
36	1	0	-0.590102	3.088889	-1.356482

Energy and Geometry for 4019* (conformer 1)
Sum of electronic and thermal free energies = -675.271686 a.u.

Center Number	Atomic Number	Atomic Type	Coordinates (Ångstroms)		
			X	Y	Z

1	6	0	-1.800588	-1.863379	-0.550915
2	6	0	-0.809453	-0.750208	-0.355449
3	6	0	-1.047477	0.580026	-0.287347
4	6	0	-2.385763	1.25042	-0.402032
5	6	0	-3.453074	0.708839	0.560791
6	6	0	-3.969083	-0.695966	0.234729
7	6	0	-2.974319	-1.842995	0.436088
8	6	0	0.232332	1.38217	-0.078731
9	6	0	1.288311	0.296583	-0.040898
10	6	0	0.62889	-0.958787	-0.208541
11	6	0	1.578899	-1.953876	-0.17229
12	6	0	2.812284	-1.792776	-0.020089
13	6	0	3.448991	-0.560325	0.143917

14	7	0	2.58626	0.482359	0.122258
15	6	0	4.912105	-0.317912	0.330896
16	6	0	0.201635	2.147407	1.253914
17	6	0	0.488291	2.347424	-1.246587
18	1	0	-1.271691	-2.818394	-0.462614
19	1	0	-2.196999	-1.822403	-1.575779
20	1	0	-2.755672	1.148192	-1.43366
21	1	0	-2.264214	2.325132	-0.228506
22	1	0	-4.304794	1.398846	0.540106
23	1	0	-3.055199	0.727256	1.584348
24	1	0	-4.326333	-0.711423	-0.805342
25	1	0	-4.84584	-0.890849	0.863718
26	1	0	-2.582259	-1.814029	1.46128
27	1	0	-3.517709	-2.789441	0.332206
28	1	0	5.478141	-0.720082	-0.514814
29	1	0	5.106545	0.752359	0.415151
30	1	0	5.270403	-0.819182	1.235393
31	1	0	1.152995	2.665727	1.407355
32	1	0	-0.599939	2.893368	1.24779
33	1	0	0.036388	1.465674	2.09436
34	1	0	0.529989	1.809517	-2.198944
35	1	0	1.439409	2.867635	-1.098295
36	1	0	-0.308939	3.095712	-1.304293

Energy and Geometry for 4019* (conformer 2)
Sum of electronic and thermal free energies = -675.270046 a.u.

Center Number	Atomic Number	Atomic Type	Coordinates (Ångstroms)		
			X	Y	Z
1	6	0	-1.806916	-1.887888	-0.103375
2	6	0	-0.816084	-0.753918	-0.080355
3	6	0	-1.043353	0.57697	0.028168
4	6	0	-2.379829	1.264985	0.069204
5	6	0	-3.463566	0.529879	-0.732403
6	6	0	-4.080285	-0.676015	-0.012913
7	6	0	-3.075632	-1.586388	0.703398

8	6	0	0.25577	1.376303	0.090179
9	6	0	1.30654	0.287558	0.013015
10	6	0	0.629899	-0.963818	-0.100194
11	6	0	1.575267	-1.961002	-0.174913
12	6	0	2.818495	-1.805085	-0.151929
13	6	0	3.472032	-0.575367	-0.040858
14	7	0	2.615106	0.469022	0.039811
15	6	0	4.947346	-0.337595	-0.002119
16	6	0	0.364208	2.157398	1.408493
17	6	0	0.40382	2.327784	-1.108324
18	1	0	-1.310072	-2.771829	0.312831
19	1	0	-2.066713	-2.1469	-1.13974
20	1	0	-2.259773	2.27835	-0.330978
21	1	0	-2.704563	1.395446	1.112999
22	1	0	-3.02364	0.209076	-1.684826
23	1	0	-4.265478	1.232557	-0.984296
24	1	0	-4.641655	-1.265159	-0.748787
25	1	0	-4.811409	-0.321609	0.724417
26	1	0	-2.77409	-1.131019	1.654942
27	1	0	-3.57558	-2.527718	0.956692
28	1	0	5.427559	-0.763383	-0.888157
29	1	0	5.153039	0.733147	0.038475
30	1	0	5.389395	-0.819136	0.875862
31	1	0	1.326772	2.675275	1.459401
32	1	0	-0.433966	2.90469	1.471293
33	1	0	0.282186	1.487635	2.27046
34	1	0	0.309128	1.786107	-2.054945
35	1	0	1.386725	2.807463	-1.078579
36	1	0	-0.359863	3.11105	-1.076188

Energy and Geometry for 4019* (conformer 3)
Sum of electronic and thermal free energies = -675.267661 a.u.

Center Number	Atomic Number	Atomic Type	Coordinates (Ångstroms)		
			X	Y	Z
1	6	0	1.748413	-1.976575	0.443881
2	6	0	0.81328	-0.805358	0.328121
3	6	0	1.076206	0.522441	0.313707
4	6	0	2.426058	1.168585	0.457061
5	6	0	3.442727	0.765224	-0.627337
6	6	0	3.512616	-0.745056	-0.922923
7	6	0	3.239187	-1.641363	0.29346
8	6	0	-0.189176	1.355995	0.139615
9	6	0	-1.264846	0.293169	0.050343
10	6	0	-0.629572	-0.979401	0.169907
11	6	0	-1.597219	-1.954162	0.0896
12	6	0	-2.827294	-1.767013	-0.060956
13	6	0	-3.439549	-0.516737	-0.177204
14	7	0	-2.558542	0.508618	-0.109585
15	6	0	-4.897381	-0.239765	-0.357761
16	6	0	-0.132756	2.1836	-1.153845
17	6	0	-0.436602	2.269365	1.350392
18	1	0	1.471761	-2.692141	-0.34328
19	1	0	1.564154	-2.495255	1.394294
20	1	0	2.833266	0.921367	1.444665
21	1	0	2.314601	2.25799	0.444896
22	1	0	4.427146	1.120646	-0.300326
23	1	0	3.210819	1.299502	-1.556318
24	1	0	4.50085	-0.967601	-1.33919
25	1	0	2.788542	-1.000262	-1.707105
26	1	0	3.781349	-2.586823	0.188752
27	1	0	3.621563	-1.17085	1.206899
28	1	0	-5.469855	-0.639393	0.484998
29	1	0	-5.068624	0.835481	-0.427661
30	1	0	-5.269002	-0.722389	-1.266812
31	1	0	-1.071549	2.729158	-1.289465
32	1	0	0.6841	2.911478	-1.104057

33	1	0	0.026455	1.540386	-2.025317
34	1	0	-0.490067	1.688282	2.276458
35	1	0	-1.380003	2.808815	1.222722
36	1	0	0.369731	3.003577	1.446576

Energy and Geometry for 4019* (conformer 4)
Sum of electronic and thermal free energies = -675.267261 a.u.

Center Number	Atomic Number	Atomic Type	Coordinates (Ångstroms)		
			X	Y	Z
1	6	0	-1.837044	-1.814053	-0.614647
2	6	0	-0.844685	-0.710003	-0.362871
3	6	0	-1.073603	0.620054	-0.243333
4	6	0	-2.389565	1.338885	-0.31013
5	6	0	-3.641419	0.449436	-0.256256
6	6	0	-3.570878	-0.590058	0.871537
7	6	0	-2.937023	-1.930474	0.454219
8	6	0	0.218057	1.401834	-0.006932
9	6	0	1.265104	0.307206	-0.028121
10	6	0	0.592932	-0.934256	-0.233374
11	6	0	1.533674	-1.939054	-0.246575
12	6	0	2.770057	-1.79434	-0.103288
13	6	0	3.420097	-0.573974	0.096655
14	7	0	2.566876	0.475929	0.124825
15	6	0	4.887681	-0.351142	0.272604
16	6	0	0.219197	2.098537	1.363789
17	6	0	0.474417	2.424431	-1.124232
18	1	0	-1.300141	-2.765912	-0.681913
19	1	0	-2.298144	-1.657382	-1.596002
20	1	0	-2.411649	1.968653	-1.211237
21	1	0	-2.431438	2.039223	0.53665
22	1	0	-3.801133	-0.046563	-1.220609
23	1	0	-4.504843	1.105619	-0.105279
24	1	0	-4.574055	-0.789454	1.263026
25	1	0	-3.00068	-0.156809	1.703484
26	1	0	-2.529806	-2.424995	1.343408

27	1	0	-3.712913	-2.594752	0.055657
28	1	0	5.439201	-0.729992	-0.593205
29	1	0	5.093049	0.713989	0.389913
30	1	0	5.252554	-0.885351	1.155372
31	1	0	1.197606	2.552927	1.546438
32	1	0	-0.537226	2.888982	1.393608
33	1	0	0.010584	1.384949	2.167717
34	1	0	0.47487	1.942337	-2.107117
35	1	0	1.444577	2.907013	-0.972365
36	1	0	-0.300528	3.197848	-1.115586

Energy and Geometry for 5014 (conformer 1)
Sum of electronic and thermal free energies = -1002.858736 a.u.

Center Number	Atomic Number	Atomic Type	Coordinates (Ångstroms)		
			X	Y	Z
1	6	0	-3.007371	1.316534	-1.217343
2	6	0	-2.056508	0.788608	-0.328196
3	6	0	-2.166977	-0.538838	0.15199
4	6	0	-3.253009	-1.291188	-0.297286
5	6	0	-4.19727	-0.764391	-1.179858
6	6	0	-4.078643	0.542207	-1.643567
7	6	0	-1.155336	-1.120045	1.154463
8	6	0	0.212077	-0.967147	0.617821
9	6	0	-1.285336	-0.38472	2.508242
10	6	0	-1.377331	-2.62327	1.408135
11	6	0	1.344904	-0.885391	0.177919
12	14	0	3.043671	-0.72295	-0.544145
13	6	0	4.293022	-1.199376	0.770705
14	6	0	3.150418	-1.880031	-2.017497
15	6	0	3.284328	1.057494	-1.082018
16	6	0	-0.992316	1.666267	0.052476
17	6	0	-0.134699	2.474918	0.338539
18	6	0	0.858022	3.363919	0.684845
19	7	0	1.696267	4.112127	0.977234
20	1	0	-2.889532	2.337702	-1.565916
21	1	0	-3.375026	-2.31436	0.036795
22	1	0	-5.02626	-1.385676	-1.504746
23	1	0	-4.808917	0.955564	-2.331231
24	1	0	-1.090927	0.685392	2.416093
25	1	0	-2.298022	-0.525024	2.898826
26	1	0	-0.571021	-0.802739	3.223072
27	1	0	-1.315481	-3.201404	0.482389
28	1	0	-0.602175	-2.983165	2.088988
29	1	0	-2.349756	-2.796659	1.878558
30	1	0	5.312728	-1.111268	0.378909
31	1	0	4.209662	-0.547813	1.646707
32	1	0	4.14507	-2.232864	1.101011

33	1	0	4.136124	-1.807319	-2.490997
34	1	0	2.993573	-2.920983	-1.716269
35	1	0	2.394825	-1.627202	-2.768802
36	1	0	4.252486	1.173991	-1.58295
37	1	0	2.502847	1.367783	-1.783848
38	1	0	3.266686	1.739165	-0.225418

Energy and Geometry for 5014 (conformer 2)
Sum of electronic and thermal free energies = -1002.857997 a.u.

Center Number	Atomic Number	Atomic Type	Coordinates (Ångstroms)		
			X	Y	Z
1	6	0	-2.999965	1.346564	-1.193931
2	6	0	-2.050549	0.796183	-0.316797
3	6	0	-2.173441	-0.53641	0.1457
4	6	0	-3.270237	-1.270296	-0.307903
5	6	0	-4.213164	-0.721053	-1.178122
6	6	0	-4.082143	0.590274	-1.624822
7	6	0	-1.163698	-1.142307	1.135351
8	6	0	0.2029	-0.996345	0.594845
9	6	0	-1.278415	-0.422881	2.499096
10	6	0	-1.401682	-2.645803	1.371578
11	6	0	1.335278	-0.916473	0.153461
12	14	0	3.039286	-0.721327	-0.548053
13	6	0	3.029566	-1.415058	-2.291131
14	6	0	3.454139	1.107178	-0.558597
15	6	0	4.236445	-1.671732	0.538921
16	6	0	-0.975608	1.658426	0.069379
17	6	0	-0.110924	2.458748	0.357874
18	6	0	0.887306	3.342187	0.702709
19	7	0	1.730865	4.086132	0.990511
20	1	0	-2.872625	2.371049	-1.529225
21	1	0	-3.402083	-2.296483	0.012864
22	1	0	-5.050928	-1.328488	-1.506618
23	1	0	-4.811266	1.021219	-2.302839
24	1	0	-1.073464	0.64627	2.419467

25	1	0	-2.29017	-0.557785	2.893992
26	1	0	-0.564352	-0.85733	3.204354
27	1	0	-1.35031	-3.213543	0.438796
28	1	0	-0.627978	-3.022642	2.044891
29	1	0	-2.374122	-2.813644	1.844009
30	1	0	4.014102	-1.295375	-2.757516
31	1	0	2.783577	-2.482104	-2.289328
32	1	0	2.293529	-0.898341	-2.915771
33	1	0	4.459644	1.266748	-0.965197
34	1	0	2.748708	1.67056	-1.178775
35	1	0	3.431173	1.524733	0.453204
36	1	0	5.258536	-1.576941	0.154806
37	1	0	4.223699	-1.292647	1.566092
38	1	0	3.983423	-2.736826	0.566294

Energy and Geometry for 5014 (conformer 3)
Sum of electronic and thermal free energies = -1002.85745 a.u.

Center Number	Atomic Number	Atomic Type	Coordinates (Ångstroms)		
			X	Y	Z
2	6	0	-2.503868	0.964973	0.000167
3	6	0	-1.095661	0.809873	-0.00024
4	6	0	-0.330307	1.978169	-0.000902
5	6	0	-0.912453	3.245367	-0.000808
6	6	0	-2.297173	3.3849	-0.000086
7	6	0	-0.424775	-0.574664	-0.000058
8	6	0	1.045339	-0.447664	0.000169
9	6	0	-0.805464	-1.369493	1.270768
10	6	0	-0.805209	-1.369545	-1.270925
11	6	0	2.262801	-0.414603	0.000397
12	14	0	4.117064	-0.389297	0.000573
13	6	0	4.716013	-2.154188	-0.211099
14	6	0	4.692692	0.681643	-1.427939
15	6	0	4.692726	0.317938	1.639448
16	6	0	-3.430993	-0.125289	0.000241
17	6	0	-4.293209	-0.978892	0.000099

18	6	0	-5.244577	-1.974509	-0.000087
19	7	0	-6.047531	-2.812805	-0.000255
20	1	0	-4.170791	2.32324	0.00072
21	1	0	0.750928	1.896306	-0.001612
22	1	0	-0.274708	4.124007	-0.001299
23	1	0	-2.758218	4.366931	0.000078
24	1	0	-0.520417	-0.815075	2.168932
25	1	0	-1.877961	-1.569778	1.305436
26	1	0	-0.278489	-2.327601	1.27044
27	1	0	-0.520336	-0.814969	-2.169048
28	1	0	-0.277971	-2.32751	-1.2707
29	1	0	-1.877671	-1.57007	-1.30559
30	1	0	5.811576	-2.185976	-0.21901
31	1	0	4.364888	-2.79176	0.606892
32	1	0	4.358032	-2.582114	-1.15337
33	1	0	5.787539	0.723452	-1.454036
34	1	0	4.346386	0.279656	-2.385816
35	1	0	4.316908	1.705991	-1.334525
36	1	0	5.787588	0.334454	1.684498
37	1	0	4.332258	1.342852	1.777018
38	1	0	4.328441	-0.284642	2.478

Energy and Geometry for 5014 (conformer 4)
Sum of electronic and thermal free energies = -1002.858793 a.u.

Center Number	Atomic Number	Atomic Type	Coordinates (Ångstroms)		
			X	Y	Z
1	6	0	3.021234	1.37429	-1.167858
2	6	0	2.065478	0.813056	-0.304745
3	6	0	2.184112	-0.525513	0.14201
4	6	0	3.283821	-1.254	-0.313324
5	6	0	4.233179	-0.694075	-1.169633
6	6	0	4.106264	0.623047	-1.600306
7	6	0	1.169189	-1.14316	1.11936
8	6	0	-0.197073	-0.990811	0.579181
9	6	0	1.405805	-2.649611	1.338235

10	6	0	1.28005	-0.440982	2.492477
11	6	0	-1.331348	-0.905335	0.143615
12	14	0	-3.039411	-0.713913	-0.550245
13	6	0	-4.097158	0.162255	0.725799
14	6	0	-2.908311	0.298507	-2.123329
15	6	0	-3.714967	-2.424328	-0.920699
16	6	0	0.983333	1.665447	0.081484
17	6	0	0.101292	2.44579	0.371435
18	6	0	-0.933506	3.28703	0.713519
19	7	0	-1.811683	3.99086	0.998808
20	1	0	2.896171	2.402801	-1.491487
21	1	0	3.413092	-2.284273	-0.004918
22	1	0	5.07293	-1.297778	-1.499935
23	1	0	4.840563	1.06209	-2.267442
24	1	0	1.35709	-3.206303	0.398671
25	1	0	2.37668	-2.823374	1.811753
26	1	0	0.629845	-3.034009	2.004635
27	1	0	1.076741	0.629373	2.425493
28	1	0	0.56301	-0.883377	3.189747
29	1	0	2.290245	-0.582222	2.88913
30	1	0	-5.118424	0.292813	0.35024
31	1	0	-4.149019	-0.411668	1.657001
32	1	0	-3.693801	1.153264	0.959325
33	1	0	-3.896483	0.425702	-2.580303
34	1	0	-2.500332	1.294275	-1.920154
35	1	0	-2.256952	-0.191913	-2.854176
36	1	0	-4.725534	-2.353764	-1.33907
37	1	0	-3.083632	-2.947217	-1.646695
38	1	0	-3.767015	-3.035297	-0.013365

Energy and Geometry for 5014 (conformer 5)
Sum of electronic and thermal free energies = -1002.857718 a.u.

Center Number	Atomic Number	Atomic Type	Coordinates (Ångstroms)		
			X	Y	Z
1	6	0	3.030112	2.264488	0.002248
2	6	0	2.476625	0.970958	0.000601
3	6	0	1.072623	0.781853	-0.001748
4	6	0	0.279419	1.931722	-0.002897
5	6	0	0.830943	3.2125	-0.001386
6	6	0	2.211887	3.385324	0.001419
7	6	0	0.4353	-0.619047	-0.00334
8	6	0	-1.036581	-0.521458	-0.003709
9	6	0	0.83521	-1.402867	-1.274831
10	6	0	0.833496	-1.405598	1.267049
11	6	0	-2.254107	-0.496155	-0.003232
12	14	0	-4.105166	-0.396285	0.000891
13	6	0	-4.755301	-1.422585	-1.42738
14	6	0	-4.726631	-1.061634	1.6403
15	6	0	-4.568176	1.410416	-0.204877
16	6	0	3.430105	-0.096429	0.001219
17	6	0	4.314178	-0.927406	0.001782
18	6	0	5.293712	-1.895314	0.002513
19	7	0	6.11859	-2.712036	0.00309
20	1	0	4.110478	2.369201	0.004201
21	1	0	-0.799738	1.82471	-0.005215
22	1	0	0.171956	4.075318	-0.002357
23	1	0	2.649268	4.378094	0.002782
24	1	0	0.538133	-0.853802	-2.172385
25	1	0	1.912182	-1.577858	-1.30882
26	1	0	0.330764	-2.373013	-1.276586
27	1	0	0.534786	-0.858641	2.165347
28	1	0	0.329199	-2.375823	1.265723
29	1	0	1.910395	-1.580571	1.302473
30	1	0	-5.851078	-1.409031	-1.440615
31	1	0	-4.399744	-1.032751	-2.386884
32	1	0	-4.430809	-2.465095	-1.344293

33	1	0	-5.820698	-1.013963	1.681624
34	1	0	-4.428628	-2.105805	1.781672
35	1	0	-4.330042	-0.479632	2.478667
36	1	0	-5.657138	1.533425	-0.198074
37	1	0	-4.154176	2.015928	0.608519
38	1	0	-4.189813	1.808948	-1.152264

Energy and Geometry for 5014 (conformer 6)
Sum of electronic and thermal free energies = -1002.857803 a.u.

Center Number	Atomic Number	Atomic Type	Coordinates (Ångstroms)		
			X	Y	Z
1	6	0	3.048582	2.258357	0.003373
2	6	0	2.485523	0.968989	0.001513
3	6	0	1.080128	0.79039	-0.001431
4	6	0	0.29562	1.946071	-0.003848
5	6	0	0.856569	3.222745	-0.002213
6	6	0	2.238748	3.385278	0.001869
7	6	0	0.432198	-0.605495	-0.002493
8	6	0	-1.039303	-0.498941	-0.00209
9	6	0	0.825925	-1.392346	-1.274129
10	6	0	0.825366	-1.395067	1.26766
11	6	0	-2.256847	-0.471527	-0.001056
12	14	0	-4.109315	-0.394722	0.00021
13	6	0	-4.685597	-0.228065	1.777502
14	6	0	-4.620609	1.104861	-1.005004
15	6	0	-4.765009	-1.97517	-0.76766
16	6	0	3.431043	-0.105423	0.001966
17	6	0	4.308731	-0.943126	0.001897
18	6	0	5.280146	-1.919181	0.001792
19	7	0	6.098767	-2.742176	0.001664
20	1	0	4.129689	2.354938	0.005961
21	1	0	-0.78414	1.846685	-0.007466
22	1	0	0.204114	4.090509	-0.004089
23	1	0	2.683489	4.374779	0.003512
24	1	0	0.532757	-0.841063	-2.171613

25	1	0	1.901576	-1.575308	-1.308351
26	1	0	0.314264	-2.358709	-1.275736
27	1	0	0.530786	-0.846239	2.166181
28	1	0	0.314233	-2.361706	1.26621
29	1	0	1.900997	-1.5777	1.302704
30	1	0	-5.779737	-0.179771	1.8203
31	1	0	-4.361716	-1.083481	2.379366
32	1	0	-4.288064	0.681788	2.239358
33	1	0	-5.712343	1.197458	-1.027429
34	1	0	-4.213149	2.025108	-0.572803
35	1	0	-4.265207	1.028995	-2.037914
36	1	0	-5.860778	-1.96365	-0.785761
37	1	0	-4.409615	-2.09249	-1.796668
38	1	0	-4.44541	-2.852914	-0.196224

Energy and Geometry for 5014‡

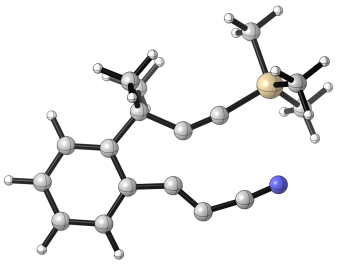

Imaginary Frequencies: -318.0645 cm^{-1}
Sum of electronic and thermal free energies = -1002.809774 a.u.

Center Number	Atomic Number	Atomic Type	Coordinates (Ångstroms)		
			X	Y	Z
1	6	0	3.469648	1.574373	-0.092503
2	6	0	2.299023	0.809407	-0.022915
3	6	0	2.347781	-0.579992	0.000489
4	6	0	3.576041	-1.23617	-0.046028
5	6	0	4.746817	-0.483042	-0.117824
6	6	0	4.693011	0.915863	-0.140583
7	6	0	0.994592	-1.250888	0.098728
8	6	0	-0.03888	-0.113858	0.041512
9	6	0	0.759241	-2.217639	-1.068926
10	6	0	0.849143	-1.98346	1.442044
11	6	0	-1.296473	-0.097821	0.006657
12	14	0	-3.156697	-0.333655	-0.066728
13	6	0	-3.931282	0.273484	1.520607
14	6	0	-3.843815	0.478493	-1.6022
15	6	0	-3.307028	-2.205629	-0.201425
16	6	0	0.954103	1.374475	0.033435
17	6	0	0.410394	2.54325	0.073919
18	6	0	-0.945222	2.734103	0.107684
19	7	0	-2.115975	2.741828	0.126804
20	1	0	3.410113	2.657983	-0.110092
21	1	0	3.623293	-2.321752	-0.026588
22	1	0	5.708335	-0.985719	-0.15694
23	1	0	5.611751	1.491172	-0.197342
24	1	0	0.807814	-1.694704	-2.027841
25	1	0	1.528107	-2.99698	-1.058024

26	1	0	-0.22089	-2.693712	-0.972399
27	1	0	0.976642	-1.294	2.28112
28	1	0	-0.137442	-2.450334	1.513362
29	1	0	1.613688	-2.764047	1.514255
30	1	0	-4.992393	-0.000574	1.539321
31	1	0	-3.448057	-0.181991	2.391206
32	1	0	-3.851234	1.360363	1.60498
33	1	0	-4.885343	0.167301	-1.743831
34	1	0	-3.813243	1.567825	-1.519285
35	1	0	-3.277105	0.178892	-2.489821
36	1	0	-4.370227	-2.475389	-0.191578
37	1	0	-2.876367	-2.577055	-1.136683
38	1	0	-2.824426	-2.71859	0.636716

Energy and Geometry for 5014*

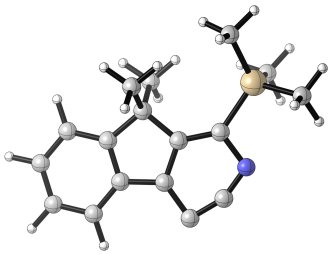

Sum of electronic and thermal free energies = -1002.861881 a.u.

Center Number	Atomic Number	Atomic Type	Coordinates (Ångstroms)		
			X	Y	Z
1	6	0	-3.612034	1.300508	0.063528
2	6	0	-2.338174	0.739144	0.002222
3	6	0	-2.144802	-0.646193	0.00171
4	6	0	-3.239579	-1.50229	0.06335
5	6	0	-4.520427	-0.947768	0.127444
6	6	0	-4.706521	0.44059	0.126574
7	6	0	-0.668804	-1.003187	-0.107282
8	6	0	-0.012043	0.375659	-0.097057
9	6	0	-1.024844	1.392451	-0.060291
10	6	0	-0.755334	2.795913	-0.064899
11	6	0	0.528953	2.692975	-0.092507
12	7	0	1.62471	2.099584	-0.106541
13	6	0	1.343006	0.718968	-0.107652
14	6	0	-0.429245	-1.725049	-1.445248
15	6	0	-0.225632	-1.874934	1.075191
16	14	0	2.984894	-0.265149	0.059953
17	6	0	3.070181	-1.906798	-0.849305
18	6	0	4.310418	0.854111	-0.650657
19	6	0	3.271053	-0.508909	1.900797
20	1	0	-3.738993	2.379599	0.063126
21	1	0	-3.109319	-2.581668	0.061214
22	1	0	-5.385565	-1.602259	0.178149
23	1	0	-5.712023	0.846813	0.175784
24	1	0	-0.778214	-1.112133	-2.281969
25	1	0	0.630635	-1.939604	-1.591851

26	1	0	-0.977953	-2.672501	-1.46044
27	1	0	0.833465	-2.135304	0.997209
28	1	0	-0.387796	-1.358404	2.026253
29	1	0	-0.796802	-2.80904	1.087319
30	1	0	4.101403	-2.267674	-0.745922
31	1	0	2.414239	-2.68502	-0.450981
32	1	0	2.872801	-1.793703	-1.920148
33	1	0	5.280794	0.346639	-0.605397
34	1	0	4.106151	1.099905	-1.698339
35	1	0	4.388836	1.791384	-0.092427
36	1	0	4.267177	-0.932864	2.072701
37	1	0	3.218009	0.451338	2.425255
38	1	0	2.534636	-1.181658	2.3514

Energy and Geometry for 5013 (conformer 1)
Sum of electronic and thermal free energies = -998.328468 a.u.

Center Number	Atomic Number	Atomic Type	Coordinates (Ångstroms)		
			X	Y	Z
1	6	0	-3.268771	2.059326	-0.00001
2	6	0	-2.598263	0.827926	0
3	6	0	-1.185283	0.80366	0.00001
4	6	0	-0.485427	2.011358	0.000011
5	6	0	-1.159779	3.230046	0.000003
6	6	0	-2.552291	3.252451	-0.000008
7	6	0	-0.445227	-0.493262	0.00002
8	6	0	1.012489	-0.436196	0.000012
9	8	0	-1.013003	-1.570571	0.000033
10	6	0	2.230157	-0.436381	0.000005
11	14	0	4.100624	-0.460382	-0.000006
12	6	0	4.628907	-1.365643	-1.549673
13	6	0	4.683586	1.319204	-0.000009
14	6	0	4.628924	-1.36564	1.549656
15	6	0	-3.415404	-0.34729	-0.000003
16	6	0	-4.225466	-1.248793	-0.000007
17	6	0	-5.118003	-2.297714	-0.000009

18	7	0	-5.877836	-3.175023	-0.000012
19	1	0	-4.353796	2.068858	-0.000018
20	1	0	0.599949	1.994984	0.000019
21	1	0	-0.597079	4.157631	0.000004
22	1	0	-3.085731	4.197381	-0.000016
23	1	0	5.722364	-1.408756	-1.606235
24	1	0	4.247472	-2.391576	-1.553827
25	1	0	4.262571	-0.861435	-2.449487
26	1	0	5.778799	1.357919	-0.000014
27	1	0	4.326121	1.851765	-0.887273
28	1	0	4.326128	1.851764	0.887257
29	1	0	5.722382	-1.408771	1.606197
30	1	0	4.262613	-0.861418	2.449473
31	1	0	4.247472	-2.391567	1.553828

Energy and Geometry for 5013 (conformer 2)
Sum of electronic and thermal free energies = -998.328102 a.u.

Center Number	Atomic Number	Atomic Type	Coordinates (Ångstroms)		
			X	Y	Z
1	6	0	-3.279772	2.05334	-0.006393
2	6	0	-2.60316	0.825299	0.000177
3	6	0	-1.190064	0.80823	0.007822
4	6	0	-0.496373	2.019379	0.008614
5	6	0	-1.176701	3.234705	0.002504
6	6	0	-2.569265	3.250057	-0.005255
7	6	0	-0.443346	-0.484646	0.014477
8	6	0	1.014413	-0.422347	0.010722
9	8	0	-1.00574	-1.564752	0.02233
10	6	0	2.232119	-0.425148	0.007183
11	14	0	4.102516	-0.460594	-0.004016
12	6	0	4.683127	0.599628	1.426117
13	6	0	4.626206	-2.244923	0.203553
14	6	0	4.646405	0.237018	-1.654251
15	6	0	-3.414456	-0.354004	-0.001668
16	6	0	-4.22019	-1.259388	-0.004019

17	6	0	-5.107729	-2.31255	-0.006333
18	7	0	-5.863195	-3.19362	-0.008232
19	1	0	-4.364816	2.057531	-0.012461
20	1	0	0.588922	2.00815	0.014436
21	1	0	-0.6187	4.165111	0.003562
22	1	0	-3.107467	4.192266	-0.010408
23	1	0	5.778369	0.621764	1.454674
24	1	0	4.325591	1.629975	1.331109
25	1	0	4.328145	0.201299	2.382055
26	1	0	5.719442	-2.320583	0.203374
27	1	0	4.258312	-2.656708	1.148873
28	1	0	4.241662	-2.866426	-0.611385
29	1	0	5.740148	0.234988	-1.720936
30	1	0	4.255684	-0.361253	-2.483587
31	1	0	4.300497	1.267656	-1.783599

Energy and Geometry for 5013 (conformer 3)
Sum of electronic and thermal free energies = -998.328090 a.u.

Center Number	Atomic Number	Atomic Type	Coordinates (Ångstroms)		
			X	Y	Z
1	6	0	-3.270799	2.057306	0.005953
2	6	0	-2.599331	0.826437	0.000394
3	6	0	-1.186333	0.803317	-0.005992
4	6	0	-0.487593	2.01159	-0.006948
5	6	0	-1.162824	3.229768	-0.001766
6	6	0	-2.555316	3.251036	0.005002
7	6	0	-0.445161	-0.492918	-0.011066
8	6	0	1.012732	-0.435893	-0.008763
9	8	0	-1.012242	-1.57058	-0.0166
10	6	0	2.230438	-0.439544	-0.007079
11	14	0	4.101215	-0.462196	0.001253
12	6	0	4.640217	-2.191803	-0.464411
13	6	0	4.671041	0.806635	-1.252091
14	6	0	4.636664	-0.013206	1.738132
15	6	0	-3.415691	-0.349321	0.001527

16	6	0	-4.22547	-1.251081	0.002803
17	6	0	-5.117809	-2.30017	0.003852
18	7	0	-5.877546	-3.17756	0.004643
19	1	0	-4.355816	2.065982	0.011047
20	1	0	0.597653	1.995864	-0.01218
21	1	0	-0.600878	4.157807	-0.002819
22	1	0	-3.089521	4.195523	0.009434
23	1	0	5.733982	-2.257937	-0.470639
24	1	0	4.25919	-2.927802	0.250738
25	1	0	4.277816	-2.465588	-1.460295
26	1	0	5.766	0.829437	-1.290486
27	1	0	4.302501	0.566725	-2.254439
28	1	0	4.321288	1.809839	-0.98806
29	1	0	5.730447	-0.012754	1.805069
30	1	0	4.279483	0.982138	2.020735
31	1	0	4.253022	-0.733863	2.467366

Energy and Geometry for 5013 (conformer 4)
Sum of electronic and thermal free energies = -998.328040 a.u.

Center Number	Atomic Number	Atomic Type	Coordinates (Ångstroms)		
			X	Y	Z
1	6	0	-3.260592	2.061363	-0.034587
2	6	0	-2.595042	0.827795	0.001006
3	6	0	-1.182646	0.79868	0.040539
4	6	0	-0.478568	2.003916	0.042132
5	6	0	-1.148077	3.224823	0.008751
6	6	0	-2.539936	3.251952	-0.030446
7	6	0	-0.447293	-0.500451	0.080129
8	6	0	1.010461	-0.449011	0.05382
9	8	0	-1.018529	-1.574671	0.131408
10	6	0	2.227891	-0.452292	0.030314
11	14	0	4.097629	-0.463386	-0.019405
12	6	0	4.583708	-0.695577	-1.812358
13	6	0	4.676384	1.188485	0.646385
14	6	0	4.679116	-1.886512	1.047196

15	6	0	-3.416525	-0.344318	-0.00927
16	6	0	-4.230301	-1.242355	-0.023957
17	6	0	-5.127137	-2.287512	-0.03833
18	7	0	-5.890692	-3.161499	-0.050011
19	1	0	-4.345091	2.074549	-0.066114
20	1	0	0.606272	1.983733	0.07194
21	1	0	-0.582117	4.150421	0.012432
22	1	0	-3.069593	4.198616	-0.058176
23	1	0	5.675453	-0.704159	-1.907027
24	1	0	4.202747	-1.643697	-2.205133
25	1	0	4.194946	0.114644	-2.437437
26	1	0	5.770947	1.237857	0.634322
27	1	0	4.294449	2.015467	0.038829
28	1	0	4.342995	1.339169	1.678298
29	1	0	5.774276	-1.92028	1.063825
30	1	0	4.326853	-1.781873	2.078306
31	1	0	4.315472	-2.843101	0.658485

Energy and Geometry for 5013 (conformer 5)
Sum of electronic and thermal free energies = -998.326683 a.u.

Center Number	Atomic Number	Atomic Type	Coordinates (Ångstroms)		
			X	Y	Z
1	6	0	3.352371	1.254425	-0.757299
2	6	0	2.244444	0.658482	-0.134026
3	6	0	2.311561	-0.693396	0.264274
4	6	0	3.485804	-1.412845	0.036277
5	6	0	4.574227	-0.819088	-0.596177
6	6	0	4.505275	0.515051	-0.995672
7	6	0	1.192488	-1.435907	0.930124
8	6	0	-0.175649	-1.130319	0.545749
9	8	0	1.427693	-2.330587	1.723287
10	6	0	-1.327152	-0.943788	0.195427
11	14	0	-3.086277	-0.670578	-0.38091
12	6	0	-3.124235	0.939499	-1.334426
13	6	0	-3.506077	-2.131163	-1.475063

14	6	0	-4.167745	-0.607892	1.144447
15	6	0	1.118066	1.497503	0.138181
16	6	0	0.22554	2.285055	0.364903
17	6	0	-0.811898	3.149183	0.637412
18	7	0	-1.690731	3.872226	0.865172
19	1	0	3.297327	2.299905	-1.042417
20	1	0	3.528236	-2.449477	0.354
21	1	0	5.474482	-1.397353	-0.776924
22	1	0	5.351253	0.98467	-1.486735
23	1	0	-4.09058	1.051278	-1.839486
24	1	0	-2.993288	1.801196	-0.672789
25	1	0	-2.339467	0.966433	-2.097557
26	1	0	-4.533906	-2.040109	-1.84413
27	1	0	-2.838345	-2.184807	-2.340848
28	1	0	-3.425913	-3.072719	-0.922559
29	1	0	-5.214417	-0.452843	0.85946
30	1	0	-4.103782	-1.542187	1.711322
31	1	0	-3.872286	0.214428	1.804118

Energy and Geometry for 5013 (conformer 6)
Sum of electronic and thermal free energies = -998.326230 a.u.

Center Number	Atomic Number	Atomic Type	Coordinates (Ångstroms)		
			X	Y	Z
1	6	0	-3.384959	1.216638	-0.740527
2	6	0	-2.26072	0.636458	-0.131181
3	6	0	-2.300898	-0.718886	0.257888
4	6	0	-3.464146	-1.457599	0.03384
5	6	0	-4.568409	-0.879207	-0.584919
6	6	0	-4.526679	0.458979	-0.974514
7	6	0	-1.165422	-1.446673	0.911015
8	6	0	0.196924	-1.115605	0.526949
9	8	0	-1.380758	-2.353679	1.695983
10	6	0	1.349782	-0.924336	0.183474
11	14	0	3.119554	-0.664625	-0.365932
12	6	0	3.304473	1.125275	-0.878787

13	6	0	4.21828	-1.088156	1.087747
14	6	0	3.385607	-1.828998	-1.807594
15	6	0	-1.149968	1.4988	0.13432
16	6	0	-0.283704	2.318412	0.349723
17	6	0	0.715675	3.231677	0.604373
18	7	0	1.557786	4.000338	0.820772
19	1	0	-3.35126	2.264904	-1.018422
20	1	0	-3.4851	-2.497064	0.344213
21	1	0	-5.459595	-1.472237	-0.762673
22	1	0	-5.385002	0.917462	-1.45459
23	1	0	4.300988	1.285508	-1.306625
24	1	0	2.565187	1.402404	-1.637446
25	1	0	3.196165	1.800887	-0.024955
26	1	0	5.272123	-0.963274	0.814833
27	1	0	4.010586	-0.435143	1.941431
28	1	0	4.069335	-2.124653	1.406636
29	1	0	4.417231	-1.751026	-2.168897
30	1	0	3.205983	-2.868382	-1.514963
31	1	0	2.716158	-1.588225	-2.639608

Energy and Geometry for 5013 (conformer 7)
Sum of electronic and thermal free energies = -998.326230 a.u.

Center Number	Atomic Number	Atomic Type	Coordinates (Ångstroms)		
			X	Y	Z
1	6	0	3.384992	1.216611	0.740521
2	6	0	2.26074	0.636446	0.131185
3	6	0	2.300894	-0.7189	-0.257881
4	6	0	3.464135	-1.457627	-0.033845
5	6	0	4.568413	-0.879248	0.584901
6	6	0	4.526704	0.458938	0.974496
7	6	0	1.165403	-1.44667	-0.910998
8	6	0	-0.196938	-1.115592	-0.526922
9	8	0	1.380719	-2.353672	-1.695977
10	6	0	-1.349797	-0.924323	-0.18345
11	14	0	-3.11958	-0.664619	0.36593

12	6	0	-3.304485	1.125284	0.878779
13	6	0	-4.218278	-1.088125	-1.087779
14	6	0	-3.38567	-1.82901	1.807569
15	6	0	1.149998	1.498803	-0.134307
16	6	0	0.283743	2.318426	-0.349707
17	6	0	-0.715624	3.231705	-0.60435
18	7	0	-1.557726	4.000377	-0.820748
19	1	0	3.351309	2.264878	1.018416
20	1	0	3.485073	-2.497093	-0.344216
21	1	0	5.459593	-1.472289	0.762646
22	1	0	5.385039	0.91741	1.454563
23	1	0	-4.301014	1.285561	1.306565
24	1	0	-2.565222	1.4024	1.637465
25	1	0	-3.196109	1.800876	0.02494
26	1	0	-5.272127	-0.963257	-0.814878
27	1	0	-4.010576	-0.43509	-1.941444
28	1	0	-4.069322	-2.124614	-1.406689
29	1	0	-4.417299	-1.751033	2.168856
30	1	0	-3.206052	-2.868393	1.514929
31	1	0	-2.716234	-1.588259	2.6396

Energy and Geometry for 5013 (conformer 8)
Sum of electronic and thermal free energies = -998.326042 a.u.

Center Number	Atomic Number	Atomic Type	Coordinates (Ångstroms)		
			X	Y	Z
1	6	0	-3.346463	1.38565	0.629835
2	6	0	-2.244861	0.705172	0.087383
3	6	0	-2.356893	-0.667112	-0.225128
4	6	0	-3.56954	-1.319339	0.005657
5	6	0	-4.652525	-0.640548	0.556053
6	6	0	-4.538936	0.713022	0.870732
7	6	0	-1.250747	-1.504902	-0.794211
8	6	0	0.122789	-1.203067	-0.427708
9	8	0	-1.503066	-2.464338	-1.502184
10	6	0	1.280085	-0.997913	-0.108764

11	14	0	3.055294	-0.643387	0.365236
12	6	0	3.805544	-2.27199	0.902111
13	6	0	3.888367	0.051405	-1.159612
14	6	0	3.018602	0.592701	1.770346
15	6	0	-1.067036	1.471797	-0.178624
16	6	0	-0.109165	2.181314	-0.395258
17	6	0	1.024539	2.923215	-0.6432
18	7	0	1.991314	3.533821	-0.84299
19	1	0	-3.254391	2.443502	0.852726
20	1	0	-3.645998	-2.372653	-0.243675
21	1	0	-5.582767	-1.16826	0.739623
22	1	0	-5.379636	1.248662	1.299323
23	1	0	4.85272	-2.128838	1.191026
24	1	0	3.270085	-2.685704	1.762649
25	1	0	3.773938	-3.009164	0.093548
26	1	0	4.938215	0.278691	-0.943132
27	1	0	3.857395	-0.665979	-1.985761
28	1	0	3.403839	0.977028	-1.487185
29	1	0	4.039328	0.819393	2.098403
30	1	0	2.550805	1.533011	1.460748
31	1	0	2.465112	0.199263	2.629138

Energy and Geometry for 5013‡

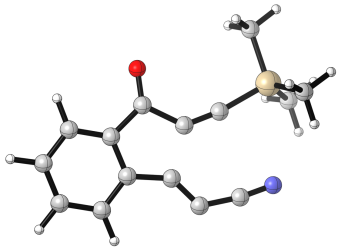

Imaginary Frequencies: -335.1549 cm^{-1}
Sum of electronic and thermal free energies = -998.280761 a.u.

Center Number	Atomic Number	Atomic Type	Coordinates (Ångstroms)		
			X	Y	Z
1	6	0	3.580391	1.331907	0.000003
2	6	0	2.377734	0.619943	0.000001
3	6	0	2.39067	-0.772404	-0.000001
4	6	0	3.580898	-1.497825	0
5	6	0	4.777798	-0.790693	0.000003
6	6	0	4.771551	0.612396	0.000005
7	6	0	1.034278	-1.345852	-0.000005
8	6	0	0.000884	-0.219922	-0.000003
9	8	0	0.737868	-2.513741	-0.000009
10	6	0	-1.254064	-0.205489	0
11	14	0	-3.121953	-0.454931	0.000002
12	6	0	-3.821704	0.28251	-1.565195
13	6	0	-3.246181	-2.32828	0.00001
14	6	0	-3.821705	0.282521	1.565194
15	6	0	1.052775	1.232463	-0.000001
16	6	0	0.532188	2.40641	-0.000003
17	6	0	-0.817707	2.648287	-0.000004
18	7	0	-1.986385	2.69375	-0.000005
19	1	0	3.574104	2.416789	0.000004
20	1	0	3.559677	-2.583133	-0.000001
21	1	0	5.722691	-1.323954	0.000004
22	1	0	5.714902	1.149631	0.000007
23	1	0	-4.880594	0.013053	-1.651882
24	1	0	-3.740204	1.372706	-1.555399

25	1	0	-3.301082	-0.10157	-2.448179
26	1	0	-4.302484	-2.622368	0.000002
27	1	0	-2.771426	-2.759258	-0.88699
28	1	0	-2.771442	-2.759248	0.887023
29	1	0	-4.880588	0.013042	1.651896
30	1	0	-3.301065	-0.101533	2.448179
31	1	0	-3.740228	1.372719	1.555379

Energy and Geometry for 5013*

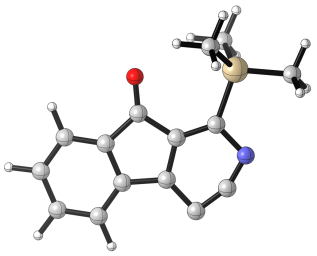

Sum of electronic and thermal free energies = -998.338977 a.u.

Center Number	Atomic Number	Atomic Type	Coordinates (Ångstroms)		
			X	Y	Z
1	6	0	-1.044843	1.330447	-0.000003
2	6	0	0.008744	0.365309	-0.000003
3	6	0	-0.609185	-0.999892	-0.000006
4	6	0	-2.088354	-0.774565	-0.000002
5	6	0	-2.340536	0.606159	-0.000002
6	6	0	-0.800358	2.729235	-0.000004
7	6	0	0.488812	2.66672	-0.000003
8	7	0	1.605955	2.10885	-0.000003
9	6	0	1.352192	0.725944	-0.000003
10	6	0	-3.119769	-1.699482	0.000002
11	6	0	-4.432343	-1.212786	0.000007
12	6	0	-4.684606	0.161594	0.000005
13	6	0	-3.637653	1.092256	0.000001
14	8	0	-0.02717	-2.065067	-0.000013
15	14	0	2.890715	-0.421351	0.000001
16	6	0	2.8572	-1.460754	-1.558191
17	6	0	4.364674	0.734027	0.000033
18	6	0	2.857165	-1.460782	1.558174
19	1	0	-2.912334	-2.765492	0.000003
20	1	0	-5.264358	-1.909751	0.000011
21	1	0	-5.71153	0.513812	0.000008
22	1	0	-3.833176	2.160565	0
23	1	0	3.774333	-2.057513	-1.624599
24	1	0	2.004267	-2.145164	-1.560106
25	1	0	2.802821	-0.830857	-2.452393
26	1	0	5.292531	0.150412	-0.000112

27	1	0	4.372426	1.37738	-0.885864
28	1	0	4.372563	1.377152	0.886094
29	1	0	3.774323	-2.0575	1.624622
30	1	0	2.802711	-0.8309	2.452382
31	1	0	2.004264	-2.145231	1.560036

Bibliography and Notes

1. Mayr, H.; Ofial, A. R., The Reactivity–Selectivity Principle: An Imperishable Myth in Organic Chemistry. *Angew. Chem. Int. Ed.* **2006,** *45*, 1844-1854.

2. Stoermer, R.; Kahlert, B., Ueber das 1- und 2-Brom-cumaron. *Ber. Dtsch. Chem. Ges* **1902,** *35*, 1633-1640.

3. Wittig, G., Phenyl-lithium, der Schlüssel zu einer neuen Chemie metallorganischer Verbindungen. *Naturwissenschaften* **1942,** *30*, 696-703.

4. Bergstrom, F. W.; Horning, C. H., The Action of Bases on Organic Halogen Compounds. V. The Action of Potassium Amide on Some Aromatic Halides (1). *J. Org. Chem.* **1946,** *11*, 334-340.

5. Gilman, H.; Avakian, S., Dibenzofuran. XXIII. Rearrangement of Halogen Compounds in Amination by Sodamide 1. *J. Am. Chem. Soc.* **1945,** *67*, 349-351.

6. Roberts, J. D.; Simmons, H. E.; Carlsmith, L. A.; Vaughan, C. W., Rearragement in the Reaction of Chlorobenzne-1-C14 with Potassium Amide 1. *J. Am. Chem. Soc.* **1953,** *75*, 3290-3291.

7. a) Wittig, G.; Pohmer, L., Intermediäre Bildung von Dehydrobenzol (Cyclohexa-dienin). *Angewandte Chemie* **1955,** *67*, 348-348. (b) Wittig, G., 1,2-Dehydrobenzene. *Angew. Chem. Int. Ed.* **1965,** *4*, 731-737. (c) Heaney, H., The Benzyne and Related Intermediates. *Chem. Rev.* **1962,** *62*, 81-97.

8. Hoffmann, R. W. Dehydrobenzene and Cycloalkynes. 11, Academic Press: New York, 1967.

9. Kametani, T.; Ogasawara, K., Benzyne reaction. Part I. Total Syntheses of (±)-Cryptaustoline and (±)-Cryptowoline by the Benzyne Reaction. *J. Chem. Soc. C* **1967**, 2208-2208.

10. Leopold, D. G.; Miller, A. E. S.; Lineberger, W. C., Determination of the singlet-triplet splitting and electron affinity of o-benzyne by negative ion photoelectron spectroscopy. *J. Am. Chem. Soc.* **1986,** *108*, 1379-1384.

11. (a) Tadross, P. M.; Stoltz, B. M., A comprehensive history of arynes in natural product total synthesis. *Chem. Rev.* **2012,** *112*, 3550-3577. (b) Gampe, C. M.; Carreira, E. M., Arynes and Cyclohexyne in Natural Product Synthesis. *Angew. Chem. Int. Ed.* **2012,** *51*, 3766-3778.

12. (a) Dubrovskiy, A. V.; Markina, N. A.; Larock, R. C., Use of benzynes for the synthesis of heterocycles. *Org. Biomol. Chem* **2013,** *11*, 191-218. (b) Sanz, R.,

Recent Applications of Aryne Chemistry to Organic Synthesis. A Review. *Org. Prep. Proced. Int* **2008,** *40*, 215-291. (c) García-López, J.-A.; Greaney, M. F., Synthesis of biaryls using aryne intermediates. *Chem. Soc. Rev.* **2016,** *45*, 6766-6798. (d) Alam, M. A.; Shimada, K.; Jahan, A.; Nasrin, D.; Zahan, M. K.-E.; Shahabuddin, M., The Advances and Applications of Arynes and Their Precursors to Synthesize the Heterocyclic Compounds: A Review. *American Journal of Heterocyclic Chemistry* **2017,** *3*, 47-54. (e) Bhunia, A.; Yetra, S. R.; Biju, A. T., Recent advances in transition-metal-free carbon-carbon and carbon-heteroatom bond-forming reactions using arynes. *Chem. Soc. Rev.* **2012,** *41*, 3140-52. (f) Bhojgude, S. S.; Bhunia, A.; Biju, A. T., Employing Arynes in Diels–Alder Reactions and Transition-Metal-Free Multicomponent Coupling and Arylation Reactions. *Acc. Chem. Res.* **2016,** *49*, 1658-1670.

13. (a) Castedo, L.; Guitian, E.; Saá, C.; Suau, R.; Saá, J. M., Regioselectivity in the [4+2] cycloaddition of benzyne. Synthesis of 11-substituted aporphines. *Tetrahedron Lett.* **1983,** *24*, 2107-2108. (b) Matsumoto, T.; Hosoya, T.; Katsuki, M.; Suzuki, K., New efficient protocol for aryne generation. Selective synthesis of differentially protected 1,4,5-naphthalenetriols. *Tetrahedron Lett.* **1991,** *32*, 6735-6736.

14. For earlier examples, see: (a) Hamura, T.; Ibusuki, Y.; Sato, K.; Matsumoto, T.; Osamura, Y.; Suzuki, K., Strain-induced regioselectivities in reactions of benzyne possessing a fused four-membered ring. *Org. Lett.* **2003,** *5*, 3551-3554. (b) Garr, A. N.; Luo, D.; Brown, N.; Cramer, C. J.; Buszek, K. R.; VanderVelde, D., Experimental and theoretical investigations into the unusual regioselectivity of 4,5-, 5,6-, and 6,7-indole aryne cycloadditions. *Org. Lett.* **2010,** *12*, 96-9. (c) Cheong, P. H. Y.; Paton, R. S.; Bronner, S. M.; Im, G. Y. J.; Garg, N. K.; Houk, K. N., Indolyne and aryne distortions and nucleophilic regioselectivites. *J. Am. Chem. Soc.* **2010,** *132*, 1267-1269.

15. For more recent examples, particularly for studies of the distortion and regioselectivity of various hetarynes, see: (a) Picazo, E.; Houk, K. N.; Garg, N. K., Computational predictions of substituted benzyne and indolyne regioselectivities. *Tetrahedron Lett.* **2015,** *56*, 3511-3514. (b) Medina, J. M.; Mackey, J. L.; Garg, N. K.; Houk, K. N., The Role of Aryne Distortions, Steric Effects, and Charges on Regioselectivities of Aryne Reactions. *J. Am. Chem. Soc.* **2014,** *136*, 15798-15805. (c) Goetz, A. E.; Garg, N. K., Enabling the Use of Heterocyclic Arynes in Chemical Synthesis. *J. Org. Chem.* **2014,** *79*, 846-851. (d) Goetz, A. E.; Garg, N. K., Regioselective reactions of 3,4-pyridynes enabled by the aryne distortion model. *Nat. Chem.* **2012,** *5*, 54. (e) Bronner, S. M.; Mackey, J. L.; Houk, K. N.; Garg, N. K., Steric Effects Compete with Aryne Distortion To Control Regioselectivities of Nucleophilic Additions to 3-Silylarynes. *J. Am. Chem. Soc.* **2012,** *134*, 13966-13969. (f) Goetz, A. E.; Bronner, S. M.; Cisneros, J. D.; Melamed, J. M.; Paton, R. S.; Houk, K. N.; Garg, N. K., An Efficient Computational Model to Predict the Synthetic Utility of Heterocyclic Arynes.

Angew. Chem. Int. Ed. **2012,** *51*, 2758-2762. (g) Cheong, P. H. Y.; Paton, R. S.; Bronner, S. M.; Im, G. Y. J.; Garg, N. K.; Houk, K. N., Indolyne and aryne distortions and nucleophilic regioselectivites. *J. Am. Chem. Soc.* **2010,** *132*, 1267-1269.

16. (a) Medina, J. M.; McMahon, T. C.; Jiménez-Osés, G.; Houk, K. N.; Garg, N. K., Cycloadditions of cyclohexynes and cyclopentyne. *J. Am. Chem. Soc.* **2014,** *136*, 14706-9. (b) McMahon, T. C.; Medina, J. M.; Yang, Y.-F.; Simmons, B. J.; Houk, K. N.; Garg, N. K., Generation and Regioselective Trapping of a 3,4-Piperidyne for the Synthesis of Functionalized Heterocycles. *J. Am. Chem. Soc.* **2015**. (c) Shah, T. K.; Medina, J. M.; Garg, N. K., Expanding the Strained Alkyne Toolbox: Generation and Utility of Oxygen-Containing Strained Alkynes. *J. Am. Chem. Soc.* **2016,** *138*, 4948-4954.

17. a) Barber, J. S.; Styduhar, E. D.; Pham, H. V.; McMahon, T. C.; Houk, K. N.; Garg, N. K., Nitrone Cycloadditions of 1,2-Cyclohexadiene. *J. Am. Chem. Soc.* **2016,** *138*, 2512-2515. (b) Barber, J. S.; Yamano, M. M.; Ramirez, M.; Darzi, E. R.; Knapp, R. R.; Liu, F.; Houk, K. N.; Garg, N. K., Diels–Alder cycloadditions of strained azacyclic allenes. *Nat. Chem.* **2018,** *10*, 953-960. (c) Yamano, M. M.; Knapp, R. R.; Ngamnithiporn, A.; Ramirez, M.; Houk, K. N.; Stoltz, B. M.; Garg, N. K., Cycloadditions of Oxacyclic Allenes and a Catalytic Asymmetric Entryway to Enantioenriched Cyclic Allenes. *Angew. Chem. Int. Ed.* **2019,** *58*, 5653-5657.

18. Campbell, C. D.; Rees, C. W., Reactive intermediates. Part I. Synthesis and oxidation of 1- and 2-aminobenzotriazole. *J. Chem. Soc. C* **1969,** *0*, 742-742.

19. Wittig, G.; Hoffmann, R. W., Dehydrobenzol aus 1.2.3-Benzothiadiazol-1.1-dioxyd. *Chemische Berichte* **1962,** *95*, 2718-2728.

20. Stiles, M.; Miller, R. G.; Burckhardt, U., Reactions of Benzyne Intermediates in Non-basic Media. *J. Am. Chem. Soc.* **1963,** *85*, 1792-1797.

21. Logullo, F. M.; Seitz, A. H.; Friedman, L., Benzenediazonium-2-carboxylate and Biphenylene. *Org. Synth.* **1968,** *48*, 12.

22. Himeshima, Y.; Sonoda, T.; Kobayashi, H., Fluoride-induced 1,2-elimination of o-trimethylsilylphenyl triflate to benzyne under mild conditions. *Chem. Lett.* **1983**, 1211-1214.

23. For a brief overview of the synthetic methods used to access various *o*-trimethylsilylphenyl triflate benzyne precursors, refer to Section 6 of ref. 12(a).
24. Diels, O.; Alder, K., Synthesen in der hydroaromatischen Reihe. *Justus Liebig's Annalen der Chemie* **1928,** *460*, 98-122.

25. For just a few of the dozens of relatively recent reviews regarding the Diels–Alder reaction and its applications in organic synthesis, refer to (a) Nicolaou, K. C.; Snyder, S. A.; Montagnon, T.; Vassilikogiannakis, G., The Diels-Alder Reaction in Total Synthesis. *Angew. Chem. Int. Ed.* **2002,** *41*, 1668-1698. (b) Juhl, M.; Tanner, D., Recent applications of intramolecular Diels–Alder reactions to natural product synthesis. *Chem. Soc. Rev.* **2009,** *38*, 2983-2992. (c) Corey, E. J., Catalytic Enantioselective Diels–Alder Reactions: Methods, Mechanistic Fundamentals, Pathways, and Applications. *Angew. Chem. Int. Ed.* **2002,** *41*, 1650-1667. (d) Funel, J.-A.; Abele, S., Industrial applications of the Diels-Alder reaction. *Angew. Chem. Int. Ed.* **2013,** *52*, 3822-63. (e) Takao, K.-I.; Munakata, R.; Tadano, K.-i., Recent advances in natural product synthesis by using intramolecular Diels-Alder reactions. *Chem. Rev.* **2005,** *105*, 4779-807.

26. Michael, A.; Bucher, J. E., Ueber die Einwirkung von Essigsäureanhydrid auf Säuren der Acetylenreihe. *Ber. Dtsch. Chem. Ges* **1895,** *28*, 2511-2512.

27. Wessig, P.; Müller, G., The dehydro-Diels-Alder reaction. *Chem. Rev.* **2008,** *108*, 2051-63.

28. For recent examples of applications of the DDA reaction in total synthesis, see (a) McGee, P.; Bétournay, G.; Barabé, F.; Barriault, L., A 11-Steps Total Synthesis of Magellanine through a Gold(I)-Catalyzed Dehydro Diels–Alder Reaction. *Angew. Chem. Int. Ed.* **2017,** *56*, 6280-6283. (b) Reddy, M. C.; Jeganmohan, M., Total synthesis of aristolactam alkaloids via synergistic C–H bond activation and dehydro-Diels–Alder reactions. *Chem. Sci.* **2017,** *8*, 4130-4135. (c) Chinta, B. S.; Sanapa, H.; Vasikarla, K. P.; Baire, B., Synthetic approach to seco-tetracenomycin natural products saccharothrixone A–C. *Tetrahedron Lett.* **2018,** *59*, 1970-1973. (d) Chinta, B. S.; Siraswar, A.; Baire, B., The dehydro Diels-Alder (DDA) reaction based approach to isofuranonaphthalenone, nodulones A-C and xestolactone A. *Tetrahedron* **2017,** *73*, 4178-4185. (e) Chinta, B. S.; Baire, B., Total synthesis of selaginpulvilins A and C. *Org. Biomol. Chem* **2018,** *16*, 262-265.

29. Calculations run by Johnson and coworkers Ajaz, A.; Bradley, A. Z.; Burrell, R. C.; Li, W. H. H.; Daoust, K. J.; Bovee, L. B.; DiRico, K. J.; Johnson, R. P., Concerted vs stepwise mechanisms in dehydro-Diels-Alder reactions. *J. Org. Chem.* **2011,** *76*, 9320-8.

30. As a demonstrative example, the heat of hydrogenation ($\Delta H°$) of acetylene to ethane (1 atm, 25 °C) is –74.4 kcal•mol^{-1}l while the $\Delta H°$ of ethylene to ethane is –32.8 kcal•mol^{-1}. The $\Delta\Delta H°$ of these values (41.6 kcal•mol^{-1}), which can be taken to be the value of $\Delta H°$ for the hydrogenation acetylene to ethylene, is 8.8 kcal•mol^{-1} more exothermic than the hydrogenation of ethylene to ethane. $\Delta H°$ values for acetylene and ethylene were taken from: Roberts, J. D.; Caserio, M. C., Alkenes and Alkynes II. Oxidation and Reduction Reactions. Acidity of Alkynes.

In *Basic Principles of Organic Chemistry*, Benjamin Inc.: Menlo Park, 1977; pp 405-444.

31. Bradley, A. Z.; Johnson, R. P., Thermolysis of 1,3,8-Nonatriyne: Evidence for Intramolecular [2 + 4] Cycloaromatization to a Benzyne Intermediate. *J. Am. Chem. Soc.* **1997,** *119*, 9917-9918.

32. (a) Jones, R. R.; Bergman, R. G., p-Benzyne. Generation as an intermediate in a thermal isomerization reaction and trapping evidence for the 1,4-benzenediyl structure. *J. Am. Chem. Soc.* **1972,** *94*, 660-661. (b) Bergman, R. G., Reactive 1,4-dehydroaromatics. *Acc. Chem. Res.* **1973,** *6*, 25-31. (c) Grissom, J. W.; Gunawardena, G. U.; Klingberg, D.; Huang, D., The chemistry of enediynes, enyne allenes and related compounds. *Tetrahedron* **1996,** *52*, 6453-6518.

33. (a) Miyawaki, K.; Suzuki, R.; Kawano, T.; Ueda, I., Cycloaromatization of a non-conjugated polyenyne system: Synthesis of 5H-benzo[d]fluoreno[3,2-b]pyrans via diradicals generated from 1-[2-{4-(2-alkoxymethylphenyl)butan-1,3-diynyl}]phenylpentan-2,4-diyn-1-ols and trapping evidence for the 1,2-didehydroben. *Tetrahedron Lett.* **1997,** *38*, 3943-3946. (b) Miyawaki, K.; Kawano, T.; Ueda, I., Multiple cycloaromatization of novel aromatic enediynes bearing a triggering device on the terminal acetylene carbon. *Tetrahedron Lett.* **1998,** *39*, 6923-6926. (c) Ueda, I.; Sakurai, Y.; Kawano, T.; Wada, Y.; Futai, M., An unprecedented arylcarbene formation in thermal reaction of non-conjugated aromatic enetetraynes and DNA strand cleavage. *Tetrahedron Lett.* **1999,** *40*, 319-322. (d) Miyawaki, K.; Kawano, T.; Ueda, I., Domino thermal radical cycloaromatization of non-conjugated aromatic hexa- and heptaynes: synthesis of fluoranthene and benzo[a]rubicene skeletons. *Tetrahedron Lett.* **2000,** *41*, 1447-1451.

34. Tsui, J. A.; Sterenberg, B. T., A Metal-Templated 4 + 2 Cycloaddition Reaction of an Alkyne and a Diyne To Form a 1,2-Aryne. *Organometallics* **2009,** *28*, 4906-4908.

35. Hoye, T. R.; Baire, B. B.; Niu, D.; Willoughby, P. H.; Woods, B. P., The hexadehydro-Diels–Alder reaction. *Nature* **2012,** *490*, 208.

36. Having said this, it is still advisable to—as one reviewer of this paper so aptly pointed out—never underestimate the power of mere heat.

37. Woods, B. P.; Baire, B.; Hoye, T. R., Rates of Hexadehydro-Diels–Alder (HDDA) Cyclizations: Impact of the Linker Structure. *Org. Lett.* **2014,** *16*, 4578-4581.

38. Xiao, X.; Woods, B. P.; Xiu, W.; Hoye, T. R., Benzocyclobutadienes: An Unusual Mode of Access Reveals Unusual Modes of Reactivity. *Angew. Chem. Int. Ed.* **2018,** *57*, 9901-9905.

39. For publications that review recent developments of the HDDA reaction, refer to: (a) Diamond, O. J.; Marder, T. B., Methodology and applications of the hexadehydro-Diels–Alder (HDDA) reaction. *Org. Chem. Front.* **2017,** *4*, 891-910. (b) Holden , C.; Greaney, M. F., The Hexadehydro-Diels–Alder Reaction: A New Chapter in Aryne Chemistry. *Angew. Chem. Int. Ed.* **2014,** *53*, 5746-5749.

40. Karmakar, R.; Mamidipalli, P.; Yun, S. Y.; Lee, D., Alder-ene reactions of arynes. *Org. Lett.* **2013,** *15*, 1938-41.

41. Pogula, V. D.; Wang, T.; Hoye, T. R., Intramolecular [4 + 2] Trapping of a Hexadehydro-Diels–Alder (HDDA) Benzyne by Tethered Arenes. *Org. Lett.* **2015,** *17*, 856-859.

42. Xiao, X.; Hoye, T. R., The domino hexadehydro-Diels–Alder reaction transforms polyynes to benzynes to naphthynes to anthracynes to tetracynes (and beyond?). *Nat. Chem.* **2018,** *10*, 838-844.

43. Willoughby, P. H.; Niu, D.; Wang, T.; Haj, M. K.; Cramer, C. J.; Hoye, T. R., Mechanism of the Reactions of Alcohols with o-Benzynes. *J. Am. Chem. Soc.* **2014,** *136*, 13657-13665.

44. Ross, S. P.; Baire, B.; Hoye, T. R., Mechanistic Duality in Tertiary Amine Additions to Thermally Generated Hexadehydro-Diels–Alder Benzynes. *Org. Lett.* **2017,** *19*, 5705-5708.

45. Chen, J.; Baire, B.; Hoye, T. R., Cycloaddition reactions of azide, furan, and pyrrole units with benzynes generated by the hexadehydro-Diels–Alder (HDDA) reaction. *Heterocycles* **2014,** *88*, 1191-1200.

46. Niu, D.; Willoughby, P. H.; Woods, B. P.; Baire, B.; Hoye, T. R., Alkane desaturation by concerted double hydrogen atom transfer to benzyne. *Nature* **2013,** *501*, 531-4.

47. (a) Reetz, M. T., Dyotropic Rearrangements, a New Class of Orbital-Symmetry Controlled Reactions. Type II. *Angew. Chem. Int. Ed* **1972,** *11*, 130-131. (b) Fernández, I.; Sierra, M. A.; Cossío, F. P., In-Plane Aromaticity in Double Group Transfer Reactions. *J. Org. Chem.* **2007,** *72*, 1488-1491. (c) Fernández, I.; Cossío, F. P.; Sierra, M. A., Dyotropic Reactions: Mechanisms and Synthetic Applications. *Chem. Rev.* **2009,** *109*, 6687-6711.

48. Niu, D.; Wang, T.; Woods, B. P.; Hoye, T. R., Dichlorination of (hexadehydro-Diels-Alder generated) benzynes and a protocol for interrogating the kinetic order of bimolecular aryne trapping reactions. *Org. Lett.* **2014,** *16*, 254-7.

49. Wang, T.; Oswood, C. J.; Hoye, T. R., Trapping of Hexadehydro-Diels–Alder Benzynes with Exocyclic, Conjugated Enals as a Route to Fused Spirocyclic Benzopyran Motifs. *Synlett* **2017,** *28*, 2933-2935.

50. Palani, V.; Chen, J.; Hoye, T. R., Reactions of Hexadehydro-Diels–Alder (HDDA)-Derived Benzynes with Thioamides: Synthesis of Dihydrobenzothiazino-Heterocyclics. *Org. Lett.* **2016,** *18*, 6312-6315.

51. Zhang, J.; Niu, D.; Brinker, V. A.; Hoye, T. R., The Phenol–Ene Reaction: Biaryl Synthesis via Trapping Reactions between HDDA-Generated Benzynes and Phenolics. *Org. Lett.* **2016,** *18*, 5596-5599.

52. Ross, S. P.; Hoye, T. R., Multiheterocyclic Motifs via Three-Component Reactions of Benzynes, Cyclic Amines, and Protic Nucleophiles. *Org. Lett.* **2018,** *20*, 100-103.

53. Hoye, J. C.; Vignesh, P.; Thomas, R., Reactions of HDDA-Derived Benzynes with Sulfides: Mechanism, Modes, and Three-Component Reactions. *J. Am. Chem. Soc.* **2016,** *138*, 4318–4321.

54. Xiao, X.; Wang, T.; Xu, F.; Hoye, T. R., CuI-Mediated Bromoalkynylation and Hydroalkynylation Reactions of Unsymmetrical Benzynes: Complementary Modes of Addition. *Angew. Chem. Int. Ed.* **2018,** *57*, 16564-16568.

55. Ross, S. P.; Hoye, T. R., Reactions of hexadehydro-Diels–Alder benzynes with structurally complex multifunctional natural products. *Nat. Chem.* **2017,** *9*, 523-530.

56. Xu, F.; Xiao, X.; Hoye, T. R., Reactions of HDDA-Derived Benzynes with Perylenes: Rapid Construction of Polycyclic Aromatic Compounds. *Org. Lett.* **2016,** *18*, 5636-5639.

57. Xu, F.; Kyle, W. H.; Russell, J. H.; Hoye, T. R., Blue-Emitting Arylalkynyl Naphthalene Derivatives via a Hexadehydro-Diels–Alder Cascade Reaction. *J. Am. Chem. Soc.* **2016,** *138*, 12739–12742.

58. Okuma, K.; Nojima, A.; Matsunaga, N.; Shioji, K., Reaction of Benzyne with Salicylaldehydes: General Synthesis of Xanthenes, Xanthones, and Xanthols. *Org. Lett.* **2009,** *11*, 169-171.

59. Yoshida, H.; Fukushima, H.; Ohshita, J.; Kunai, A., Arynes in a three-component coupling reaction: straightforward synthesis of benzoannulated iminofurans. *Angew. Chem. Int. Ed.* **2004,** *43*, 3935-8.

60. (a) Rokita, S. E. Quinone Methides. 1, Wiley: Hoboken, 2009. (b) Willis, N. J.; Bray, C. D., ortho-Quinone Methides in Natural Product Synthesis. *Chem. Eur. J.* **2012,** *18*, 9160-9173. (c) Yang, B.; Gao, S., Recent advances in the application of Diels–Alder reactions involving o-quinodimethanes, aza-o-quinone methides and o-quinone methides in natural product total synthesis. *Chem. Soc. Rev.* **2018,** *47*, 7926-7953. (d) Singh, M. S.; Nagaraju, A.; Anand, N.; Chowdhury, S., ortho-Quinone methide (o-QM): a highly reactive, ephemeral and versatile intermediate in organic synthesis. *RSC Adv.* **2014,** *4*, 55924-55959. (e) Bai, W.-J.; David, J. G.; Feng, Z.-G.; Weaver, M. G.; Wu, K.-L.; Pettus, T. R. R., The Domestication of ortho-Quinone Methides. *Acc. Chem. Res.* **2014**.

61. (a) Yoshida, H.; Watanabe, M.; Fukushima, H.; Ohshita, J.; Kunai, A., A 2:1 Coupling Reaction of Arynes with Aldehydes via *o*-Quinone Methides: Straightforward Synthesis of 9-Arylxanthenes. *Org. Lett.* **2004,** *6*, 4049-4051. (b) Yoshida, H.; Ito, Y.; Ohshita, J., Three-component coupling using arynes and DMF: straightforward access to coumarins via ortho-quinone methides. *Chem. Commun.* **2011,** *47*, 8512-8512.

62. The use of styrene also did not yield the desired three-component reaction product.

63. There are only two reported examples of such a reaction in the literature: (a) Heaney, H.; McCarty, C. T., Reactions of arynes with carbonyl compounds. *J. Chem. Soc. D: Chem. Comm.* **1970**, 123a-123a. (b) Jyuzo, N.; Masayuki, Y.; Osamu, S., Reaction of benzyne generated from 1-(2-carboxylphenyl)-3,3-dimethyltriazene with benzaldehyde and some other carbonyl compounds. *Chem. Lett.* **1973,** *2*, 451-454.

64. This proposed preference was based on the assumption that the partial positive charge on the carbonyl carbon, which would develop increasing positive charge during the trapping even, would be more effectively stabilized by an aryl rather than an alkyl substituent.

65. The use of acetaldehyde, formaldehyde, and acetone as the third-component also failed to yield their desired mixed benzodioxane products.

66. When this same reaction was carried out in acetonitrile (like the HDDA reactions in Figure 2.3) rather than benzene, the yield of product **2023** was merely 5%.

67. Similarly, when acetonitrile was used as the reaction solvent instead of benzene, the yield was significantly lower (11%).

68. Vanoye, L.; Favre-Réguillon, A.; Aloui, A.; Philippe, R.; de Bellefon, C., Insights in the aerobic oxidation of aldehydes. *RSC Adv.* **2013,** *3*, 18931-18937.

69. (a) Tambar, U. K.; Stoltz, B. M., The Direct Acyl-Alkylation of Arynes. *J. Am. Chem. Soc.* **2005,** *127*, 5340-5341. (b) Tadross, P. M.; Virgil, S. C.; Stoltz, B. M., Aryne Acyl-Alkylation in the General and Convergent Synthesis of Benzannulated Macrolactone Natural Products: An Enantioselective Synthesis of (−)-Curvularin. *Org. Lett.* **2010,** *12*, 1612-1614. (c) Yoshida, H.; Watanabe, M.; Ohshita, J.; Kunai, A., Facile insertion reaction of arynes into carbon–carbon σ-bonds. *Chem. Commun.* **2005**, 3292-3294.

70. In contrast to other 1,3-dicarbonyl compounds, molecular traps that contain a protic amide (such as β-keto amides and malonamide esters) yield α-arylation products from reaction with Kobayashi benzyne: (a) Mohanan, K.; Coquerel, Y.; Rodriguez, J., Transition-Metal-Free α-Arylation of β-Keto Amides via an Interrupted Insertion Reaction of Arynes. *Org. Lett.* **2012,** *14*, 4686-4689. (b) Dhokale, R. A.; Thakare, P. R.; Mhaske, S. B., Transition-Metal-Free C-Arylation at Room Temperature by Arynes. *Org. Lett.* **2012,** *14*, 3994-3997. (c) Gupta, E.; Kant, R.; Mohanan, K., Decarbethoxylative Arylation Employing Arynes: A Metal-Free Pathway to Arylfluoroamides. *Org. Lett.* **2017,** *19*, 6016-6019.

71. It should also be noted that, while they are not 1,3-dicarbonyl compounds per se, β-enamino esters and ketones yield α-arylation products under the Kobayashi conditions: (a) Ramtohul, Y. K.; Chartrand, A., Direct C-Arylation of β-Enamino Esters and Ketones with Arynes. *Org. Lett.* **2007,** *9*, 1029-1032. (b) Picazo, E.; Anthony, S. M.; Giroud, M.; Simon, A.; Miller, M. A.; Houk, K. N.; Garg, N. K., Arynes and Cyclic Alkynes as Synthetic Building Blocks for Stereodefined Quaternary Centers. *J. Am. Chem. Soc.* **2018,** *140*, 7605-7610.

72. Wang, T.; Naredla, R. R.; Thompson, S. K.; Hoye, T. R., The pentadehydro-Diels–Alder reaction. *Nature* **2016,** *532*, 484.

73. Krause, N.; Hashmi, A. S. K. Modern Allene Chemistry. Wiley-VCH: Weinheim, 2004.

74. (a) Myers, A. G.; Kuo, E. Y.; Finney, N. S., Thermal generation of .alpha.,3-dehydrotoluene from (Z)-1,2,4-heptatrien-6-yne. *J. Am. Chem. Soc.* **1989,** *111*, 8057-8059. (b) Myers, A. G.; Dragovich, P. S.; Kuo, E. Y., Studies on the thermal generation and reactivity of a class of (.sigma.,.pi.)-1,4-biradicals. *J. Am. Chem. Soc.* **1992,** *114*, 9369-9386.

75. This cycloaromatization is probably most well-known for being integral to the mechanism of cytotoxicity for certain ene-diyne natural products such as neocarzinostatin. For relevant references, see: (a) Myers, A. G.; Proteau, P. J.;

Handel, T. M., Stereochemical assignment of neocarzinostatin chromophore. Structures of neocarzinostatin chromophore-methyl thioglycolate adducts. *J. Am. Chem. Soc.* **1988,** *110*, 7212-7214. (b) Nagata, R.; Yamanaka, H.; Murahashi, E.; Saito, I., DNA cleavage by acyclic eneyne-allene systems related to neocarzinostatin and esperamicin-calicheamicin. *Tetrahedron Lett.* **1990,** *31*, 2907-2910. (c) Nicolaou, K. C.; Maligres, P.; Shin, J.; De Leon, E.; Rideout, D., DNA-cleavage and antitumor activity of designed molecules with conjugated phosphine oxide-allene-ene-yne functionalities. *J. Am. Chem. Soc.* **1990,** *112*, 7825-7826.

76. One limitation in using the Myers–Saito reaction to access α,3-dehydrotoluene products is the tendency of certain allenyl enyne substrate to undergo a Schmittel cyclization. (a) Schmittel, M.; Strittmatter, M.; Kiau, S., Switching from the Myers reaction to a new thermal cyclization mode in enyne-allenes. *Tetrahedron Lett.* **1995,** *36*, 4975-4978. (b) Schmittel, M.; Keller, M.; Kiau, S.; Strittmatter, M., A Surprising Switch from the Myers–Saito Cyclization to a Novel Biradical Cyclization in Enyne–Allenes: Formal Diels–Alder and Ene Reactions with High Synthetic Potential. *Chem. Eur. J.* **1997,** *3*, 807-816.

77. While there exist countless examples of incorporations of alkynes into cycloaromatization processes, there are only a few examples of cycloaromatization reactions that involve nitriles. This will be an important premise to the work presented in Chapters 4 and 5.

78. Given the remarkable ease with which nitriles were incorporated into the PDDA reaction, it is interesting to note the following reported failure to incorporate a nitrile into a Myers–Saito cyclizaion: Gillmann, T.; Heckhoff, S., Aza-enyne allenes: Thermal reaction behavior of 2,4,5-hexatrienenitriles. *Tetrahedron Lett.* **1996,** *37*, 839-840.

79. Jung, M. E.; Piizzi, G., gem-Disubstituent Effect: Theoretical Basis and Synthetic Applications. *Chem. Rev.* **2005,** *105*, 1735-1766.

80. Admittedly, the formation of **3023** could occur through a competitive stepwise process. I did not attempt to locate the TS structures and intermediates for such a process.

81. Cyclic olefins are known to undergo Alder-Ene reactions with arynes: Chen, Z.; Liang, J.; Yin, J.; Yu, G.-A.; Liu, S. H., Alder-ene reaction of aryne with olefins. *Tetrahedron Lett.* **2013,** *54*, 5785-5787. This type of reaction was also observed when triyne **3025** was heated by itself in 1,4-cyclohexadiene.

82. Heating HDDA substrates in the presence of an added 1,3-diyne trap also does not result in an analogous HDDA–HDDA cascade, as the 1,3-diyne moiety more readily forms an alkynyl benzocyclobutadiene product in lieu of a naphthalyne

product (ref 29). The 1,3-diyne trap must be tethered to the benzyne precursor in order for this HDDA–HDDA cascade to occur (ref 38).

83. Wermuth, C. G., Are pyridazines privileged structures? *Med. Chem. Commun.* **2011,** *2*, 935-941.

84. The installation of the cyanoalkyne moiety proved to be somewhat troublesome but will be not be discussed here. The synthesis of cyanoalkyne substrates will be covered in more detail in Chapter 5.

85. Reux, D.; Pochat, F., Single step synthesis of 2,4-dicyanonaphthylamines from synthetic equivalents of α-cyanoalkynes. *J. Chem. Soc., Chem. Commun.* **1991**, 1419-1420.

86. The nitrile could also replace the end alkyne of the 1,3-diyne to make a substrate in which an alkyne is tethered to a cyanoalkyne moiety. The aza-HDDA reactions of such substrates will be the topic of the following chapter in this thesis (Chapter 5).

87. Vitaku, E.; Smith, D. T.; Njardarson, J. T., Analysis of the Structural Diversity, Substitution Patterns, and Frequency of Nitrogen Heterocycles among U.S. FDA Approved Pharmaceuticals. *J. Med. Chem.* **2014,** *57*, 10257-10274.

88. (a) Murakami, K.; Yamada, S.; Kaneda, T.; Itami, K., C–H Functionalization of Azines. *Chem. Rev.* **2017,** *117*, 9302-9332. (b) Allais, C.; Grassot, J.-M.; Rodriguez, J.; Constantieux, T., Metal-Free Multicomponent Syntheses of Pyridines. *Chem. Rev.* **2014,** *114*, 10829-10868. (c) Bull, J. A.; Mousseau, J. J.; Pelletier, G.; Charette, A. B., Synthesis of Pyridine and Dihydropyridine Derivatives by Regio- and Stereoselective Addition to N-Activated Pyridines. *Chem. Rev.* **2012,** *112*, 2642-2713.

89. For the original report of this reaction—sometimes referred to as the Bönnemann reaction—see: Bönnemann, H.; Brinkmann, R.; Schenkluhn, H., Eine einfache, kobalt-katalysierte Pyridin-Synthese. *Synthesis* **1974,** *1974*, 575-577.

90. For relatively recent reviews on this chemistry, see: (a) Varela, J. A.; Saá, C., Construction of Pyridine Rings by Metal-Mediated [2 + 2 + 2] Cycloaddition. *Chem. Rev.* **2003,** *103*, 3787-3802. (b) Heller, B.; Hapke, M., The fascinating construction of pyridine ring systems by transition metal-catalysed [2 + 2 + 2] cycloaddition reactions. *Chem. Soc. Rev.* **2007,** *36*, 1085-1094. (c) Domínguez, G.; Pérez-Castells, J., Recent advances in [2+2+2] cycloaddition reactions. *Chem. Soc. Rev.* **2011,** *40*, 3430-3444. (d) Varela, J. A.; Saá, C., Recent Advances in the Synthesis of Pyridines by Transition-Metal-Catalyzed [2+2+2] Cycloaddition. *Synlett* **2008,** *2008*, 2571-2578.

91. (a) Levine, R.; Leake, W. W., Rearrangement in the Reaction of 3-Bromopyridine with Sodium Amide and Sodioacetophenone. *Science* **1955,** *121*, 780-780. (b) May, C.; Moody, C. J., A new precursor to 3,4-didehydropyridine, and its use in the synthesis of the antitumour alkaloid ellipticine. *Journal of the Chemical Society, Perkin Transactions 1* **1988**, 247-250. (c) Snieckus, V.; Tsukazaki, M., Synthetic Connections to the Directed ortho Metalation Reaction. 3,4-Pyridynes from 4-Trialkylsilyl-3-pyridyl Triflates. *Heterocycles* **1992,** *33*, 533-536. (d) Vinter-Pasquier, K.; Jamart-Grégoire, B.; Caubère, P., Complex Base-Induced Generation of 3,4-Didehydropyridine Derivatives: New Access to Aminopyridines or Pyridones. *Heterocycles* **1997,** *45*, 2113-2129. (e) Walters, M. A.; Shay, J. J., 2,3-Pyridyne Formation by Fluoride-Induced Desilylation-Elimination. *Synth. Commun.* **1997,** *27*, 3573-3579. (f) Lin, W.; Chen, L.; Knochel, P., Preparation of functionalized 3,4-pyridynes via 2-magnesiated diaryl sulfonates. *Tetrahedron* **2007,** *63*, 2787-2797.

92. (a) Goetz, A. E.; Garg, N. K., Regioselective reactions of 3,4-pyridynes enabled by the aryne distortion model. *Nat. Chem.* **2012,** *5*, 54. (b) Enamorado, M. F.; Ondachi, P. W.; Comins, D. L., A Five-Step Synthesis of (S)-Macrostomine from (S)-Nicotine. *Org. Lett.* **2010,** *12*, 4513-4515. (c) Díaz, M.; Cobas, A.; Guitián, E.; Castedo, L., Synthesis of Ellipticine by Hetaryne Cycloadditions − Control of Regioselectivity. *European Journal of Organic Chemistry* **2001,** *2001*, 4543-4549. (d) Zoltewicz, J. A.; Nisi, C., Trapping of 3,4-pyridyne by thiomethoxide ion in ammonia. *J. Org. Chem.* **1969,** *34*, 765-766. (e) May, C.; Moody, C. J., A concise synthesis of the antitumour alkaloid ellipticine. *J. Chem. Soc., Chem. Commun.* **1984**, 926-927.

93. The thermodynamic instability of alkynes (as demonstrated by DFT calculations related to DDA reactions) was briefly discussed in section 1.2.1. The relative stability of alkynes compared to nitrile was shown as part of the *in silico* studies of the PDDA reaction in section 3.3.2.

94. An additional demonstrative example of this can be seen in the (computed) □H° value for the addition of H_2 to ethyne (to ethene) vs. that for its addition to hydrogen cyanide (to methanimine). The former is -47.1 kcal•mol^{-1} while the latter is -11.7 kcal•mol^{-1}. Lan, Y.; Danheiser, R. L.; Houk, K. N., Why Nature Eschews the Concerted [2 + 2 + 2] Cycloaddition of a Nonconjugated Cyanodiyne. Computational Study of a Pyridine Synthesis Involving an Ene–Diels–Alder–Bimolecular Hydrogen-Transfer Mechanism. *J. Org. Chem.* **2012,** *77*, 1533-1538.

95. While there do exist scattered examples of the participation of nitriles in the Diels–Alder reaction, they required either prohibitively high temperatures or the use of strongly activated nitriles such as tosyl cyanide. (a) Boger, D. L.; Weinreb, S. M. Hetero Diels–Alder Methodology in Organic Synthesis. Academic Press: San Diego, 1987. (b) van Leusen, A. M.; Jagt, J. C., Cycloaddition reactions of

sulfonyl cyanides. *Tetrahedron Lett.* **1970,** *11*, 971-973. (c) Sasaki, M.; Hamzik, P. J.; Ikemoto, H.; Bartko, S. G.; Danheiser, R. L., Formal Bimolecular [2 + 2 + 2] Cycloaddition Strategy for the Synthesis of Pyridines: Intramolecular Propargylic Ene Reaction/Aza Diels–Alder Reaction Cascades. *Org. Lett.* **2018,** *20*, 6244-6249.

96. Nitriles are known to undergo thermal 1,3-dipolar cycloadditions with azides to give tetrazoles. As is the case with nitrile Diels–Alder reactions, activated cyano groups such as tosyl and acyl nitriles are required for the reactions to proceed at reasonable temperatures. (a) Huisgen, R., 1,3-Dipolar Cycloadditions. Past and Future. *Angew. Chem. Int. Ed* **1963,** *2*, 565-598. (b) Demko, Z. P.; Sharpless, K. B., A Click Chemistry Approach to Tetrazoles by Huisgen 1,3-Dipolar Cycloaddition: Synthesis of 5-Sulfonyl Tetrazoles from Azides and Sulfonyl Cyanides. *Angew. Chem. Int. Ed.* **2002,** *41*, 2110-2113. (c) Demko, Z. P.; Sharpless, K. B., A Click Chemistry Approach to Tetrazoles by Huisgen 1,3-Dipolar Cycloaddition: Synthesis of 5-Acyltetrazoles from Azides and Acyl Cyanides. *Angew. Chem. Int. Ed.* **2002,** *41*, 2113-2116. (d) Himo, F.; Demko, Z. P.; Noodleman, L.; Sharpless, K. B., Mechanisms of Tetrazole Formation by Addition of Azide to Nitriles. *J. Am. Chem. Soc.* **2002,** *124*, 12210–12216.

97. Rare examples of the participation of unactivated nitriles can been seen in the following two publications: Sakai, T.; Danheiser, R. L., Cyano Diels−Alder and Cyano Ene Reactions. Applications in a Formal [2 + 2 + 2] Cycloaddition Strategy for the Synthesis of Pyridines. *J. Am. Chem. Soc.* **2010,** *132*, 13203-13205. (b) You, X.; Xie, X.; Chen, H.; Li, Y.; Liu, Y., Cyano-Schmittel Cyclization through Base-Induced Propargyl-Allenyl Isomerization: Highly Modular Synthesis of Pyridine-Fused Aromatic Derivatives. *Chem. Eur. J.* **2015,** *21*, 18699-18705.

98. Hoye, T. R.; Baire, B.; Wang, T., Tactics for probing aryne reactivity: mechanistic studies of silicon–oxygen bond cleavage during the trapping of (HDDA-generated) benzynes by silyl ethers. *Chem. Sci.* **2014,** *5*, 545-545.

99. (a) Marell, D. J.; Furan, L. R.; Woods, B. P.; Lei, X.; Bendelsmith, A. J.; Cramer, C. J.; Hoye, T. R.; Kuwata, K. T., Mechanism of the Intramolecular Hexadehydro-Diels–Alder Reaction. *J. Org. Chem.* **2015,** *80*, 11744-11754. (b) Liang, Y.; Hong, X.; Yu, P.; Houk, K. N., Why Alkynyl Substituents Dramatically Accelerate Hexadehydro-Diels–Alder (HDDA) Reactions: Stepwise Mechanisms of HDDA Cycloadditions. *Org. Lett.* **2014,** *16*, 5702-5705. (c) Yu, P.; Yang, Z.; Liang, Y.; Hong, X.; Li, Y.; Houk, K. N., Distortion-Controlled Reactivity and Molecular Dynamics of Dehydro-Diels–Alder Reactions. *J. Am. Chem. Soc.* **2016,** *138*, 8247-8252. (d) Chen, M.; He, C. Q.; Houk, K. N., Mechanism and Regioselectivity of an Unsymmetrical Hexadehydro-Diels–Alder (HDDA) Reaction. *J. Org. Chem.* **2019,** *84*, 1959-1963.

100. Wang, T.; Niu, D.; Hoye, T. R., The Hexadehydro-Diels–Alder Cycloisomerization Reaction Proceeds by a Stepwise Mechanism. *J. Am. Chem. Soc.* **2016,** *138*, 7832-7835.

101. This computational process involves starting from the geometry of the diradical **4014$_{\text{diradical}}$**, and optimizing the geometry of the structure as the distance between the carbon atom and nitrogen atom of the forming C–N bond is gradually decreased. It was observed that the C–C bond that was formed in the first step to access **4014$_{\text{diradical}}$** started to cleave as the new C–N bond was formed.

102. (a) Armaly, A. M.; DePorre, Y. C.; Groso, E. J.; Riehl, P. S.; Schindler, C. S., Discovery of Novel Synthetic Methodologies and Reagents during Natural Product Synthesis in the Post-Palytoxin Era. *Chem. Rev.* **2015,** *115*, 9232-9276. (b) Nicolaou, K. C.; Vourloumis, D.; Winssinger, N.; Baran, P. S., The Art and Science of Total Synthesis at the Dawn of the Twenty-First Century. *Angew. Chem. Int. Ed.* **2000,** *39*, 44-122. (c) Nicolaou, K. C.; Snyder, S. A., The Essence of Total Synthesis. *Proc Natl Acad Sci* **2004,** *101*, 11929-11936.

103. Trost, B. M.; O'Boyle, B. M.; Hund, D., Investigation of a Domino Heck Reaction for the Rapid Synthesis of Bicyclic Natural Products. *Chem. Eur. J.* **2010,** *16*, 9772-9776.

104. Deno, N. C.; Potter, N. H., Mechanism of oxidation of alcohols by aqueous bromine. *J. Am. Chem. Soc.* **1967,** *89*, 3555-3556.

105. Palou, J., Oxidation of some organic compounds by aqueous bromine solutions. *Chem. Soc. Rev.* **1994,** *23*, 357-357.

106. When saying “standard conditions,” I refer to Sonogashira reaction conditions that I have used in the synthesis of HDDA substrates. Specifically, the conditions involve coupling of an aryl bromide with 1.1–1.5 equivalents of terminal alkyne in the presence of 1–2 mol% of $Pd(PPh_3)_2Cl_2$ and CuI using triethylamine as the solvent.

107. Zhang, L.; Li, B., A series of 4,5-diazafluoren-9-one-derived ligands and their Cu(I) complexes: Synthesis, characterization and photophysical properties. *Inorganica Chimica Acta* **2009,** *362*, 4857-4861.

108. (a) Ye, F.; Tran, C.; Jullien, L.; Le Saux, T.; Haddad, M.; Michelet, V.; Ratovelomanana-Vidal, V., Synthesis of Fluorescent Azafluorenones and Derivatives via a Ruthenium-Catalyzed [2 + 2 + 2] Cycloaddition. *Org. Lett.* **2018,** *20*, 4950-4953. (b) Gao, M.; Su, H.; Lin, Y.; Ling, X.; Li, S.; Qin, A.; Tang, B. Z., Photoactivatable aggregation-induced emission probes for lipid droplets-specific live cell imaging. *Chem. Sci.* **2017,** *8*, 1763-1768.

109. (a) Mueller, D.; Davis, R. A.; Duffy, S.; Avery, V. M.; Camp, D.; Quinn, R. J., Antimalarial Activity of Azafluorenone Alkaloids from the Australian Tree Mitrephora diversifolia. *J. Nat. Prod.* **2009,** *72*, 1538-1540. (b) Wijeratne, E. M. K.; De Silva, L. B.; Kikuchi, T.; Tezuka, Y.; Gunatilaka, A. A. L.; Kingston, D. G. I., Cyathocaline, an Azafluorenone Alkaloid from Cyathocalyx zeylanica. *J. Nat. Prod.* **1995,** *58*, 459-462. (c) Hufford, C. D.; Liu, S.; Clark, A. M.; Oguntimein, B. O., Anticandidal Activity of Eupolauridine and Onychine, Alkaloids from Cleistopholis patens. *J. Nat. Prod.* **1987,** *50*, 961-964. (d) Koyama, J.; Morita, I.; Kobayashi, N.; Osakai, T.; Usuki, Y.; Taniguchi, M., Structure–activity relations of azafluorenone and azaanthraquinone as antimicrobial compounds. *Bioorg. Med. Chem. Lett.* **2005,** *15*, 1079-1082. (e) Manpadi, M.; Uglinskii, P. Y.; Rastogi, S. K.; Cotter, K. M.; Wong, Y.-S. C.; Anderson, L. A.; Ortega, A. J.; Van slambrouck, S.; Steelant, W. F. A.; Rogelj, S.; Tongwa, P.; Antipin, M. Y.; Magedov, I. V.; Kornienko, A., Three-component synthesis and anticancer evaluation of polycyclic indenopyridines lead to the discovery of a novel indenoheterocycle with potent apoptosis inducing properties. *Org. Biomol. Chem* **2007,** *5*, 3865-3872. (f) Addla, D.; Bhima; Sridhar, B.; Devi, A.; Kantevari, S., Design, synthesis and antimicrobial evaluation of novel 1-benzyl 2-butyl-4-chloroimidazole embodied 4-azafluorenones via molecular hybridization approach. *Bioorg. Med. Chem. Lett.* **2012,** *22*, 7475-7480. (g) Goulart, M. O. F.; Santana, A. E. G.; De Oliveira, A. B.; De Oliveira, G. G.; Maia, J. G. S., Azafluorenones and azaanthraquinone from Guatteria dielsiana. *Phytochemistry* **1986,** *25*, 1691-1695.

110. You, X.; Xie, X.; Chen, H.; Li, Y.; Liu, Y., Cyano-Schmittel Cyclization through Base-Induced Propargyl-Allenyl Isomerization: Highly Modular Synthesis of Pyridine-Fused Aromatic Derivatives. *Chem. Eur. J.* **2015,** *21*, 18699-18705.

111. Tomás-Mendivil, E.; Heinrich, C. F.; Ortuno, J.-C.; Starck, J.; Michelet, V., Gold-Catalyzed Access to 1*H*-Isochromenes: Reaction Development and Mechanistic Insight. *ACS Catalysis* **2017,** *7*, 380-387.

112. Corey, E. J.; Katzenellenbogen, J. A.; Gilman, N. W.; Roman, S. A.; Erickson, B. W., Stereospecific total synthesis of the dl-C18 Cecropia juvenile hormone. *J. Am. Chem. Soc.* **1968,** *90*, 5618-5620.

113. Corey, E. J.; Gilman, N. W.; Ganem, B. E., New methods for the oxidation of aldehydes to carboxylic acids and esters. *J. Am. Chem. Soc.* **1968,** *90*, 5616-5617.

114. Nagata, W.; Yoshioka, M., Alkylaluminum cyanides as potent reagents for hydrocyanation. *Tetrahedron Lett.* **1966,** *7*, 1913-1918.

115. Nagata, W.; Yoshioka, M.; Hirai, S., Hydrocyanation. IV. New hydrocyanation methods using hydrogen cyanide and an alkylaluminum, and an alkylaluminum cyanide. *J. Am. Chem. Soc.* **1972,** *94*, 4635-4643.

116. Nicolaou, K. C.; Vassilikogiannakis, G.; Kranich, R.; Baran, P. S.; Zhong, Y.-L.; Swaminathan, N., New Synthetic Technology for the Mild and Selective One-Carbon Homologation of Hindered Aldehydes in the Presence of Ketones. *J. Am. Chem. Soc.* **2000,** *2*, 1895-1898.

117. Nicolaou, K. C.; Vassilikogiannakis, G.; Montagnon, T., The Total Synthesis of Coleophomones B and C. *Angew. Chem. Int. Ed.* **2002,** *41*, 3276-3281.

118. Nicolaou, K. C.; Montagnon, T.; Vassilikogiannakis, G.; Mathison, C. J. N., The Total Synthesis of Coleophomones B, C, and D. *J. Am. Chem. Soc.* **2005,** *127*, 8872–8888.

119. Evans, D. A.; Truesdale, L. K.; Carroll, G. L., Cyanosilylation of aldehydes and ketones. A convenient route to cyanohydrin derivatives. *J. Chem. Soc., Chem. Commun.* **1973,** *0*, 55-55.

120. Cossfo, F. P.; Aizpurua, J. M.; Palomo, C., Synthetic applications of chromium(VI) reagents in combination with chlorotrimethylsilane. *Can. J. Chem.* **1986,** *64*, 225-231.

121. Corey, E. J.; Schmidt, G., A simple route to Δ2-butenolides from conjugated aldehydes. *Tetrahedron Lett.* **1980,** *21*, 731-734.

122. Janosik, T.; Johnson, A.-L.; Bergman, J., Synthesis of the marine alkaloids rhopaladins A, B, C and D. *Tetrahedron* **2002,** *58*, 2813-2819.

123. Kandemir, H.; Wood, K.; Kumar, N.; Black, D. S., Synthesis of 5-(7′-indolyl)oxazoles and 2,5-di-(7′-indolyl)oxazoles. *Tetrahedron* **2013,** *69*, 2193-2198.

124. Sindhu, K. S.; Thankachan, A. P.; Sajitha, P. S.; Anilkumar, G., Recent developments and applications of the Cadiot–Chodkiewicz reaction. *Org. Biomol. Chem* **2015,** *13*, 6891-6905.

125. Baire, B.; Niu, D.; Willoughby, P. H.; Woods, B. P.; Hoye, T. R., Synthesis of complex benzenoids via the intermediate generation of o-benzynes through the hexadehydro-Diels-Alder reaction. *Nat. Protoc.* **2013,** *8*, 501-508.

126. Wittig, G.; Pohmer, L., Intermediäre Bildung von Dehydrobenzol (Cyclohexa-dienin). *Angewandte Chemie* **1955,** *67*, 348-348.

127. Bhojgude, S. S.; Biju, A. T., Arynes in transition-metal-free multicomponent coupling reactions. *Angew. Chem. Int. Ed.* **2012,** *51*, 1520-2.

128. Appel, R., Tertiary Phosphane/Tetrachloromethane, a Versatile Reagent for Chlorination, Dehydration, and P-N Linkage. *Angew. Chem. Int. Ed.* **1975,** *14*, 801-811.

129. (a) Mitsunobu, O.; Masaaki Yamada, Preparation of Esters of Carboxylic and Phosphoric Acid via Quaternary Phosphonium Salts. *Bull. Chem. Soc. Jpn.* **1967,** *40*. (b) Hughes, D. L., The Mitsunobu Reaction. *Org. React.* **1992,** *42*, 335.

130. Wilk, B. K., A Convenient Preparation of Alkyl Nitriles by the Mitsunobu Procedure. *Synth. Commun.* **2006,** *23*, 2481-2484.

131. Pérez, I. P.; Agustín, C.; Diego, P.; Enrique, G.; Dolores, 1,7-Naphthodiyne: a new platform for the synthesis of novel, sterically congested PAHs. *Chem. Commun.* **2016,** *52*, 5534-5537.

132. Mehta, G.; Kotha, S., Recent chemistry of benzocyclobutenes. *Tetrahedron* **2001,** *57*, 625-659.

133. Woodward, R. B.; Hoffmann, R., Conservation of Orbital Symmetry. *Angew. Chem. Int. Ed.* **1969,** *8*, 781-853.

134. Karmakar, R.; Yun, S. Y.; Chen, J.; Xia, Y.; Lee, D., Benzannulation of Triynes to Generate Functionalized Arenes by Spontaneous Incorporation of Nucleophiles. *Angew. Chem. Int. Ed.* **2015,** *54*, 6582-6586.

135. For examples, see: (a) Casarini, A.; Dembech, P.; Reginato, G.; Ricci, A.; Seconi, G., Terminal 1-halo- 1 and 1-pseudohalo-1-alkynes via bis(trimethylsilyl)peroxide (BTMSPO) promoted Umpolung transfer of Halides and pseudohalides. *Tetrahedron Lett.* **1991,** *32*, 2169-2170. (b) Kim, J.-G.; Lee, E. H.; Jang, D. O., One-pot synthesis of conjugated alkynenitriles from aldehydes. *Tetrahedron Lett.* **2007,** *48*, 2299-2301. (c) Yamamoto, Y.; Asatani, T.; Kirai, N., Copper-Catalyzed Stereoselective Hydroarylation of 3-Aryl-2- propynenitriles with Arylboronic Acids. *Advanced Synthesis & Catalysis* **2009,** *351*, 1243-1249. (d) Vatèle, J.-M., One-Pot Oxidative Conversion of Alcohols into Nitriles by Using a TEMPO/PhI(OAc)2/NH4OAc System. *Synlett* **2014,** *25*, 1275-1278.

136. Southwick, P. L.; Christman, D. R., Reactions of Iodine—Amine Complexes with Unsaturated Compounds. II. An Investigation of the Scope of the Reaction with the Iodine—Morpholine Complex. *J. Am. Chem. Soc.* **1953,** *75*, 629-632.

137. Mori, K.; Tominaga, M.; Takigawa, T.; Matsui, M., A Mild Transesterification Method. *Synthesis* **1973,** *1973*, 790-791.

138. (a) Otera, J.; Yano, T.; Kawabata, A.; Nozaki, H., Novel distannoxane-catalyzed transesterification and a new entry to α, β-unsaturated carboxylic acids.

Tetrahedron Lett. **1986,** *27*, 2383-2386. (b) Otera, J.; Danoh, N.; Nozaki, H., Novel template effects of distannoxane catalysts in highly efficient transesterification and esterification. *J. Org. Chem.* **1991,** *56*, 5307-5311.

139. For a good (albeit somewhat dated) overview of the use of organotin catalysts in transesterification reactions, refer to section VIII of the following review: Otera, J., Transesterification. *Chem. Rev.* **1993,** *93*, 1449-1470.

140. Several equivalents were used because the catalyst was several years old and this was a trial experiment. Otera's catalyst is usually capable of effectively catalyzing transesterification reactions at very low loadings.

141. Attempts to neutralize the hydrogen fluoride with a mildly basic workup of $NaHCO_3$ resulted in the formation of the aforementioned cyclic ether **5021**.

142. The addition of 5.0 molar equivalents of piperidine to a solution of substrate **5015** in *o*-DCB gave a black solution within a matter of seconds at room temperature.

143. Recall that this was seen to some extent in the reactions of the class I aza-HDDA substrates in Chapter 4.

144. The anticipated product of this reaction would actually not be **5025h** but rather its carbonyl-bridged precursor that would give **5025h** through a chelotropic elimination of carbon monoxide.

145. Deprotonation and substitution on propargylic, benzylic methylenes is precedented but not very common. For a few examples, see (a) Miura, K.; Okajima, S.; Hondo, T.; Nakagawa, T.; Takahashi, T.; Hosomi, A., Acid-Catalyzed Cyclization of Vinylsilanes Bearing a Hydroxy Group: A New Method for Stereoselective Synthesis of Disubstituted Tetrahydrofurans1. *J. Am. Chem. Soc.* **2000,** *122*, 11348-11357. (b) Yan, J.; Zhu, J.; Matasi, J. J.; Herndon, J. W., Relative Asymmetric Induction in the Intramolecular Reaction between Alkynes and Cyclopropylcarbene−Chromium Complexes: Stereocontrolled Synthesis of Five-Membered Rings Fused to Oxygen Heterocycles. *J. Org. Chem.* **1999,** *64*, 1291-1301. (c) Feldman, K. S.; Bruendl, M. M.; Schildknegt, K.; Bohnstedt, A. C., Inter- and Intramolecular Addition/Cyclizations of Sulfonamide Anions with Alkynyliodonium Triflates. Synthesis of Dihydropyrrole, Pyrrole, Indole, and Tosylenamide Heterocycles. *J. Org. Chem.* **1996,** *61*, 5440-5452. (d) Tarasova, O. A.; Brandsma, L.; Nedolya, N. A.; Afonin, A. V.; Ushakov, I. A.; Klyba, L. V., New Approach to the Synthesis of Strained Cyclic Systems: I. Iminocyclobutenes and Iminothietanes from 1,3-Dilithio-3-phenylpropyne and Methyl Isothiocyanate. *Russ. J. Org.* **2003,** *39*, 1451-1457.

146. Deprotonation/dialkylation of a benzylic, propargylic methylene is even more rare. Only two examples could be found in the literature: (a) Kinoshita, K.; Asoh,

K.; FuruchiI, N.; Ito, T.; Kawada, H.; Ishii, N.; Sakamoto, H.; Hong, W.; Park, M.; Ono, Y.; Kato, Y.; Morikami, K.; Emura, T.; Oikawa, N. Tetracyclic Compound. US2012083488, April 5th, 2012. (b) Aquila, B.; Dakin, L.; Ezhuthachan, J.; Lee, S.; Lyne, P.; Pontz, T.; Zheng, X. Quinazolineone Derivatives and Their Use as B-RAF Inhibitors WO2006024834 March 9th, 2006.

147. You may notice that intermediate **5034** itself could be converted to a cyanoalkyne aza-HDDA substrate. DFT calculations indicated that such a substrate would cyclize at tractable temperatures ($\Delta G^{\ddagger} = 32.8$ kcal•mol^{-1}). Unfortunately, the attempts to synthesize this substrate from **5034** (not discussed in this thesis) met with failure.

148. Imbri, D.; Tauber, J.; Opatz, T., A High-Yielding Modular Access to the Lamellarins: Synthesis of Lamellarin G Trimethyl Ether, Lamellarin η and Dihydrolamellarin η. *Chem. Eur. J.* **2013,** *19*, 15080-15083.